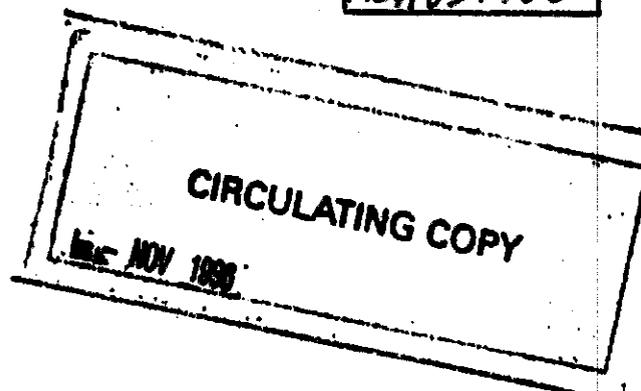


BRL R 1921

BRL

ADA031985



REPORT NO. 1921

PROJECT DIPOLE WEST - MULTIBURST ENVIRONMENT
(NON-SIMULTANEOUS DETONATIONS)

Ralph E. Reisler
Burnett A. Pettit

September 1976

Approved for public release; distribution unlimited.

USA BALLISTIC RESEARCH LABORATORIES
ABERDEEN PROVING GROUND, MARYLAND

Destroy this report when it is no longer needed.
Do not return it to the originator.

Secondary distribution of this report by originating
or sponsoring activity is prohibited.

Additional copies of this report may be obtained
from the National Technical Information Service,
U.S. Department of Commerce, Springfield, Virginia
22151.

The findings in this report are not to be construed as
an official Department of the Army position, unless
so designated by other authorized documents.

REPORT DOCUMENTATION PAGE		READ INSTRUCTIONS BEFORE COMPLETING FORM
1. REPORT NUMBER Report No. 1921	2. GOVT ACCESSION NO.	3. RECIPIENT'S CATALOG NUMBER
4. TITLE (and Subtitle) PROJECT DIPOLE WEST - MULTIBURST ENVIRONMENT (NON-SIMULTANEOUS DETONATIONS)	5. TYPE OF REPORT & PERIOD COVERED Final	
	6. PERFORMING ORG. REPORT NUMBER	
7. AUTHOR(s) Ralph E. Reisler Burnett A. Pettit	8. CONTRACT OR GRANT NUMBER(s) DNA 001-73-C-0229	
9. PERFORMING ORGANIZATION NAME AND ADDRESS USA Ballistic Research Laboratories Aberdeen Proving Ground, Maryland 21005	10. PROGRAM ELEMENT, PROJECT, TASK AREA & WORK UNIT NUMBERS N99QAXA-A111-04	
11. CONTROLLING OFFICE NAME AND ADDRESS U.S. Army Material Development & Readiness Command 5001 Eisenhower Avenue Alexandria, Virginia 22304	12. REPORT DATE September 1976	
	13. NUMBER OF PAGES 385	
14. MONITORING AGENCY NAME & ADDRESS (if different from Controlling Office) Defense Nuclear Agency Washington, D.C. 20305	15. SECURITY CLASS. (of this report) Unclassified	
	15a. DECLASSIFICATION/DOWNGRADING SCHEDULE	
16. DISTRIBUTION STATEMENT (of this Report) Approved for public release; distribution unlimited.		
17. DISTRIBUTION STATEMENT (of the abstract entered in Block 20, if different from Report)		
18. SUPPLEMENTARY NOTES		
19. KEY WORDS (Continue on reverse side if necessary and identify by block number) Multiburst Detonations Hydrodynamic Airblast Codes Non-Simultaneous Detonations Pentolite Charges		
20. ABSTRACT (Continue on reverse side if necessary and identify by block number) DIPOLE WEST (Non-Simultaneous Detonations) is a series of five high explosive experiments conducted by USA Ballistic Research Laboratories at the Defence Research Establishment, Suffield, in Alberta, Canada, during the fall of 1974 and spring of 1975. One of the experiments involved detonation of a single 216-pound pentolite charge; the remaining experiments consisted of two 216-pound pentolite charges for each event. The charges were detonated non-simultaneously, with times between detonations of 0, 3, 5, and 10 milliseconds.		

20. Abstract

Purpose of the series was to obtain information on the phenomenology of strong shock on shock, shock on fireball, and fireball flow interactions from the detonation of multiple high explosive charges. Density, particle velocity, stagnation pressure, and overpressure were measured at and near the ground surface as well as at and near the plane midway between charges. Measurement techniques included pressure transducers and high speed photography.

A Mach stem seen between the charges for shots with 0 and 3 millisecond separation times was not observed on the 5 and 10 millisecond shots. Comparisons made with the AFWL HULL hydrodynamic air blast code show good correlation.

FOREWORD

Project DIPOLE WEST was sponsored by the Defense Nuclear Agency and executed under the direct management of Mr. James F. Moulton, Jr., Chief, Aerospace Systems Division. Mr. John H. Keefer, Ballistic Research Laboratories, conceived the project and was responsible for its general supervision. Contributions were also made by Dr. John Dewey, University of Victoria; Mr. A. P. R. Lambert, Canadian General Electric; Mr. Charles Needham, Air Force Weapons Laboratory; and Mr. John Wisot-ski, Denver Research Institute. This report was edited by Dr. Lynn Kennedy of the Albuquerque Office of General Electric - TEMPO.

The planning, fielding, and analyzing of the results of a large experiment of this type require the dedicated effort of many well trained people. We would particularly like to record our appreciation for assistance so willingly supplied by the Defense Research Establishment, Suffield. In addition to those previously mentioned, the following organizations and personnel contributed significantly to the success of this operation.

AIR FORCE WEAPONS LABORATORY
Capt. Dan Matuska

BENDIX CORPORATION
Mr. Ted Maxfield

CANADIAN ARSENALS
Mr. John B. Marchand

DEFENSE NUCLEAR AGENCY
Mr. Clifton W. Lewis

DEFENCE RESEARCH ESTABLISHMENT SUFFIELD
Mr. Ron Bengston
Mr. Roy Brown
Mr. M. L. Fach
Mr. J. Francis
Mr. Joe Godin
Mr. George Hosking
Mr. Ken Jackson
Mr. R. A. Klymchuk
Mr. Brian Laidlaw
Mr. S. May
Mr. John A. McCallum
Mr. C. C. McIvor
Mr. J. H. Pinnell
Mr. Gordon P. Smart
Mr. C. C. Sutherland
Mr. F. Trafford

Mr. R. H. Withers
Mr. Richard C. M. Wyld

DENVER RESEARCH INSTITUTE

Mr. Bob Marchese
Mr. Larry Brown
Mr. Ray Bjarnason

GENERAL ELECTRIC COMPANY - TEMPO

Mr. Paul Burda
Mr. Warren Chan
Mr. Harry Pearce
Ms. Ellen Stewart

UNIVERSITY OF VICTORIA

Mr. David Classen
Mr. Douglas McMillin

CONVERSION FACTORS

U.S. customary units of measurement used in this study were converted to metric (SI) units as follows:

<u>Multiply</u>	<u>By</u>	<u>To Obtain</u>
inches	2.54	centimeters
feet	0.3048	meters
pounds (mass)	0.4536	kilograms
pounds (force) per square inch	6.895	kilopascals
pounds (mass) per cubic foot	16.02	kilograms per cubic meter
feet per second	0.3048	meters per second

TABLE OF CONTENTS

	<u>Page</u>
FOREWORD	3
LIST OF ILLUSTRATIONS	7
LIST OF TABLES	13
1. INTRODUCTION	15
1.1 Background	15
1.2 Objectives	15
1.3 Canadian Contribution	16
2. TEST PLANNING AND OPERATION	18
2.1 Operational Planning	18
2.1.1 Environmental Impact	18
2.1.2 Experimental Layout	18
2.1.3 Site Preparation	23
2.1.4 Explosive Preparation	23
2.1.5 Project Schedule	32
2.2 Data Acquisition Systems	32
2.2.1 Air Blast Pressure Instrumentation	39
2.2.2 Photographic Instrumentation	40
2.3 Predictions and Calculations	42
2.4 Data Reduction	47
2.4.1 Photo-Optical Analysis	47
2.4.2 Air Blast Pressure Analysis	62
3. RESULTS	64
3.1 General Observations	64
3.2 Photographic Results	68
3.3 Air Blast Results	73

TABLE OF CONTENTS (Continued)

	<u>Page</u>
4. DISCUSSION OF RESULTS	122
4.1 Instrument Performance	122
4.2 Pressure Records	122
4.3 Triple Point Paths	125
4.4 Comparison of Experimental and Calculated Results . . .	129
4.5 Comparison with Other HE Data	139
4.6 Comparison Among Events of Present Series	151
5. CONCLUSIONS AND RECOMMENDATIONS	154
REFERENCES	155
APPENDIX	157
DISTRIBUTION LIST	379

LIST OF ILLUSTRATIONS

<u>Figure</u>	<u>Page</u>
2.1 Map of Suffield Military Reserve Showing DIPOLE WEST Site	19
2.2 Diagram of the Charge Handling System	21
2.3 Diagram Showing Gage Mount Locations on Gun Barrels	22
2.4 Type I Total Head Probe and Type III Overpressure Baffle	24
2.5 Field Layout of DIPOLE WEST Site	25
2.6 Detail of Field Layout, Ground Zero Area	26
2.7 Ground Zero Area with Stabilized Surface	27
2.8 Seat Belt Strap Sling Charge Suspension System	33
2.9 Photograph of Charges in Place	35
2.10 Calculated Position of Ideal Reflecting Surface for Different Values of Charge Detonation Non-Simultaneity	41
3.1 Shot 12 Fireballs at ~ 0.05 Second After Detonation	65
3.2 Shot 13 Fireballs at ~ 0.05 Second After Detonation of the Upper Charge	66
3.3 Shot 14 Fireball at ~ 0.05 Second After Detonation	68
3.4 Shot 15 Fireballs at ~ 0.05 Second After Detonation of the Upper Charge	69
3.5 Shot 16 Fireballs at ~ 0.05 Second After Detonation of the Upper Charge	70
3.6(A) Fireballs of Non-Simultaneous Events at 1.5 and 6.2 Milliseconds After Detonation	71
3.6(B) Fireballs of Non-Simultaneous Events at 11.2 and 16.2 Milliseconds After Detonation	72
3.7 Frame from Photographic Record of Shot 12 Showing Shock Wave System	74
3.8 Reconstructed Triple Point Paths and Position of the Ideal Reflecting Surface; Shot 12	75

LIST OF ILLUSTRATIONS (Continued)

<u>Figure</u>	<u>Page</u>
3.9 Frame from Photographic Record of Shot 16 Showing Shock Wave System	76
3.10 Reconstructed Triple Point Path and Shock Wave Diagram; Shot 16	77
3.11 Frame from Photographic Record of Shot 15 Showing Shock Wave System	78
3.12 Reconstructed Triple Point Path and Shock Wave Diagram; Shot 15	79
3.13 Frame from Photographic Record of Shot 13 Showing Shock Wave System	80
3.14 Reconstructed Triple Point Path and Shock Wave Diagram; Shot 13	81
3.15 Air Blast Parameters at Ground Level Versus Ground Range; Shot 12	85
3.16 Air Blast Parameters at 3, 10, and 20 Feet Versus Ground Range; Shot 12	86
3.17 Air Blast Parameters at 27, 30, and 33 Feet Versus Ground Range; Shot 12	87
3.18 Air Blast Parameters at Ground Level Versus Ground Range; Shot 13	90
3.19 Air Blast Parameters at 3, 10, and 20 Feet Versus Ground Range; Shot 13	91
3.20 Air Blast Parameters at 27, 30, and 33 Feet Versus Ground Range; Shot 13	92
3.21 Air Blast Parameters at Ground Level Versus Ground Range; Shot 14	95
3.22 Air Blast Parameters at 3, 10, and 20 Feet Versus Ground Range; Shot 14	96
3.23 Air Blast Parameters at 27, 30, and 33 Feet Versus Ground Range; Shot 14	97

LIST OF ILLUSTRATIONS (Continued)

<u>Figure</u>		<u>Page</u>
3.24	Comparison of Pressure Records at 20-Foot Range from Gage Lines 1 and 2, Shot 15	99
3.25	Comparison of Pressure Records at 60-Foot Range from Gage Lines 1 and 2, Shot 15	100
3.26	Comparison of Pressure Records at 400-Foot Range from Gage Lines 1 and 2, Shot 15	101
3.27	Air Blast Parameters at Ground Level Versus Ground Range; Shot 15	104
3.28	Air Blast Parameters at 3, 10, and 20 Feet Versus Ground Range; Shot 15	105
3.29	Air Blast Parameters at 27, 30, and 33 Feet Versus Ground Range; Shot 15	106
3.30	Air Blast Parameters at Ground Level Versus Ground Range; Shot 16	109
3.31	Air Blast Parameters at 3, 10, and 20 Feet Versus Ground Range; Shot 16	110
3.32	Air Blast Parameters at 27, 30, and 33 Feet Versus Ground Range; Shot 16	111
3.33	Comparison of Pressure Records at Station 10.0E from Shots 12, 13, and 15	112
3.34	Comparison of Pressure Records at Station 20.0 from Shots 12, 13, and 15	113
3.35	Comparison of Pressure Records at Station 30.0 from Shots 12, 13, and 15	114
3.36	Comparison of Pressure Records at Station 2-40.0 from Shots 12, 13, and 15	115
3.37	Comparison of Pressure Records at Station 50.0S from Shots 12, 13, and 15	116
3.38	Comparison of Pressure Records at Station 2-60.0 from Shots 12, 13, and 15	117

LIST OF ILLUSTRATIONS (Continued)

<u>Figure</u>		<u>Page</u>
3.39	Comparison of Pressure Records at Station 90.0 from Shots 12, 13, and 15	118
3.40	Comparison of Pressure Records at Station 110.0 from Shots 12, 13, and 15	119
3.41	Comparison of Pressure Records at Station 245.0 from Shots 12, 13, and 15	120
3.42	Comparison of Pressure Records at Station 800.0 from Shots 12, 13, and 15	121
4.1	Overpressure Record from Shot 12, Station 40.10S, Illustrating Multiple Shock Structure of the Pressure Pulse	123
4.2	Overpressure Records at 20-Foot Ground Stations Showing Double Peak Phenomenon	124
4.3	Comparison of Mach Stem Position-Time Curves at the Ideal Reflecting Plane and at the Ground Surface; Shot 12	126
4.4	Comparison of Triple Point Paths Above and Below the Ideal Reflecting Plane; Shot 12	127
4.5	Triple Point Paths from Shot 12 Compared to Those from DIPOLE WEST Shot 8	128
4.6	Comparison of Triple Point Paths Above the Ground Surface for Shots 12 and 13	130
4.7	Comparison of Mach Stem Position-Time Curves for Shots 12 and 13	131
4.8	Calculated and Measured Triple Point Paths; Shot 15	132
4.9	Calculated and Measured Triple Point Paths; Shot 16	133
4.10	Pressure Contours from AFWL HULL Three Millisecond Delay Calculation at Seven Milliseconds After Detonation of the Lower Charge	134
4.11	Pressure Contours from AFWL HULL Three Millisecond Delay Calculation at Ten Milliseconds After Detonation of the Lower Charge	135

LIST OF ILLUSTRATIONS (Continued)

<u>Figure</u>		<u>Page</u>
4.12	Pressure Contours from AFWL HULL Ten Millisecond Delay Calculation at Seven Milliseconds After Detonation of the Lower Charge	136
4.13	Pressure Contours from AFWL HULL Ten Millisecond Delay Calculation at Ten Milliseconds After Detonation of the Lower Charge	137
4.14	Overpressure Records at the South 50-Foot Ground Station Showing Differences Caused by Varying Detonation Delay Time	138
4.15	Comparison Between Calculated and Experimental Air Blast Parameters at Ground Level; Shot 12	140
4.16	Comparison Between Calculated and Experimental Air Blast Parameters at Ground Level; Shot 13	141
4.17	Comparison Between Calculated and Experimental Air Blast Parameters at Ground Level; Shot 14	142
4.18	Comparison Between Calculated and Experimental Air Blast Parameters at Ground Level; Shot 15	143
4.19	Comparison Between Calculated and Experimental Arrival Times at 3 and 10 Feet Above Ground	144
4.20	Comparison Between Calculated and Experimental Arrival Times at 20 and 30 Feet Above Ground	145
4.21	Comparison Between Calculated and Experimental Overpressures at 3 and 10 Feet Above Ground	146
4.22	Comparison Between Calculated and Experimental Overpressures at 20 and 30 Feet Above Ground	147
4.23	Comparison Between Calculated and Experimental Overpressure-Impulses at 3 and 10 Feet Above Ground	148
4.24	Comparison Between Calculated and Experimental Overpressure-Impulses at 20 and 30 Feet Above Ground	149
4.25	Comparison of Shot 12 Data with That from DIPOLE WEST 8	150

LIST OF ILLUSTRATIONS (Continued)

<u>Figure</u>		<u>Page</u>
4.26	Maximum Overpressure at Ground Level Versus Ground Range for All Events	152
4.27	Maximum Overpressure-Impulse at Ground Level Versus Ground Range for All Events	153

LIST OF TABLES

<u>Table</u>	<u>Page</u>
2.1 Gage Position Survey Data	28
2.2 Survey Data of Charge Positions	34
2.3 Shot Schedule and Conditions; Non-Simultaneous Detonations	36
2.4 Weather Conditions at Shot Times	37
2.5 Detailed Shot Day Schedule; Shot 12	38
2.6 Survey Data, Photomarkers and Cameras	43
2.7 Cameras for Shots 12 through 16	46
2.8 AFWL HULL Calculation, Two 216-Pound Pentolite Spheres, Simultaneous Detonation	48
2.9 AFWL HULL Calculation, Two 216-Pound Pentolite Spheres, Three Millisecond Time Separation	52
2.10 AFWL HULL Calculation, Two 216-Pound Pentolite Spheres, Five Millisecond Time Separation	56
2.11 AFWL HULL Calculation, Two 216-Pound Pentolite Spheres, Ten Millisecond Time Separation	59
3.1 Measured Air Blast Parameters; Shot 12	83
3.2 Measured Air Blast Parameters; Shot 13	88
3.3 Measured Air Blast Parameters; Shot 14	93
3.4 Measured Air Blast Parameters; Shot 15	102
3.5 Measured Air Blast Parameters; Shot 16	107
4.1 Scaling Factors	151

This page Left Intentionally Blank

CHAPTER I

INTRODUCTION

1.1 Background

DIPOLE WEST is the name for a series of high explosive tests conducted by the U. S. Army Ballistic Research Laboratories at the Defence Research Establishment Suffield (DRES) in Alberta, Canada. The present report is intended to cover Shots 12 through 16 of the series. Shots 1 through 11, fired in the summer and fall of 1973, are described in an earlier report (*Reference 1*). An additional nine events, Shots 17 through 25, were fired in the summer of 1975. These are to be described in a future report.

The five events discussed here comprise that portion of the series concerned with non-simultaneous detonations. Shots 12, 13, 14, and 15 were detonated during late October and early November of 1974. Shot 16 was fired in June of 1975. 216-pound pentolite charges were used for all five events.

Shot 14 consisted of a single charge detonated at a height-of-burst (HOB) of 15 feet above the ground surface. The other four events contained, in addition to the 15-foot charge, a second charge at 45 feet. The configurations for these events were identical (within limits of experimental practicality) except for the difference between detonation times of the two charges. Shot 12 detonations were simultaneous (to within 5 microseconds), while the lower detonation was delayed by 10, 5, and 3 milliseconds for Shots 13, 15, and 16 respectively.

1.2 Objectives

The objectives of the non-simultaneous events in the DIPOLE WEST series are the same as those of the earlier experiments; namely, to examine the air blast phenomenology of strong shock on shock, shock on fireball, and fireball flow interactions from the detonation of multiple high explosive charges. Whereas the earlier experiments involved simultaneous detonations with varying charge separations, heights of burst, charge orientations, and ground surface conditions, the present series deals exclusively with effects of varying the time between detonation of the two charges.

1. J.H. Keefer and R.E. Reisler, "Multiburst Environment - Simultaneous Detonations, Project DIPOLE WEST," BRL Report No. 1766, USA Ballistic Research Laboratories, Aberdeen Proving Ground, Maryland 21005, March 1975. AD #A009485.

As before, major emphasis is given to comparison of the experimental data with the results of theoretical hydrodynamic calculations. It is anticipated that, if analysis of the data so indicates, computer codes will be upgraded to reproduce the experimental results more adequately. Specifically, calculations with the most modern hydrodynamic codes indicate that, for the configuration described, a delay in detonation of the lower charge of 10 milliseconds or more will alter the shock interaction to the extent that a Mach stem is not formed between the two charges. An experimental investigation of this effect is one of the objectives of this test series.

A broader objective, which is of interest to the defense community, is that of verification of the validity of the Low Altitude Multi-Burst (LAMB) model (Reference 2). This model has been developed for prediction of the free field blast environment produced by multiple nuclear explosions occurring in close time and space proximity. High explosive simulation techniques are used to model the nuclear detonations for these experiments.

This objective has application in the analysis of fratricide problems related to rapid and closely spaced interceptor bursts engaging a swarm of attacking reentry vehicles. It also bears on analyses of the blast degradation of targeting accuracy of follow-on reentry vehicles in a multi-missile attack on closely spaced targets.

The present report addresses only the immediate objectives of the field tests in order to make the basic experimental results available to the broadest audience. Subsequent reports will address problems related to defense related objectives.

Air blast parameters of interest for this study are overpressure, overpressure impulse, dynamic pressure, dynamic pressure impulse, propagation velocity, Mach stem formation, and Mach stem growth rate. Information was obtained from pressure transducers and from high speed photography.

1.3 Canadian Contribution

As previously mentioned, the DIPOLE WEST tests were conducted at the Defence Research Establishment Suffield (DRES) range near Medicine Hat in Alberta, Canada. The site constructed for the 1973 DIPOLE WEST series was again utilized. Only a few changes were required for this series.

2. C.E. Needham and L.A. Wittwer, "The Air Force Weapons Laboratory Low Altitude Multiple Burst (LAMB) Model," AFWL-DYT-75-2 (unpublished).

As in the past, technical and logistic support by DRES personnel was of excellent quality and was generously supplied. DRES staff members with the technical knowledge and experience required for safe and efficient operation of the tests were available, and their expertise was extremely valuable. DRES support included firing and control system operation, power and its distribution on-site, photography, radio communications, munitions handling, machine shop assistance, meteorological service, and general supervision. Equipment and material provided by DRES included two 200-foot walk-up towers, cable and hoist equipment, photo markers, smoke puff grids, and backdrops. The Canadian contribution to the success of this test series was a very significant one, and it is much appreciated.

CHAPTER 2

TEST PLANNING AND OPERATION

2.1 Operational Planning

Planning for this series of DIPOLE WEST experiments began immediately upon completion of the 1973 series in November of that year. Because of other commitments of the DRES range and personnel, however, fielding operations could not begin until late in the summer of 1974.

2.1.1 Environmental Impact

An assessment of the impact of the DIPOLE WEST series of experiments on the environment had been carried out by DASIAC, General Electric - TEMPO, prior to firing of the 1973 events. Because the site previously established was again used, and because the same configuration and type of explosive were to be employed, it was felt that the previously prepared environmental impact assessment would also apply to this series. In fact, the charges used were smaller (216 lbs each) than those used in 1973 (1080 lbs each), so it was assumed that the environmental impact would be even less than that for the earlier series.

The conclusions reached in the environmental assessment are stated fully in *Reference 3* and summarized in *Reference 1*. Briefly, they are:

(1) The tests will have no significant adverse environmental impact, including very little impact on environmental systems and no impact on endangered species.

(2) The test preparatory activities will have no more than minor environmental impacts which will be short-lived.

2.1.2 Experimental Layout

As previously mentioned, the site used for previous DIPOLE WEST trials was used again for the non-simultaneous series. This site is in the south part of the DRES range, approximately 12 miles east of the DRES main laboratory. A diagram of the Suffield Military Reserve showing the location of the experimental area is given in Figure 2.1.

3. DASIAC Staff, "Environmental Impact Assessment for DIPOLE WEST," General Electric Company - TEMPO, Santa Barbara, California 93102, May 1973.

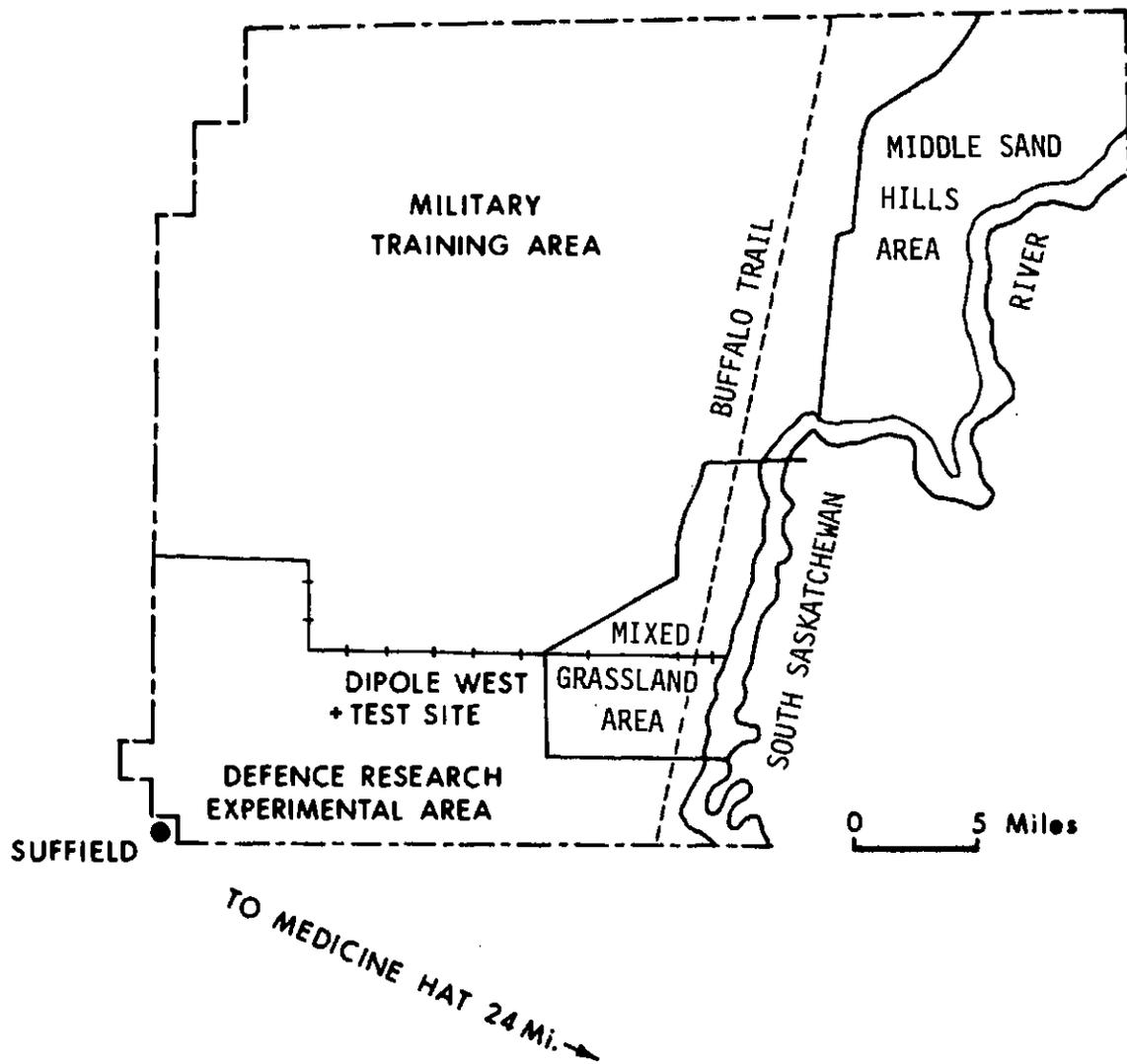


Figure 2.1. Map of Suffield Military Reserve Showing DIPOLE WEST Site

The site had been extensively examined and surveyed prior to its selection in order to determine ground conditions in detail and to ensure that lines of site from the main camera position would provide adequate coverage of shock phenomena against the canvas backdrop and smoke puff array. Features of the site are described in the following paragraphs.

2.1.2.1 Charge Suspension Towers. Two 200-foot towers are used for suspension of the charges over ground zero. The towers are of aluminum, constructed in a collapsible, walk-up style. They are 400 feet apart with ground zero midway between them. A 5/8-inch wire cable stretches between the tops of the towers with the ends run through pulleys. Additional pulleys at ground level are anchored in concrete bases. A stationary winch at a position 600 feet south of ground zero provides power for raising the charges. A diagram of the charge handling system, showing positions of the towers and winch, is given in Figure 2.2. The towers are permanently lighted to comply with Canadian aircraft warning regulations.

2.1.2.2 Permanent Camera Shelters. Permanent camera shelters are available mounted on concrete bases. The main camera position has shelters at 30 and 50 feet above ground as well as at ground level. The elevated shelters are supported by four 60-foot power poles, which are securely guyed to prevent motion. Although six camera positions are available, only four of these were used for the present series of shots (see *Reference 1*).

2.1.2.3 Gun Barrels. Four "gun barrels" are available for use as instrument mounts for elevated pressure gage measurements. These are actual surplus gun barrels modified so the end of the larger barrel fits into the breech of a smaller barrel. A length of 6-inch diameter, 0.432 inch wall thickness, "extra heavy" pipe is added at the smaller end. The barrels are 54 feet long after the addition, and are mounted vertically at ranges of 20, 30, 40 and 60 feet from ground zero.

Pressure transducers are mounted on the gun barrels on U-shaped brackets. The bracket arms extend two feet from the barrels so that the measurement points are not perturbed by the barrel. A side-on overpressure gage is mounted on one side with an 18-inch diameter steel baffle plate. A stagnation pressure gage within a probe is attached to the other side of the U-mount. The elevated instrumentation is illustrated fully in *Reference 1*. Figure 2.3 is a diagram showing gage mount locations on the barrels.

2.1.2.4 Surface Gage Mounts. A number of concrete block mounts are available for surface and 3-foot elevation pressure measurements. These mounts are of three types: (I) ground baffle with a total head probe at the three-foot level, (II) simple ground baffle for measurement of overpressure at ground level, and (III) side-on overpressure baffle at the three-foot level. These gage

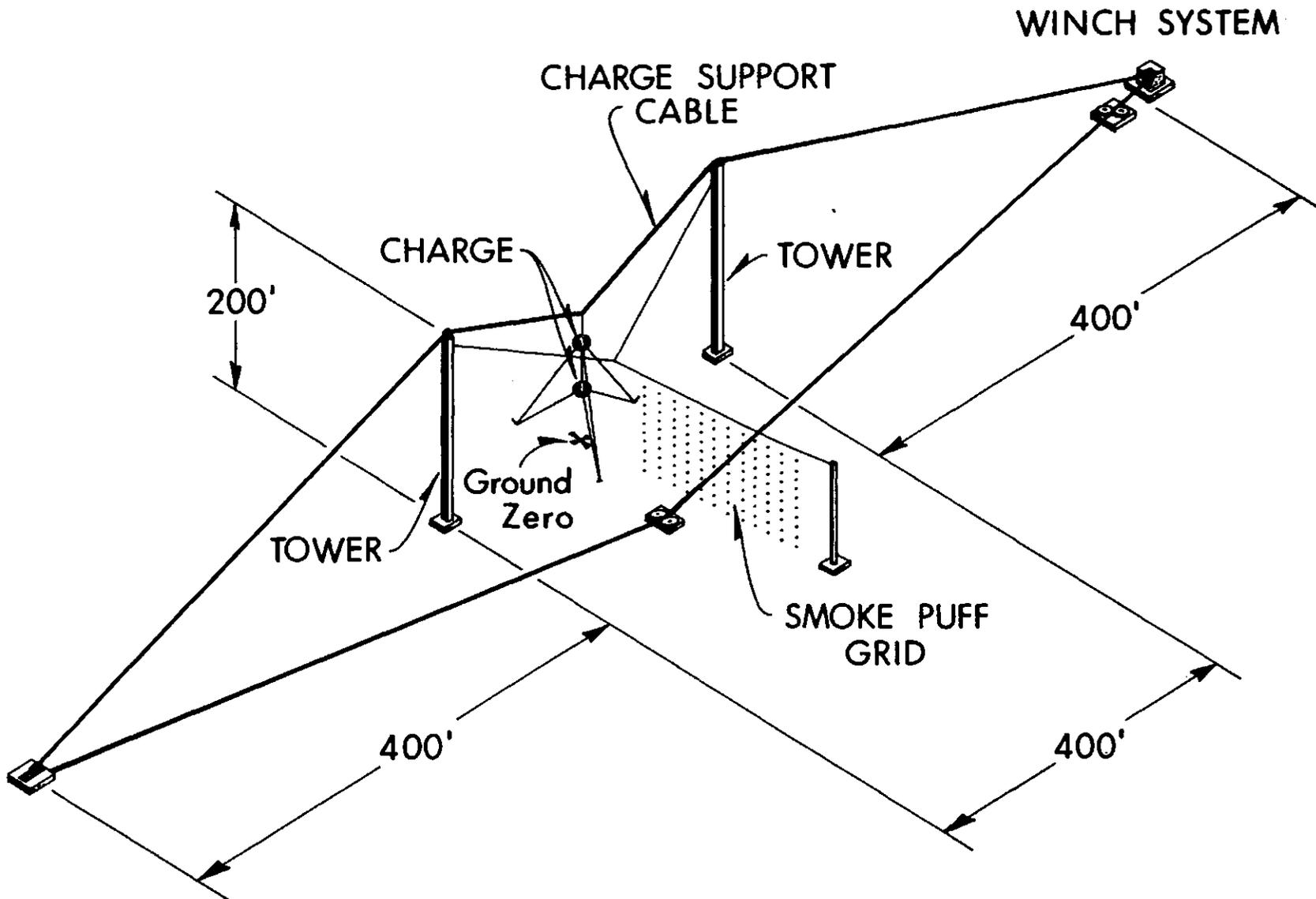


Figure 2.2. Diagram of the Charge Handling System

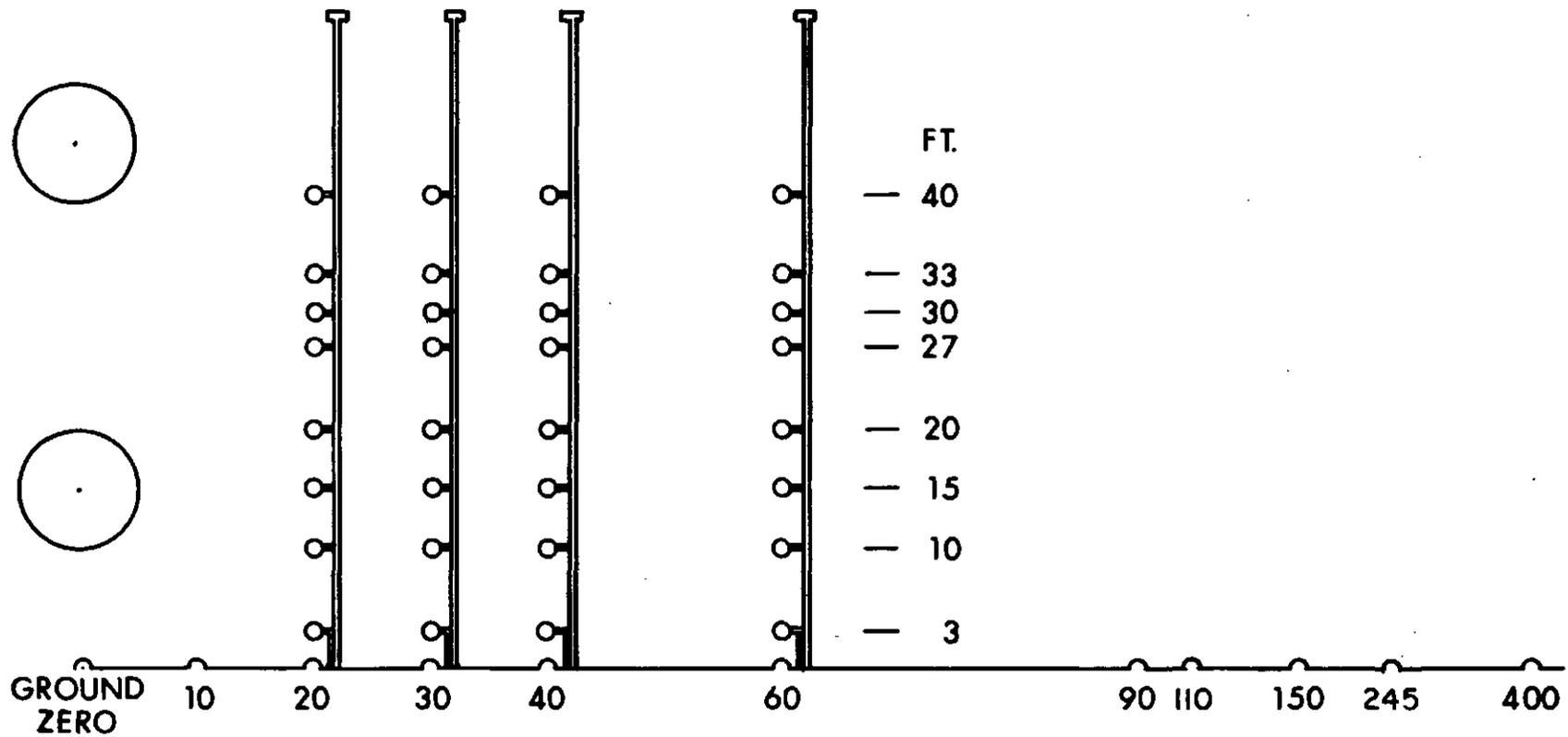


Figure 2.3. Diagram Showing Gage Mount Locations on Gun Barrels

mounts are of a standard design and are described more fully in Reference 4. Figure 2.4 shows a type I total head probe and a type III overpressure baffle mounted so that the sensors are equidistant from ground zero.

2.1.2.5 Back Drops and Smoke Puff Array. Poles for suspending the smoke puff array and for mounting the ten 30 x 50-foot canvas backdrops are available at locations appropriate for viewing from the camera positions. These features, along with most of those described in the previous paragraphs, may be generally located in the site layout diagram shown in Figure 2.5.

2.1.2.6 Electrical Wiring. The wiring for control, power, and firing lines remains unchanged from the previous series.

2.1.3 Site Preparation

Operations for DIPOLE WEST in 1974 began in July with preparation of the test site. The rough, soft surface used for Shot 11 in 1973 had grown over with weeds during the winter and spring months. These weeds were removed, and the area was raked and harrowed.

Earth moving and grading equipment was used to bring the level of the site to that of ground zero over a 400-foot radius. In order to bring all ground-level gages to the same elevation as that of the gage at ground zero, many of the existing gage mounts were modified. A number of additional gage mounts were also installed on the layout. The revised field layout of the ground zero area is shown in Figure 2.6.

"Soil cement" was applied to the ground surface over a radius of 200 feet from ground zero, and this in turn was topped with tar. This produced a firm, stabilized surface. Figure 2.7 is a photograph of the area showing the stabilized surface.

Positions of all the gage mounts were surveyed prior to conducting the tests. This survey data is presented in Table 2.1.

Site preparation activities were arranged by the CGE/DRES Project Office under the direction of Mr. Arthur Lambert. Work was done under direct local contracts.

2.1.4 Explosive Preparation

Pentolite was chosen as the explosive to be used for the non-simultaneous detonations because past experience indicates that

4. R.E. Reisler, (Ballistic Research Laboratories), "Basic Air Blast Studies," Operation SNOWBALL Project Descriptions, Vol. 1, DASA 1516-1, July 1964.

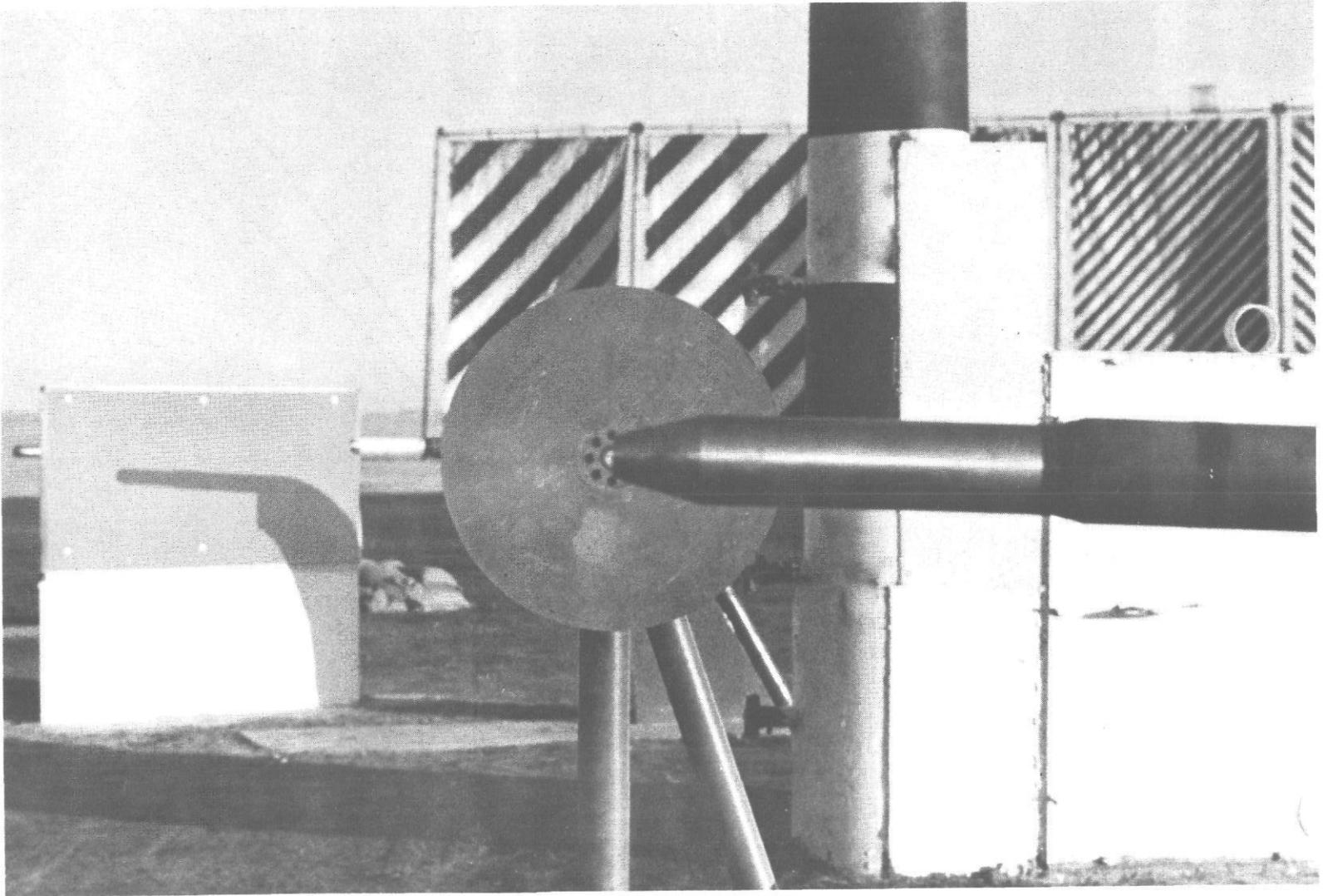


Figure 2.4. Type I Total Head Probe and Type III Overpressure Baffle

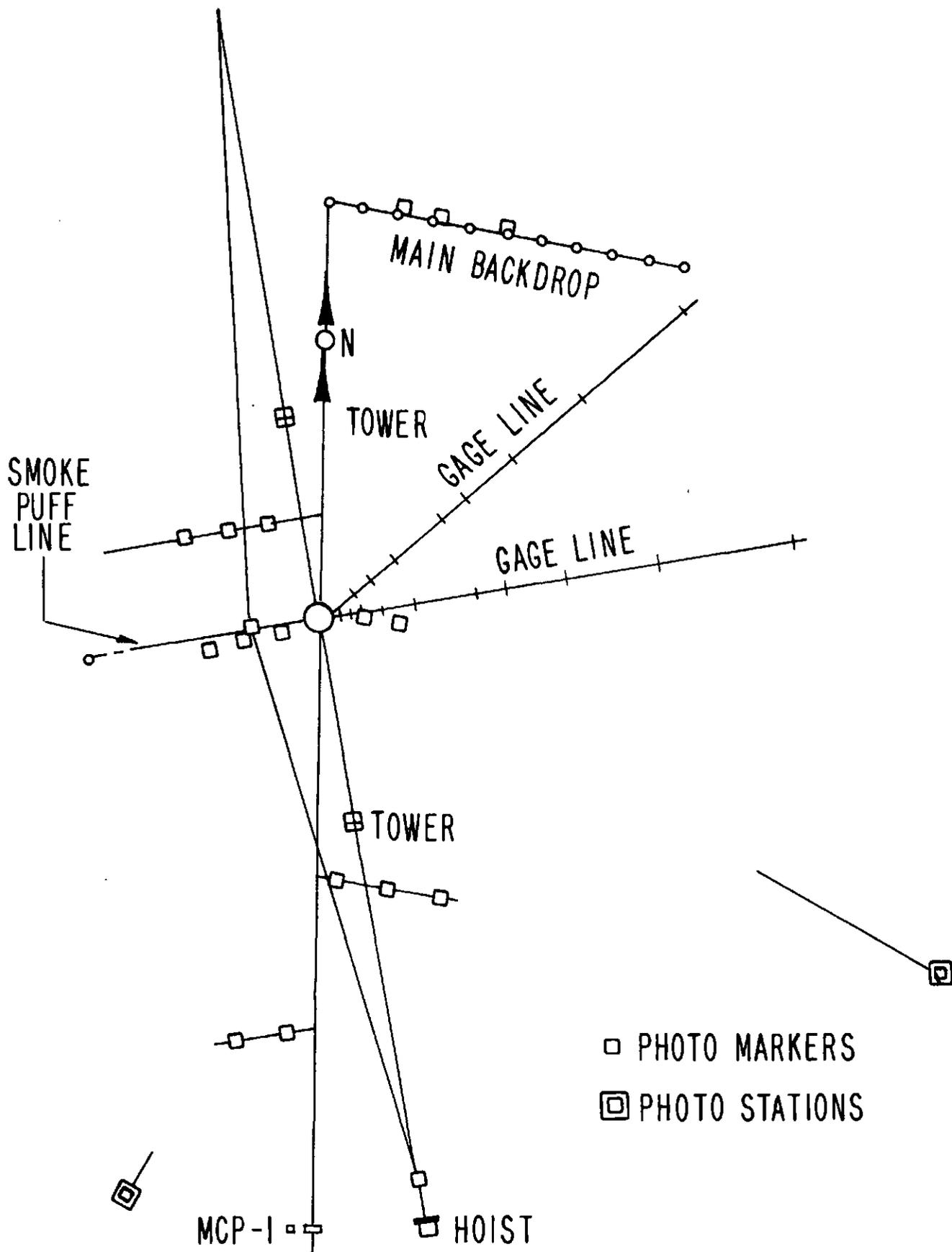


Figure 2.5. Field Layout of DIPOLE WEST Site

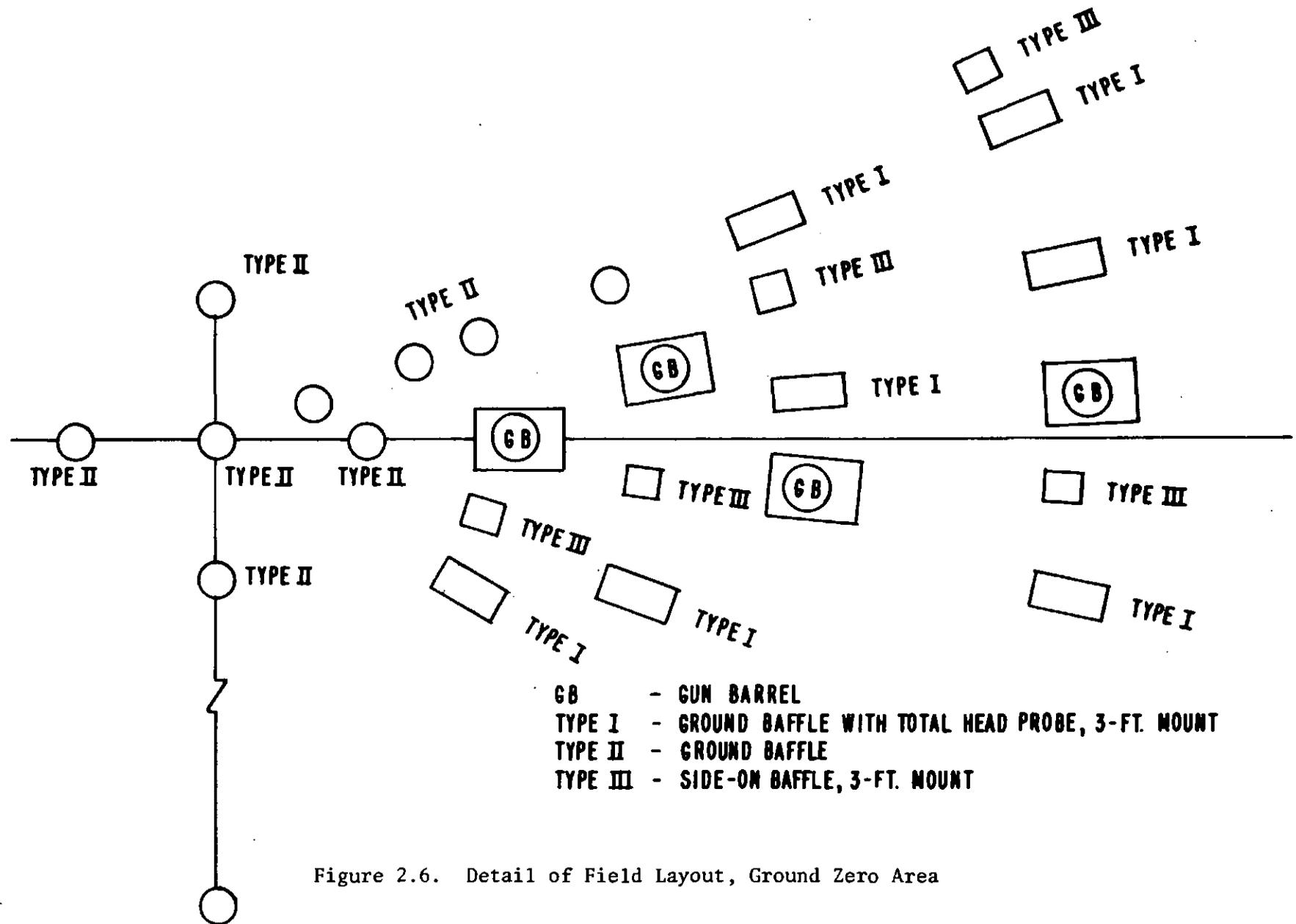


Figure 2.6. Detail of Field Layout, Ground Zero Area

Table 2.1. Gage Position Survey Data

Code	Station	Bearing	Distance (feet)	Elevation (feet)
1	20.10	84° 07' 37"	19.88	2326.37
2	20.10	76° 25' 18"	19.89	2326.37
1	20.15	83° 52' 20"	19.86	2331.38
2	20.15	76° 07' 46"	19.99	2331.36
1	20.20	84° 12' 46"	19.89	2336.38
2	20.20	76° 24' 22"	19.89	2336.39
1	20.27	83° 53' 34"	19.84	2343.35
2	20.27	76° 14' 11"	19.95	2343.38
1	20.30	84° 08' 44"	19.85	2346.40
2	20.30	76° 17' 57"	19.85	2346.37
1	20.33	83° 43' 18"	19.79	2349.32
2	20.33	75° 59' 43"	19.97	2349.33
1	20.40	84° 04' 43"	19.82	2356.41
2	20.40	76° 11' 32"	19.82	2356.34
1	30.10	69° 25' 01"	29.03	2326.52
2	30.10	72° 34' 31"	30.78	2326.47
1	30.20	68° 23' 02"	30.02	2336.46
2	30.20	73° 31' 20"	29.94	2336.44
1	30.27	68° 52' 31"	29.87	2343.44
2	30.27	73° 59' 42"	30.07	2343.45
1	30.30	68° 29' 34"	20.02	2346.24
2	30.30	73° 40' 04"	29.94	2346.34
1	30.33	68° 52' 56"	29.94	2349.43
2	30.33	74° 00' 04"	30.07	2349.43
1	40.10	86° 13' 23"	39.92	2326.56
2	40.10	82° 20' 17"	39.90	2326.51
1	40.20	86° 12' 55"	39.94	2336.59
2	40.20	82° 21' 38"	39.89	2336.58
1	40.27	86° 02' 23"	39.90	2343.50
2	40.27	82° 12' 10"	39.98	2343.48
1	40.30	86° 10' 17"	39.92	2346.56
2	40.30	82° 18' 39"	39.91	2346.55
1	40.33	86° 06' 44"	39.95	2349.47
2	40.33	82° 09' 53"	39.98	2349.44
1	60.10	78° 26' 54"	59.72	2326.40
2	60.10	75° 51' 18"	59.86	2326.38
1	60.20	78° 27' 22"	59.73	2336.40
2	60.20	75° 53' 57"	59.79	2336.42
1	60.27	78° 28' 46"	59.73	2343.23
2	60.27	75° 54' 46"	59.78	2343.34

Table 2.1. Gage Position Survey Data (Continued)

Code	Station	Bearing	Distance (feet)	Elevation (feet)
1	60.30	78° 25' 20"	59.72	2346.37
2	60.30	75° 51' 16"	59.82	2346.38
1	60.33	78° 27' 26"	59.75	2349.32
2	60.33	75° 54' 09"	59.81	2349.33
II	0.0	0° 00' 00"	0.00	2316.31
II	10.N	350° 00' 09"	10.03	2316.28
II	10.S	170° 00' 30"	9.99	2316.28
II	10.W		10.01	2316.22
II	10.E	80° 00' 03"	10.00	2316.23
I	20.0	108° 54' 14"	20.10	2316.54
I	20.3	108° 54' 14"	20.34	2319.41
III	20.3		20.15	2319.41
I	30.0	99° 15' 25"	29.95	2316.41
I	30.3	99° 15' 25"	30.10	2319.33
III	30.3		30.15	2319.43
I	40.0	65° 43' 46"	39.98	2316.43
I	40.3	65° 43' 46"	40.09	2319.34
III	40.3		40.11	2319.26
I	60.0	89° 35' 17"	60.04	2316.39
I	60.3	89° 35' 17"	60.28	2319.29
III	60.3		60.15	2319.26
II	90.0	80° 00' 00"	90.05	2316.07
II	110.0	80° 00' 00"	109.95	2315.84
II	150.0	80° 00' 00"	149.94	2315.73
II	245.0	80° 00' 00"	244.94	2315.11
II	400.0	80° 00' 00"	400.00	2314.51
II	800.0	105° 40' 56"	814.56	2319.89
II	Trailer	121° 33' 20"	1651.45	2320.97
II	50.0N	349° 59' 20"	50.02	2316.21
II	50.0S	170° 00' 17"	49.97	2316.42
II	2-15.0	44° 55' 54"	15.01	2316.32
II	2-20.0	44° 52' 20"	20.07	2316.26
II	2-30.0	44° 50' 14"	30.03	2316.21
I	2-40.0	44° 56' 08"	40.00	2316.16
I	2-40.3	44° 57' 42"	40.16	2319.14
I	2-60.0	67° 56' 12"	60.03	2316.21
I	2-60.0	50° 40' 02"	59.99	2316.09
I	2-60.3	67° 57' 12"	60.13	2319.25
III	2-60.3	44° 55' 37"	60.14	2319.04
I	2-90.0	44° 55' 27"	90.03	2315.96
I	2-110.0	44° 55' 21"	110.05	2315.85

Table 2.1. Gage Position Survey Data (Continued)

Code	Station	Bearing	Distance (feet)	Elevation (feet)
1	60.30	78° 25' 20"	59.72	2346.37
2	60.30	75° 51' 16"	59.82	2346.38
1	60.33	78° 27' 26"	59.75	2349.32
2	60.33	75° 54' 09"	59.81	2349.33
II	0.00	0° 00' 00"	0.00	2316.31
II	10.N	350° 00' 09"	10.03	2316.28
II	10.S	170° 00' 30"	9.99	2316.28
II	10.W		10.01	2316.22
II	10.E	80° 00' 03"	10.00	2316.23
I	20.0	108° 54' 14"	20.10	2316.54
I	20.3	108° 54' 14"	20.34	2319.41
III	20.3		20.15	2319.41
I	30.0	99° 15' 25"	29.95	2316.41
I	30.3	99° 15' 25"	30.10	2319.33
III	30.3		30.15	2319.43
I	40.0	65° 43' 46"	39.98	2316.43
I	40.3	65° 43' 46"	40.09	2319.34
III	40.3		40.11	2319.26
I	60.0	89° 35' 17"	60.04	2316.39
I	60.3	89° 35' 17"	60.28	2319.29
III	60.3		60.15	2319.26
II	90.0	80° 00' 00"	90.05	2316.07
II	110.0	80° 00' 00"	109.95	2315.84
II	150.0	80° 00' 00"	149.94	2315.73
II	245.0	80° 00' 00"	244.94	2315.11
II	400.0	80° 00' 00"	400.00	2314.51
II	800.0	105° 40' 56"	814.56	2319.89
II	Trailer	121° 33' 20"	1651.45	2320.97
II	50.ON	349° 59' 20"	50.02	2316.21
II	50.OS	170° 00' 17"	49.97	2316.42
II	2-15.0	44° 55' 54"	15.01	2316.32
II	2-20.0	44° 52' 20"	20.07	2316.26
II	2-30.0	44° 50' 14"	30.03	2316.21
I	2-40.0	44° 56' 08"	40.00	2316.16
I	2-40.3	44° 57' 42"	40.16	2319.14
I	2-60.0	67° 56' 12"	60.03	2316.21
I	2-60.0	50° 40' 02"	59.99	2316.09
I	2-60.3	67° 57' 12"	60.13	2319.25
III	2-60.3	44° 55' 37"	60.14	2319.04
I	2-90.0	44° 55' 27"	90.03	2315.96
I	2-110.0	44° 55' 21"	110.05	2315.85

Table 2.1. Gage Position Survey Data (Continued)

Code	Station	Bearing	Distance (feet)	Elevation (feet)
I	2-150.0	44° 55' 37"	150.10	2315.62
II	2-245.0	44° 57' 35"	245.09	2315.12
II	2-400.0	44° 59' 21"	400.14	2314.29

Code Key:

- 1 - Side-on Baffle, Gun Barrel
- 2 - Total Head Probe, Gun Barrel
- I - Ground Baffle with Total Head Probe, 3-Foot Mount
- II - Ground Baffle
- III - Side-on Baffle, 3-Foot Mount

this explosive is comparatively free from jetting or other anomalies of detonation. The firm of Canadian Arsenals Limited, St. Paul L'Ermite, Quebec, had provided cast pentolite spheres for the earlier DIPOLE WEST events, and so were familiar with the casting techniques. They were again asked to provide charges for this series. The smaller charges (216 lbs) required that a new spun aluminum mold be made at DRES, but otherwise no particular problems were encountered in obtaining the charges.

All munitions handling and firing and control system operation were handled very efficiently by DRES personnel. The charges were brought to the site several hours before shot time in a pickup truck. A "seat belt" strap sling arrangement made from one-inch nylon webbing was used to suspend the charges in position. This suspension system is shown in Figure 2.8. A cable of appropriate length was attached to the strap sling at one end and to the 5/8-inch overhead supporting and hoisting cable at the other end.

All charges were armed on the ground and then raised to the desired height. As the charges were raised by the power winch, their positions were monitored from two survey points. When the specified elevations were reached (15 and 45 feet), tethering ropes attached to the charges were secured and a final position survey was taken. Survey data of charge positions for each shot are given in Table 2.2. Figure 2.9 is a photograph of the charges in place.

2.1.5 Project Schedule

As previously mentioned, this series of DIPOLE WEST events could not be scheduled until late in the summer because of other commitments of the DRES range and personnel. Further delays were experienced in the field due to a number of trivial but nonetheless annoying problems. Once firing actually began, however, operations ran smoothly, and all four events of the fall series were completed within a nine-day period at the end of October, 1974. The fifth non-simultaneous detonation, Shot 16, was fired as the first event of the spring series on June 10, 1975. A shot schedule, along with details of shot configurations, is given in Table 2.3. Weather conditions at shot time for each event, which were provided by the DRES meteorological service, are given in Table 2.4.

An example of a detailed schedule of operations for shot day is given in Table 2.5. This particular schedule is for Shot 12, but operation schedules for all events were quite similar.

2.2 Data Acquisition Systems

The systems used to acquire data on the non-simultaneous events of DIPOLE WEST were of two general types:

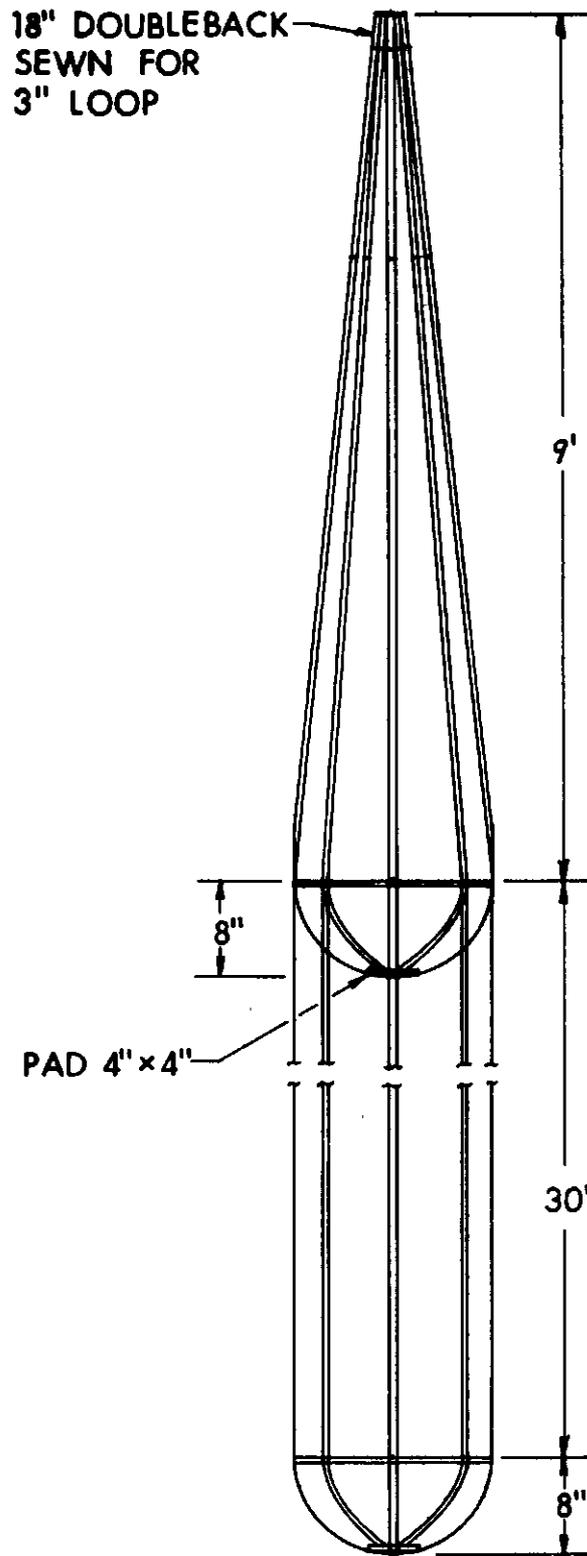


Figure 2.8. Seat Belt Strap Sling Charge Suspension System

Table 2.2. Survey Data of Charge Positions

Ground Zero (GZ) - Distance - 0 feet
 Elevation - 2316.31 feet

			Shot 12	Shot 13	Shot 14	Shot 15	Shot 16
34 BOTTOM CHARGE	Bearing	-	48 17' 27.9"	276 26' 41.1"	83 15' 18.7"	100 01' 32.6"	285 32' 37.5"
	Distance	-	0.303'	0.469'	0.298'	0.393'	0.306'
	Height above GZ	-	14.735'	14.857'	14.860'	14.87'	15.05'
TOP CHARGE	Bearing	-	53 35' 23.5"	228 25' 29.4"		123 50' 26.8"	332 42' 56.8"
	Distance	-	0.280'	0.913'		0.214'	0.764'
	Height above GZ	-	44.847'	44.874'		44.96'	45.34'

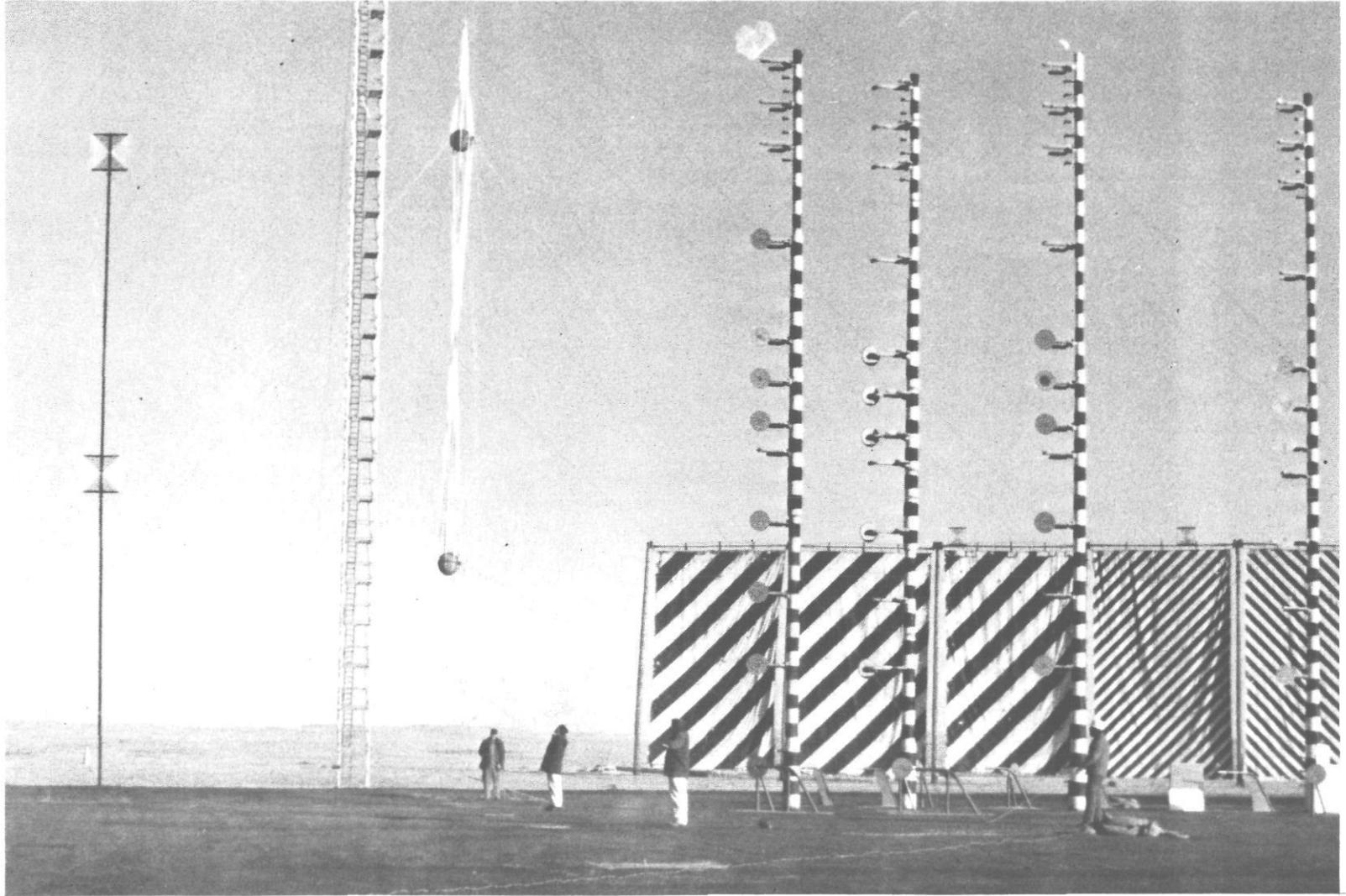


Figure 2.9. Photograph of Charges in Place

Table 2.3. Shot Schedule and Conditions; Non-Simultaneous Detonations

Shot No.	Date Fired	Total Charge Weight (lbs)	No. and Material of Charges	Distance Between Charges (ft)	Burst (ft)		Time Between Detonations (msec)
					1st	2nd	
12	24 Oct 74	432	2 Pent	30.11	44.85	14.74	0
13	28 Oct 74	432	2 Pent	30.02	44.87	14.86	10.09
14	30 Oct 74	216	1 Pent	-	-	14.86	-
15	1 Nov 74	432	2 Pent	30.09	44.96	14.87	5.09
16	10 Jun 75	432	2 Pent	30.29	45.34	15.05	2.90

Table 2.4. Weather Conditions at Shot Times

Shot No.	12	13	14	15	16
Firing Time	1100 MDST	1200 MST	1500 MST	1200 MST	1450 MST
Wind Conditions					
2 meters: Direction	297°	Calm	110°	071°	295°
Speed (mph)	2.1		4.8	6.7	2.7
14 meters: Direction	297°	Calm	110°	071°	290°
Speed (mph)	0.7		5.4	7.2	4.7
Temperature (°F)	43.3	63.0	39.8	35.7	73.2
Relative Humidity (%)	65	67	86	68	27
Sky Condition	Scattered Cirrus Bright Sunshine	3/10 Cirrus Bright Sunshine	Overcast Strato- Cumulus	Overcast Strato- Cumulus	Scattered Cirrus Bright Sunshine
Ambient Pressure (mb)	939.5	914.4	928.0	929.0	936.6

Table 2.5. Detailed Shot Day Schedule; Shot 12

0700 MDST	Z-4:00	<ol style="list-style-type: none"> 1. Power on at BRL Trailer 2. Meteorological Forecast 3. Trial Director to Site 4. CGE Representative to Site 5. BRL Group to Site for Check Out of Instruments, etc. 6. DRI and DRES Photo Groups to Site 7. Control Opens 8. TSS Crew to Site for Raising of Backdrops, etc. 9. TSS Survey Crew to Site 10. Munitions Personnel to Site for Smoke Puffs and Charge Suspension 11. Medical Attendant and Ambulance to Site 12. CFB Operator and Mechanic to Hoist Equipment 13. Meteorological Personnel to Site
0845 MDST	Z-2:15	Road Blocks Out and Reported in Position
0855 MDST	Z-2:05	Power Off and Radio Silence Warning Given; Area Cleared
0900 MDST	Z-2:00	<ol style="list-style-type: none"> 1. Power Off 2. Charge Suspension and Arming Party to Ground Zero
1000 MDST	Z-1:00	Ground Zero Area Cleared; Personnel Return to Tech Ops or to Bunkers
1001 MDST	Z-0:59	<ol style="list-style-type: none"> 1. Power On 2. Re-entry for Photo Personnel if Necessary
1010 MDST	Z-0:50	Meteorological Report from DRES to Control
1030 MDST	Z-0:30	Report from Road Blocks That All Traffic Stopped
1040 MDST	Z-0:20	Photo Personnel Report Under Cover or at Operations
1045 MDST	Z-0:15	<ol style="list-style-type: none"> 1. BRL Trailer Report Under Cover 2. Trial is "Go"
1058 MDST	Z-0:02	Console On
1059 MDST	Z-0:01	Count Down
1100 MDST	Zero	
1101 MDST	Z + 0:01	Control Instruct Munitions to Clear Ground Zero Area
1105 MDST	Z + 0:05	Re-entry as Directed to Ground Zero

- 1) magnetic tape systems for recording pressure signals from sensors placed in the blast field, and
 - 2) hi-speed cameras for recording smoke puff trajectories and the passage of the shock front over the back drop system.
- These data acquisition systems are discussed in the following sections.

2.2.1 Air Blast Pressure Instrumentation

Two types of sensors were placed in the blast field. These were electronic overpressure transducers and electronic stagnation pressure transducers. The basic units of the pressure data acquisition system were four 32-track magnetic tape recorders (Sangamo Model 4784's). Twenty seven channels on each recorder were available for frequency modulated data recording at a frequency response of dc to 70 kHz, two channels were used for direct recording of the time zeros (one from each charge), one channel contained a 200 kHz speed reference signal, and one channel recorded an IRIG B time reference from WWV. Bay Lab 5503 dc amplifiers were used with the recorders to amplify transducer output signals to the required level.

Timing signals for the remote operation of the recorders were supplied by the DRES control bunker equipment. Manual supervision of this remote operation was provided.

Tyco Instruments Model HFG pressure transducers were used for both side-on overpressure and stagnation pressure measurements. This transducer is basically a Wheatstone bridge with two active semiconductor strain gage arms and two dummy arms. The strain gages are bonded to a force summing column, which is in turn attached to a force collecting diaphragm. In addition, several quartz piezoelectric transducers, manufactured by PCB Piezotronics, Inc., were used.

The pressure transducers were mounted on the gun barrels with U-shaped brackets as previously described, or in surface level or 3-foot level mounts. Gages to measure overpressure were mounted in the center of an 18-inch diameter steel baffle plate oriented so that the shock swept across the plate from one edge to the other. Total head gages were mounted in probes directed toward the blast. Surface level overpressure gages were installed in concrete blocks.

The gages were calibrated statically in their mounted positions prior to detonation of the events. The calibration level was reproduced on tape as a system gain check five seconds before each event. In all cases, the pressure calibration level was chosen so that predicted peak pressure to be recorded fell between 80 and 100% of this level. All gages were recalibrated if it became necessary to move or remount them for any reason.

Additional details concerning the pressure data

acquisition system and the calibration procedures used are given in Reference 1.

2.2.2 Photographic Instrumentation

Provisions for shock profile and shock wave radius-time studies by photo-optical means were made by setting up a backdrop line against which the shock wave could be photographed. The backdrop line began at a point on the MCP-GZ (Main Camera Position-Ground Zero) line 400 feet from GZ on the side away from the MCP. (See Figure 2.5, the site layout diagram). It extended along a line making an angle of 80° to the MCP-GZ line to a distance of 325 feet. Ten 30 x 50-foot stripe-patterned canvas drops were used to provide background for the photography. Prior to the series, a few of the drops were damaged by wind. Replacements from DRES stocks had strips of widths different from those originally used.

In order to observe, against the backdrop, whether or not a Mach stem is produced by the reflection of the shock at ground surface, it was necessary to have a camera as close as possible to the ground. The camera for these observations was placed at the minimum practical height of 3 feet. An additional 3-foot level camera station, located approximately 150 feet to the west of the main camera position, was used to avoid the partial blockage of the field of view by the south charge tower.

In order to see the Mach stem, if there is one, at the reflecting surface between charges, it was likewise necessary to have a camera on or above the line of sight from the top of the backdrop through the reflecting surface. In the case of simultaneous detonations, this reflecting surface is the horizontal plane at 30 feet above ground, halfway between charges. As detonation of the lower charge is delayed, however, the reflecting surface moves downward and becomes non-planar. The calculated position of this surface for a number of different delay times is shown in Figure 2.10. A camera position at 30 feet was used to view shock interactions at the reflecting surface.

For particle trajectory analysis, a smoke puff grid was produced by firing small charges in an established pattern (Reference 5). The smoke puffs were placed along a line which passed through ground zero and made an angle of 80° with the MCP-GZ line on the opposite side from the backdrop line. Twenty one drops (vertical lines of smoke puffs) were used for the shots in the non-simultaneous series. Vertical spacing of the puffs was five feet, starting at five feet

5. B.J. Holsgrove and R.A. Klymchuk, "Statically Oriented Smoke Puff Grids," Suffield Technical Paper No. 352, Defence Research Establishment Suffield, Ralston, Alberta, Canada, September 1970.

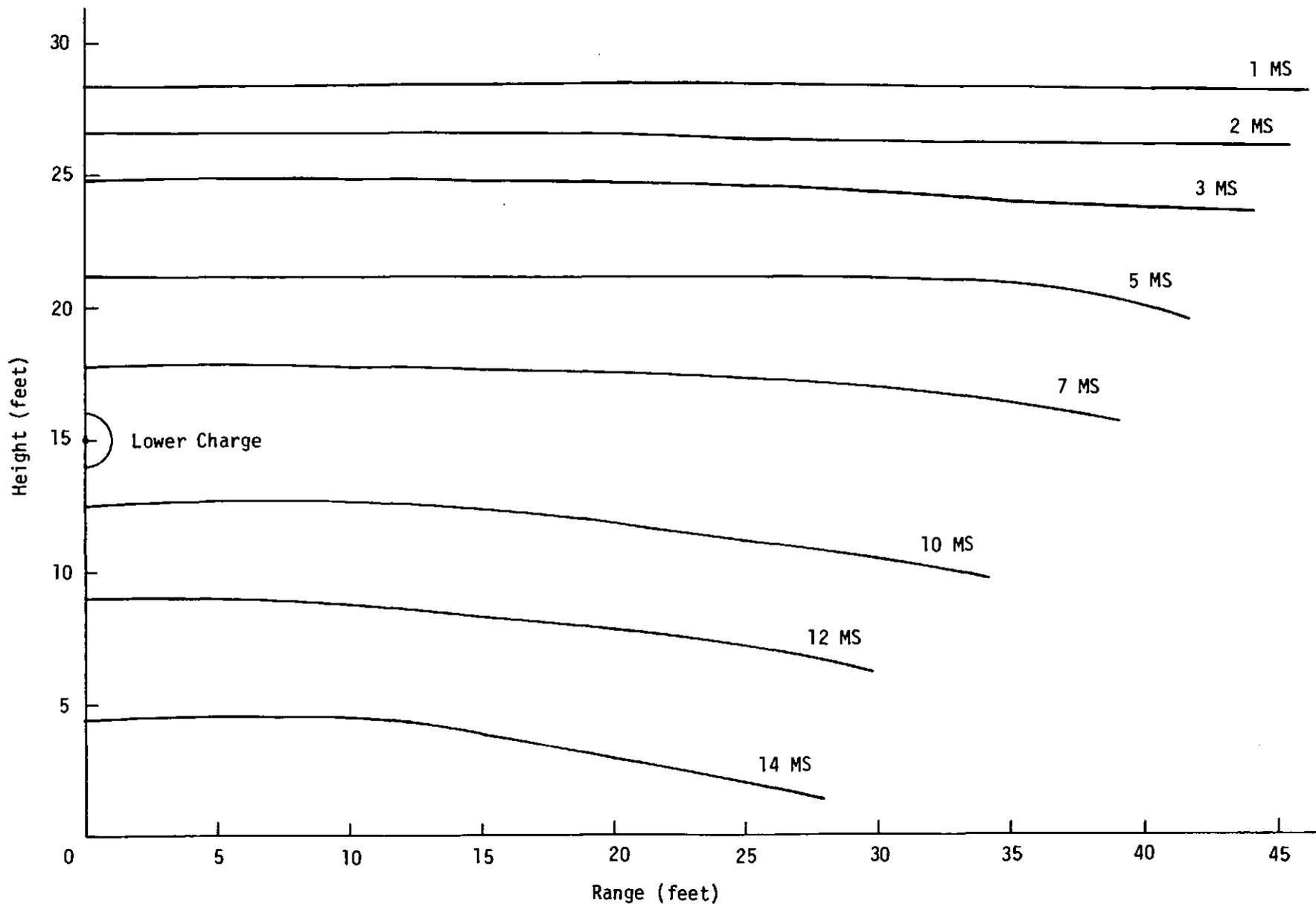


Figure 2.10. Calculated Position of Ideal Reflecting Surface for Different Values of Charge Detonation Non-Simultaneity

above the ground and extending through 45 feet. There were thus fifteen smoke puffs per drop. Horizontal spacing of the drops was five feet, beginning at 45 feet from ground zero. White smoke puffs were used for the lower nine stations on each drop for contrast with the prairie background, while red smoke puffs were used at the higher positions for contrast with the sky.

To observe the smoke puffs, two cameras were used at the main camera position at an elevation of 30 feet. Both cameras were centered accurately in azimuth and elevation on a central elevated marker so that the image plane of the camera was parallel to the plane of the smoke puffs. Such an arrangement requires a minimum of geometrical correction in the subsequent analysis of the film records.

For basic photographic documentation, a number of photographic markers were placed at various positions within the field of view of the cameras. Some of these markers were at ground level, while others were mounted on poles or on top of the backdrops. The positions of these markers can be seen in the site layout diagram, Figure 2.5. For Shots 12 through 15, photomarker locations were the same as had been used for the simultaneous detonations. For Shot 16, some rearrangements were made. Surveyed positions for all of the photomarkers and cameras are given in Table 2.6. The cameras used, with their framing rates and fields-of-view, are listed in Table 2.7.

2.3 Predictions and Calculations

In order to calibrate the air blast pressure gages to reasonable values, it was necessary to make predictions of peak overpressure and total head pressure values to be expected at the various gage locations. This was done by BRL personnel using scaling rules to extrapolate information gained from a large number of earlier HE tests. The technique is standardized and has been used on many occasions with a high degree of success. The accuracy of the technique is attested to by the fact that only a few recorded pressures exceeded band edge of the recording system.

More formal calculations were made at the Air Force Weapons Laboratory using their hydrodynamic computer code HULL. The calculation was begun as a one-dimensional spherically symmetric problem for detonation of the first (upper) charge. At time of detonation of the second (lower) charge, the calculation was reformatted into two dimensions in cylindrical symmetry, with the results of the one-dimensional calculation superimposed as input conditions. Calculations were carried out for the simultaneous case and for non-simultaneities of 3, 5, and 10 milliseconds, corresponding to the experimental conditions.

Results obtained from the calculations, in the form of "station

Table 2.6. Survey Data, Photomarkers and Cameras

Station	Bearing	Distance (feet)	Elevation (feet)
Shots 12-15: Photomarkers			
W1	257° 21' 32"	35.54	2318.10
W2	260° 22' 01"	70.37	2318.03
W3	261° 30' 11"	105.15	2317.35
E2	96° 50' 21"	69.82	2318.24
E3	99° 40' 16"	99.84	2317.89
300-1	176° 20' 50"	304.31	2312.99
300-2	170° 08' 25"	314.37	2313.09
300-3	164° 22' 57"	328.04	2313.27
W300-1	183° 42' 13"	315.18	2331.58
W300-2	187° 37' 45"	318.05	2331.64
BD-1	10° 00' 11"	393.55	2367.00
BD-2	17° 12' 07"	396.90	2366.77
BD-3	24° 02' 00"	405.75	2366.99
BD-1A	21° 10' 18.4"	392.50	2319.28
BD-2A	31° 16' 15.9"	412.88	2319.22
BD-3A	38° 19' 03.8"	444.74	2319.34
Shots 12-15: Vertical Position Markers			
1a	333° 24' 43"	106.19	2348.89
1b	333° 24' 40"	106.42	2383.78
2a	317° 56' 24"	121.91	2348.64
2b	317° 48' 50"	122.41	2383.61
3a	305° 18' 51"	149.20	2348.38
3b	305° 12' 35"	149.41	2383.34
Shots 12-15: Camera Positions (United States)			
U.S.-1	181° 41' 16.2"	602.28	2315.73
U.S.-2	181° 30' 28"	602.28	2315.80
U.S.-3	181° 19' 32.2"	601.82	2315.79
U.S.-4	181° 12' 43.9"	601.83	2315.85
U.S.-5	181° 54' 13"	602.25	2313.70
U.S.-6	181° 36' 18"	602.28	2313.68
U.S.-7	181° 21' 06.2"	601.99	2314.04
U.S.-8	180° 07' 25.4"	600.63	2314.52
U.S.-9	179° 57' 11.2"	600.69	2314.48
U.S.-10	179° 49' 50.7"	600.37	2314.58
U.S.-11	179° 41' 34.6"	600.49	2314.51

Table 2.6. Survey Data, Photomarkers and Cameras (Continued)

Station	Bearing	Distance (feet)	Elevation (feet)
U.S.-12	180° 42' 15"	600.63	2340.70
U.S.-13	180° 37' 46"	600.63	2340.72
U.S.-14	180° 12' 37"	600.66	2340.72

Shots 12-15: Camera Positions (Canada)

CAN-1	180° 00' 45"	599.58	2340.85
CAN-2	179° 57' 18"	600.68	2340.89
CAN-3	179° 49' 54"	600.50	2340.89
CAN-4	196° 30' 08"	575.96	2313.32
CAN-5	196° 21' 41.4"	576.13	2313.32
CAN-6	118° 51' 30"	2294.02	2312.24

Shot 16: Photomarkers

1-1	2° 37' 10.8"	395.90	2367.85
1-2	16° 29' 32"	396.11	2367.75
1-3	29° 48' 15.8"	416.65	2368.11
1-4	41° 10' 45.3"	457.31	2367.99
2-1	2° 07' 39.5"	372.38	2322.57
2-2	16° 53' 02.2"	371.15	2322.43
2-3	30° 53' 20.9"	393.95	2322.41
2-4	42° 42' 44.8"	437.20	2322.43
3-1	96° 50' 47.5"	69.81	2317.53
3-2	103° 47' 39.6"	141.85	2317.58
4-1	177° 12' 01.9"	303.40	2332.37
4-2	171° 54' 41.6"	311.20	2332.36
4-3	166° 50' 33.5"	322.27	2332.32
5-1	333° 03' 02.2"	105.85	2316.67
5-2	332° 46' 42.2"	106.88	2348.93
5-3	332° 38' 29.9"	106.84	2383.81
5-4	318° 05' 42.0"	121.68	2316.59
5-5	317° 54' 37.0"	122.41	2348.55
5-6	317° 27' 33.2"	122.00	2383.63
5-7	305° 26' 11.2"	148.95	2316.59
5-8	305° 19' 39.4"	149.24	2348.51
5-9	305° 06' 14.9"	149.17	2383.45
6-1	184° 47' 27.7"	304.52	2327.35
6-2	188° 19' 20.9"	308.68	2327.45

Table 2.6. Survey Data, Photomarkers and Cameras (Continued)

Station	Bearing	Distance (feet)	Elevation (feet)
Shot 16: Camera Positions (United States)			
U.S.-1	181° 12' 43.9"	601.82	2315.85
U.S.-2	181° 36' 18"	602.28	2313.37
U.S.-3	181° 21' 06.2"	601.99	2313.74
U.S.-4	181° 53' 45"	602.25	2312.95
U.S.-5	180° 07' 25.4"	600.63	2314.52
U.S.-6	179° 57' 11.2"	600.68	2314.48
U.S.-7	179° 49' 50.7"	600.37	2314.87
U.S.-8	179° 41' 34.6"	600.49	2314.71
U.S.-9	180° 42' 15"	600.63	2340.70
U.S.-10	180° 37' 46"	600.63	2340.71
U.S.-11	180° 25' 37"	600.65	2340.70
Shot 16: Camera Positions (Canada)			
CAN-1	179° 57' 44.2"	601.27	2341.02
CAN-2	179° 51' 03.9"	601.34	2340.56
CAN-3	179° 46' 18.1"	601.27	2340.99
CAN-4	179° 38' 40.7"	601.15	2340.85

Table 2.7. Cameras for Shots 12 thru 16

<u>Camera Type</u>	<u>Position</u>	<u>Framing Rate</u>	<u>View</u>	<u>Field-of-View</u>
16mm Fastax	MCP1	4,500	Smoke Puffs	20-80
16mm Fastax	MCP1	4,500	Backdrop	20-80
16mm Fastax	MCP1 30'	4,500	Smoke Puffs	20-80
16mm Fastax	MCP1 30'	4,500	Backdrop	20-80
16mm Milliken	MCP1 30'	400	Fireball/Cloud	120-0-120
16mm Dynafax	MCP1	25,000	Fireball	60-0-60
16mm Hycam	MCP1	6,000	Fireball	60-0-60
16mm Eastman	MCP1	3,000	Smoke Puffs	0-120
16mm Eastman	MCP1	3,000	Backdrop	0-120
70mm Hulcher	MCP1	20	Fireball/Cloud	90-0-90
70mm Hulcher	MCP1	20	Fireball/Cloud	250-0-250
16mm Fastax	60'	6,000	Strobe/Gage	59-61

listings", are given in Tables 2.8, 2.9, 2.10 and 2.11. In using these tables, it should be kept in mind that time is measured from detonation of the second charge. In the experimental results presented in Chapter 3, time is measured from detonation of the first charge. Therefore, in comparing experimental and calculated arrival times, it is necessary to add an amount equal to the difference in detonation time to the calculated results. Each of these calculations required approximately 30 hours of CDC 6600 computer time.

One other thing should be pointed out about the calculations. The calculation for the simultaneous detonation (Table 2.8) was zoned more finely in the region of the ground surface, which was treated as an ideal reflecting plane, than were the non-simultaneous calculations. For these latter calculations, the region of interest, and hence of finest zoning, was the shock interaction region between the charges. For ground level comparisons between calculations and data, therefore, results from the simultaneous calculation are more precise and should be used. If time is measured from detonation of the second charge, then these ground level results (or at least the initial portions of the pressure pulse waveform) will be equally valid for all events.

2.4 Data Reduction

2.4.1 Photo-Optical Analysis

Data analysis for the photo-optical results is being carried out at the University of Victoria, British Columbia. Basic film reading equipment is available there, and the necessary computer program analysis systems were developed for use with data from the earlier DIPOLE WEST events.

A computer program, REDUCE, is used for the shock wave analysis. This program provides geometrical scaling in terms of the surveyed positions of the camera, charges, and photomarkers, and reduces the photogrammetric shock wave data to distance-time values. A further geometrical correction is required because the shock front trajectory viewed from a fixed camera position lies along the semi-circular path for which the camera-GZ line is a diameter.

The resulting shock radius-time (R-t) data is then fitted by a least squares program to a curve of the form

$$R = A + Bt + C \ln(1 + t) + D \sqrt{\ln(1 + t)}.$$

The data are weighted inversely with observed radius so as to obtain a fit with constant percentage error throughout the range of the input data. Outputs from this second program, SHOCK, are fitted shock radius values, scaled times and distances, shock velocities, peak particle velocities, peak overpressures (in both atm and psi),

Table 2.8. AFWL HULL Calculation, Two 216-Pound Pentolite Spheres,
Simultaneous Detonation

a. Coordinates, Arrival Times, Overpressures

Station Number	Range (ft)	Height (ft)	Arrival Time (ms)	Peak Overpressure (psi)	Overpressure Impulse (psi-ms)
1	0.00	0.	2.38	507.66	325.15
2	.33	0.	2.38	515.03	325.18
3	.72	0.	2.38	511.47	324.71
4	1.12	0.	2.39	509.51	323.70
5	1.51	0.	2.40	506.95	322.31
6	1.90	0.	2.42	502.97	320.29
7	2.30	0.	2.43	497.20	317.61
8	2.69	0.	2.45	490.11	315.05
9	3.08	0.	2.48	484.16	311.53
10	3.48	0.	2.50	477.33	305.26
11	3.87	0.	2.53	469.71	302.43
12	4.27	0.	2.56	460.43	296.68
13	4.66	0.	2.60	449.92	292.99
14	5.05	0.	2.64	440.94	287.41
15	5.45	0.	2.68	432.26	283.10
16	5.84	0.	2.73	422.50	275.27
17	6.23	0.	2.77	410.03	271.18
18	6.63	0.	2.83	398.63	266.45
19	7.02	0.	2.88	388.30	258.40
20	7.41	0.	2.94	378.26	254.03
21	7.81	0.	3.00	363.79	249.68
22	8.20	0.	3.06	352.40	241.92
23	8.60	0.	3.13	341.67	237.63
24	8.99	0.	3.20	329.50	229.27
25	9.38	0.	3.27	318.59	225.12
26	9.78	0.	3.35	308.55	217.05
27	10.17	0.	3.43	296.23	213.90
28	10.56	0.	3.51	286.61	205.18
29	10.96	0.	3.59	275.05	201.87
30	11.35	0.	3.68	264.03	193.68
31	11.75	0.	3.77	254.41	190.95
32	12.14	0.	3.87	243.15	183.51
33	12.53	0.	3.96	234.78	180.54
34	12.93	0.	4.06	224.28	174.37
35	13.32	0.	4.16	215.41	172.39
36	13.71	0.	4.27	205.33	165.89
37	14.11	0.	4.37	196.74	163.79
38	14.50	0.	4.48	187.33	157.58
39	14.90	0.	4.59	177.43	152.66
40	15.29	0.	4.70	168.14	150.30
41	15.68	0.	4.82	158.62	145.80

Table 2.8. AFWL HULL Calculation, Two 216-Pound Pentolite Spheres, Simultaneous Detonation (Continued)

Station Number	Range (ft)	Height (ft)	Arrival Time (ms)	Peak Overpressure (psi)	Overpressure Impulse (psi-ms)
42	16.08	0.	4.93	149.11	140.88
43	16.47	0.	5.05	139.00	139.87
44	16.86	0.	5.17	128.84	134.41
45	17.26	0.	5.29	120.63	130.86
46	17.65	0.	5.41	114.31	127.13
47	18.04	0.	5.54	108.30	123.89
48	18.44	0.	5.67	102.54	124.28
49	18.83	0.	5.80	97.27	122.05
50	19.23	0.	5.93	92.44	118.40
51	19.62	0.	6.03	89.22	116.56
52	20.01	0.	6.16	85.14	113.46
53	20.41	0.	6.30	81.35	111.52
54	20.80	0.	6.44	77.91	109.41
55	21.19	0.	6.59	74.76	107.83
56	21.59	0.	6.73	71.87	105.91
57	21.98	0.	6.88	69.22	104.20
58	22.38	0.	7.03	66.75	102.89
59	22.77	0.	7.18	64.52	101.01
60	23.16	0.	7.33	62.41	99.23
61	23.56	0.	7.49	60.40	97.26
62	23.95	0.	7.65	58.54	96.86
63	24.34	0.	7.81	56.71	96.38
64	24.74	0.	8.02	54.64	95.59
65	25.13	0.	8.18	53.03	94.42
66	25.52	0.	8.35	51.50	93.13
67	25.92	0.	8.52	50.02	92.06
68	26.31	0.	8.69	48.61	91.40

b. Dynamic Pressures, Phase Durations

Station Number	Horizontal Dynamic Pressure Peak (psi)	Vertical Dynamic Pressure Peak* (psi)	Positive Phase Duration (ms)	Horizontal Dynamic Pressure Impulse (psi-ms)	Vertical Dynamic Pressure Impulse (psi-ms)
1	.05	-41.39	3.52	.10	-3.47
2	.32	-40.20	3.52	.23	-3.40
3	1.60	-40.37	3.52	.81	-3.42
4	3.61	-39.85	3.52	1.76	-3.38
5	6.65	-39.33	3.52	3.15	-3.36
6	10.40	-39.06	3.52	4.90	-3.31

Table 2.8. AFWL HULL Calculation, Two 216-Pound Pentolite Spheres, Simultaneous Detonation (Continued)

Station Number	Horizontal Dynamic Pressure Peak (psi)	Vertical Dynamic Pressure Peak* (psi)	Positive Phase Duration (ms)	Horizontal Dynamic Pressure Impulse (psi-ms)	Vertical Dynamic Pressure Impulse (psi-ms)
7	14.94	-38.69	3.52	7.78	-3.26
8	20.18	-37.91	3.51	10.19	-3.22
9	26.01	-37.06	3.50	12.83	-3.18
10	32.23	-36.46	3.48	15.70	-3.09
11	38.79	-35.09	3.48	19.12	-2.88
12	45.86	-34.23	3.46	22.40	-2.74
13	53.26	-33.62	3.44	25.83	-2.74
14	60.80	-31.97	3.41	29.98	-2.52
15	68.61	-30.93	3.38	33.60	-2.43
16	76.33	-30.02	3.36	38.02	-2.36
17	84.19	-29.21	3.35	41.76	-2.31
18	91.62	-27.25	3.33	45.48	-2.05
19	98.81	-26.48	3.33	49.86	-1.92
20	105.84	-25.29	3.34	53.31	-1.86
21	112.66	-23.90	3.35	56.79	-1.83
22	119.03	-21.95	3.36	60.95	-1.46
23	124.98	-20.94	3.38	64.31	-1.46
24	130.80	-19.89	3.41	67.87	-1.39
25	136.19	-18.70	3.42	70.94	-1.24
26	141.06	-16.56	3.44	73.87	-1.16
27	146.32	-14.73	3.47	76.91	-.96
28	149.95	-13.87	3.53	80.00	-.91
29	154.49	-12.72	3.54	82.32	-.88
30	157.81	-10.94	3.57	85.58	-.70
31	160.59	-9.81	3.64	87.55	-.66
32	163.97	-8.33	3.67	90.62	-.50
33	166.89	-6.93	3.69	92.54	-.47
34	170.54	-5.73	3.74	95.61	-.34
35	172.04	-4.46	3.81	97.57	-.31
36	175.13	-3.55	3.84	100.38	-.22
37	178.10	-2.48	3.89	102.83	-.17
38	180.28	-1.71	3.97	105.03	-.12
39	181.70	-.98	4.01	108.02	-.08
40	183.48	-.51	4.07	110.93	-.05
41	184.13	-.18	4.14	113.12	-.03
42	183.84	-.04	4.20	115.20	-.02
43	182.86	-.04	4.23	117.36	-.01
44	181.16	.29	4.31	118.93	.02
45	178.45	.52	4.37	121.14	.03
46	174.05	.55	4.46	122.69	.03

Table 2.8. AFWL HULL Calculation, Two 216-Pound Pentolite Spheres, Simultaneous Detonation (Continued)

Station Number	Horizontal Dynamic Pressure Peak (psi)	Vertical Dynamic Pressure Peak* (psi)	Positive Phase Duration (ms)	Horizontal Dynamic Pressure Impulse (psi-ms)	Vertical Dynamic Pressure Impulse (psi-ms)
47	168.43	.46	4.52	123.31	.03
48	161.46	.33	4.60	124.26	.02
49	153.69	.26	4.66	124.36	.02
50	145.32	.23	4.74	123.53	.02
51	139.16	.20	4.84	122.98	.02
52	130.61	.17	4.87	121.98	.02
53	122.31	.14	5.00	120.59	.02
54	114.29	.12	5.05	119.15	.01
55	106.56	.09	5.12	117.51	.01
56	99.49	.07	5.17	115.52	.01
57	92.76	.06	5.24	113.30	.01
58	86.60	.04	5.32	111.02	.01
59	80.78	.03	5.41	108.77	.01
60	75.40	.03	5.51	106.22	.01
61	70.44	.02	5.56	103.61	.00
62	65.86	.02	5.68	101.32	.00
63	61.60	.01	5.77	98.86	.00
64	56.79	.01	5.83	95.62	.00
65	53.26	.01	5.94	93.00	.00
66	50.02	.00	6.05	90.27	.00
67	47.05	.00	6.06	87.64	.00
68	44.33	.00	6.17	85.12	.00

*Negative sign indicates dynamic pressure peak in the downward direction.

Table 2.9. AFWL HULL Calculation, Two 216-Pound Pentolite Spheres,
Three Millisecond Time Separation

a. Coordinates, Arrival Times, Overpressures

Station Number	Range (ft)	Height (ft)	Arrival Time (ms)	Peak Overpressure (psi)	Overpressure Impulse (psi-ms)
1	0.	3.	1.35	129.8	153.5
2	0.	10.	5.61	70.91	163.3
3	10.	3.	2.38	93.50	141.8
4	10.	10.	1.27	265.3	115.0
5	10.	15.	1.04	307.8	109.1
6	10.	20.	1.27	263.7	131.3
7	20.	3.	5.29	47.08	112.4
8	20.	10.	4.04	63.43	70.09
9	20.	15.	3.82	66.08	108.3
10	20.	20.	4.06	62.45	99.74
11	20.	30.	3.02	39.36	103.9
12	20.	40.	1.07	61.83	67.24
13	20.	50.	1.25	61.27	68.20
14	25.	3.	7.34	40.17	103.1
15	25.	10.	6.13	37.73	108.1
16	25.	15.	5.91	38.99	101.5
17	25.	20.	6.15	37.34	92.93
18	25.	30.	5.10	31.98	95.25
19	25.	40.	3.20	34.06	57.07
20	25.	50.	3.25	36.30	58.27
21	30.	3.	9.92	36.84	100.9
22	30.	10.	8.67	24.80	103.6
23	30.	15.	8.47	25.34	98.25
24	30.	20.	8.75	36.98	86.92
25	30.	30.	7.60	26.50	86.80
26	30.	40.	5.86	22.67	51.04
27	30.	50.	5.86	22.95	52.06
28	40.	3.	15.11	23.74	95.96
29	40.	10.	14.70	18.86	94.05
30	40.	15.	14.54	20.12	90.76
31	40.	20.	13.98	22.36	85.24
32	40.	30.	13.69	19.85	73.28
33	40.	40.	11.99	12.97	65.42
34	40.	50.	11.99	13.21	42.24
35	50.	3.	21.07	15.28	90.05
36	50.	10.	21.41	17.03	83.98
37	50.	15.	20.54	14.03	80.27
38	50.	20.	20.00	14.45	76.94
39	50.	30.	19.87	15.09	61.85
40	50.	40.	18.78	8.45	57.83

Table 2.9. AFWL HULL Calculation, Two 216-Pound Pentolite Spheres,
Three Millisecond Time Separation (Continued)

Station Number	Range (ft)	Height (ft)	Arrival Time (ms)	Peak Overpressure (psi)	Overpressure Impulse (psi-ms)
41	50.	50.	18.76	8.48	52.88
42	60.	3.	27.66	11.35	81.75
43	60.	10.	27.68	14.41	78.11
44	60.	15.	27.11	10.35	73.08
45	60.	20.	26.62	10.25	68.52
46	60.	30.	26.45	10.77	61.15
47	60.	40.	26.07	7.03	50.76
48	60.	50.	26.05	6.12	47.39
49	82.5	3.	43.41	9.31	64.68
50	82.5	10.	43.16	8.23	63.05
51	82.5	15.	43.12	8.09	61.02
52	82.5	20.	43.04	7.22	58.39
53	82.5	30.	42.78	6.08	51.91
54	82.5	40.	43.32	5.81	45.91
55	82.5	50.	43.58	3.59	40.28
56	90.	3.	48.82	8.38	60.05
57	90.	10.	48.69	7.28	58.79
58	90.	15.	48.65	7.05	57.16
59	90.	20.	48.69	6.71	55.05
60	90.	30.	48.54	5.24	49.97
61	90.	40.	49.07	5.11	44.10
62	90.	50.	49.78	3.69	38.90

b. Dynamic Pressures, Phase Durations

Station Number	Horizontal Dynamic Pressure Peak (psi)	Vertical Dynamic Pressure Peak* (psi)	Positive Phase Duration (ms)	Horizontal Dynamic Pressure Impulse (psi-ms)	Vertical Dynamic Pressure Impulse (psi-ms)
1	0.	-146.	4.51	0.	-89.8
2	0.	12.7	6.17	0.	3.92
3	47.0	-57.3	4.65	39.3	-36.4
4	377.	-81.6	2.12	101.	-22.5
5	544.	-5.10	1.37	146.	-6.47
6	372.	89.7	4.56	94.7	22.7
7	28.6	-10.3	5.62	48.9	-7.67
8	59.3	-3.41	4.06	53.6	-2.50
9	66.8	-0.96	11.6	53.5	-2.20
10	57.6	3.61	5.63	54.6	2.48

Table 2.9. AFWL HULL Calculation, Two 216-Pound Pentolite Spheres,
Three Millisecond Time Separation (Continued)

Station Number	Horizontal Dynamic Pressure Peak (psi)	Vertical Dynamic Pressure Peak* (psi)	Positive Phase Duration (ms)	Horizontal Dynamic Pressure Impulse (psi-ms)	Vertical Dynamic Pressure Impulse (psi-ms)
11	19.2	-10.1	6.74	36.4	-10.5
12	55.6	-3.75	4.08	47.3	-2.73
13	54.6	3.96	4.12	45.6	6.12
14	22.2	-3.88	6.38	44.4	-2.68
15	25.5	-0.94	11.2	42.0	-1.07
16	27.9	-0.76	11.6	40.1	-1.60
17	24.9	1.01	6.36	44.9	2.08
18	14.3	-4.04	7.42	31.6	-5.06
19	21.9	1.23	5.12	32.8	2.09
20	24.0	0.81	5.25	31.8	2.65
21	19.1	-1.16	15.5	37.9	-0.86
22	12.3	-0.32	11.3	32.4	0.63
23	13.1	-0.74	11.5	30.5	-1.39
24	20.8	0.50	6.95	37.3	1.88
25	10.3	-1.66	8.07	25.9	-2.17
26	10.5	1.21	6.18	21.9	2.35
27	10.7	0.29	6.22	21.1	1.56
28	11.7	-0.15	15.6	30.6	0.22
29	5.34	0.13	11.3	22.2	0.50
30	7.50	-0.37	11.6	22.3	-0.97
31	10.1	0.28	12.9	27.7	-0.71
32	6.60	-0.30	9.08	18.3	0.62
33	3.71	0.62	14.0	12.3	1.50
34	3.83	0.33	8.31	11.1	1.36
35	5.12	-0.05	15.0	20.5	-0.07
36	5.26	-0.17	15.4	19.2	0.24
37	4.13	-0.20	12.8	17.8	-0.45
38	4.56	0.15	14.0	17.0	0.40
39	4.89	0.18	10.6	15.2	0.81
40	1.64	0.20	14.0	8.26	0.91
41	1.66	0.24	17.9	6.66	0.99
42	2.87	-0.02	15.0	15.6	-0.03
43	4.45	0.03	15.7	16.4	0.19
44	2.31	-0.08	16.9	13.3	0.18
45	2.37	0.04	14.6	11.8	0.33
46	2.62	0.11	17.1	10.2	0.60
47	1.05	0.06	14.4	6.29	0.57
48	0.88	0.13	17.8	4.44	0.65
49	1.94	0.00	16.8	9.79	0.01
50	1.56	0.01	17.3	8.81	0.08
51	1.50	0.01	17.6	8.05	0.15

Table 2.9. AFWL HULL Calculation, Two 216-Pound Pentolite Spheres,
Three Millisecond Time Separation (Continued)

Station Number	Horizontal Dynamic Pressure Peak (psi)	Vertical Dynamic Pressure Peak* (psi)	Positive Phase Duration (ms)	Horizontal Dynamic Pressure Impulse (psi-ms)	Vertical Dynamic Pressure Impulse (psi-ms)
52	1.18	0.02	18.2	6.94	0.21
53	0.87	0.02	21.6	5.22	0.31
54	0.78	0.03	20.0	4.08	0.35
55	0.30	0.03	24.3	2.63	0.32
56	1.59	0.00	17.8	8.25	0.01
57	1.22	0.00	17.9	7.43	0.06
58	1.15	0.01	18.2	6.80	0.12
59	1.04	0.01	18.4	6.06	0.17
60	0.65	0.02	21.3	4.49	0.26
61	0.61	0.02	23.3	3.48	0.31
62	0.31	0.02	24.3	2.38	0.28

*Negative sign indicates dynamic pressure peak in the downward direction.

Table 2.10. AFWL HULL Calculation, Two 216-Pound Pentolite Spheres,
Five Millisecond Time Separation

a. Coordinates, Arrival Times, Overpressures

Station Number	Range (ft)	Height (ft)	Arrival Time (ms)	Peak Overpressure (psi)	Overpressure Impulse (psi-ms)
1	0.	0.	2.13	357.5	313.4
2	10.	0.	3.16	242.8	219.1
3	10.	3.	2.40	111.8	134.4
4	10.	10.	1.26	221.6	112.2
5	10.	15.	0.99	233.3	103.7
6	20.	0.	5.84	91.97	139.4
7	20.	3.	5.22	41.05	114.6
8	20.	10.	3.99	51.40	115.7
9	20.	15.	3.74	53.24	97.06
10	25.	0.	7.64	53.24	118.1
11	25.	3.	7.41	38.87	110.7
12	25.	10.	6.08	30.76	106.6
13	25.	15.	5.86	36.00	104.0
14	30.	0.	9.76	36.03	110.9
15	30.	3.	9.94	35.27	107.4
16	30.	10.	8.58	21.01	102.7
17	30.	15.	8.27	32.25	98.21
18	40.	0.	14.86	20.52	104.1
19	40.	3.	14.97	21.52	103.4
20	40.	10.	14.23	17.07	94.75
21	40.	15.	13.45	18.26	89.82
22	50.	0.	20.87	16.37	94.59
23	50.	3.	20.82	16.62	94.04
24	50.	10.	20.32	13.95	88.53
25	50.	15.	19.47	12.14	82.15
26	60.	0.	27.11	14.28	83.84
27	60.	3.	27.05	13.71	83.36
28	60.	10.	26.79	12.18	79.72
29	60.	15.	26.06	8.88	74.74
30	82.5	0.	42.13	8.64	64.63
31	82.5	3.	42.14	8.60	64.49
32	82.5	10.	42.21	8.09	62.78
33	82.5	15.	42.23	7.44	61.12
34	90.	0.	47.32	7.50	59.88
35	90.	3.	47.33	7.47	59.60
36	90.	10.	47.45	7.13	58.25
37	90.	15.	47.58	6.81	57.24
38	150.	0.	93.09	3.24	33.78
39	150.	3.	93.11	3.23	33.76
40	150.	10.	93.22	3.09	33.06
41	150.	15.	93.54	3.18	33.12

Table 2.10. AFWL HULL Calculation, Two 216-Pound Pentolite Spheres,
Five Millisecond Time Separation (Continued)

b. Dynamic Pressures, Phase Durations

Station Number	Horizontal Dynamic Pressure Peak (psi)	Vertical Dynamic Pressure Peak* (psi)	Positive Phase Duration (ms)	Horizontal Dynamic Pressure Impulse (psi-ms)	Vertical Dynamic Pressure Impulse (psi-ms)
1	0.82	-26.1	3.62	1.15	-5.10
2	105.	-9.25	3.66	66.5	-1.70
3	62.0	-84.0	4.47	38.1	-39.4
4	272.	-75.1	2.06	9.91	-22.0
5	372.	-8.32	1.18	148.	-13.5
6	102.	0.01	5.05	104.	-0.01
7	22.9	-8.75	7.26	46.4	-7.33
8	43.2	-2.89	10.4	51.7	-4.25
9	48.4	-0.86	5.67	58.1	-2.61
10	59.8	0.07	11.3	92.2	0.02
11	19.8	-3.01	8.78	43.3	-2.05
12	19.0	-0.81	10.5	40.1	-2.48
13	24.4	-0.61	11.5	46.5	-1.62
14	30.8	0.01	10.8	69.4	0.01
15	17.9	-0.41	10.7	38.0	-0.42
16	9.65	-0.72	10.1	32.4	-1.95
17	18.9	-0.89	11.1	39.4	-1.75
18	9.73	0.00	12.3	37.8	0.00
19	9.96	0.07	12.2	33.1	0.06
20	5.88	-0.61	12.8	24.9	-1.15
21	7.24	-0.30	12.4	26.1	-0.98
22	5.76	0.00	13.4	25.1	0.00
23	6.09	-0.02	13.5	25.4	0.03
24	3.94	-0.17	14.0	19.4	-0.21
25	3.40	-0.11	15.2	17.4	-0.32
26	4.45	0.00	13.8	19.5	0.00
27	4.18	0.00	13.9	19.2	0.01
28	3.22	0.02	14.2	15.6	0.15
29	1.87	-0.05	16.6	12.5	0.30
30	1.77	0.00	16.5	10.1	0.00
31	1.75	0.00	16.5	9.99	0.01
32	1.55	0.01	16.4	9.06	0.09
33	1.28	0.01	17.1	8.00	0.17
34	1.35	0.00	16.8	8.21	0.00
35	1.34	0.00	17.4	8.16	0.01
36	1.22	0.01	17.3	7.54	0.07
37	1.09	0.01	17.2	6.88	0.14

Table 2.10. AFWL HULL Calculation, Two 216-Pound Pentolite Spheres,
Five Millisecond Time Separation (Continued)

Station Number	Horizontal Dynamic Pressure Peak (psi)	Vertical Dynamic Pressure Peak* (psi)	Positive Phase Duration (ms)	Horizontal Dynamic Pressure Impulse (psi-ms)	Vertical Dynamic Pressure Impulse (psi-ms)
38	0.26	0.00	20.9	2.15	0.00
39	0.26	0.00	20.9	2.15	0.00
40	0.24	0.00	20.8	2.04	0.01
41	0.25	0.00	20.5	2.02	0.02

*Negative sign indicates dynamic pressure peak in the downward direction.

Table 2.11. AFWL HULL Calculation, Two 216-Pound Pentolite Spheres,
Ten Millisecond Time Separation

a. Coordinates, Arrival Times, Overpressures

Station Number	Range (ft)	Height (ft)	Arrival Time (ms)	Peak Overpressure (psi)	Overpressure Impulse (psi-ms)
1	0.	0.	2.17	381.	323.
2	0.	3.	1.40	172.	153.
3	10.	0.	3.17	237.	218.
4	10.	3.	2.38	108.	146.
5	10.	10.	1.27	225.	125.
6	10.	15.	1.07	281.	123.
7	20.	0.	5.86	97.8	162.
8	20.	3.	5.20	44.0	135.
9	20.	10.	3.98	62.2	95.3
10	20.	15.	2.09	15.7	105.
11	25.	0.	7.62	61.6	143.
12	25.	3.	7.20	31.5	132.
13	25.	10.	5.94	42.5	106.
14	25.	15.	3.97	13.2	90.5
15	30.	0.	9.66	43.8	132.
16	30.	3.	9.66	39.8	126.
17	30.	10.	8.19	30.4	98.4
18	30.	15.	6.25	24.0	74.0
19	40.	0.	14.4	28.3	105.
20	40.	3.	14.5	28.8	103.
21	40.	10.	13.5	15.6	86.1
22	40.	15.	15.0	14.6	71.8
23	50.	0.	19.8	18.7	83.1
24	50.	3.	19.9	18.5	82.4
25	50.	10.	20.1	13.8	75.1
26	50.	15.	19.7	9.46	67.2
27	60.	0.	25.9	12.9	68.6
28	60.	3.	26.0	12.6	67.9
29	60.	10.	26.6	11.9	64.3
30	60.	15.	27.0	9.46	60.1
31	82.5	0.	41.3	6.58	47.4
32	82.5	3.	41.4	6.60	47.4
33	82.5	10.	41.9	6.58	46.6
34	82.5	15.	42.6	6.27	45.6
35	90.	0.	46.7	5.66	42.9
36	90.	3.	46.8	5.54	42.7
37	90.	10.	47.3	5.55	42.4
38	90.	15.	47.9	5.35	41.8
39	150.	0.	93.9	2.10	22.8
40	150.	3.	94.0	2.10	22.7
41	150.	10.	94.2	2.00	22.2
42	150.	15.	94.6	2.01	22.2

Table 2.11. AFWL HULL Calculation, Two 216-Pound Pentolite Spheres,
Ten Millisecond Time Separation (Continued)

b. Dynamic Pressures, Phase Durations

Station Number	Horizontal Dynamic Pressure Peak (psi)	Vertical Dynamic Pressure Peak* (psi)	Positive Phase Duration (ms)	Horizontal Dynamic Pressure Impulse (psi-ms)	Vertical Dynamic Pressure Impulse (psi-ms)
1	1.01	-27.2	3.66	0.78	-5.16
2	1.14	-233.	4.38	0.90	-96.7
3	99.1	-8.82	4.03	60.3	-1.56
4	56.9	-80.2	5.39	37.1	-38.5
5	276.	-71.4	2.66	94.6	-28.6
6	382.	6.51	1.41	138.	22.6
7	105.	-0.03	6.11	108.	-0.01
8	24.9	-10.8	6.98	52.5	-9.72
9	60.7	-4.48	4.68	64.8	-10.9
10	43.1	-3.79	5.57	50.1	-8.43
11	70.4	0.11	7.44	107.	0.02
12	22.7	-4.74	7.76	52.0	-3.96
13	32.7	-2.05	8.89	50.7	-6.22
14	20.6	-2.34	6.35	36.6	-5.16
15	42.3	0.02	8.02	90.2	0.01
16	20.2	-1.88	8.01	48.6	-1.14
17	18.2	-0.92	9.42	40.7	-2.54
18	12.4	-0.84	7.31	27.6	-1.55
19	17.2	0.00	9.07	55.5	0.00
20	15.5	0.02	9.00	42.6	0.11
21	5.68	0.39	10.8	25.4	1.65
22	4.81	0.54	12.5	15.7	2.31
23	7.94	0.00	10.3	30.0	0.01
24	7.72	0.04	10.2	28.8	0.22
25	3.93	0.17	11.1	17.0	1.08
26	2.18	0.31	12.8	11.6	1.77
27	3.93	0.00	11.7	17.3	0.00
28	3.80	0.02	11.9	16.8	0.10
29	3.13	0.13	12.0	13.2	0.74
30	1.90	0.17	13.0	9.26	1.07
31	1.09	0.00	14.6	6.24	0.00
32	1.09	0.00	14.5	6.21	0.02
33	1.05	0.02	15.1	5.80	0.17
34	0.93	0.05	15.4	5.17	0.32
35	0.80	0.00	15.9	4.81	0.00
36	0.78	0.00	15.8	4.73	0.01
37	0.76	0.01	16.2	4.50	0.10
38	0.69	0.03	16.3	4.14	0.21

Table 2.11. AFWL HULL Calculation, Two 216-Pound Pentolite Spheres,
Ten Millisecond Time Separation (Continued)

Station Number	Horizontal Dynamic Pressure Peak (psi)	Vertical Dynamic Pressure Peak* (psi)	Positive Phase Duration (ms)	Horizontal Dynamic Pressure Impulse (psi-ms)	Vertical Dynamic Pressure Impulse (psi-ms)
39	0.11	0.00	21.3	0.98	0.00
40	0.11	0.00	21.3	0.97	0.00
41	0.10	0.00	21.1	0.93	0.00
42	0.10	0.00	20.6	0.92	0.01

*Negative sign indicates dynamic pressure peak in the downward direction.

and peak density ratios.

The above procedure has been successfully applied to the photographic data from the earlier DIPOLE WEST events (Shots 8 through 11). Reference 6 gives the results of that analysis, plus additional details about the process. A similar report is to be produced covering the data from Shots 12 through 16.

The program for evaluation of the particle trajectories from photography of the smoke puff array is somewhat more involved than that for the shocks. It has been applied to the data from Shots 8 through 11, however, and a report on that analysis is in preparation. A report covering Shots 12 through 16 particle trajectory analysis is also to be prepared.

2.4.2 Air Blast Pressure Analysis

Digitization and plotting of air blast pressures recorded on magnetic tape were carried out by the Albuquerque office of GE-TEMPO, using equipment, personnel, and computer programs available at the Air Force Weapons Laboratory. The 32-track analog tapes used for Shots 12 through 16 were first dubbed to 14-track format at the DNA Playback Center, Nevada Test Site. They were then taken to Albuquerque for analog-to-digital processing.

The calibration tapes made prior to each shot were first digitized and the digits were listed. These tapes contain the static pressure and electronic or shunt calibration levels. The digitized calibration levels were averaged and compared by hand, and in all cases the shunt calibration was within two percent of the pressure calibration.

The calculated pressure equivalents of the shunt calibrations were used with the shunt calibrations on the data tapes, recorded five seconds before shot time, in order to calibrate the data. Digitizing rate for the data was 100 kilosamples/second.

In order to determine zero time (the time from start of digitizing to detonation) accurately, the DET ZERO files were listed and the number of samples from start to the DET ZERO pulse was counted. This method was also used to obtain an accurate determination of the time between the two detonations.

The digitized data were run through a computer program, ADDGEN3, which translates the raw digital data to units of pressure.

6. J.M. Dewey, D.F. Classen and D.J. McMillin, "Photogrammetry of the Shock Front Trajectories on DIPOLE WEST Shots 8, 9, 10 and 11," UVIC-PF 1-75, University of Victoria, British Columbia, Canada, July 1975.

Outputs from ADDGEN3 are large working plots (from which the tables of results appearing in Chapter 3 were prepared) and "engineering unit" (EU) computer tapes. The EU tapes were used, finally, as input to another computer program, ROTATE, which prepared the small plots appearing in the Appendix.

The EU tapes were also used to calculate Mach numbers and dynamic pressures from the overpressure and total pressure records. These results will appear in a final report on the DIPOLE WEST multi-burst detonations, to be published later.

CHAPTER 3

RESULTS

3.1 General Observations

The five shots of the DIPOLE WEST non-simultaneous detonation series were successfully carried out between October 24, 1974 and June 10, 1975. Four of the shots comprised the fall 1974 series, while the final event was fired as the first shot in the spring 1975 series. Tables 2.3, 2.4, and 2.5 give firing data and environmental conditions for each of the shots. Fireball anomalies of minor significance were observed on all events, but these occurred in directions which did not affect the instrumentation, except in the cases of Shots 12 and 15.

Two pentolite charges, fired simultaneously on October 24, comprised the first event of the non-simultaneous series. This event was designated Shot 12, because it was the twelfth DIPOLE WEST event. Configuration was equivalent to that of two earlier shots in the series (Shots 7 and 8) for which the charges were at heights of 25 and 75 feet above a hard surface. In the earlier events, size of the charges was 1080 pounds each. Shot 12, using 216-pound charges at 15 and 45 feet above the surface, was a scaled down version of these events.

A photograph of the Shot 12 fireballs, taken at approximately 0.05 seconds after detonation time, is given in Figure 3.1. Some irregularities are evident in the fireball indicating the occurrence of minor jetting. Pressure-time histories recorded at stations 10.0N, 10.0S, 20.0, 20.3, 30.0 and 30.3 (as reproduced in the Appendix) for Shot 12 show the effects of these anomalies when they are directed along a gage line. The records show many small shocks and perturbations, rather than clean, exponentially decaying waves as generally observed. Figure 3.1, and all of the photographs presented in this section, are reproduced from DRES and DRI (Denver Research Institute) film.

Shot 13, fired on October 28, was the first of the non-simultaneous detonations. Configuration was the same as for Shot 12, but in this case detonation of the lower charge was delayed by approximately 10 milliseconds. Detonation of the second charge occurred successfully even though the shock wave from the first charge had engulfed the lower charge before it was detonated. The results in terms of shock wave interactions are not as easy to interpret, however, as those for cases in which the time separation was not so large. Figure 3.2 shows the Shot 13 fireballs at approximately 0.05 second after detonation of the upper charge.

Shot 14 was a single 216-pound pentolite charge at the 15-foot level, fired to provide single charge data for comparison with those from the double charge events. It was detonated on October 30. This

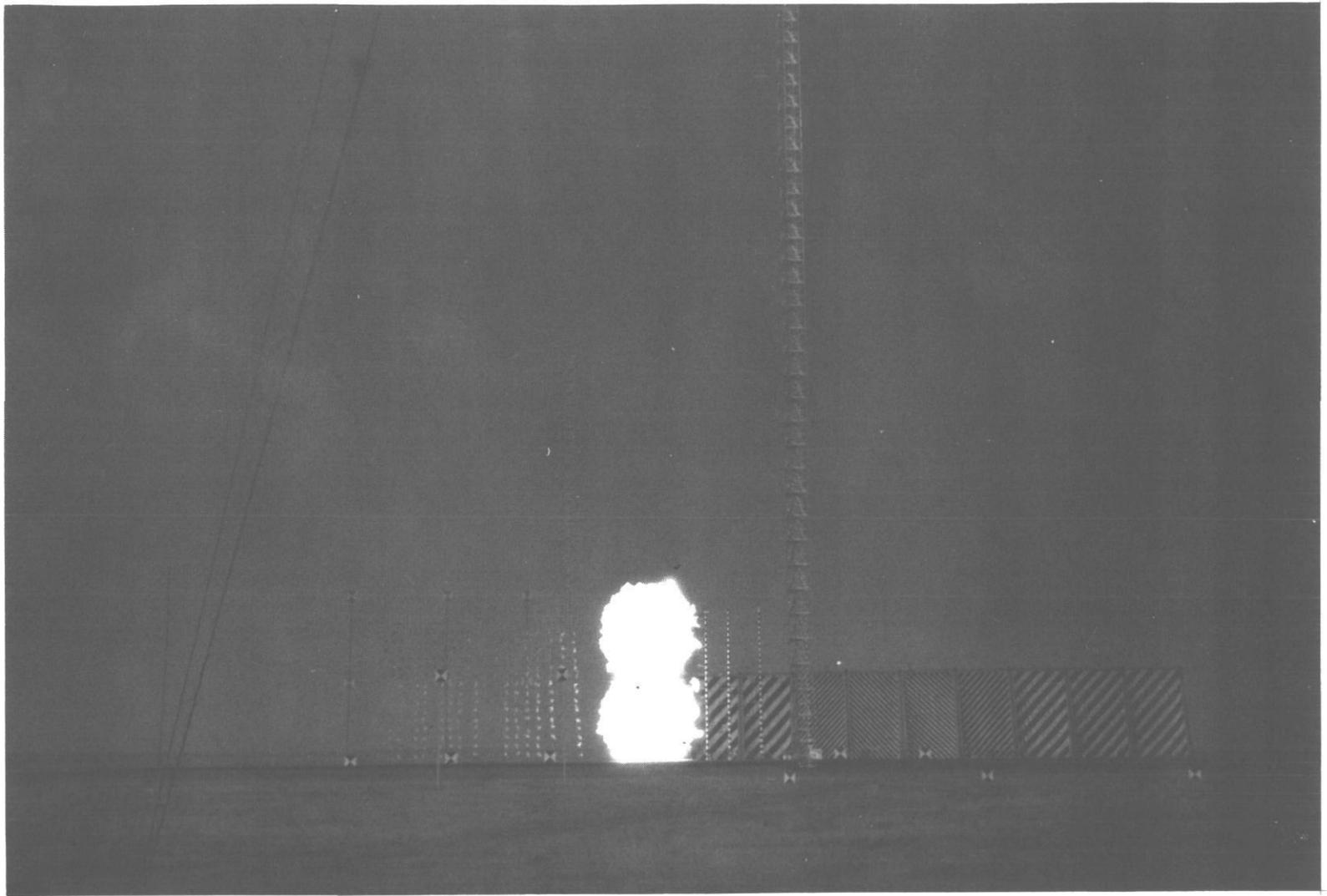


Figure 3.1. Shot 12 Fireballs at ~ 0.05 Second After Detonation

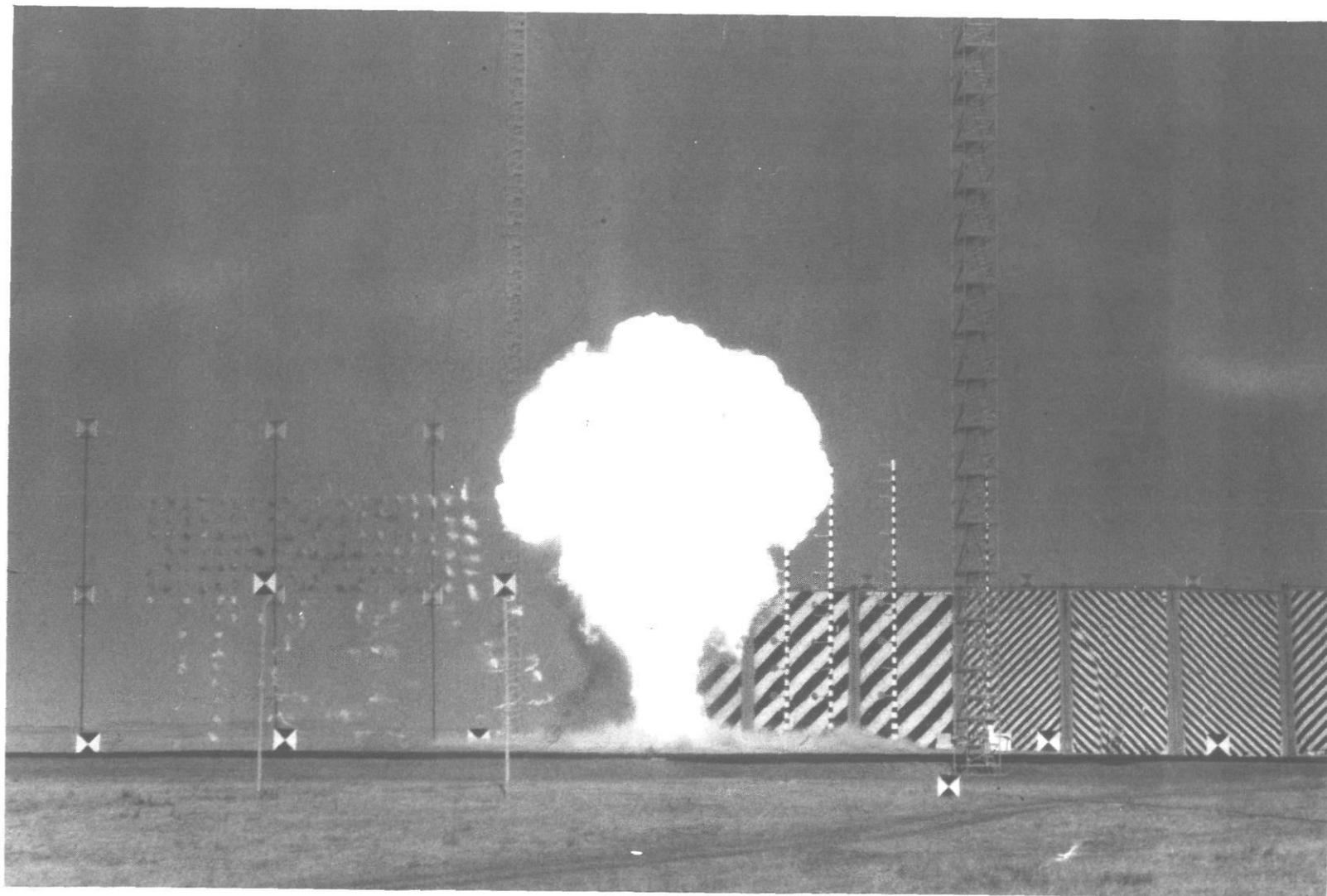


Figure 3.2. Shot 13 Fireballs at ~ 0.05 Second After Detonation of the Upper Charge

charge produced a symmetrical fireball, as can be seen in Figure 3.3, and classical exponentially decaying pressure-time histories, as seen in the Appendix.

As the final event in the fall series, Shot 15 was detonated on November 1st. Configuration was identical to the previous double-burst events, but this time the difference in detonation times was 5 milliseconds. The detonation was again satisfactory, but as it was growing quite late in the season and because it was desired to examine and evaluate the data before another shot, operations were suspended following Shot 15 until spring. Shot 15 fireballs are shown in Figure 3.4. Photographic data from Shot 15 is of minimal quality due to poor lighting at shot time. Also, the infrared colored film records indicate the presence of a jet toward the ground in the direction of the gage line on this event. The pressure-time records for stations 10.0S, 10.0E, and 40.0 display the effects of this anomaly on the gages.

The first event of the spring series, Shot 16, was fired as the final non-simultaneous detonation. It was fired on June 10, 1975, in a configuration identical to that of the fall double charge events, except that delay time between detonation of the upper and lower charges was only 3 milliseconds. These fireballs at approximately 0.05 second are shown in Figure 3.5.

In general, the entire series was run smoothly and efficiently. Excellent data was obtained except in a few cases. Further analysis remains to be completed, but it is felt that all of the objectives of the series were satisfactorily met.

3.2 Photographic Results

Shock front and particle trajectory photography results were in general quite satisfactory. Some difficulty was experienced in observing the shock fronts against the backdrop in the region of the charge support tower. Also, there was a fairly high incidence of smoke puff failure. This latter problem has been traced to a fault in squib manufacture.

Photogrammetric analysis of data recorded by the cameras was not completed in time for inclusion in this preliminary report. A separate report covering this analysis will be published at a later date by Dr. John Dewey, University of Victoria. Some preliminary information, however, can be presented.

A sequence from high speed photographs of the four double-burst detonations is shown in Figure 3.6, parts A and B. The effects of the delay time on fireball development and flowfield interaction are clearly illustrated. The fireball from the lower charge, the second to be detonated, rises upward through the first fireball so that after a

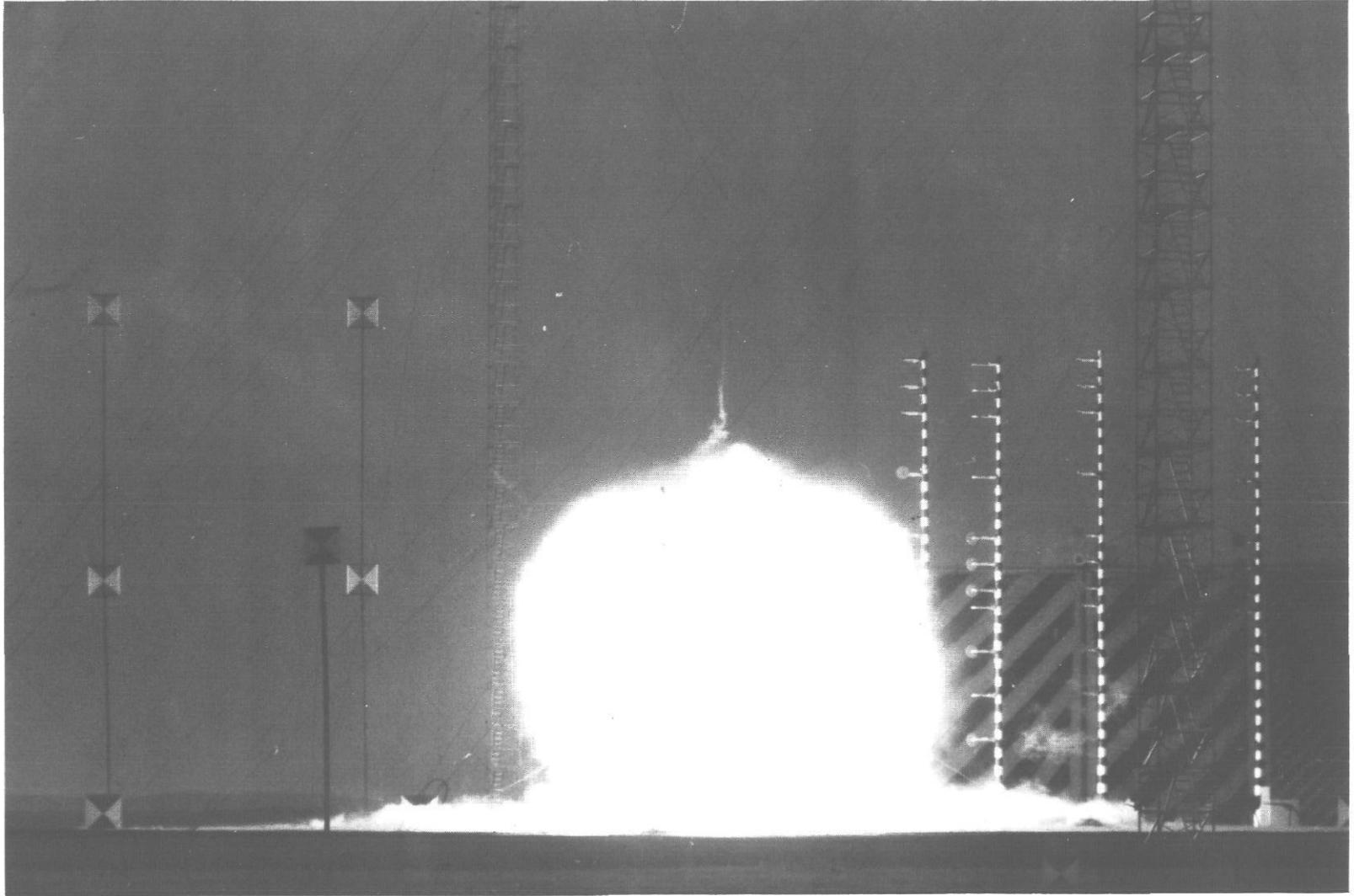


Figure 3.3. Shot 14 Fireball at ~ 0.05 Second After Detonation

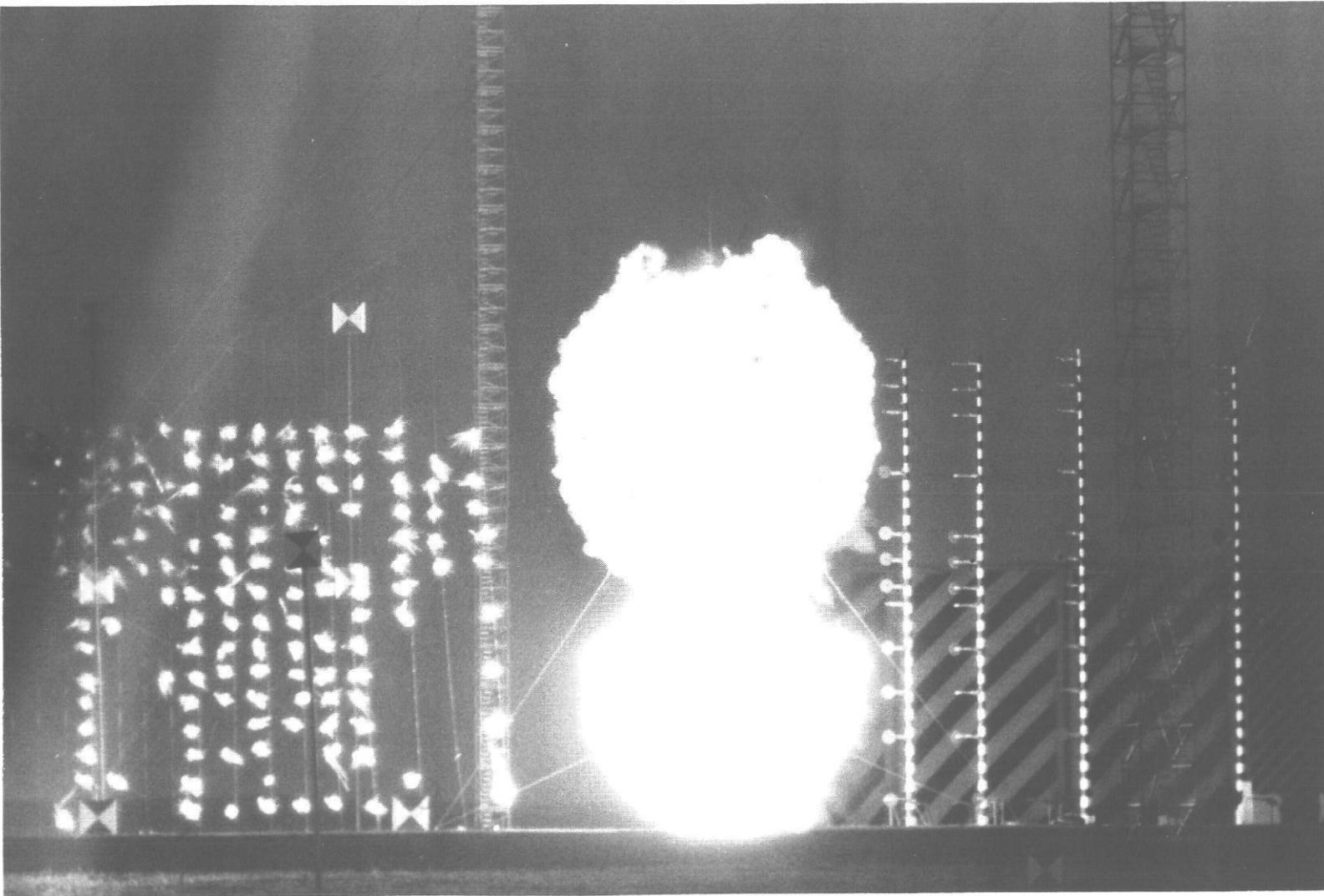


Figure 3.4. Shot 15 Fireballs at ~ 0.05 Second After Detonation of the Upper Charge

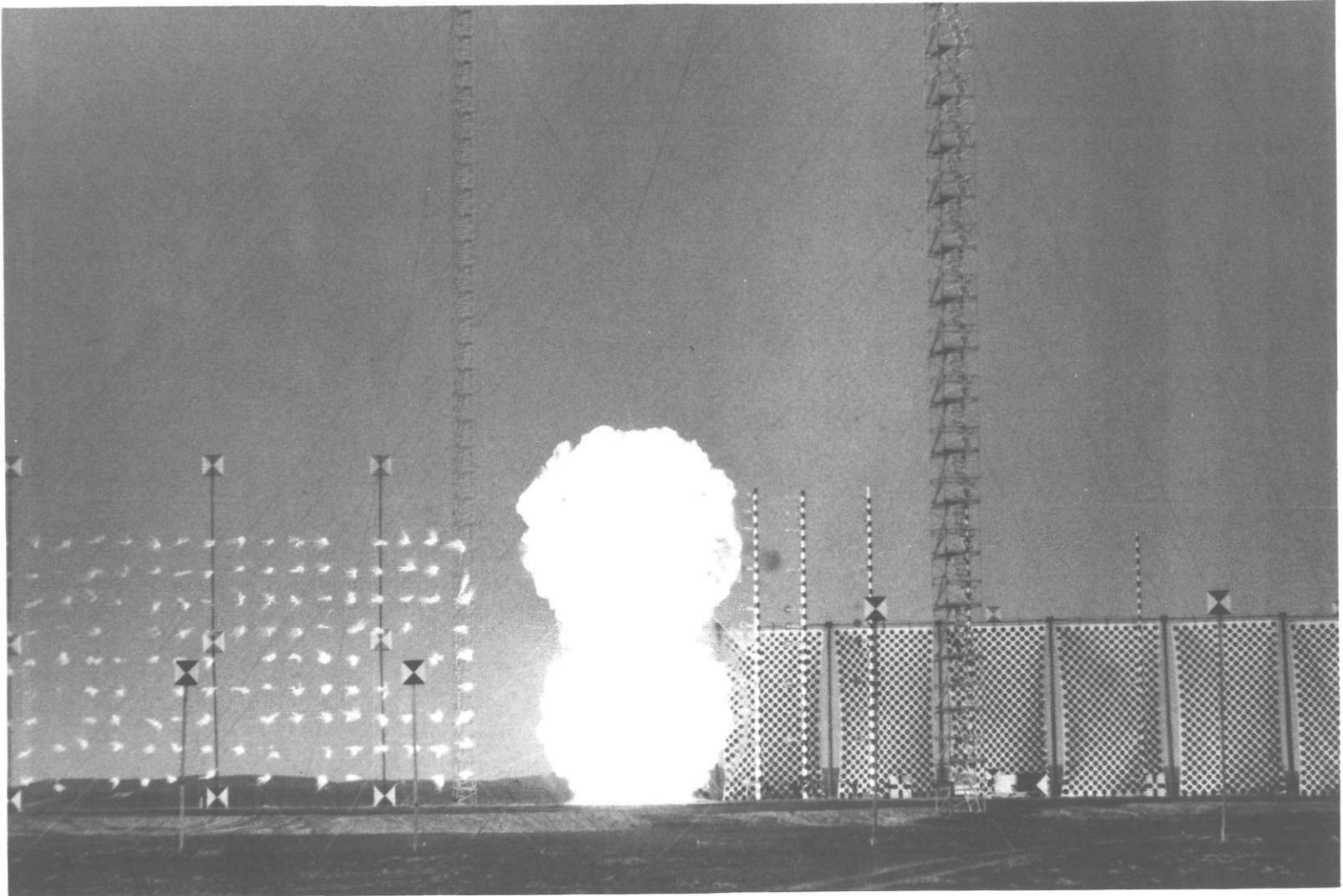


Figure 3.5. Shot 16 Fireballs at ~ 0.05 Second After Detonation of the Upper Charge

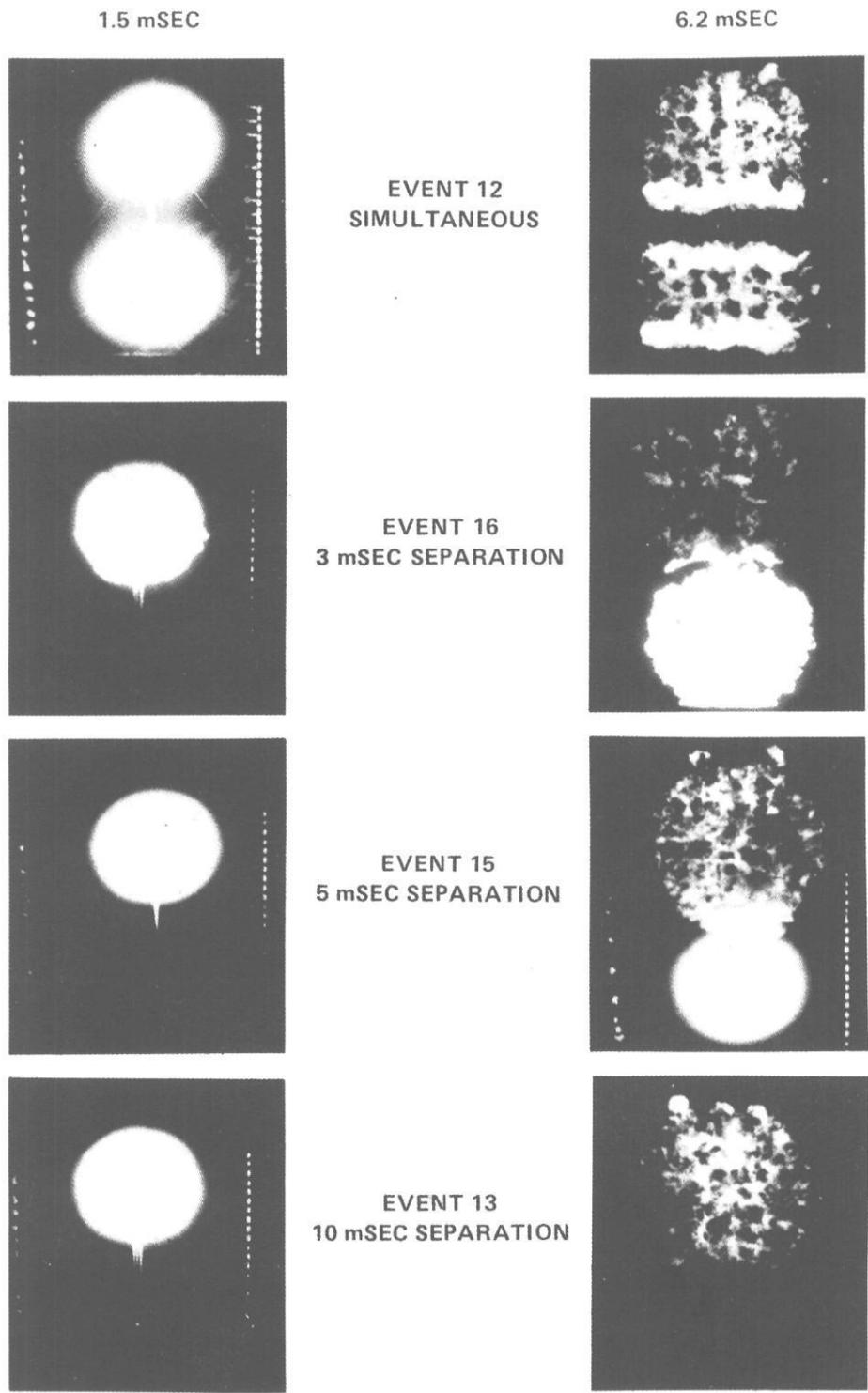


Figure 3.6(A). Fireballs of Non-Simultaneous Events at 1.5 and 6.2 Milliseconds After Detonation

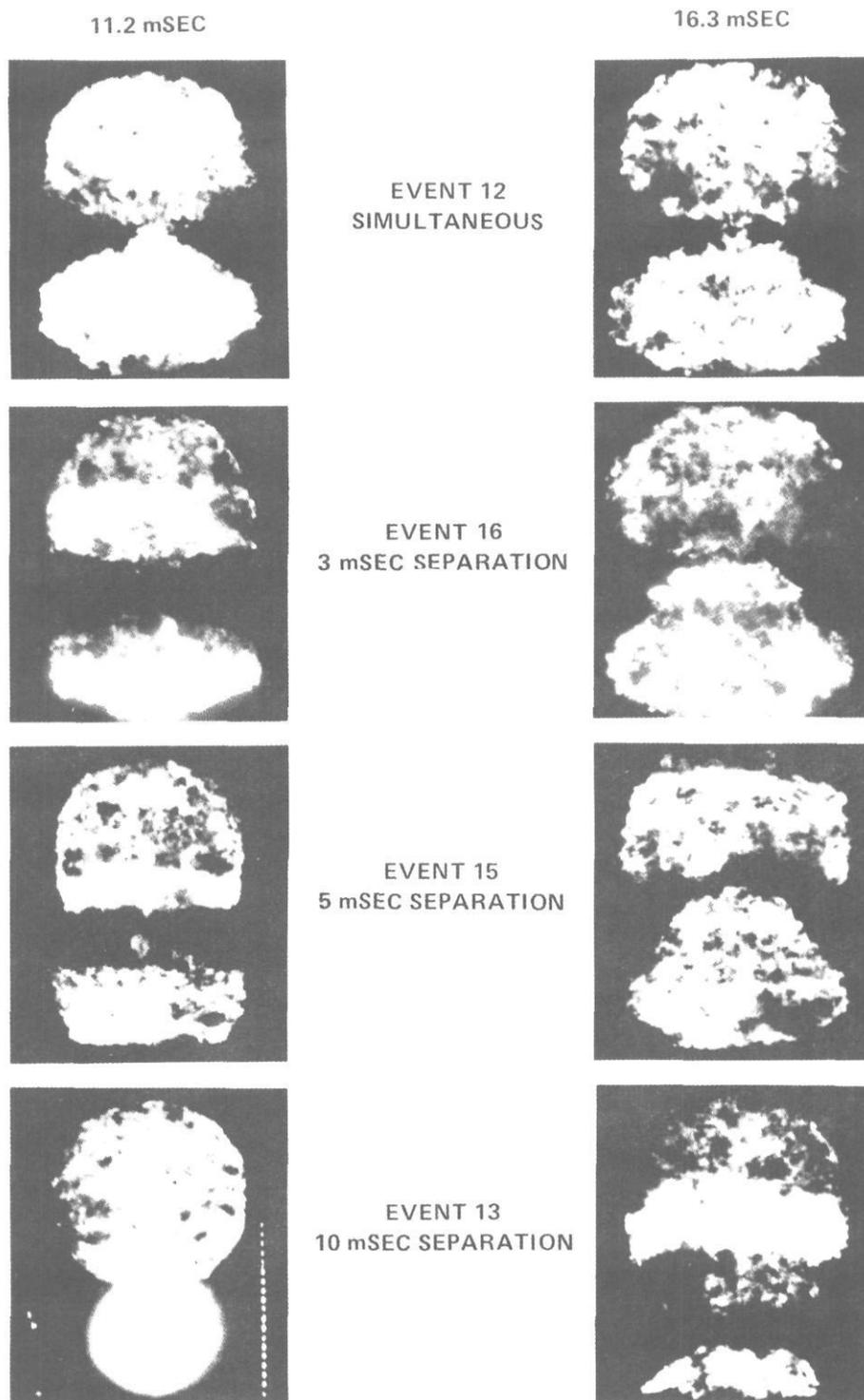


Figure 3.6(B). Fireballs of Non-Simultaneous Events at 11.2 and 16.3 Milliseconds After Detonation

very short time the detonation appears as a single fireball and subsequently a single cloud. Calculations performed for non-simultaneous detonations exhibit the same phenomena.

Figure 3.7 is a single frame from the film records of Shot 12. Time of the frame is approximately 15.7 milliseconds after detonation of the charges. Configuration of the shock system can be clearly ascertained in each case. In order to circumvent loss of clarity imposed in the process of reproducing this photograph for publication (and similar photographs shown in Figures 3.9, 3.11, and 3.13 for Shots 16, 15, and 13 respectively), lines indicating shock front positions have been drawn on a reproduction of the photograph, and this is shown in the lower half of the figure. The positions of the triple points and the general configuration of the shock systems may be observed.

Reconstructed paths of the triple points, as indicated by preliminary analysis of photographic data from Shot 12, are shown in Figure 3.8. The ideal reflecting plane, as expected for the case of simultaneous detonations, is flat and located midway between charges.

Similar photographs (at approximately 18.3 milliseconds after detonation of the upper charges for Shots 13 and 15, and at approximately 13 milliseconds for Shot 16) for the other double-burst events and accompanying sketches showing triple point paths are given in Figures 3.9 through 3.14. Differences in shock system configuration and increased distortion of the ideal reflecting surface as the non-simultaneity becomes more severe are apparent.

3.3 Air Blast Results

The air blast overpressure and total pressure records have all been digitized and plotted as described in Section 2.4.2. These plots are included as an Appendix to this report. The event number, station location, and recorder and channel numbers are given in the title for each plot. Also plotted is the integral over time, or impulse, from each record.

The station location codes, appearing in the tabulated results of this section as well as in the Appendix, may be interpreted as follows. The number before the decimal point indicates the range of the transducer location in feet from ground zero. The number after the decimal point indicates the elevation above ground in feet. Hence ST (Station) 60.27 would refer to gages on the 60-foot gun barrel at the 27-foot level.

The letters S or T following the elevation indicate whether the transducer was mounted in a side-on baffle or total head probe configuration. The prefix 2- means the transducer was located on the secondary gage line (line 2) rather than on the primary line. Other indicators are E, W, N, and S, for gages located to the east, west, north, and

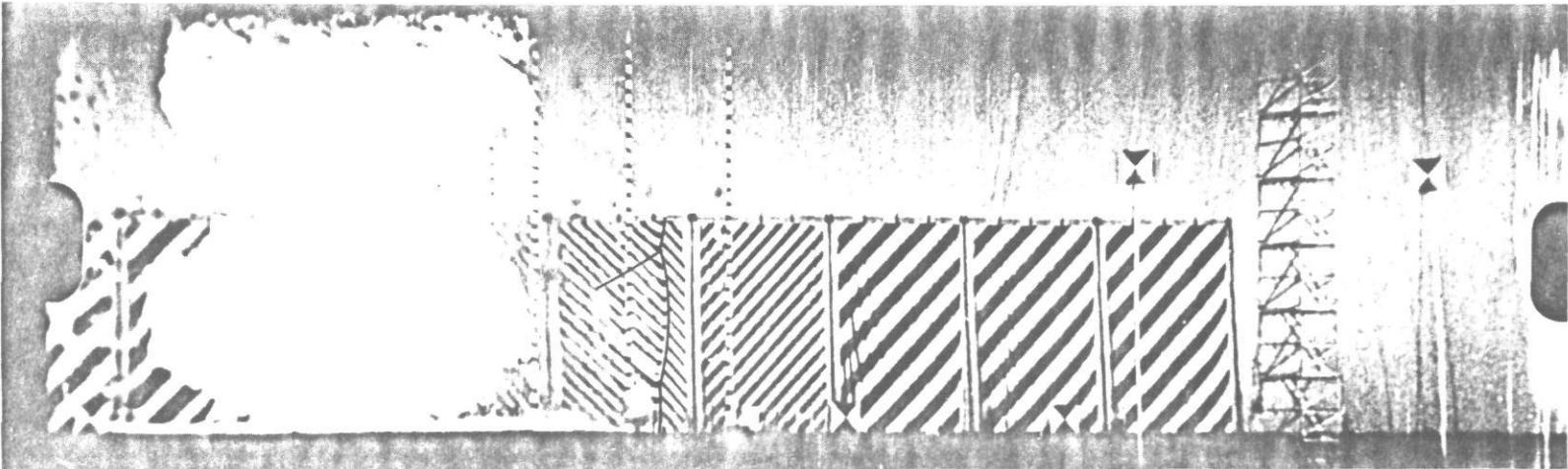
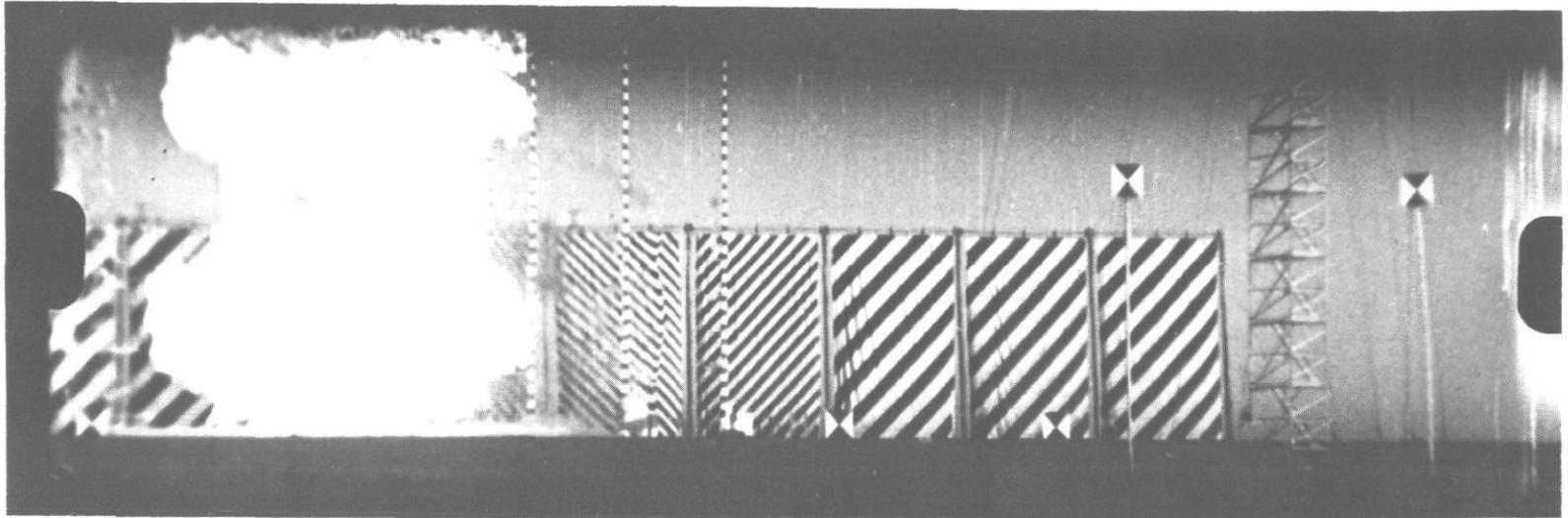


Figure 3.7. Frame from Photographic Record of Shot 12 Showing Shock Wave System

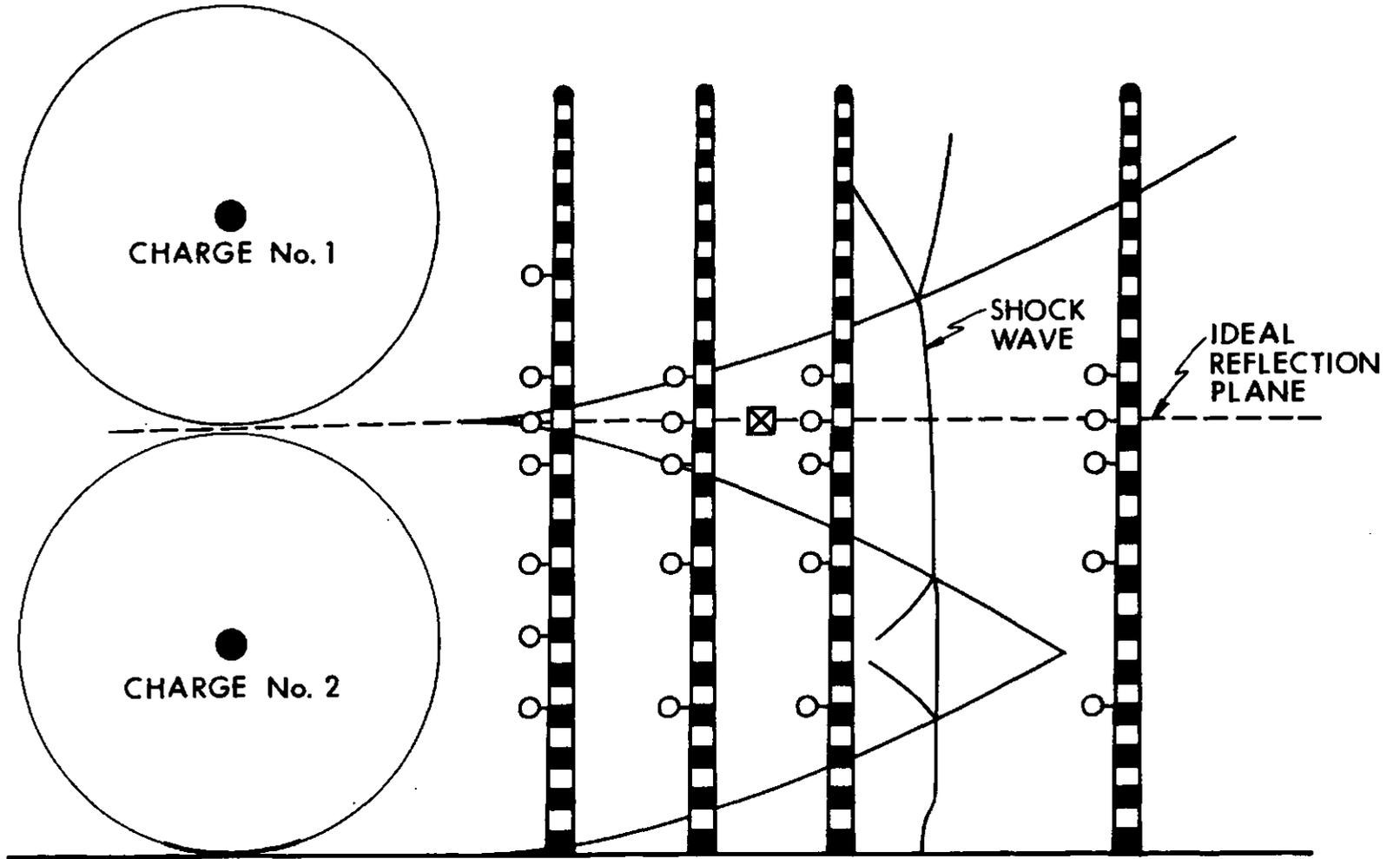


Figure 3.8. Reconstructed Triple Point Paths and Position of the Ideal Reflecting Surface; Shot 12

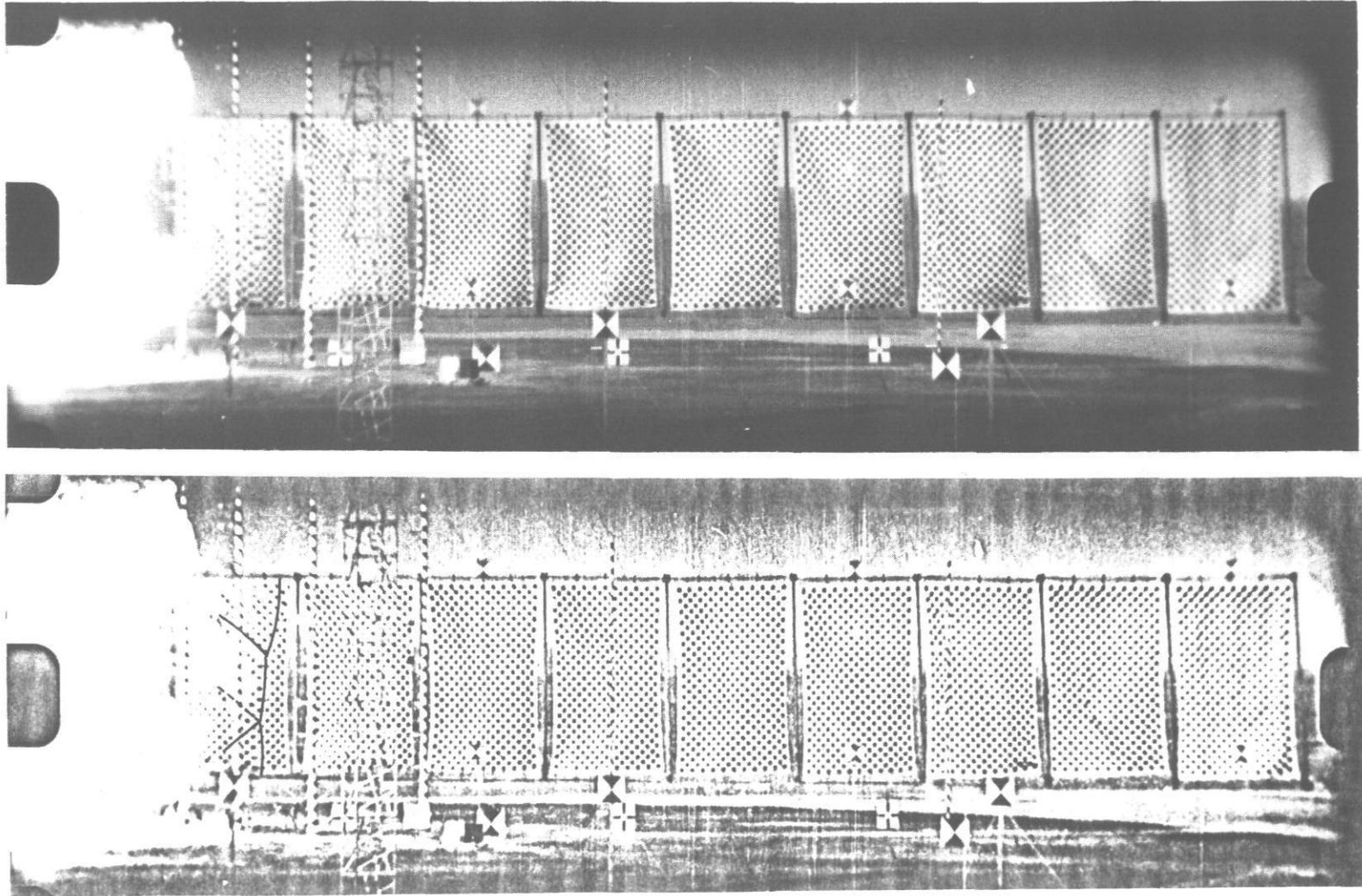


Figure 3.9. Frame from Photographic Record of Shot 16 Showing Shock Wave System

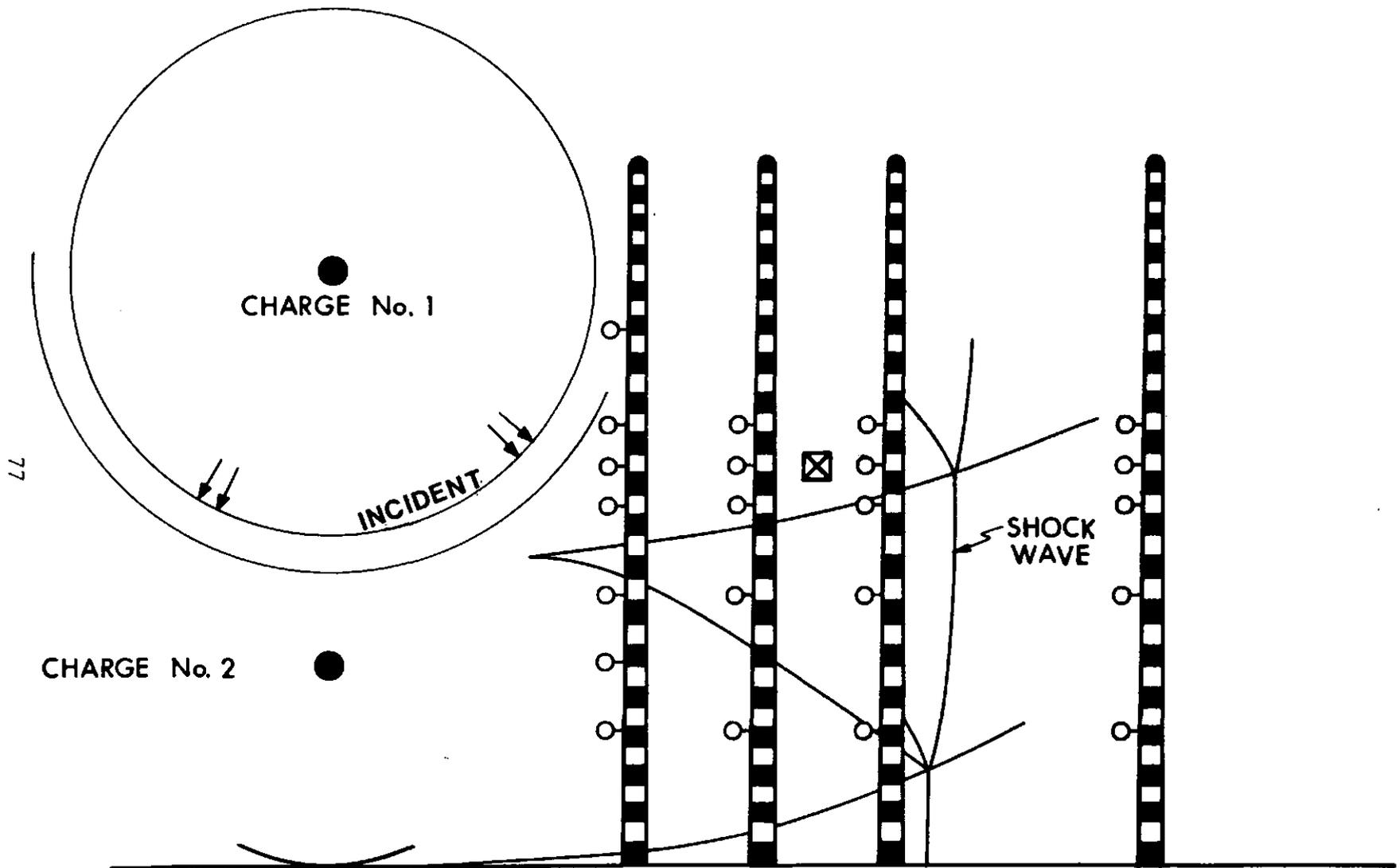


Figure 3.10. Reconstructed Triple Point Path and Shock Wave Diagram; Shot 16

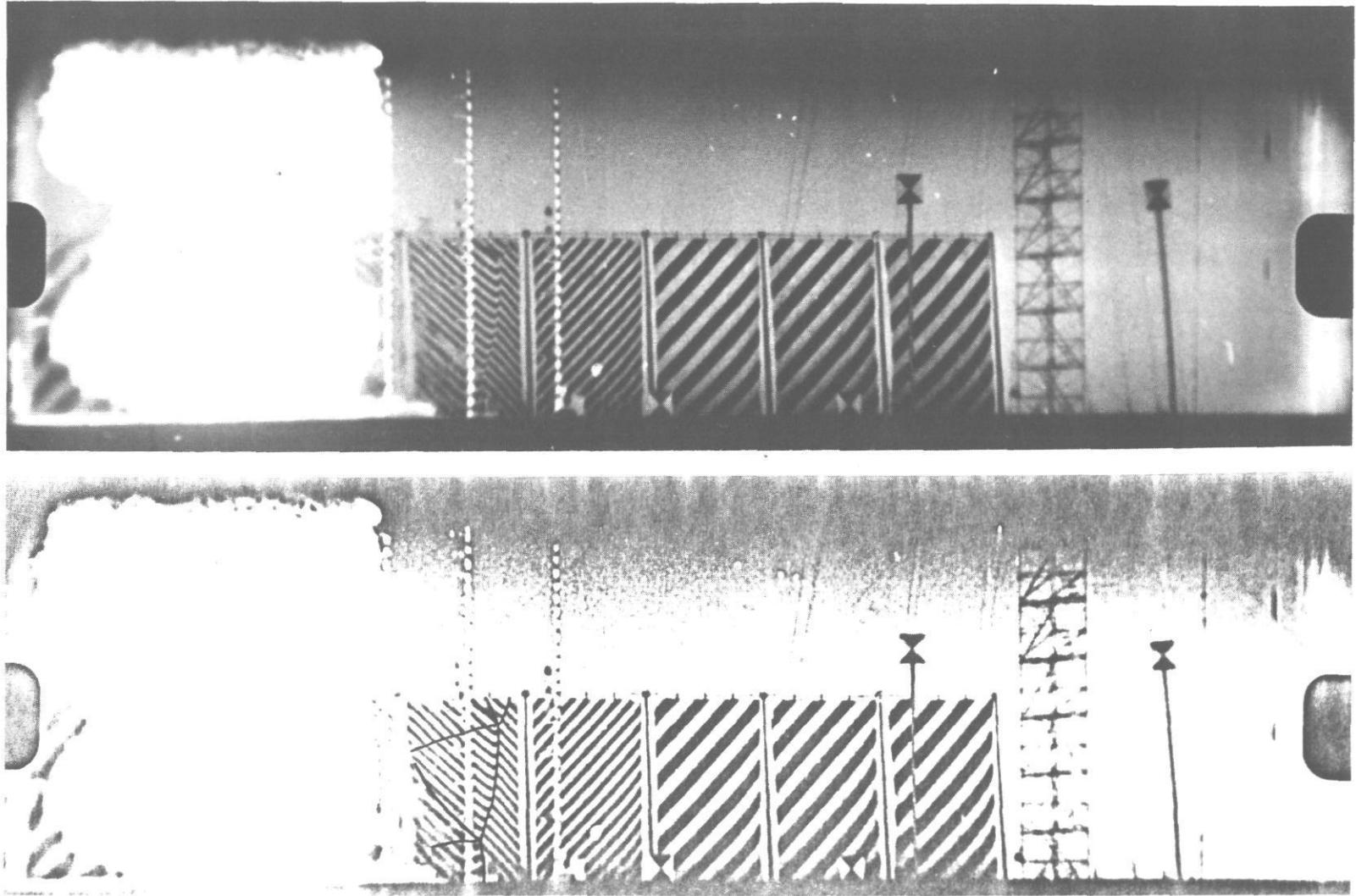


Figure 3.11. Frame from Photographic Record of Shot 15 Showing Shock Wave System

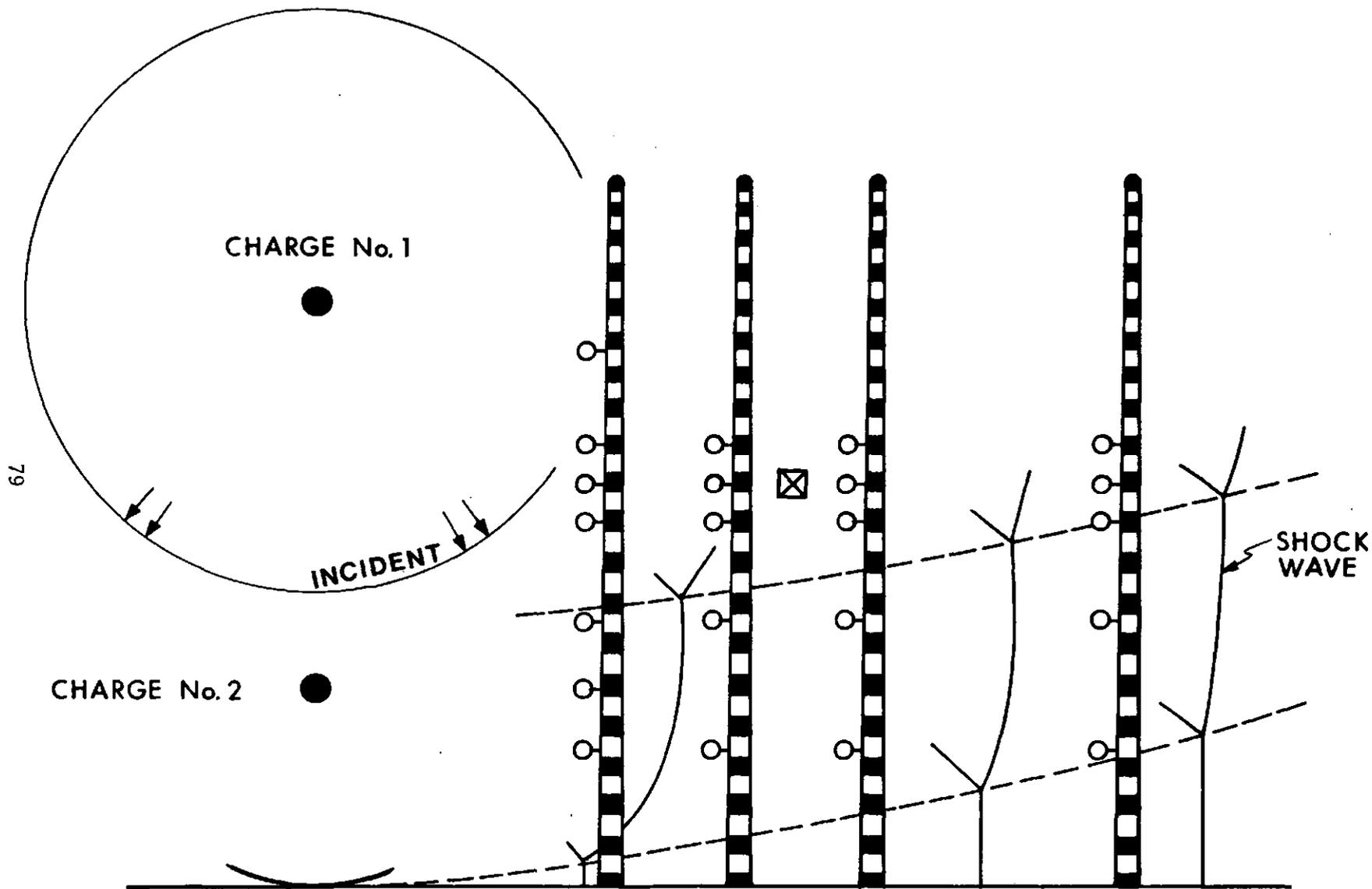


Figure 3.12. Reconstructed Triple Point Path and Shock Wave Diagram; Shot 15

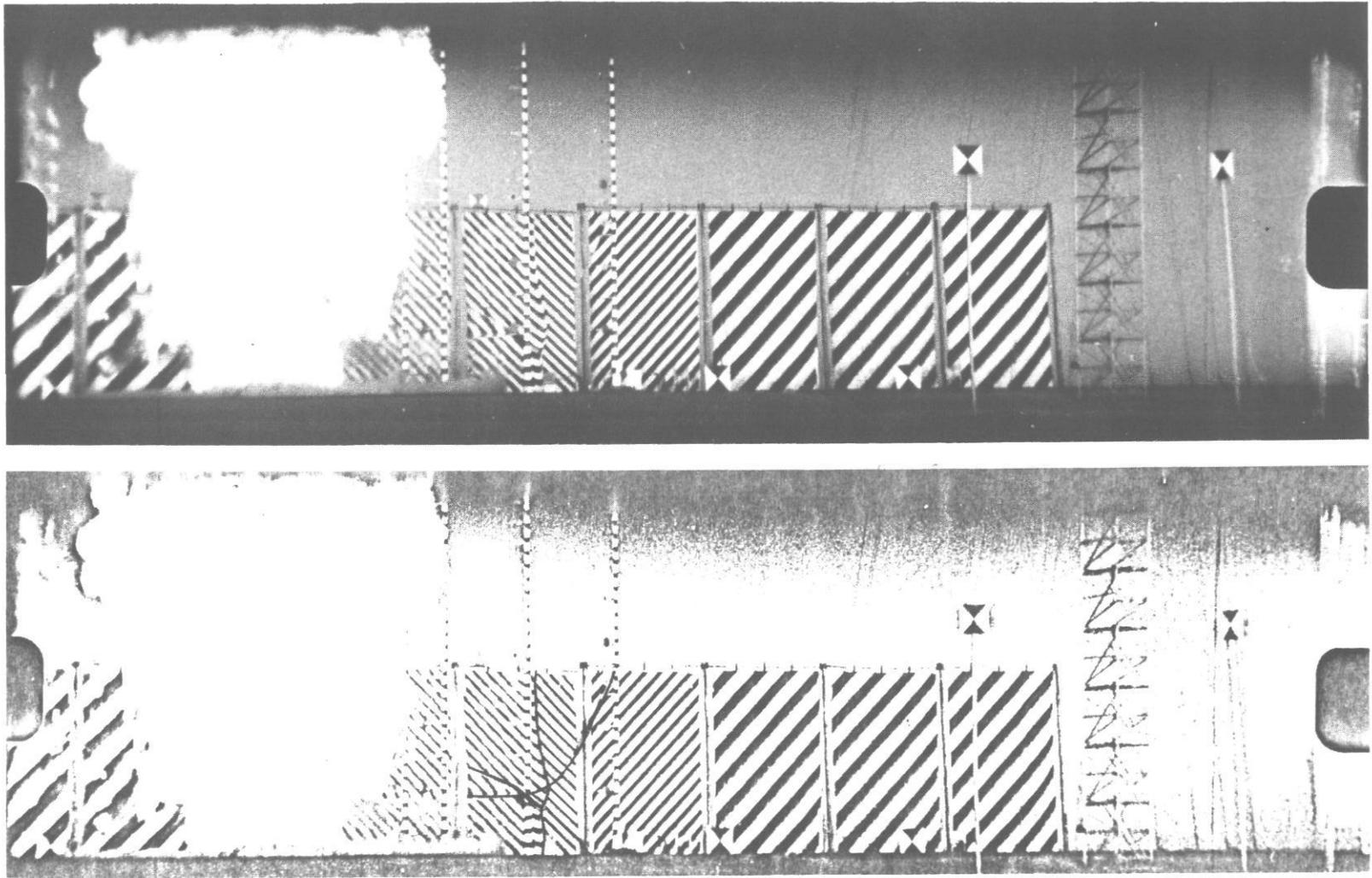


Figure 3.13. Frame from Photographic Record of Shot 13 Showing Shock Wave System

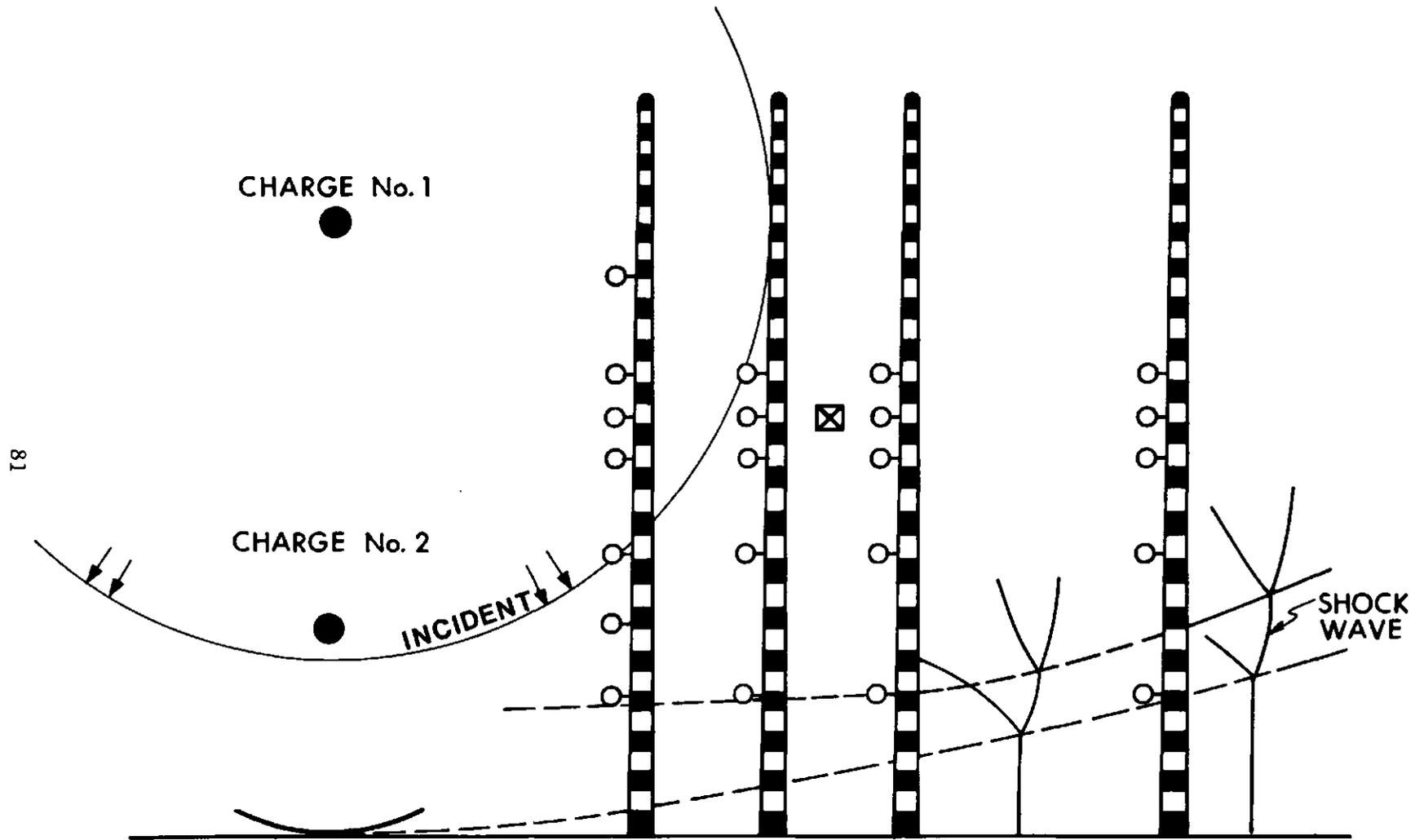


Figure 3.14. Reconstructed Triple Point Path and Shock Wave Diagram; Shot 13

south of ground zero. There is no problem with confusion of the S for side-on baffle with the S for south because all of the side-on baffles are at elevations of three feet or more, whereas all gages not on the primary gage line are mounted in ground baffles. Additional indicators are M, indicating a position midway between gage lines 1 and 2, and X, for crystal gages.

The quality of records from the eighty-two channels of overpressure and total head pressure instrumentation on Shot 12 was good. Three channels returned unuseable data, and records from an additional two channels were of poor quality. Some perturbations are evident in the waveforms recorded from ground stations out to a range of thirty feet. These perturbations may have been caused by jetting from the fireball, as seen in Figure 3.1.

A tabulation of air blast parameters obtained from Shot 12 is given in Table 3.1. The records are identified by recording system and channel number as well as by station number as described above. Parameters included are arrival time, maximum initial pressure, maximum secondary pressure (if a significant reflected pulse is evident), positive phase duration, and maximum overpressure impulse.

The tabulated information is plotted as functions of ground range in Figures 3.15, 3.16, and 3.17. The parameters measured at the surface level are given in the first plot; information from gages at the 3, 10, and 20-foot levels is given in the second plot; and the 27, 30 and 33-foot elevation data are given in the third. Reasonable consistency of data from station to station at the same level is obtained.

Good pressure-time information was also obtained from all but three of the channels instrumented for Shot 13. Table 3.2 is a listing of recorded air blast parameters. These parameters are plotted as functions of ground range for each instrumented elevation in Figures 3.18 through 3.20.

For Shot 14, eighty of the eighty-three instrumented channels returned good data, and some information was obtained from the other three. Waveforms recorded at surface and near-surface stations show minor perturbations out to range 30 feet. The piezoelectric gage at 1652 feet (Trailer) yielded a questionable record. Air blast parameters are tabulated in Table 3.3 and plotted as functions of ground range in Figures 3.21 through 3.23.

Data acquisition for Shot 15 was again excellent. Eighty-two of the eighty-six instrumented channels yielded good data; four records were poor to unuseable. Jetting, seen in the photograph of the fireball (Figure 3.4), is thought to have caused the perturbations and odd pressure spikes seen in records at some of the ground stations out to forty feet. Other ground stations show excellent agreement between records obtained from gage lines 1 and 2. A few of these latter records are

Table 3.1. Measured Air Blast Parameters; Shot 12

System-Channel	Station	Arrival Time (ms)	Primary Pressure (psi)	Secondary Pressure (psi)	Pos. Phase Duration (ms)	Overpressure Impulse (psi-ms)
3-3	0.0	2.13	650		3.1	393
4-3	10.0E	3.06	384		4.0 ¹	263
3-4	10.0W	3.10	364		3.9	265
4-4	10.0N	2.70	230		3.4	233
3-5	10.0S	2.81	525		4.3	281
1-3	20.0	4.60	80	90 ²	6.4	173 ³
3-25	2-20.0	5.63	92	92 ²	5.2	147
1-4	20.3S	4.87	53	50	5.3	111
1-5	20.3T	4.40	143	135	6.4	239
4-6	20.10S	3.80	62.5		12.7	156
4-7	20.10T	3.98	230		12.5	230
3-7	20.15S	3.73	72		4.9	162
3-8	20.15T	3.79	275		4.7	229
4-8	20.20S	3.96	64		11.6	136
4-9	20.20T	4.02	218		11.1	230
2-3	20.27S	5.02	55.5		5.1	135
2-4	20.27T	5.13	180		5.5	219
1-6	20.30S	5.42	108		5.0	167
1-7	20.30T	5.58	350		5.7	352
2-5	20.33S	4.98	59	76	5.7	141
2-6	20.33T	5.07	170	145	5.4	206
3-9	20.40S	3.86	74		6.9	120
3-10	20.40T	3.97	270		6.5	195
1-8	30.0	9.1	47.5		7.3	105
1-20	2-30.0	9.5	41		7.4	100
1-9	30.3S	9.1	31.8	44	7.2	96
1-10	30.3T	8.7	108	70	6.1	167
4-10	30.10S	8.4	29	21	11.8	123
4-11	30.10T	8.5	60	40	11.1	172
4-12	30.20S	8.6	27.5	20.3	11.2	110
4-13	30.20T	8.6	60	35	12.0	158
2-7	30.27S	9.6	45.4		7.0	108
2-8	30.27T	9.6	110		7.0	162
1-11	30.30S	9.4	47		7.3	112
1-12	30.30T	9.4	110		7.1	213
2-9	30.33S	9.6	47		7.0	112
2-10	30.33T	9.6	90		7.7	156
2-11	40.0	14.3	25.5		9.3	85
2-26	2-40.0	14.5	29		18.2	125 ⁴
2-12	40.3S	14.6	28.5		17.9	113
2-13	40.3T	14.5	42		17.1	158
2-27	2-40.3T	14.6	55		18.2	172
4-14	40.10S	11.9	4	19	14.2	105 ⁵
4-15	40.10T	11.2	10		14.6	325

Table 3.1. Measured Air Blast Parameters; Shot 12 (Continued)

System-Channel	Station	Arrival Time (ms)	Primary Pressure (psi)	Secondary Pressure (psi)	Pos. Phase Duration (ms)	Overpressure Impulse (psi-ms)
4-16	40.20S	14.3	17	21	11.7	109
4-17	40.20T	14.4	28	28	12.1	137
2-14	40.27S	14.4	29		17.8	104
2-15	40.27T	14.6	60		18.0	160
1-13	40.30S	14.3	31.5		8.9	90
1-14	40.30T	14.4	60		7.6	124
2-16	40.33S	14.4	31.5		9.3	87
2-17	40.33T	14.5	55		10.9	138
4-5	50.0N	20.7	18.5		18.7	104
3-6	50.0S	20.4	18.5		18.3	106
2-18	60.0	27.0	-		-	- ⁶
3-26	2-60.0	26.9	14	12	19.5	99.5
3-27	2-60.0M	27.0	11.6	10	18.6	88
2-19	60.3S	26.9	14		19.1	92
2-20	60.3T	27.1	-		-	- ⁶
2-24	2-60.3	27.0	13	8.5	19.2	92
2-25	2-60.3MT	27.0	-		-	- ⁶
4-18	60.10S	27.2	12.5	18	19.1	90
4-19	60.10T	27.4	20	17	18.6	103
4-20	60.20S	27.2	12.3	13.0	14.8	79
4-21	60.20T	27.4	20	18	14.4	93.5
1-15	60.27S	26.8	13.6		16.2	79
1-16	60.27T	26.9	-		-	- ⁶
2-21	60.30S	26.8	14.5		18.4	72
2-22	60.30T	26.8	19		18.4	94
1-17	60.33S	26.8	11.5		19.8	68.6
1-18	60.33T	26.8	-		-	- ⁶
4-22	90.0	49.4	9.5		20.1	69.4
4-26	2-90.0	49.2	8.7		20.6	70.5
4-23	110.0	64.5	7.4		23.0	52.8
1-21	2-110.0	64.5	7.8		22.0	59.3
3-23	150.0	96	5.0		25	42.4
1-22	2-150.0	96	4.7		25	43.6
4-24	245.0	176	2.2		31	28.0
1-23	2-245.0	176	2.25		31	27.0
4-25	400.0	312	1.2		35	17.3
1-24	2-400.0	312	1.1		35	16.2
3-24	800.0	685	0.45		27	6.25

¹ Disturbance near base line; extrapolation made through zero

² Double peak phenomena

³ Poor record

⁴ Reflection in positive phase

⁵ Multiple shocks

⁶ Bad record

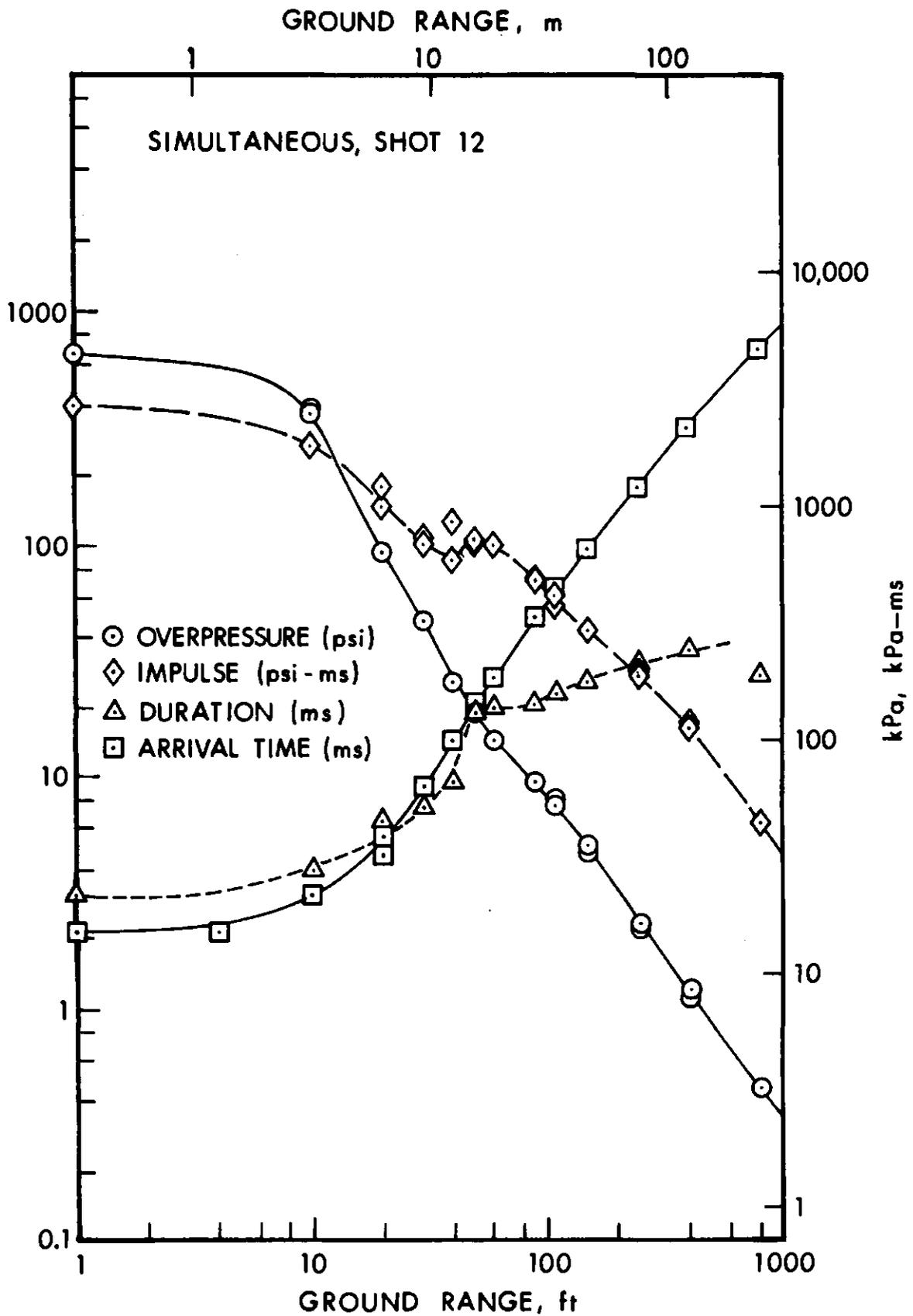


Figure 3.15. Air Blast Parameters at Ground Level Versus Ground Range; Shot 12

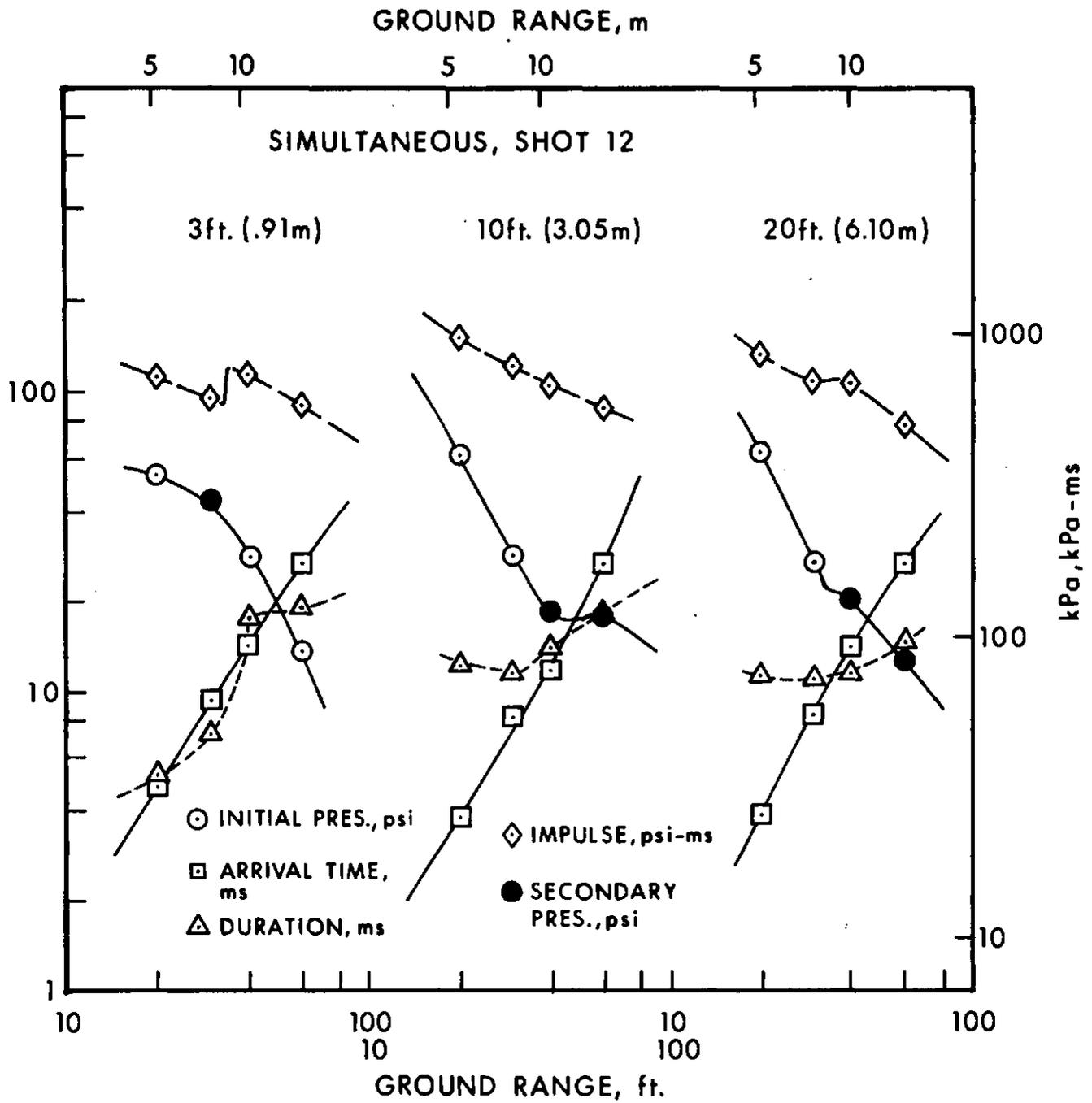


Figure 3.16. Air Blast Parameters at 3, 10, and 20 Feet Versus Ground Range; Shot 12

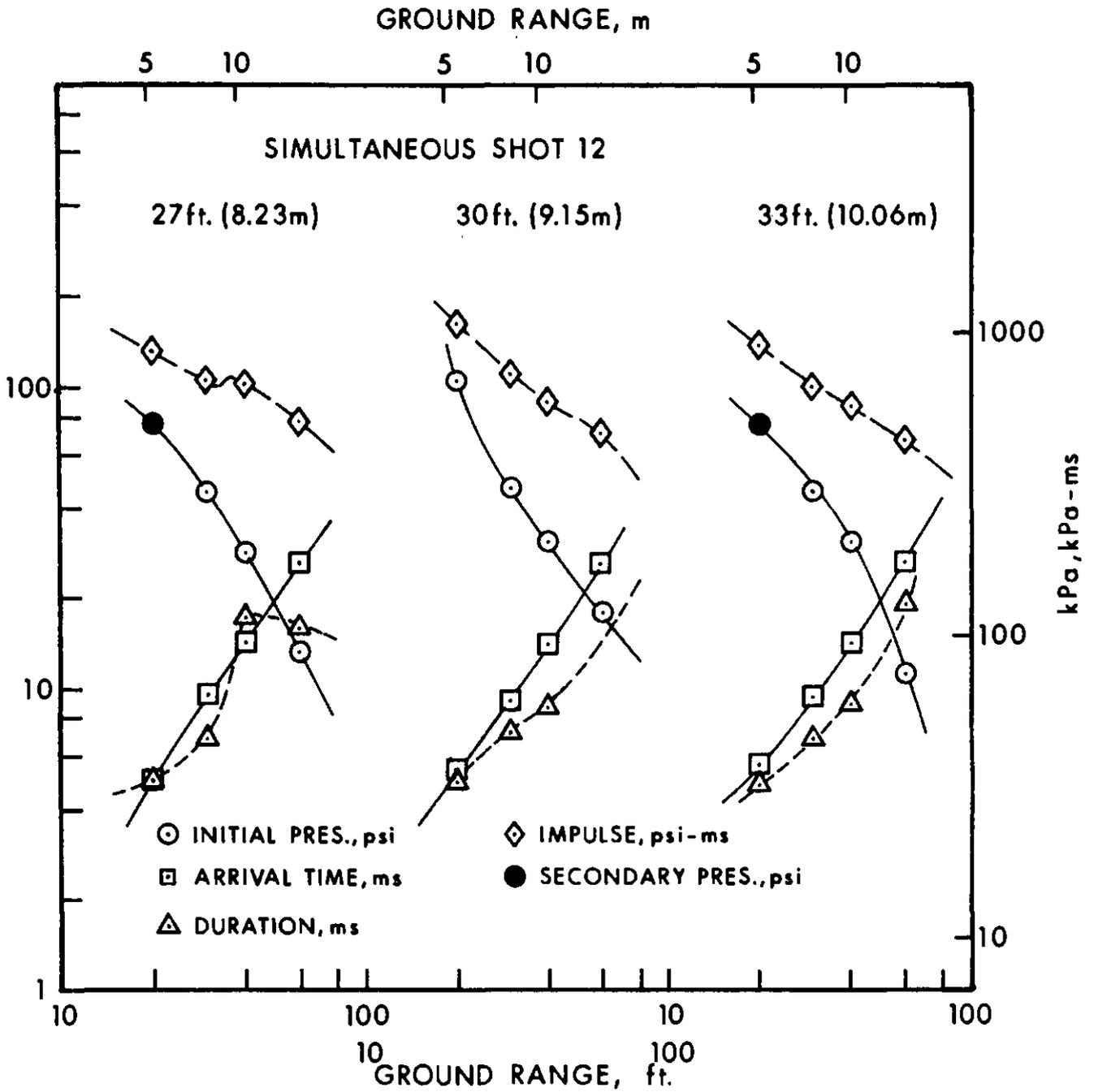


Figure 3.17. Air Blast Parameters at 27, 30, and 33 Feet Versus Ground Range; Shot 12

Table 3.2. Measured Air Blast Parameters; Shot 13

System-Channel	Station	Arrival Time ¹ (ms)	Primary Pressure (psi)	Secondary Pressure (psi)	Pos. Phase Duration (ms)	Overpressure Impulse (psi-ms)
3-3	0.0	12.27	760		2.4	372
4-3	10.0E	13.22	402		2.6	296
3-4	10.0W	13.02	402		4.6	330
4-4	10.0N	13.10	402		3.8	290
3-5	10.0S	13.10	442		3.1	308
1-3	20.0	15.62	95	98 ²	6.9	188
3-25	2-20.0	15.60	102	121 ²	8.0	188
1-4	20.3S	15.10	53	76	7.7	166
1-5	20.3T	15.19	180	230	7.4	283
4-6	20.10S	14.21	92		4.8	133
4-7	20.10T	14.25	275		4.2	197
3-7	20.15S	11.60	19	89	6.5	121
3-8	20.15T	11.71	43	275	5.3	174
4-8	20.20S	9.39	23.5	52	9.3	107
4-9	20.20T	9.42	50	200	9.3	179
2-3	20.27S	6.80	35	50.4	5.3	123
2-4	20.27T	6.87	100	180	5.1	200
1-6	20.30S	5.90	43	44	5.1	66
1-7	20.30T	6.02	110	135	4.9	87
2-5	20.33S	5.25	47	30.5	5.3	69
2-6	20.33T	5.30	150	55	4.8	114
3-9	20.40S	4.23	65		3.4	74
3-10	20.40T	4.30	220		3.0	133
1-8	30.0	19.05	55		8.2	149
1-20	2-30.0	19.2			9.0	126 ³
1-9	30.3S	19.15	52		9.9	143
1-10	30.3T	19.10	115		8.0	240
4-10	30.10S	18.20	49	27	10.1	132
4-11	30.10T	18.20	90	30	11.8	188
4-12	30.20S	13.65	15.2	25	10.7	89.5
4-13	30.20T	13.80	25	45	11.1	128
2-7	30.27S	11.35	20	25.3	6.6	100
2-8	30.27T	11.40	33	50	6.6	135
1-11	30.30S	10.50	22	24	6.7	54
1-12	30.30T	10.55	40	45	7.0	71
2-9	30.33S	9.80	25	23	6.6	54.5
2-10	30.33T	10.0	42	39	6.2	71.5
2-11	40.0	23.7	35		11.3	128
2-26	2-40.0	23.65	40		10.8	137
2-12	40.3S	23.7	37		11.6	117.5
2-13	40.3T	23.7	70		11.0	188
2-27	2-40.3T	23.65	80		11.5	202
4-14	40.10S	23.1	27.5	23.4	12.3	119
4-15	40.10T	23.25	45	30	12.0	155

Table 3.2. Measured Air Blast Parameters; Shot 13 (Continued)

System-Channel	Station	Arrival Time ¹ (ms)	Primary Pressure (psi)	Secondary Pressure (psi)	Pos. Phase Duration (ms)	Overpressure Impulse (psi-ms)
4-16	40.20S	19.0	11.6	18	11.8	86
4-17	40.20T	19.25	16	28	12.0	105
2-14	40.27S	16.85	13.5	18	14.4	82.5
2-15	40.27T	17.0	24	32	14.3	107.5
1-13	40.30S	16.15	14.5	15	14.8	79
1-14	40.30T	16.25	22	26	15.0	107
2-16	40.33S	15.5	16	15.5	15.8	80
2-17	40.33T	15.65	22	23	15.8	105
4-5	50.0N	28.6	-	-	-	- ⁴
3-6	50.0S	28.3	28.0	-	13.7	110
2-18	60.0	34.8	19	-	15.4	97
3-26	2-60.0	34.5	20.0	-	15.8	101.5
3-27	2-60.0M	34.8	16.8	-	16.1	88
2-19	60.3S	34.7	-	-	-	- ⁴
2-20	60.3T	34.6	32	-	15.8	134
2-24	2-60.3	34.5	18.0	-	16.1	92
2-25	2-60.3TM	34.8	31	-	13.4	116
4-18	60.10S	35.0	20.5	-	14.8	95.5
4-19	60.10T	34.8	-	-	-	- ⁴
4-20	60.20S	32.1	6.2	11.2	20.8	83.3
4-21	60.20T	32.1	7	16	18.4	90.1
1-15	60.27S	30.3	6.8	9.0	25.2	77
2-21	60.30S	29.8	6.8	8	26.5	70.3
2-22	60.30T	29.8	9.0	10	26.5	86.8
1-17	60.33S	29.2	6.1	6.3	28.1	65.0
4-22	90.0	54.7	10.0	-	18.6	67.9
4-26	2-90.0	54.8	9.5	-	19.0	68.5
4-23	110.0	69.1	6.4	-	22.9	51.0
1-21	2-110.0	68.9	7.0	-	20.6	55.0
3-23	150.0	99.7	4.7	-	24.8	42.4
1-22	2-150.0	99.9	4.6	-	24.8	41.8
4-24	245.0	178	2.4	-	30	26.3
1-23	2-245.0	178	2.6	-	29	25.9
4-25	400.0	312	1.2	-	34	15.7
1-24	2-400.0	311	1.1	-	34	15.4
3-24	800.0	676	.45	-	31	6.5

¹ Time referenced to detonation of top charge

² Double peak phenomena

³ Peak clipped; data poor

⁴ Bad record

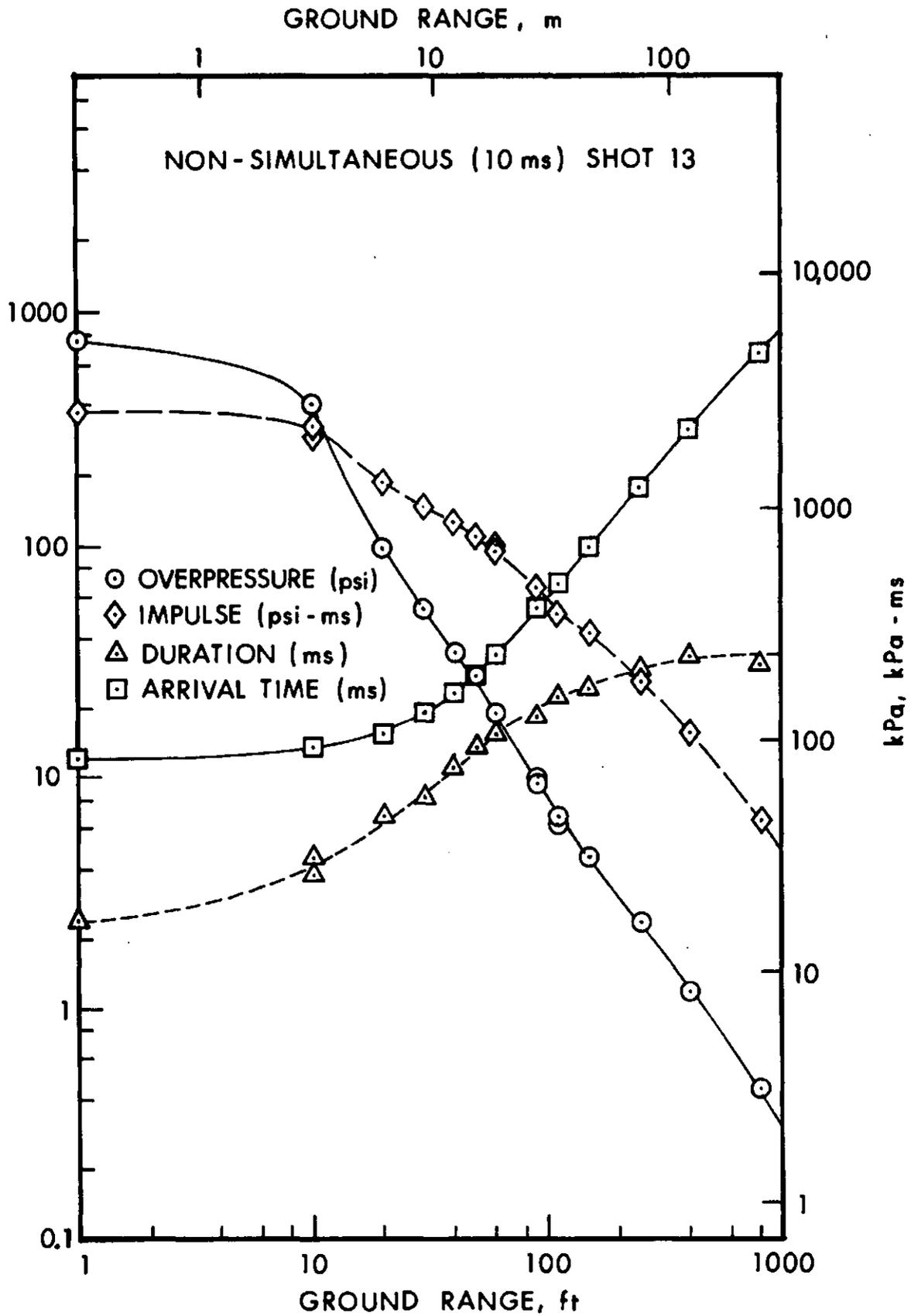


Figure 3.18. Air Blast Parameters at Ground Level Versus Ground Range; Shot 13

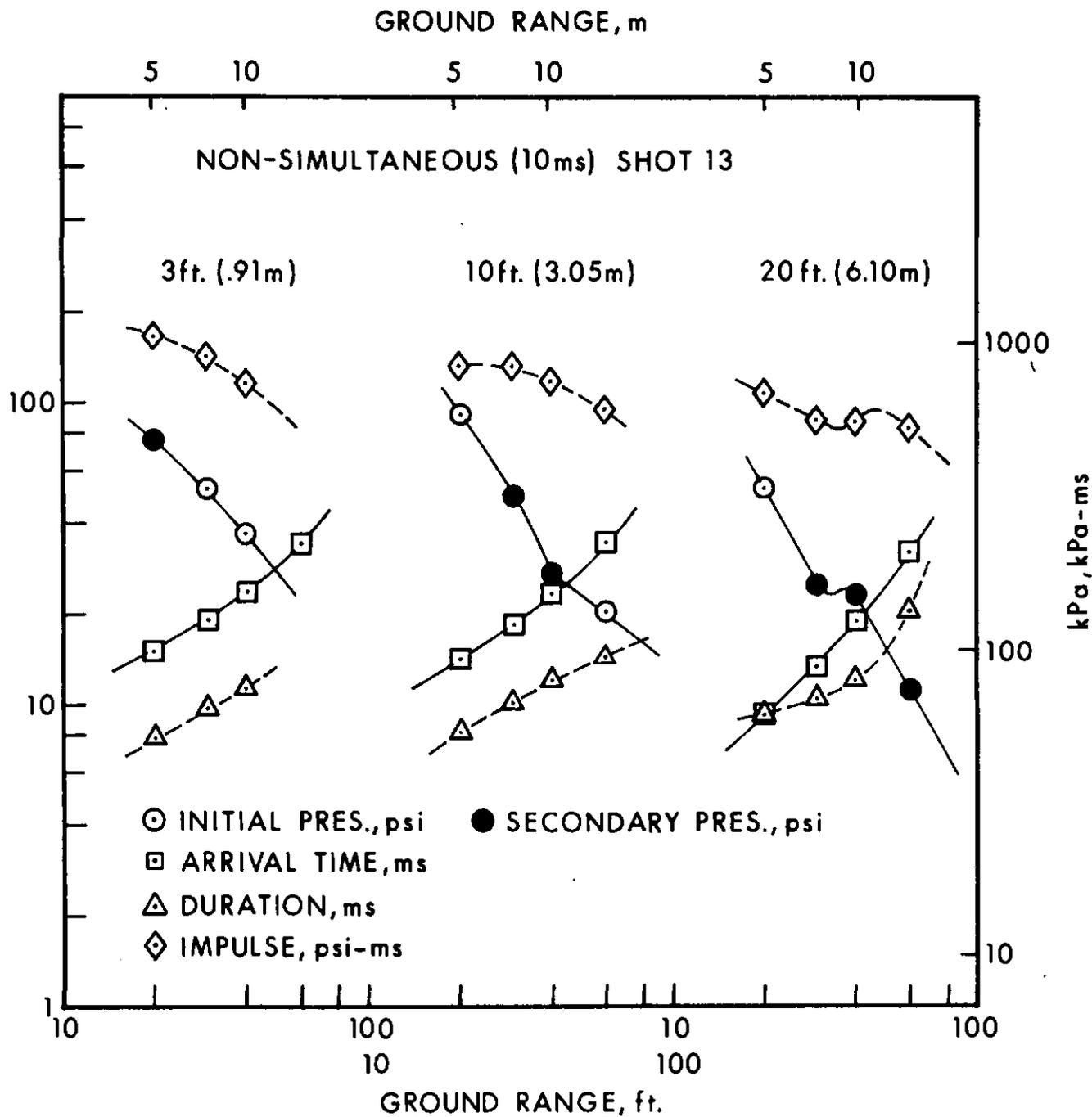


Figure 3.19. Air Blast Parameters at 3, 10, and 20 Feet Versus Ground Range; Shot 13

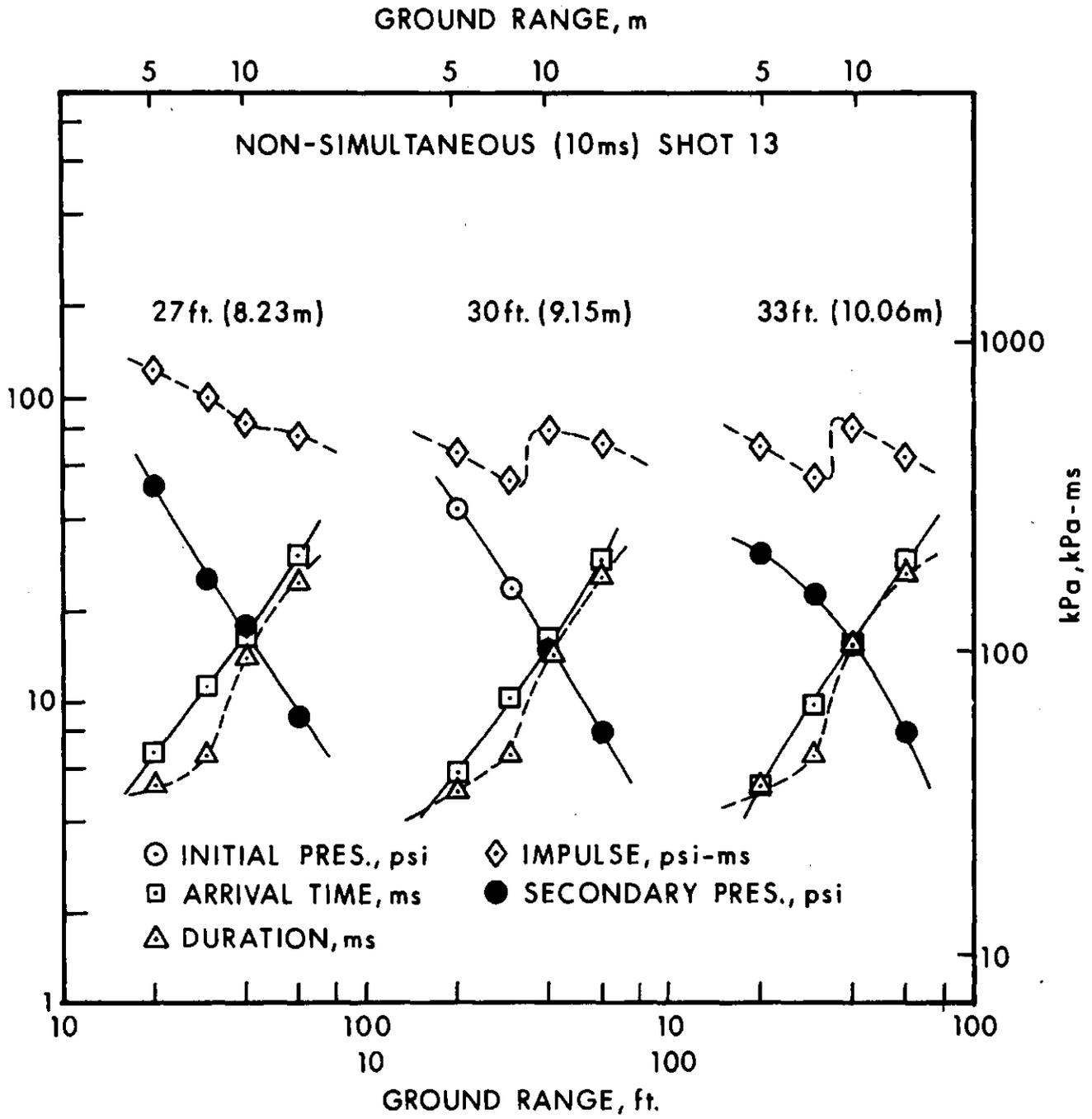


Figure 3.20. Air Blast Parameters at 27, 30, and 33 Feet Versus Ground Range; Shot 13

Table 3.3. Measured Air Blast Parameters; Shot 14

System-Channel	Station	Arrival Time (ms)	Primary Pressure (psi)	Secondary Pressure (psi)	Pos. Phase Duration (ms)	Overpressure Impulse (psi-ms)
3-3	0.0	2.20	650		-	- ¹
4-3	10.0E	3.10	355		3.7	274
3-4	10.0W	2.92	365		3.8	273
4-4	10.0N	3.15	370		3.7	268
3-5	10.0S	2.95	415		3.1	288
1-25	2-15.0X ²	4.05	156		6.4	210 ³
1-3	20.0	5.40	95		5.7	145
3-25	2-20.0	5.74	95		5.5	146
1-4	20.3S	5.04	47	61	5.9	116
1-5	20.3T	5.00	160	180	4.2	191
4-6	20.10S	4.00	59.5		11.3	116
4-7	20.10T	4.17	240		11.5	195
3-7	20.15S	3.90	70		4.5	101
3-8	20.15T	3.99	250		4.3	169
4-8	20.20S	4.15	62		5.1	76
4-9	20.20T	4.26	230		5.2	149
2-3	20.27S	5.23	50		5.1	72.5
2-4	20.27T	5.19	130		5.1	111
1-6	20.30S	5.88	38.4		4.9	68
1-7	20.30T	5.80	54.0		3.0	62.5
2-5	20.33S	6.79	45.5		6.2	71
2-6	20.33T	6.91	95		6.6	96.5
3-9	20.40S	9.28	29		6.7	58.5
3-10	20.40T	9.44	60		7.3	53.5
1-8	30.0	9.20	90 ⁴		8.1	108
1-20	2-30.0	9.4	29		8.5	92
1-9	30.3S	9.5	42		8.3	99
1-10	30.3T	9.4	140		7.0	236
4-10	30.10S	8.7	29.5		11.3	100
4-11	30.10T	8.8	50		11.2	139
4-12	30.20S	8.8	27		6.7	59
4-13	30.20T	8.9	50		6.7	86
2-7	30.27S	9.4	22.5		7.2	56
2-8	30.27T	9.85	47		7.75	80.5
1-11	30.30S	10.6	24.5		7.2	54
1-12	30.30T	10.6	40		7.4	68.5
2-9	30.33S	11.45	22		6.6	54
2-10	30.33T	11.3	32		7.7	63
2-11	40.0	14.7	26		9.8	83
2-26	2-40.0	14.75	26		9.6	86.7
2-12	40.3S	14.8	27		9.2	83
2-13	40.3T	14.75	49		9.8	111
2-27	2-40.3PT	14.9	55		10.2	121
4-14	40.10S	14.5	18	20	12.5	80

Table 3.3. Measured Air Blast Parameters; Shot 14 (Continued)

System-Channel	Station	Arrival Time (ms)	Primary Pressure (psi)	Secondary Pressure (psi)	Pos. Phase Duration (ms)	Overpressure Impulse (psi-ms)
4-15	40.10T	14.7	26	28	12.5	105
4-16	40.20S	14.6	16.5		13.4	79
4-17	40.20T	14.75	25.0		13.5	96
2-14	40.27S	15.6	19		15.1	70.0
2-15	40.27T	15.75	24		15.6	85
1-13	40.30S	16.2	16.5		16.6	68.8
1-14	40.30T	16.3	24		16.5	85
2-16	40.33S	16.8	17.5		17.2	64.3
2-17	40.33T	17.1	20		17.4	76.5
4-5	50.0N	20.8	19.5		11.6	69.3
3-6	50.0S	19.9	19.0		10.9	69.0
2-18	60.0	27.3	13.5		14.9	59.5
3-26	2-60.0	27.4	13.5		14.0	60.2
3-27	2-60.0M	27.5	10.7		13.6	52.1
2-19	60.3S	27.6	11.8		12.8	57.3
2-20	60.3T	27.6	18		15.5	70
2-24	2-60.3PS	27.6	13.5		14.4	55.6
2-25	2-60.3PTM	27.5	16.4		15.7	59.2
4-18	60.10S	27.8	13		14.4	59.0
4-19	60.10T	27.8	17.5		15.7	69.7
4-20	60.20S	28.8	7.3	7.8	15.2	55.3
4-21	60.20T	28.8	9.5	10.0	14.2	60.5
1-15	60.27S	29.6	8.0	7.0	16.2	55.1
2-21	60.30S	30.2	7.5	5.9	16.6	49.2
2-22	60.30T	30.2	8.5	6.0	16.8	58.3
1-17	60.33S	30.8	6.2	7.0	17.8	46.7
1-26	2-80.0X ²	42.0	8.35		19.0	52.8
4-22	90.0	50	6.2		20	40.1
4-26	2-90.0	50	6.0		21	40.6
4-23	110.0	66	3.6		23	29.6
1-21	2-110.0	66	4.4		22	34.1
3-23	150.0	100	3.3		25	24.4
1-22	2-150.0	100	3.1		24	24.7
4-24	245.0	182	1.3		29	14.6
1-23	2-245.0	182	1.5		28	15.6
4-25	400.0	322	0.8		31	9.6
1-24	2-400.0	321	0.7		32	9.2
3-24	800.0	700	0.25		28	3.72
1-27	TrailerX ²	1453.5	0.010, 0.0115		49	0.24 ¹

- ¹ Poor record
- ² Piezoelectric gage
- ³ Noisy base line
- ⁴ Very sharp spike

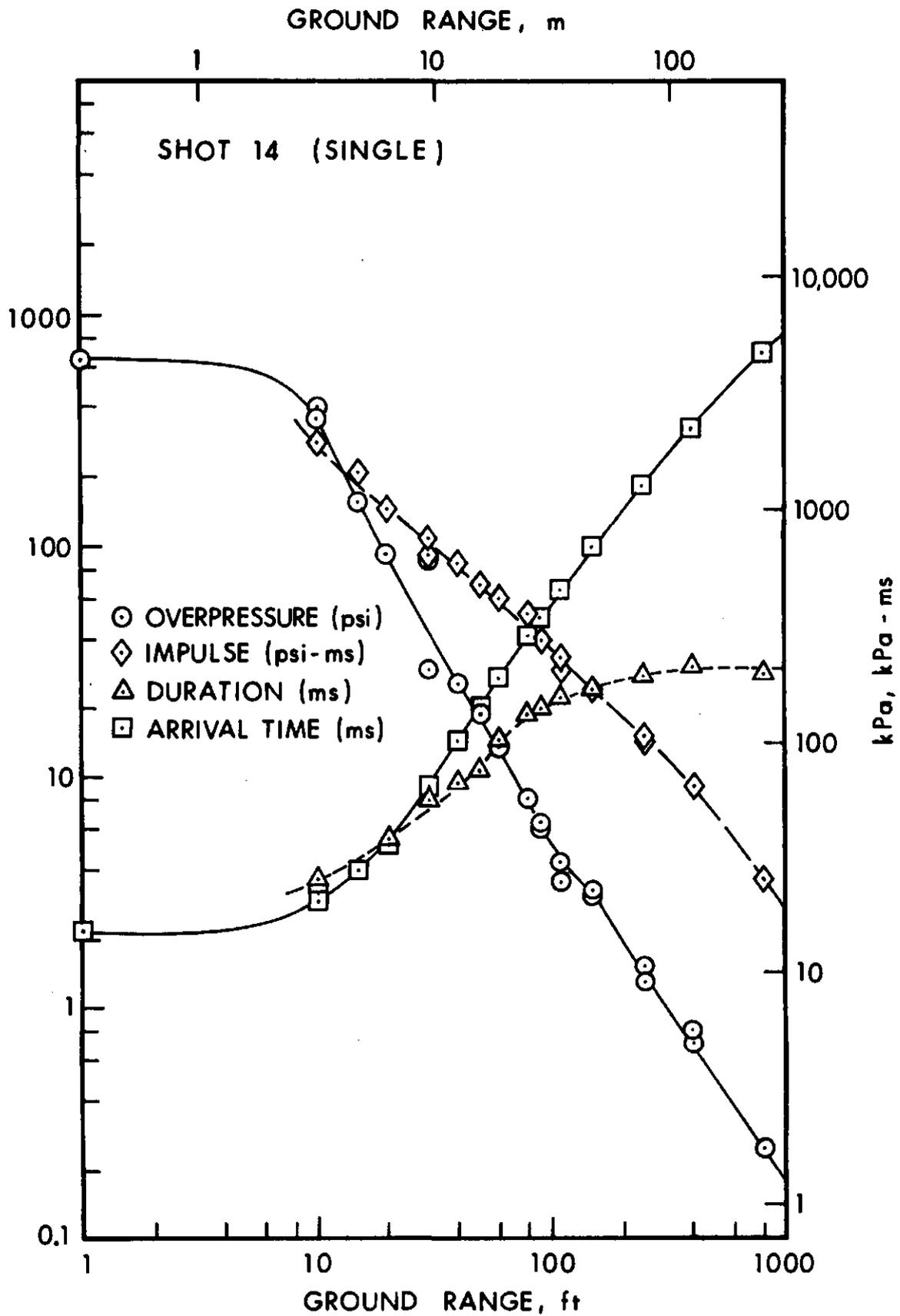


Figure 3.21. Air Blast Parameters at Ground Level Versus Ground Range; Shot 14

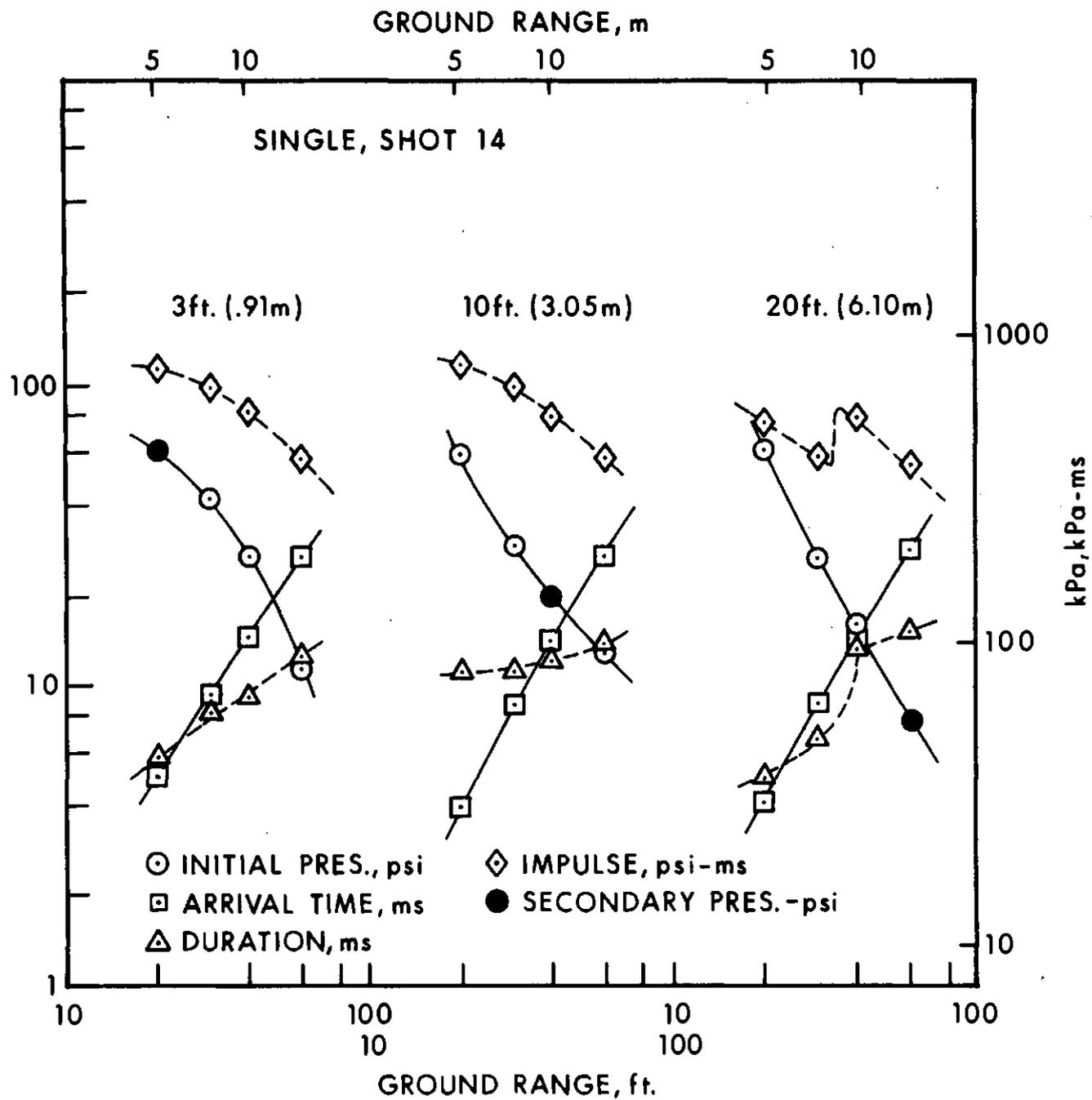


Figure 3.22. Air Blast Parameters at 3, 10, and 20 Feet Versus Ground Range; Shot 14

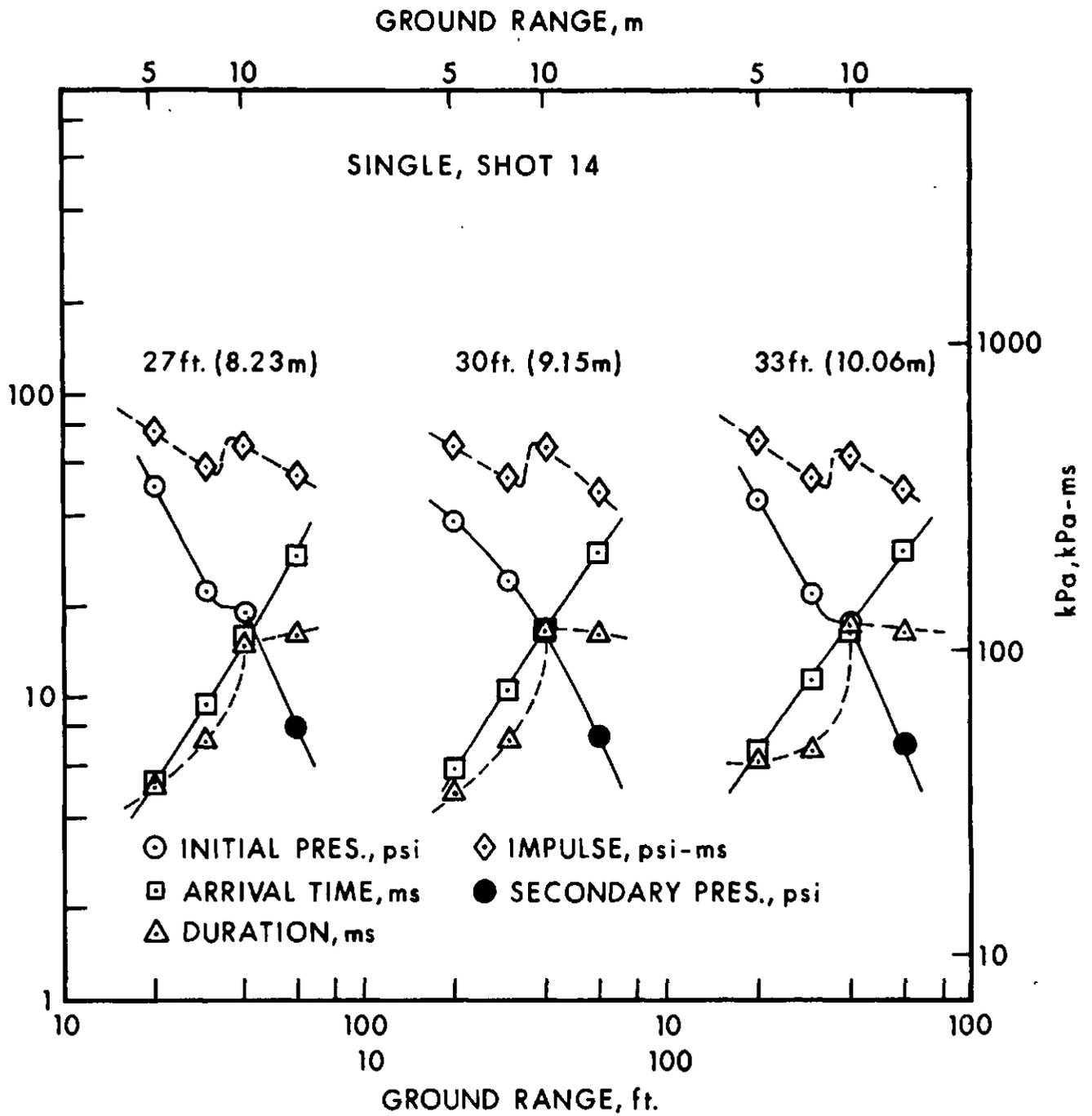


Figure 3.23. Air Blast Parameters at 27, 30, and 33 Feet Versus Ground Range; Shot 14

compared in Figures 3.24, 3.25 and 3.26. The good agreement in these cases indicates that, at least at these stations, the shock wave was symmetrical.

The tabulation of air blast parameters from Shot 15 is given in Table 3.4. Plots of these parameters are presented as functions of ground range in Figures 3.27 through 3.29.

Only two channels failed to return data of useable quality on Shot 16. Table 3.5 is the tabulation of air blast parameters for this event; Figures 3.30 through 3.32 are the plots of these parameters versus ground range.

Comparisons of pressure-time records at the same stations from Shot 12 (simultaneous detonation), Shot 13 (10 msec delay) and Shot 15 (5 msec delay) are shown in Figures 3.33 through 3.42. Note that, for ranges of 90 feet or greater from ground zero, the pressure records from the three events are nearly identical, whereas at lower ranges some significant differences occur, both in the main pressure pulse and in details of the reflected and secondary pulses. These differences, of course, are to be expected as results of the different separations in charge detonation times.

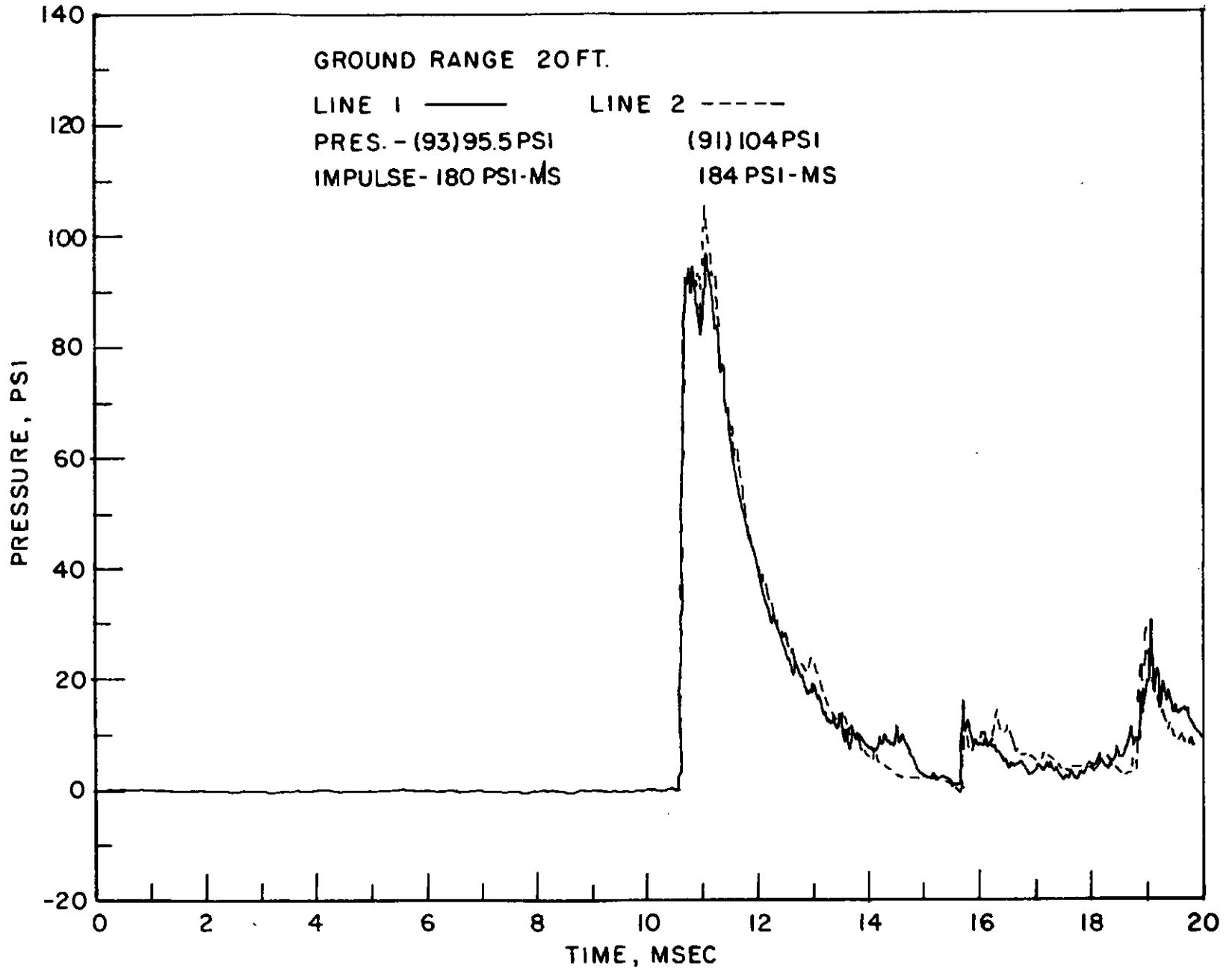


Figure 3.24. Comparison of Pressure Records at 20-Foot Range from Gage Lines 1 and 2; Shot 15

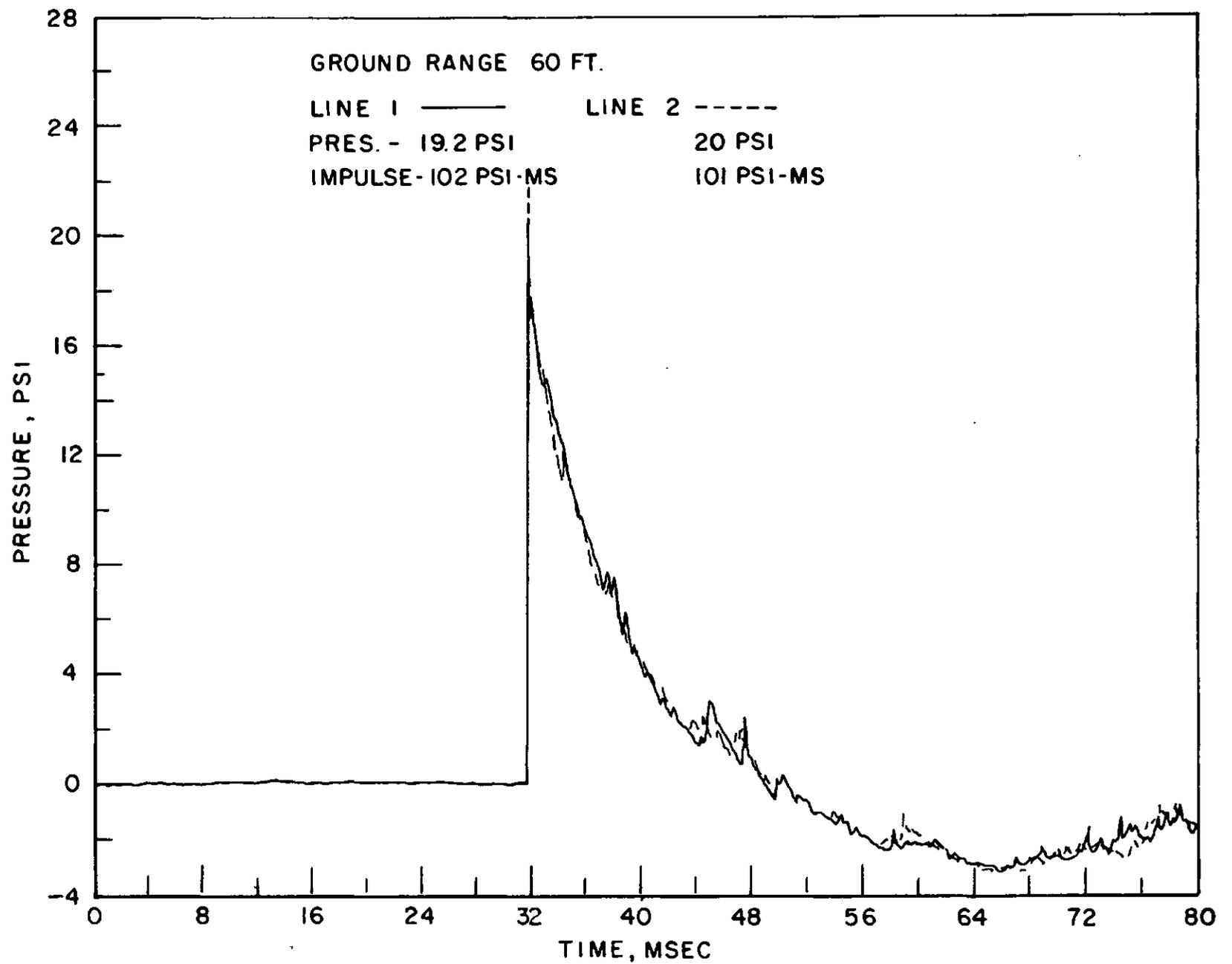


Figure 3.25. - Comparison of Pressure Records at 60-Foot Range from Gage Lines 1 and 2; Shot 15

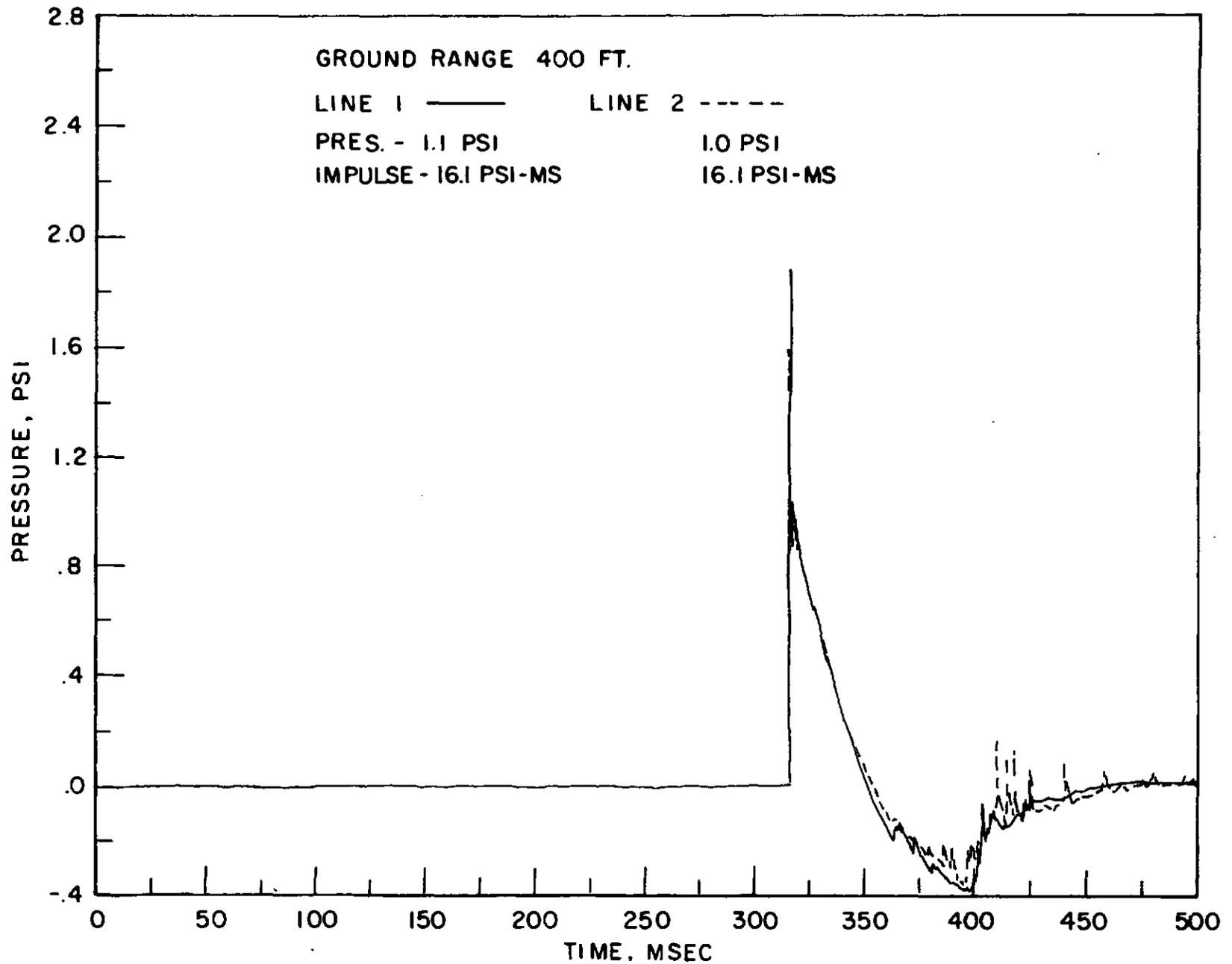


Figure 3.26. Comparison of Pressure Records at 400-Foot Range from Gage Lines 1 and 2; Shot 15

Table 3.4. Measured Air Blast Parameters; Shot 15

System-Channel	Station	Arrival Time ¹ (ms)	Primary Pressure (psi)	Secondary Pressure (psi)	Pos. Phase Duration (ms)	Overpressure Impulse (psi-ms)
3-3	0.0	7.23	840		2.1	432
4-3	10.0E	7.91	255		2.7	240
3-4	10.0W	8.12	335		3.7	260
4-4	10.0N	8.17	354		3.1	272
3-5	10.0S	7.89	227	240	3.1	235 ²
1-25	2-15.0X ³	9.2	-		-	- ⁴
1-3	20.0	10.60	93	95.5 ⁵	5.0	180
3-25	2-20.0	10.74	91	104 ⁵	5.0	184
1-4	20.3S	10.05	48	59.5	-	160 ⁶
1-5	20.3T	10.08	192	166	6.3	260
4-6	20.10S	8.96	61		8.2	145
4-7	20.10T	9.00	220		11.0	234
3-7	20.15S	8.83	67.5		5.0	146
3-8	20.15T	8.38	210		5.9	270
4-8	20.20S	8.85	93		5.6	138
4-9	20.20T	8.81	320		5.9	340
2-3	20.27S	6.64	36.7	48	7.0	120
2-4	20.27T	6.70	110	140	7.7	176
1-6	20.30S	5.77	44	32	5.1	70
1-7	20.30T	5.90	125	114	4.2	91
2-5	20.33S	5.02	51.8	25	5.1	77.5
2-6	20.33T	5.10	170	52	5.1	119
3-9	20.40S	4.04	71		4.9	82.5
3-10	20.40T	4.10	250		4.0	150
1-8	30.0	14.35	45		13.5	148
1-20	2-30.0	14.6	41.6		12.6	141
1-9	30.3S	14.45	38		13.5	140
1-10	30.3T	14.45	120		13.5	272
4-10	30.10S	13.60	36	22	9.9	132
4-11	30.10T	13.60	40	34	10.9	180
4-12	30.20S	12.8	42.2		8.3	104
4-13	30.20T	12.85	70		8.7	162
2-7	30.27S	11.2	20.2	29.6	9.5	104
2-8	30.27T	11.25	32	46.5	9.4	144
1-11	30.30S	10.4	23	27.5	11.8	106
1-12	30.30T	10.5	37.5	42.5	11.0	145
2-9	30.33S	9.8	26.5	23	6.6	59
2-10	30.33T	9.75	45	40	6.1	78
2-11	40.0	19.7	23	38	15.5	128
2-26	2-40.0	19.8	28.3	34	15.1	139
2-12	40.3S	19.8	30.2		14.7	133
2-13	40.3T	19.7	36	47	10.0	174
2-27	2-40.3PT	19.8	48		15.1	187
4-14	40.10S	18.7	24	26	13.6	118
4-15	40.10T	19.0	45	31	12.3	164

Table 3.4. Measured Air Blast Parameters; Shot 15 (Continued)

System-Channel	Station	Arrival Time ¹ (ms)	Primary Pressure (psi)	Secondary Pressure (psi)	Pos. Phase Duration (ms)	Overpressure Impulse (psi-ms)
4-16	40.20S	18.0	26		14.0	107.5
4-17	40.20T	18.0	43		15.0	150
2-14	40.27S	16.8	14.0	22.0	10.7	91
2-15	40.27T	17.0	19	27	11.0	117
1-13	40.30S	16.1	15	20	11.7	91
1-14	40.30T	16.2	23	29	12.1	118
2-16	40.33S	15.4	16.5	21	12.9	89.5
2-17	40.33T	15.7	22	30	13.2	117
4-5	50.0N	25.6	27.0		16.7	117
3-6	50.0S	25.0	26.5		16.3	113
2-18	60.0	31.7	19.2		17.3	102
3-26	2-60.0	31.6	19.5		17.6	101
3-27	2-60.0M	31.9	16		17.2	90
2-19	60.3S	31.9	19		14.0	96.5
2-20	60.3T	31.8	28		17.7	130
2-24	2-60.3PS	31.6	18.5		19.2	97
2-25	2-60.3PTM	31.7	27		17.3	121
4-18	60.10S	31.6	16.8		16.1	98
4-19	60.10T	31.6	23.5		18.4	124
4-20	60.20S	30.6	12.0	10.8	18.4	84.5
4-21	60.20T	30.7	17	13	17.1	97.5
1-15	60.27S	30.5	14.0		22.6	81
2-21	60.30S	30.1	6.5	10	22.3	71
2-22	60.30T	30.1	8	14	17.9	89
1-17	60.33S	29.6	6.6	8.0	24.4	66.3
1-26	2-80.0X ³	45.0	12.8		21.0	95
4-22	90.0	52.5	10		22.0	71
4-26	2-90.0	52.0	9.5		22.0	72
1-19	2-100.0X ³	59.5	9.0		-	- ⁷
4-23	110.0	67.4	6.0		25.0	53.6
1-31	2-110.0	67.0	7.0		24.0	61.0
3-23	150.0	99.2	5.0		26.3	44
1-22	2-150.0	99.0	4.5		26.5	44
1-16	2-200.0X ³	140.4	3.25		27.0	31.2
4-24	245.0	179	1.9		31	25.3
1-23	2-245.0	180	2.15		32	27.1
4-25	400.0	316	1.1		35	16.1
1-24	2-400.0	317	1.0		37	16.1
3-24	800.0	691	0.52		31	6.1
1-27	Trlr #1X ³	1449.4	0.018		51.5	0.395
1-18	Trlr #2X ³	1449.4	-		-	- ⁸

¹Time referenced to detonation of top charge; ²Second peak due to jetting; ³Piezoelectric gage; ⁴Bad gage; ⁵Double peak phenomena; ⁶Questionable--record does not return to zero; ⁷Poor duration--bad gage; ⁸Bad record

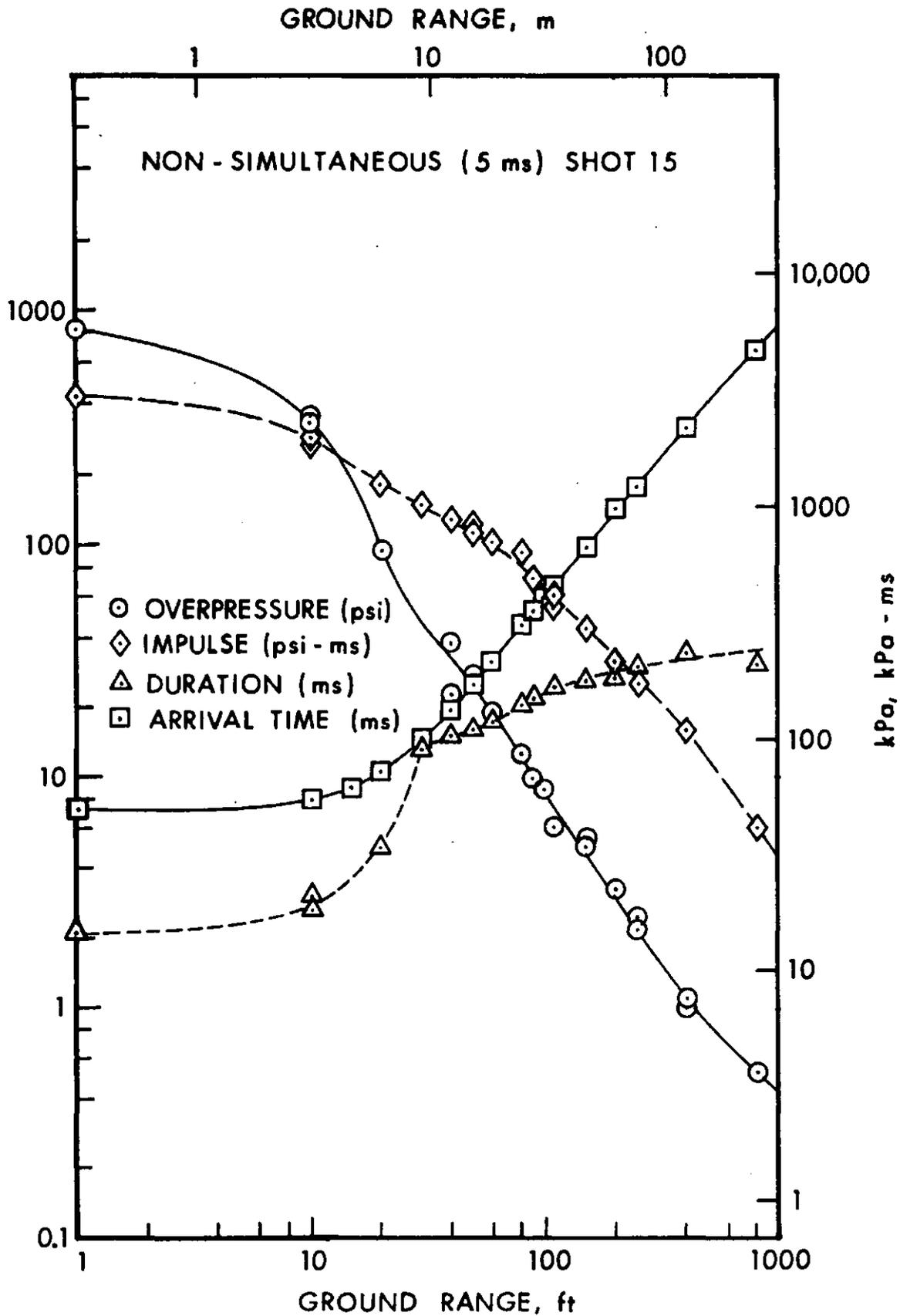


Figure 3.27. Air Blast Parameters at Ground Level Versus Ground Range; Shot 15

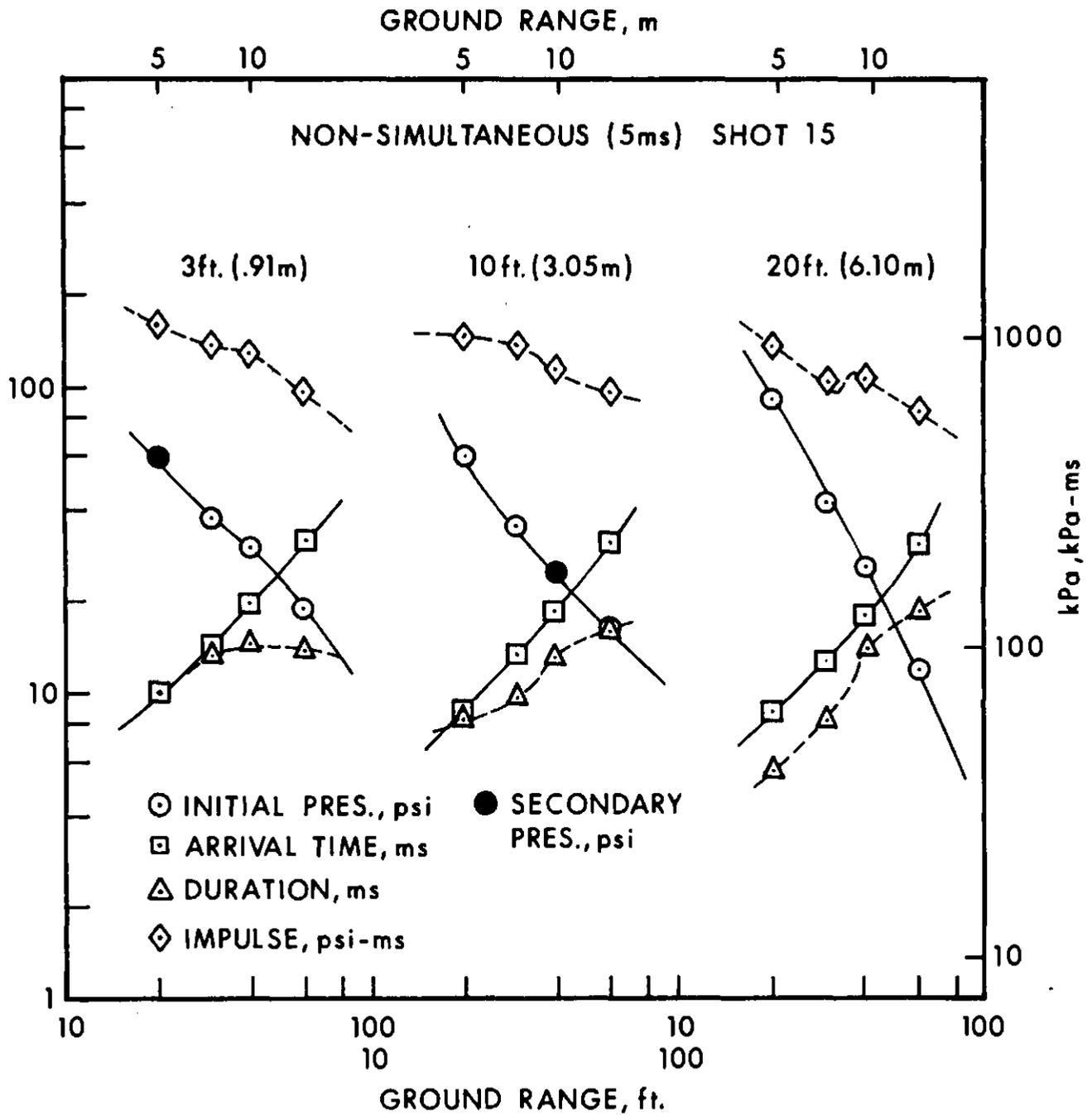


Figure 3.28. Air Blast Parameters at 3, 10, and 20 Feet Versus Ground Range; Shot 15

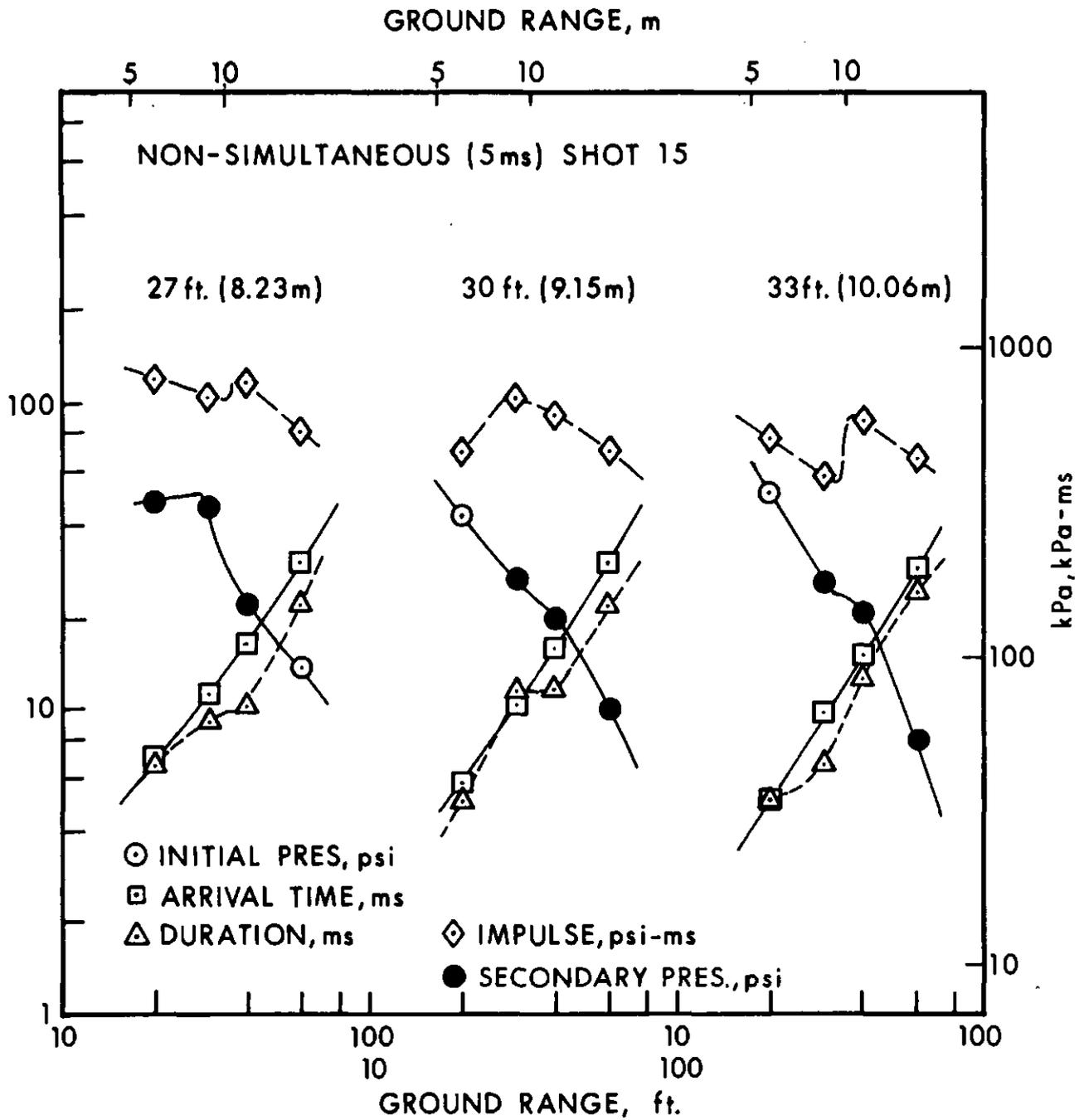


Figure 3.29. Air Blast Parameters at 27, 30, and 33 Feet Versus Ground Range; Shot 15

Table 3.5. Measured Air Blast Parameters; Shot 16

System-Channel	Station	Arrival Time ¹ (ms)	Primary Pressure (psi)	Secondary Pressure (psi)	Pos. Phase Duration (ms)	Overpressure Impulse (psi-ms)
3-3	0.0	5.02	820		3.08	400
4-4	10.0N	5.8	398		4.0	272
3-5	10.0S	5.88	372		3.52	262
4-3	10.0E	5.86	340		6.64 ²	304
3-4	10.0W	5.85	358		4.15	248
1-3	20.0	8.4	94	90 ³	5.3	142
1-19	2-20.0X ⁴	8.28	108		5.02	137
1-4	20.3S	7.8	47	61	5.3	110
1-5	20.3T	7.8	128	123	5.7	204
4-6	20.10S	6.8	64		11.5 ⁵	152
4-7	20.10T	6.85	160		1.75 ⁵	79
3-7	20.15S	6.65	64.5		10.65	131
3-8	20.15T	6.7	200		8.8	186
4-8	20.20S	6.85	60.5	48	5.55	111
4-9	20.20T	6.85	187.5	107.5	5.95	212
2-3	20.27S	6.45	39	74	6.05	135
2-4	20.27T	6.42	84	132	5.58	184
1-6	20.30S	5.55	43.4	52	7.05	119
1-7	20.30T	5.65	100	86	5.85	166
2-5	20.33S	4.9	54	32	8.5	112
2-6	20.33T	4.9	120	65	8.3	172
3-9	20.40S	3.85	69.2		6.15	85
3-10	20.40T	3.92	170		4.28	119
1-8	30.0	12.1	42.8		14.4	135
1-22	2-30.0X ⁴	12	47.0		13.1	92 ⁶
1-9	30.3S	12.1	41.0		13.1	131
1-10	30.3T	12.1	89		16.5	217
4-10	30.10S	11.2	29.2	33.2	10.0	123.5
4-11	30.10T	11.2	41.0	46.5	10.8	176
4-12	30.20S	11.0	46.0		12.3	121
4-13	30.20T	11.1	86		11.5	179
2-7	30.27S	10.6	22.0	40	7.4	105
2-8	30.27T	10.7	35	60	7.3	146
1-11	30.30S	9.8	24.4	32	8.4	101
1-12	30.30T	9.9	40	45	8.7	141
2-9	30.33S	9.18	25	27.5	10.8	95
2-10	30.33T	9.2	40	37	10.8	141
2-11	40.0	16.4	25	20	15.6	118
2-25	2-40.0	16.9	29.2		15.1	126
2-12	40.3S	16.9	27.7	21.2	15.1	120
2-13	40.3T	16.8	41	35	15.4	179
2-26	2-40.3T	16.9	45	32.5	16.1	178
4-14	40.10S	16.8	16.0	20, 30.7	11.2	109
4-15	40.10T	17	22.8	24.6, 42	11.25	142
4-16	40.20S	15.8	25.0	10.0	14.7	99

Table 3.5. Measured Air Blast Parameters; Shot 16 (Continued)

System-Channel	Station	Arrival Time ¹ (ms)	Primary Pressure (psi)	Secondary Pressure (psi)	Pos. Phase Duration (ms)	Overpressure Impulse (psi-ms)
4-17	40.20T	15.8	43.5	10.05	13.0	143
2-14	40.27S	15.9	26.2	9.7	8.9	85
2-15	40.27T	15.8	50.0	15.0	9.4	122
1-13	40.30S	15.5	14.6	21.0	10.3	84
1-14	40.30T	15.4	20.0	29.4	10.2	102
2-16	40.33S	14.6	15.2	16.5	11.1	83.5
2-17	40.33T	14.7	21.0	23	11.4	107
4-5	50.0N	22.3	15.2	15.4	16.4	104
3-6	50.0S	22.4	18.0	15.6	16.6	109
2-18	60.0	28.8	12.2	16.2	17.2	97
2-23	2-60.0	28.7	11.6	15.2	16.7	93
2-19	60.3	31	15.6	14.0	15	96
2-24	2-60.3	28.8	15.0	12.0	17.2	90
2-20	60.3T	28.9	23.0	17.5	17.1	125
4-18	60.10S	28.6	17.6		17.8	92.4
4-19	60.10T	28.6	26.2		17.8	120
4-20	60.20S	27.8	11.6	9.7	18.2	75
4-21	60.20T	28.7	17.5 ⁷			
1-15	60.27S	27.6	13.0	6.5	16.4	74
1-16	60.27T	27.6	22.4 ⁷			
2-21	60.30S	27.6	10.9	5.2	16.8	67
2-22	60.30T	27.6	15.0	5.9	16.8	84
1-17	60.33S	27.8	10.5	4.0	20.2	68
1-18	60.33T	27.8	15.5	5.0	18.2	86
4-22	90.0	48.5	9.0		22	65
3-25	2-90.0X ⁴	48.2	7.6		22.3	62
4-23	110.0	62.8	6.5		23.2	53.6
3-26	2-110.0X ⁴	62.8	6.0		23.2	50
3-23	150.0	92.8	4.4		25.7	42.4
3-27	2-150.0X ⁴	93	4.4		24.5	37.2
4-24	245.0X ⁴	169.8	2.25		27.2	23.6
4-26	2-245.0X ⁴	169.4	2.70		28.6	27.3
4-25	400.0X ⁴		- ⁷		-	-
4-27	2-400.0X ⁴	307	1.08		26.7 ²	13.3
3-24	800.0X ⁴	658	0.575		44	9.9
1-21	Trailer	1381	0.46		36	7.05

¹Time referenced to detonation of top charge

²Poor duration, gage problem

³Double peak phenomena

⁴Piezoelectric gage

⁵Duration questionable--zero shift

⁶Rapid decay--gage problem

⁷Bad record

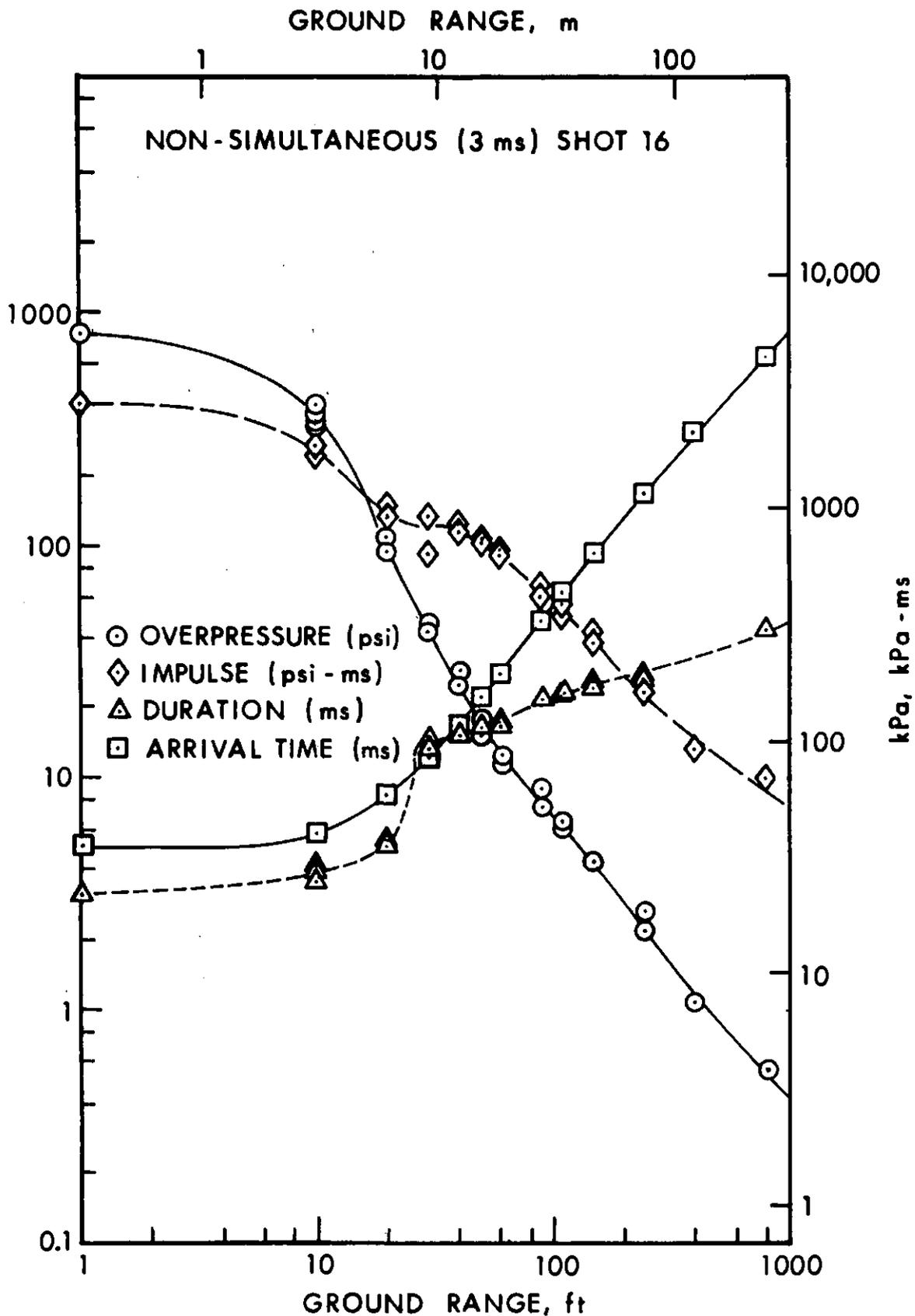


Figure 3.30. Air Blast Parameters at Ground Level Versus Ground Range; Shot 16

GROUND RANGE, m

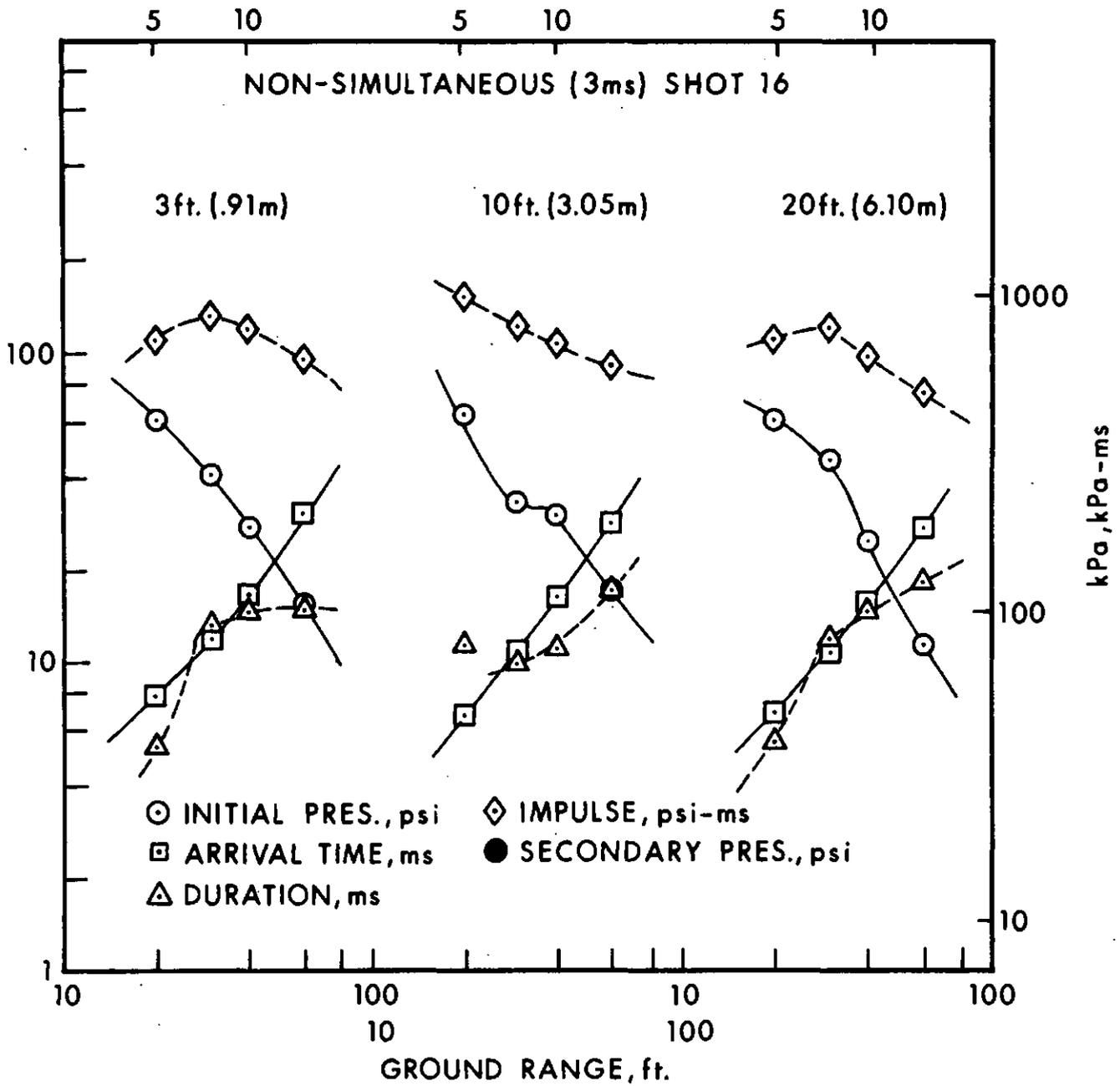


Figure 3.31. Air Blast Parameters at 3, 10, and 20 Feet Versus Ground Range; Shot 16

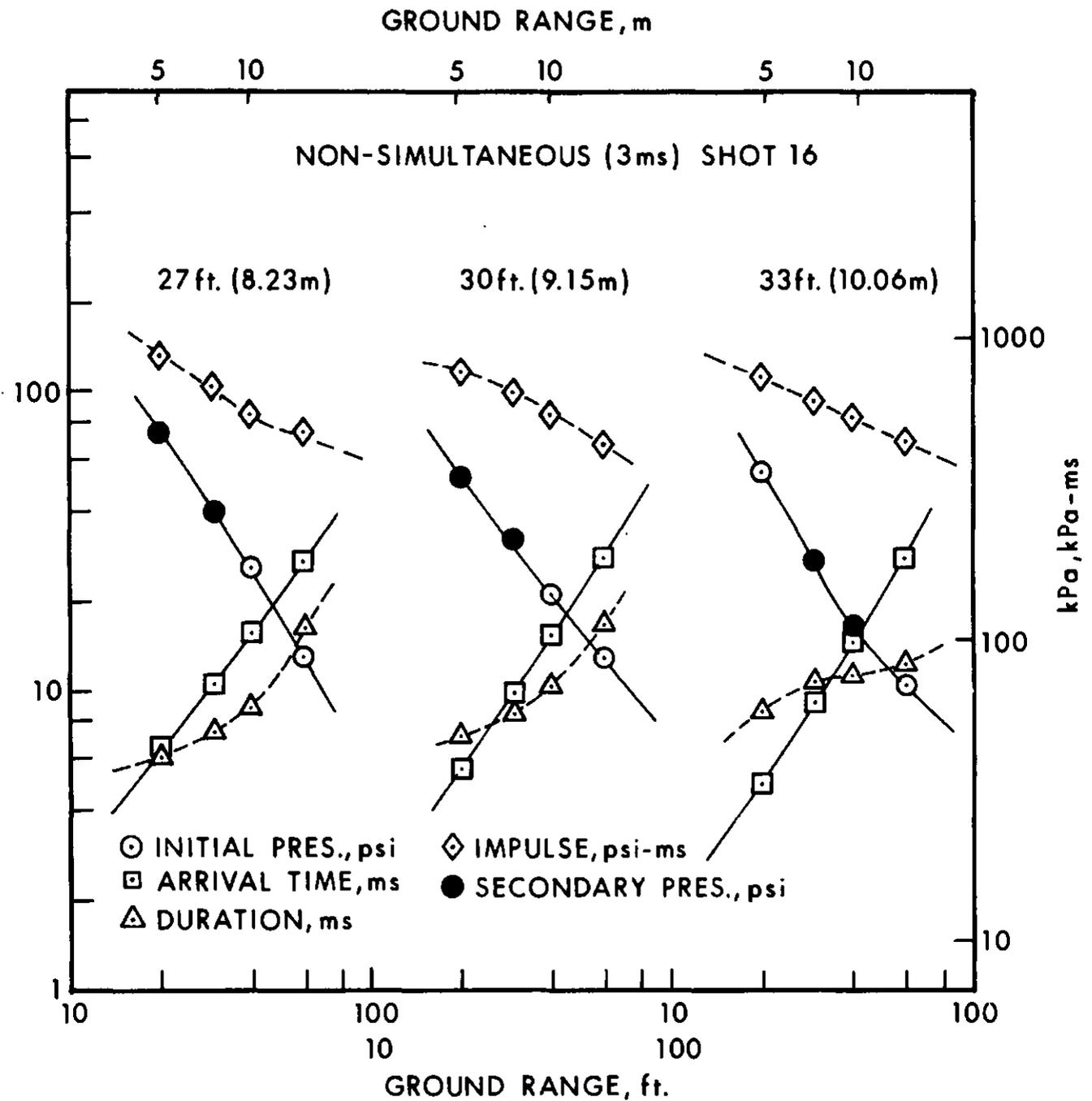


Figure 3.32. Air Blast Parameters at 27, 30, and 33 Feet Versus Ground Range; Shot 16

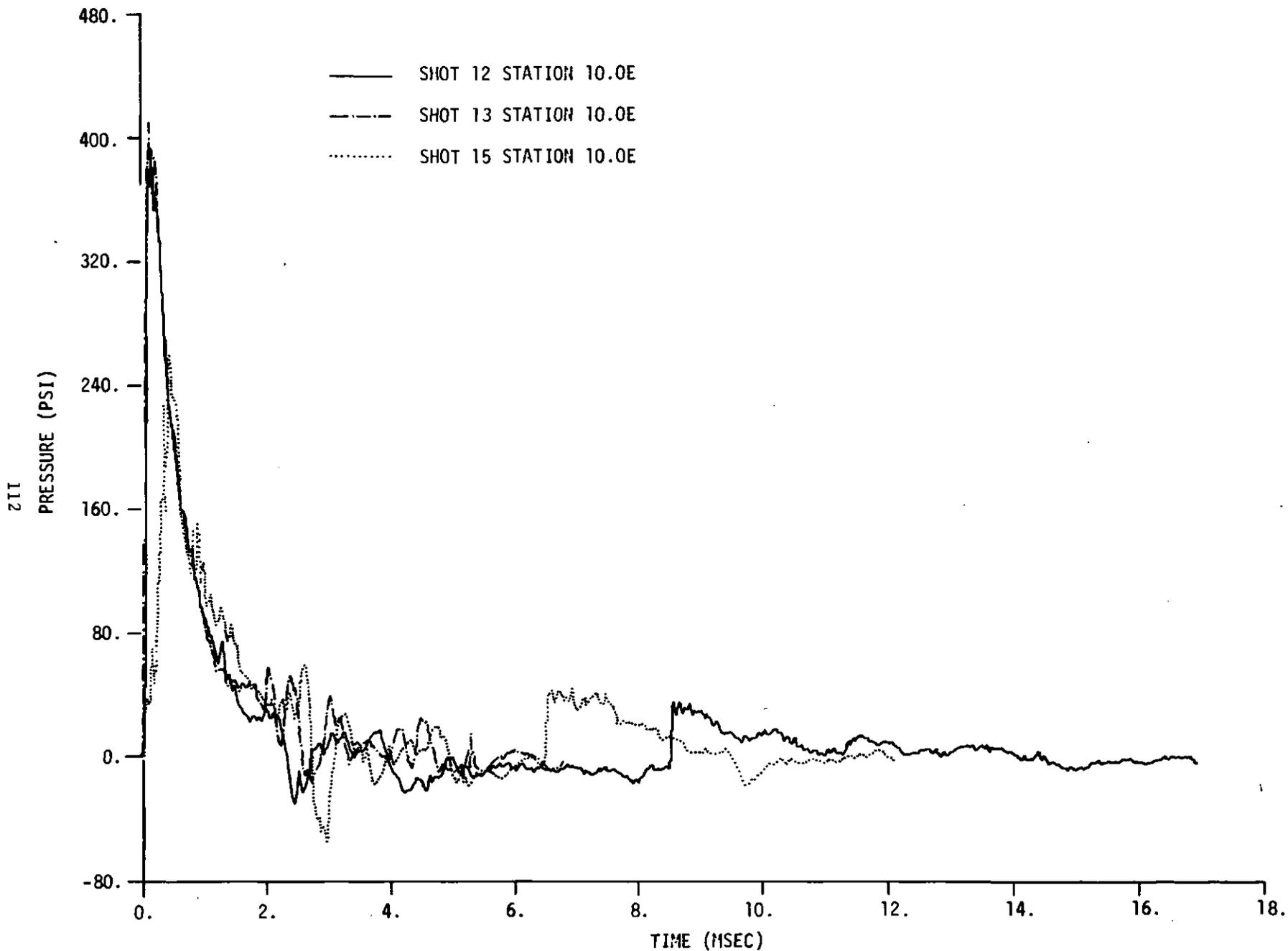


Figure 3.33. Comparison of Pressure Records at Station 10.0E from Shots 12, 13, and 15

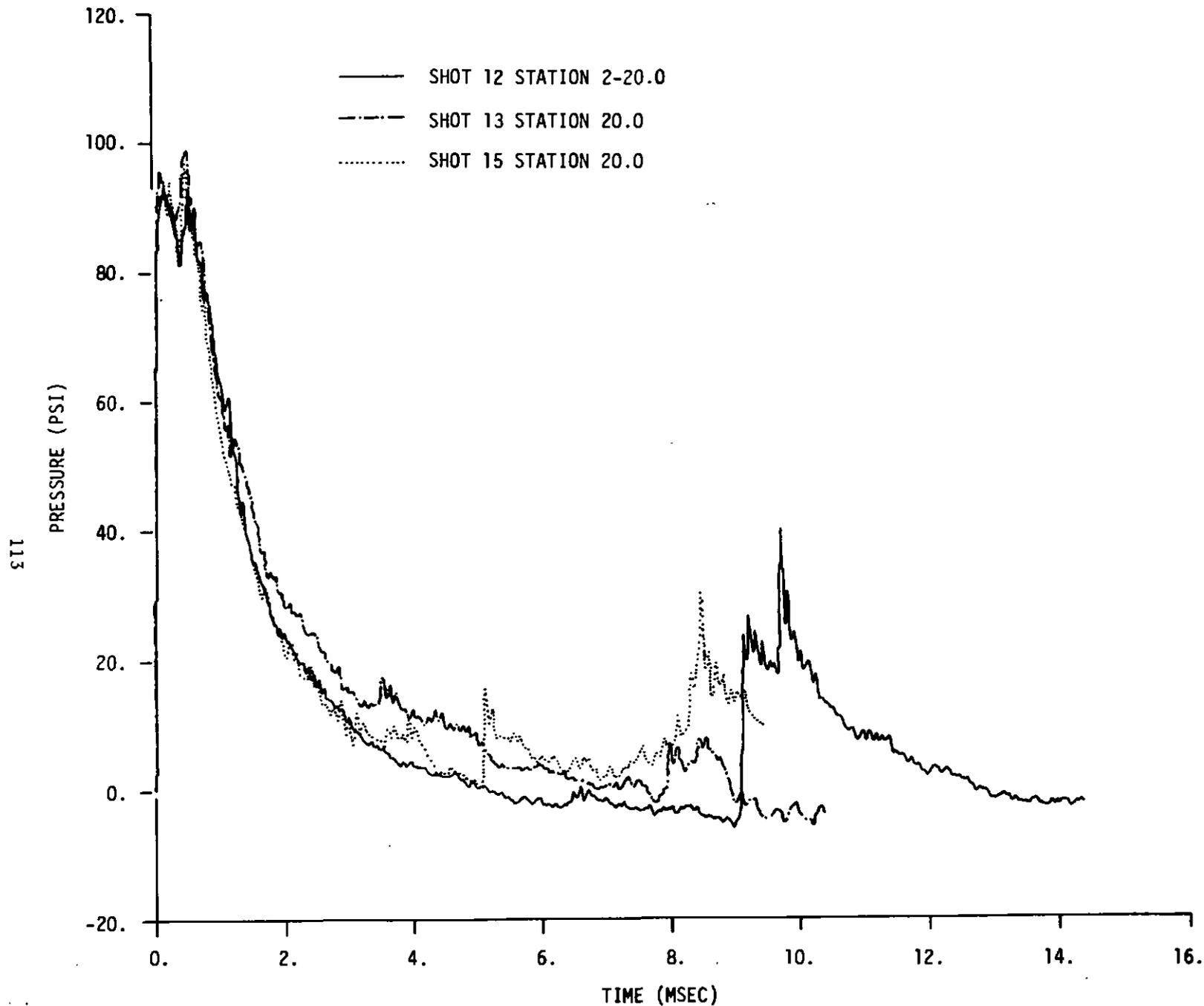


Figure 3.34. Comparison of Pressure Records at Station 20.0 from Shots 12, 13, and 15

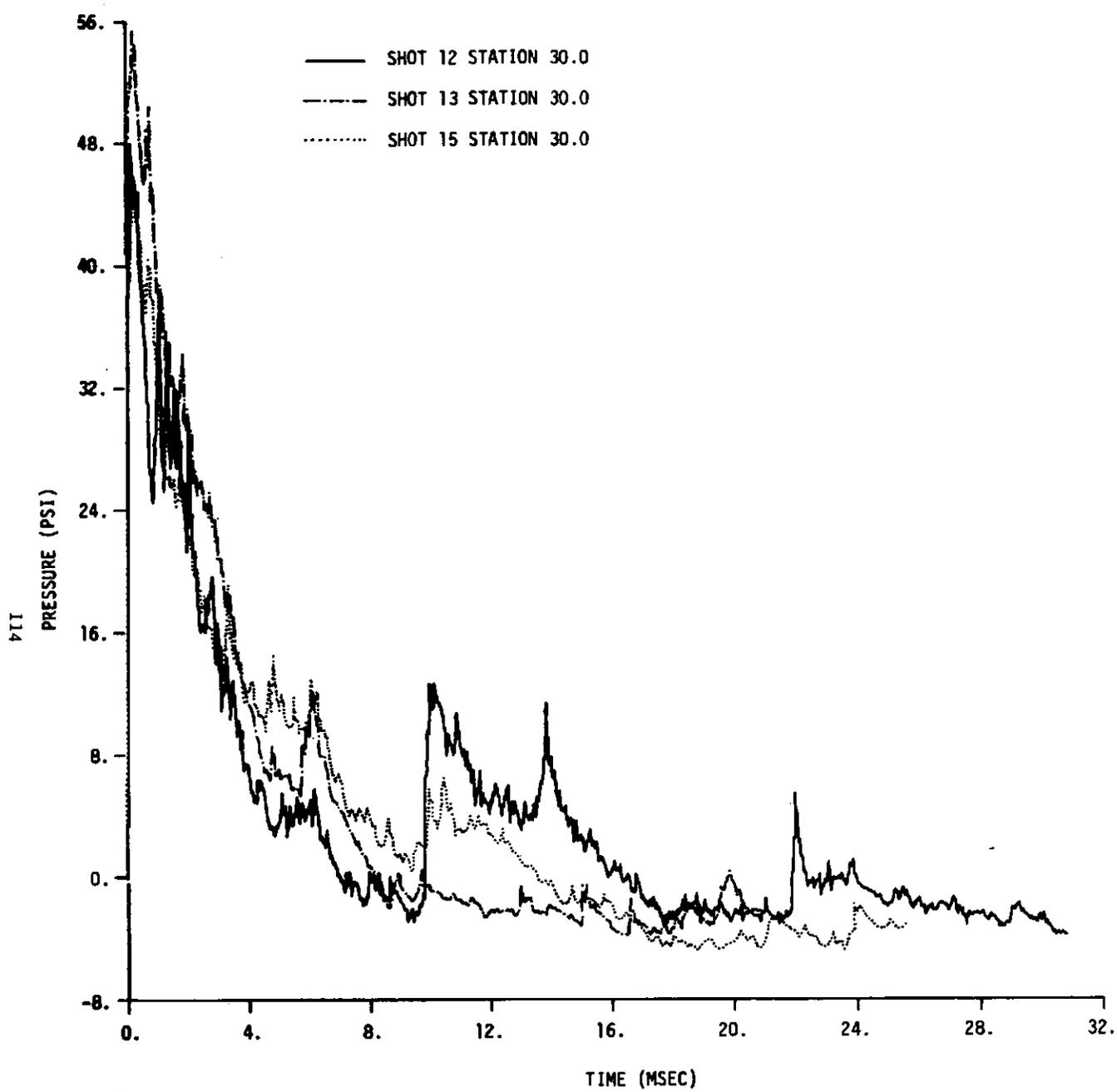


Figure 3.35. Comparison of Pressure Records at Station 30.0 from Shots 12, 13, and 15

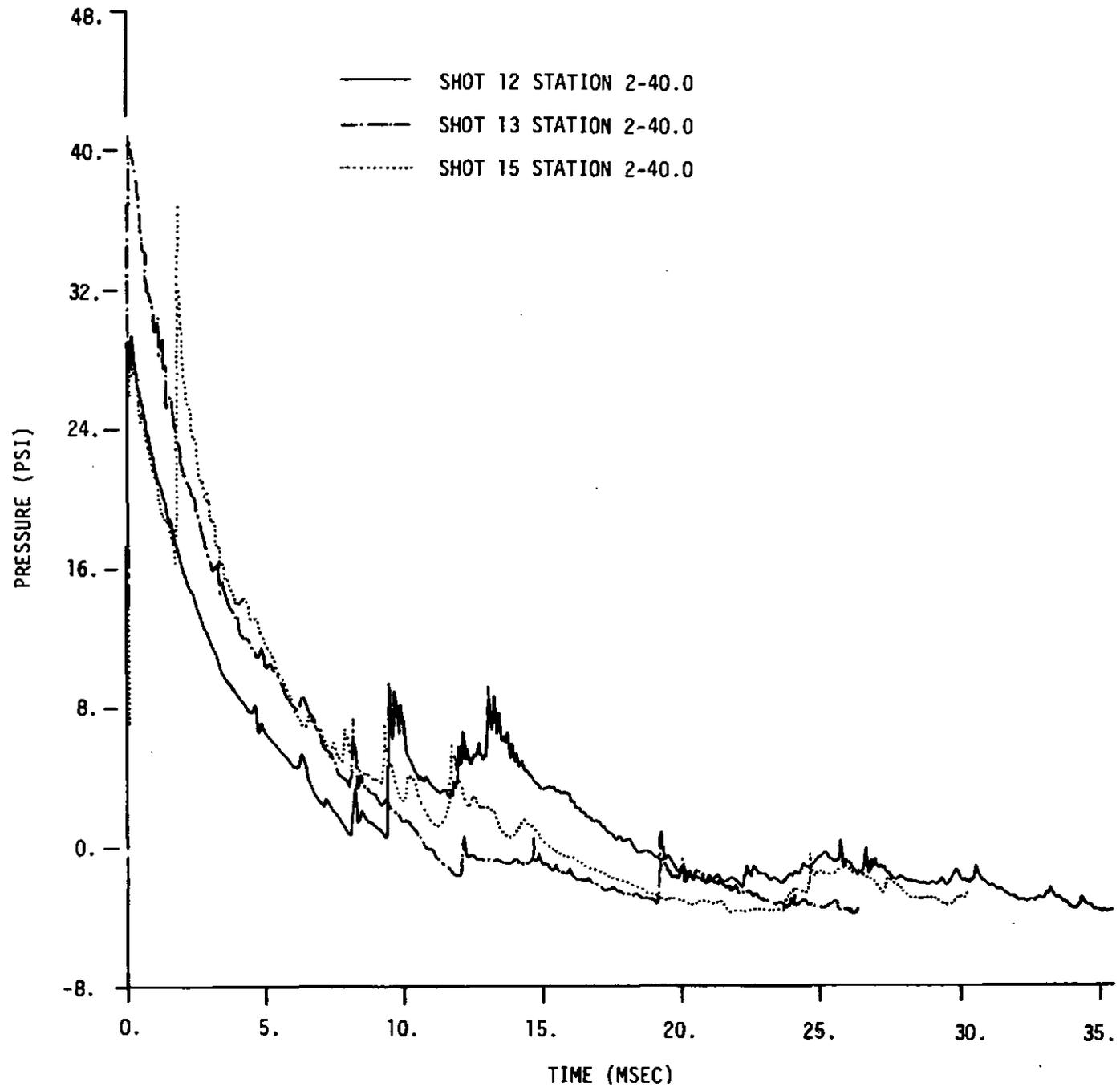


Figure 3.36. Comparison of Pressure Records at Station 2-40.0 from Shots 12, 13, and 15

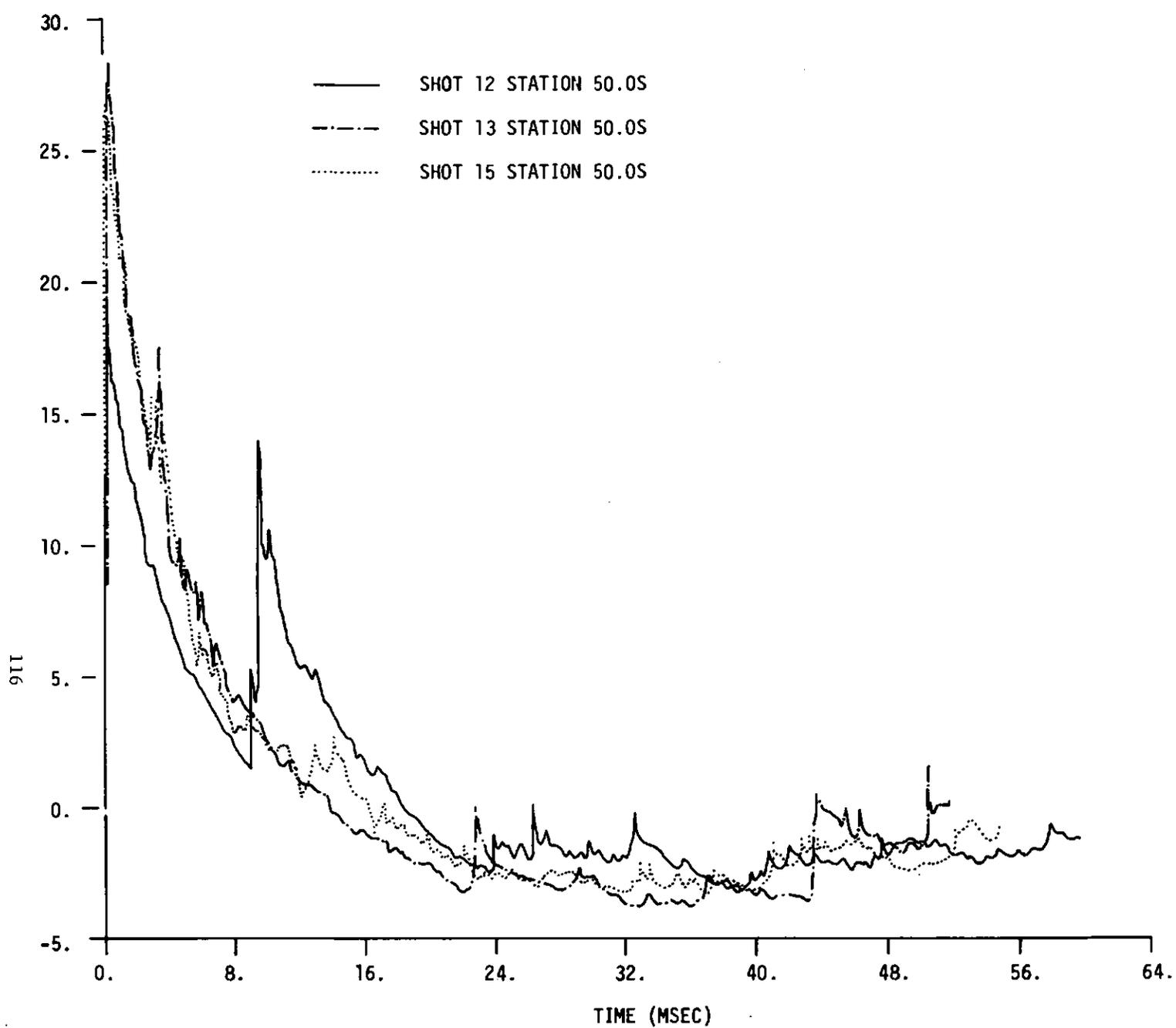


Figure 3.37. Comparison of Pressure Records at Station 50.0S from Shots 12, 13, and 15

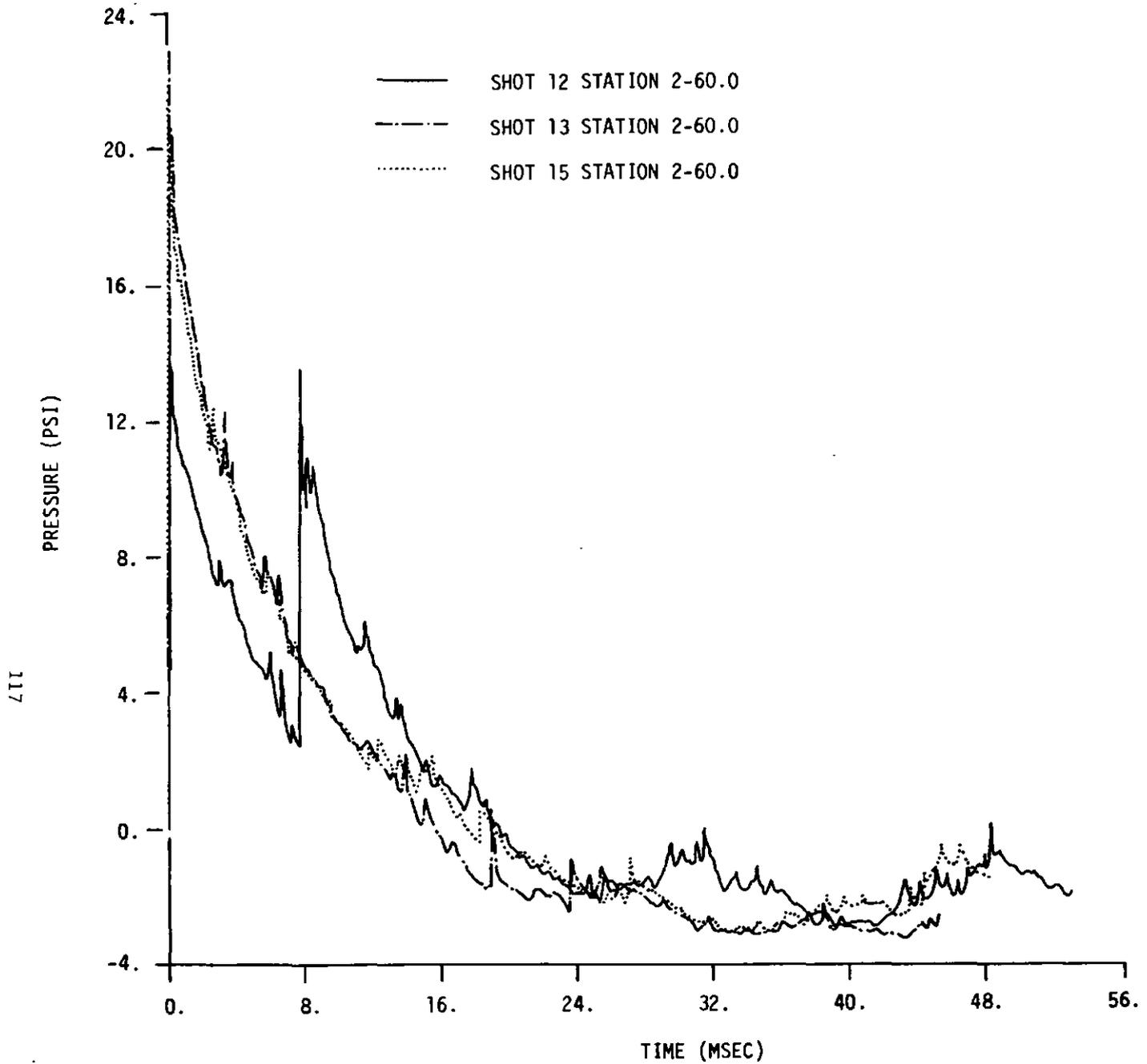


Figure 3.38. Comparison of Pressure Records at Station 2-60.0 from Shots 12, 13, and 15

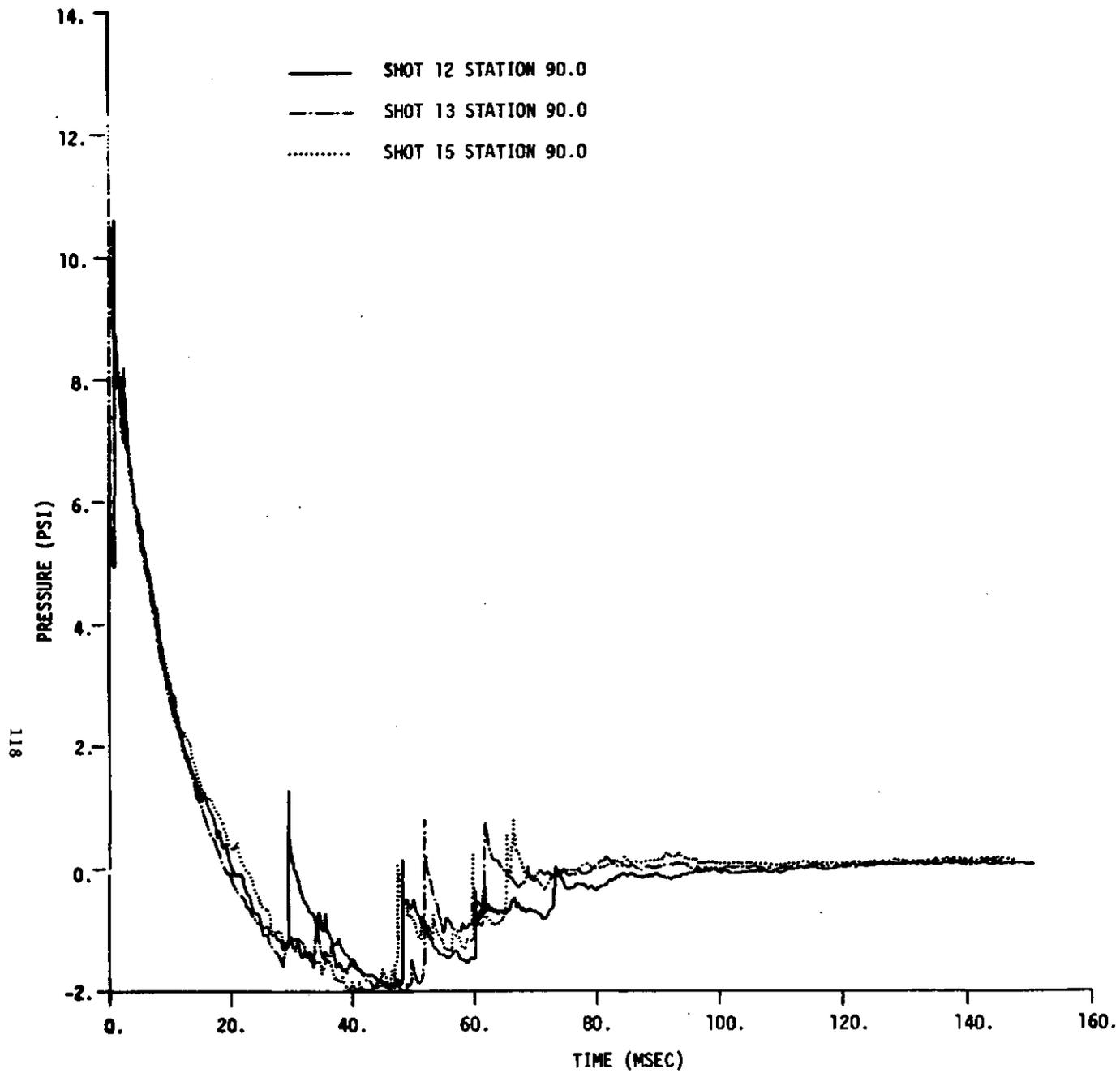


Figure 3.39. Comparison of Pressure Records at Station 90.0 from Shots 12, 13, and 15

611

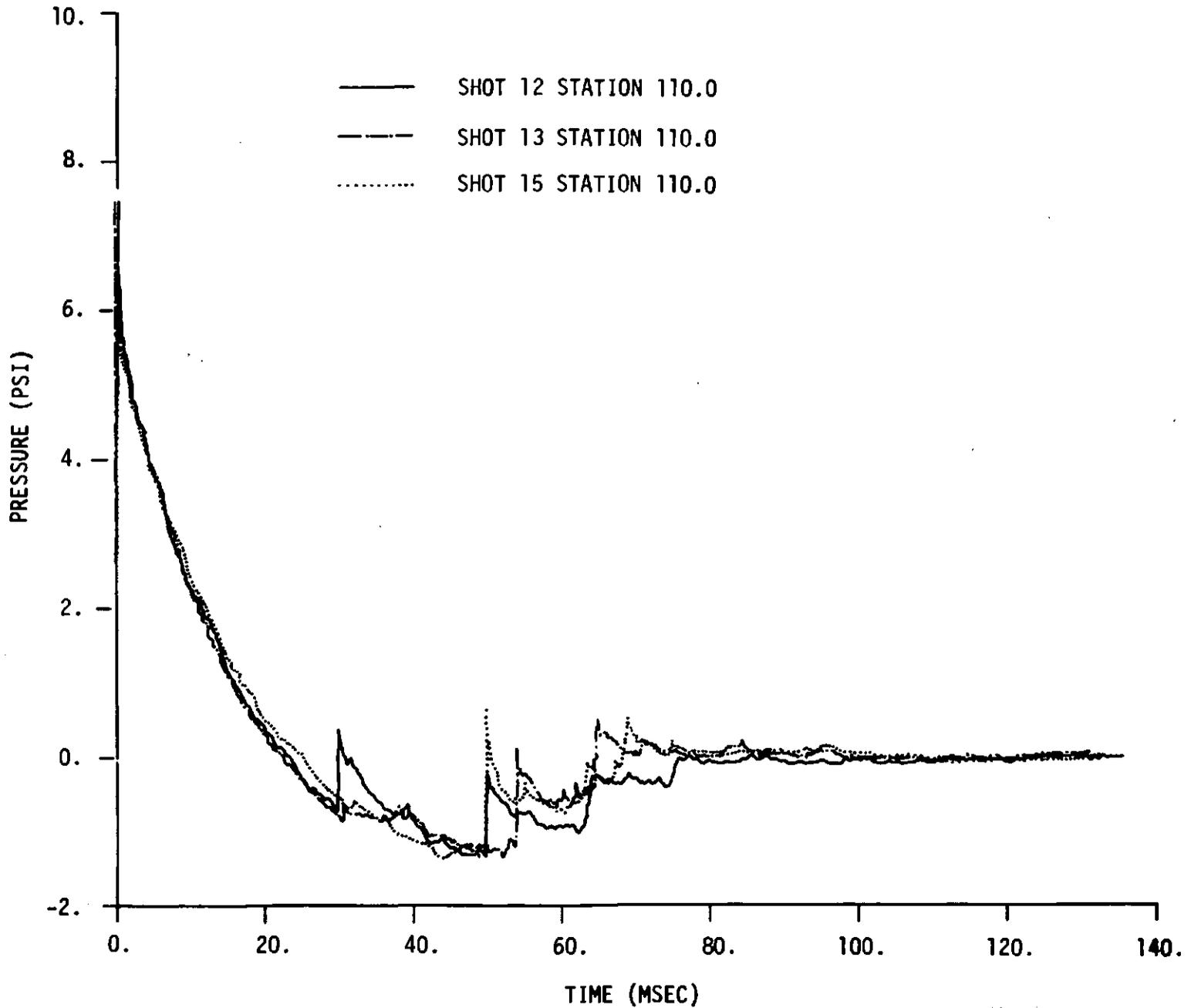


Figure 3.40. Comparison of Pressure Records at Station 110.0 from Shots 12, 13, and 15

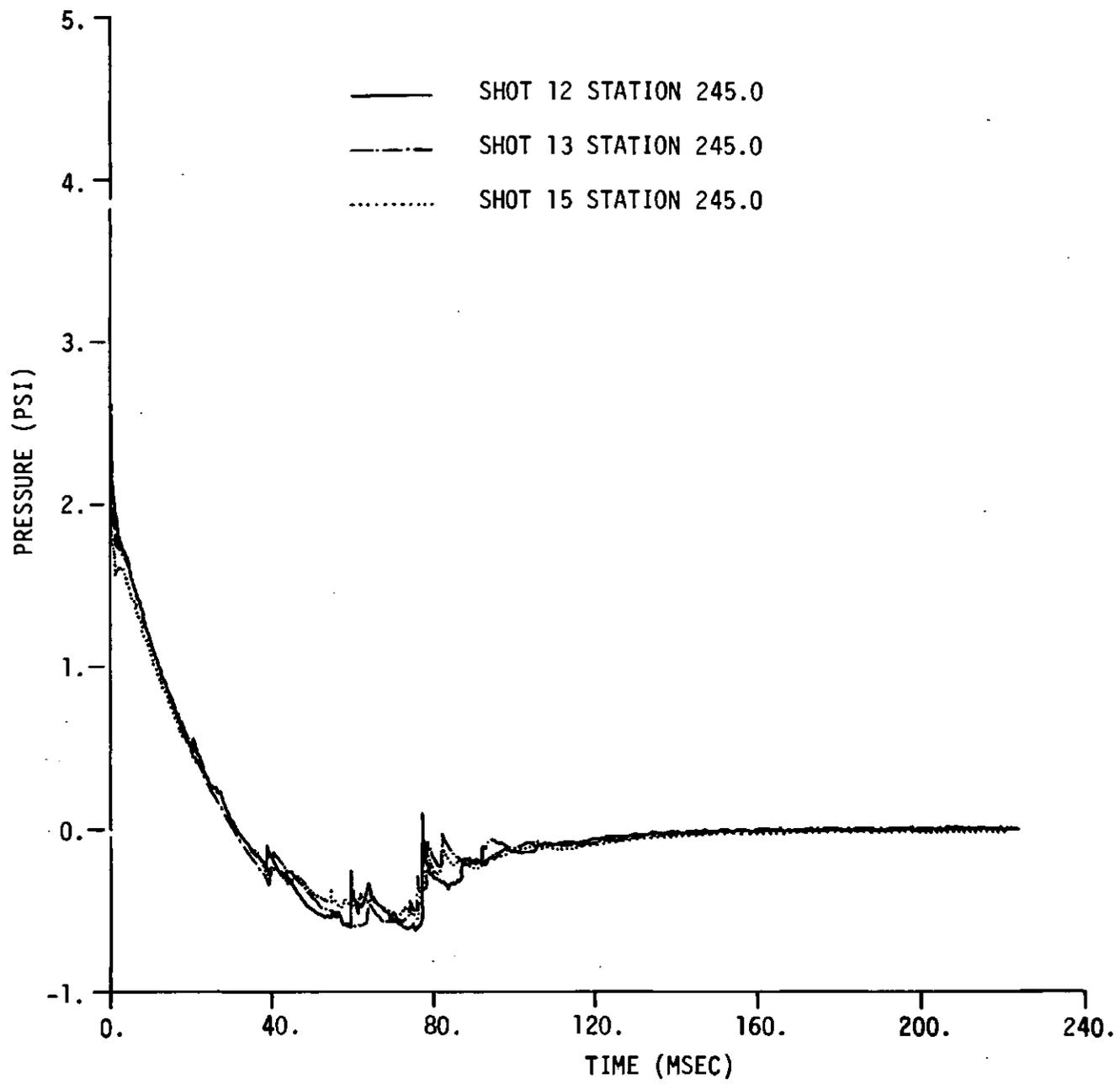


Figure 3.41. Comparison of Pressure Records at Station 245.0 from Shots 12, 13, and 15

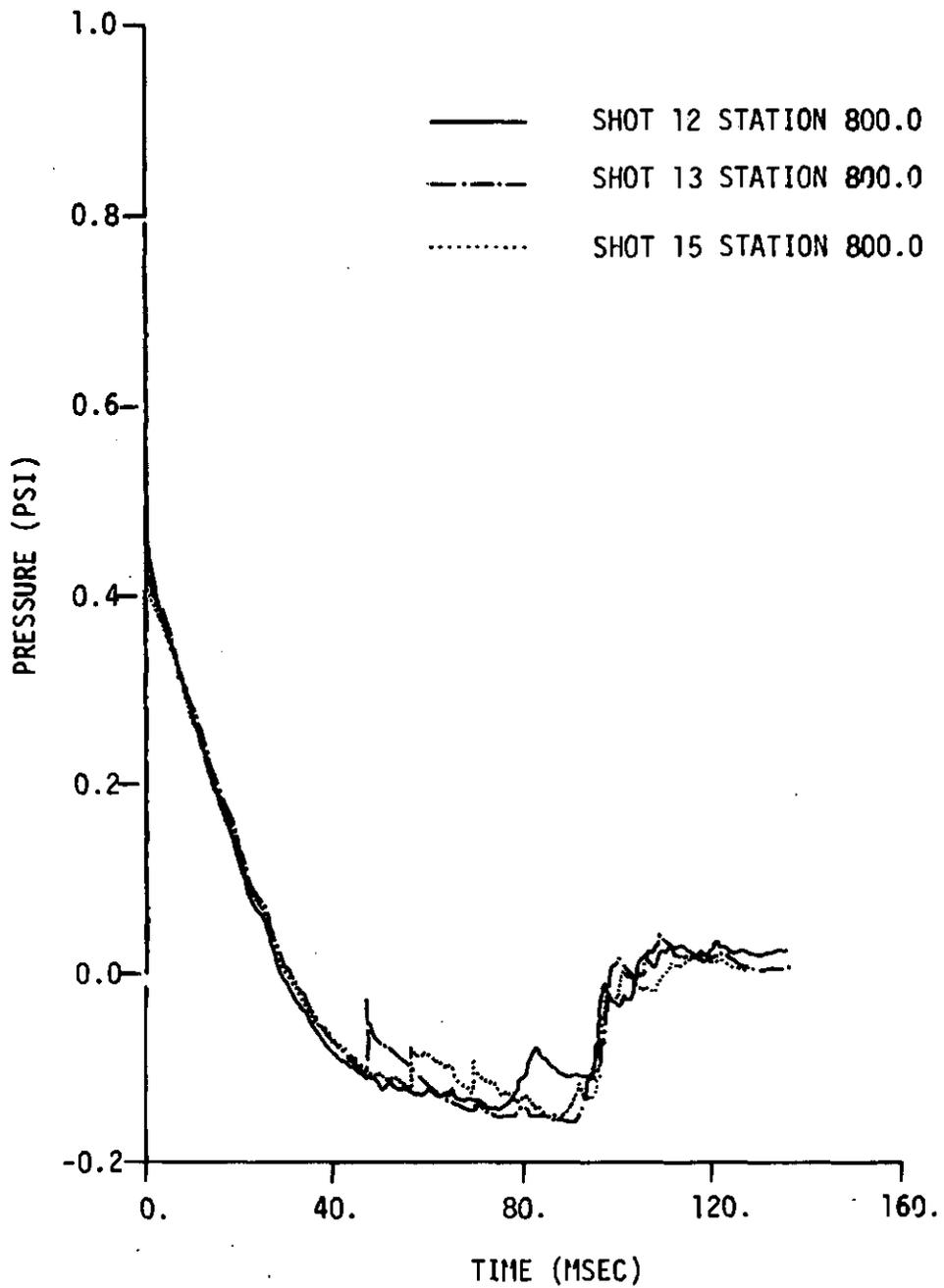


Figure 3.42. Comparison of Pressure Records at Station 800.0 from Shots 12, 13, and 15

CHAPTER 4

DISCUSSION OF RESULTS

4.1 Instrument Performance

The quality of the gage records and film obtained by the instrumentation systems was excellent throughout the series. A few very minor losses of data did occur, but these were not serious in terms of overall results. The Tyco pressure transducers functioned well in repeated shots; the PCB piezoelectric transducers, or crystal gages, which were used on an experimental basis, also performed satisfactorily.

Between 80 and 86 channels of air blast pressure data were recorded on each event. There were only scattered occurrences of gage breakdown, recording system saturation, or excessive noise. Five out of 82 channels of data were lost or partially obscured on Shot 12, resulting in a data return of 94%. Only three channels were lost on Shot 13, three on Shot 14, four on Shot 15, and two on Shot 16, so that overall data return was better than 95%.

All cameras operated satisfactorily, although on Shot 15 lighting was poor and the photographic records are of correspondingly poor quality. Also, some difficulty was experienced with a larger than normal rate of detonation failure in the smoke puffs. This problem was traced to a fault in manufacture of the squib detonators, and was corrected.

4.2 Pressure Records

In general, pressure records obtained from multiple detonations can be quite complicated. An example is shown in Figure 4.1. This is the overpressure history obtained at ST 40.20 (range 40 feet, elevation 20 feet) in Shot 12, the simultaneous detonation event. It illustrates graphically the multiple shocks that are typical of such detonations. The first, or initial, shock comes directly from detonation of the lower charge. The second shock is the reflection of this incident wave from the ideal reflecting surface between charges (positions of this surface for different degrees of non-simultaneity are shown in Figure 2.10). The third shock appearing in the record is a reflection of the initial shock from the ground. Origin of the small fourth shock is not entirely clear. It may result from reflection of the second shock at the ground surface, or may be a coalescence of several minor shocks.

Secondary peaks not related to the multiple detonation configuration may also be identified. Pressure records obtained from the 20-foot range ground stations on all five events are shown in Figure 4.2. All of the records exhibit a second peak of approximately the same size as

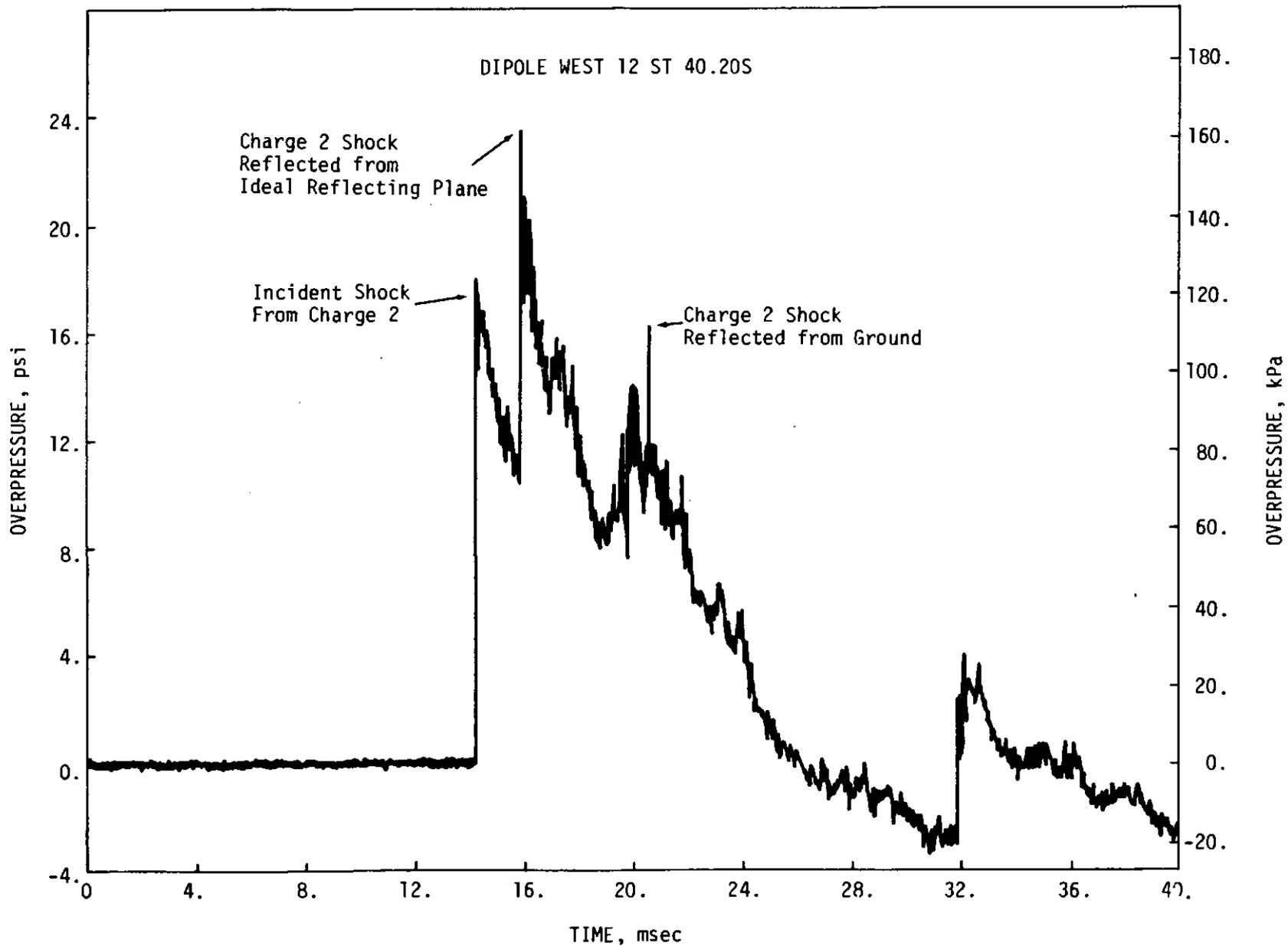


Figure 4.1. Overpressure Record from Shot 12, Station 40.20, Illustrating Multiple Shock Structure of the Pressure Pulse

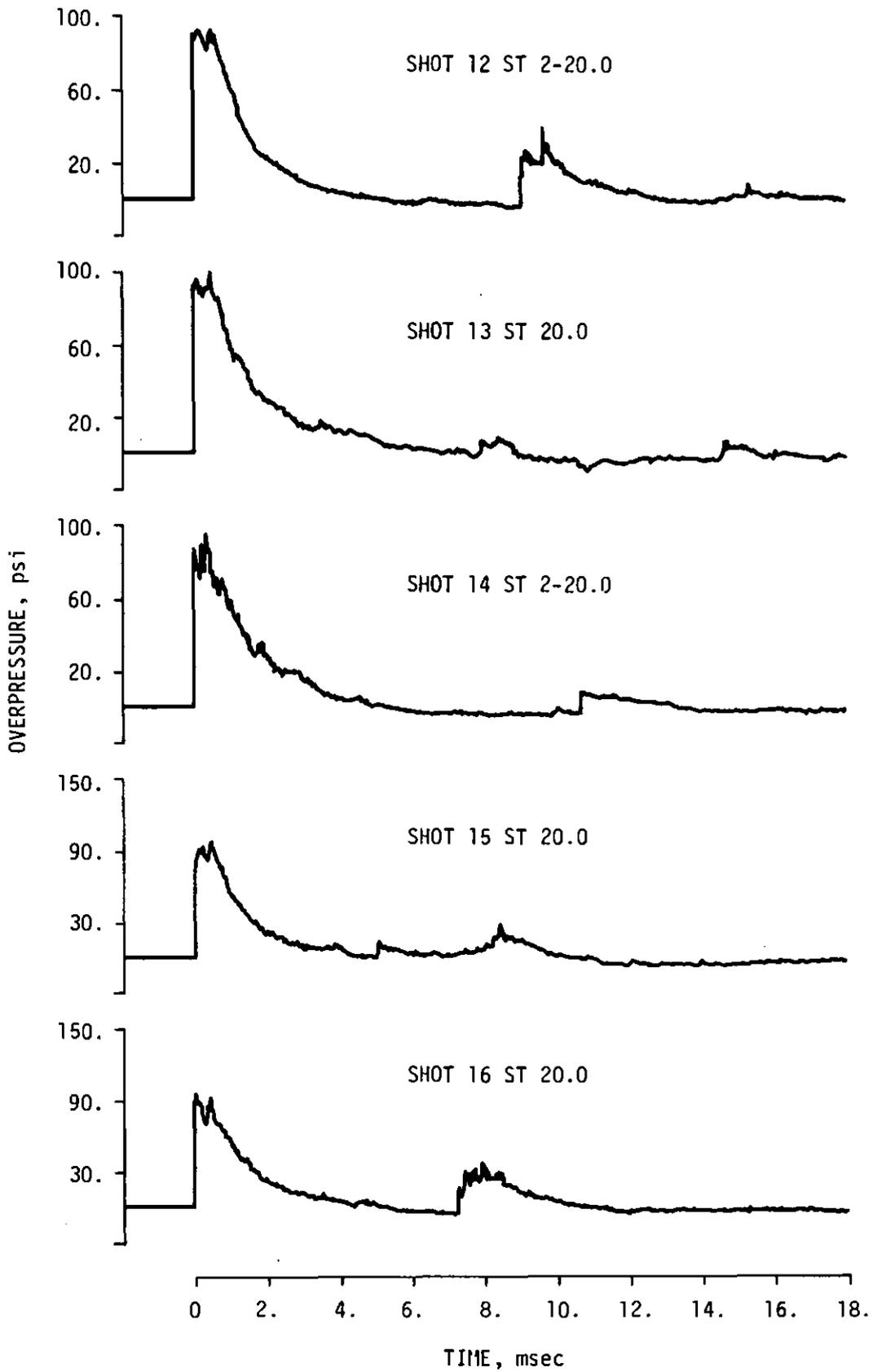


Figure 4.2. Overpressure Records at 20-Foot Ground Stations Showing Double Peak Phenomenon

the initial peak, occurring about a half millisecond later in time. This second peak may be compared to those discussed by Carpenter in Reference 7. According to Carpenter, secondary peaks of this type appear in the moderate to high overpressure regions beginning about 100 psi, near the transition between regular and Mach reflection. This is just the region in which the DIPOLE WEST 20-foot ground stations are located. A turbulent-like flow is associated with this region and is considered to be responsible for generating the second peak. The magnitude of this second peak is generally the same as or slightly larger than that of the initial peak in this pressure range. This phenomenon has been observed in shock tube as well as in field experiments (Reference 8).

4.3 Triple Point Paths

Preliminary analysis of photographic records has allowed triple point paths to be determined and Mach stem position-time curves to be plotted for some of the events. These results are discussed in the following paragraphs.

Mach stem position-time curves from Shot 12, measured near the ground surface and at the ideal reflecting plane, are compared in Figure 4.3. The curves are nearly identical, indicating very little drag occurred as a result of energy absorption at the real ground surface.

Figure 4.4 compares triple point paths above and below the ideal reflecting surface for Shot 12. The curves are again nearly identical, as they should be for this simultaneous detonation case. The slight difference may be due to a slight non-simultaneity in charge detonation times (thought to be less than 5 microseconds) or to small inaccuracies in charge positioning.

In Figure 4.5, the Shot 12 triple point paths are compared to those obtained from an earlier event in the DIPOLE WEST series, Shot 8. Shot 8, however, was fired with 1080-pound charges at heights of burst 24.5 and 74.3 feet. Scaling the Shot 8 data to 216-pound charges, the physical configuration should be identical to that for Shot 12. Correspondence of the Shot 8 and Shot 12 triple point paths is good but less

7. H.J. Carpenter and H.L. Brode, "Height of Burst at High Overpressure," R&D Associates, Marina del Rey, California - Paper presented at Fourth International Symposium on the Military Applications of Blast Simulation, 9-12 September 1974.

8. B.P. Bertrand, "Measurement of Pressure in Mach Reflection of Strong Shock Waves in a Shock Tube," BRL Memo Report 2196, USA Ballistics Research Laboratories, Aberdeen Proving Ground, Maryland 21005, June 1972. AD #746613.

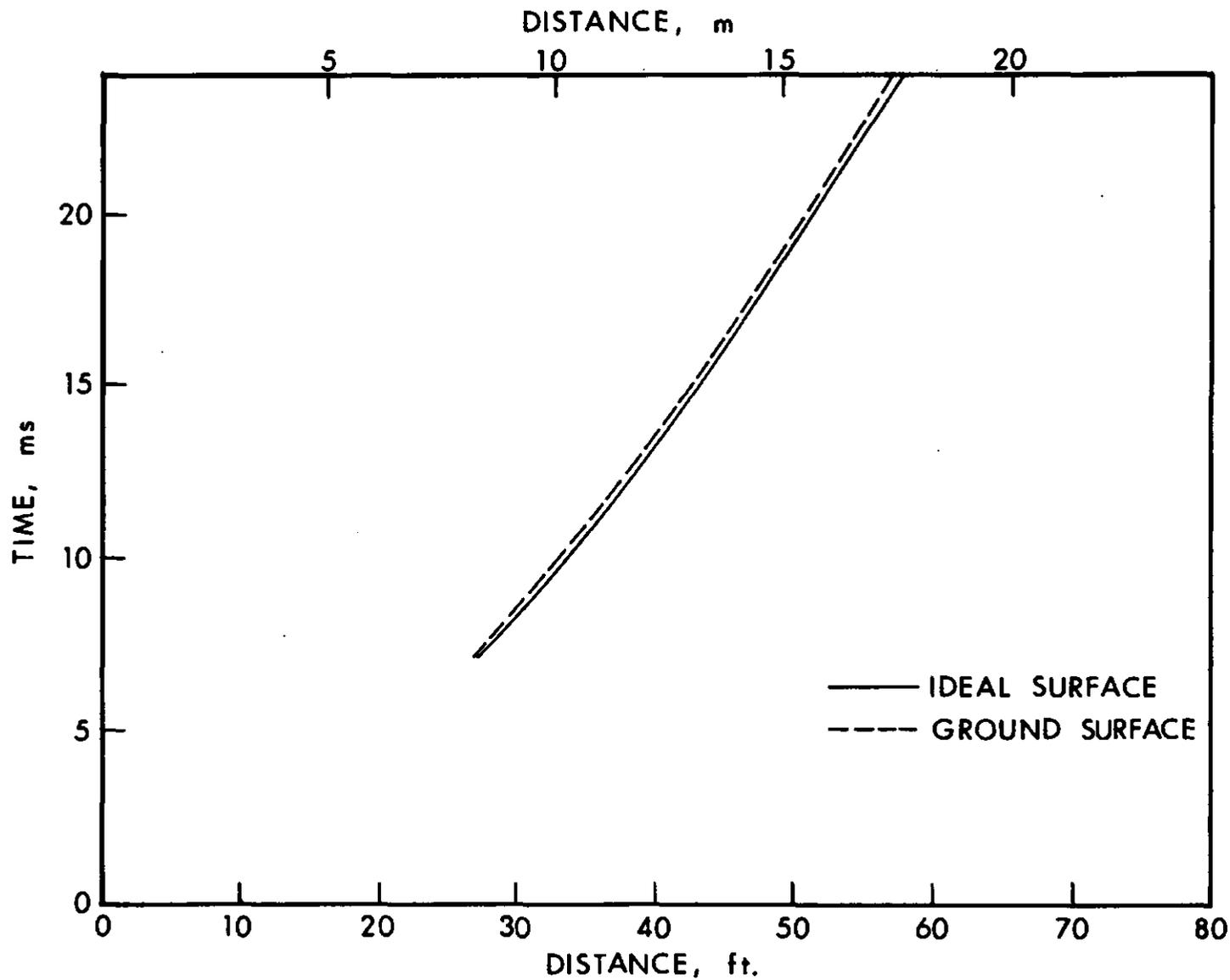


Figure 4.3. Comparison of Mach Stem Position-Time Curves at the Ideal Reflecting Plane and at the Ground Surface; Shot 12

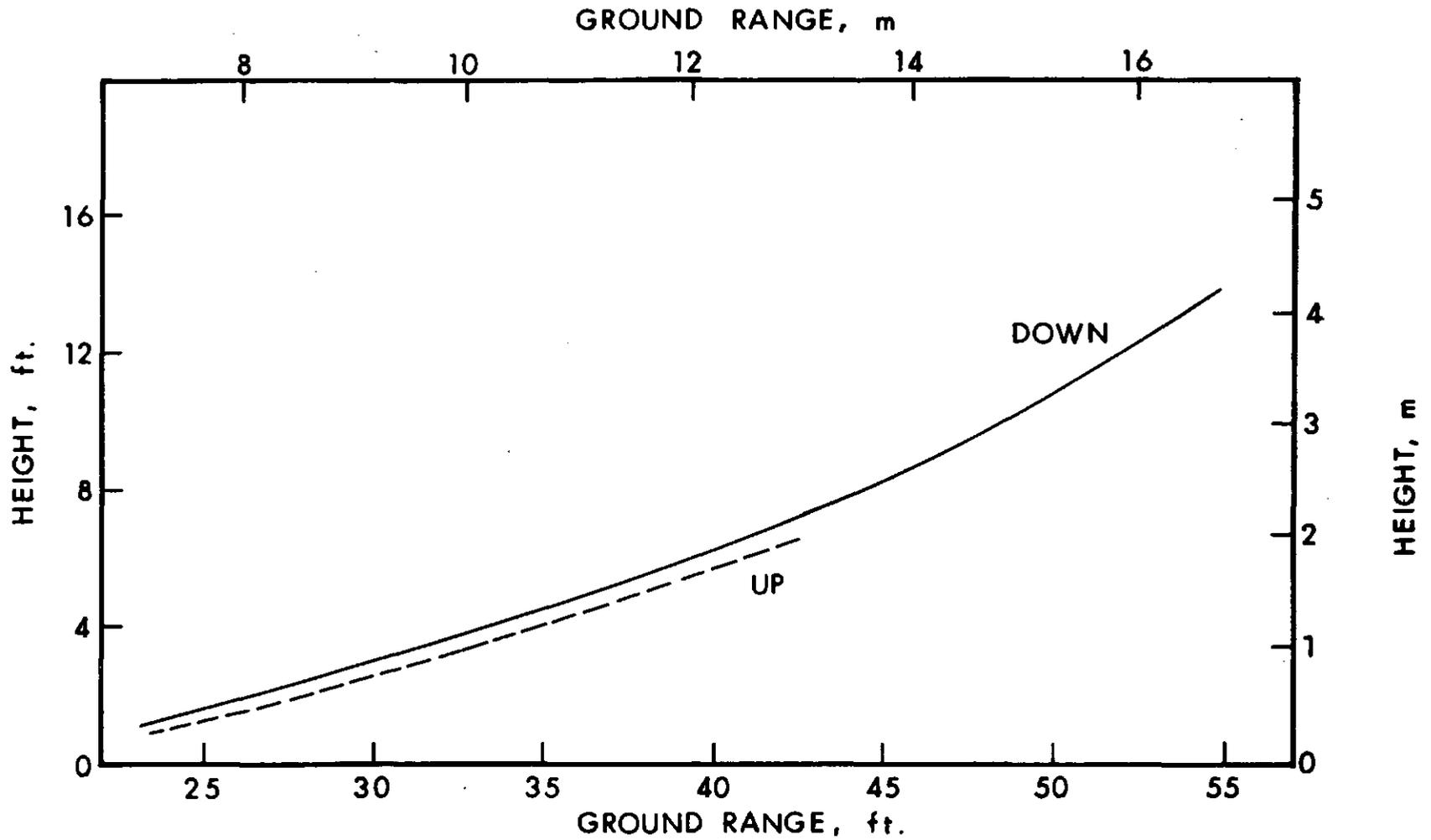


Figure 4.4. Comparison of Triple Point Paths Above and Below the Ideal Reflecting Plane; Shot 12

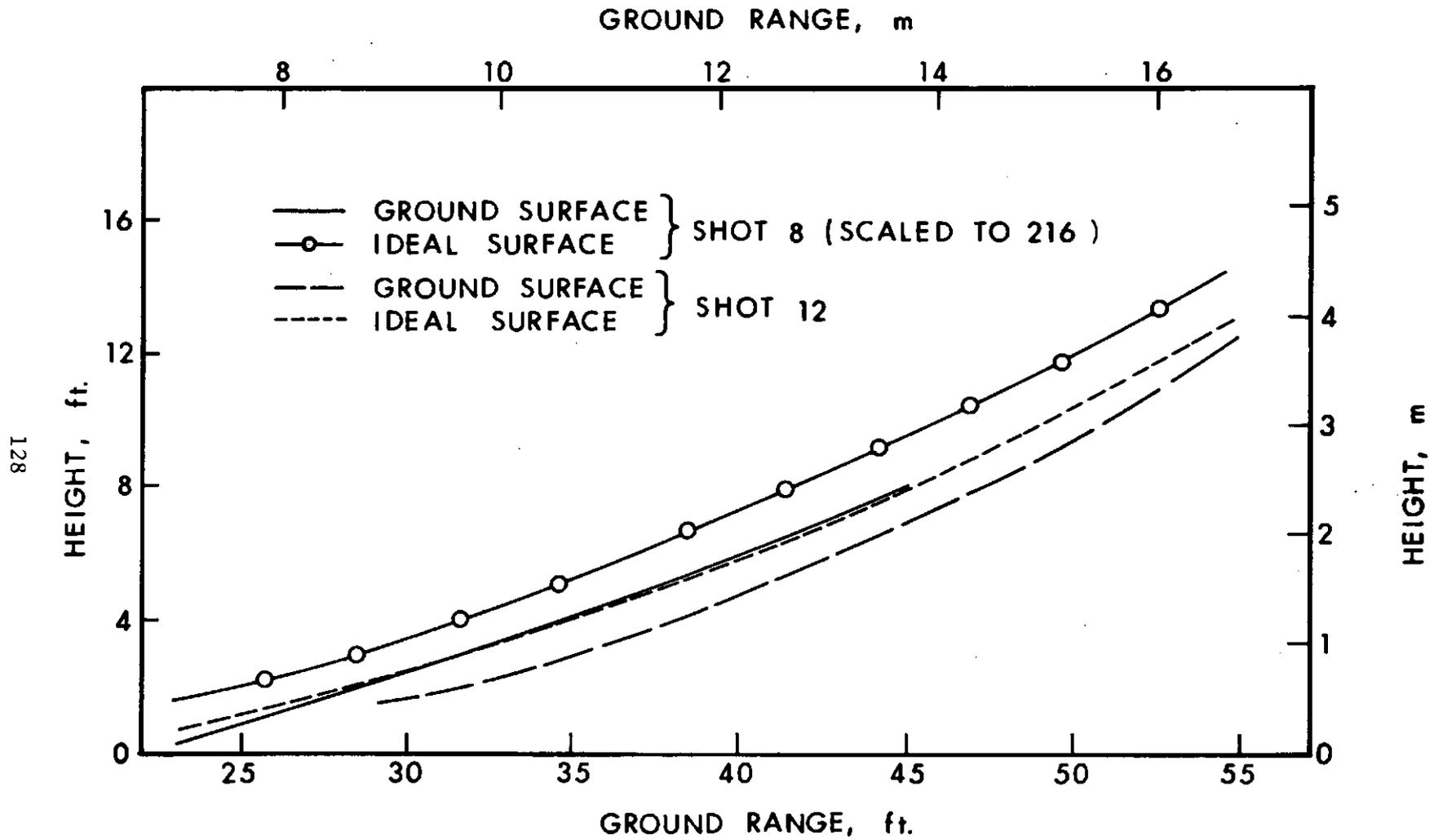


Figure 4.5. Triple Point Paths from Shot 12 Compared to Those from DIPOLE WEST Shot 8

than perfect. The difference may be due to imperfect physical correspondence of the shot configurations.

The Shot 12 triple point path arising from the ground surface is again compared in Figure 4.6. This time, comparison is with a similar triple point path generated by Shot 13. Shot 13 is the event for which delay time for detonation of the lower charge was 10 milliseconds. The shock wave from the upper charge had engulfed the lower charge before it was detonated. Differences between the Shot 12 and Shot 13 triple point paths are therefore due to the fact that the lower charge shock in Shot 13 was generated in an already disturbed medium and overtook the upper charge shock before being reflected from the ground (and hence forming a triple point). Figure 4.7 is a comparison of Mach stem position in time as a function of range for the same two events.

Figures 4.8 and 4.9 are sketches of predicted triple point paths as obtained from the HULL calculations for Shots 15 and 16, respectively. Note that for Shot 15, in which the detonation time delay was 5 milliseconds, the triple point paths are highly distorted from the simultaneous case configuration. The triple point path below the reflection plane is uncertain; the data from the calculation was very difficult to ascertain. Those predicted for Shot 16, for which the time delay was 3 milliseconds, look very similar to those generated by simultaneous detonations. In neither case do the photographic results agree very well with the calculations, and further work is required to resolve this discrepancy.

4.4 Comparison of Experimental and Calculated Results

In Section 1.2 it was pointed out that hydrocode (HULL) calculations had predicted that a delay in detonation of the lower charge by 10 milliseconds or more would alter shock interactions to the extent that a Mach stem would not be formed at the reflection plane between charges. It was also mentioned that determination of whether or not this was the case was one of the objectives of this study. Figures 4.10 through 4.13 are calculated pressure contour plots which illustrate this behavior. In Figures 4.10 and 4.11, from the 3-millisecond time separation case, a well defined Mach stem can be seen forming both at the ground and at the reflection plane between charges (note that in these plots distances are measured in meters rather than in feet). In Figures 4.12 and 4.13, however, which are plotted at identical times after detonation of the lower charge for the 10-millisecond time separation case, although the ground level Mach stem forms as before, behavior at the upper reflection region does not show this development.

This effect is also illustrated in Figure 4.14, in which overpressure waveforms recorded at Station 50.0S are shown. The waveforms

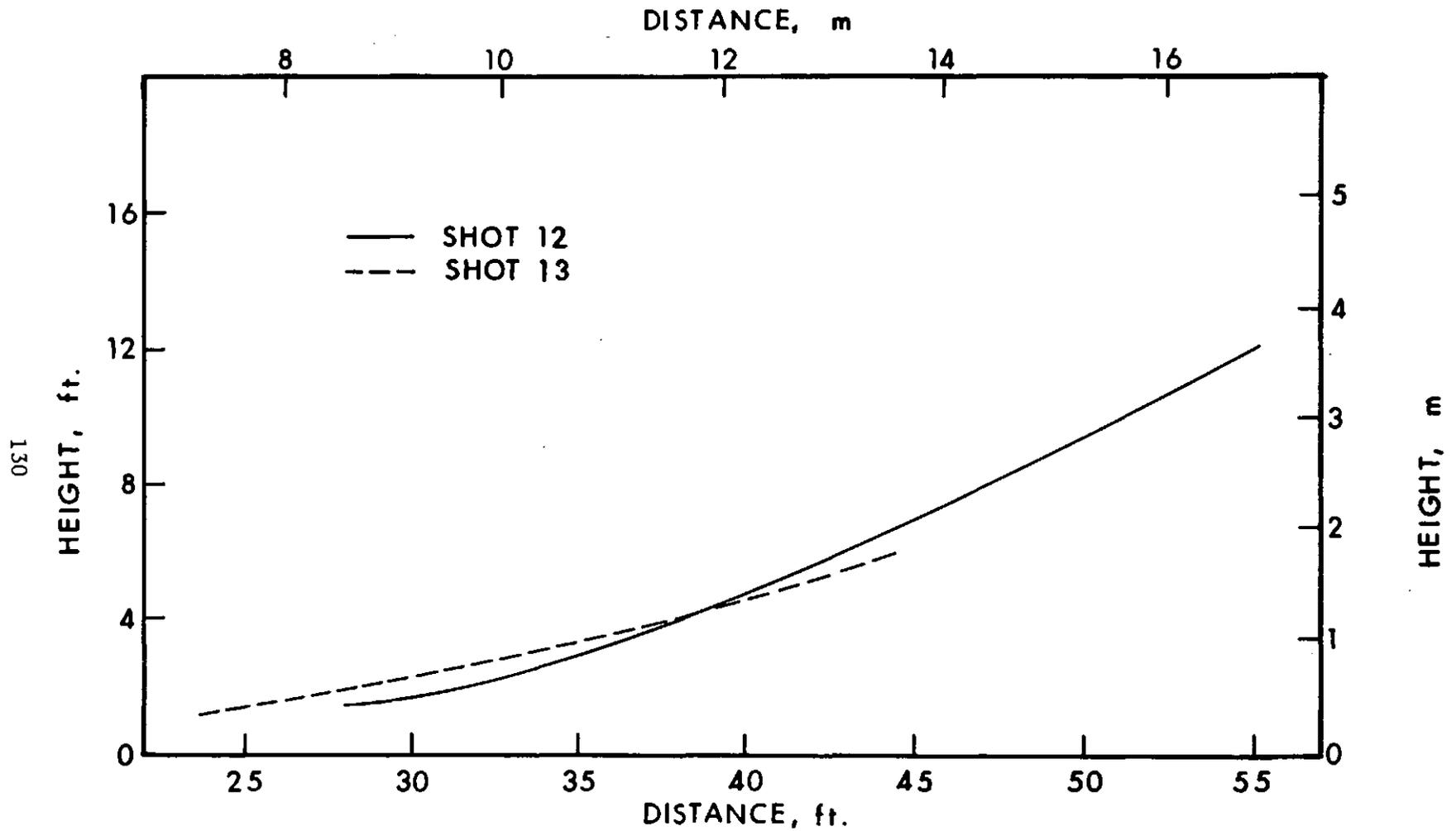


Figure 4.6. Comparison of Triple Point Paths Above the Ground Surface for Shots 12 and 13

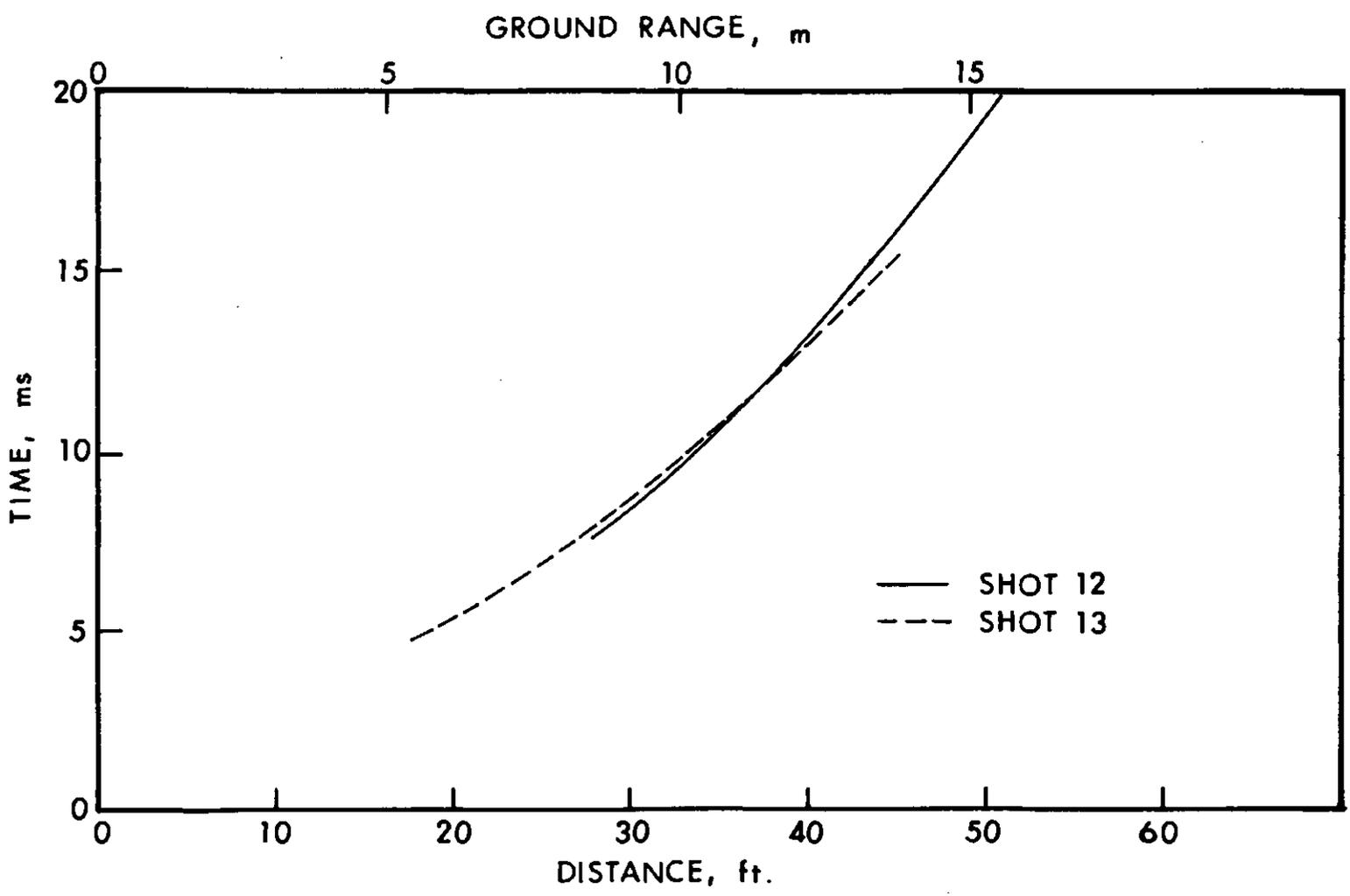


Figure 4.7. Comparison of Mach Stem Position-Time Curves for Shots 12 and 13

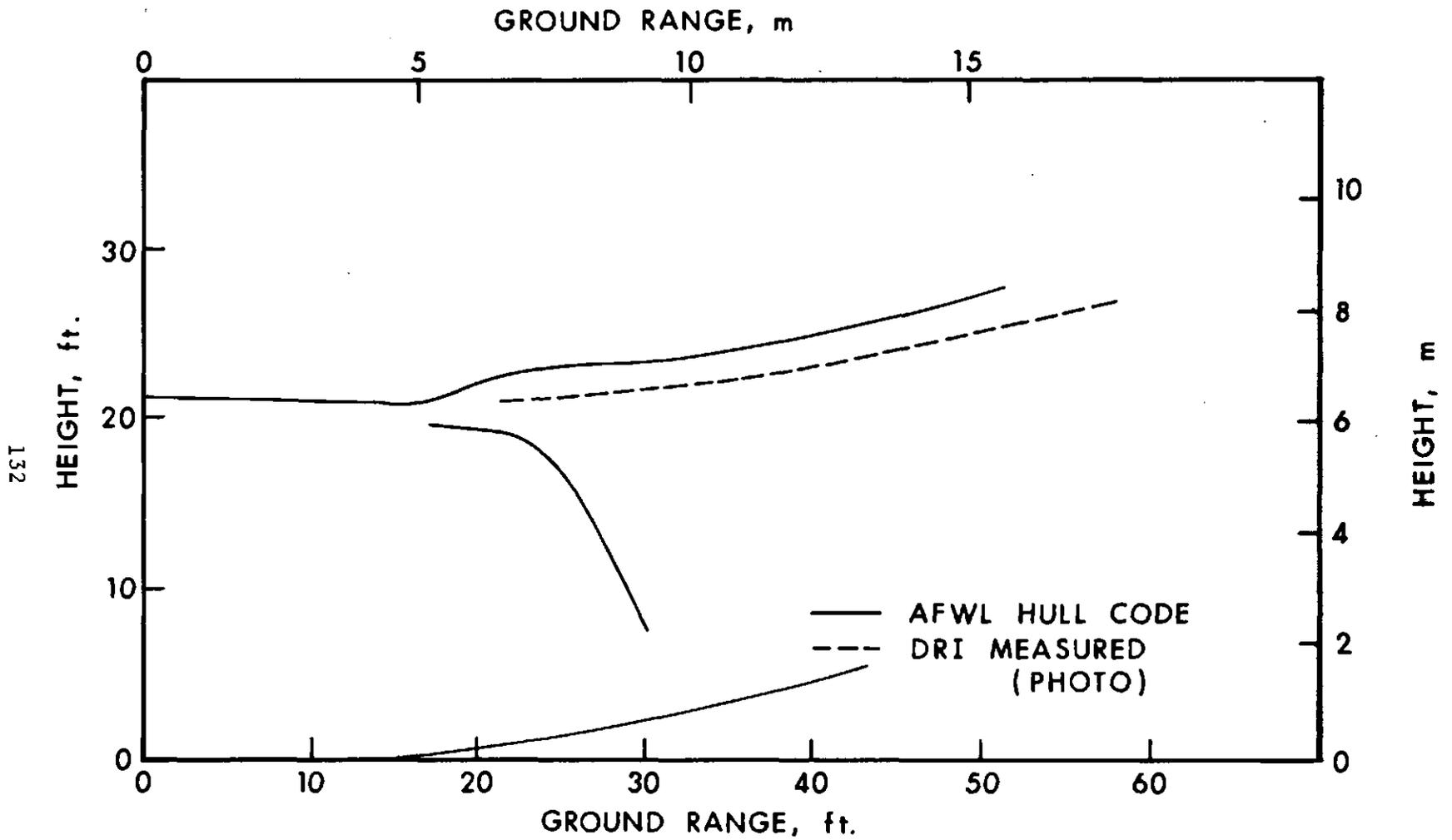


Figure 4.8. Calculated and Measured Triple Point Paths; Shot 15

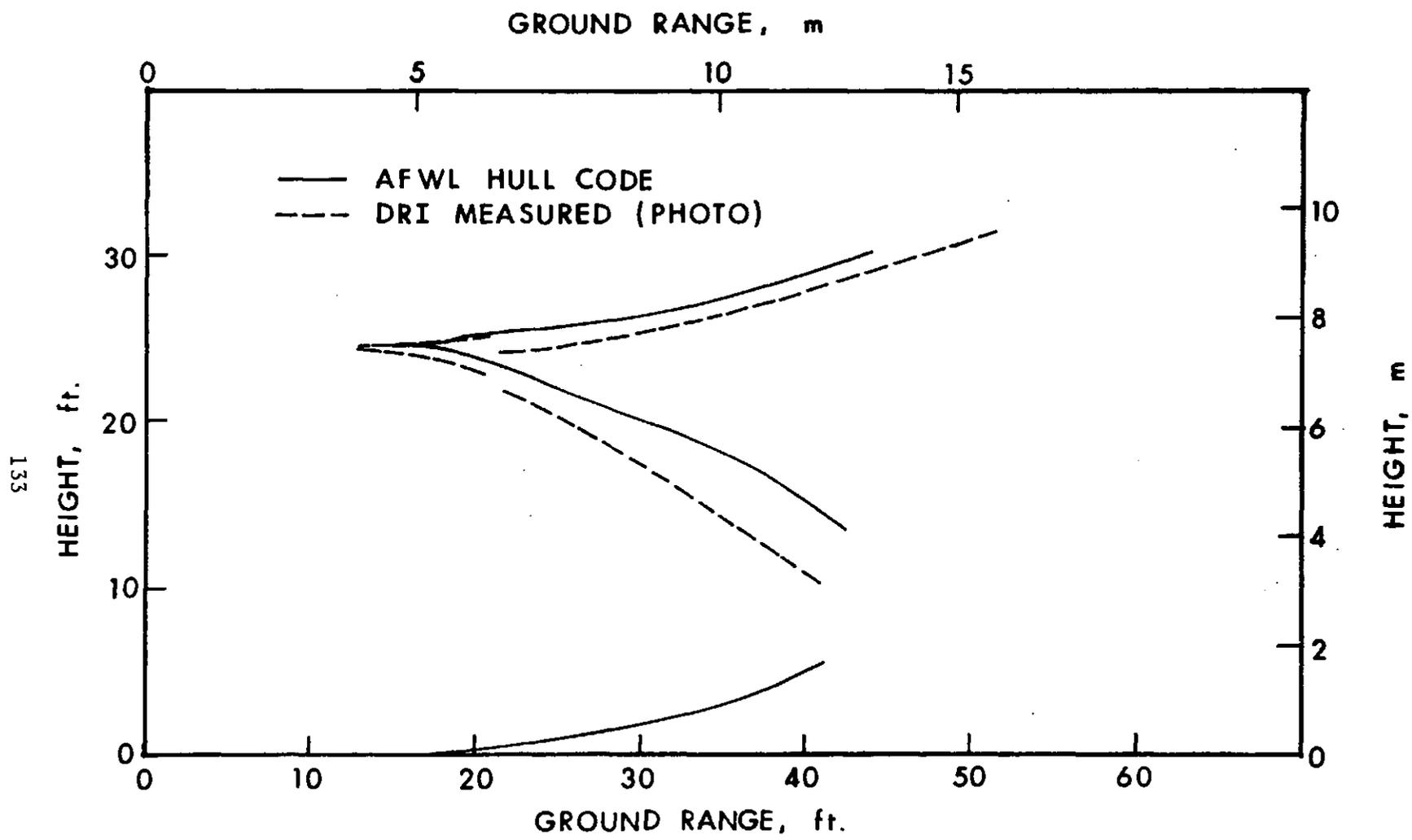


Figure 4.9. Calculated and Measured Triple Point Paths; Shot 16

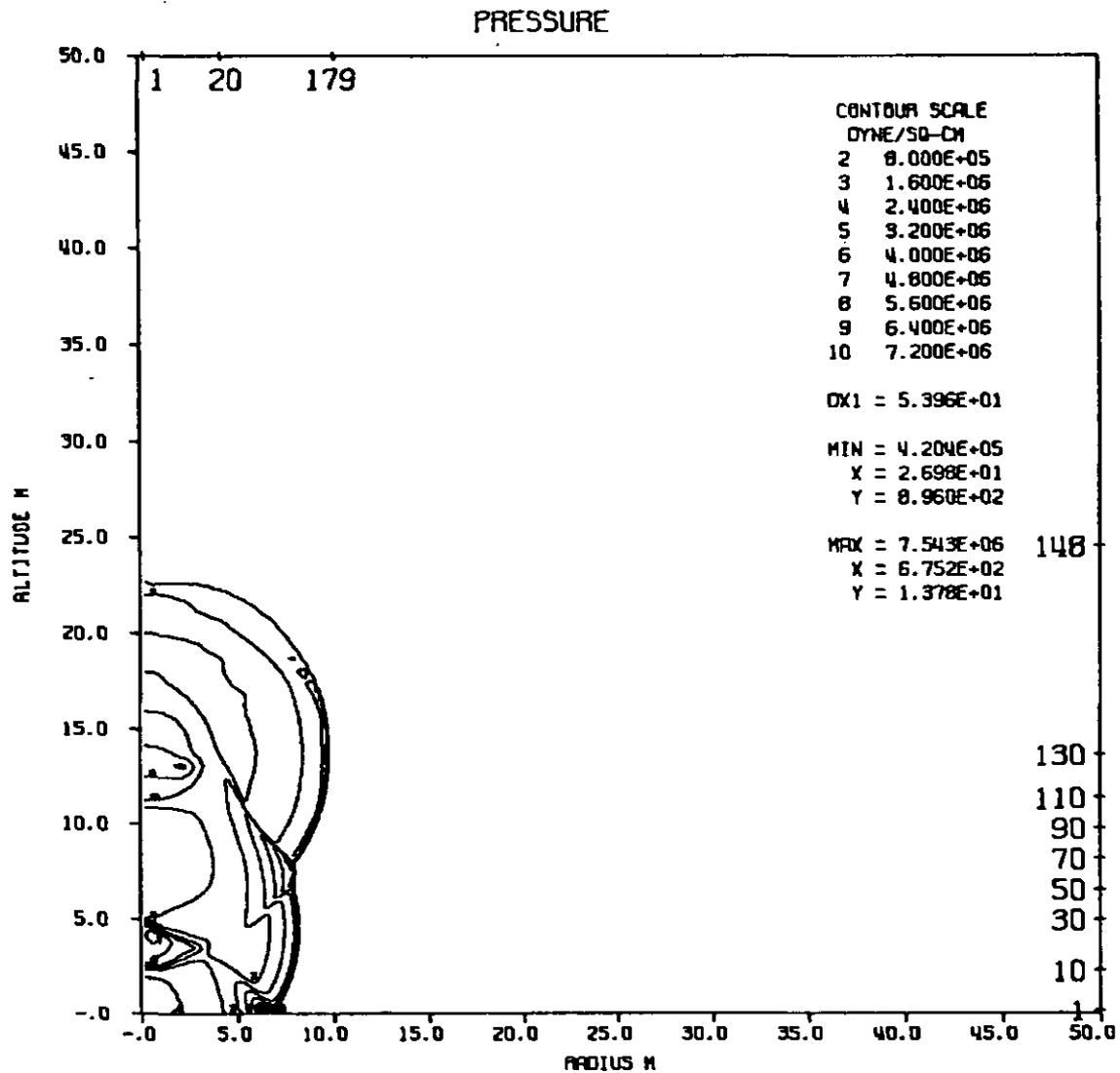


Figure 4.10. Pressure Contours from AFWL HULL Three Millisecond Delay Calculation at Seven Milliseconds After Detonation of the Lower Charge

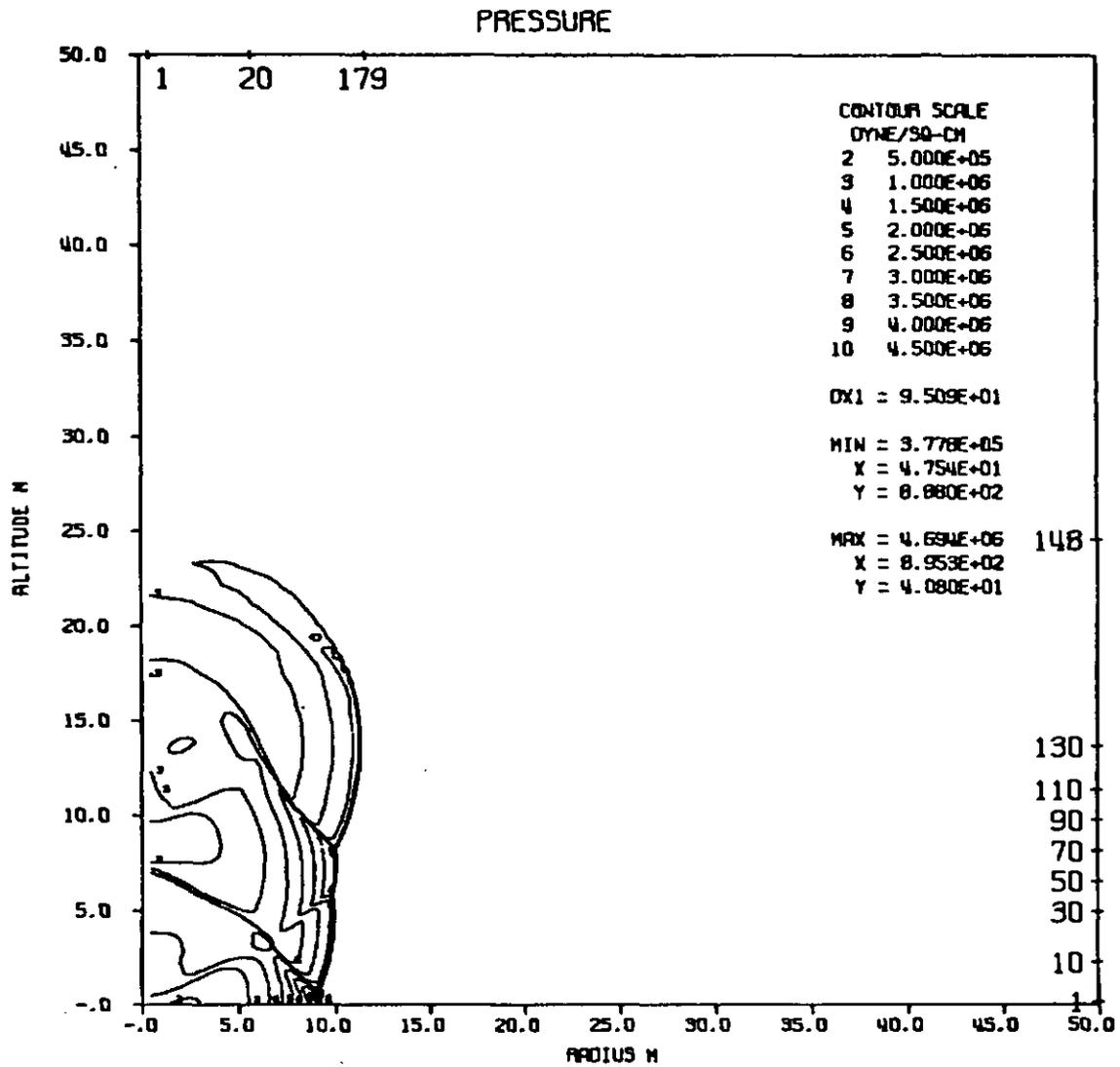


Figure 4.11. Pressure Contours from AFWL HULL Three Millisecond Delay Calculation at Ten Milliseconds After Detonation of the Lower Charge

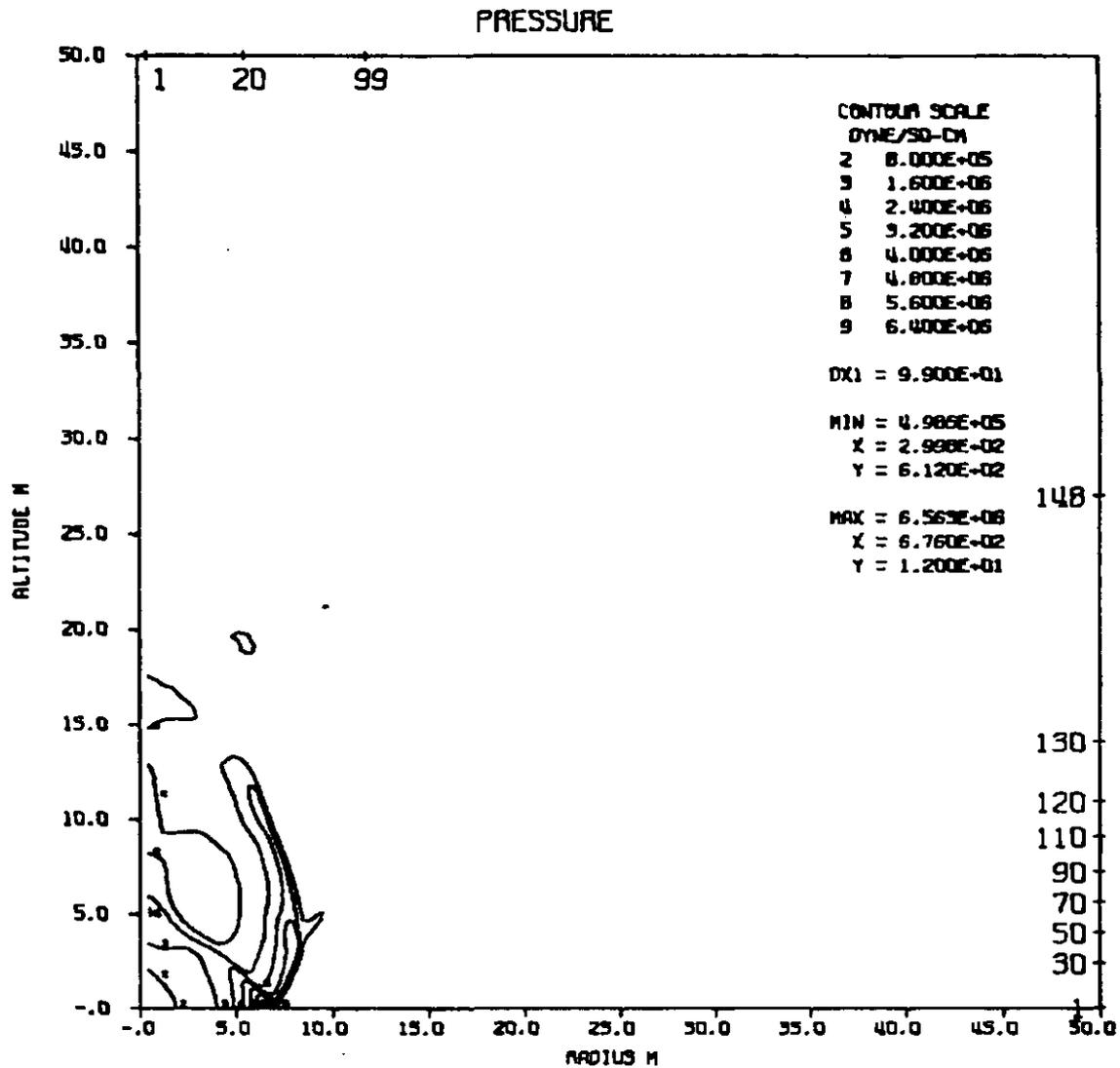


Figure 4.12. Pressure Contours from AFWL HULL Ten Millisecond Delay Calculation at Seven Milliseconds After Detonation of the Lower Charge

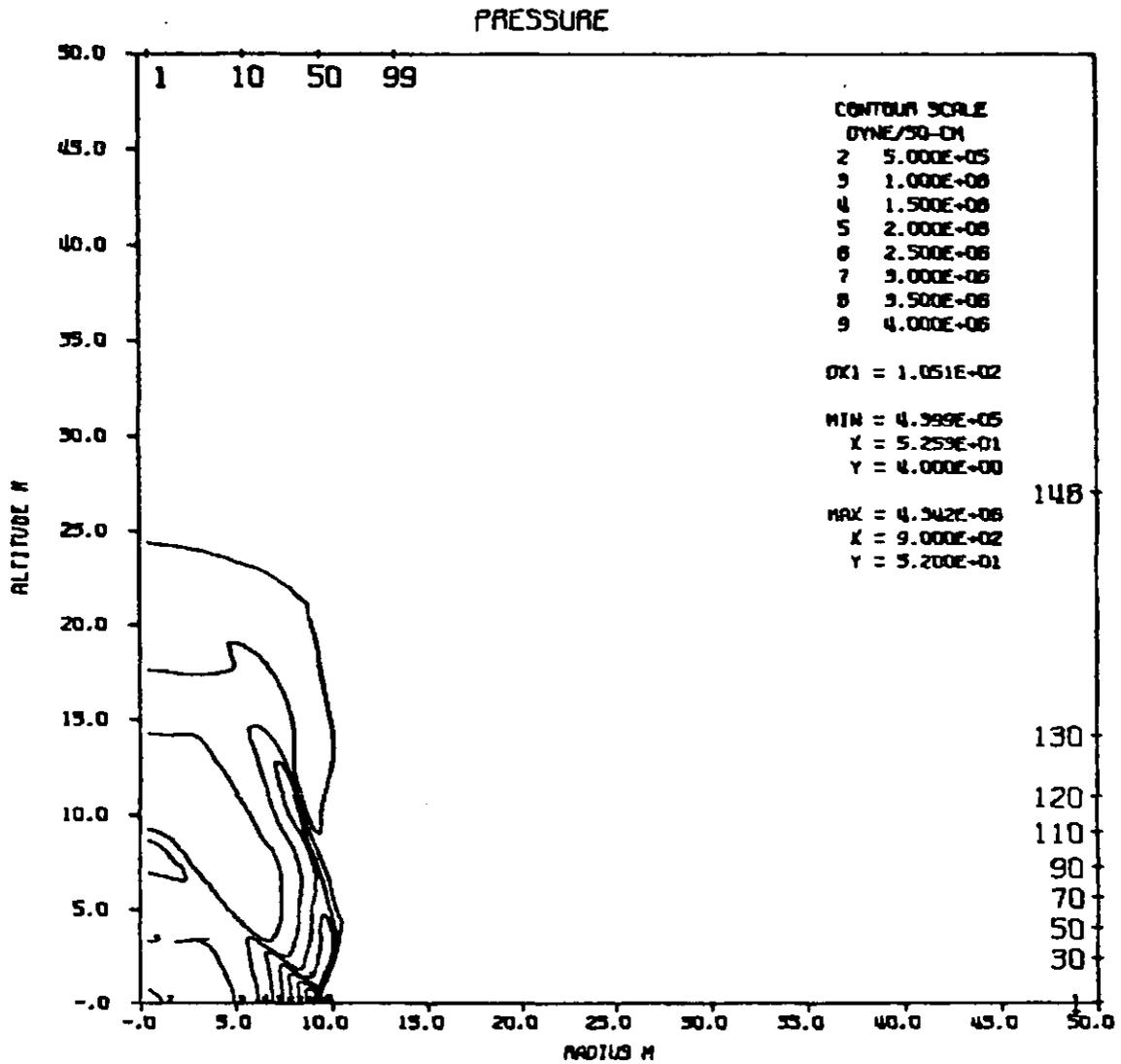


Figure 4.13. Pressure Contours from AFWL HULL Ten Millisecond Delay Calculation at Ten Milliseconds After Detonation of the Lower Charge

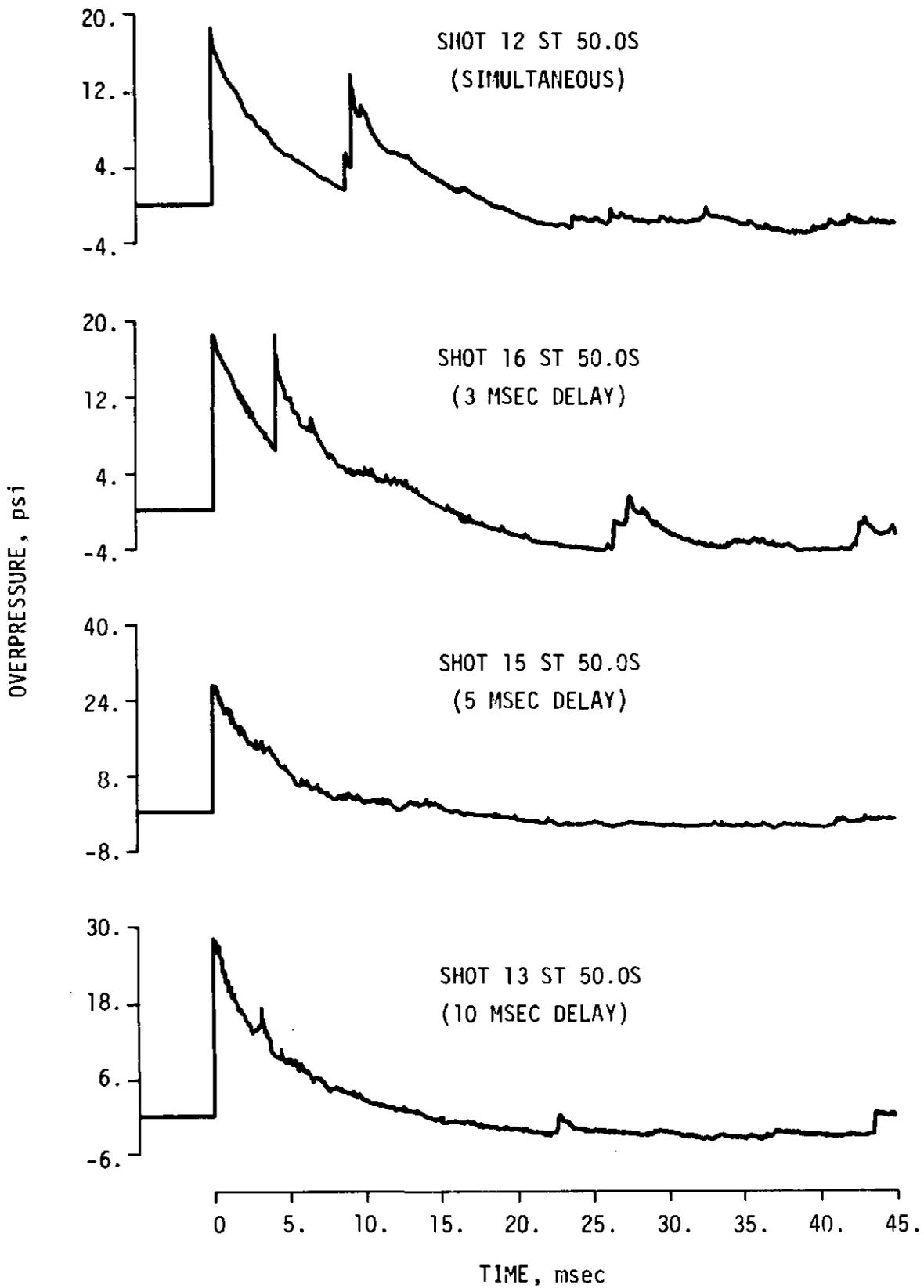


Figure 4.14. Overpressure Records at the South 50-Foot Ground Station Showing Differences Caused by Varying Detonation Delay Time

for the simultaneous and three-millisecond delay cases exhibit a well-defined second peak which may be attributed to the Mach stem from the ideal reflecting surface. Waveforms from the five- and ten-millisecond delay events, however, show no such secondary peaks.

Comparisons between calculated results and experimental data for all of the event configurations are given in Figures 4.15 through 4.24. Information for these comparisons was taken directly from the tables of Sections 2.3 (calculations) and 3.4 (experiment) except in the case of Shot 12, the simultaneous detonation, for which the HULL results were scaled from an earlier calculation, and Shot 14, the single detonation, for which tabulated HULL results have not been included. Overpressure, arrival time, and overpressure impulse comparisons are made at ground level and at elevations of 3, 10, 20, and 30 feet. Positive phase duration comparisons are made only at ground level. Unfortunately, the Shot 16 (3 ms. non-simultaneity) calculation did not print out ground level station information. This is, however, the only calculation from which information at the 20- and 30-foot levels is available.

Comparison indicates quite good agreement between calculation and experiment. In the case of arrival times, agreement is typically excellent, and experimental data points fall almost exactly on the curve calculated for the particular configuration and non-simultaneity of the event. For the other parameters, correspondence is not so precise although it is still quite good. Shot-to-shot differences are not large enough, in either the calculated or experimental results, to definitely associate a given calculation with a given set of data. All data and calculations fall within a "reasonable" band, and there is not enough experimental data to determine whether kinks in the calculated curves are real or are figments of the calculations.

4.5 Comparison With Other HE Data

In Section 4.3, a comparison was made between triple point paths from Shot 12, the simultaneously detonated event, and Shot 8, an earlier event from the DIPOLE WEST series for which the physical configuration was directly scalable. In Figure 4.25, air blast parameters at ground level from the same two events are compared. This time, the Shot 12 results have been scaled up to the 1080-pound charges of Shot 8. Correspondence of air blast parameters between the two events is excellent.

Sachs scaling factors appropriate for reducing the results from events of this series to the reference standard one-pound charge at sea level are given in Table 4.1. These factors take into account actual ambient pressures and temperatures measured at the site at shot times.

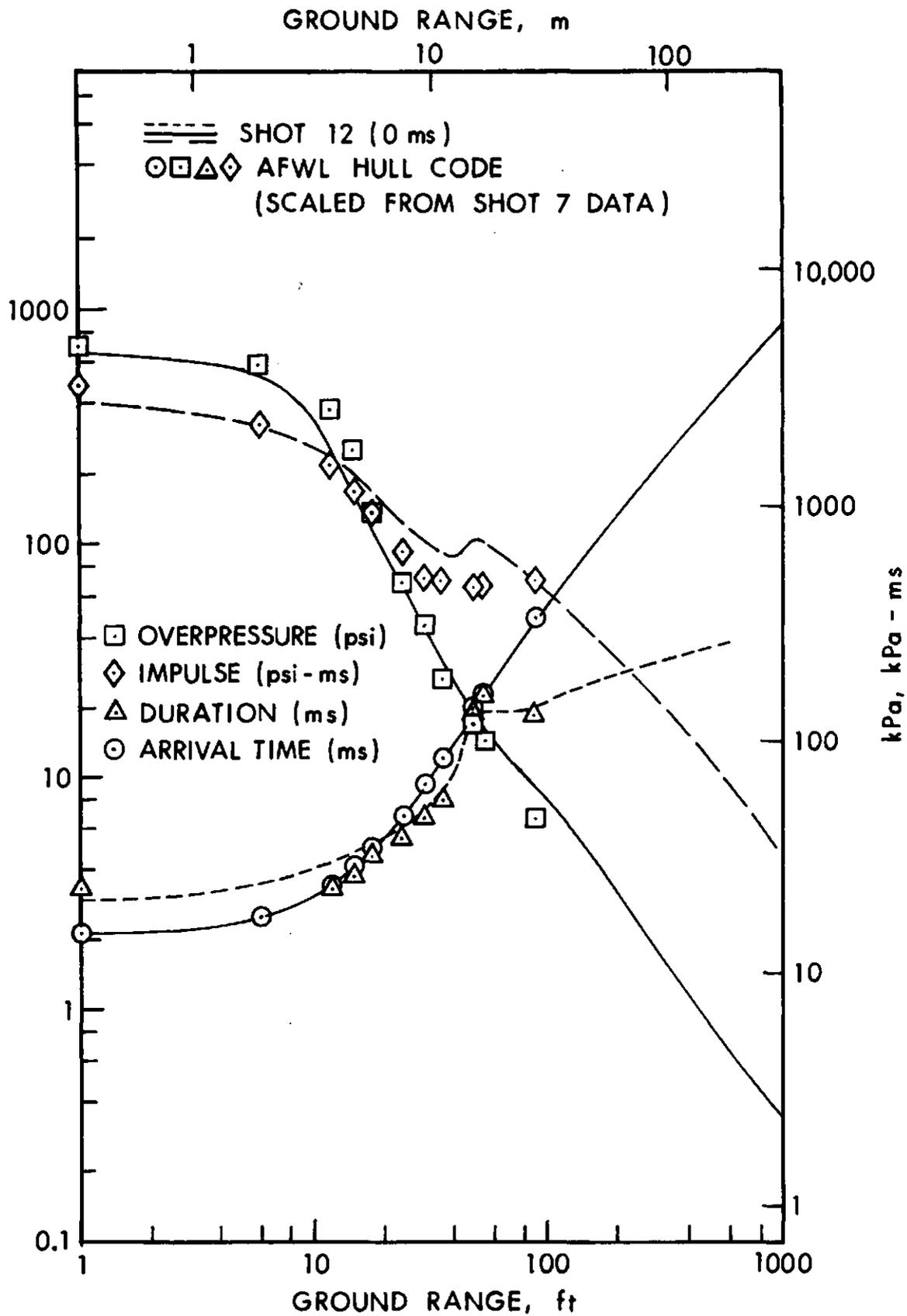


Figure 4.15. Comparison Between Calculated and Experimental Air Blast Parameters at Ground Level; Shot 12

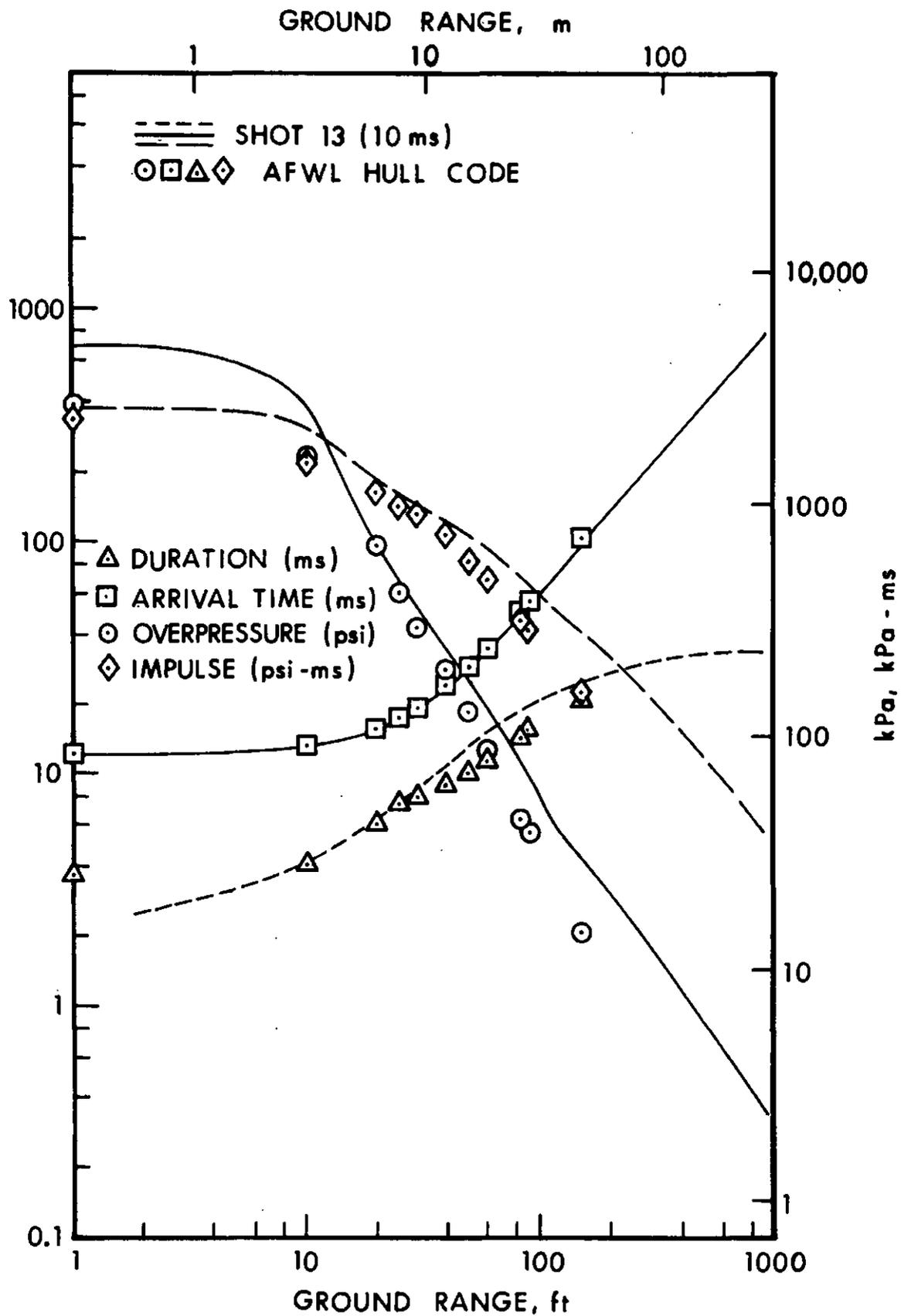


Figure 4.16. Comparison Between Calculated and Experimental Air Blast Parameters at Ground Level; Shot 13

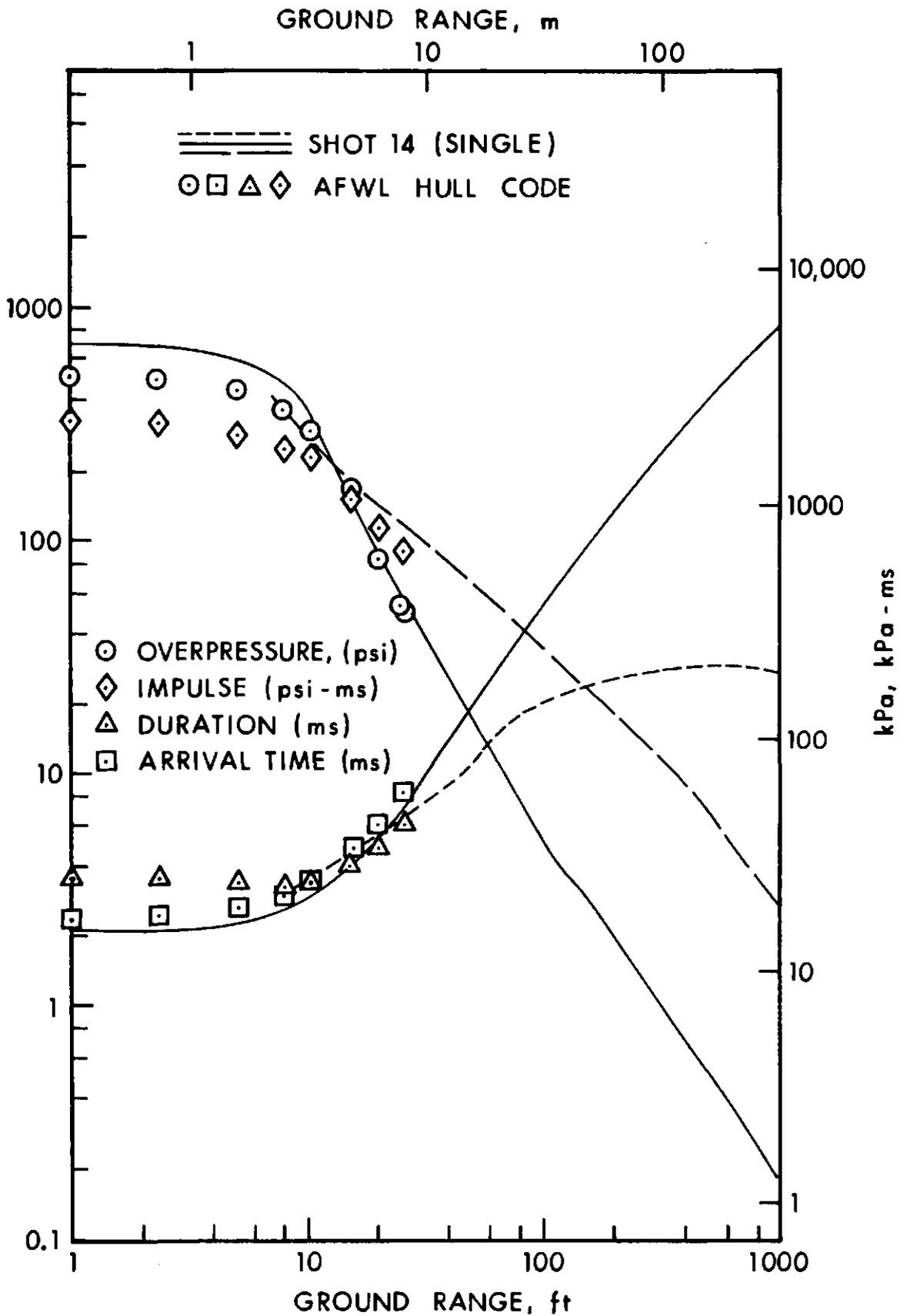


Figure 4.17. Comparison Between Calculated and Experimental Air Blast Parameters at Ground Level; Shot 14

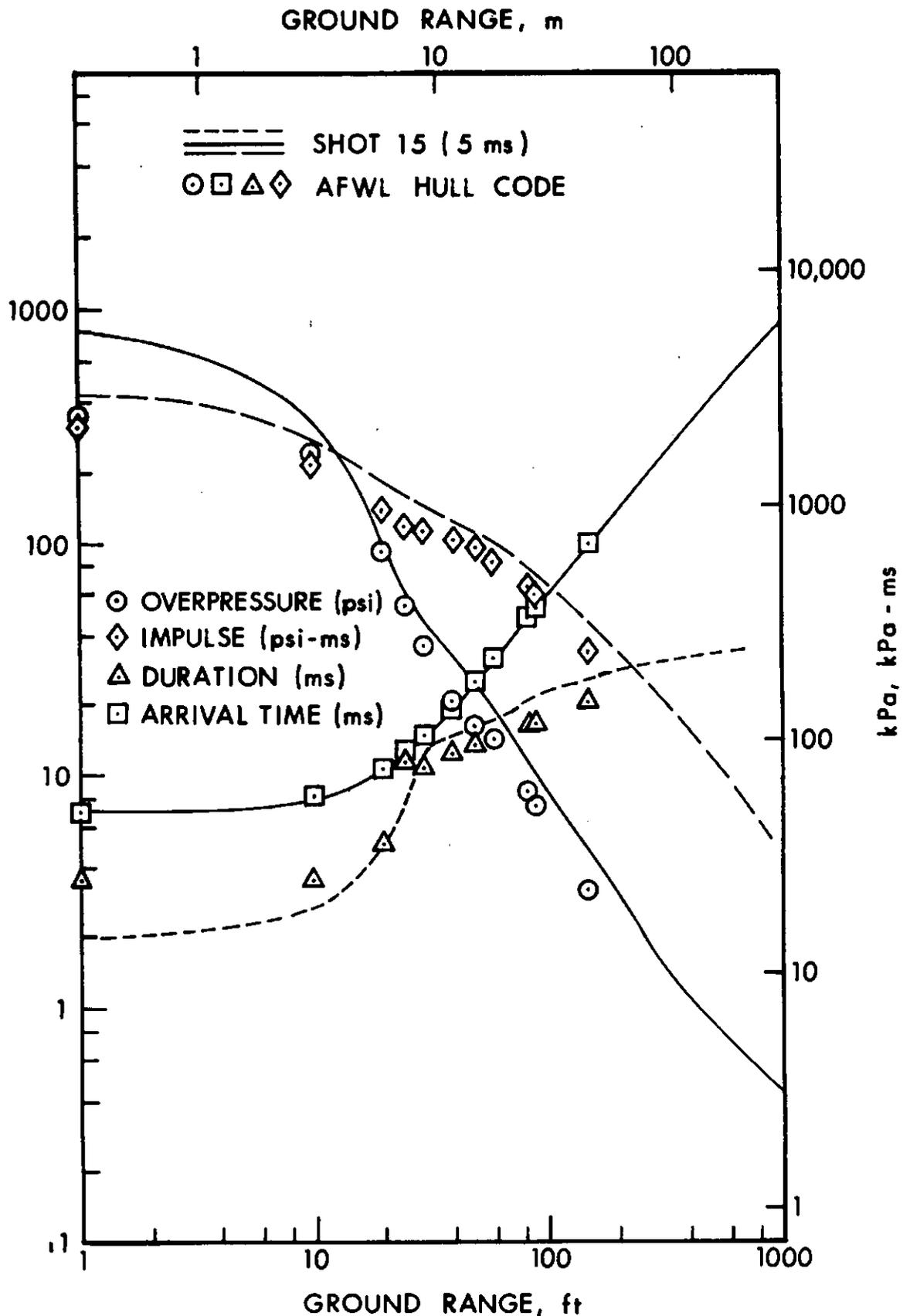


Figure 4.18. Comparison Between Calculated and Experimental Air Blast Parameters at Ground Level; Shot 15

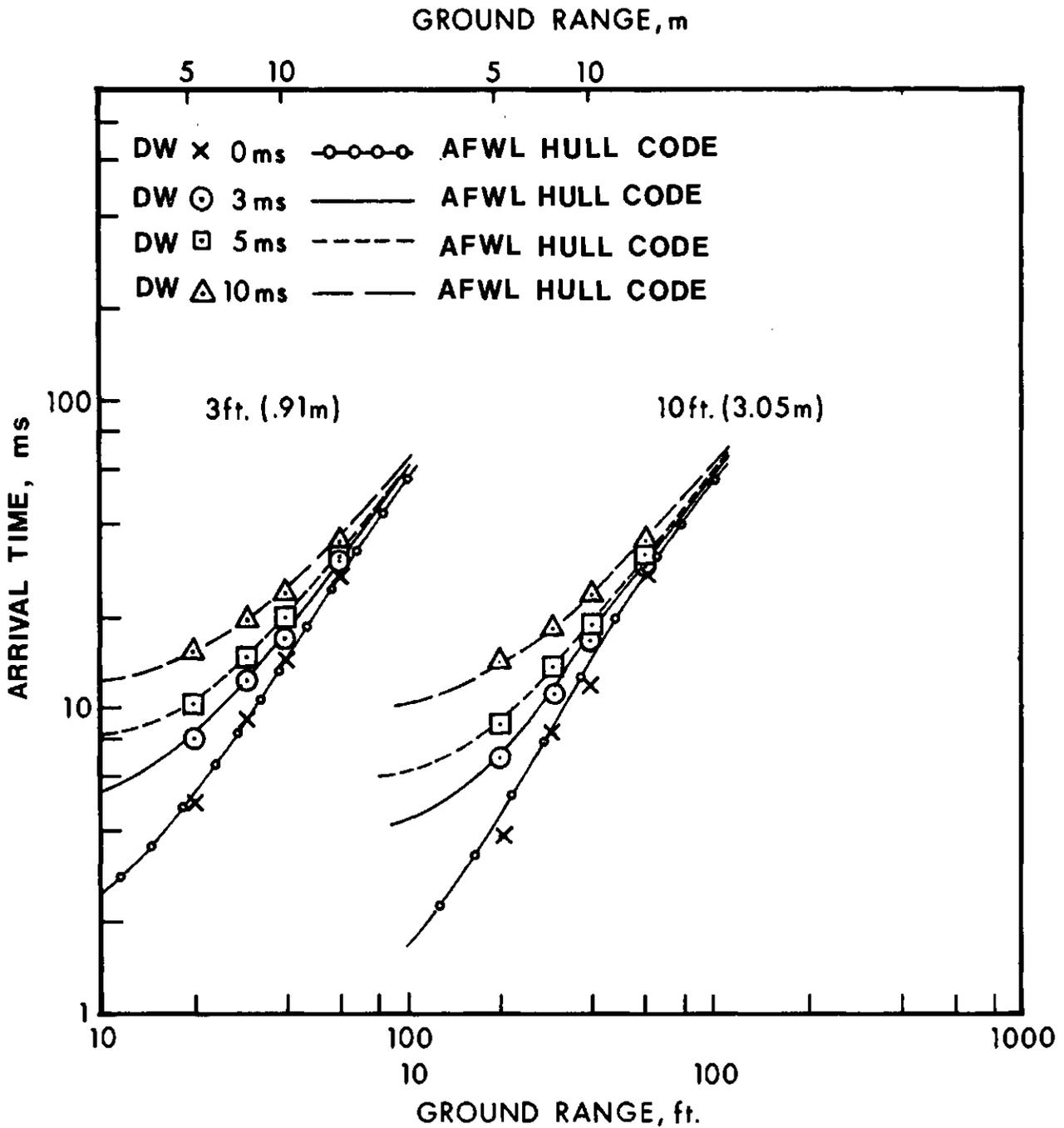


Figure 4.19. Comparison Between Calculated and Experimental Arrival Times at 3 and 10 Feet Above Ground

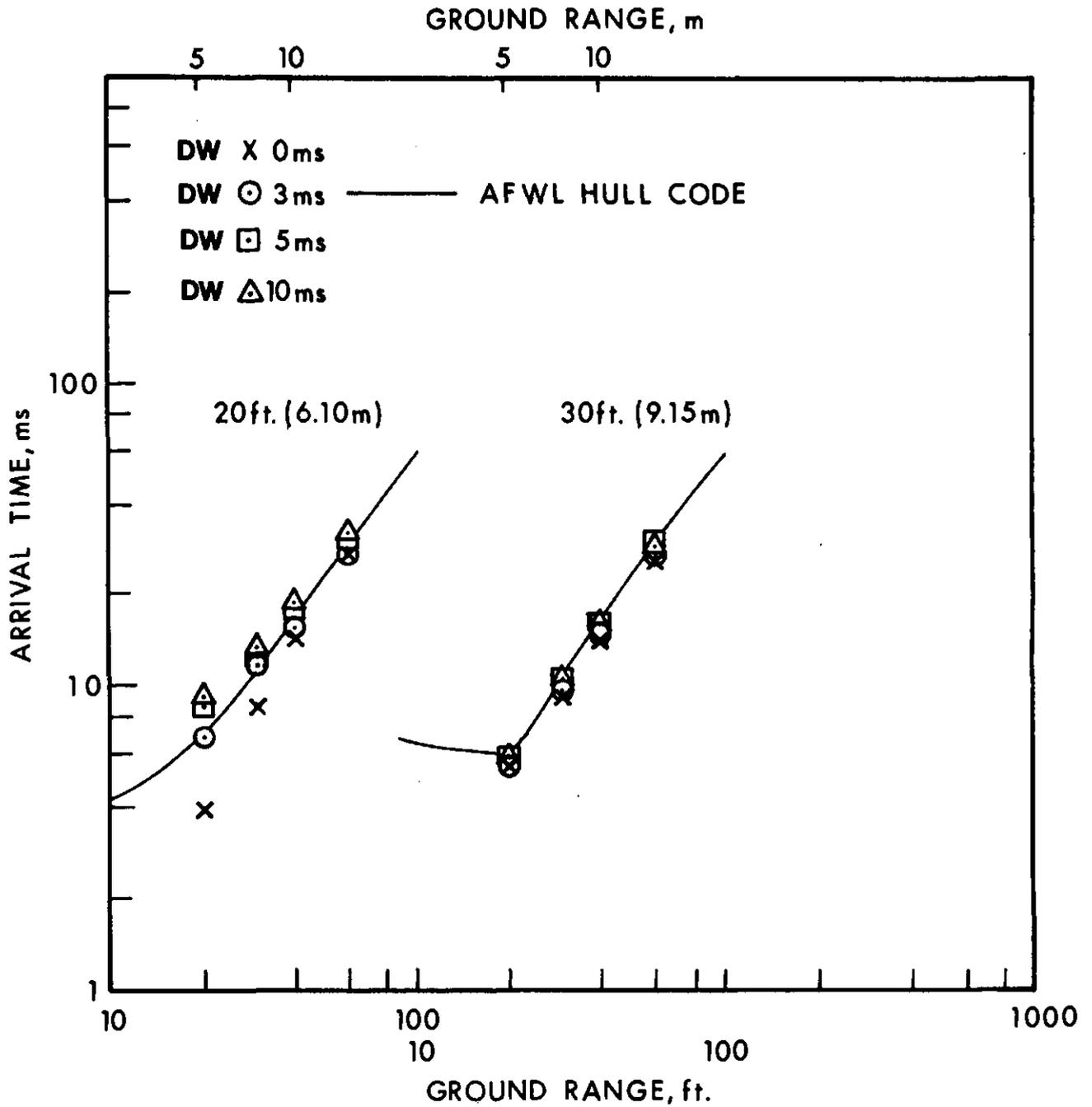


Figure 4.20. Comparison Between Calculated and Experimental Arrival Times at 20 and 30 Feet Above Ground

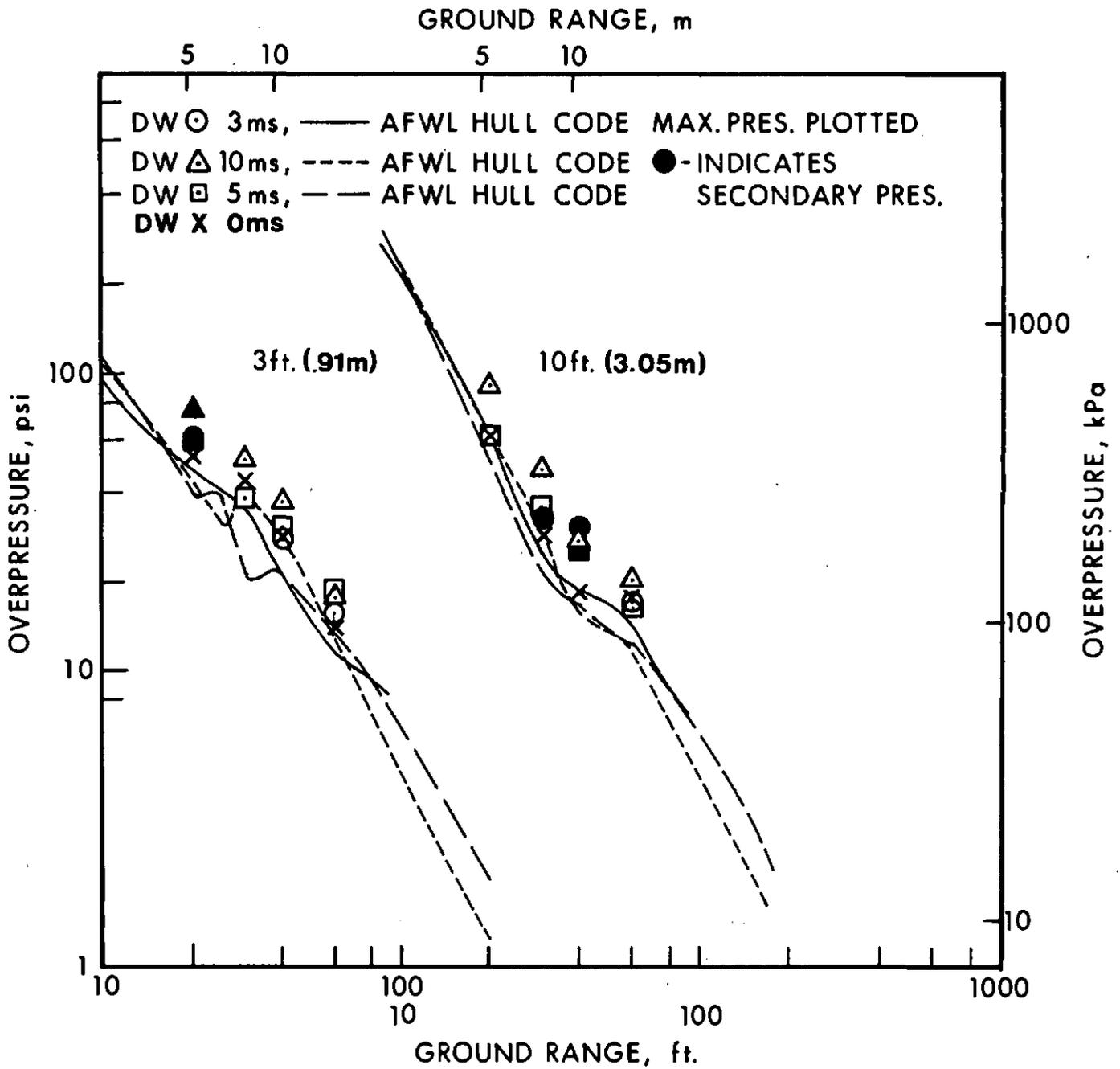


Figure 4.21. Comparison Between Calculated and Experimental Overpressures at 3 and 10 Feet Above Ground

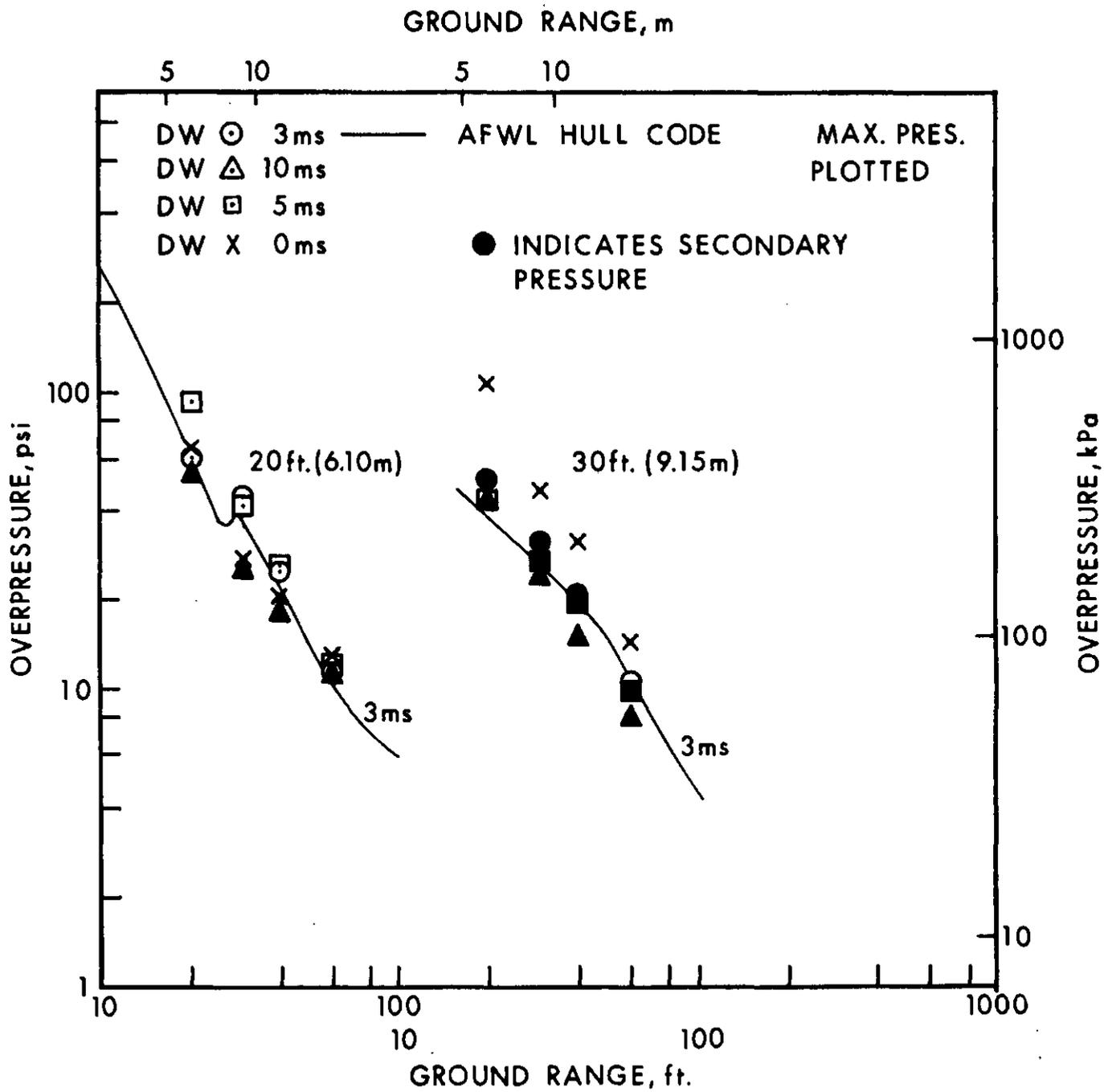


Figure 4.22. Comparison Between Calculated and Experimental Overpressures at 20 and 30 Feet Above Ground

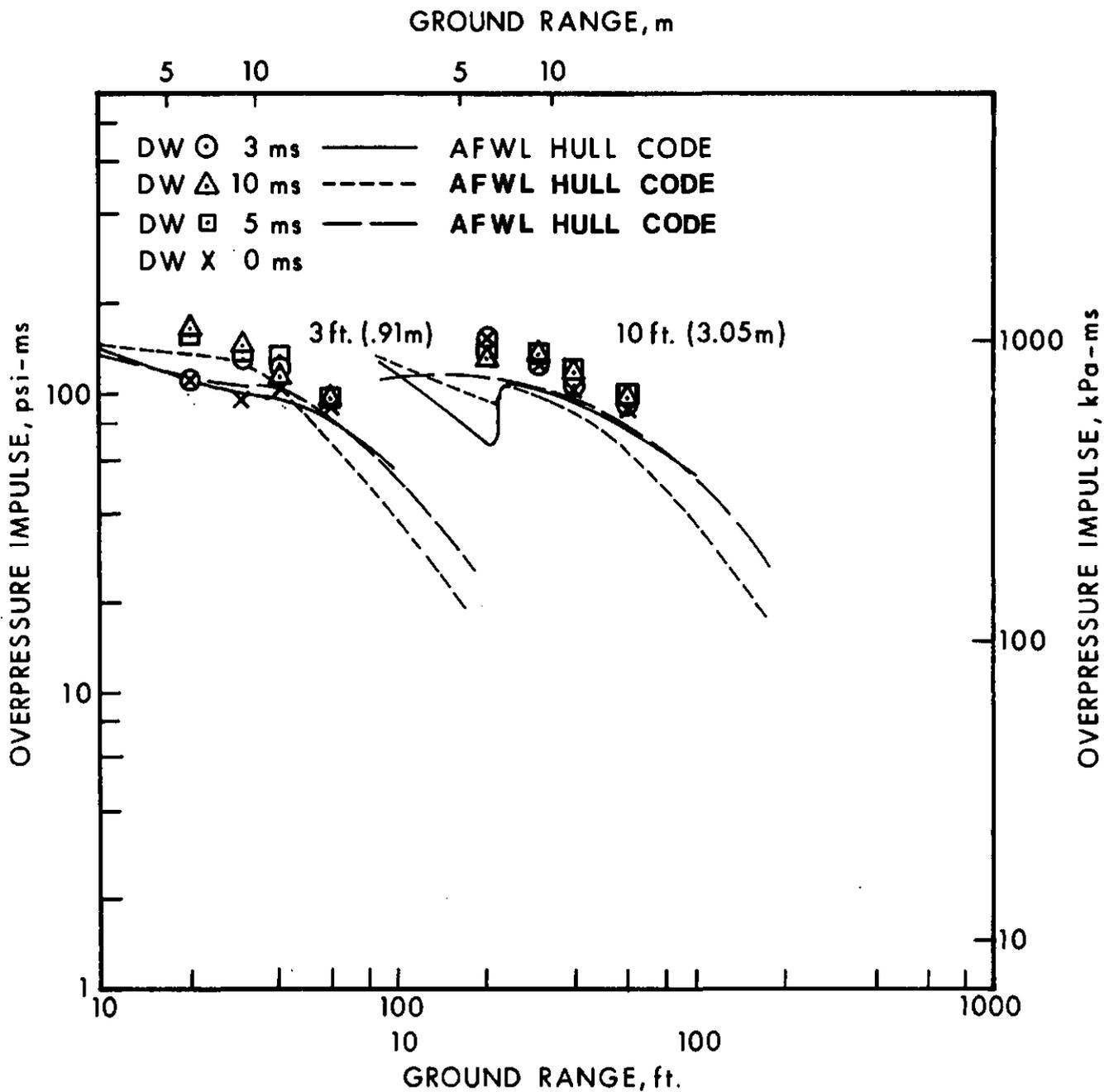


Figure 4.23. Comparison Between Calculated and Experimental Overpressure-Impulses at 3 and 10 Feet Above Ground

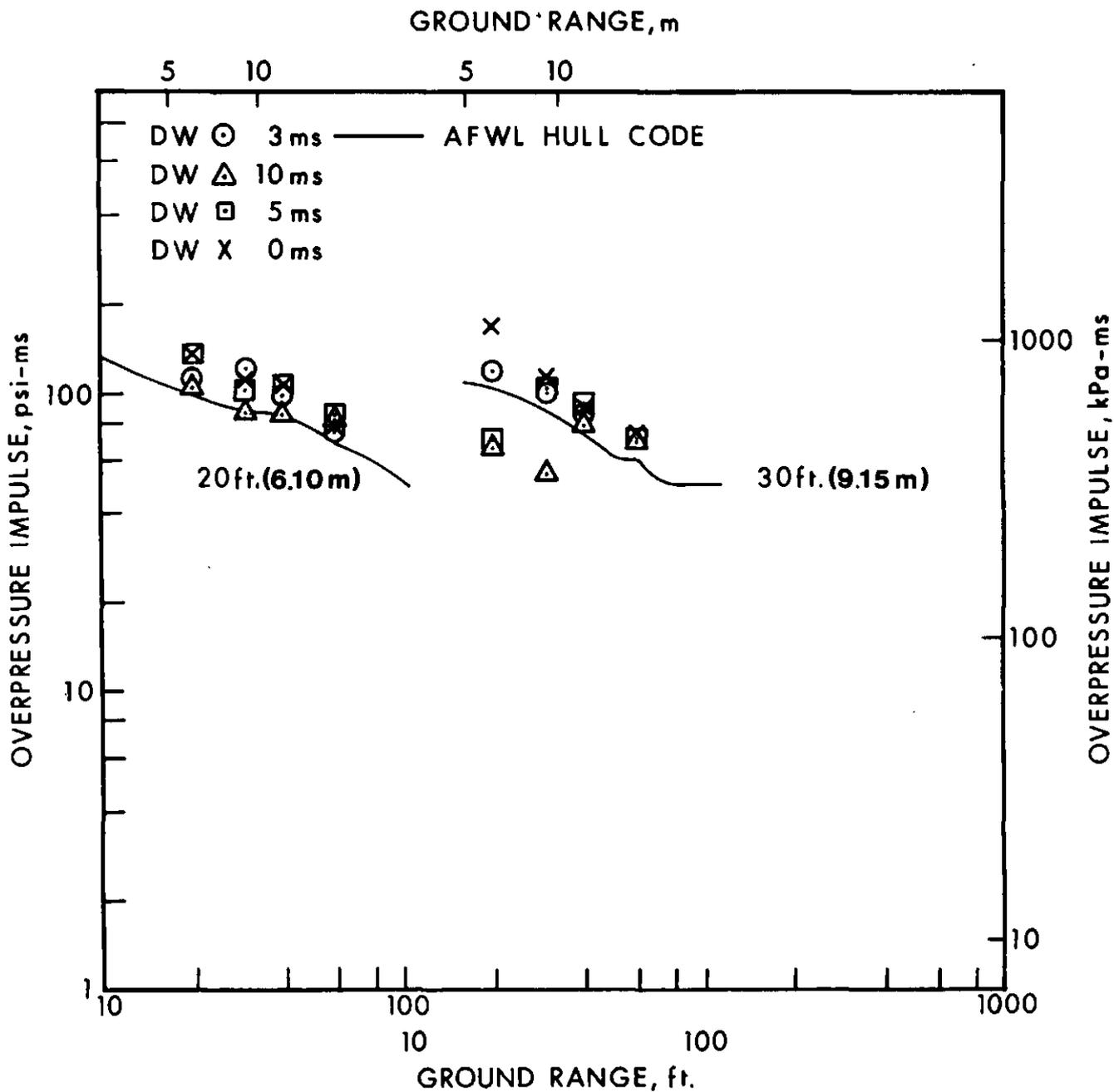


Figure 4.24. Comparison Between Calculated and Experimental Overpressure-Impulses at 20 and 30 Feet Above Ground

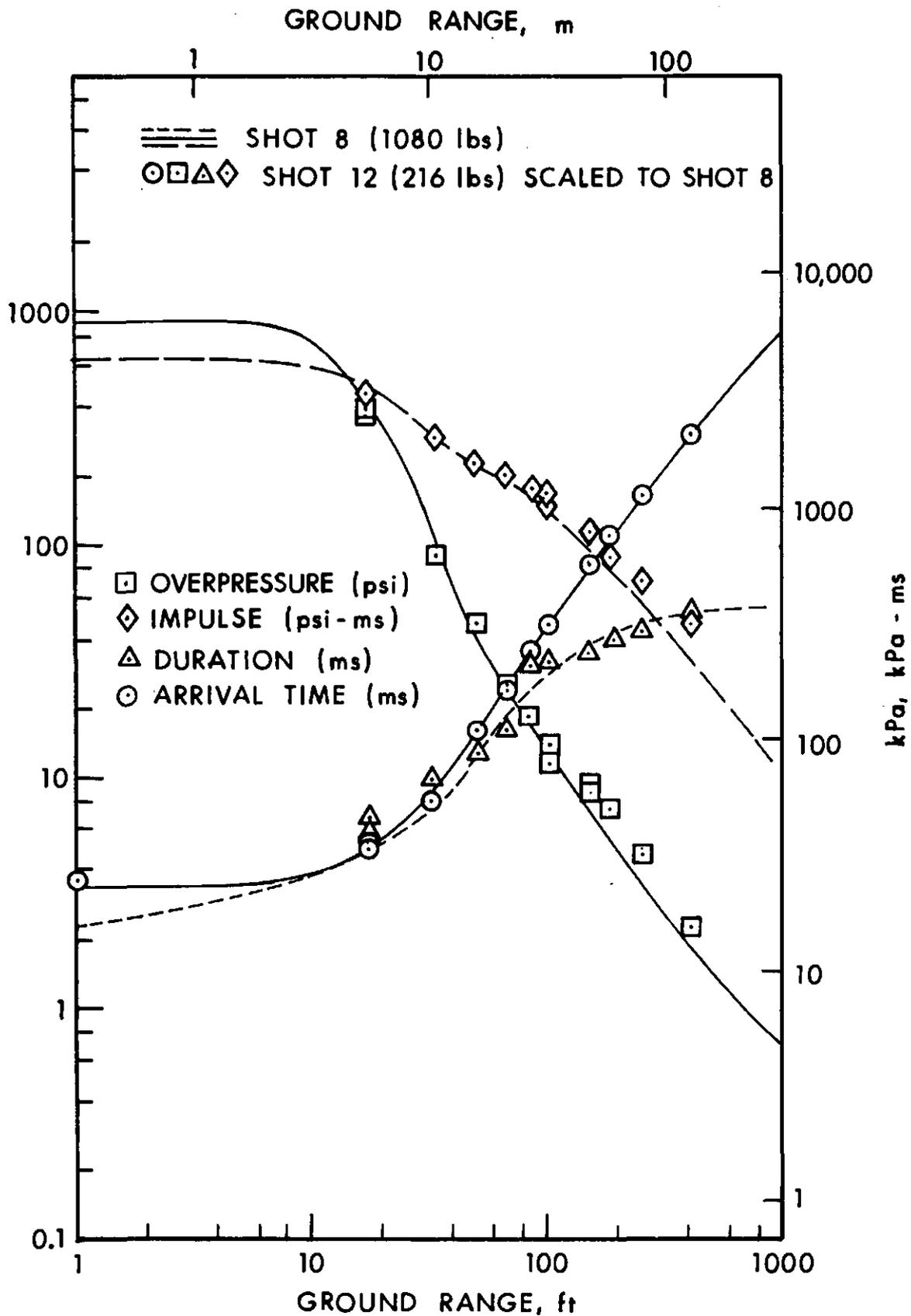


Figure 4.25. Comparison of Shot 12 Data with That from DIPOLE WEST 8

Table 4.1. Scaling Factors

Shot	Pressure	Distance	Time	Impulse
12	1.078	0.1625	0.1600	0.1725
13	1.108	0.1611	0.1636	0.1813
14	1.092	0.1618	0.1588	0.1734
15	1.091	0.1619	0.1582	0.1726
16	1.082	0.1623	0.1645	0.1780

4.6 Comparison Among Events of Present Series

Maximum overpressure curves at the ground surface for all five events are plotted together in Figure 4.26. Similar plots for maximum overpressure-impulse are given in Figure 4.27. As can be seen, these curves are almost identical for the four double-burst events, regardless of the non-simultaneity. For Shot 14, in which only a single charge was detonated, the pressure and impulse curves fall somewhat below those from the other events. This is particularly noticeable, on these logarithmic plots, at the higher values of ground range.

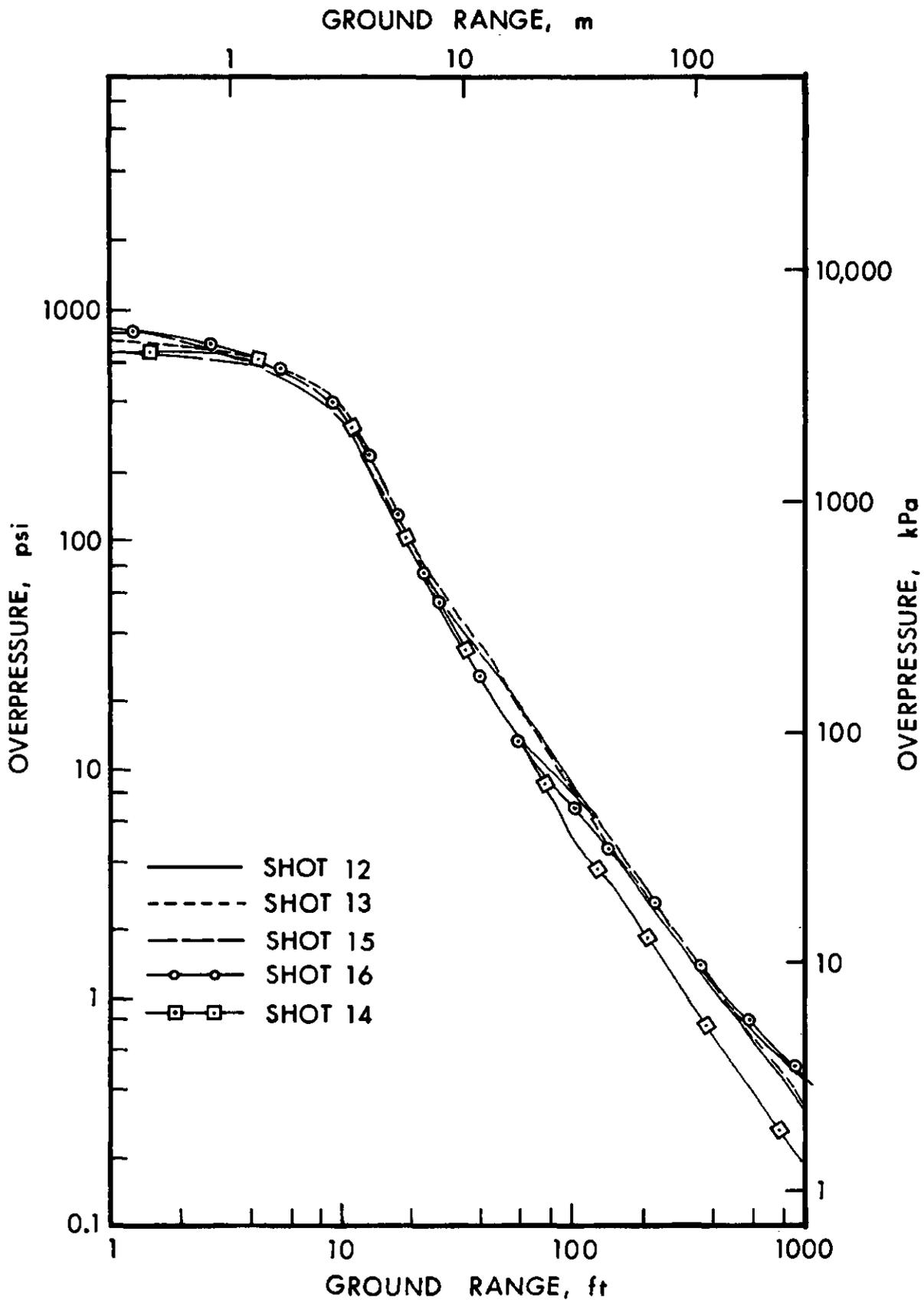


Figure 4.26. Maximum Overpressure at Ground Level Versus Ground Range for All Events

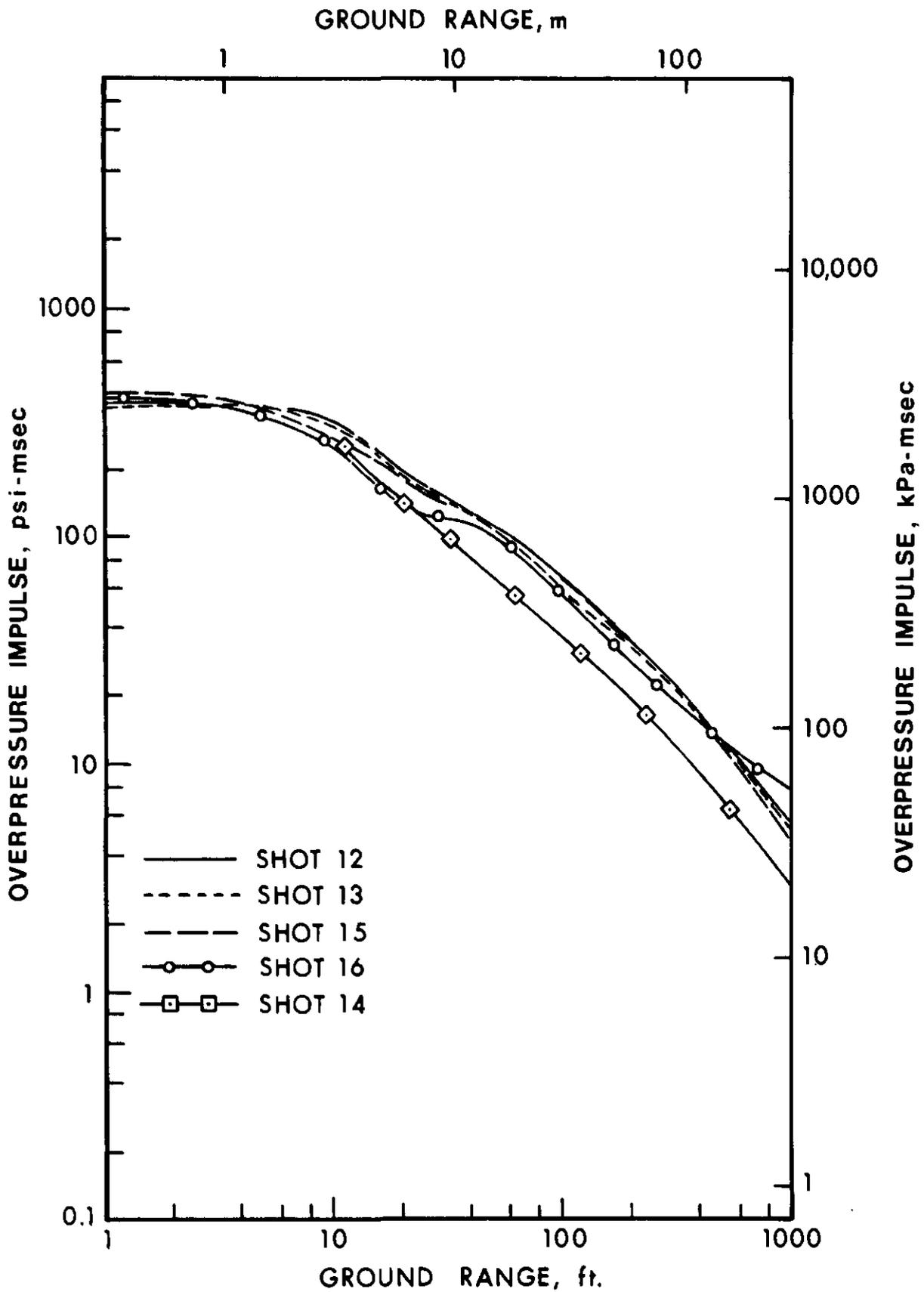


Figure 4.27. Maximum Overpressure-Impulse at Ground Level Versus Ground Range for All Events

CHAPTER 5

CONCLUSIONS AND RECOMMENDATIONS

In this series of high-explosive detonations, experimental data was successfully gathered on the rise and expansion of fireballs and on the interactions of shock waves generated by the non-simultaneous detonation of multiple bursts. Paths of the triple points and Mach stem regions were identified. A Mach region was not observed in the area of the reflection plane between charges for separation times of 5 and 10 milliseconds, whereas it was observed in the cases for separation times of 0 (simultaneous detonation) and 3 milliseconds. Theoretical calculations had predicted the absence of this Mach region in the 10 millisecond time separation case.

Overpressure blast parameters show good general correlation with those obtained from theoretical AFWL-HULL calculations. Sachs scaling relationships were also found to be valid for these multiburst detonations.

Data on dynamic pressure, dynamic pressure impulse, particle velocity, and density were being processed as this report went to press and were not available for publication. These data will be published at a later date.

One of the major recommendations made in the earlier report on simultaneous detonations (*Reference 1*) was for consideration of a series of non-simultaneously detonated events. This recommendation has been carried out with the present DIPOLE WEST shots. No additional recommendations, other than those mentioned in *Reference 1*, have become evident at this time.

REFERENCES

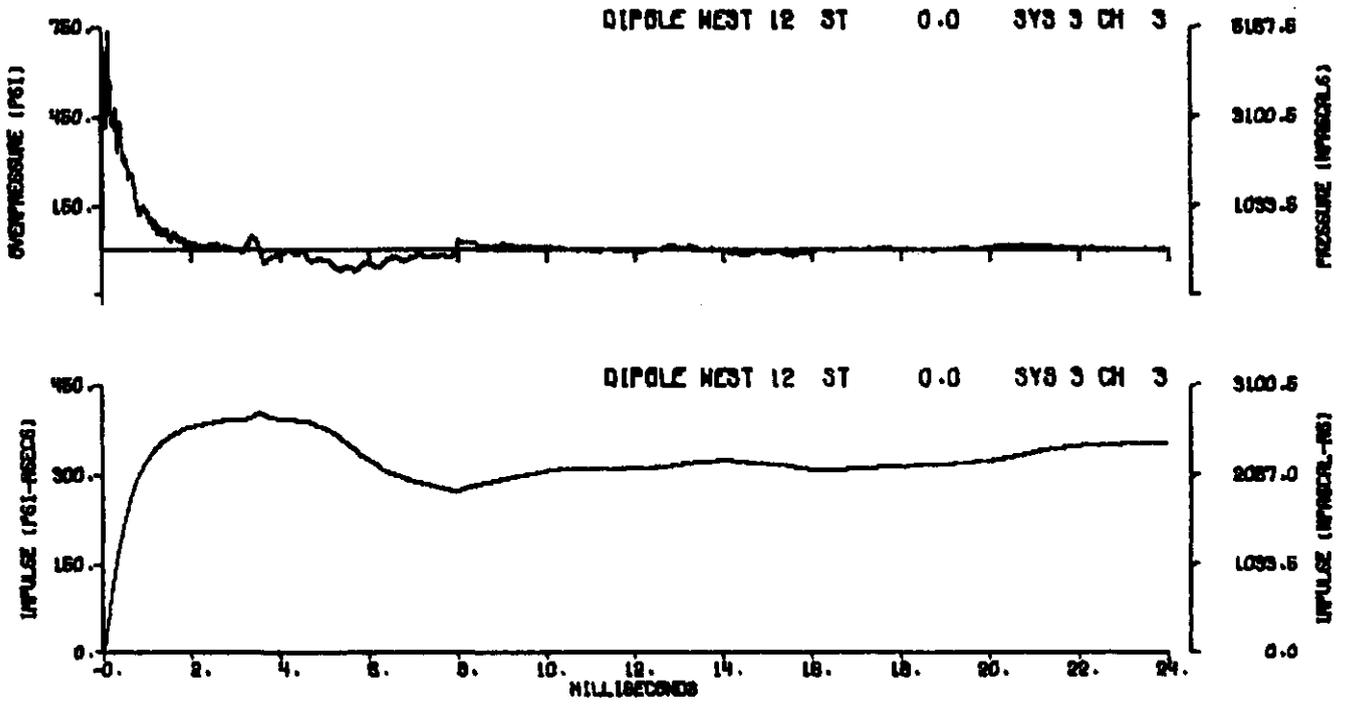
1. J.H. Keefer and R.E. Reisler, "Multiburst Environment - Simultaneous Detonations, Project DIPOLE WEST," BRL Report No. 1766, USA Ballistic Research Laboratories, Aberdeen Proving Ground, Maryland 21005, March 1975. AD #A009485.
2. C.E. Needham and L.A. Wittwer, "The Air Force Weapons Laboratory Low Altitude Multiple Burst (LAMB) Model," AFWL-DYT-75-2 (unpublished).
3. DASIAC Staff, "Environmental Impact Assessment for DIPOLE WEST," General Electric Company - TEMPO, Santa Barbara, California 93102, May 1973.
4. R.E. Reisler (Ballistic Research Laboratories), "Basic Air Blast Studies," Operation SNOWBALL Project Descriptions, Vol. 1, DASA 1516-1, July 1964.
5. B.J. Holsgrove and R.A. Klymchuk, "Statically Oriented Smoke Puff Grids," Suffield Technical Paper No. 352, Defence Research Establishment Suffield, Ralston, Alberta, Canada, September 1970.
6. J.M. Dewey, D.F. Classen and D.J. McMillin, "Photogrammetry of the Shock Front Trajectories on DIPOLE WEST Shots 8, 9, 10 and 11," UVIC-PF-1-75, University of Victoria, British Columbia, Canada, July 1975.
7. H.J. Carpenter and H.L. Brode, "Height of Burst at High Overpressure," R&D Associates, Marina del Rey, California - Paper presented at Fourth International Symposium on the Military Applications of Blast Simulation, 9-12 September 1974.
8. B.P. Bertrand, "Measurement of Pressure in Mach Reflection of Strong Shock Waves in a Shock Tube," BRL Memo Report 2196, USA Ballistic Research Laboratories, Aberdeen Proving Ground, Maryland 21005, June 1972. AD #746613.

This page Left Intentionally Blank

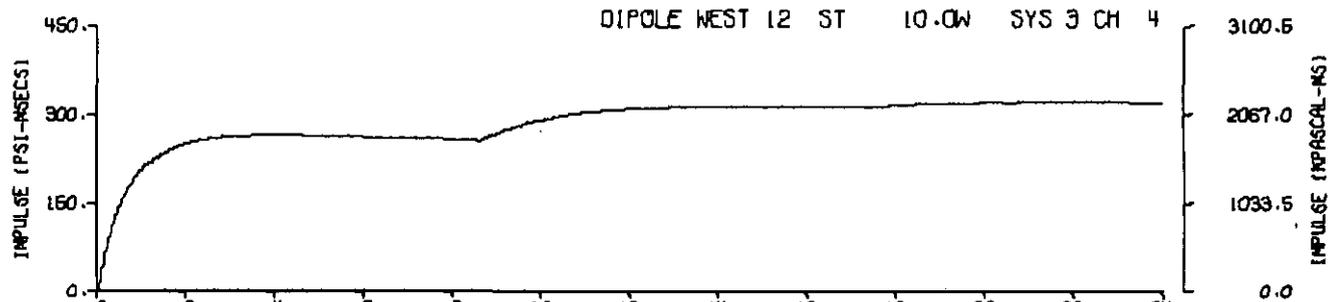
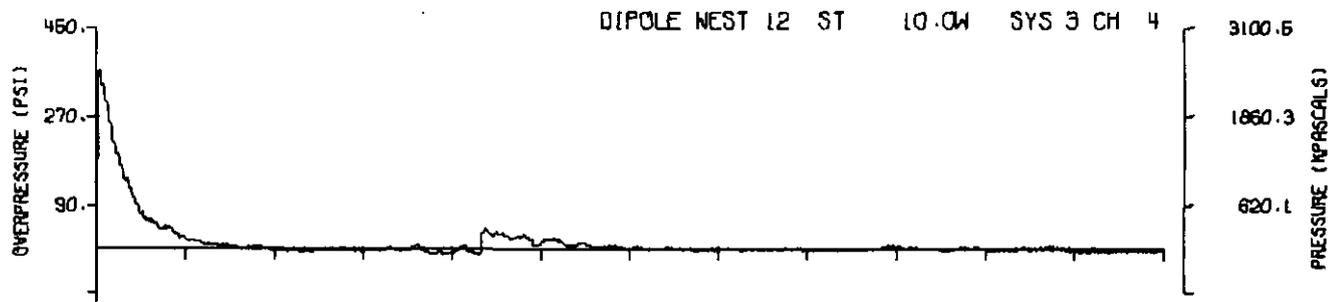
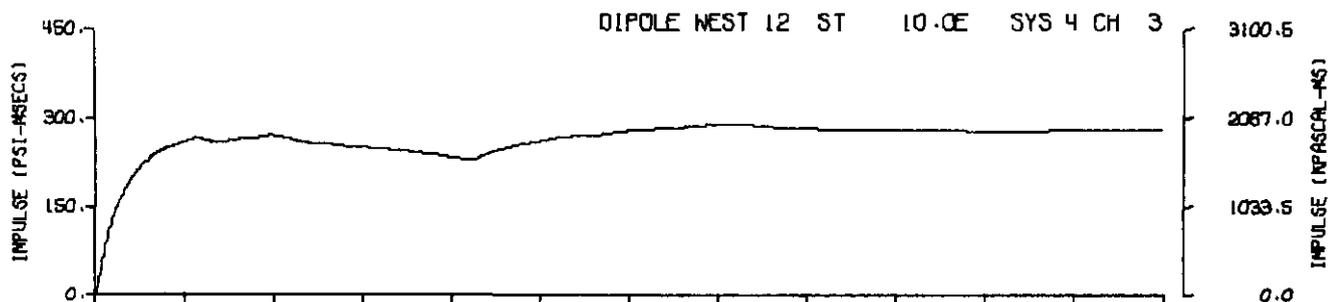
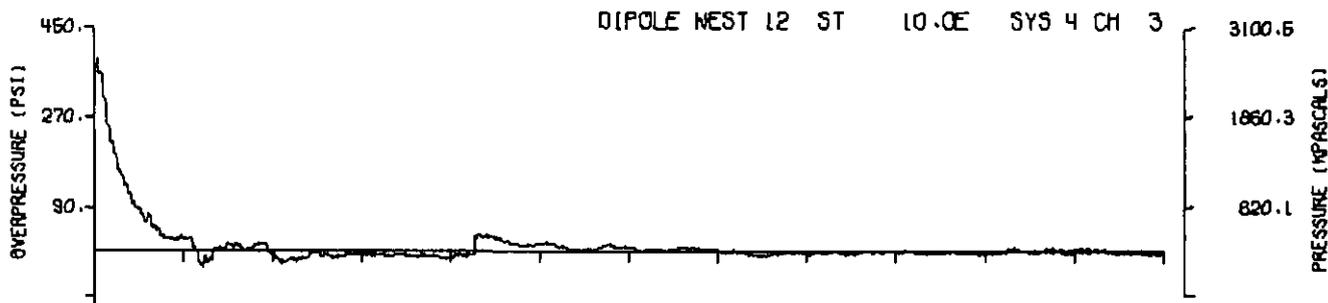
APPENDIX. PRESSURE TIME DATA

The air blast pressure records obtained from each of the shots are reproduced in this appendix. The records are organized according to event and station location. Each page is identified by event and item number; that is, A12.1 is the first page of records from Shot 12 (Shot 12, Item 1) and A16.43 is the last page of records from Shot 16.

The pressure records are plotted first in each case, followed by their integrals, the "overpressure-impulse" records. Pressure scales in pounds per square inch (psi) are given to the left of each record, and in kilopascals (kPa) to the right. Similarly, impulse scales are given in both psi-milliseconds and kPa-milliseconds.

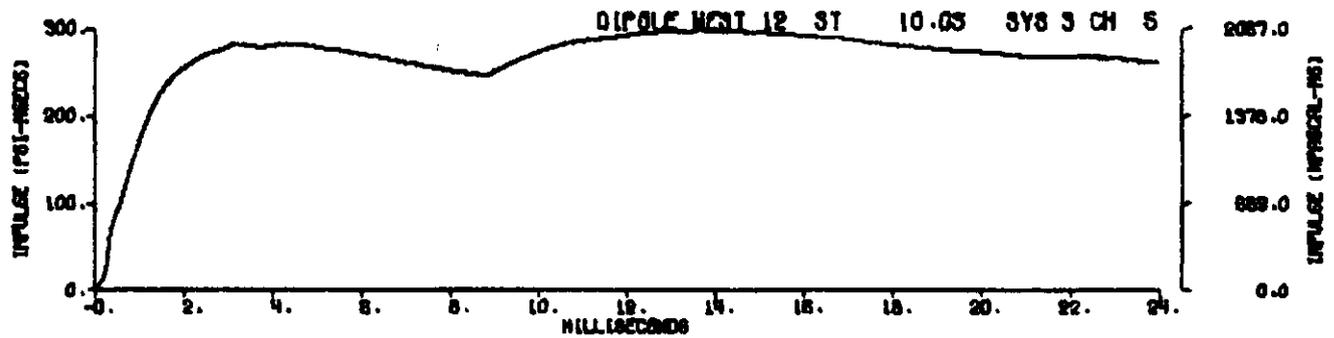
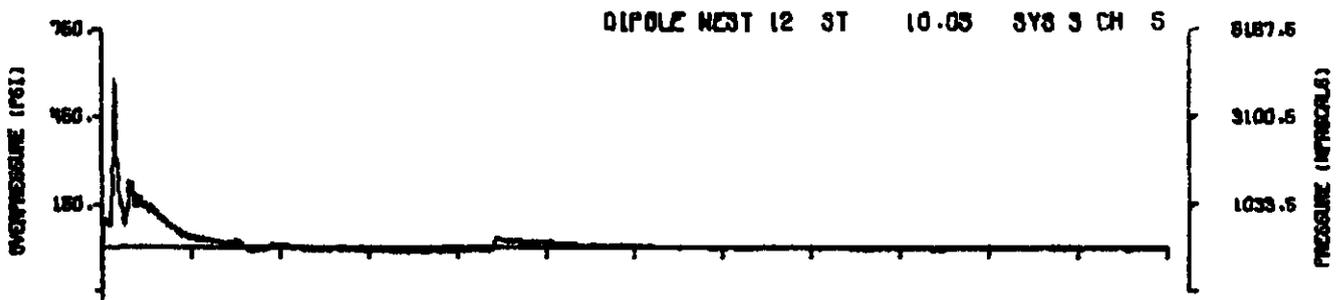
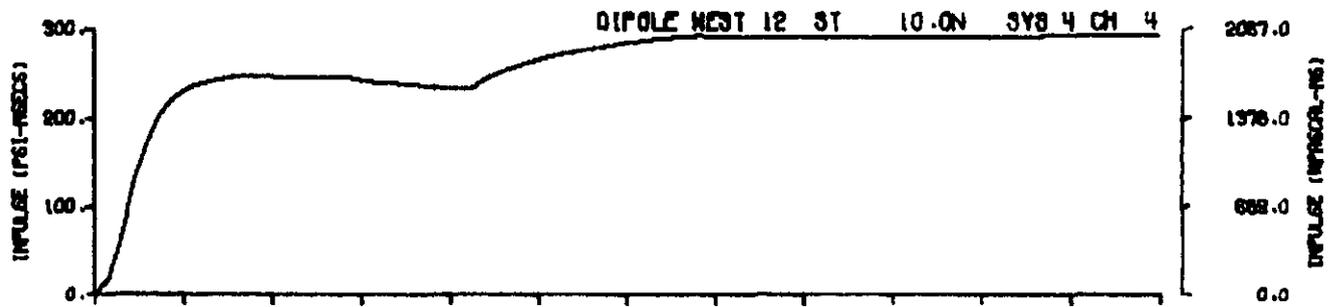
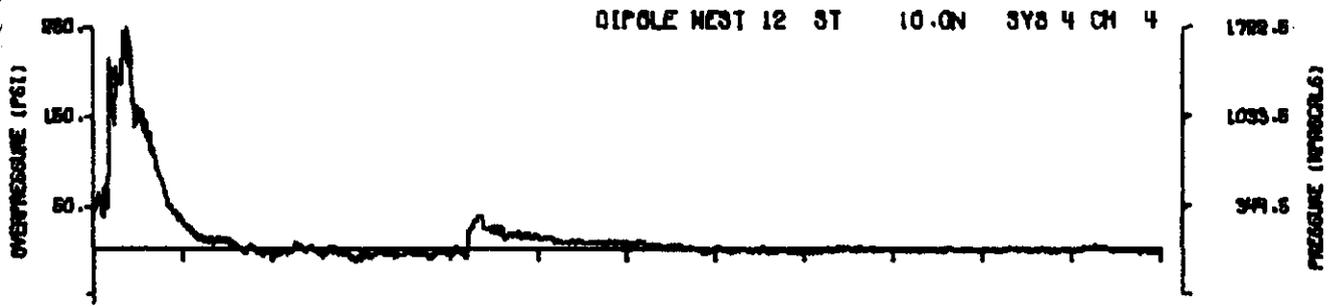


A12.1

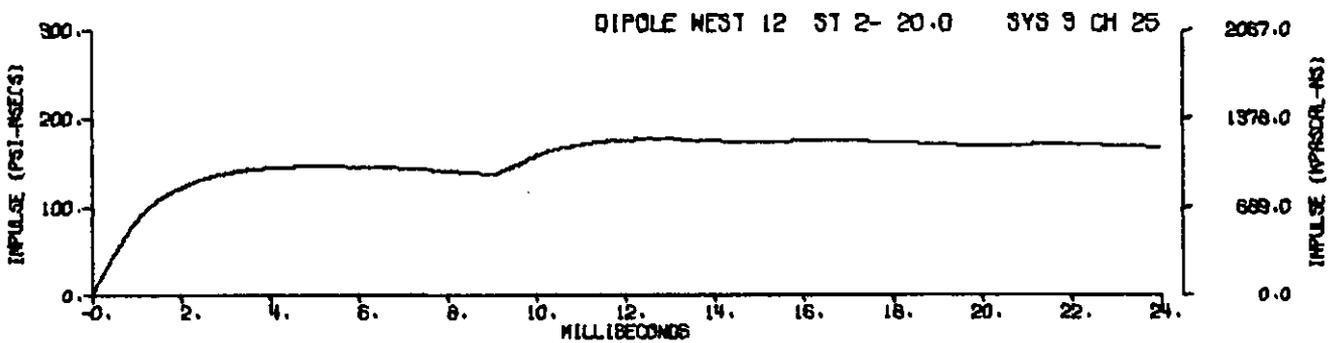
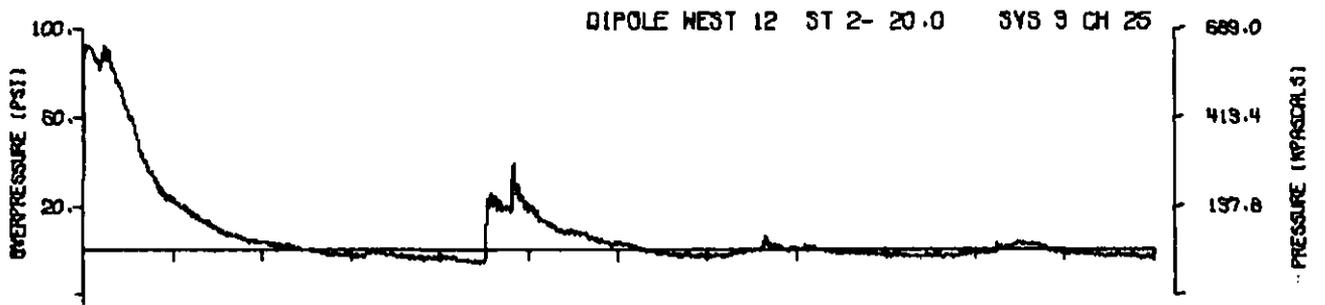
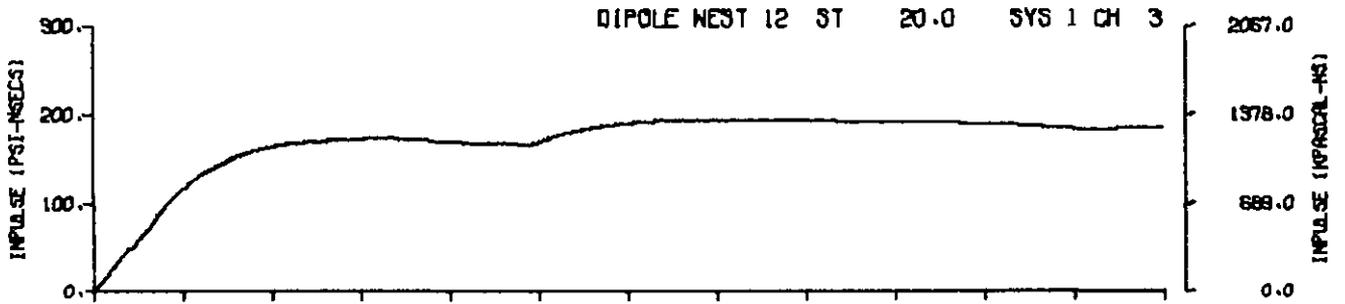
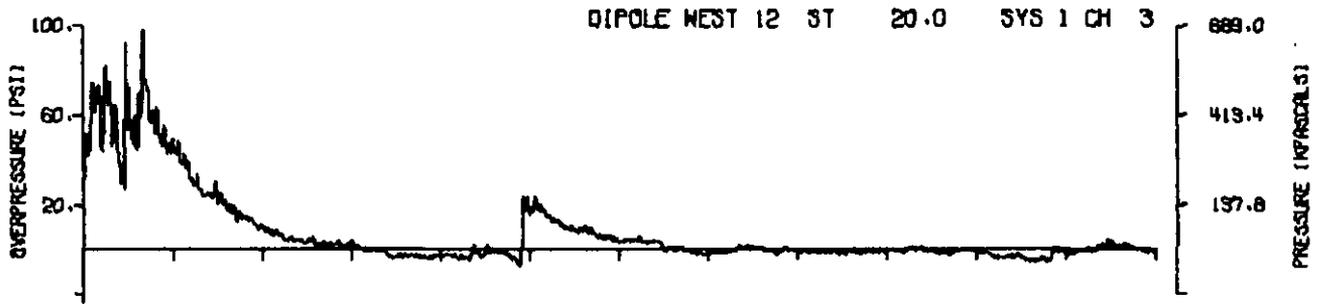


MILLISECONDS

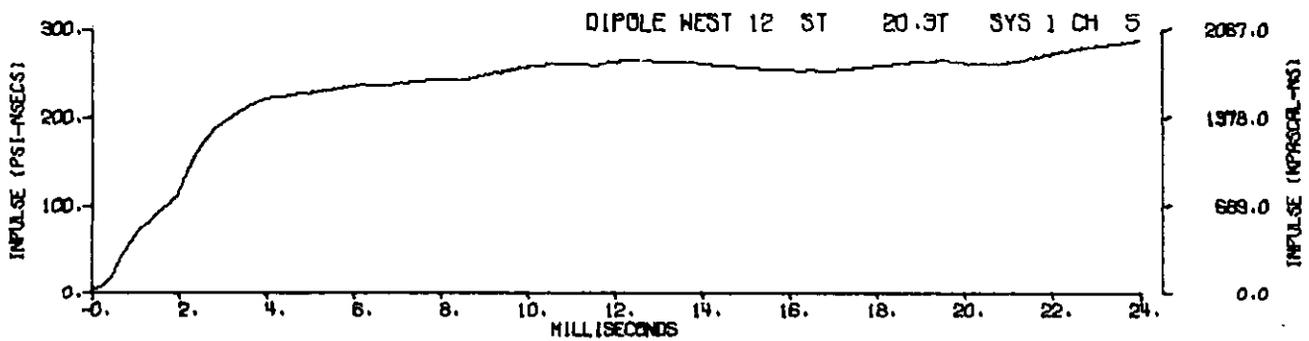
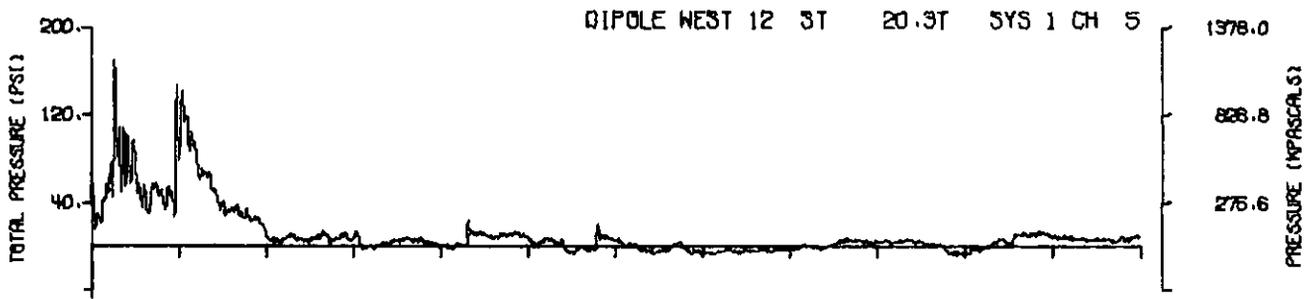
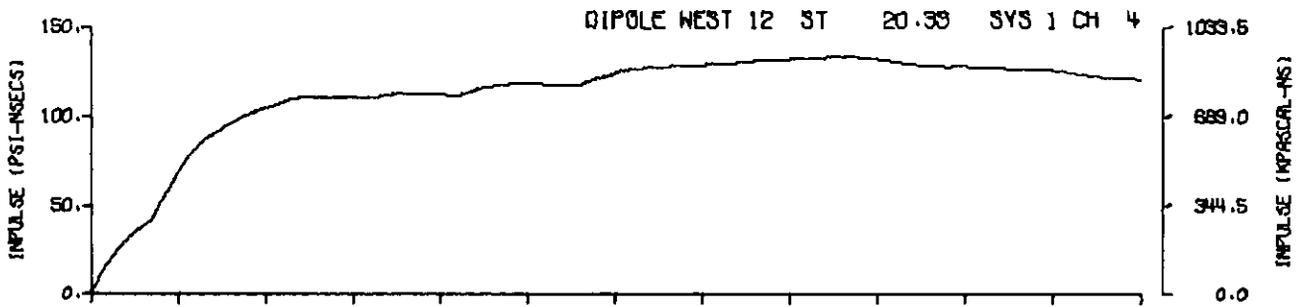
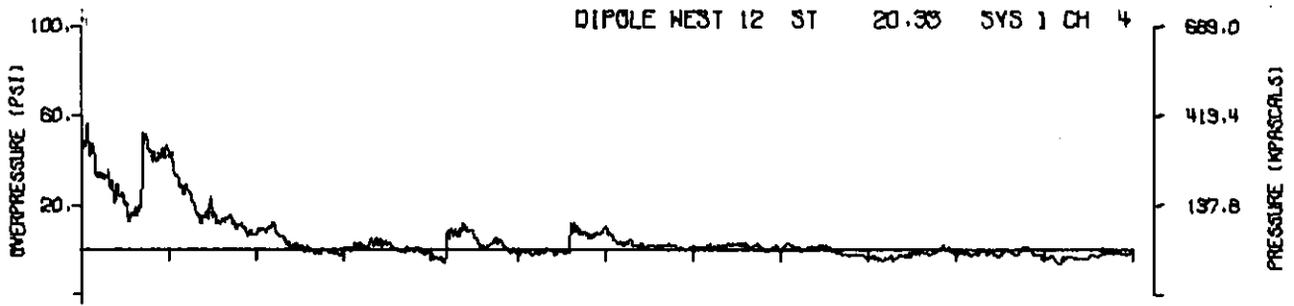
A12.2



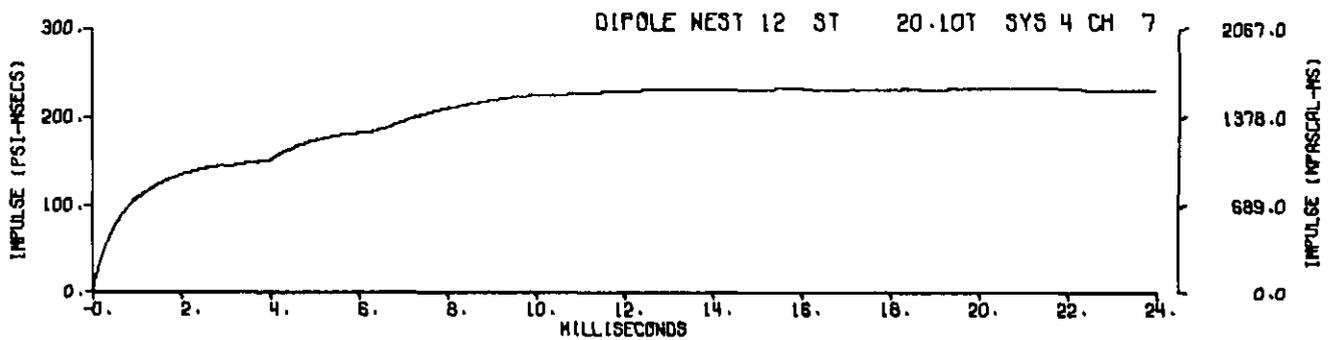
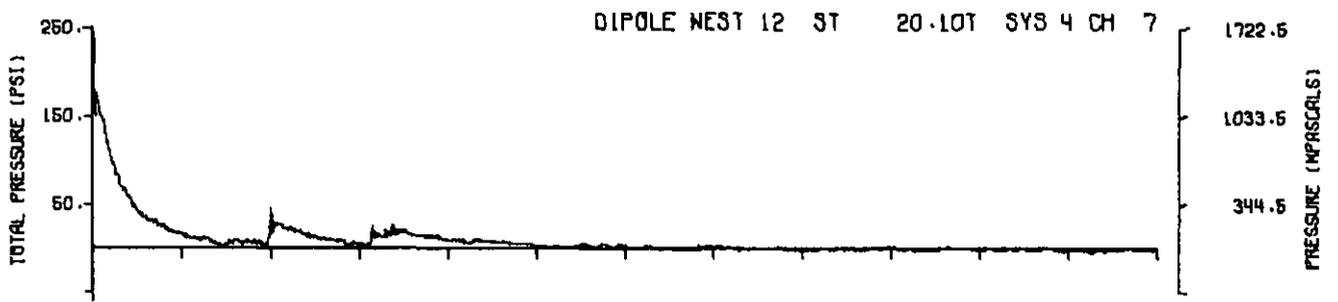
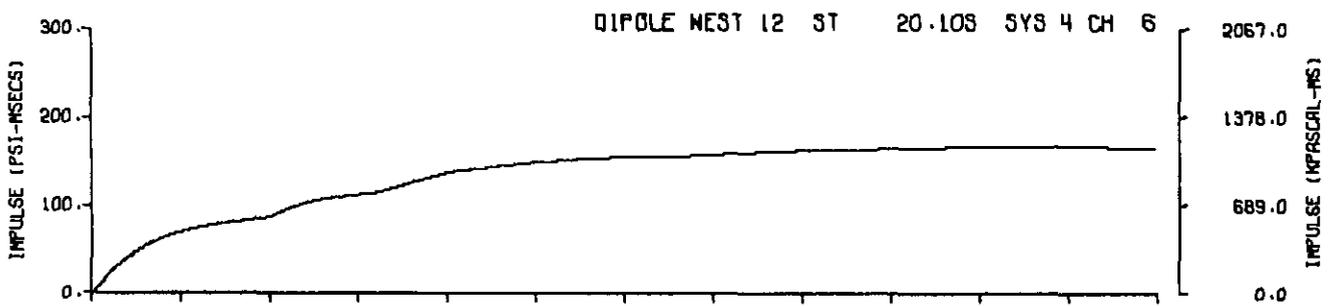
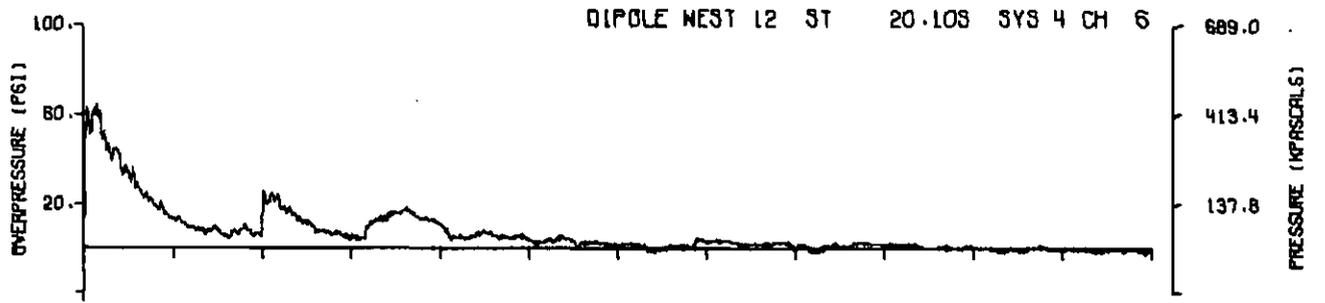
A12.3



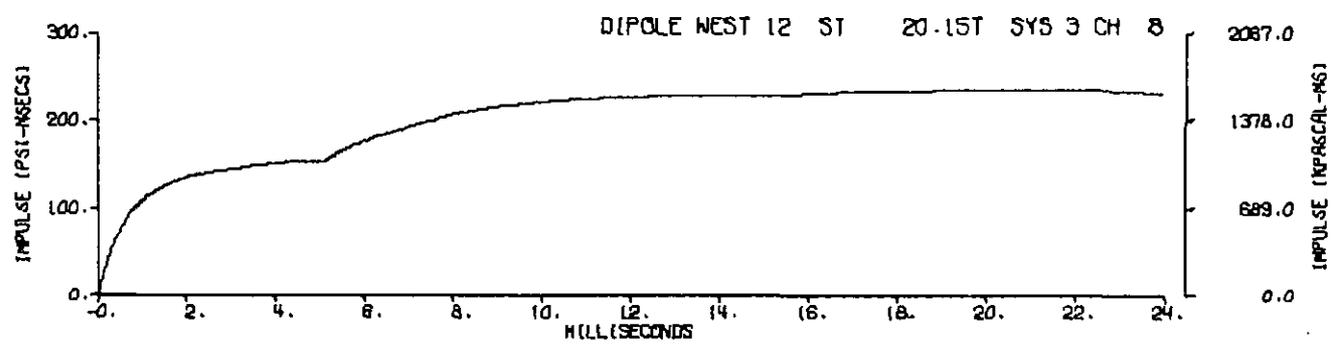
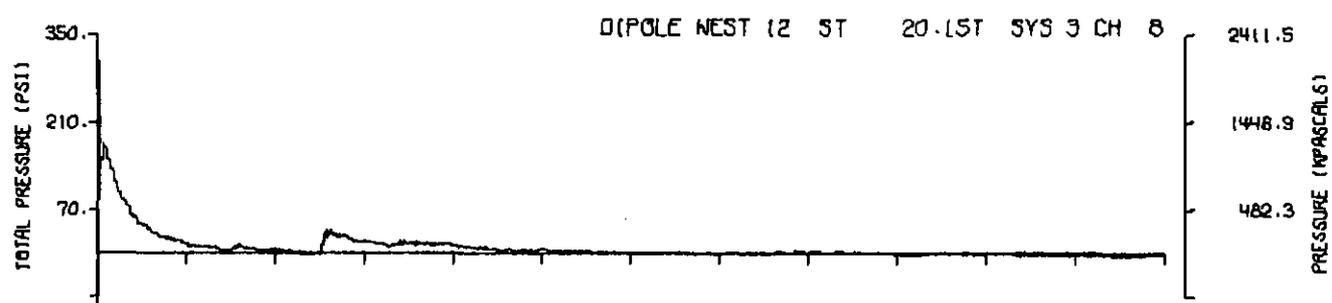
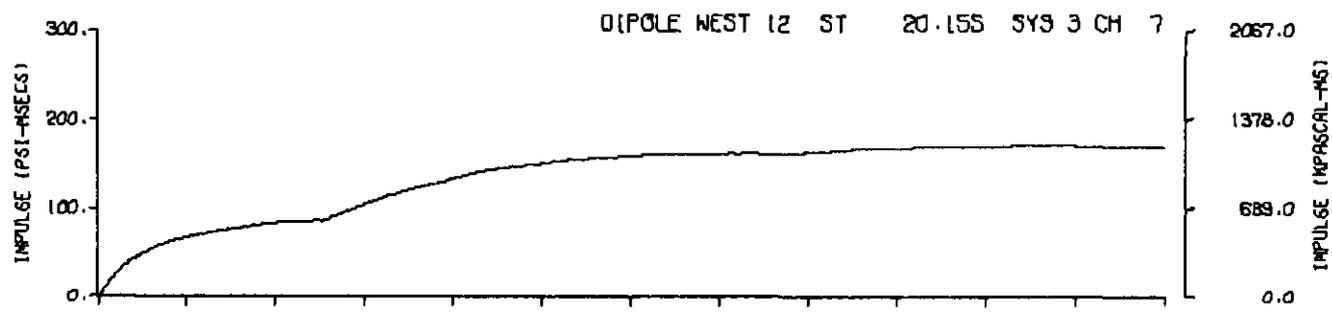
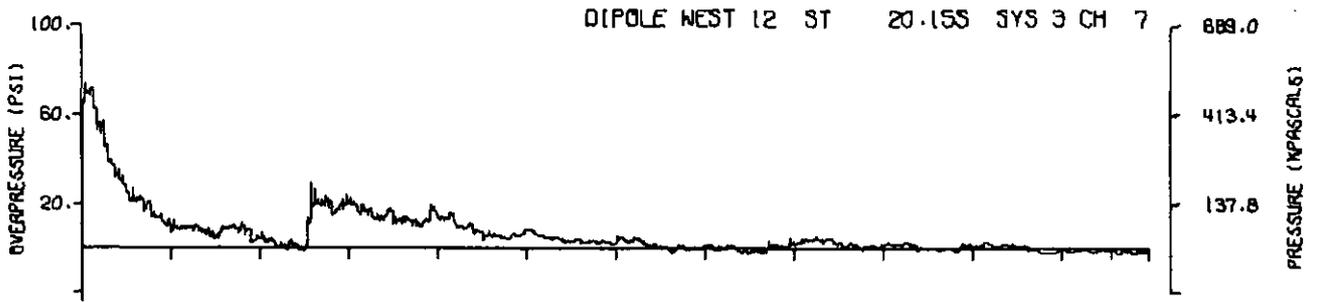
A12.4



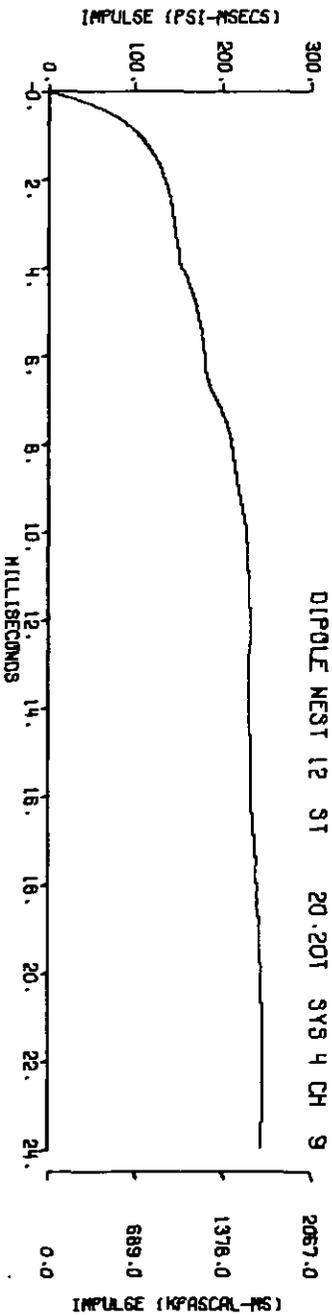
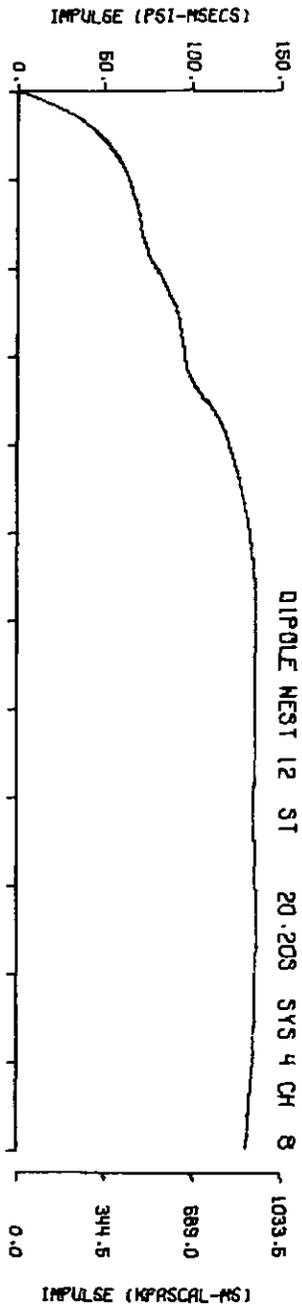
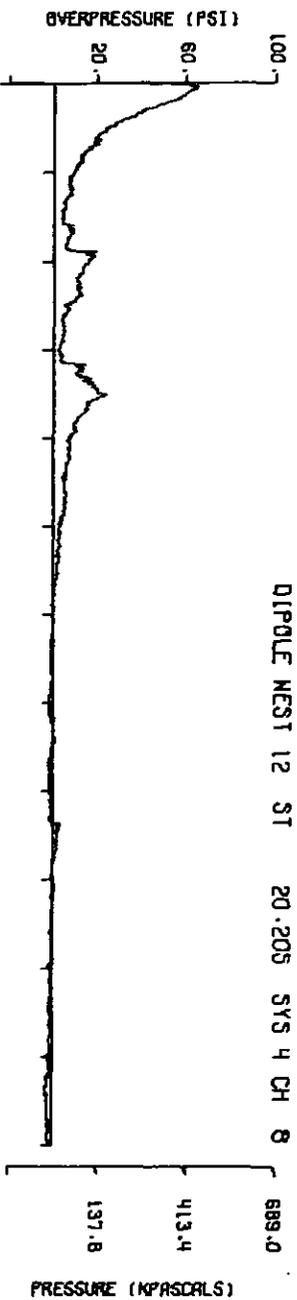
A12.5



A12.6

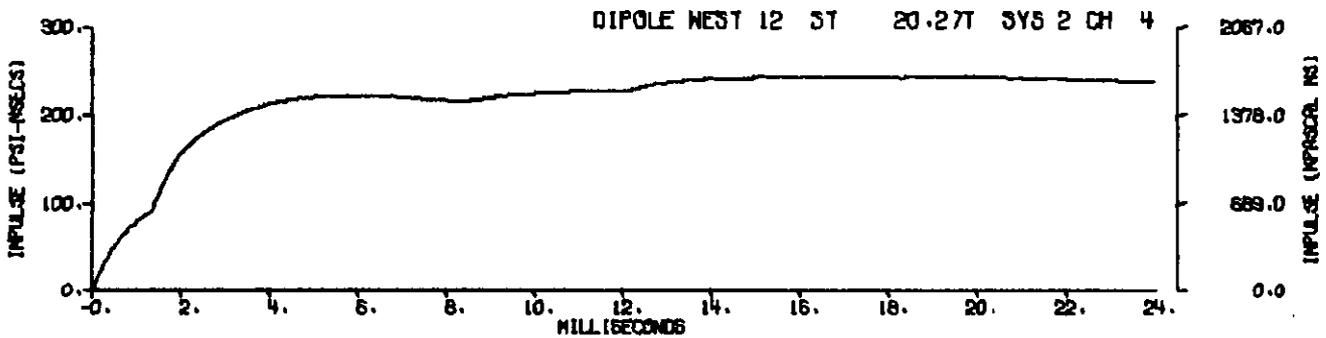
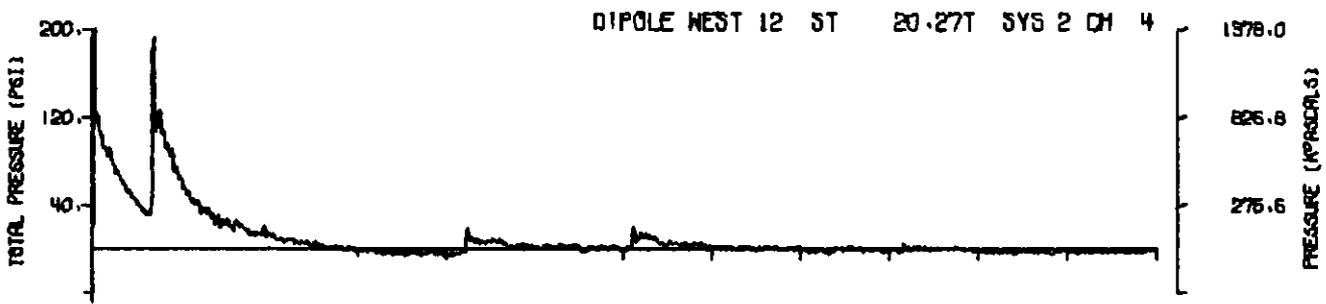
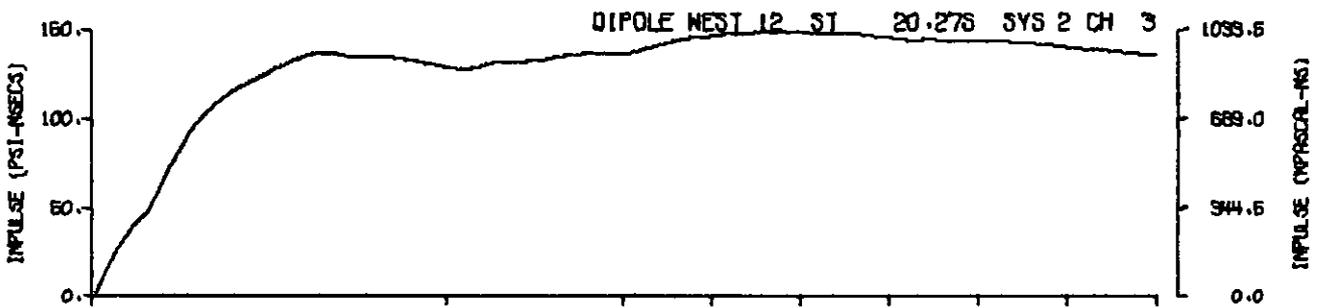
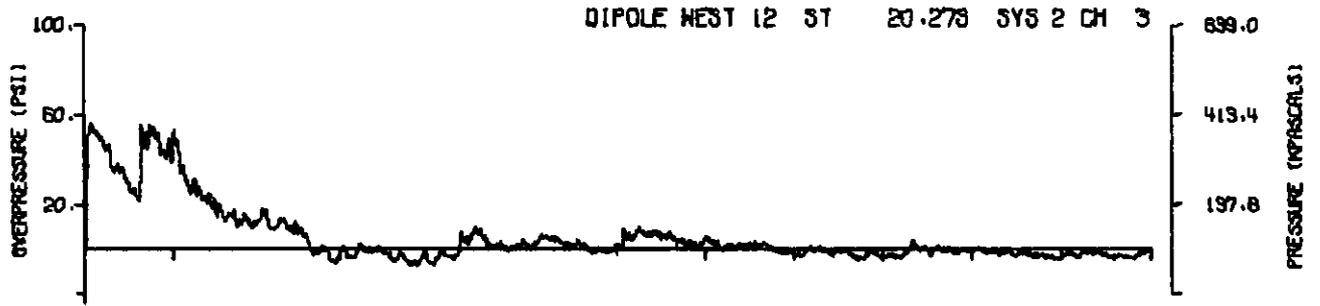


A12.7



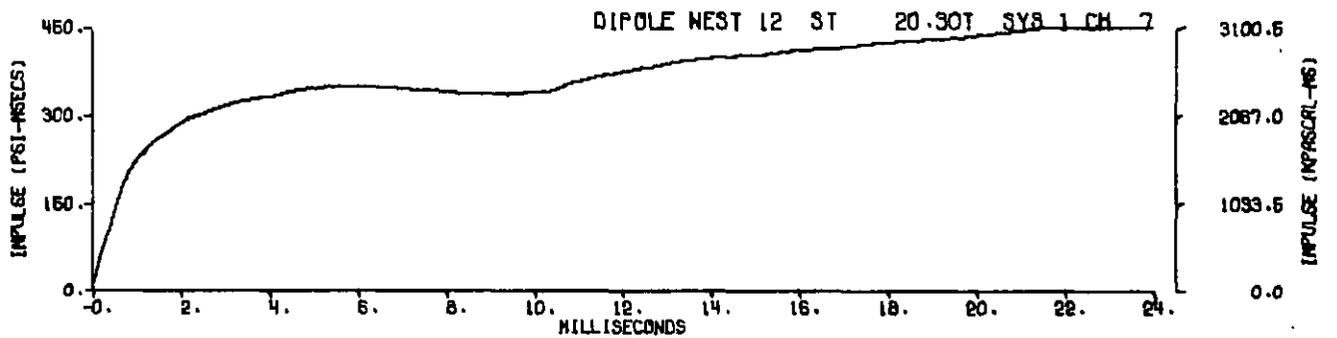
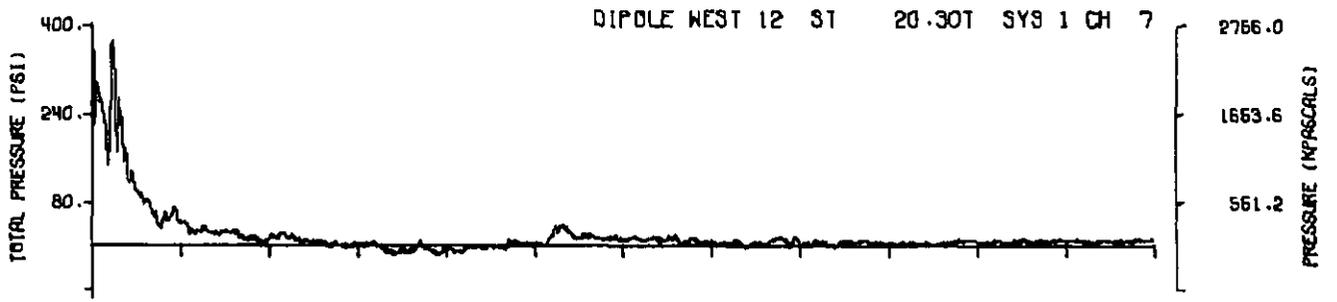
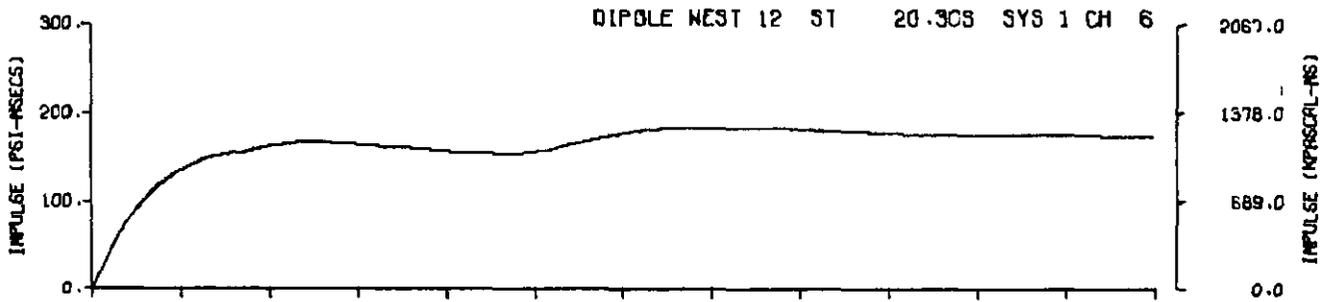
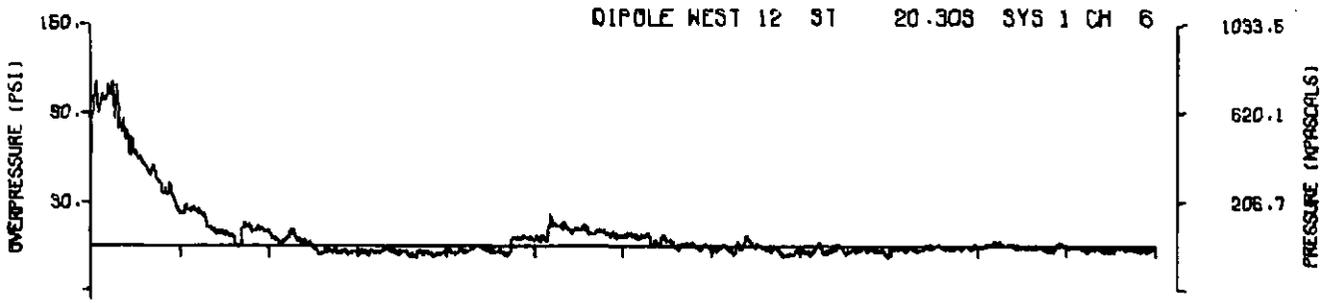
A12.8

165

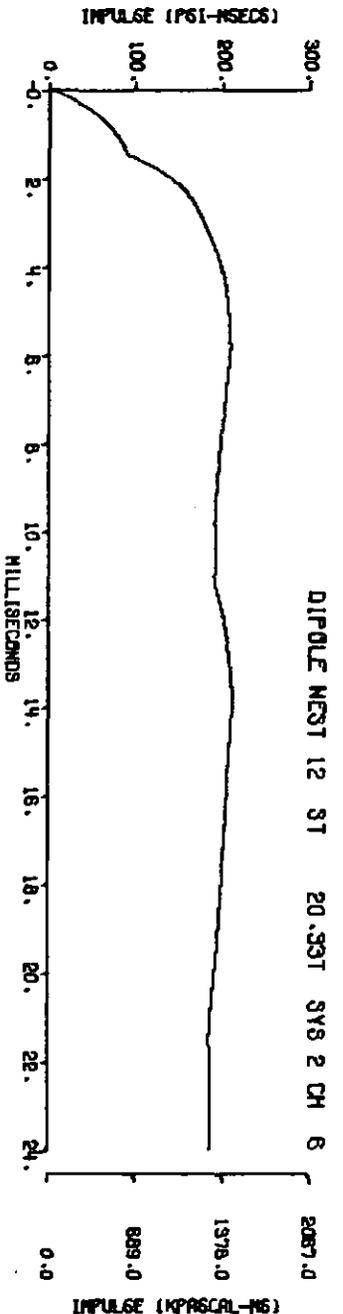
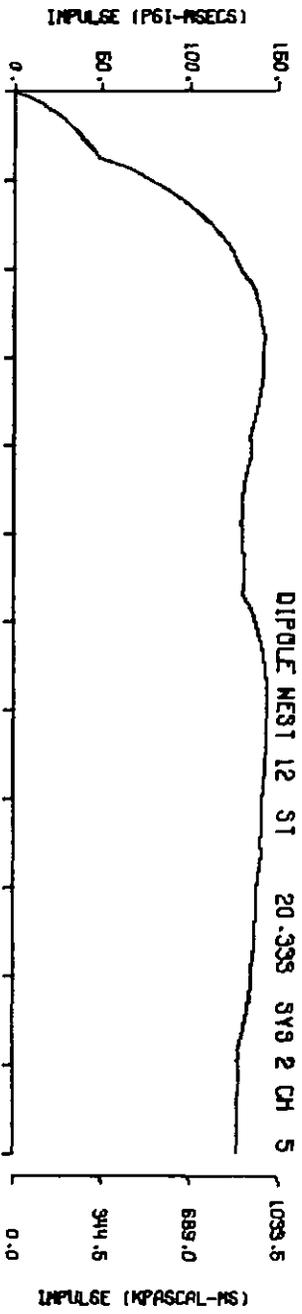
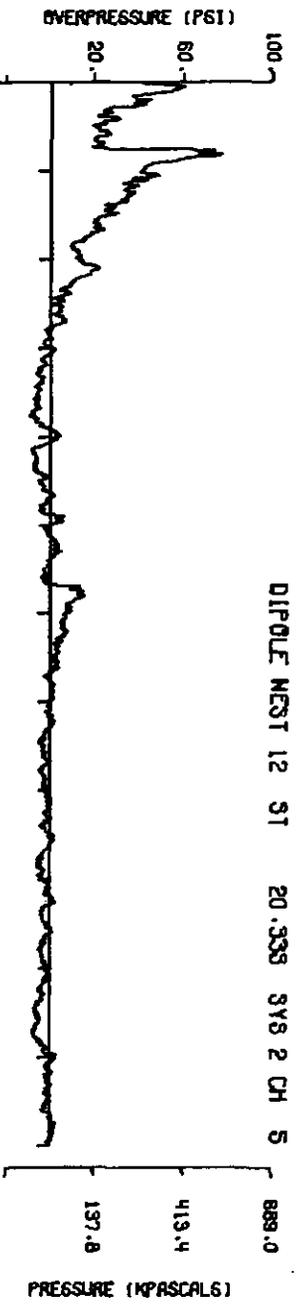


MILLISECONDS

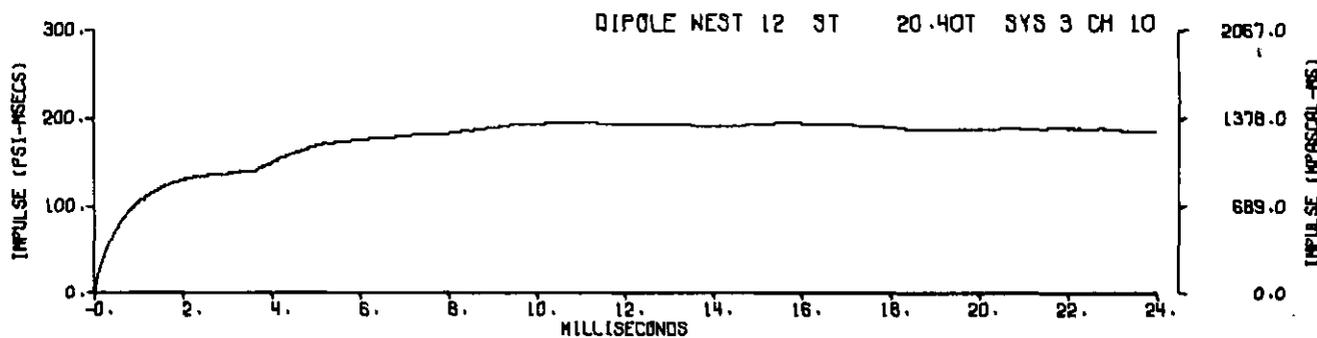
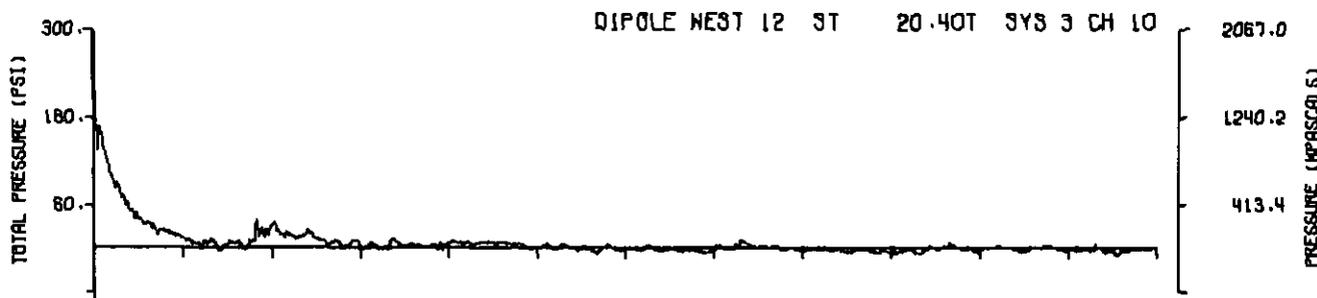
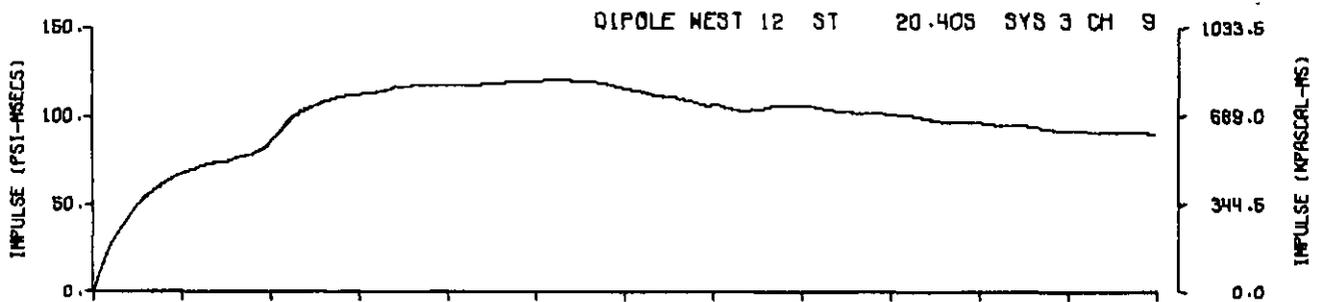
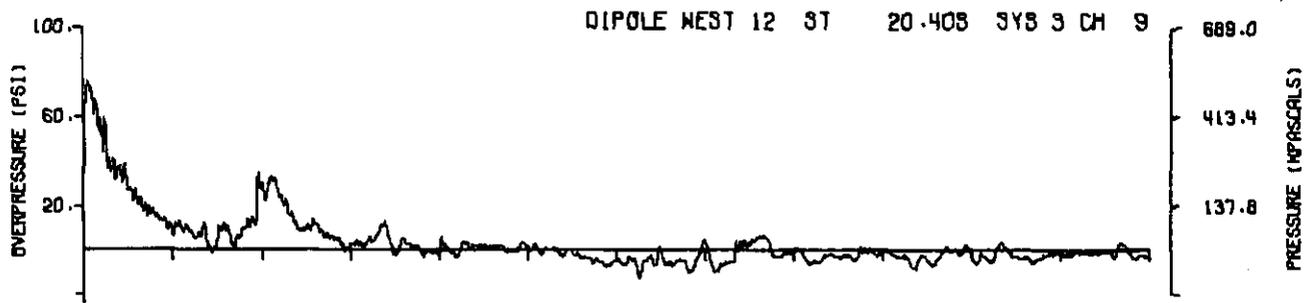
A12.9



A12.10

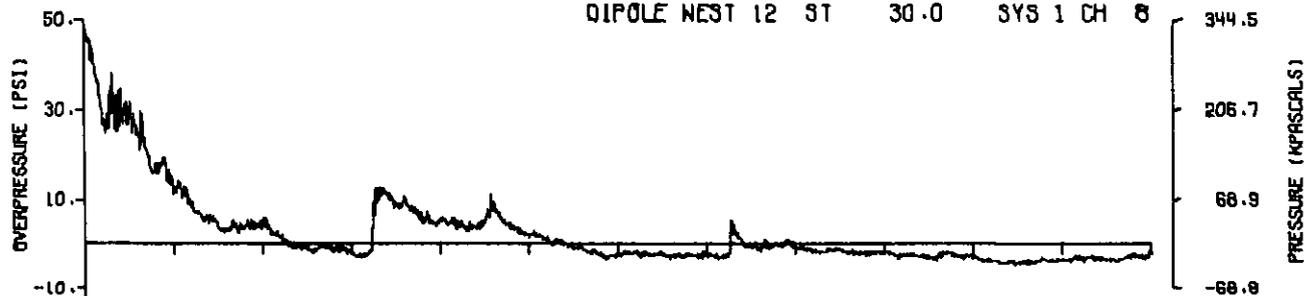


A12.11

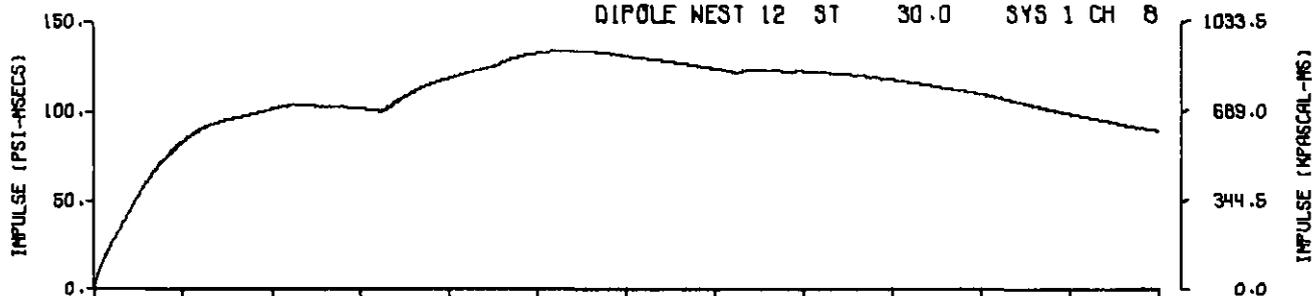


A12.12

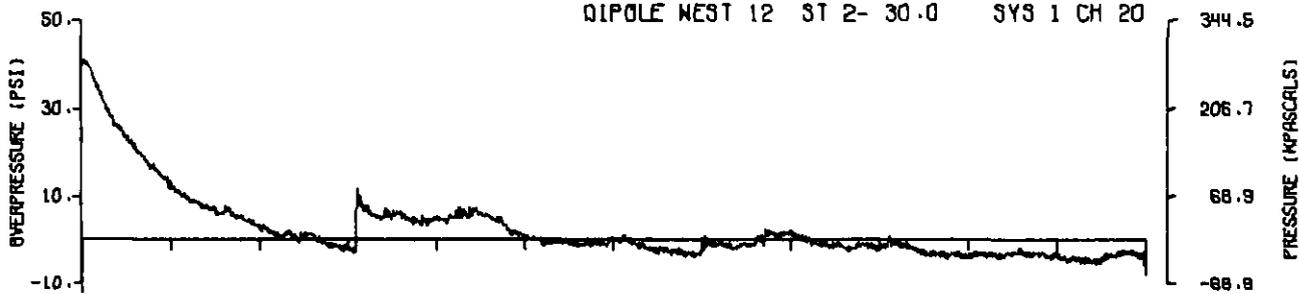
DIPOLE WEST 12 ST 30.0 SYS 1 CH 8



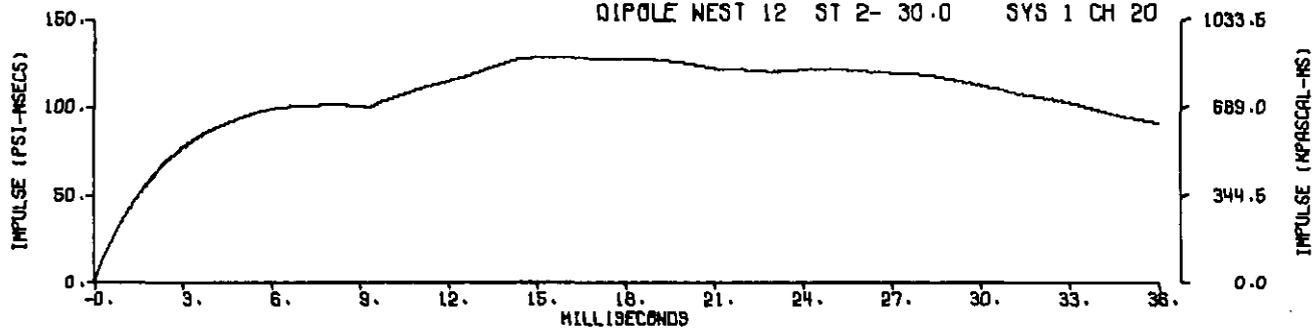
DIPOLE WEST 12 ST 30.0 SYS 1 CH 8



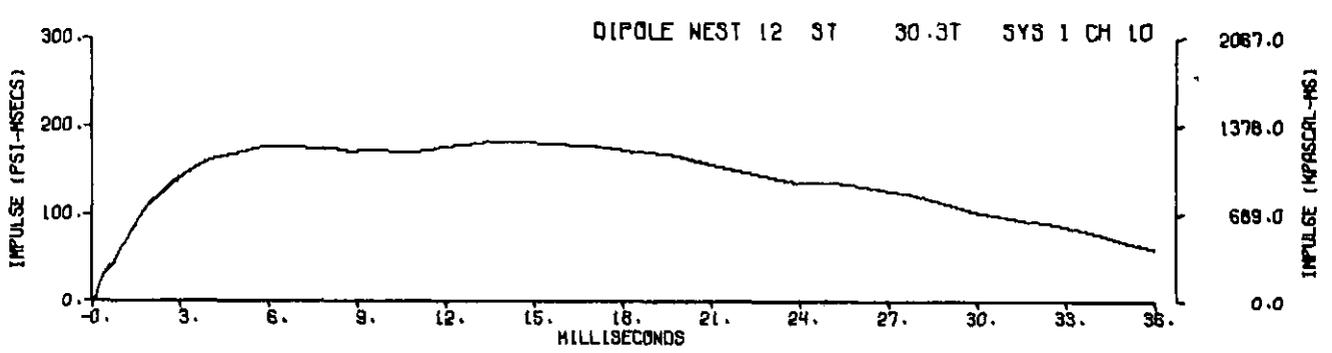
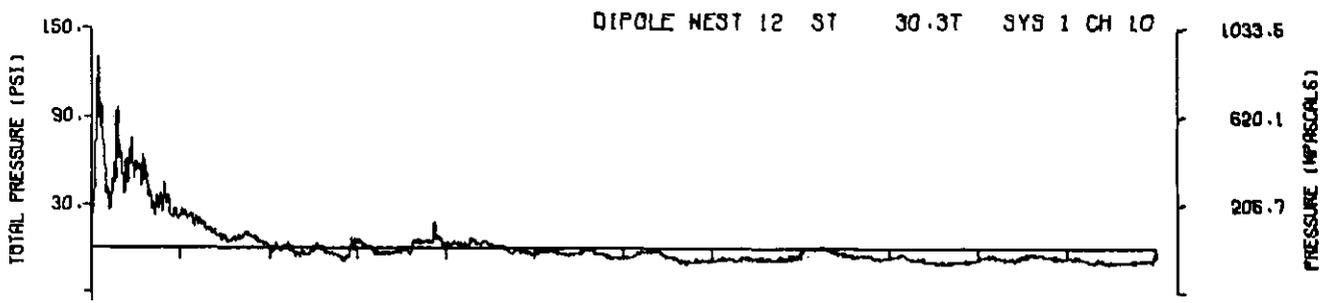
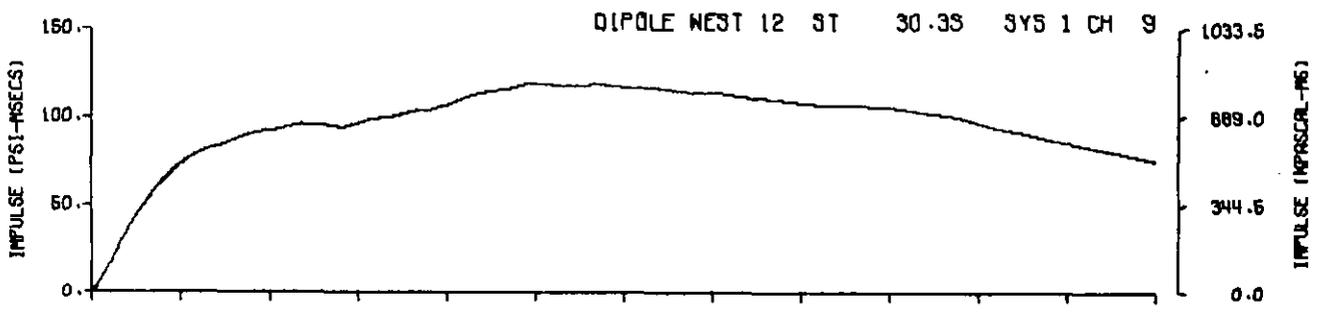
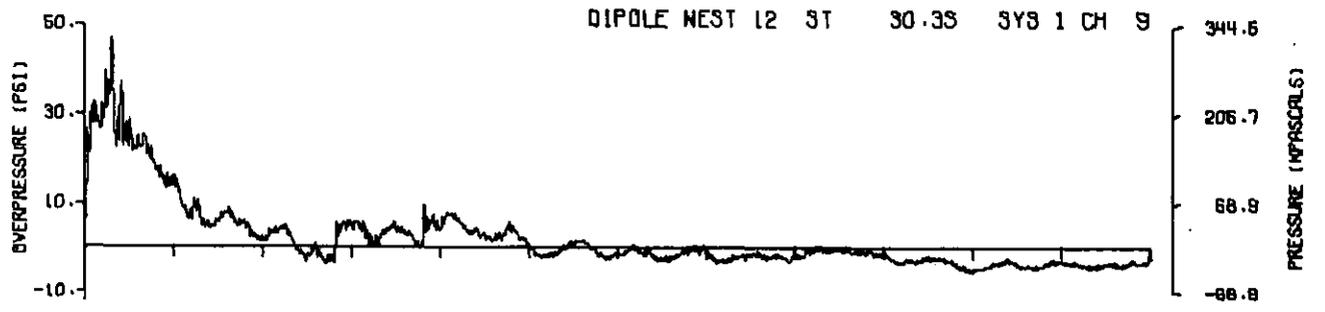
DIPOLE WEST 12 ST 2- 30.0 SYS 1 CH 20



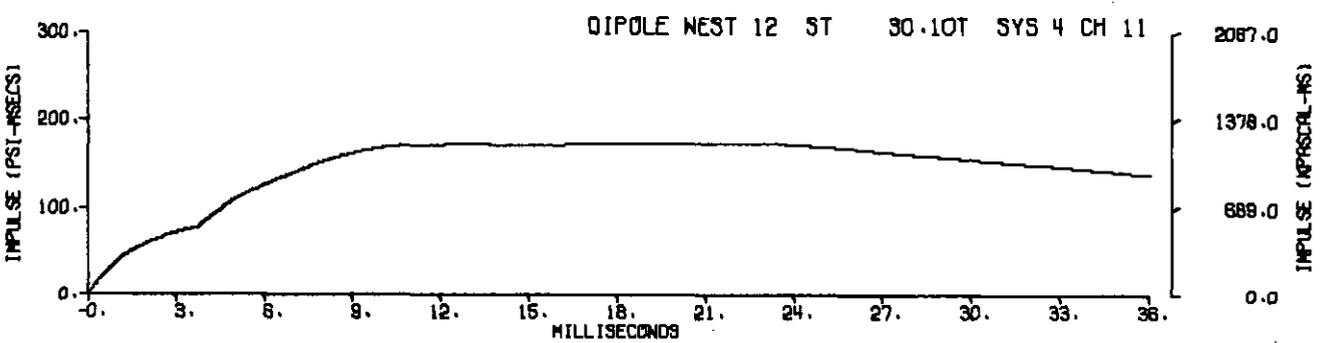
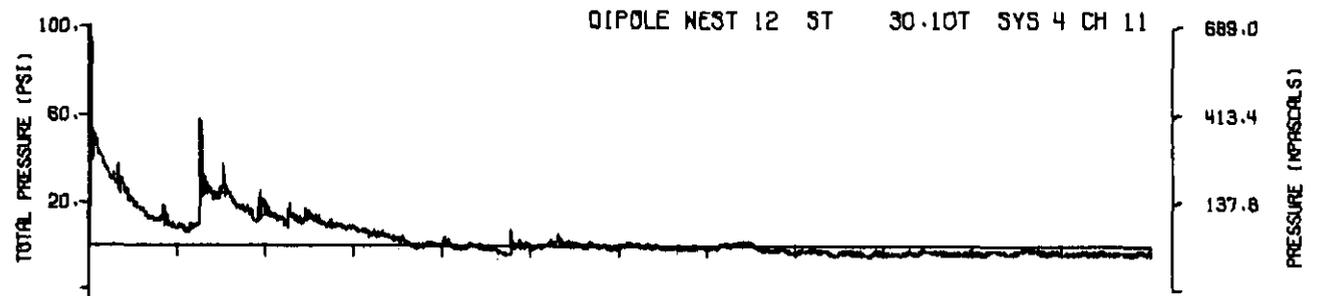
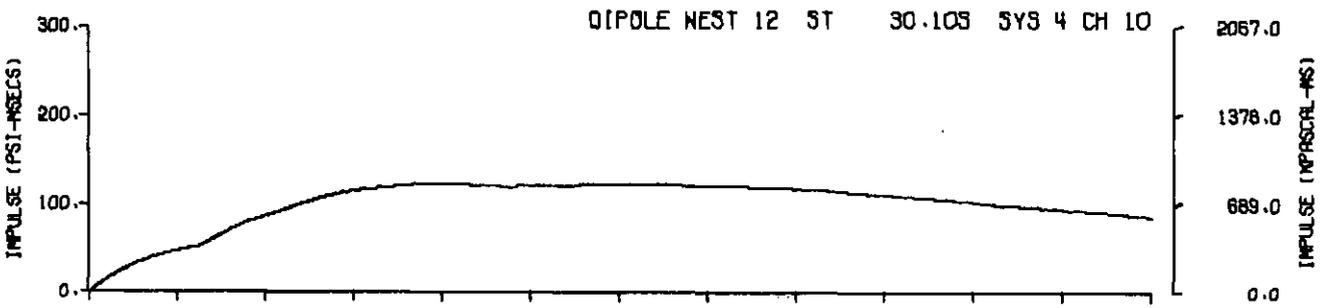
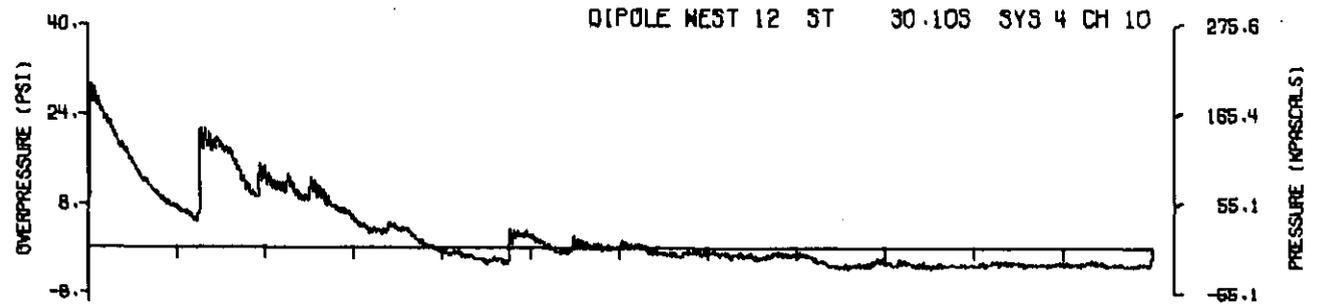
DIPOLE WEST 12 ST 2- 30.0 SYS 1 CH 20



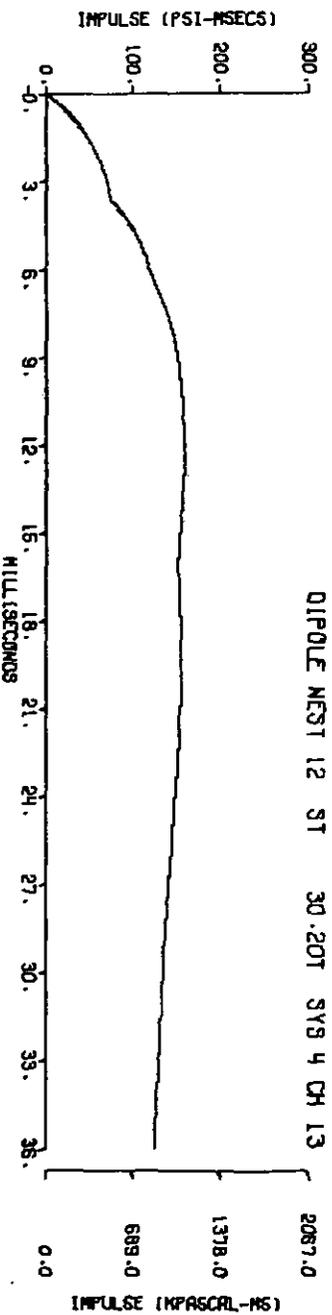
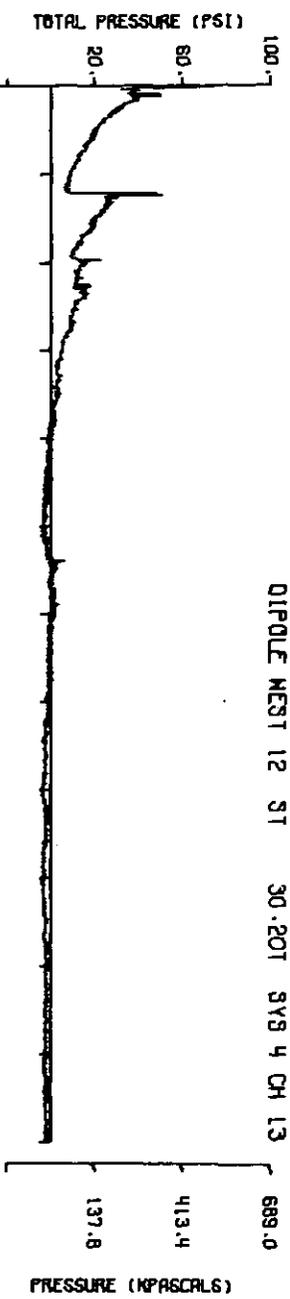
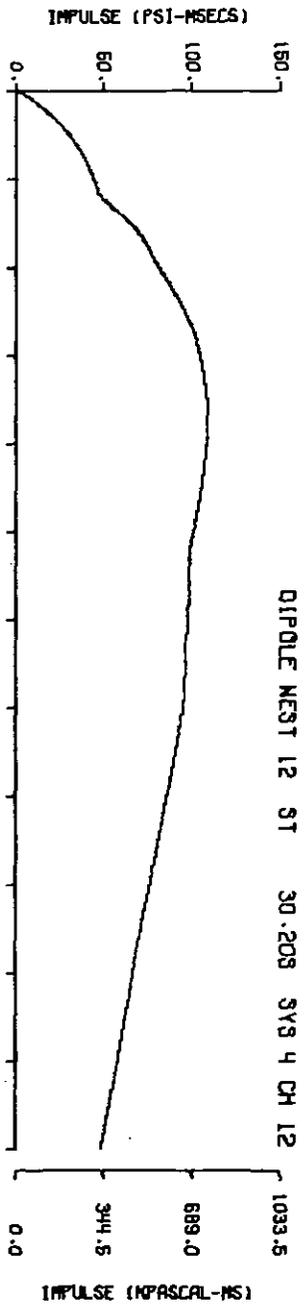
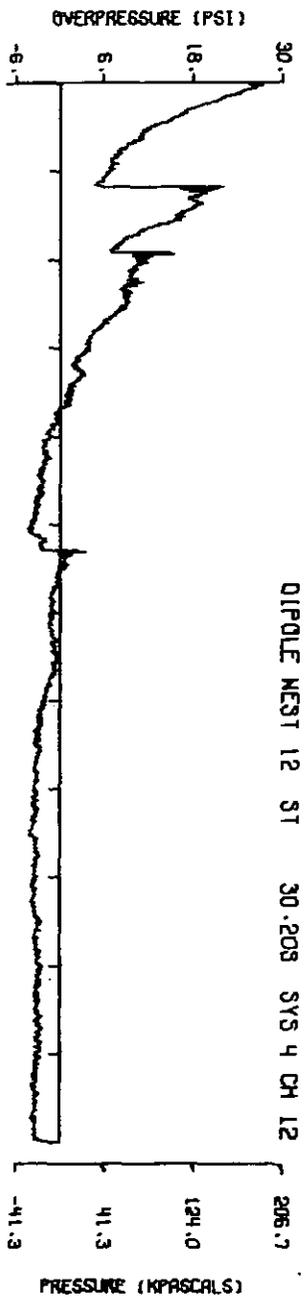
A12.13



A12.14



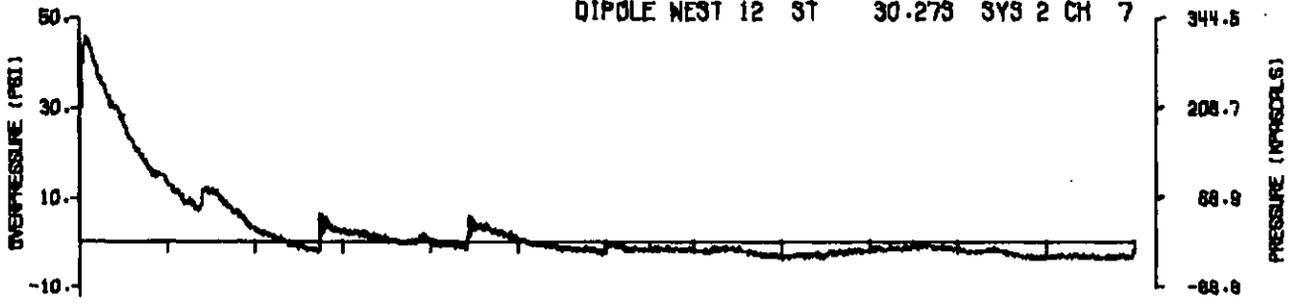
A12.15



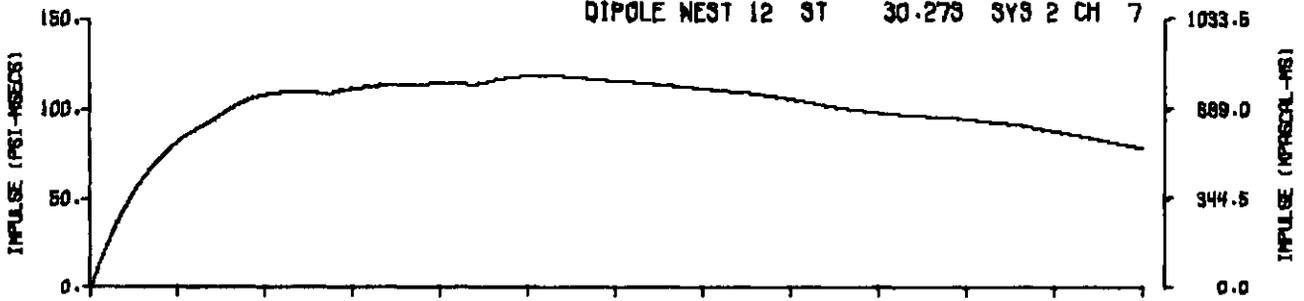
A12.16

173

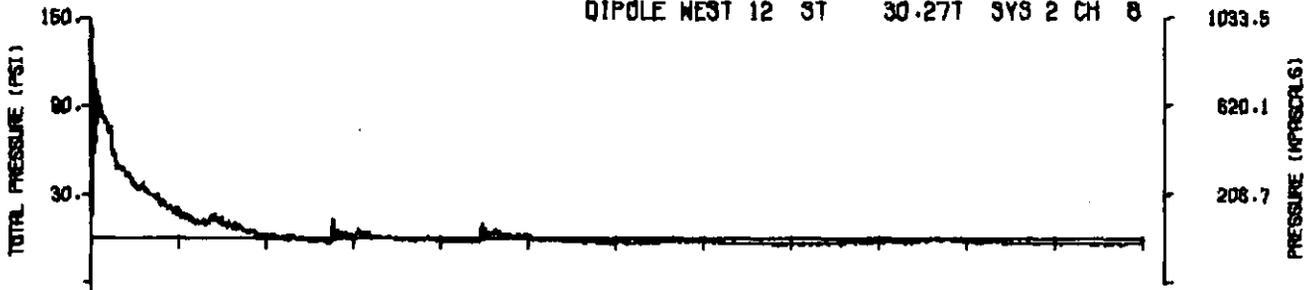
DIPOLE WEST 12 ST 30.275 SYS 2 CH 7



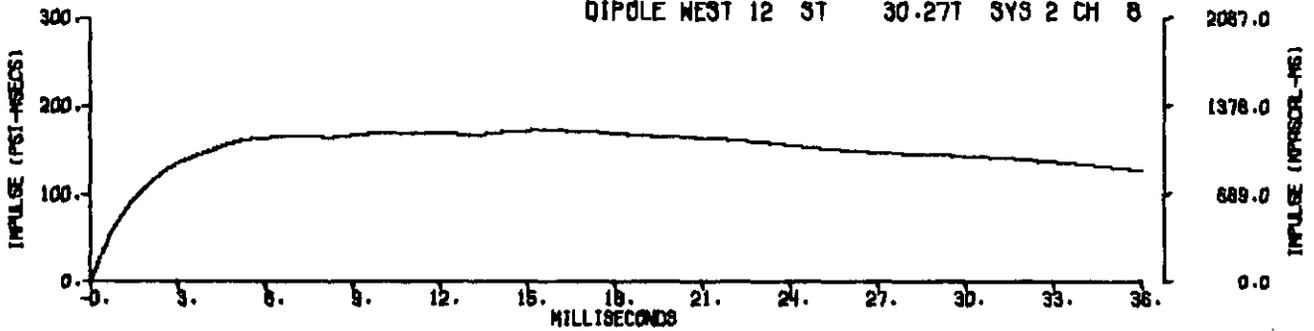
DIPOLE WEST 12 ST 30.275 SYS 2 CH 7



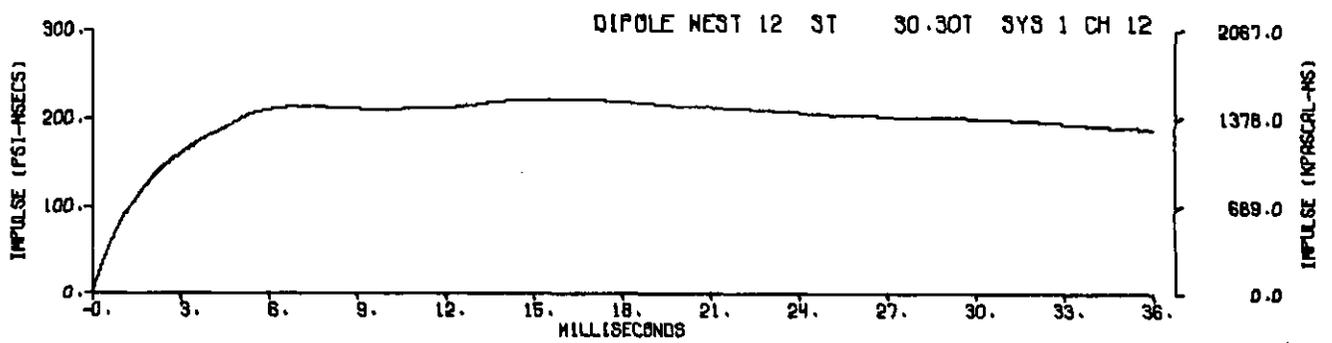
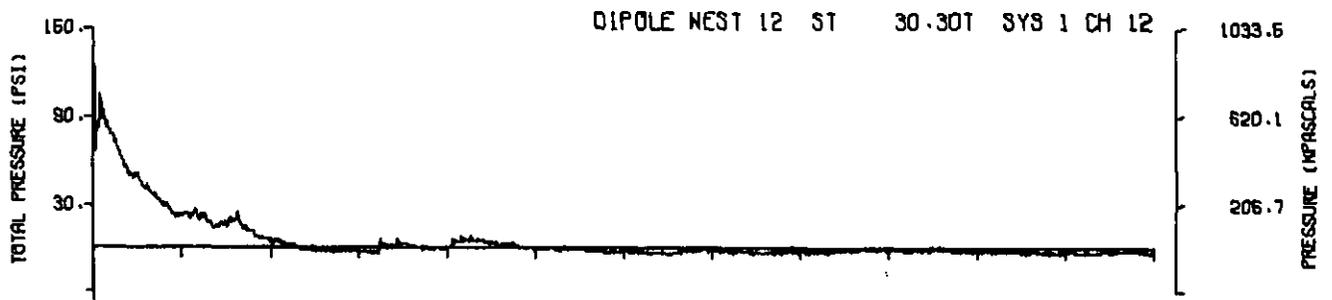
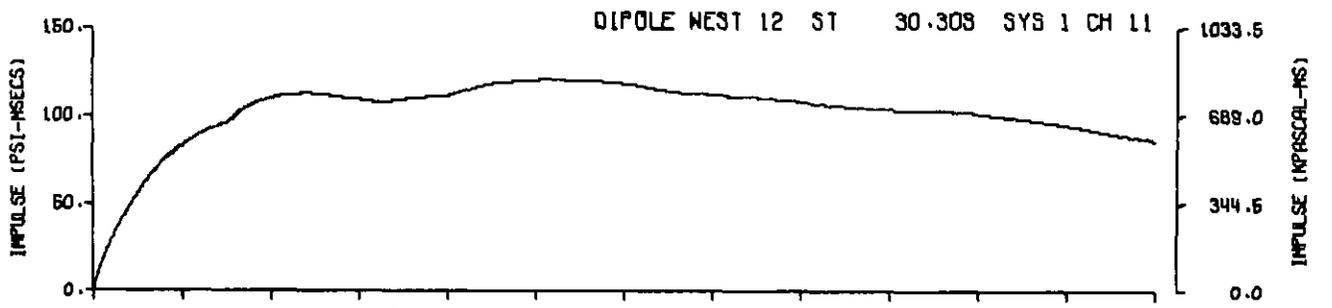
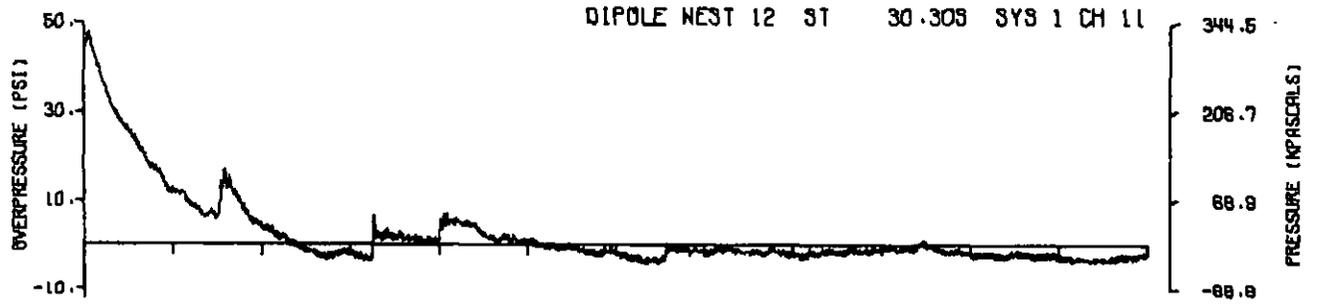
DIPOLE WEST 12 ST 30.271 SYS 2 CH 8



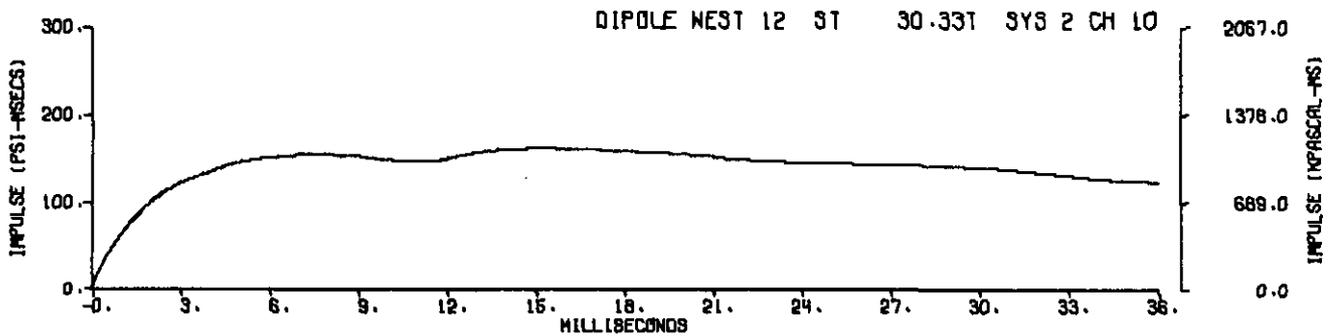
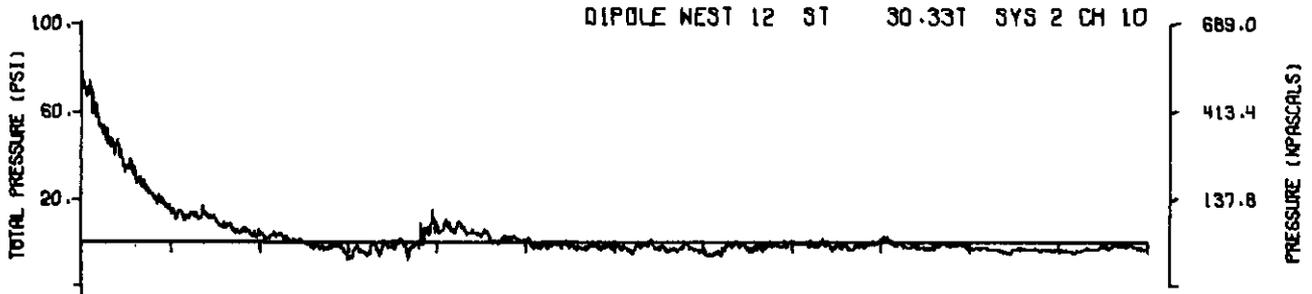
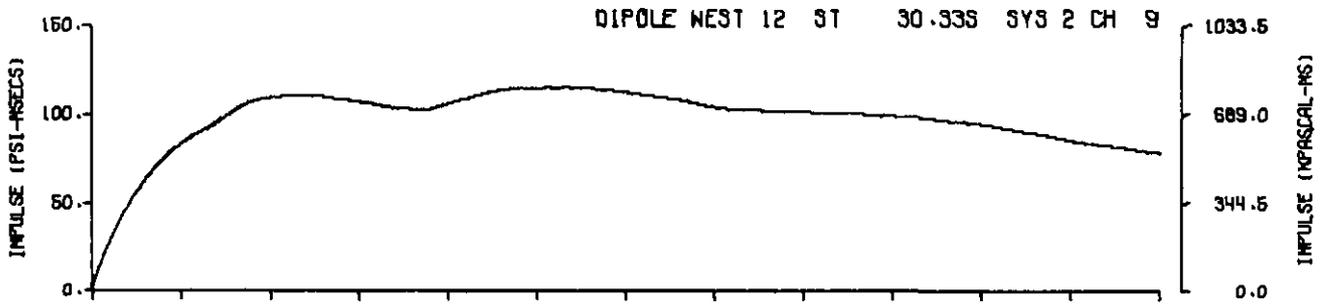
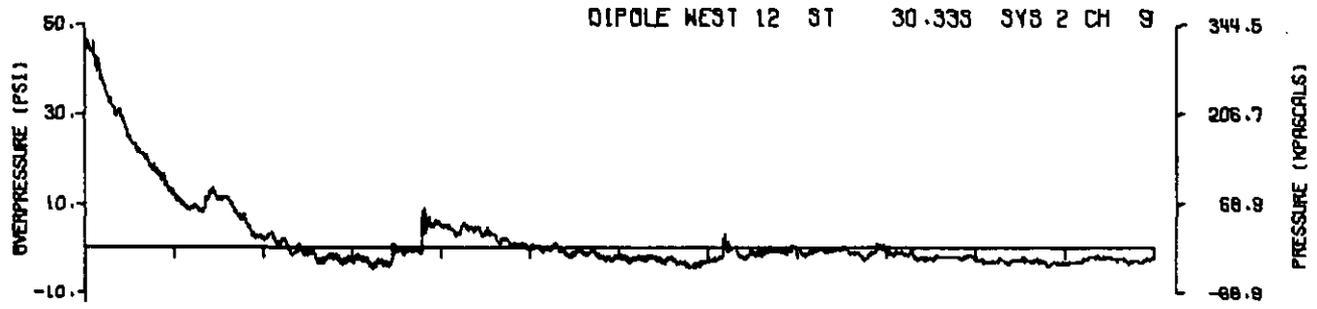
DIPOLE WEST 12 ST 30.271 SYS 2 CH 8



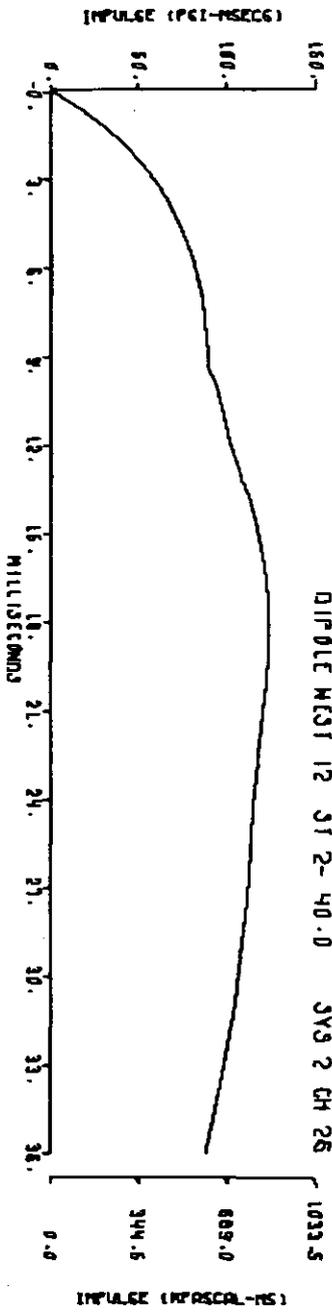
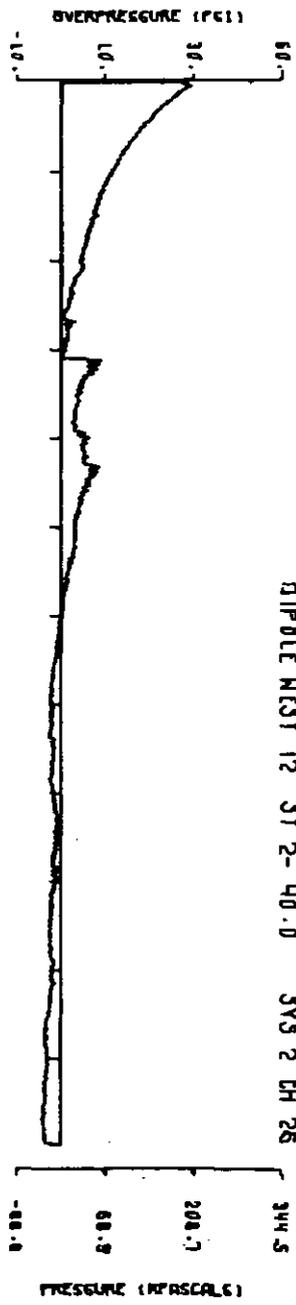
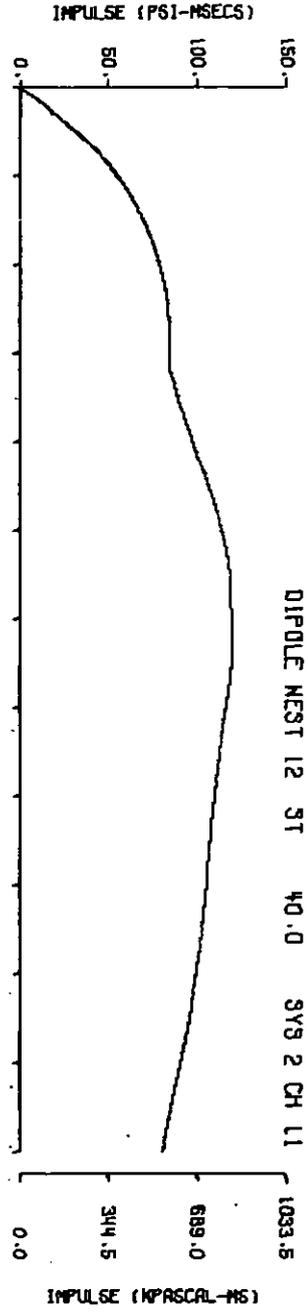
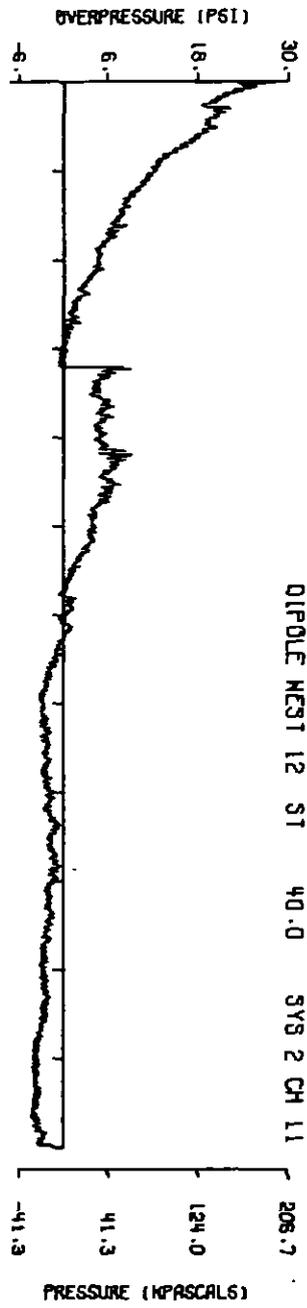
A12.17

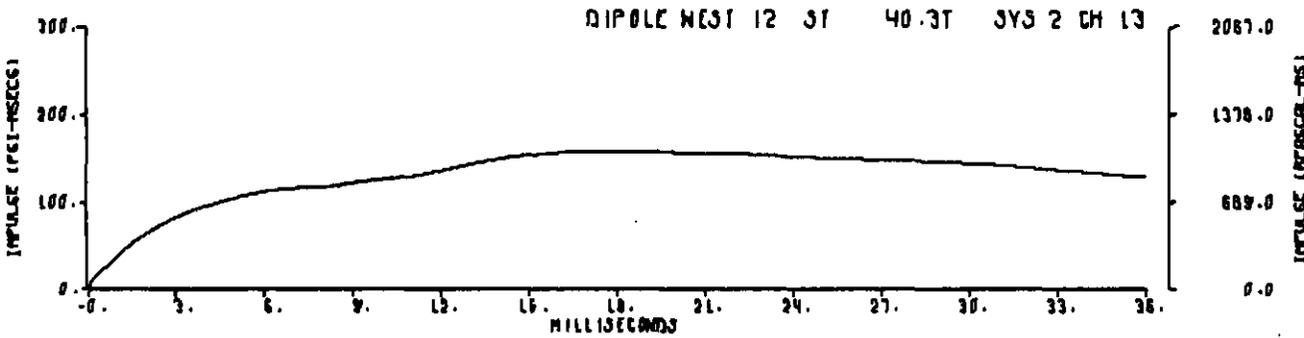
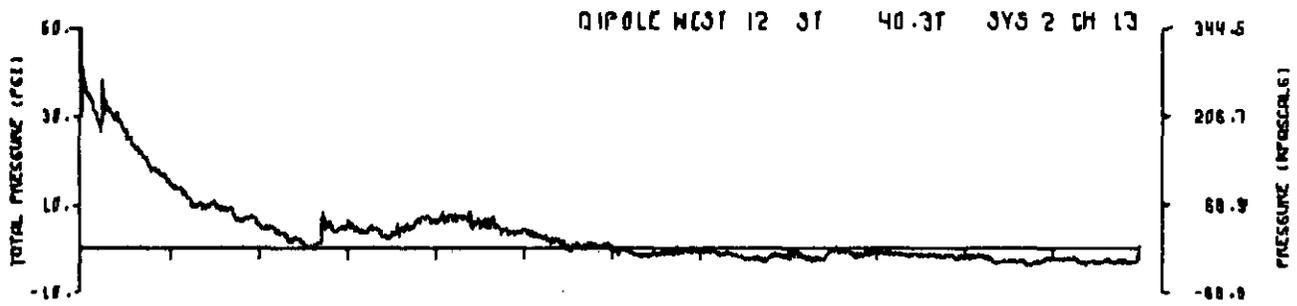
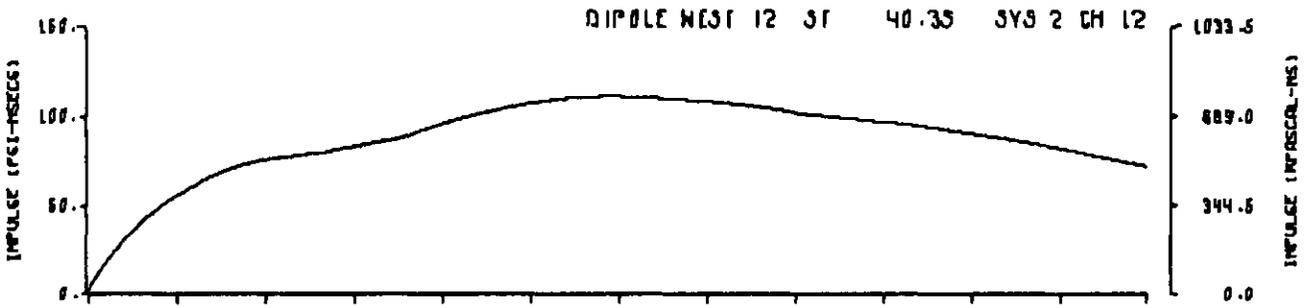
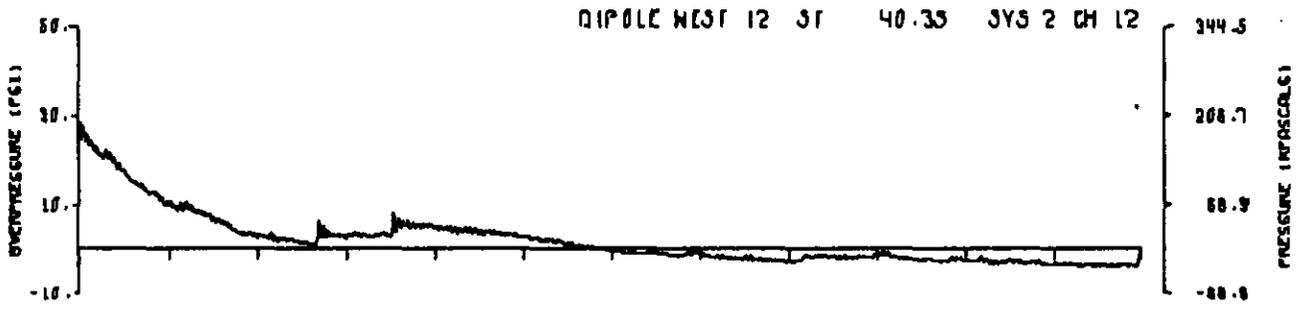


A12.18

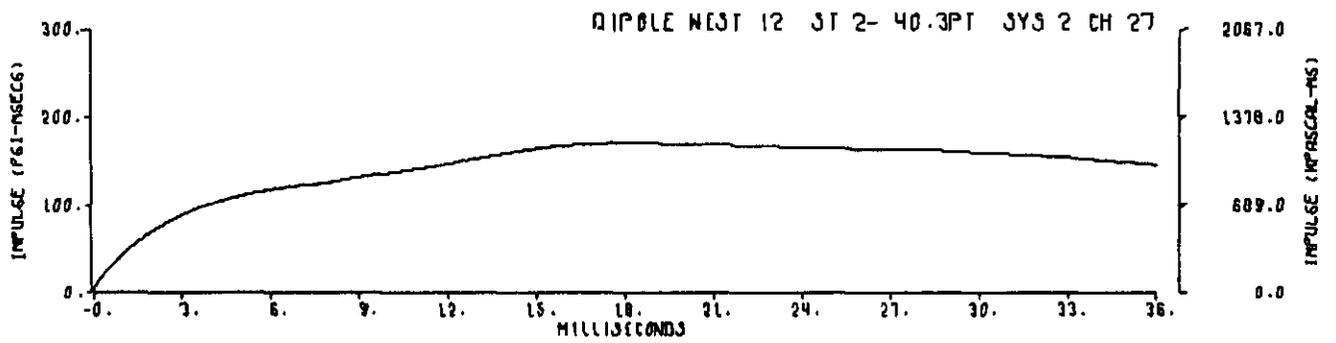
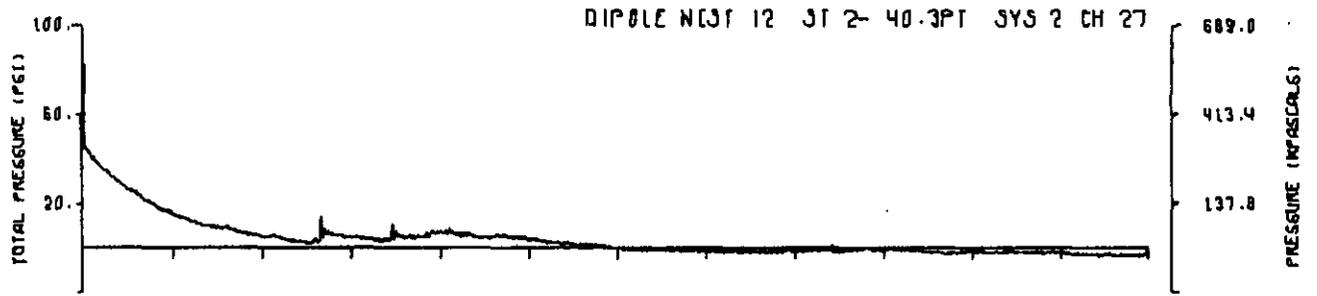


A12.19

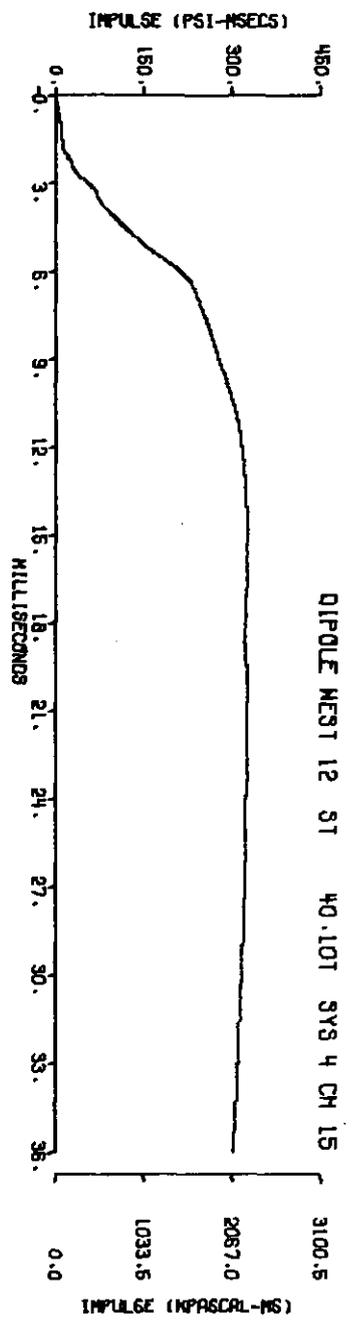
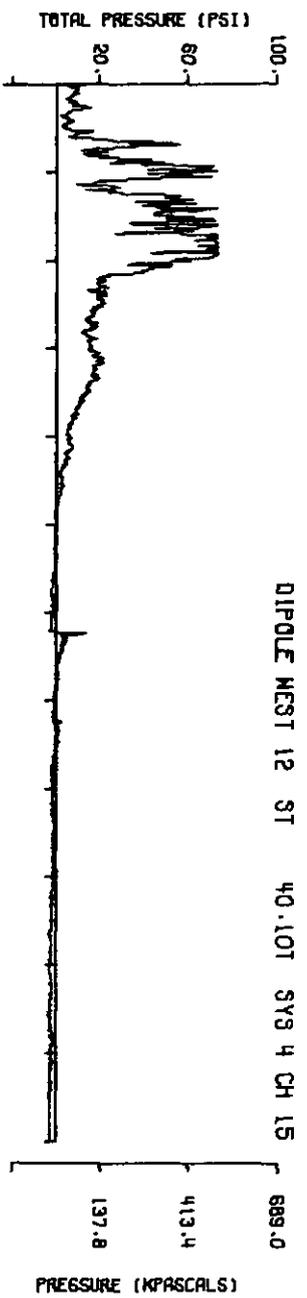
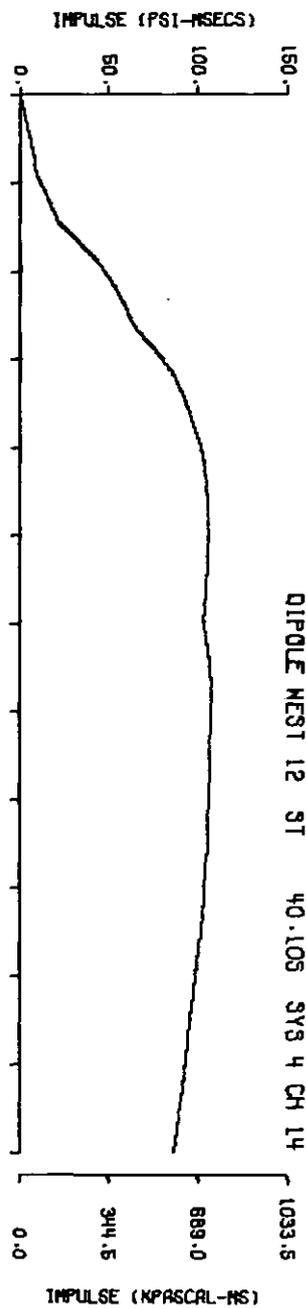
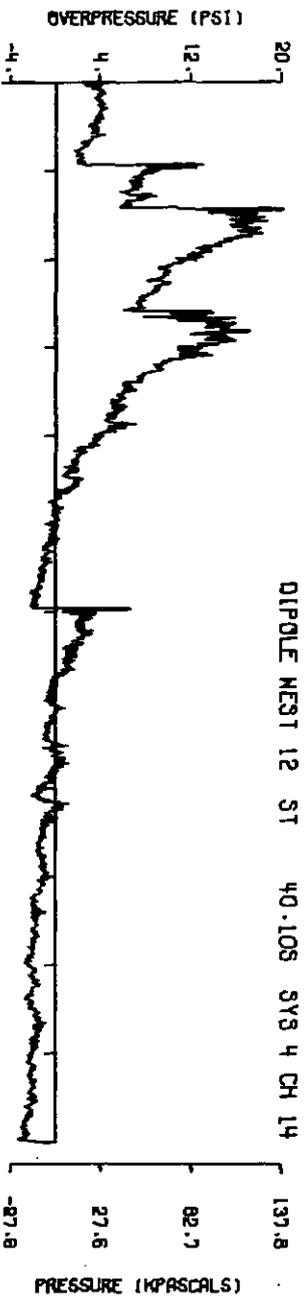




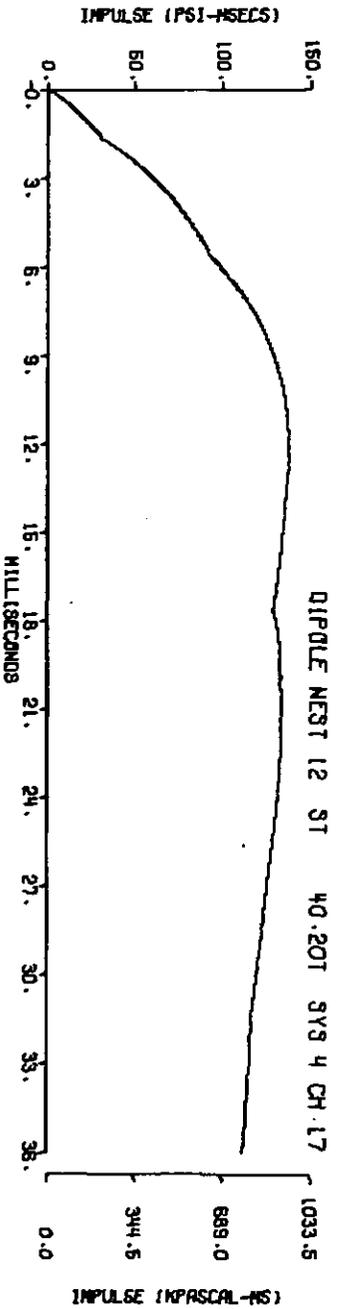
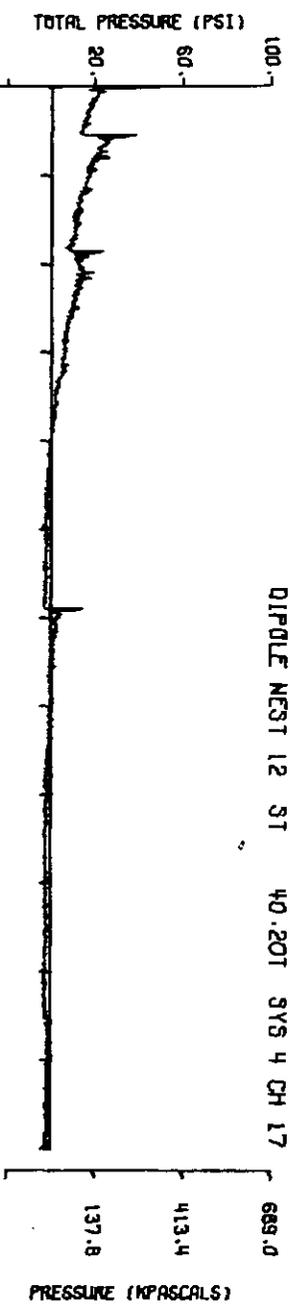
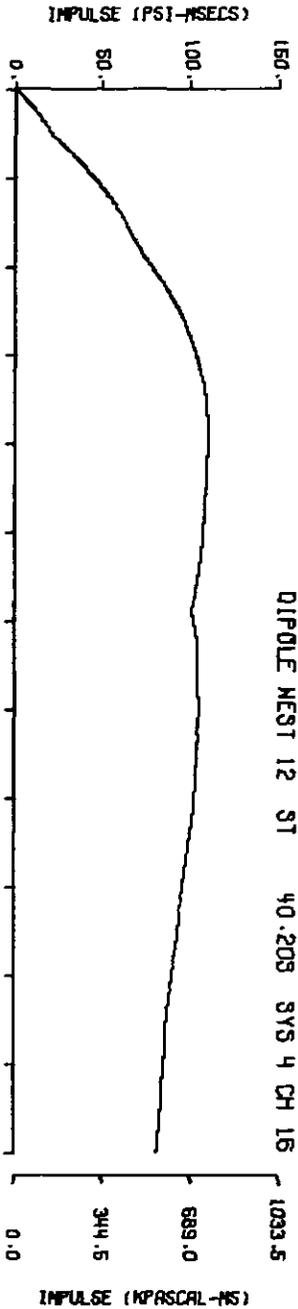
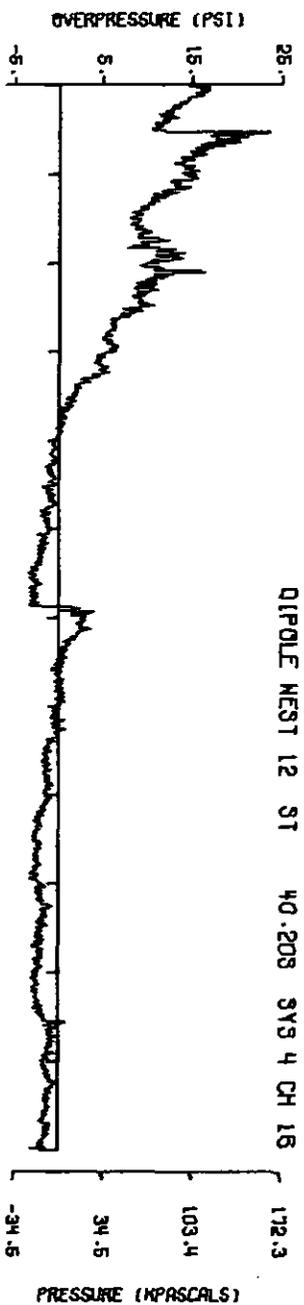
A12.21



A12.22

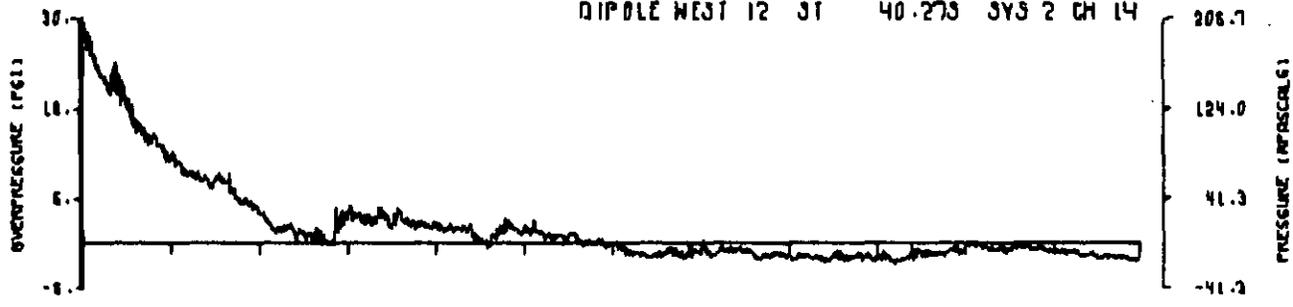


A12.23
180

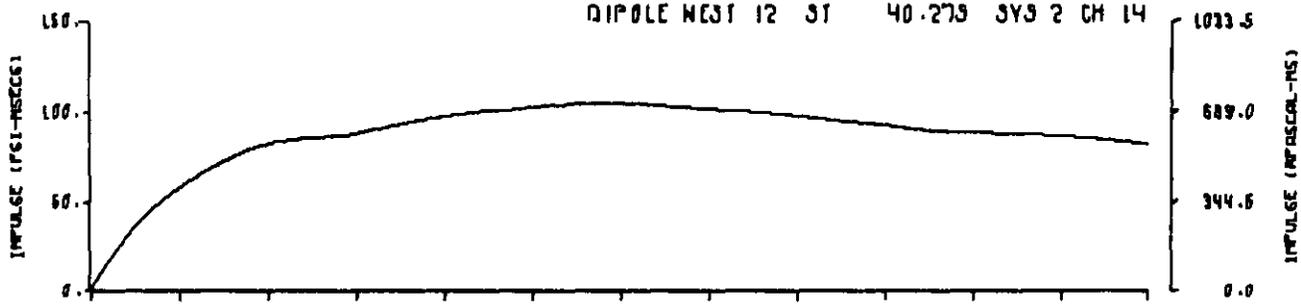


A12.24
181

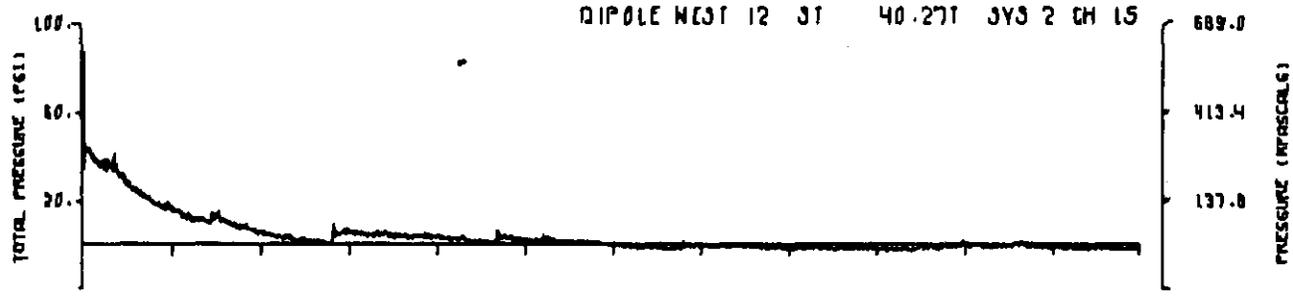
DIPOLE WEST 12 ST 40.273 SYS 2 CH 14



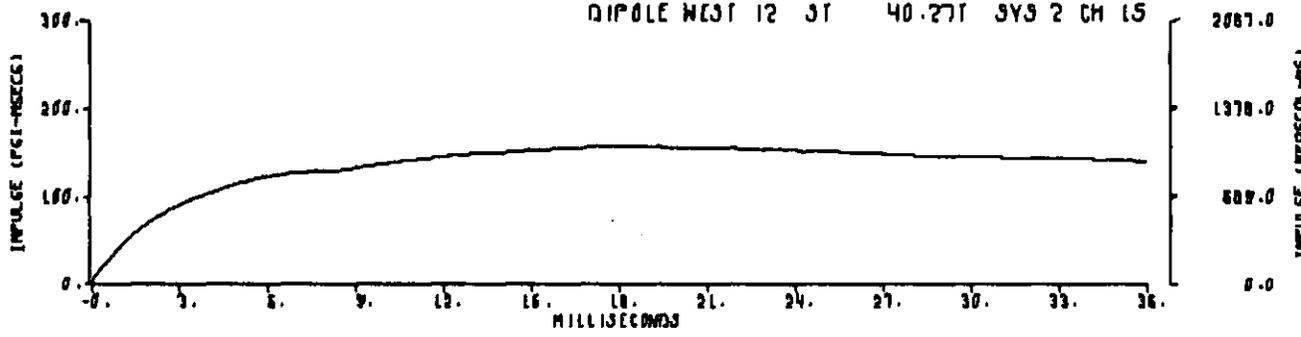
DIPOLE WEST 12 ST 40.273 SYS 2 CH 14



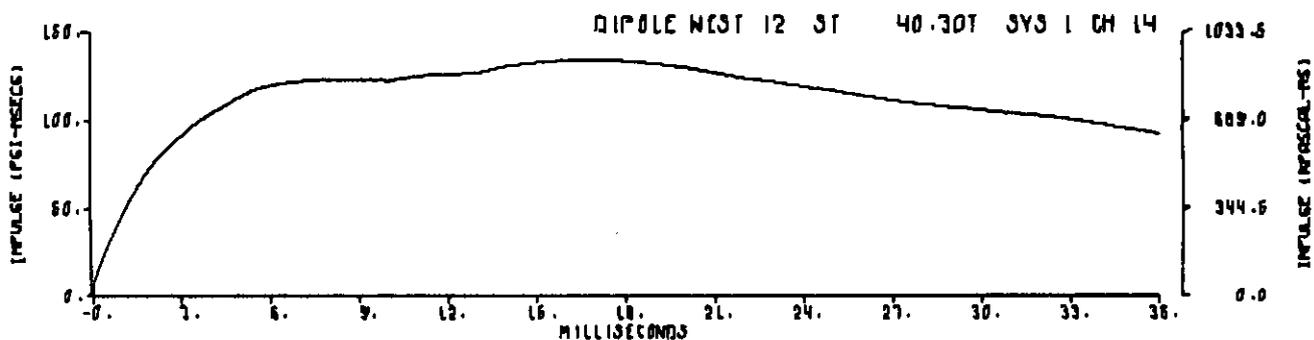
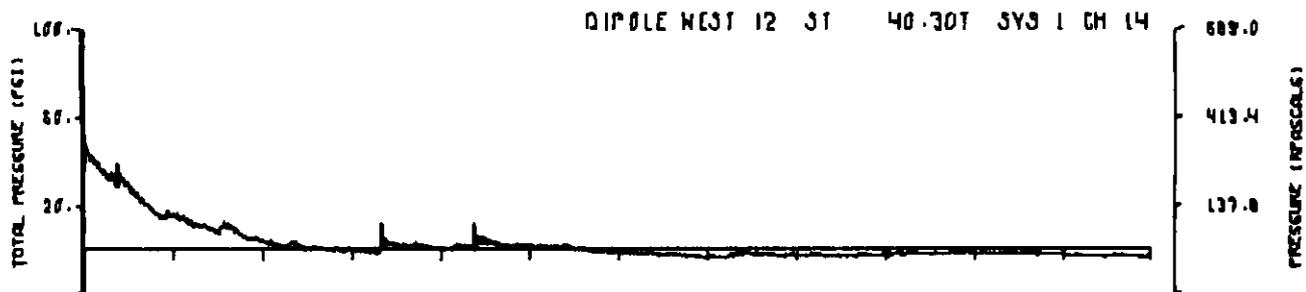
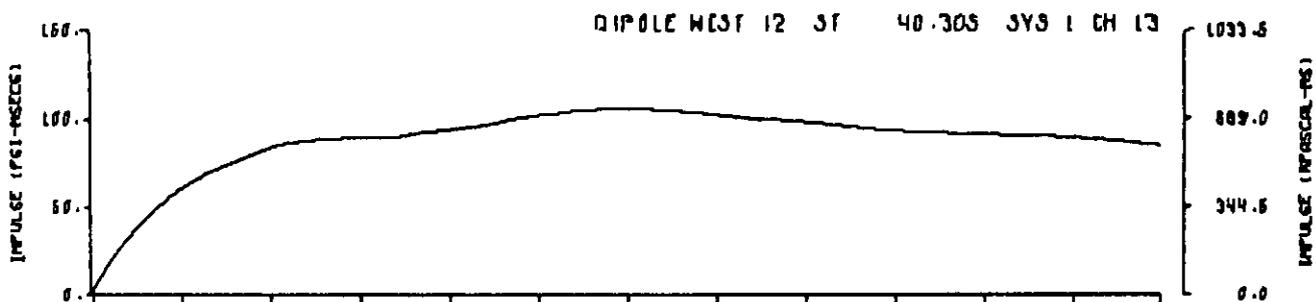
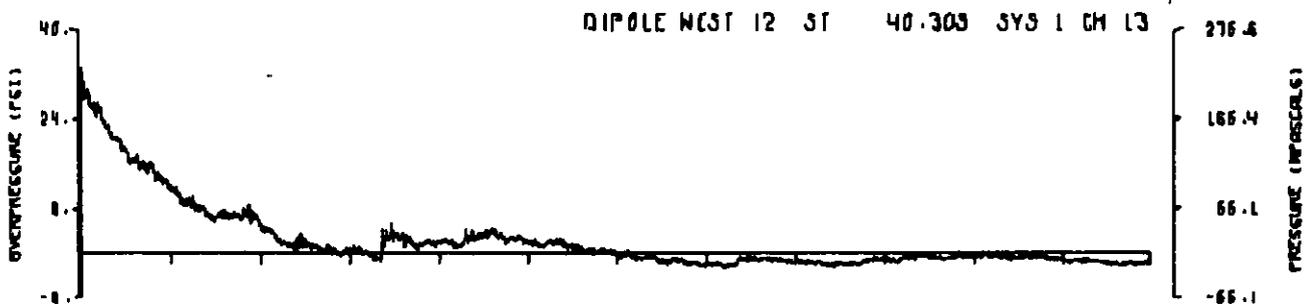
DIPOLE WEST 12 ST 40.271 SYS 2 CH 15



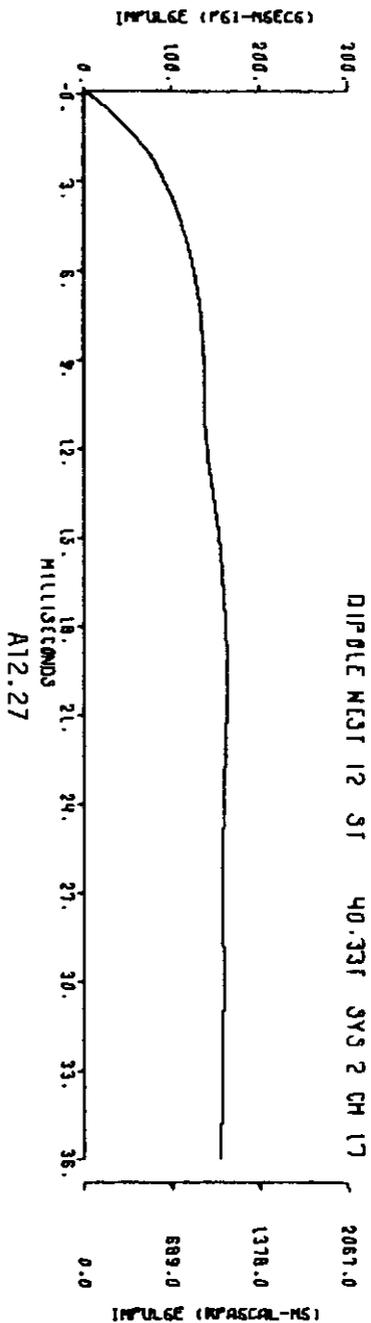
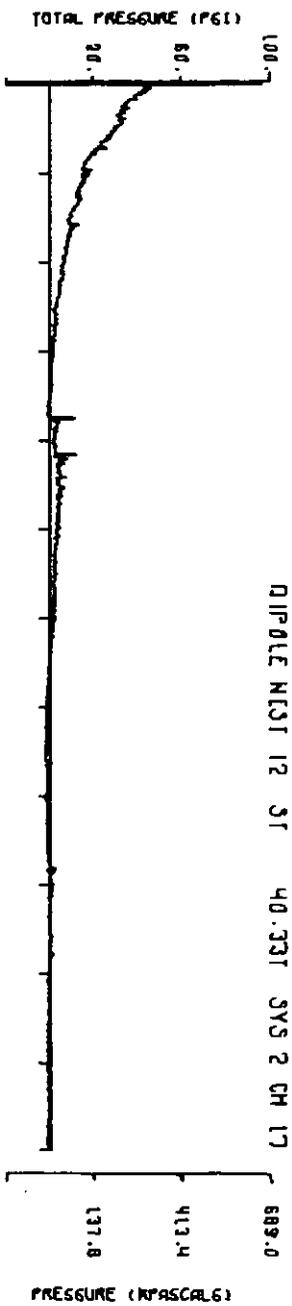
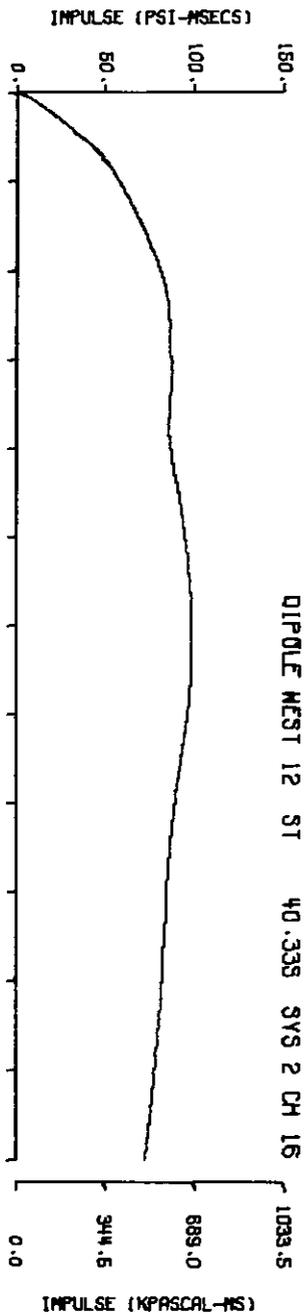
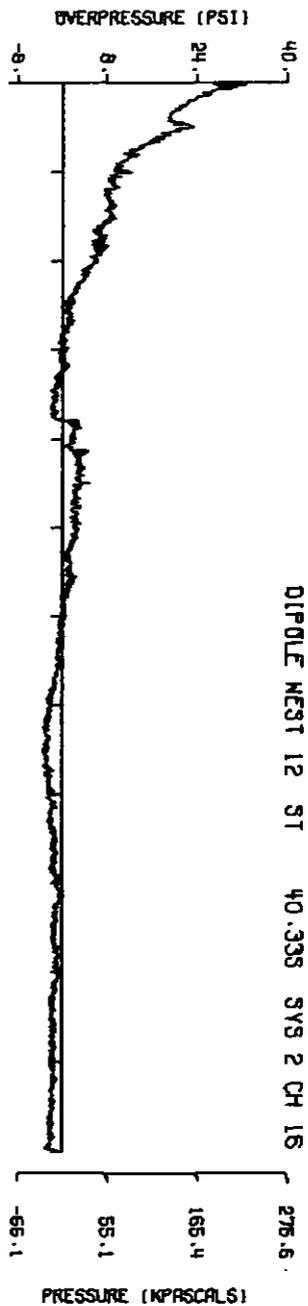
DIPOLE WEST 12 ST 40.271 SYS 2 CH 15

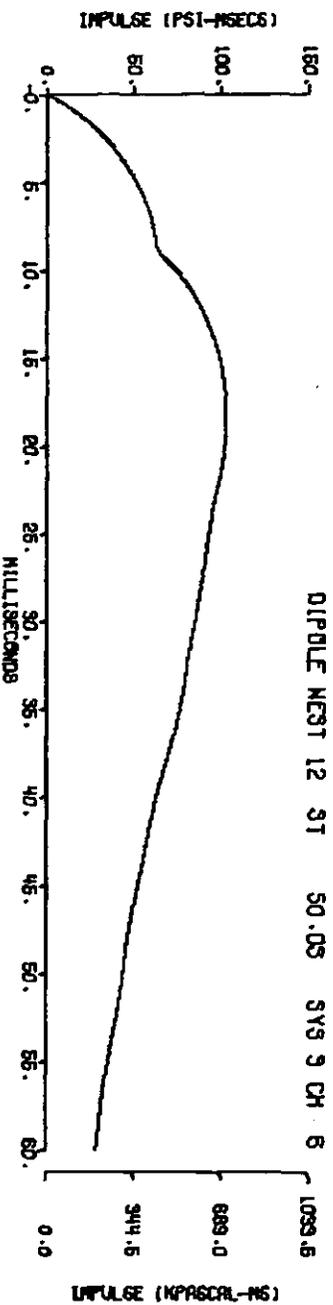
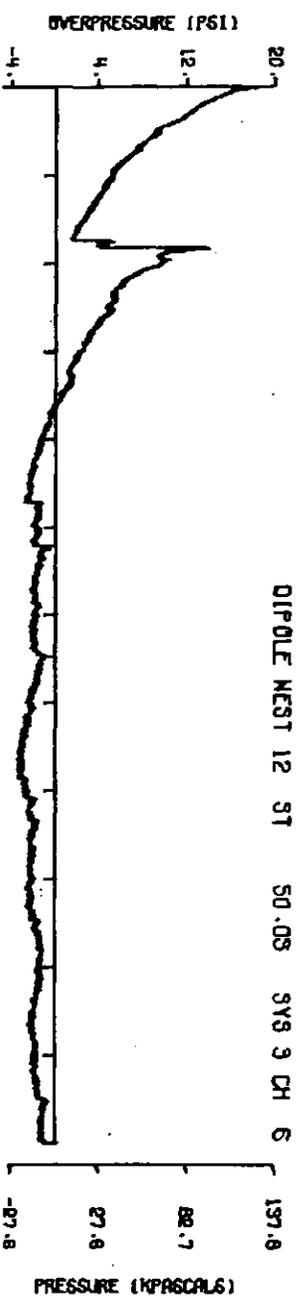
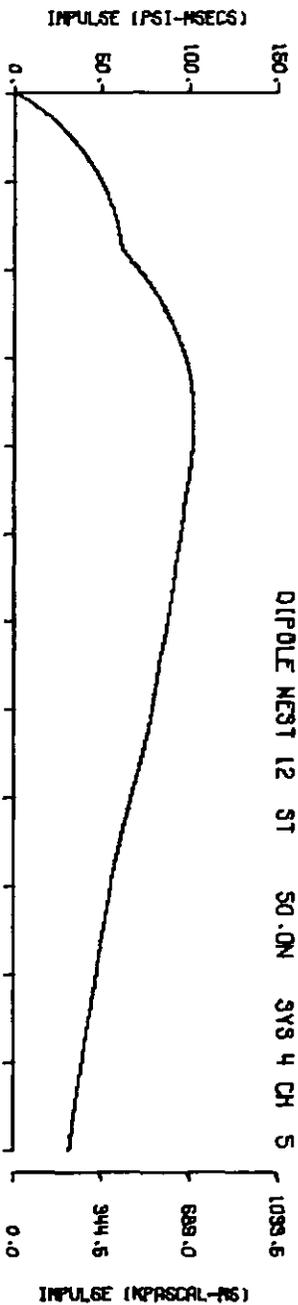
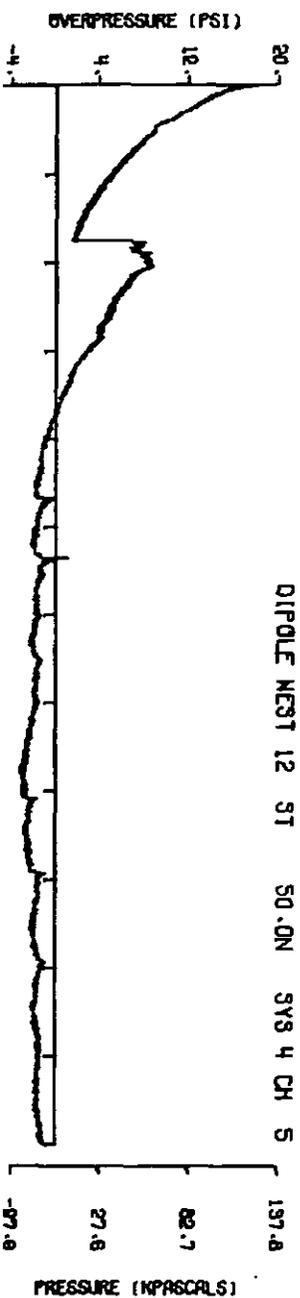


A12.25



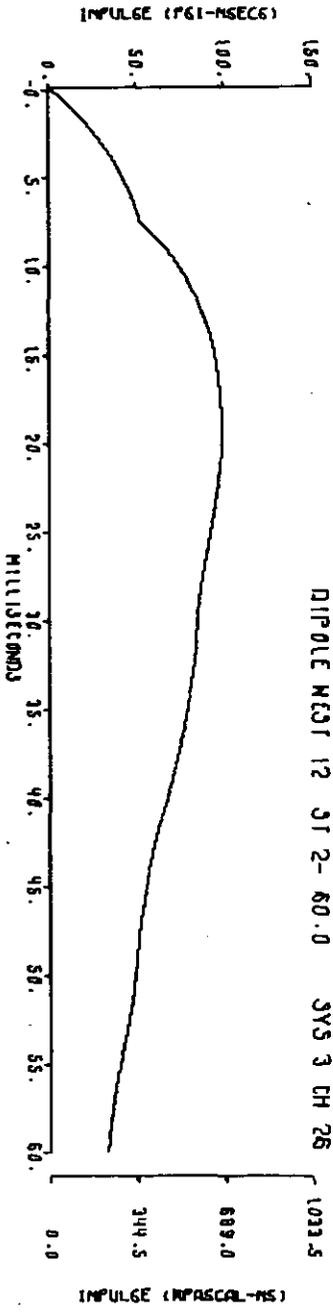
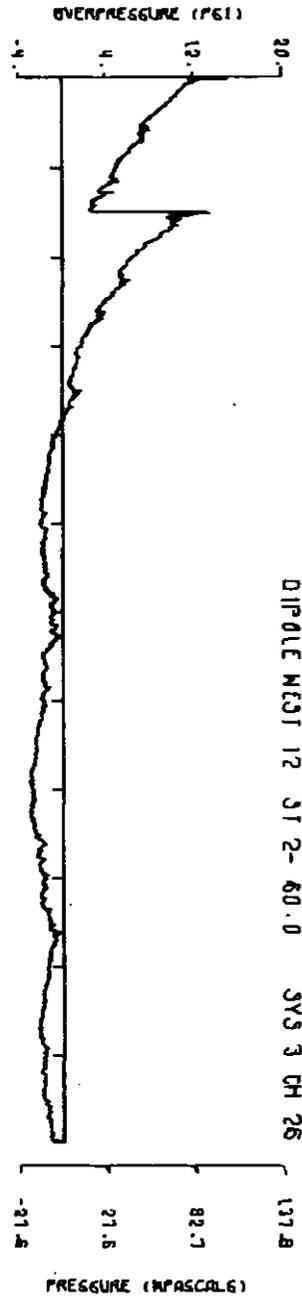
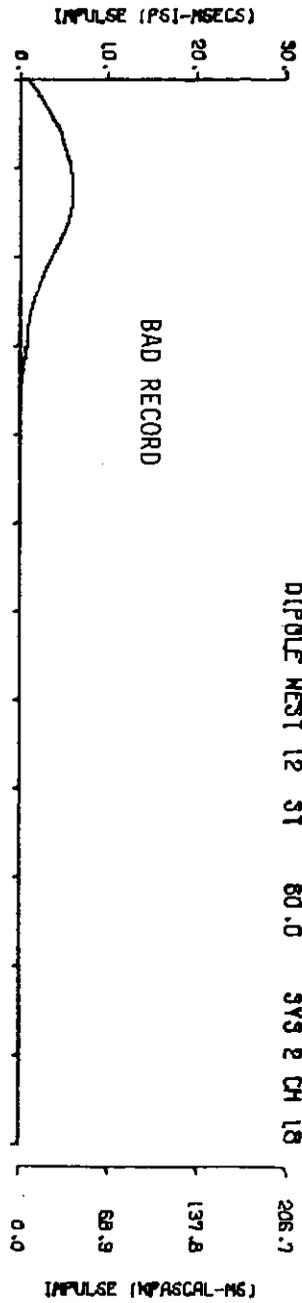
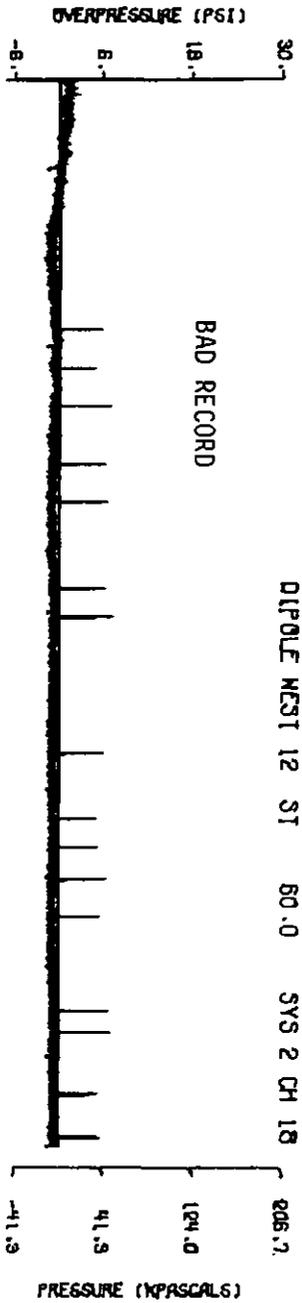
A12.26



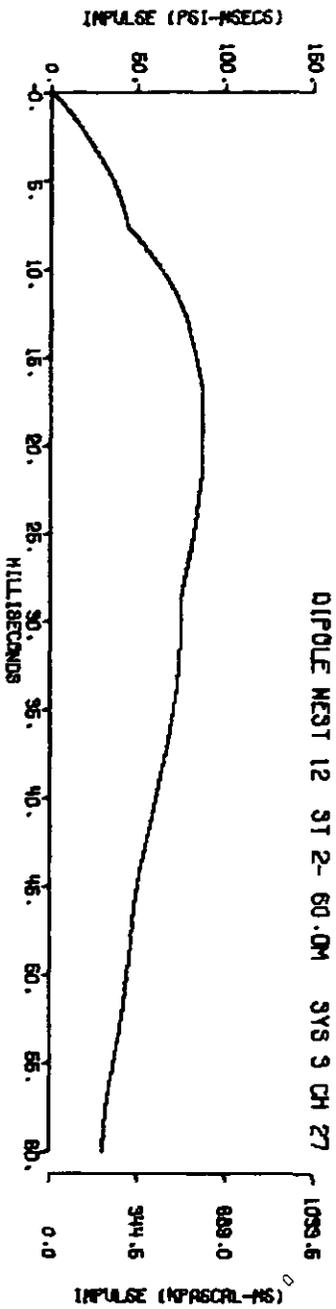
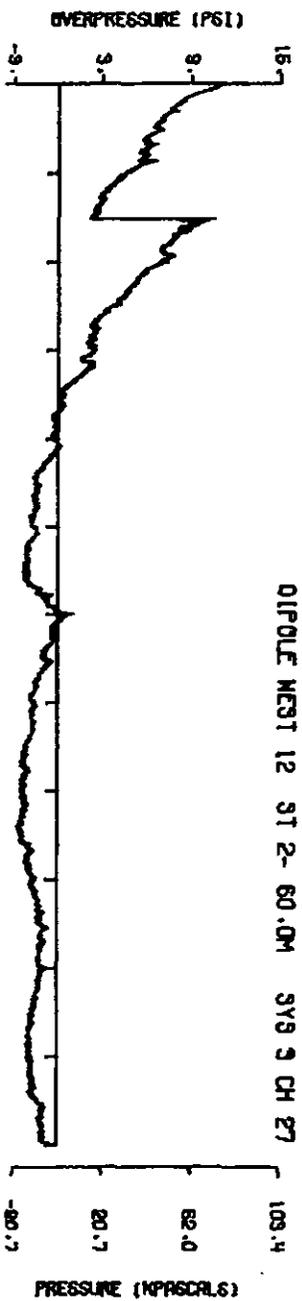


A12.28

185

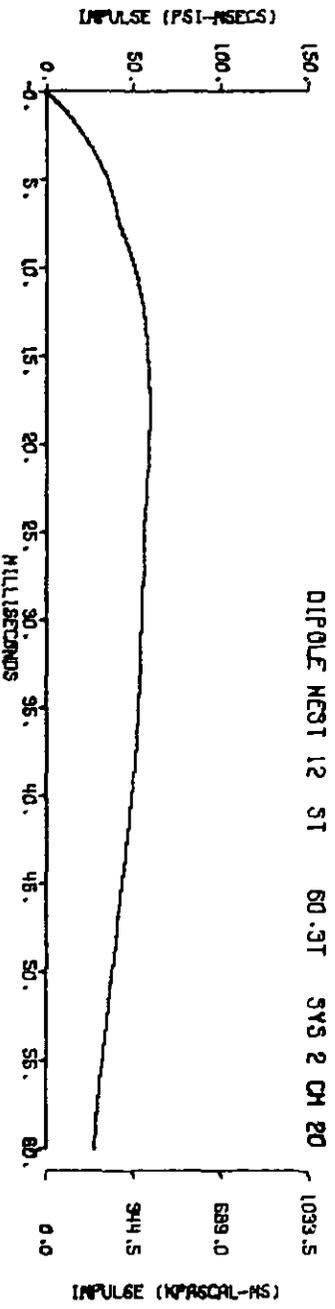
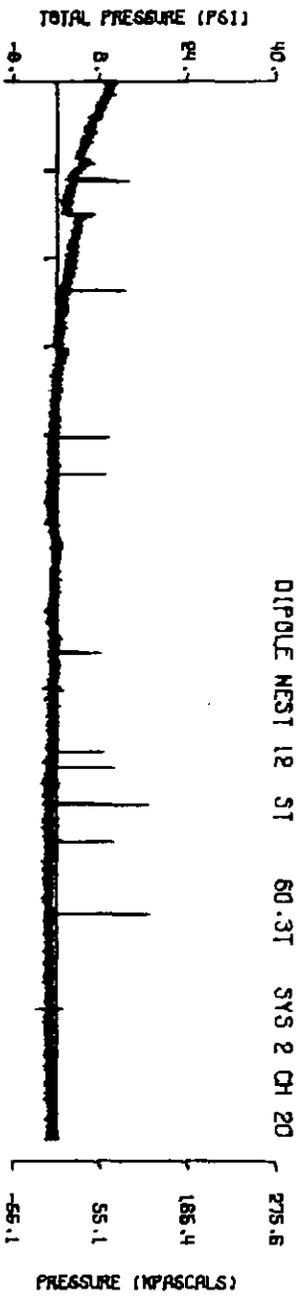
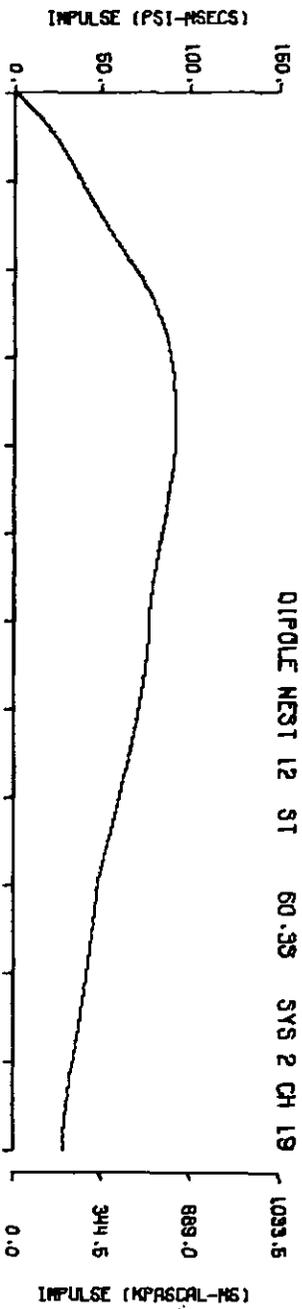
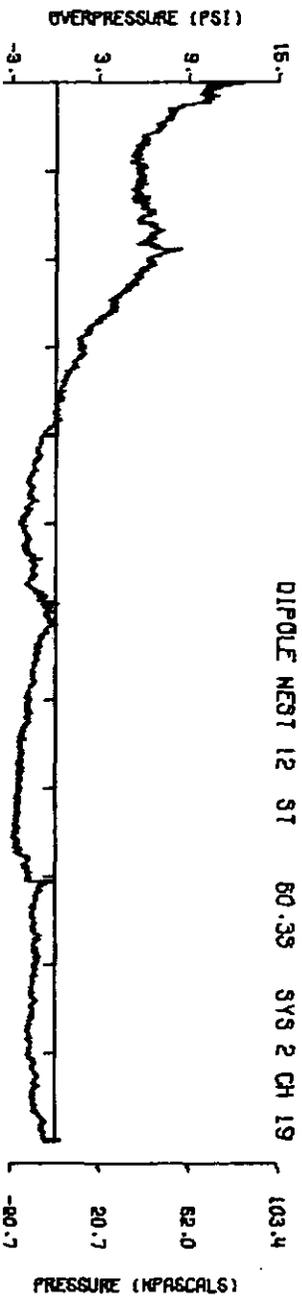


A12.29
186



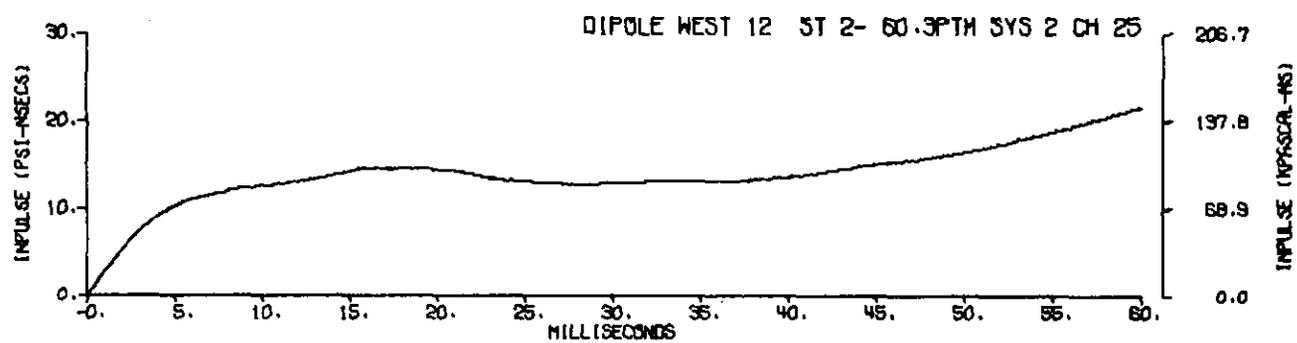
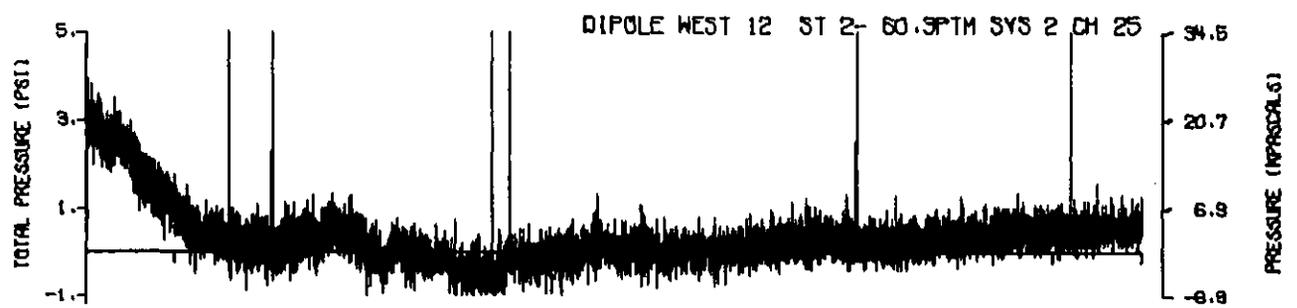
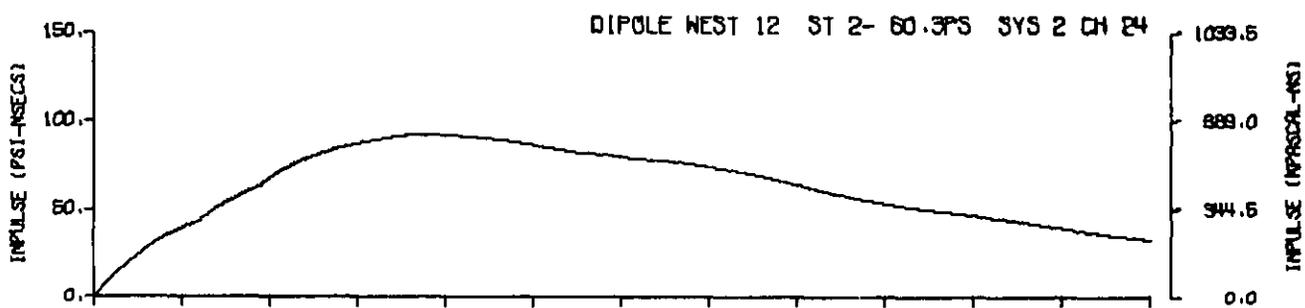
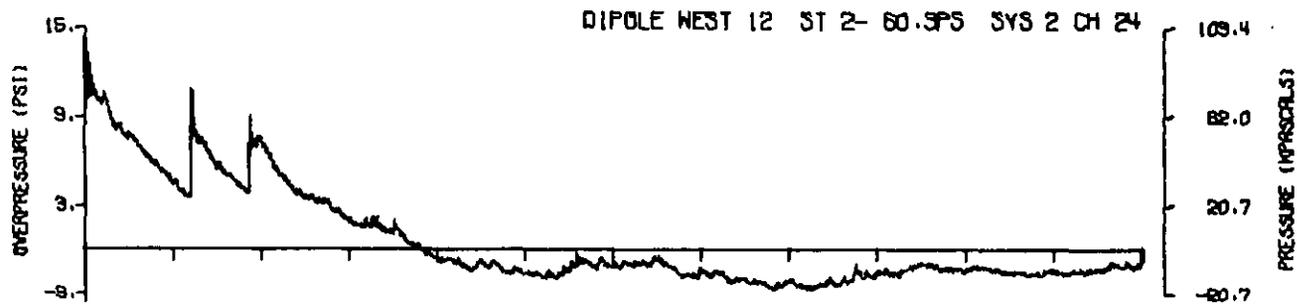
A12.30

187

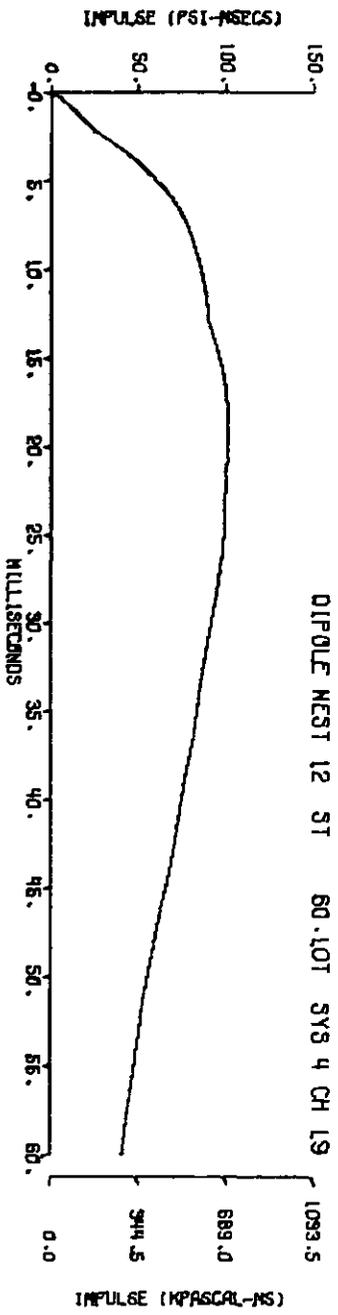
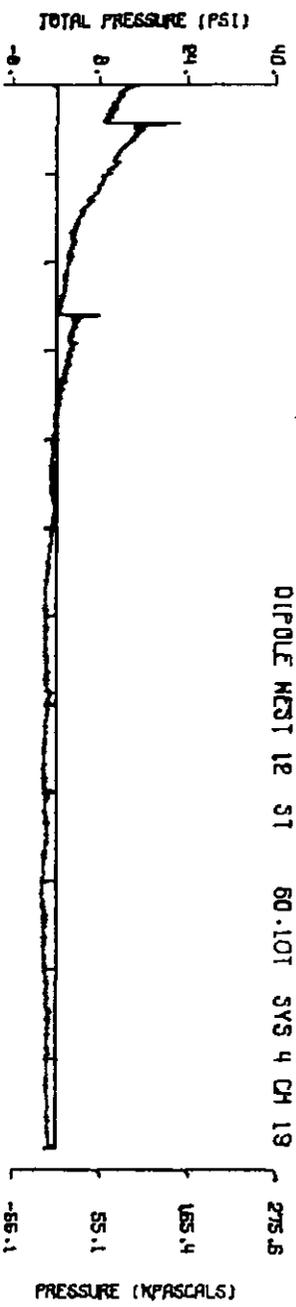
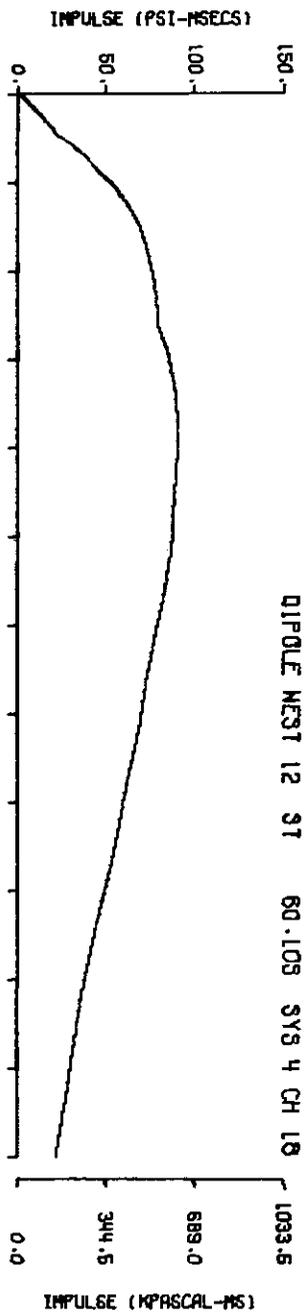
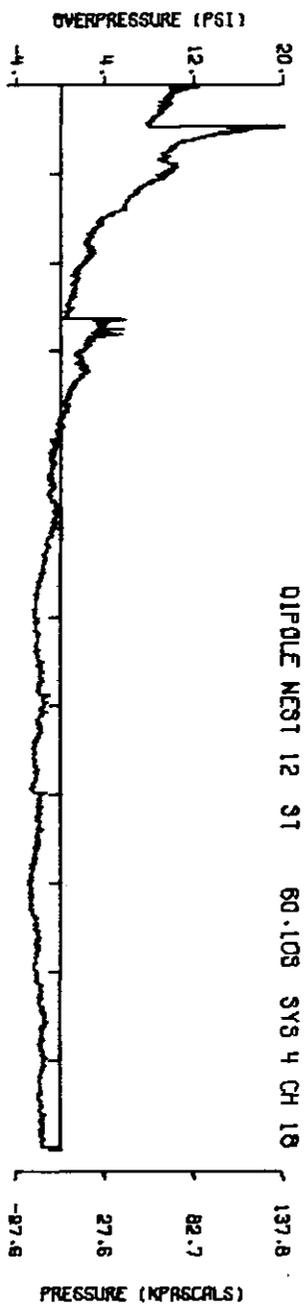


A12.31

188

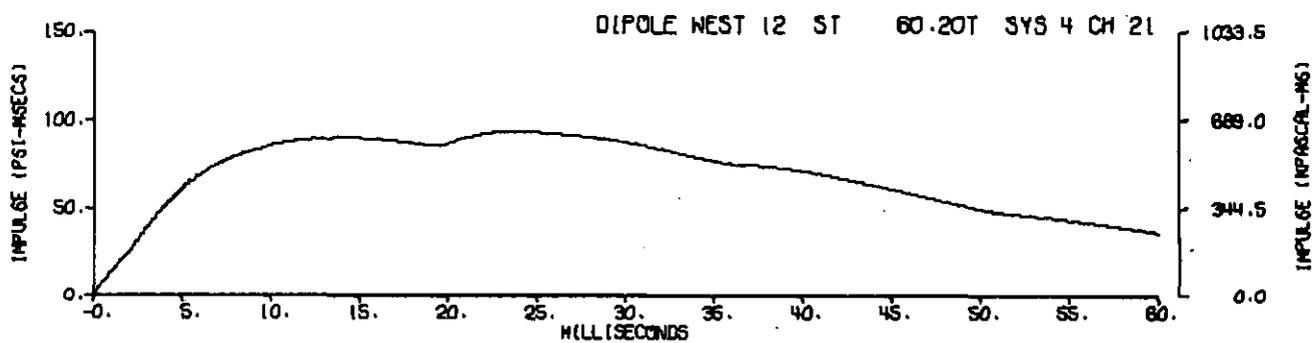
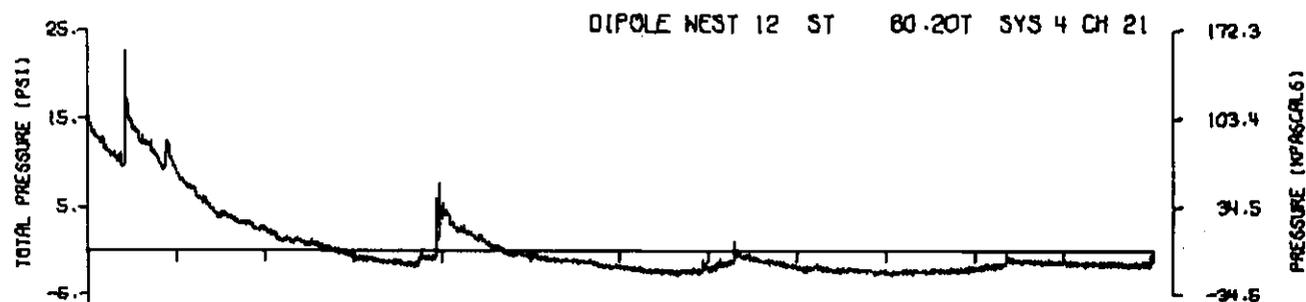
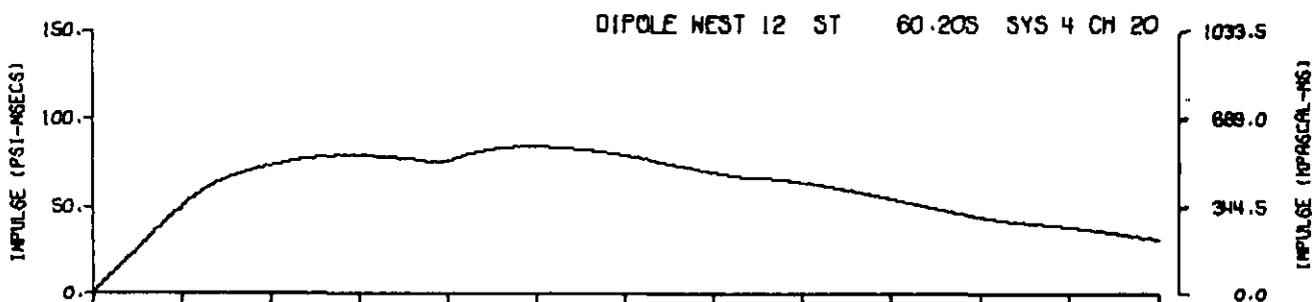
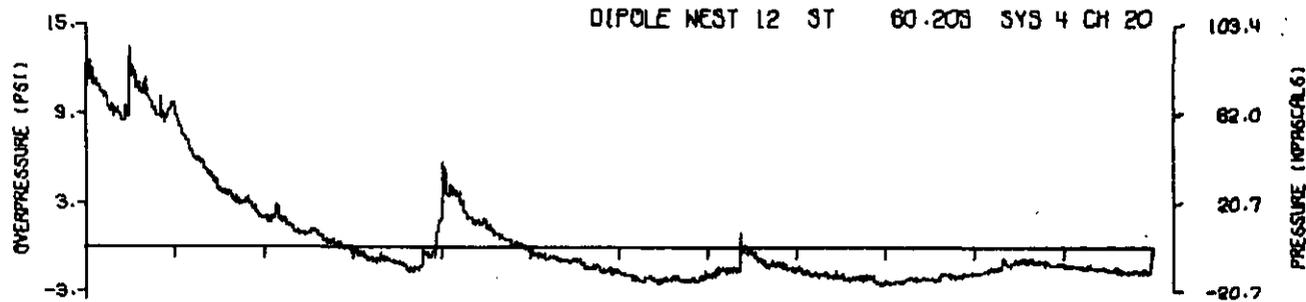


A12.32

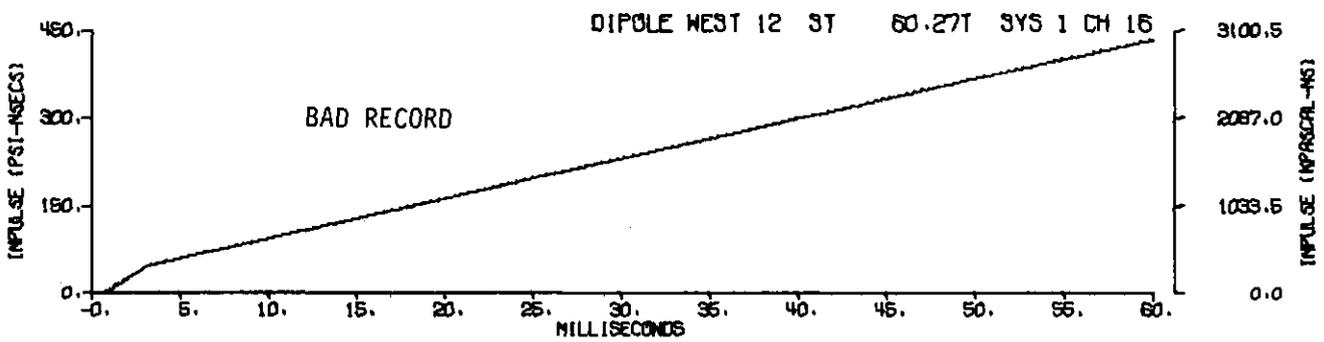
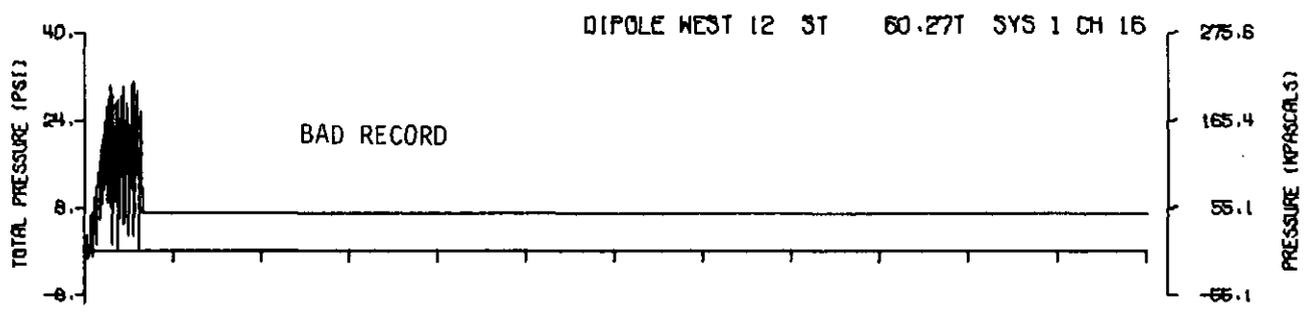
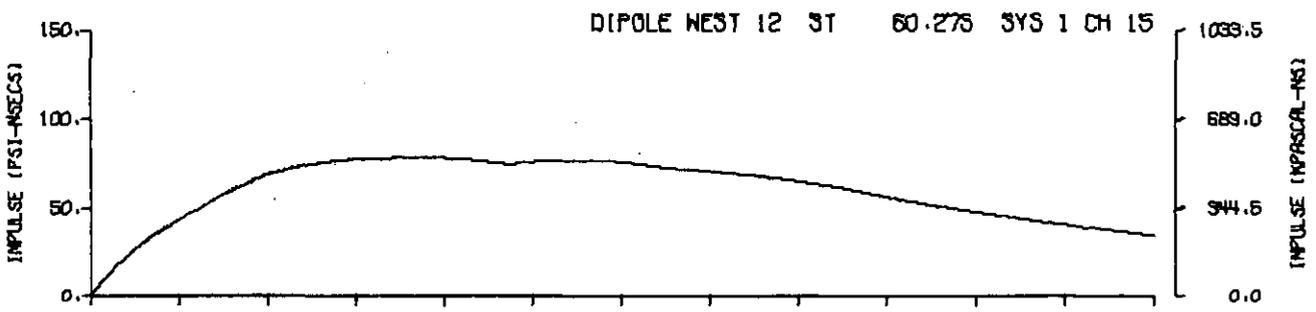
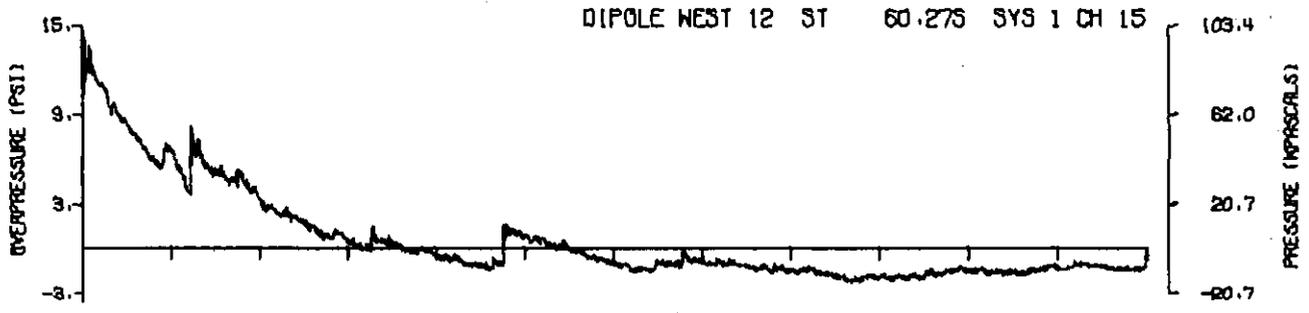


A12.33

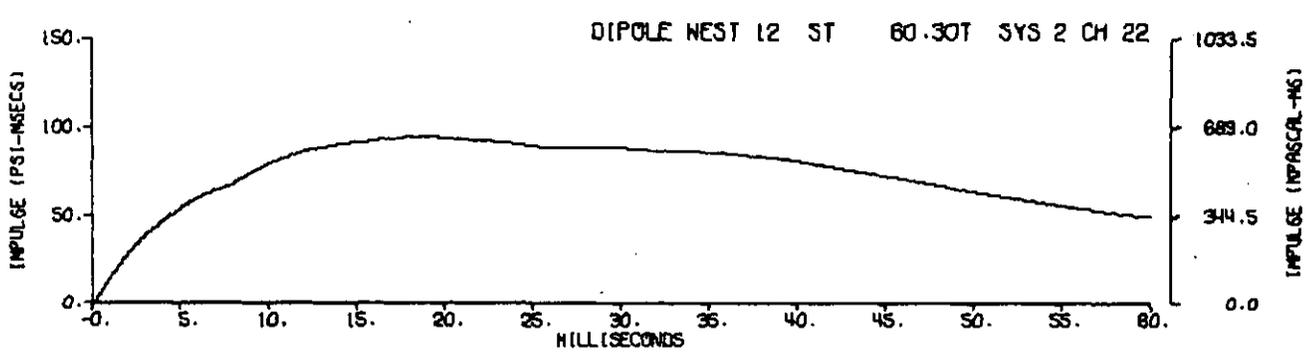
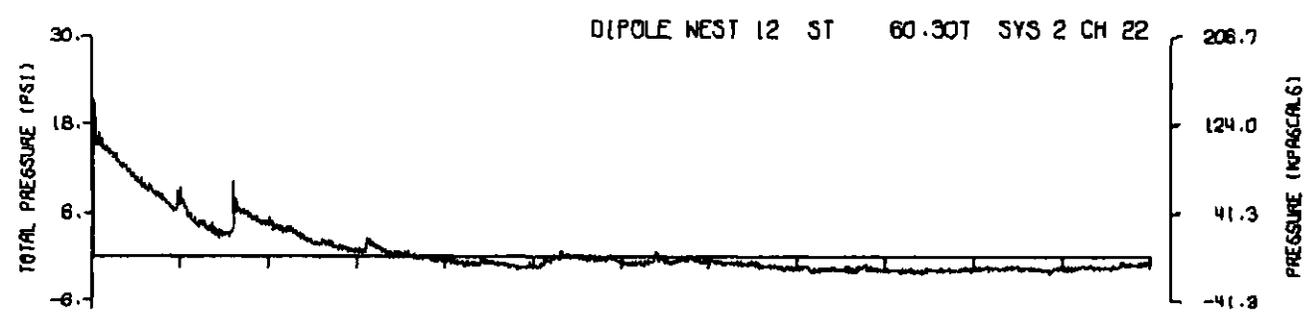
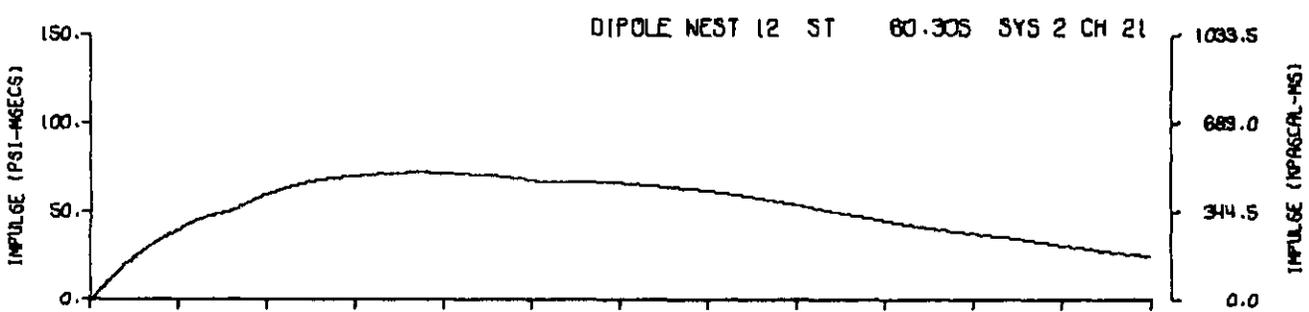
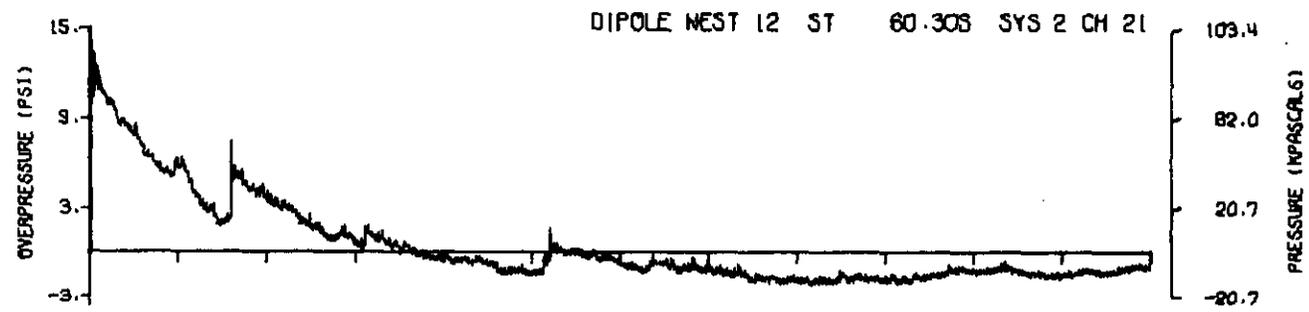
190



A12.34

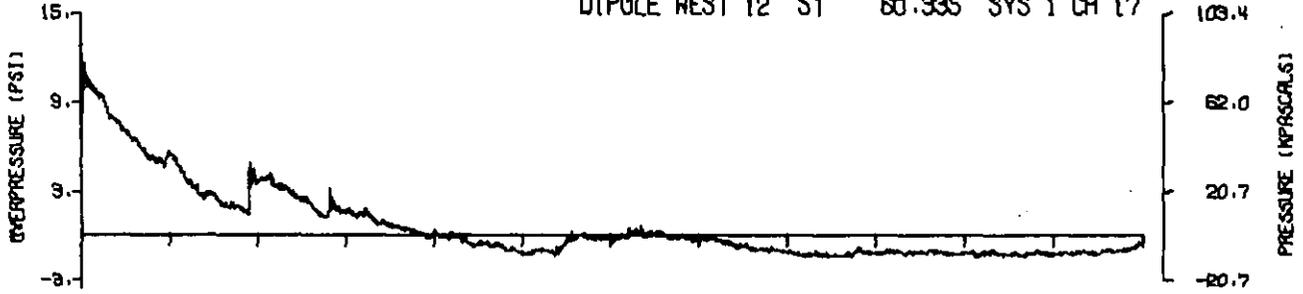


A12.35

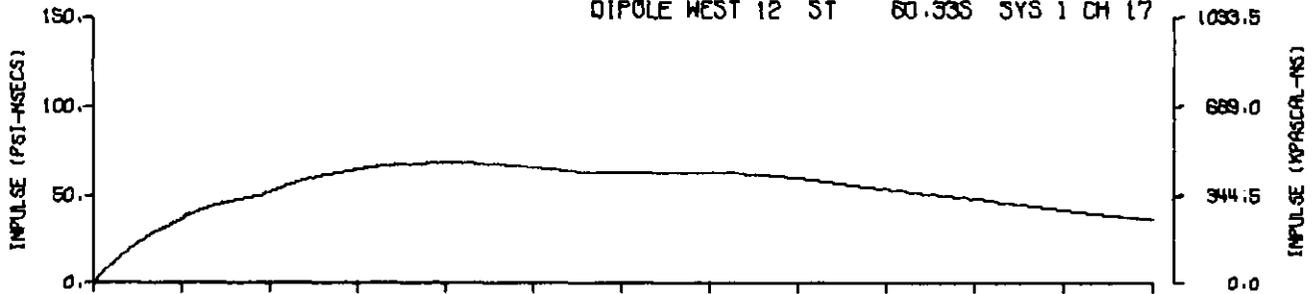


A12.36

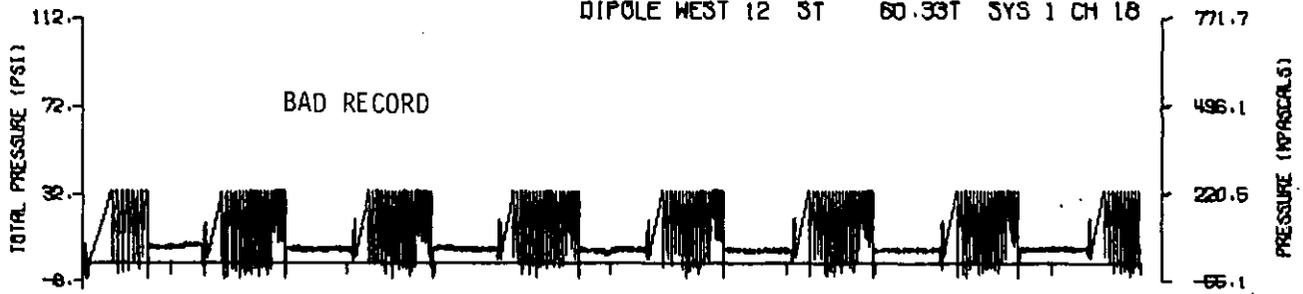
DIPOLE WEST 12 ST 60.33S SYS 1 CH 17



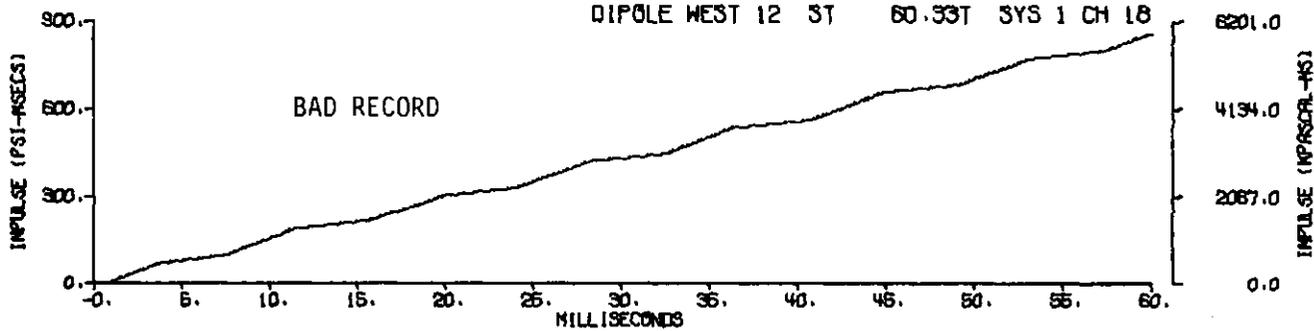
DIPOLE WEST 12 ST 60.33S SYS 1 CH 17



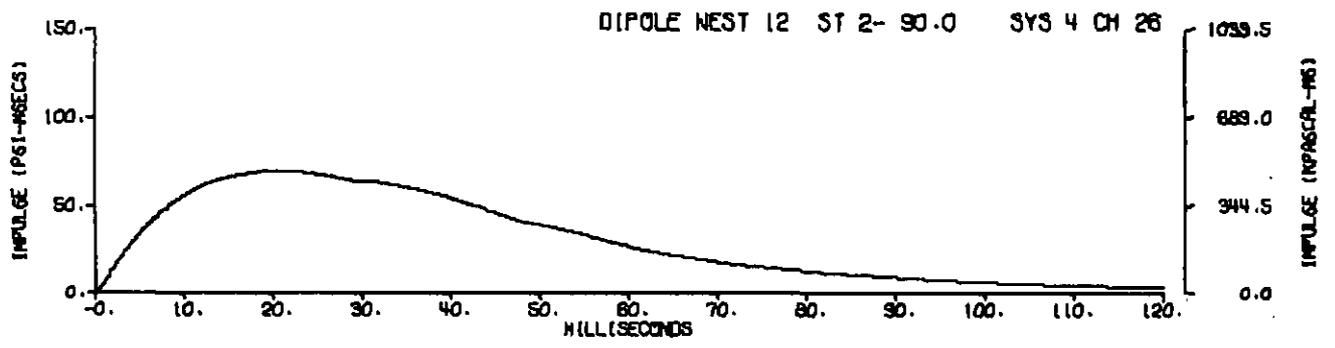
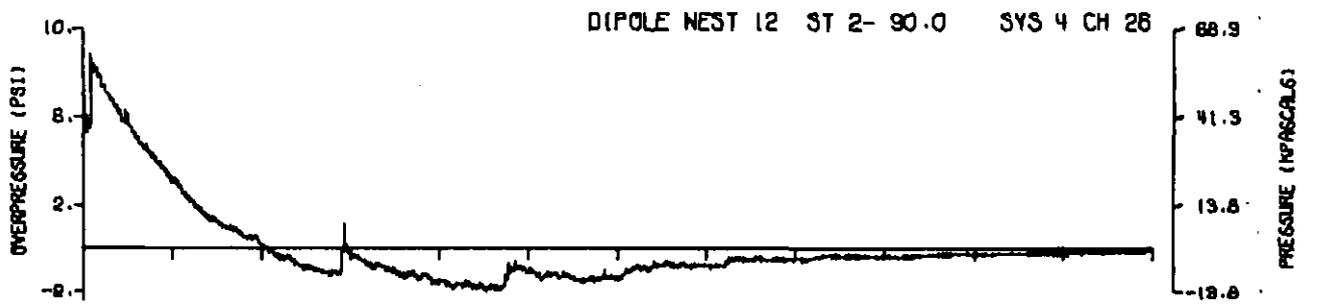
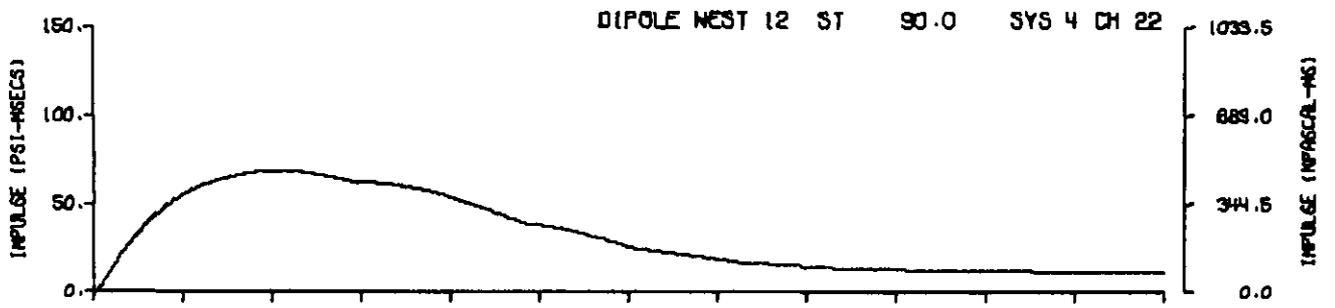
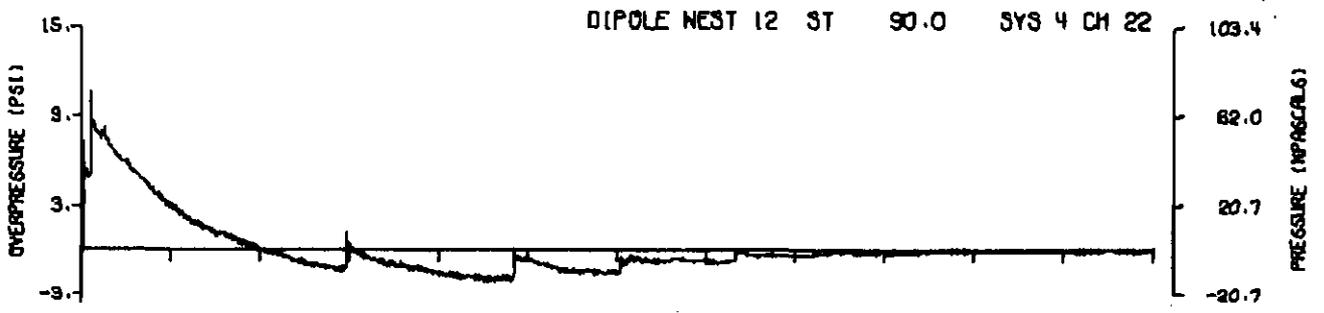
DIPOLE WEST 12 ST 60.33T SYS 1 CH 18



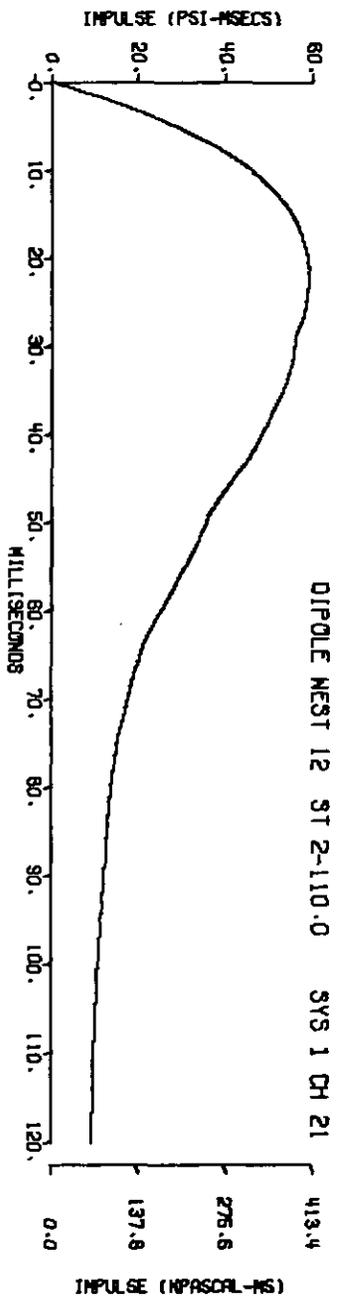
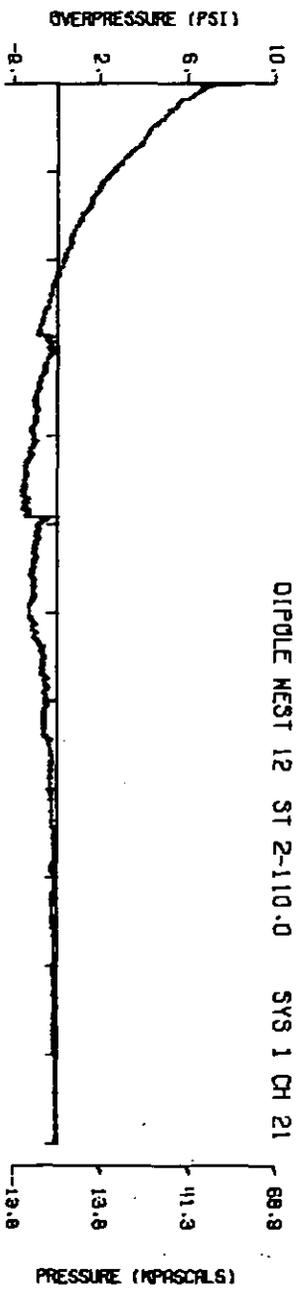
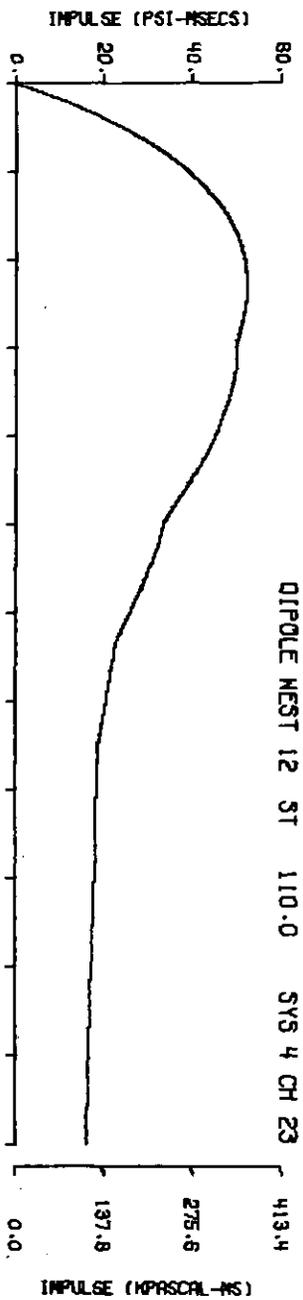
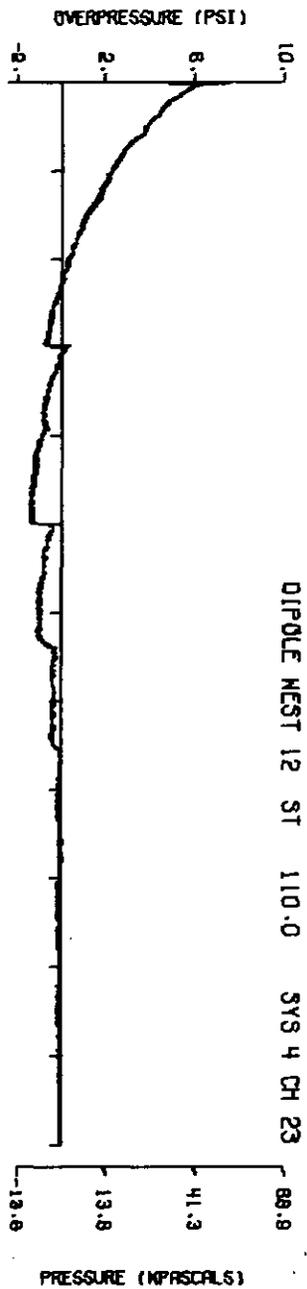
DIPOLE WEST 12 ST 60.33T SYS 1 CH 18

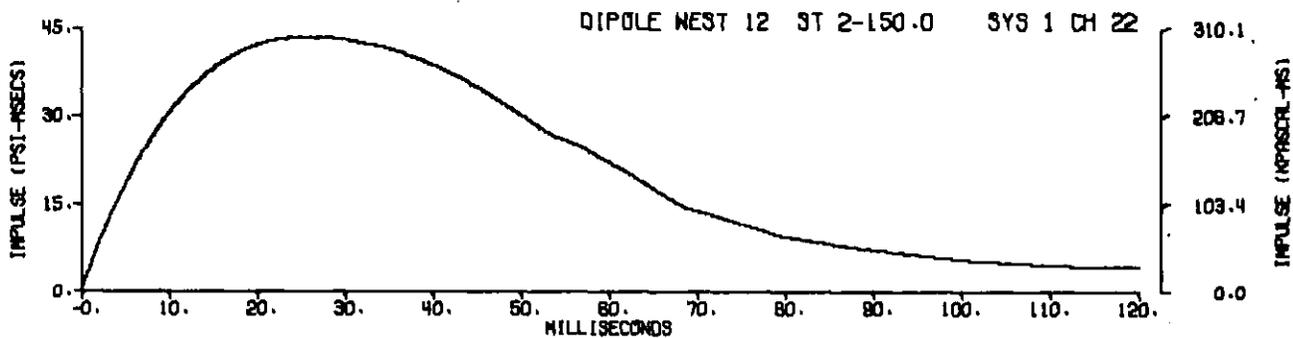
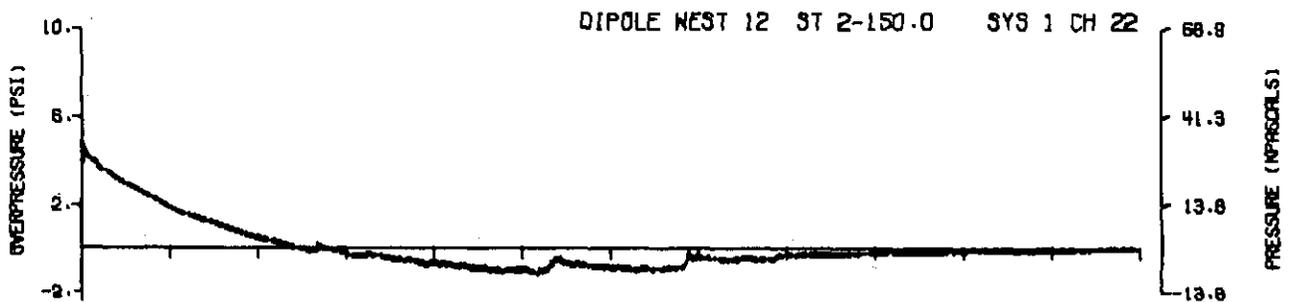
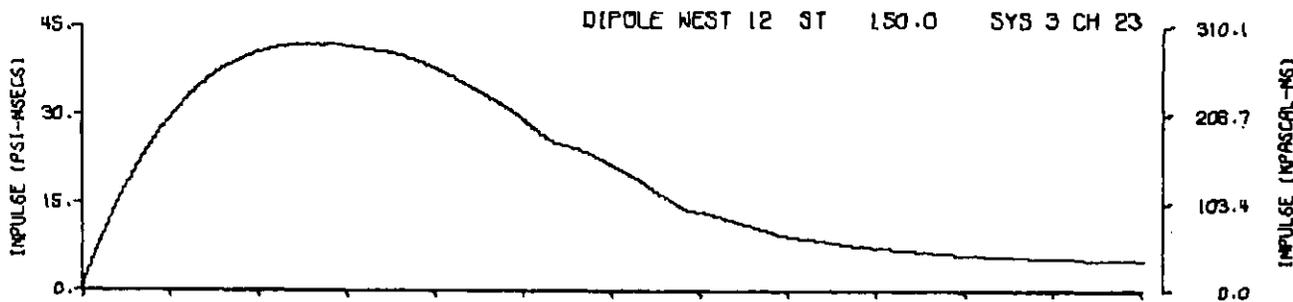
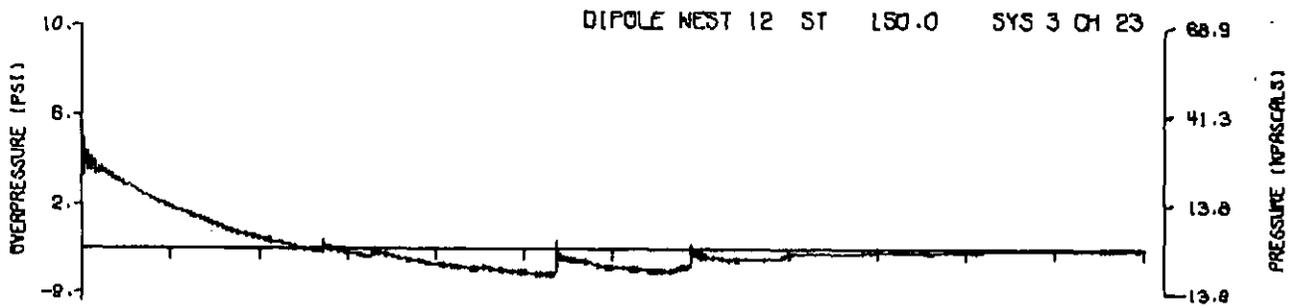


A12.37

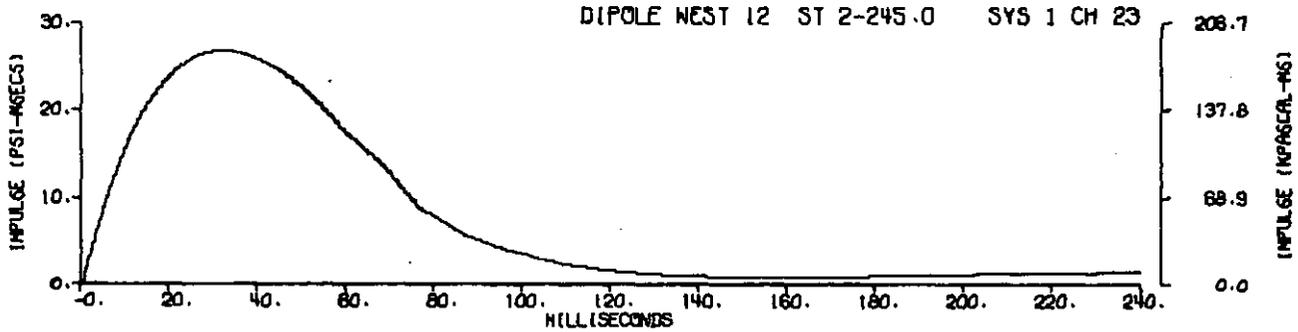
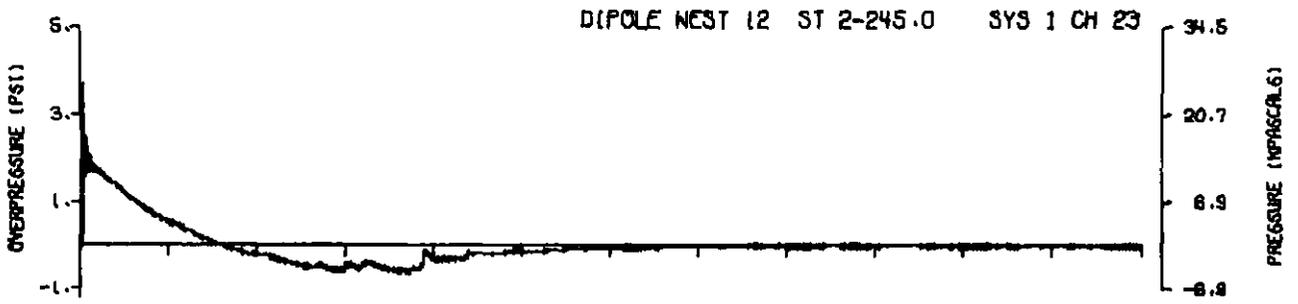
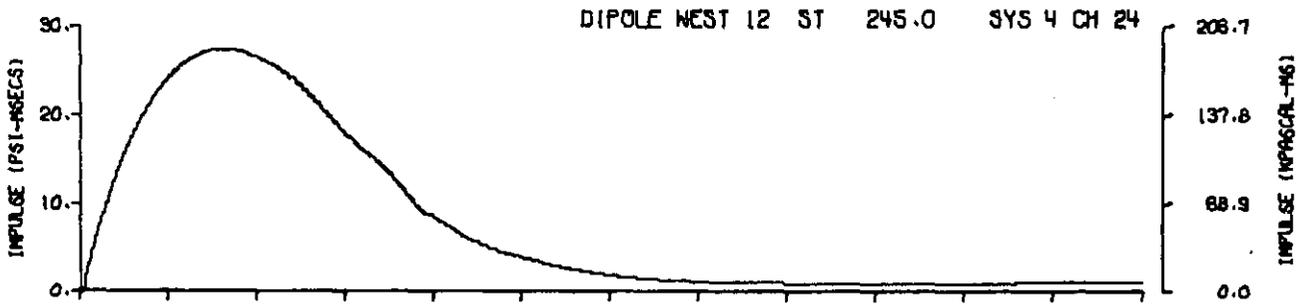
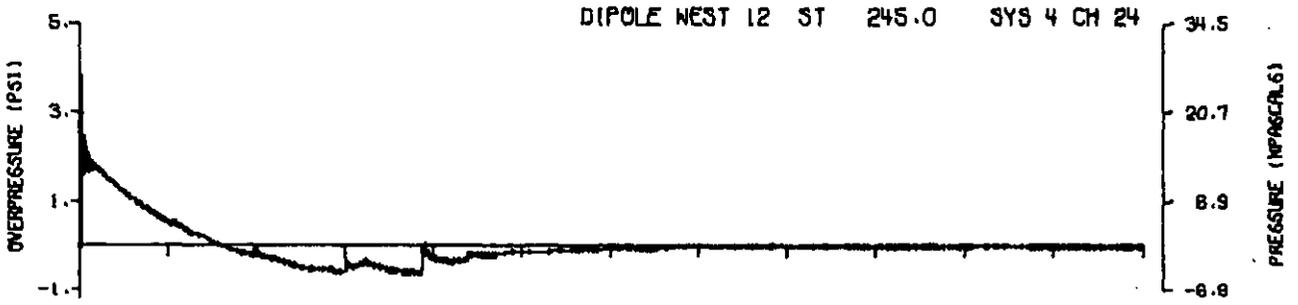


A12.38

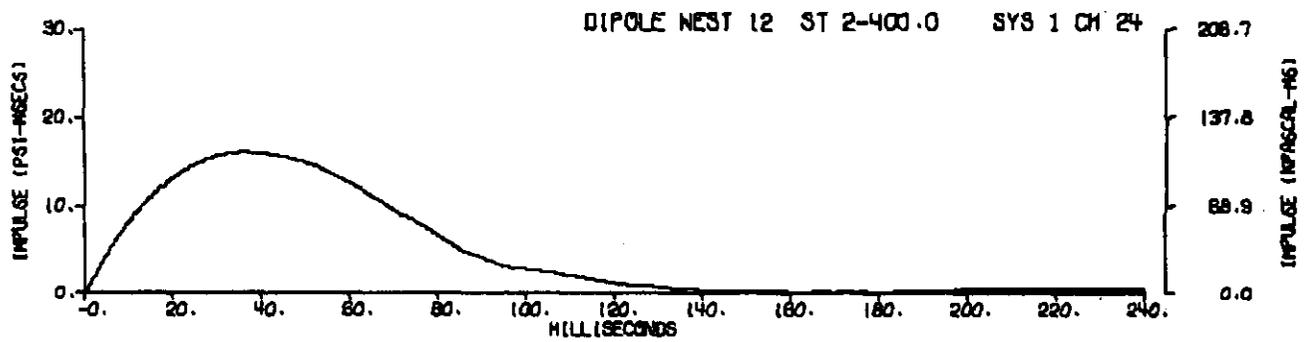
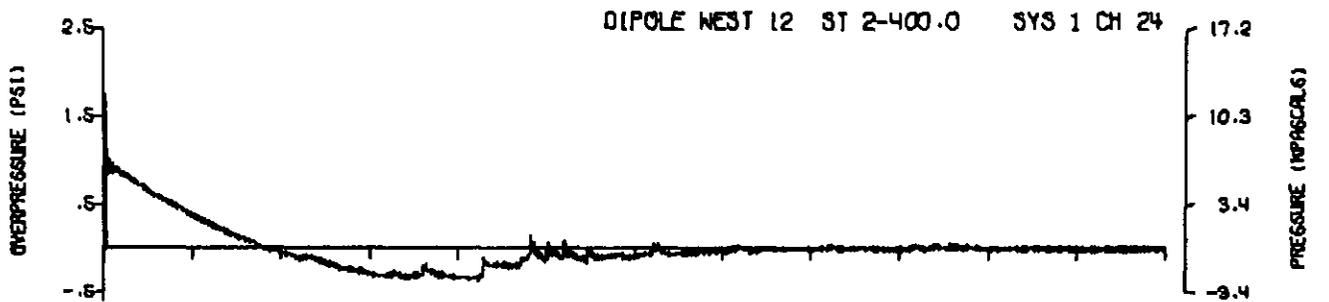
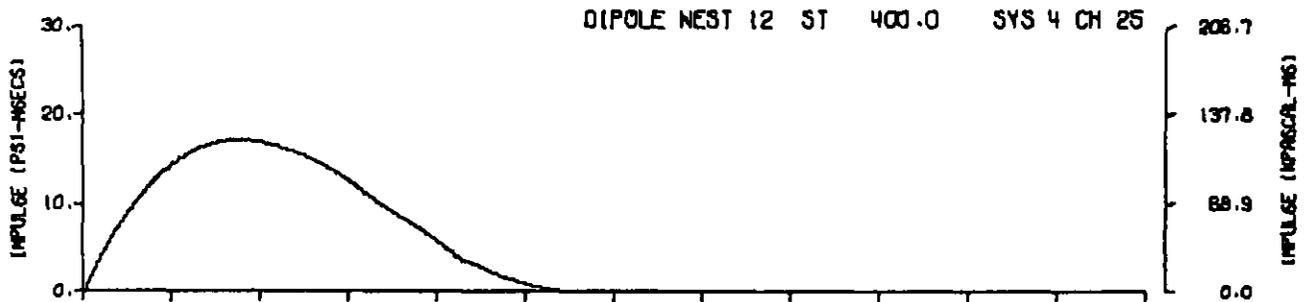
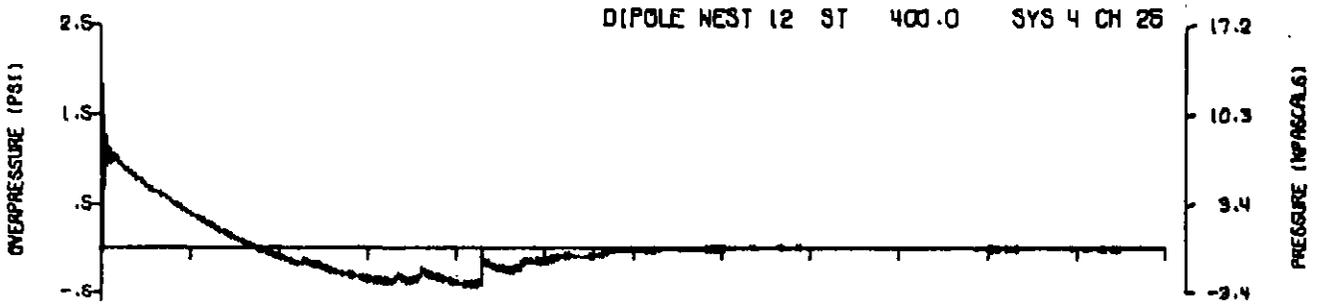




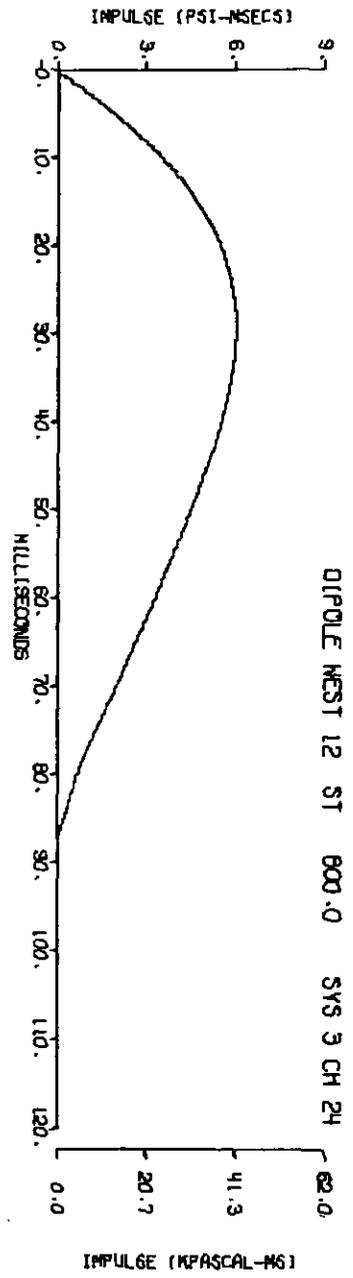
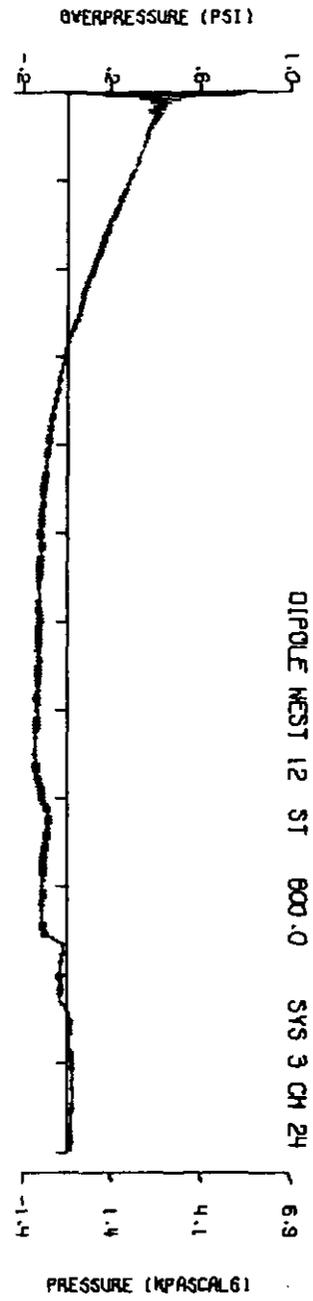
A12.40



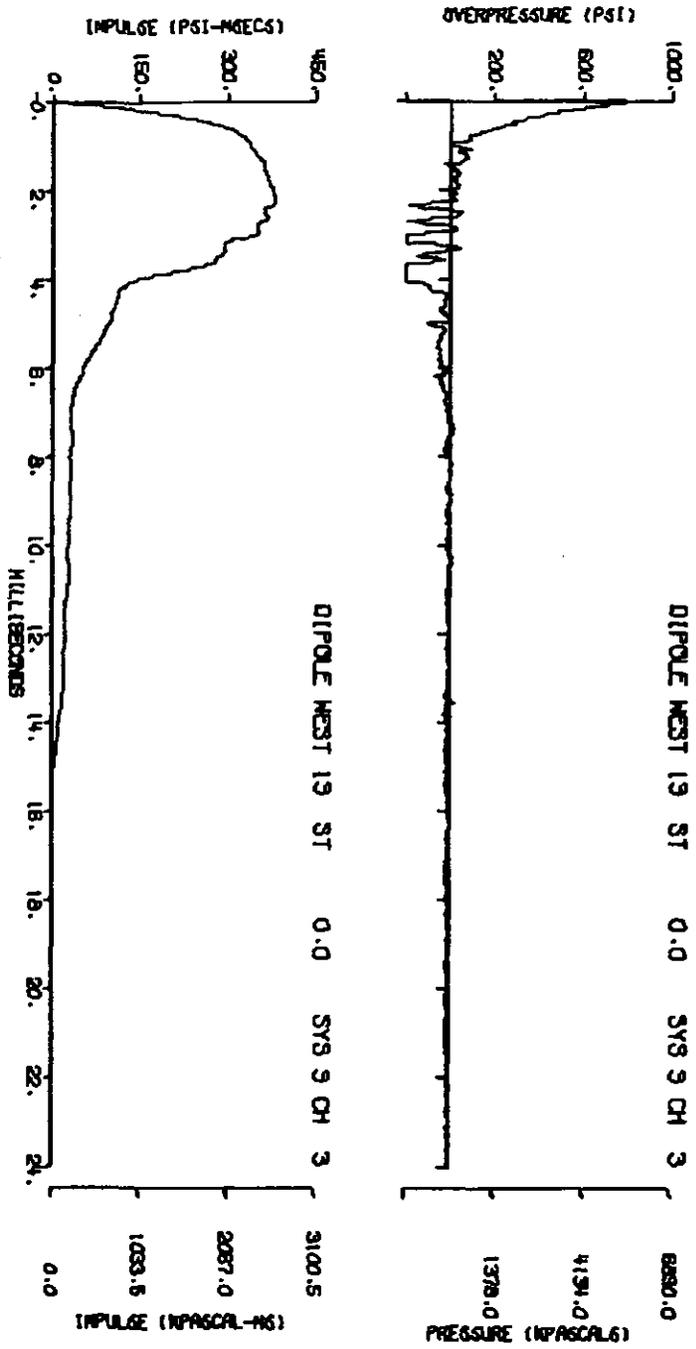
A12.41



A12.42

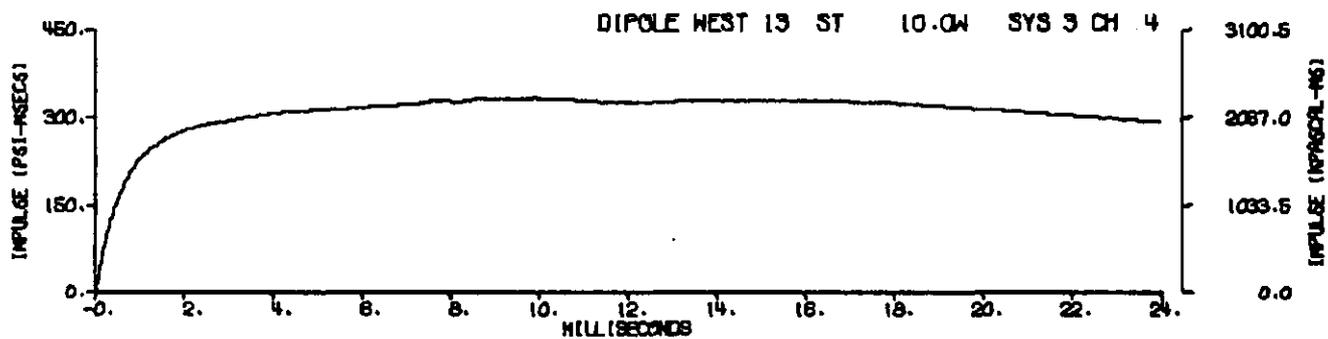
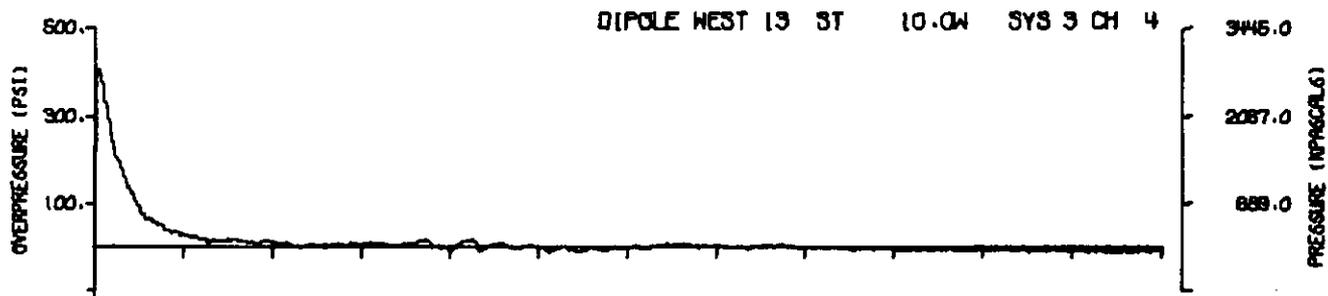
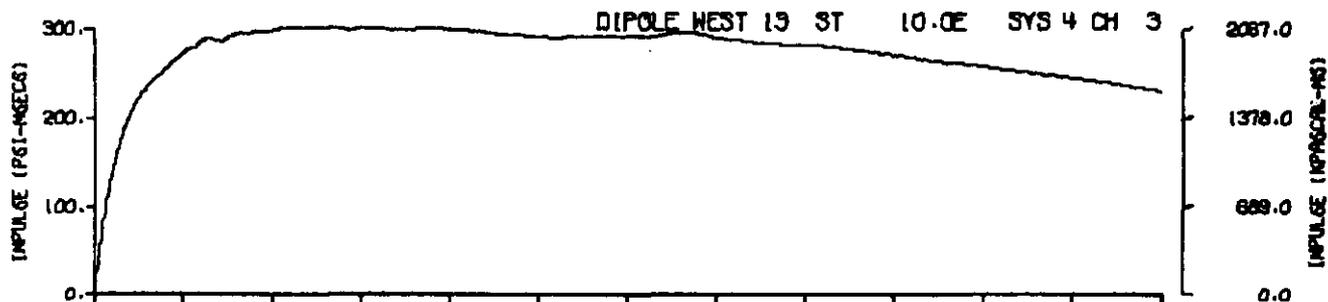
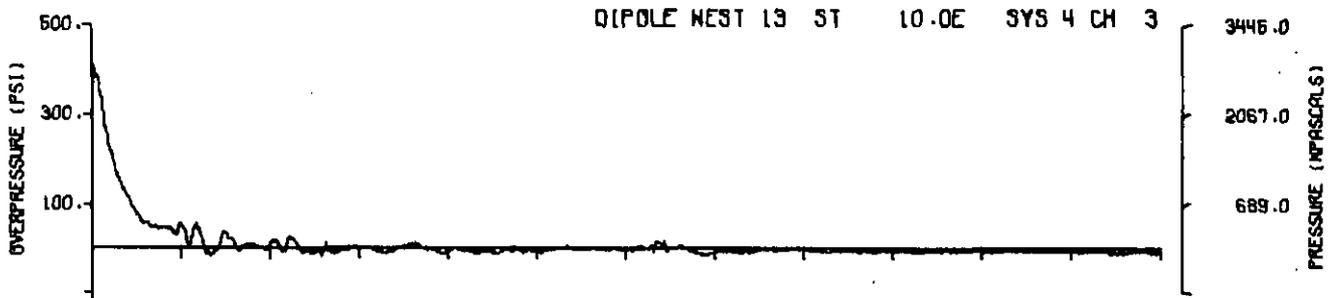


A12.43
200

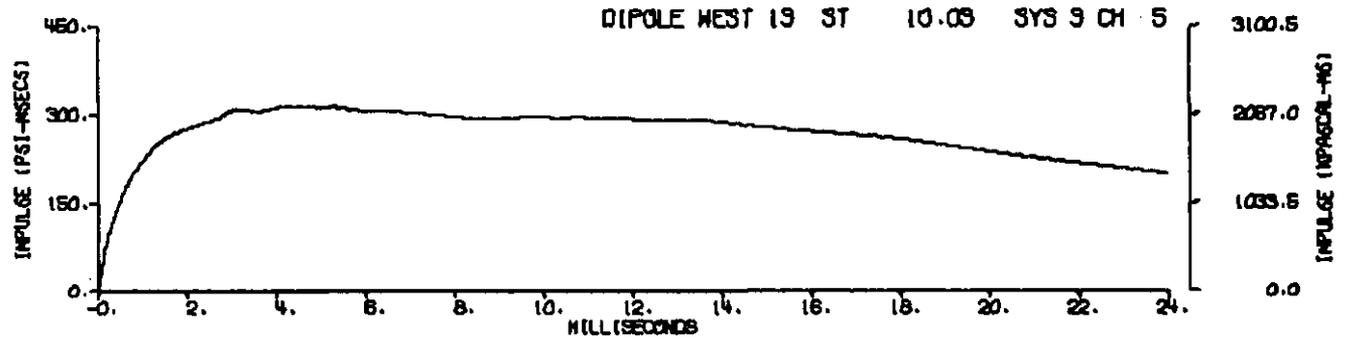
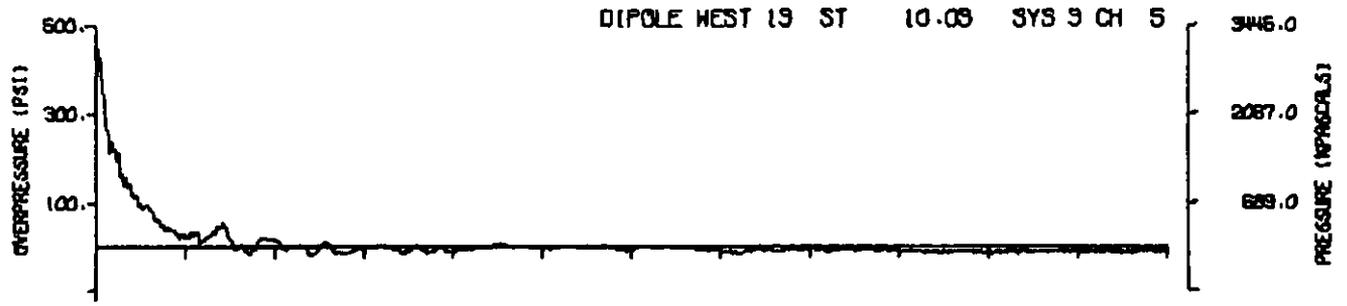
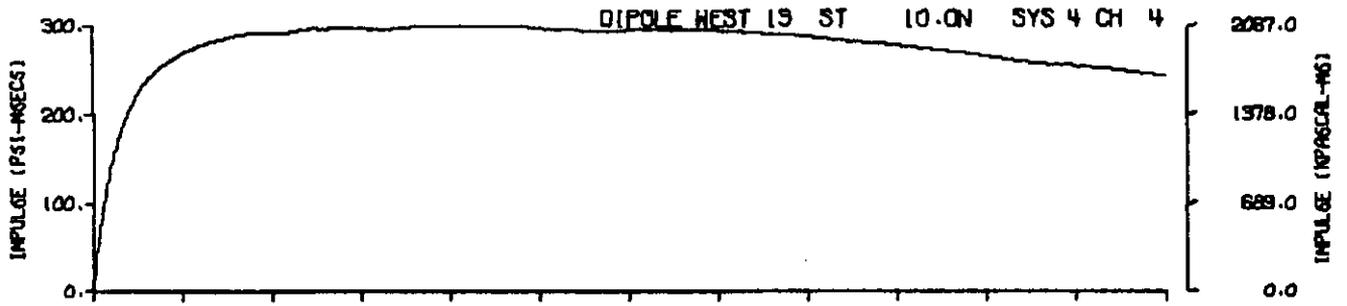
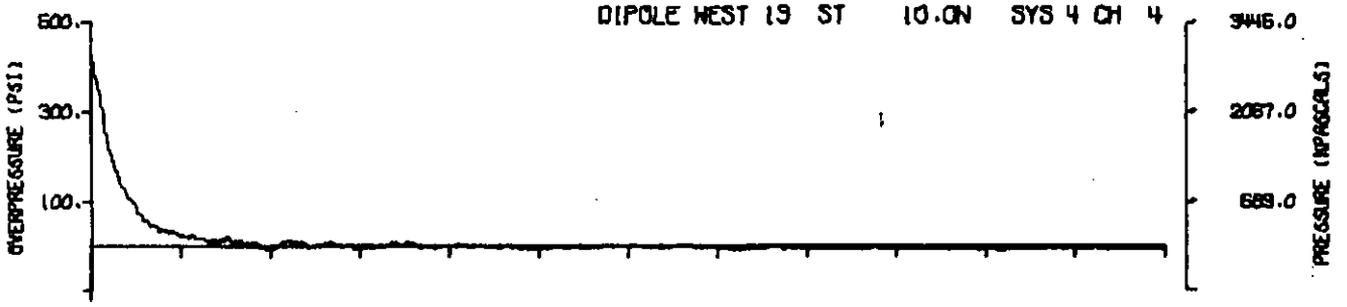


A13.1

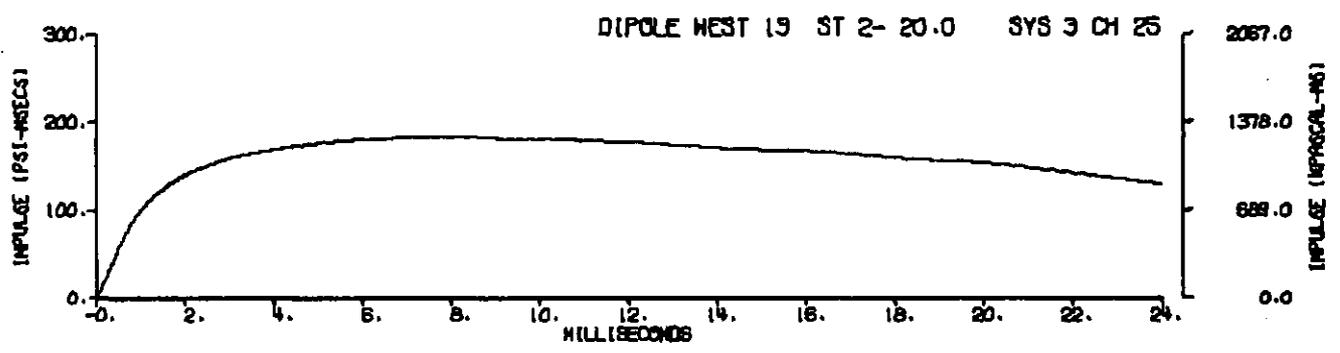
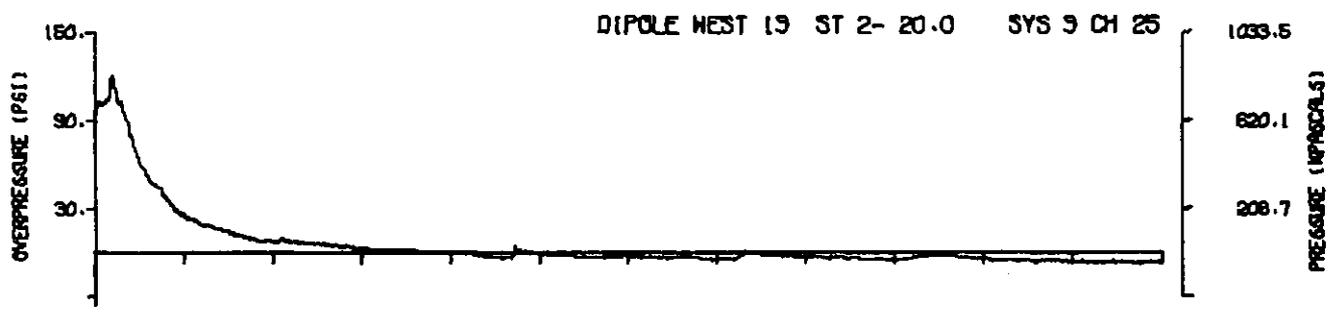
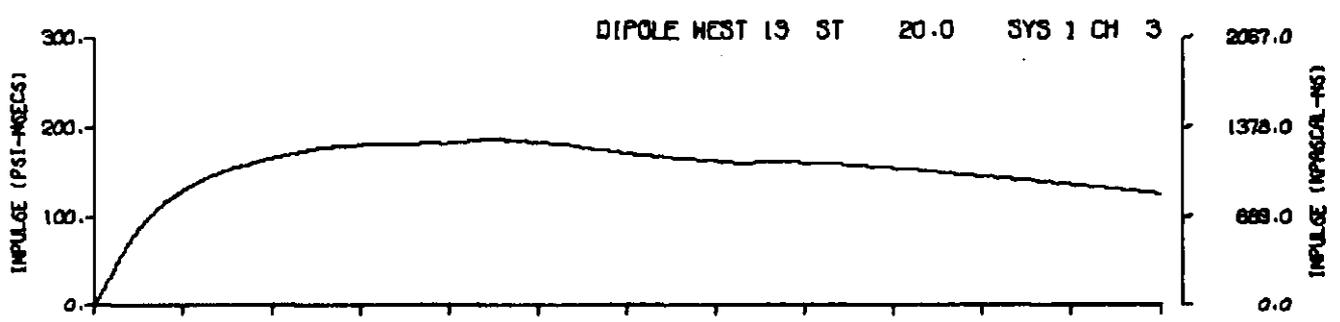
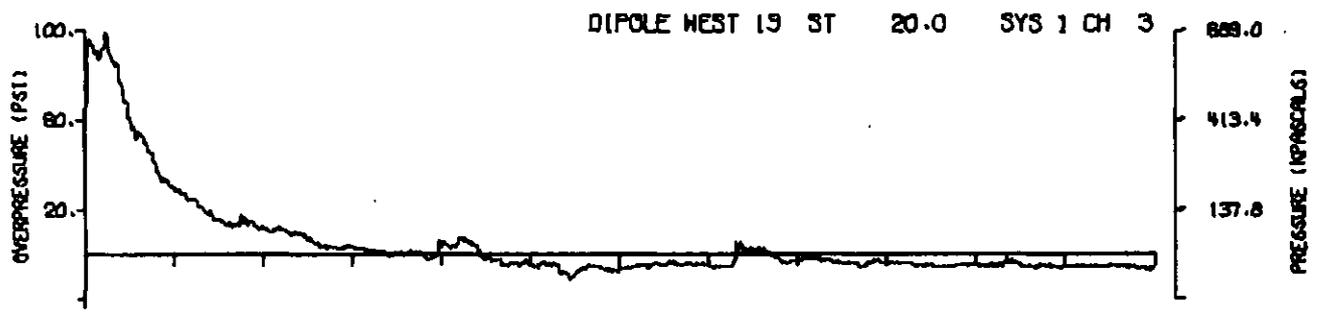
201



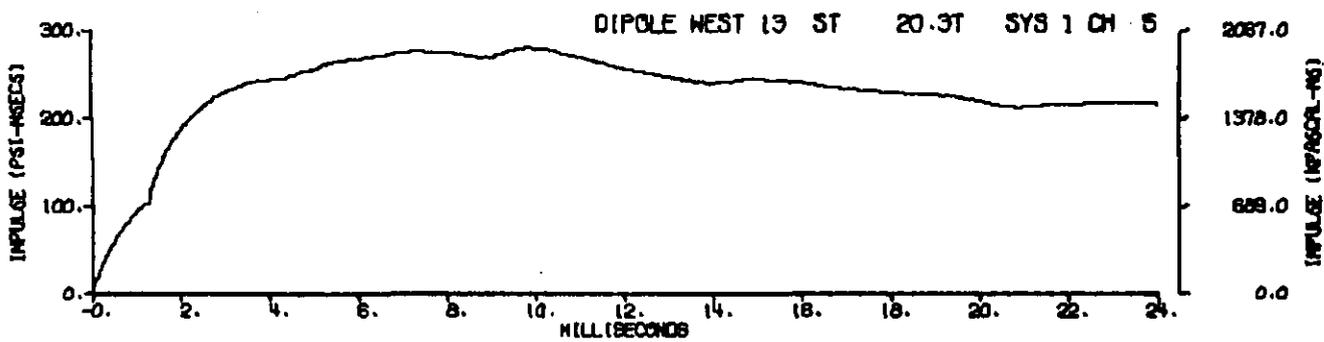
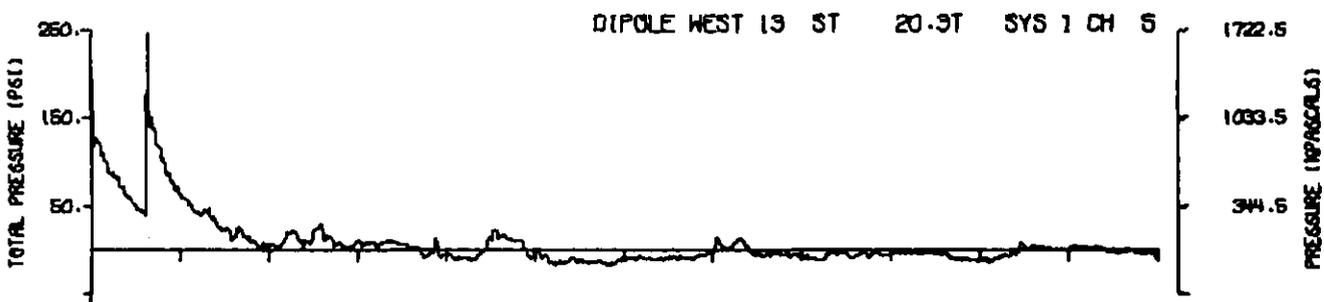
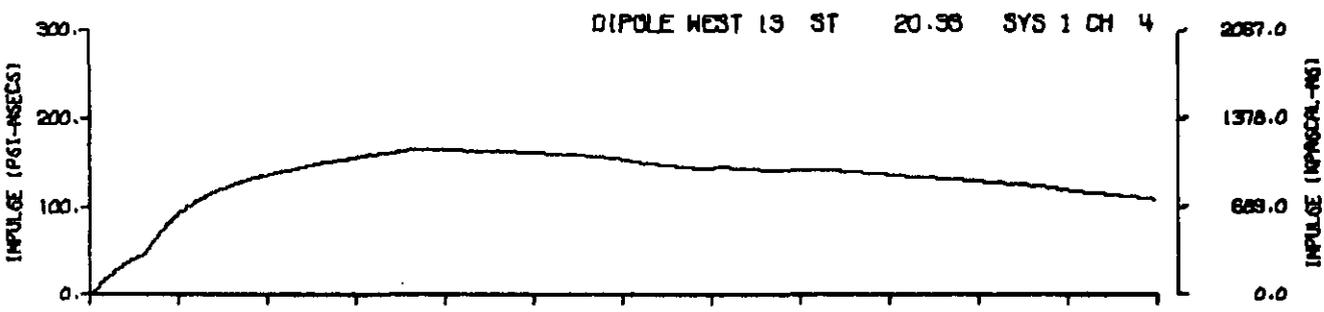
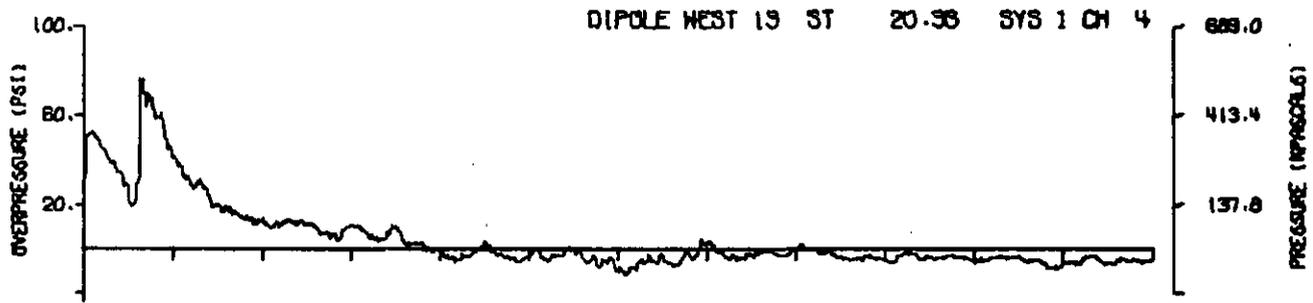
A13.2



A13.3

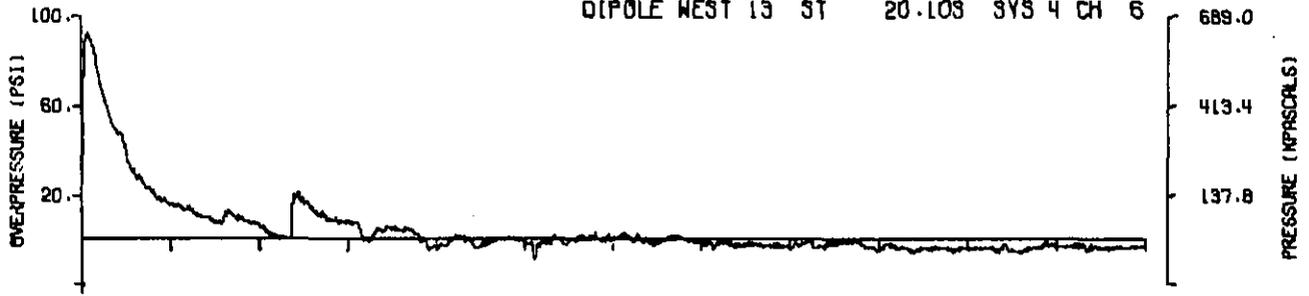


A13.4

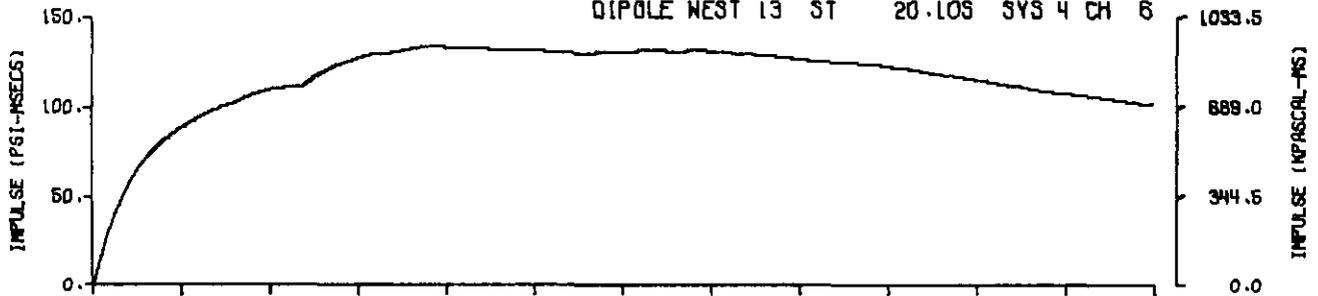


A13.5

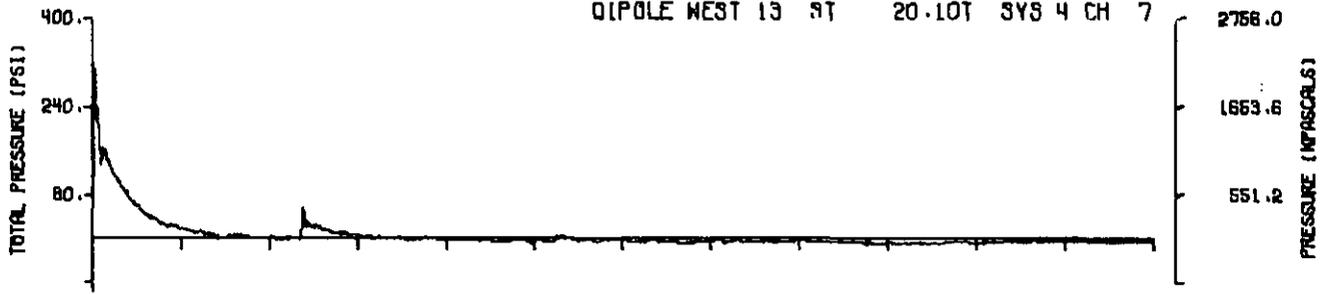
DIPOLE WEST 13 ST 20.103 SYS 4 CH 6



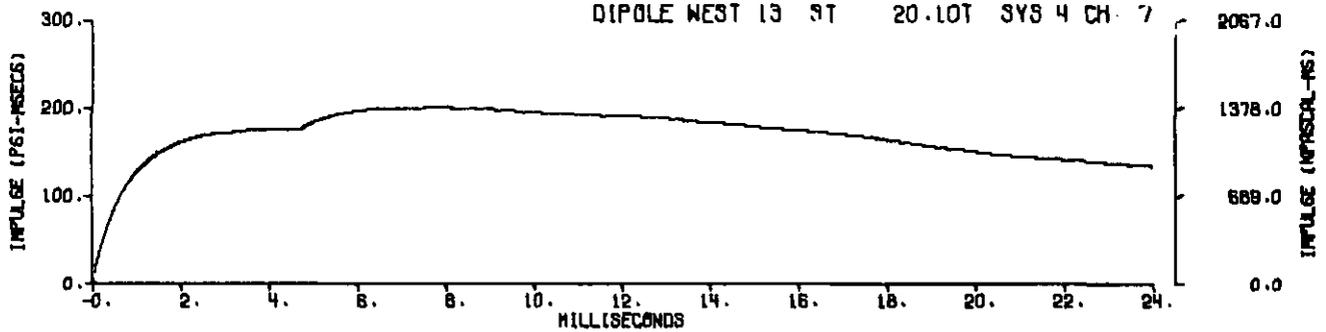
DIPOLE WEST 13 ST 20.103 SYS 4 CH 6



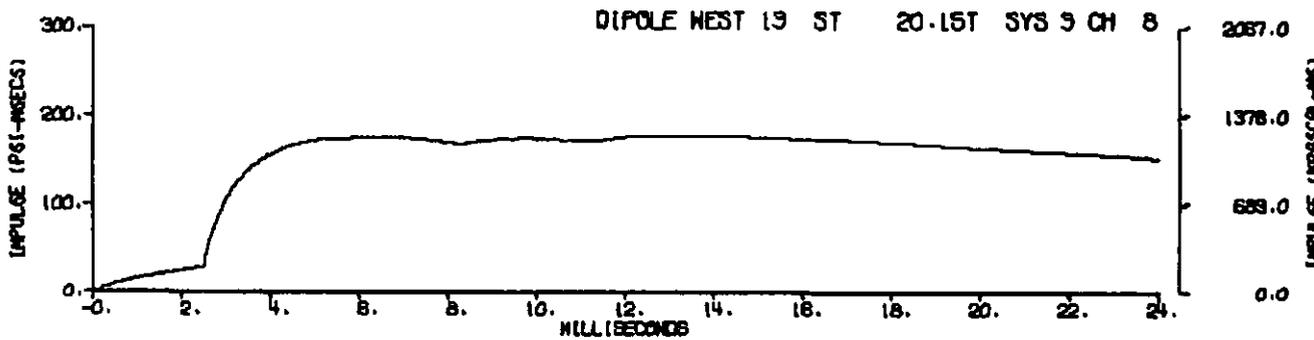
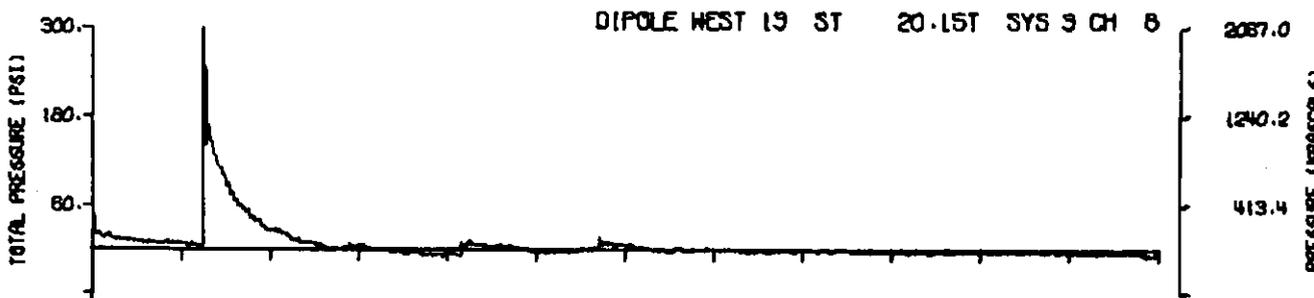
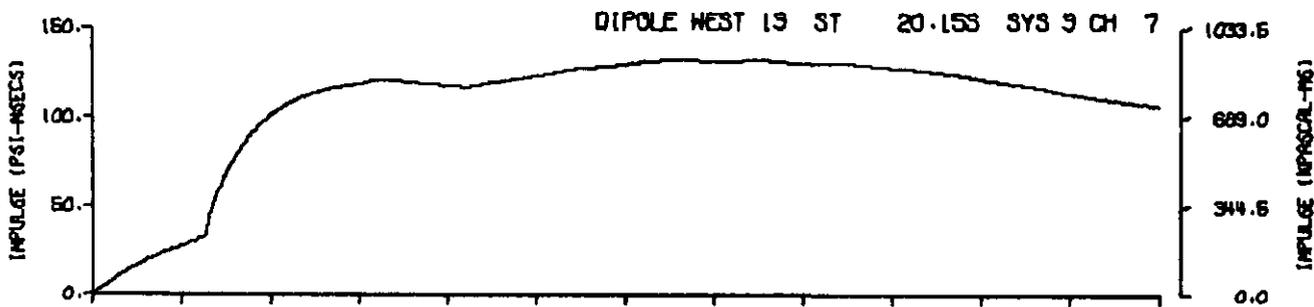
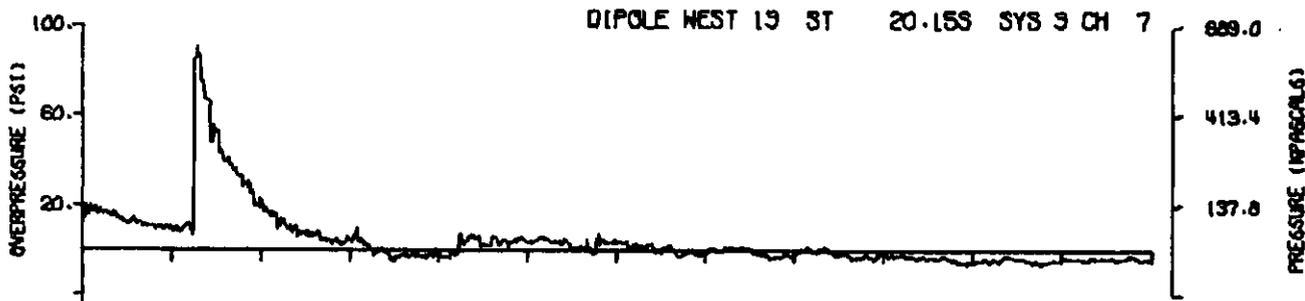
DIPOLE WEST 13 ST 20.107 SYS 4 CH 7



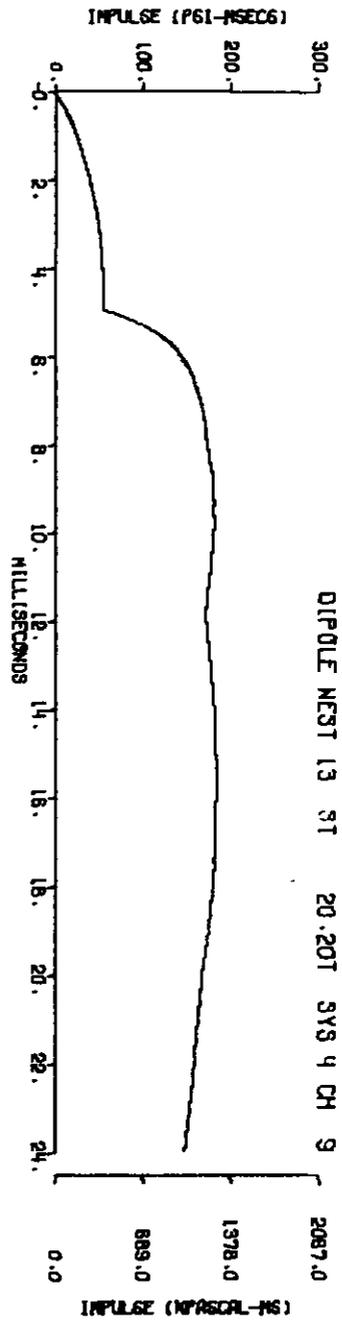
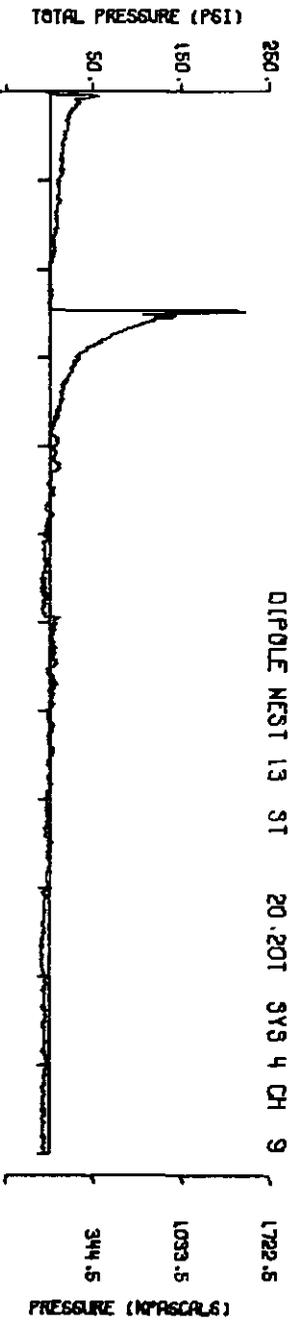
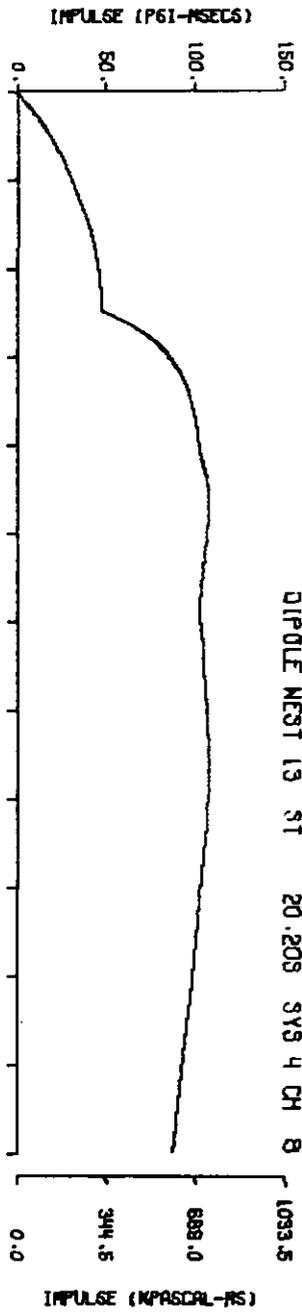
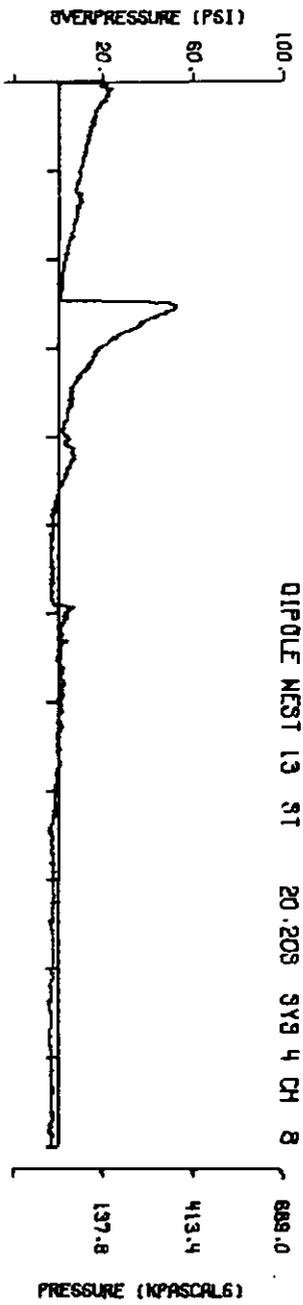
DIPOLE WEST 13 ST 20.107 SYS 4 CH 7



A13.6

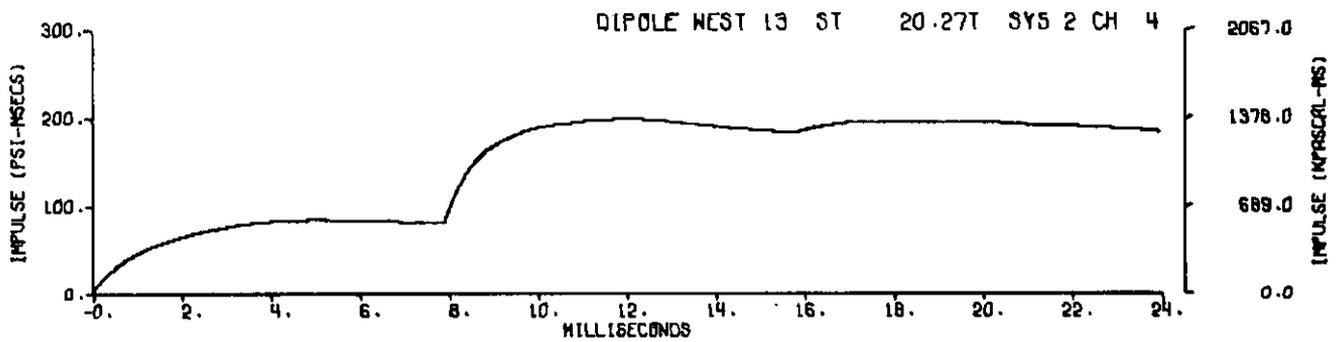
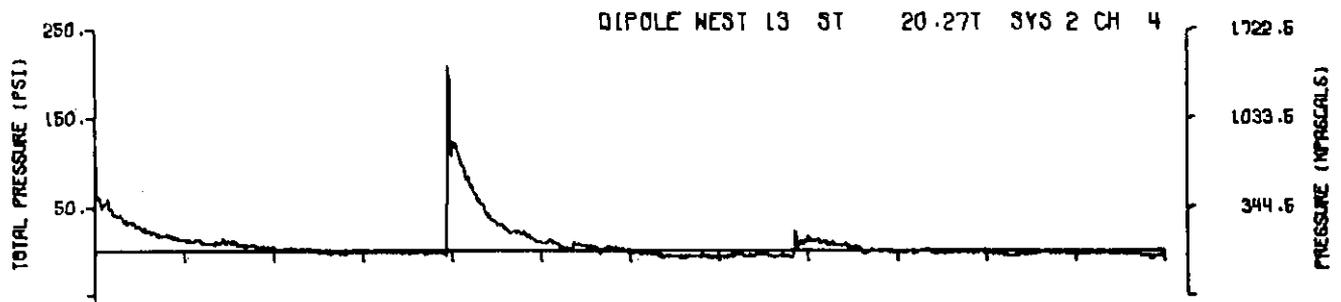
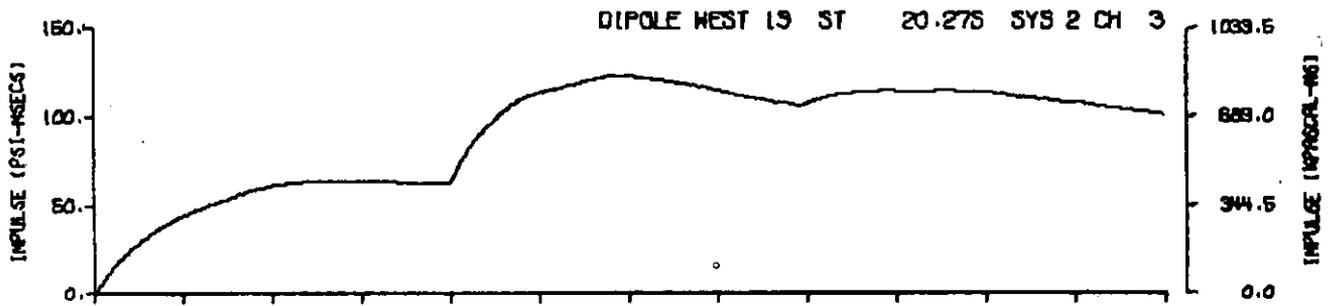
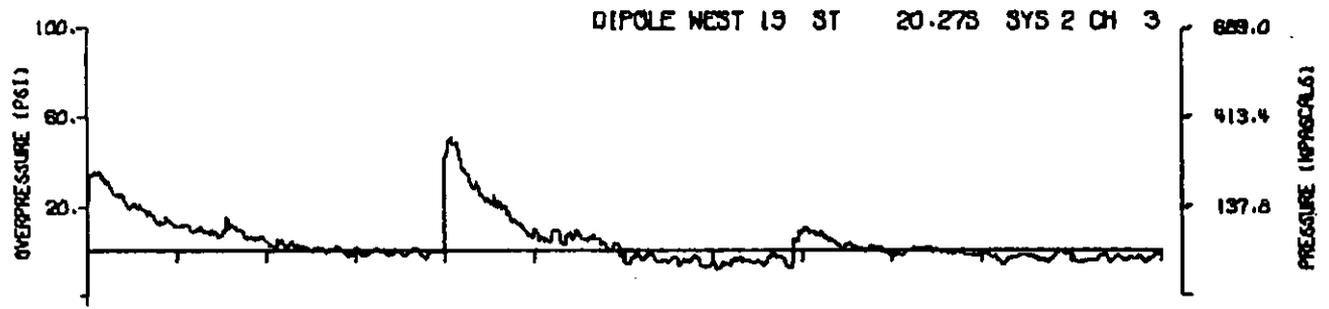


A13.7

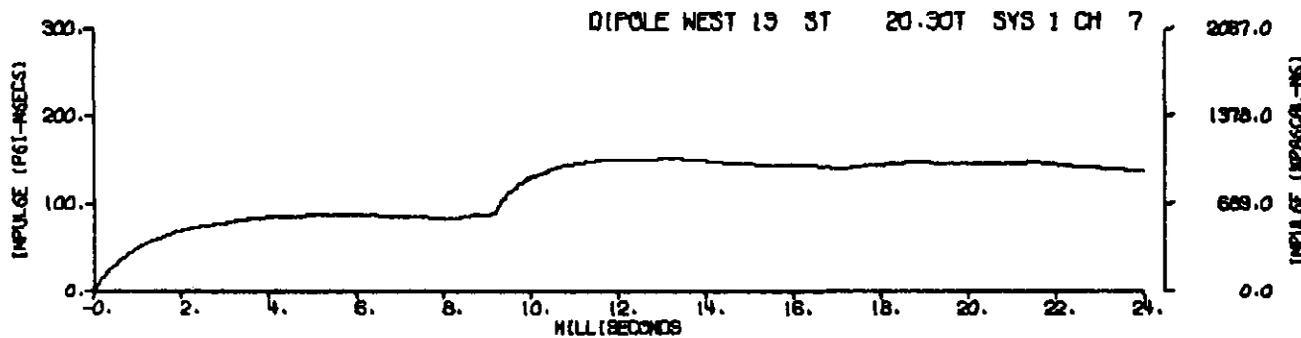
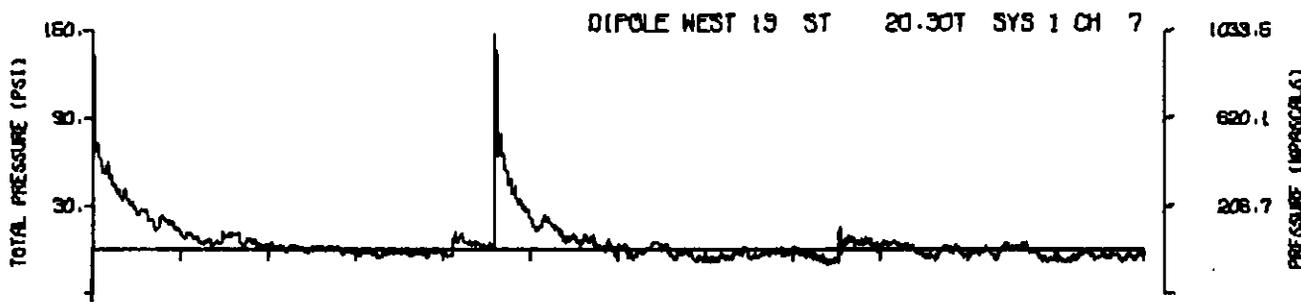
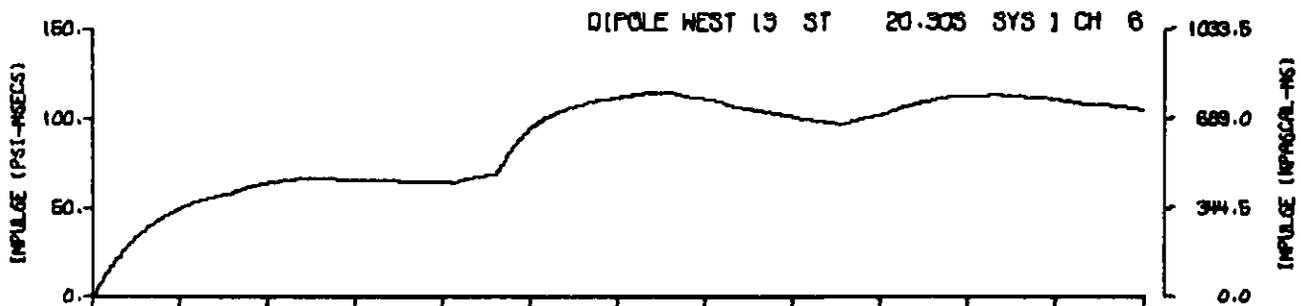
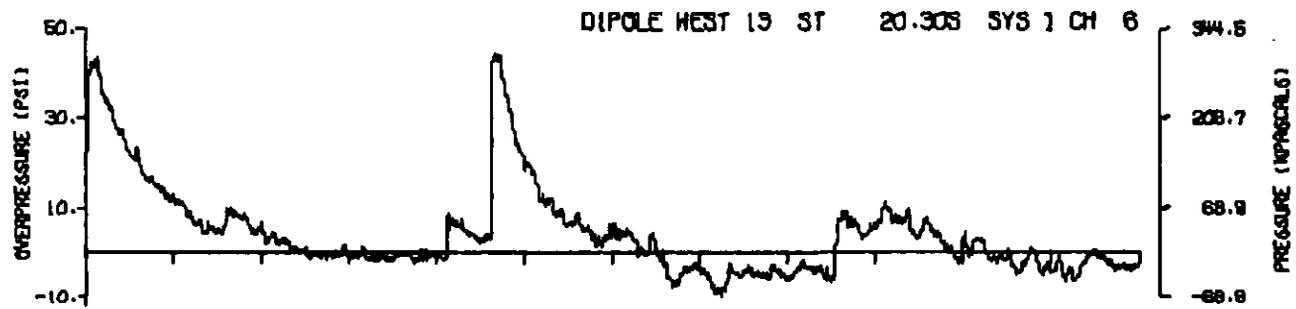


A13.8

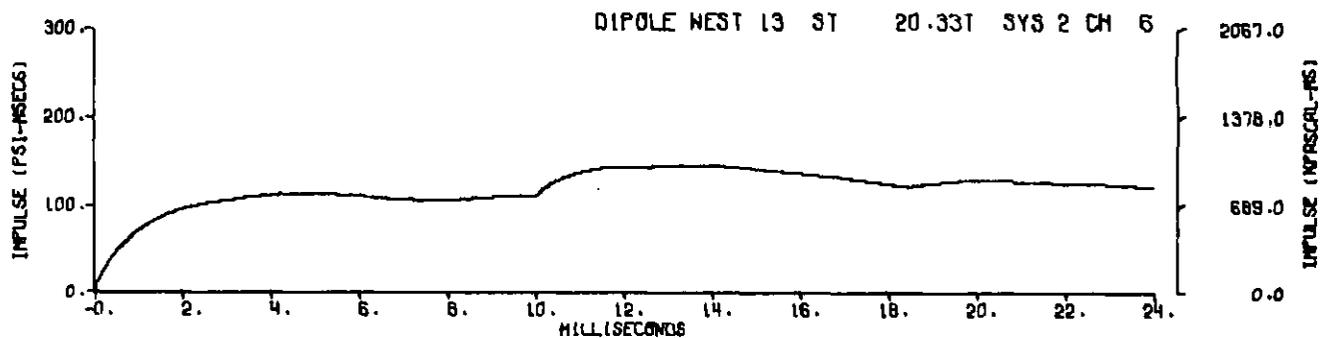
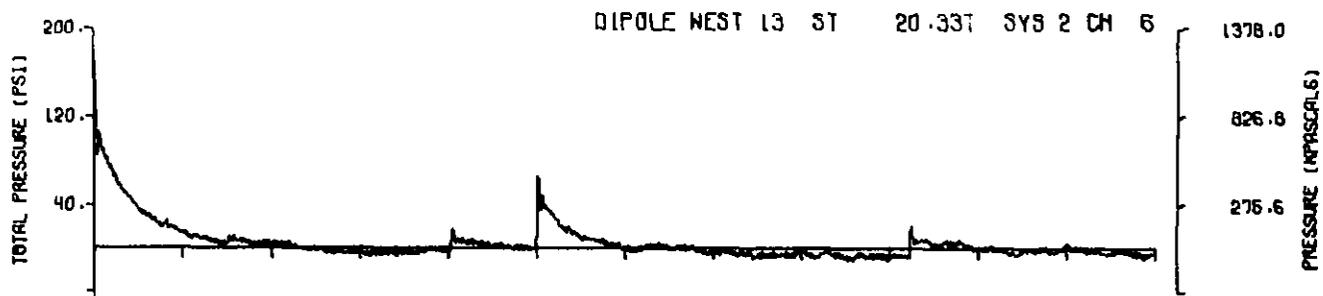
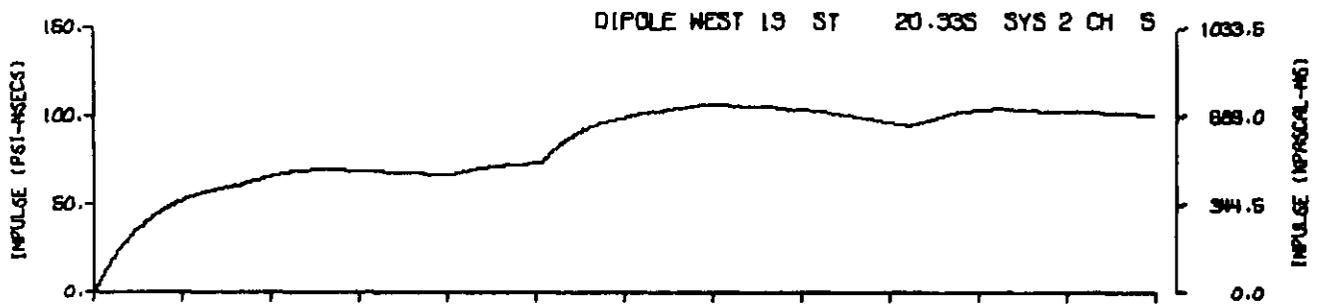
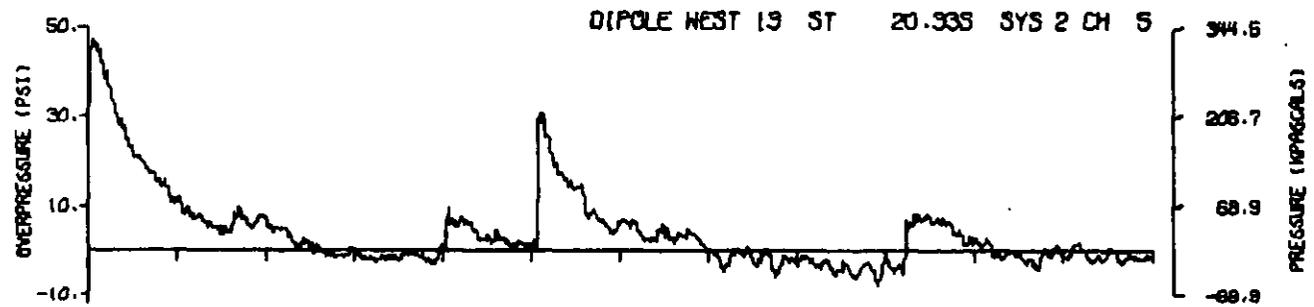
208



A13.9

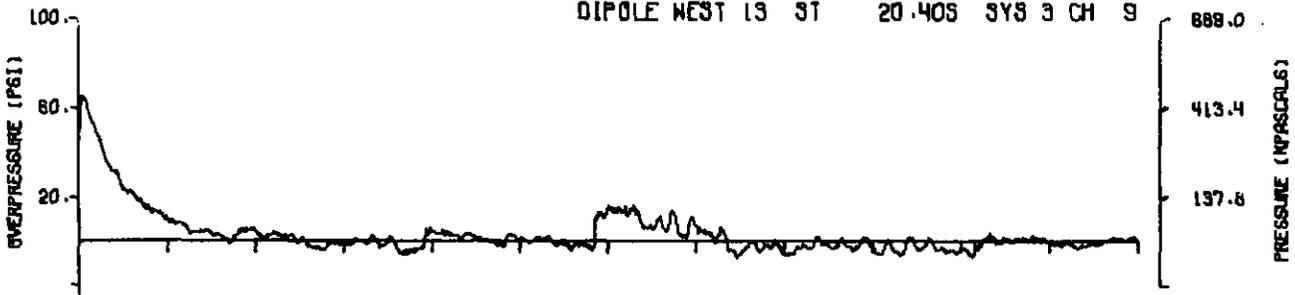


A13.10

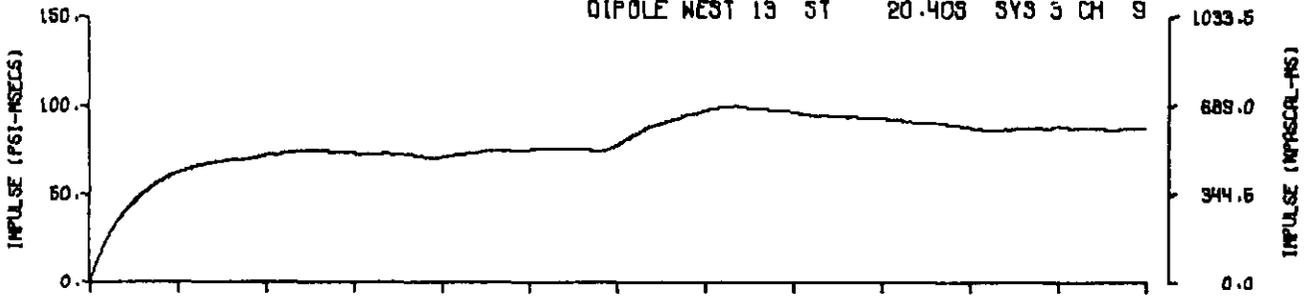


A13.11

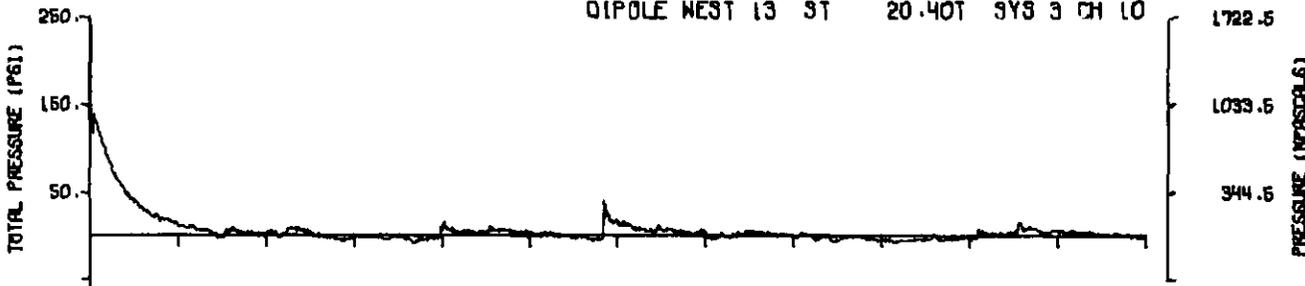
DIPOLE WEST 13 ST 20.405 SYS 3 CH 9



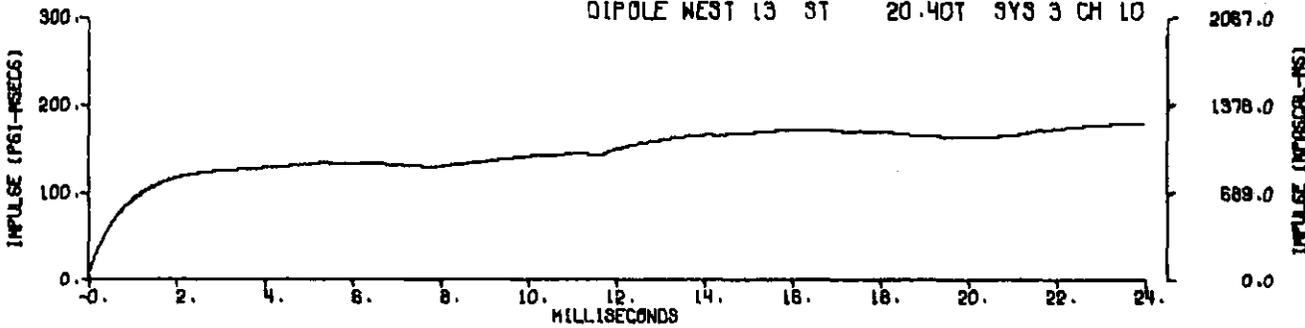
DIPOLE WEST 13 ST 20.405 SYS 3 CH 9



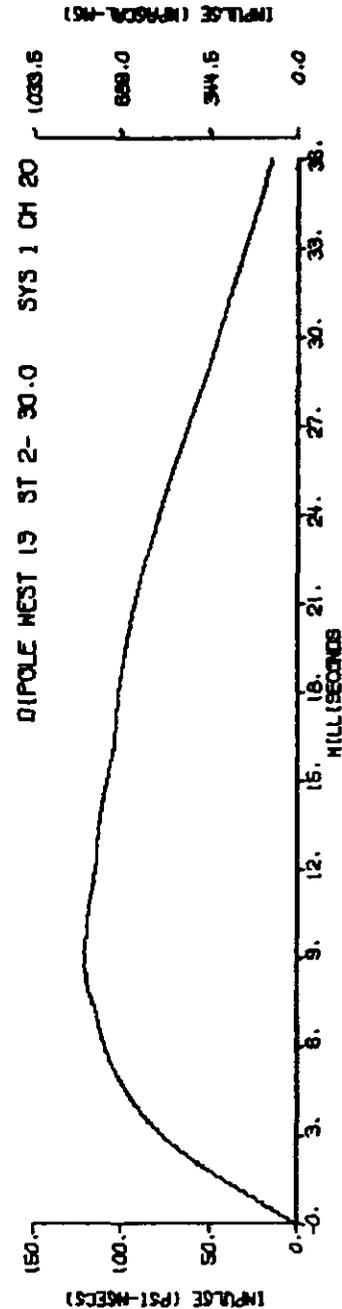
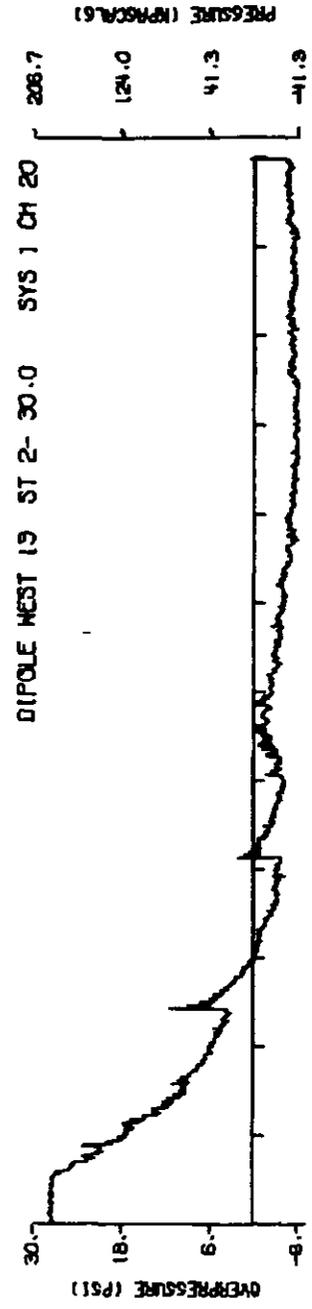
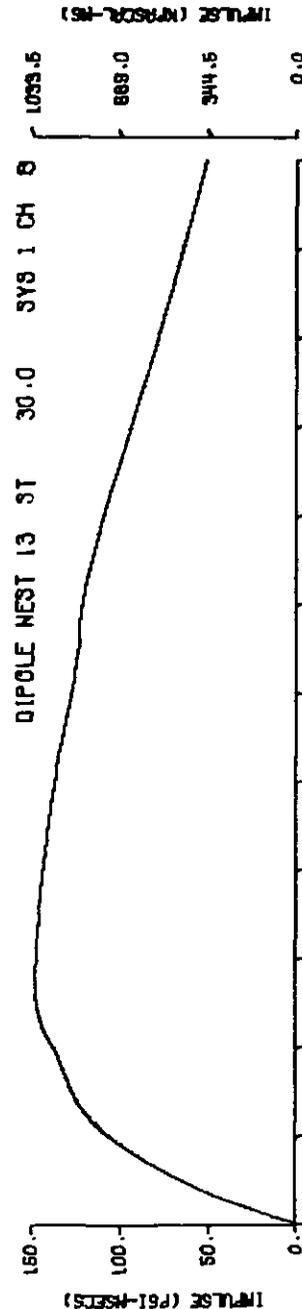
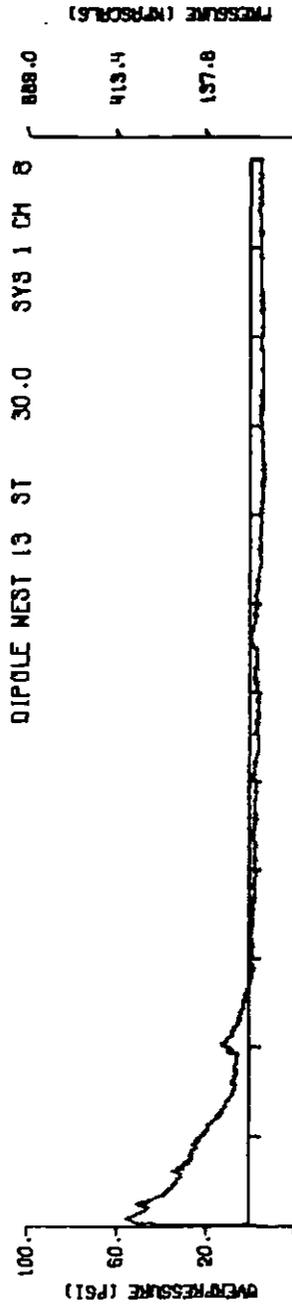
DIPOLE WEST 13 ST 20.405 SYS 3 CH 10



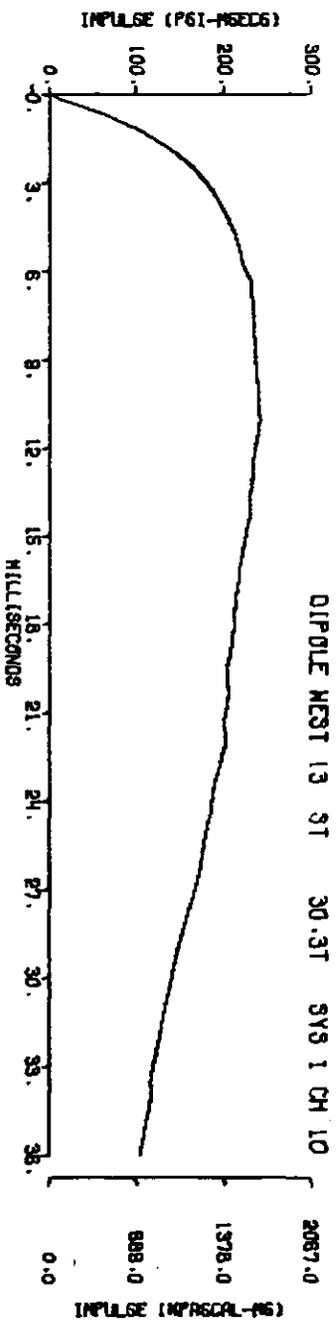
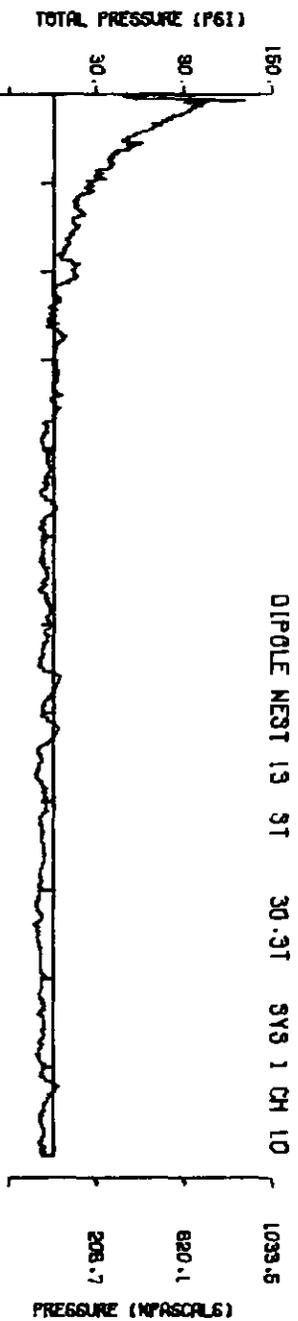
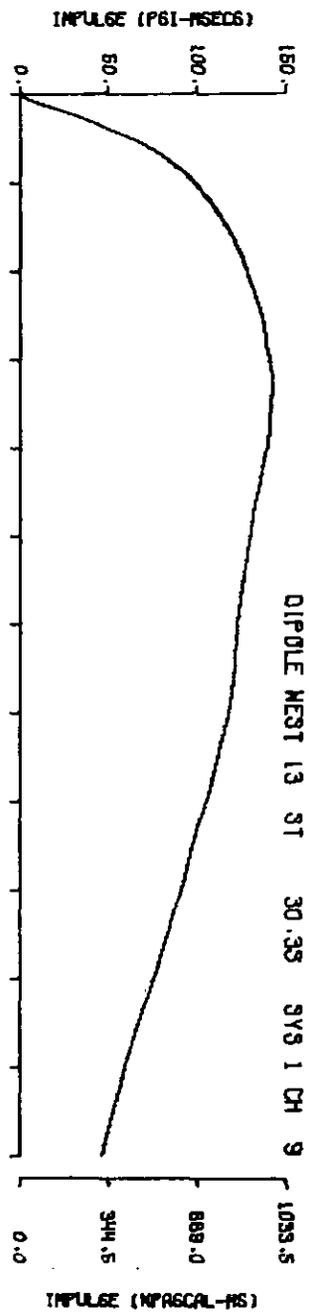
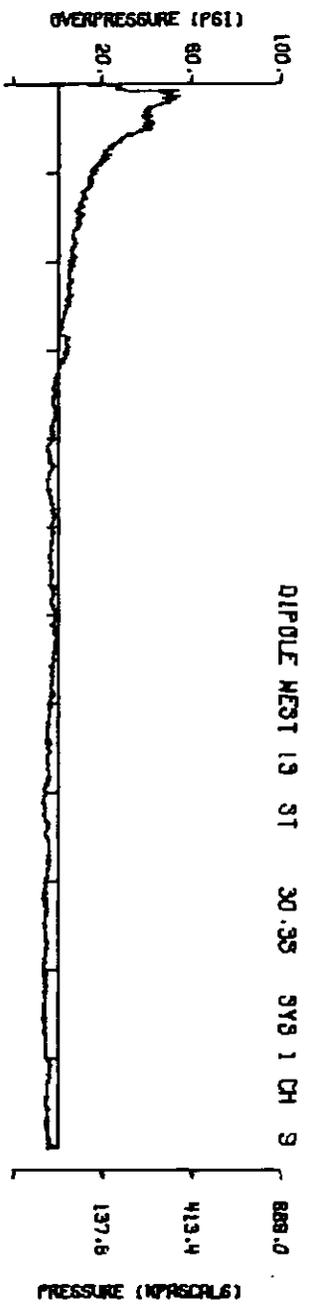
DIPOLE WEST 13 ST 20.405 SYS 3 CH 10



A13.12

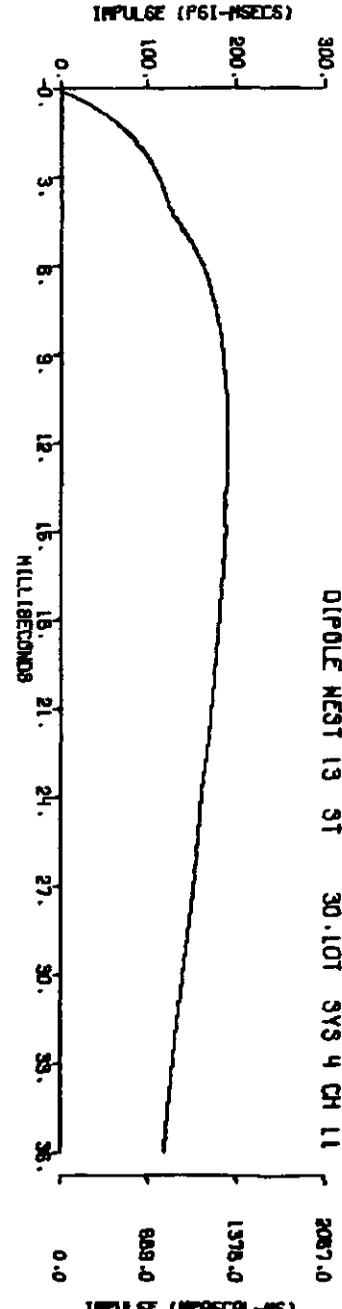
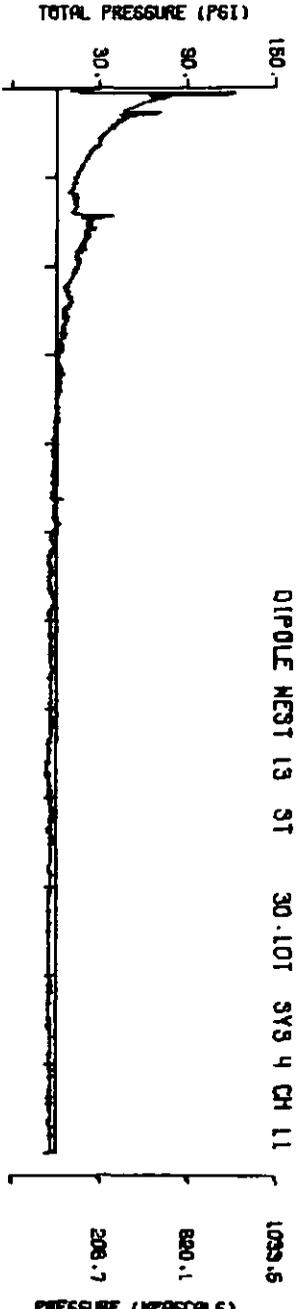
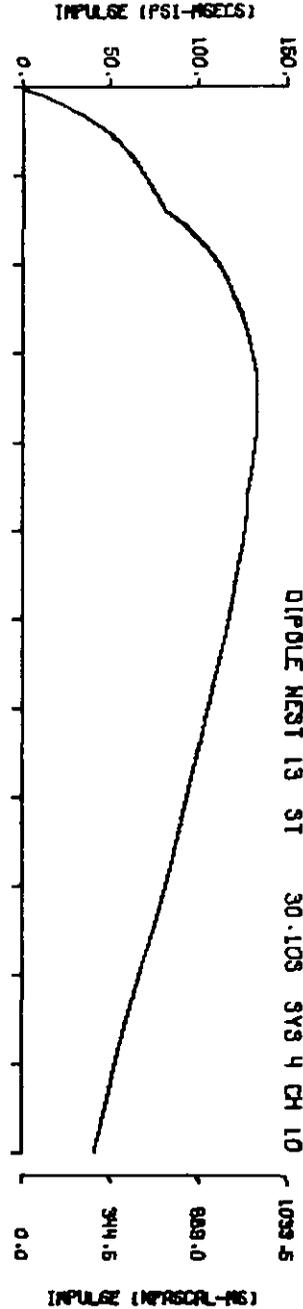
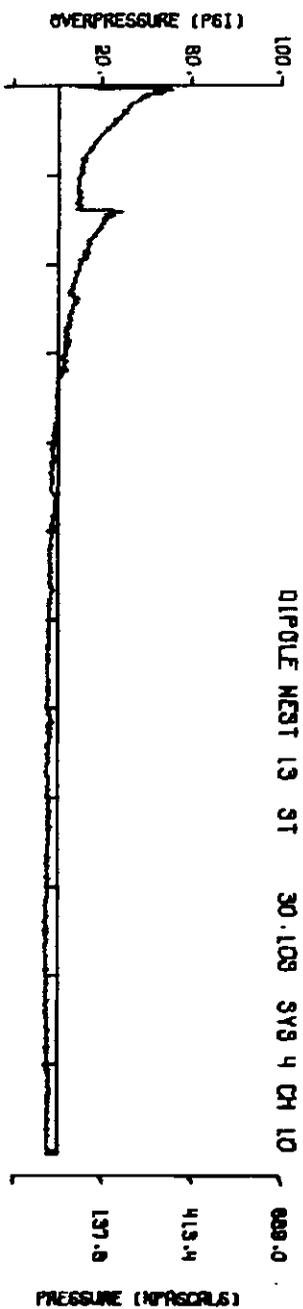


A13.13

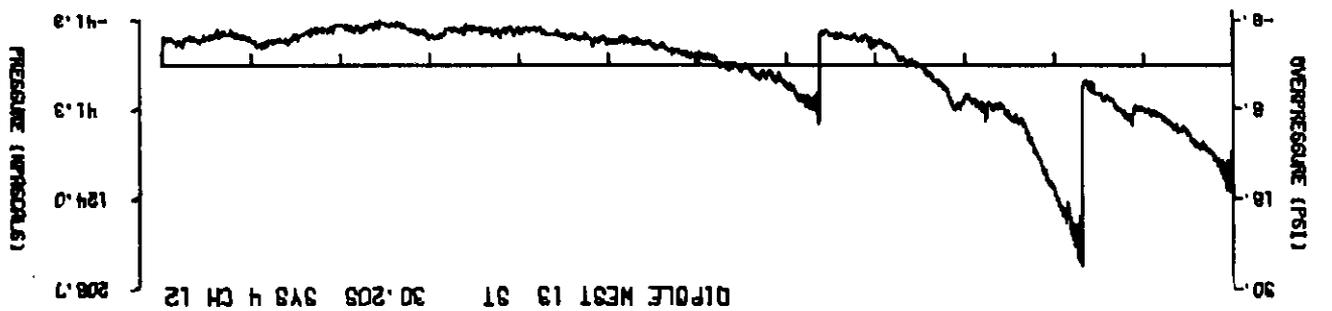
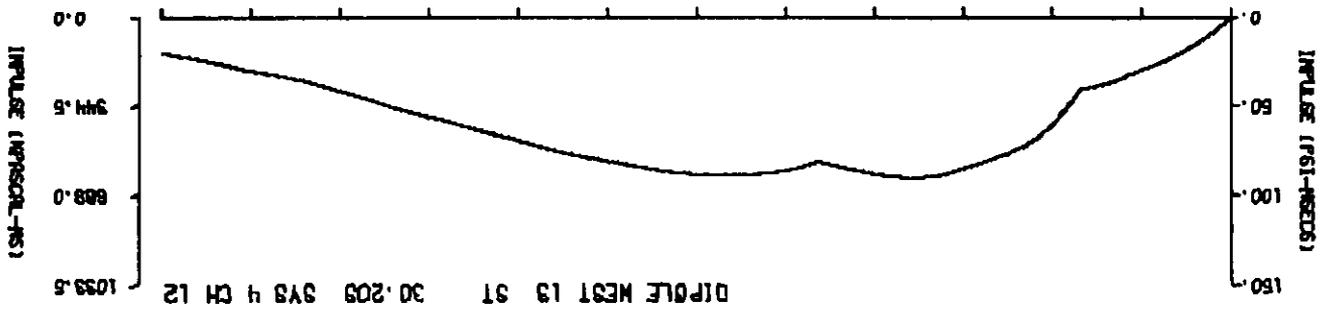
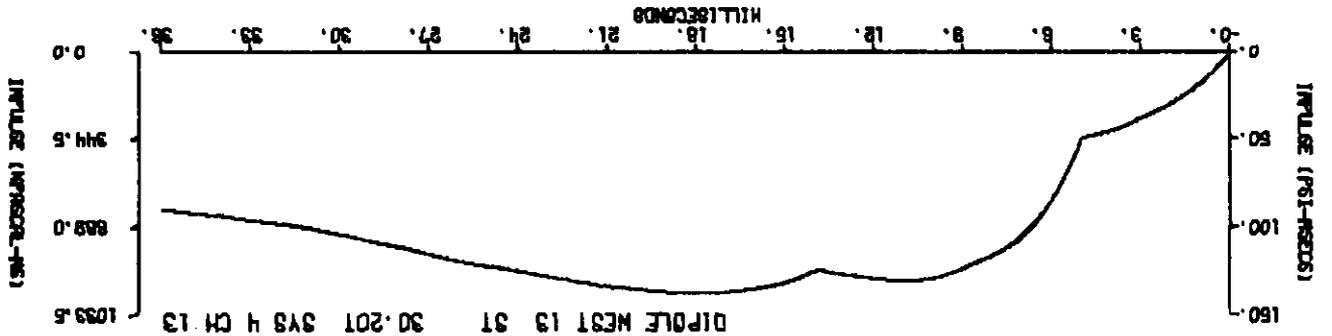


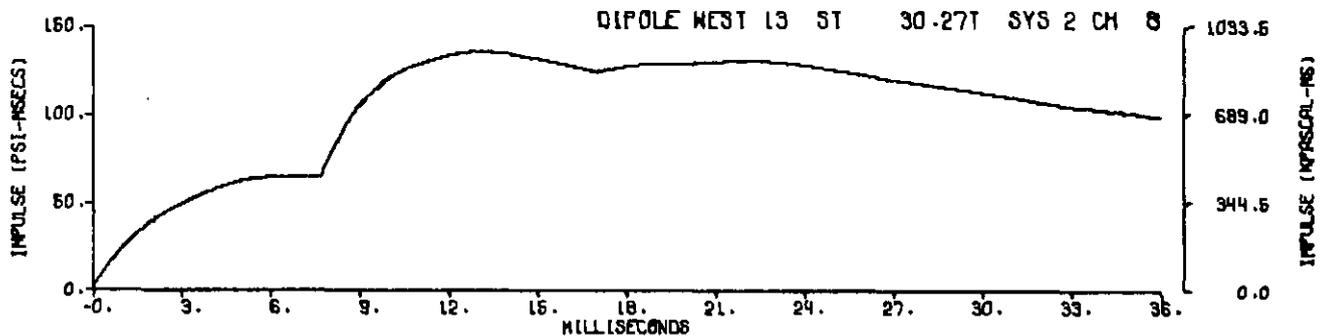
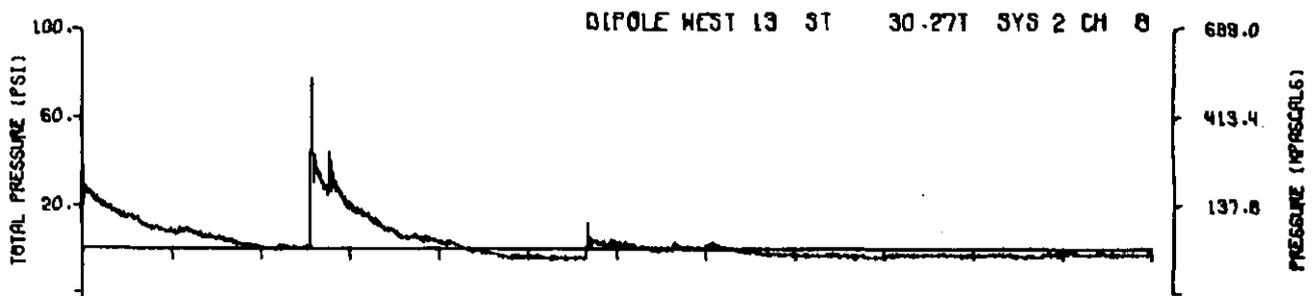
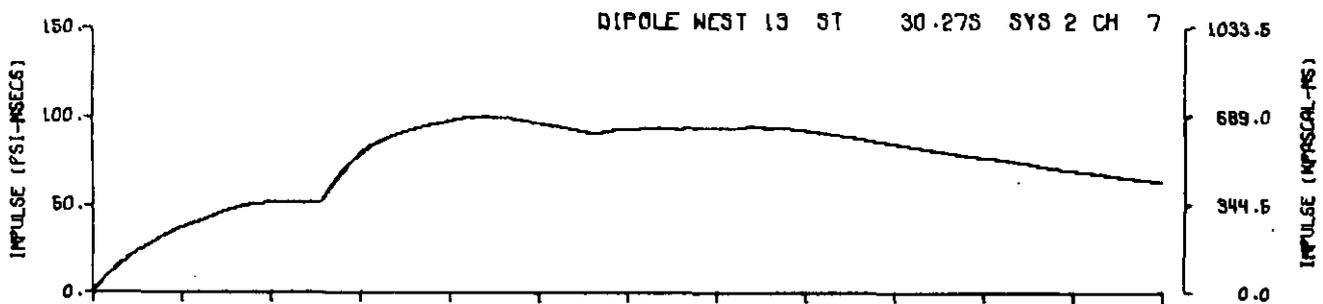
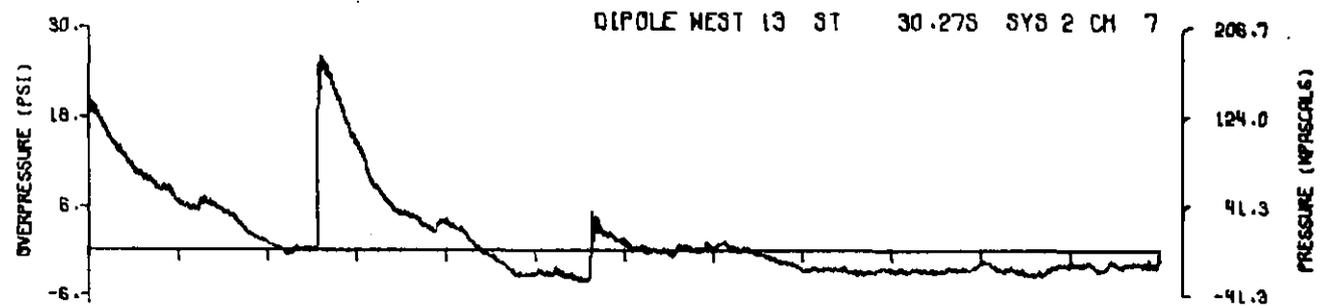
A13.14

214

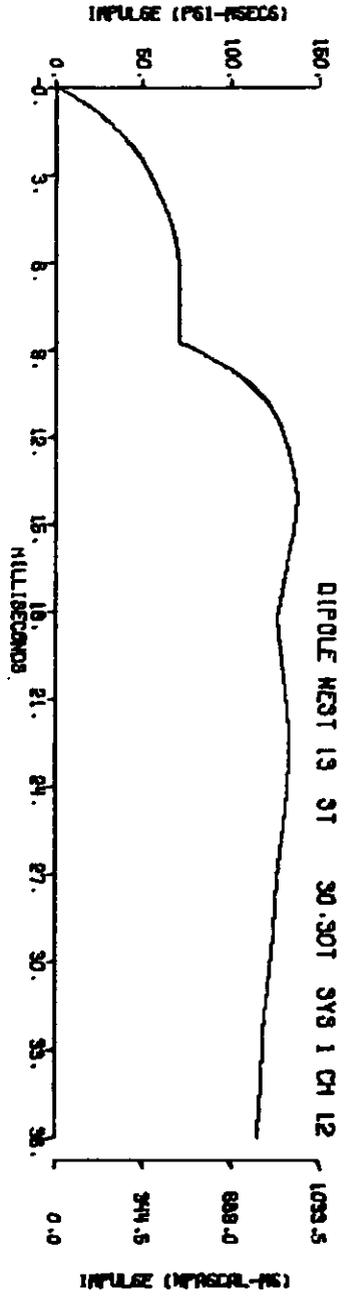
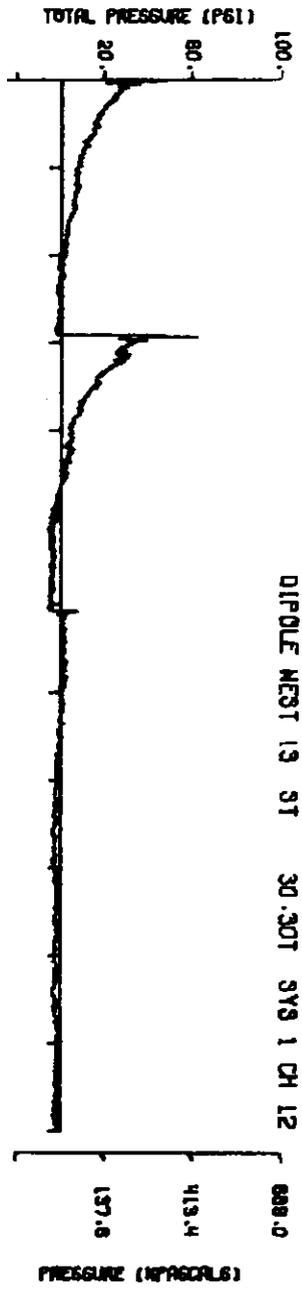
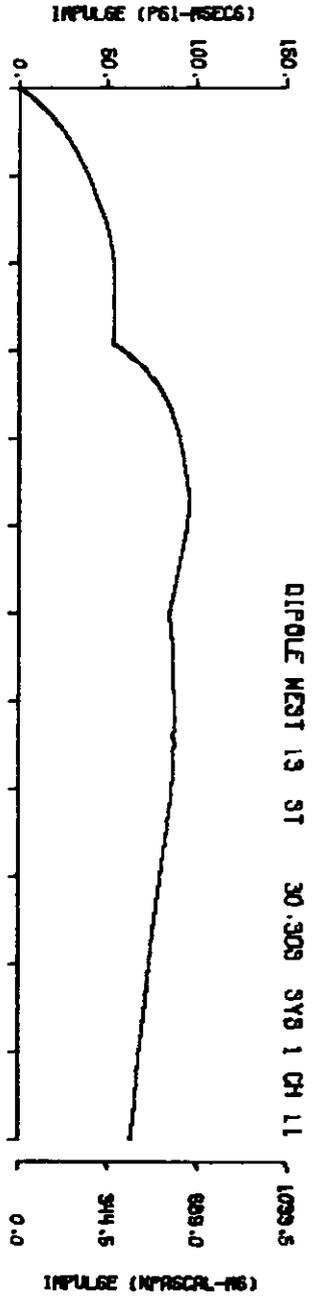
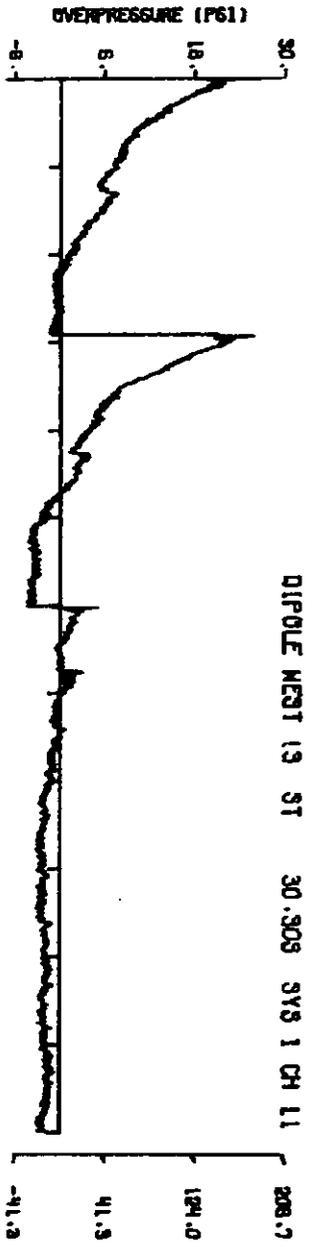


A13.15
215

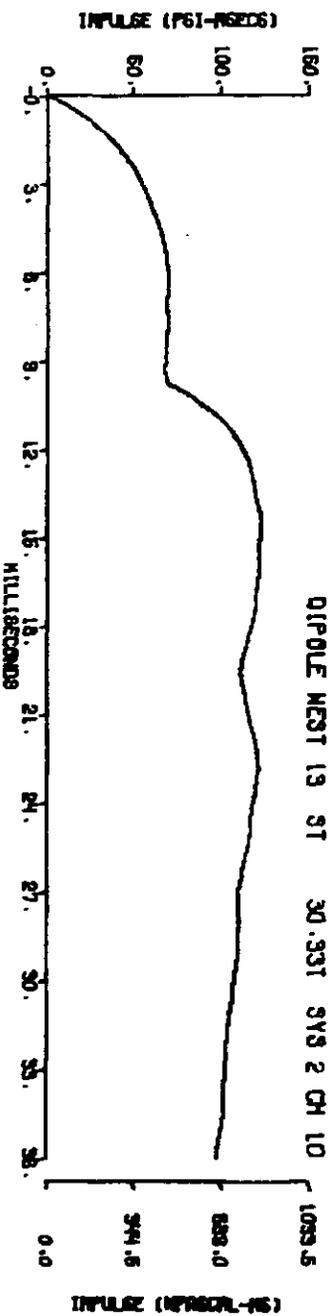
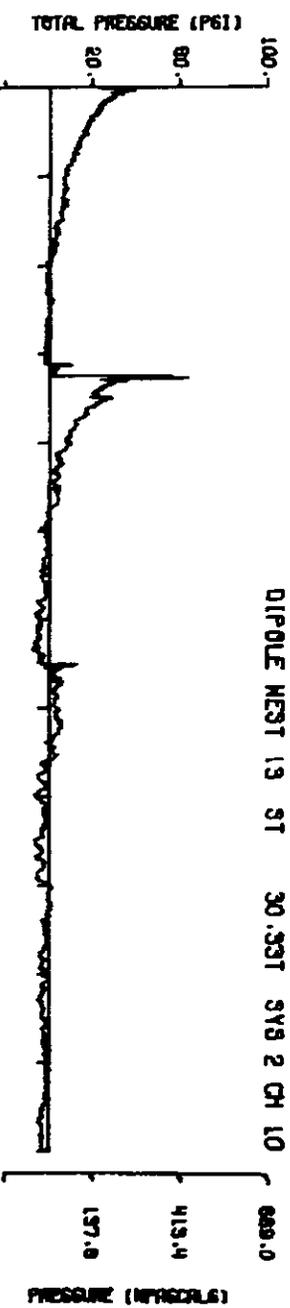
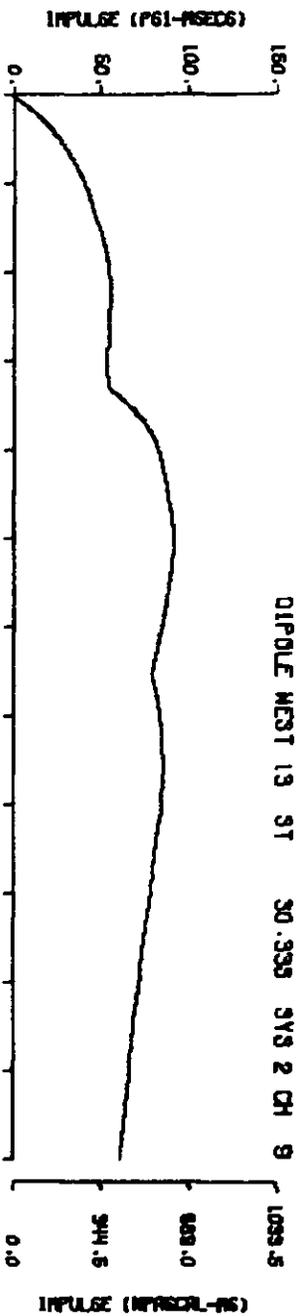
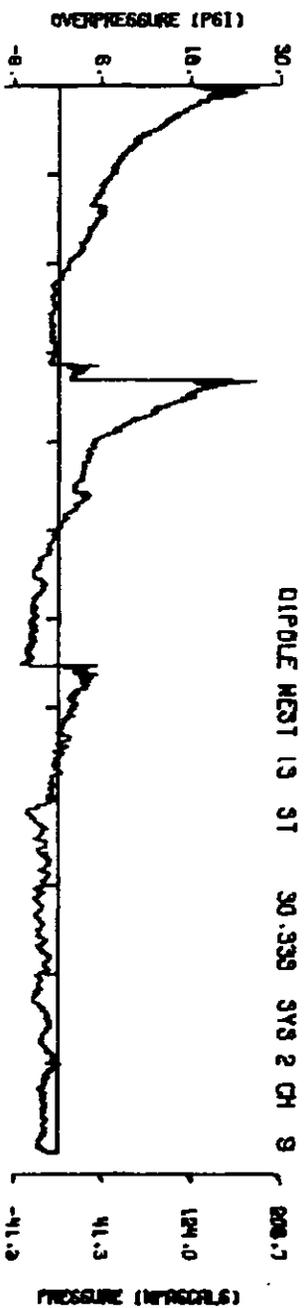




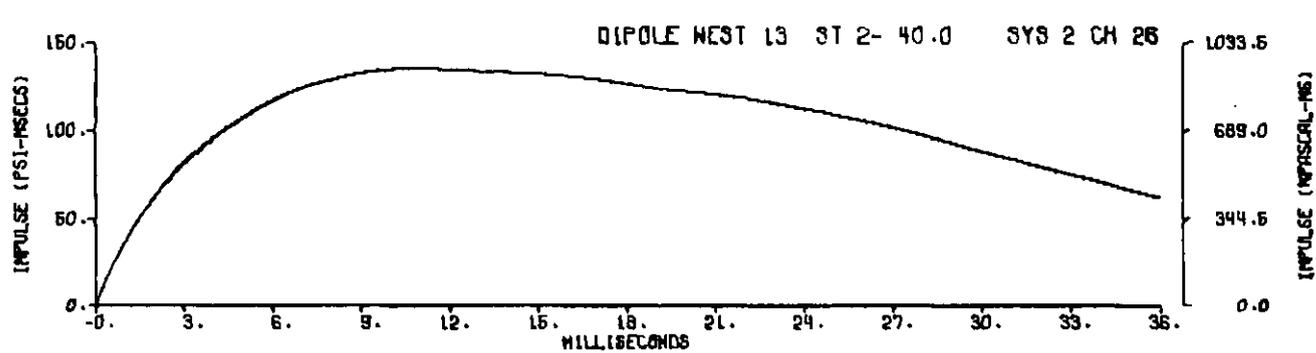
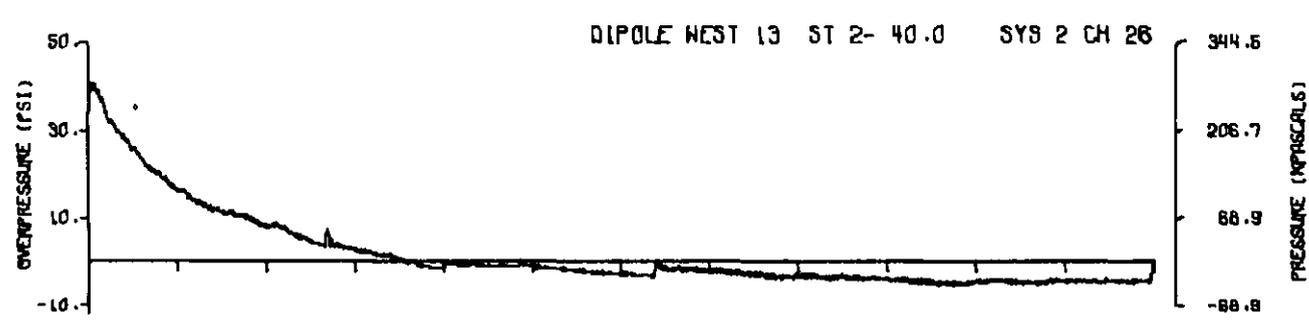
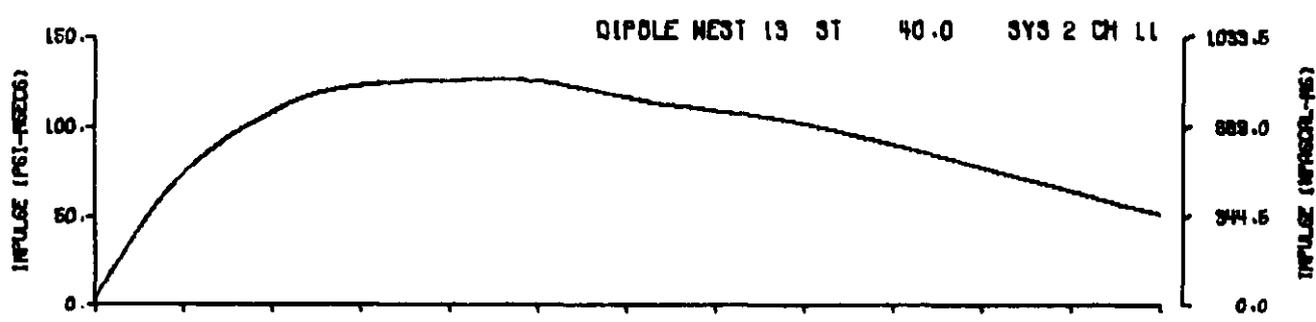
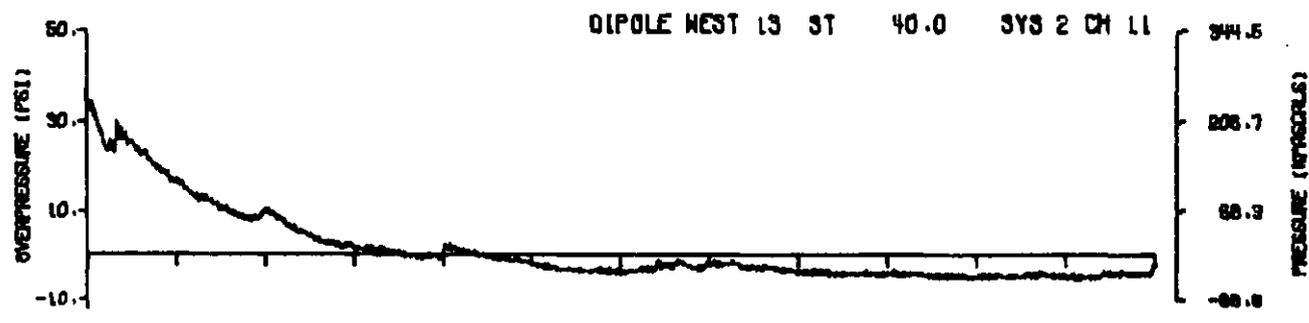
A13.17



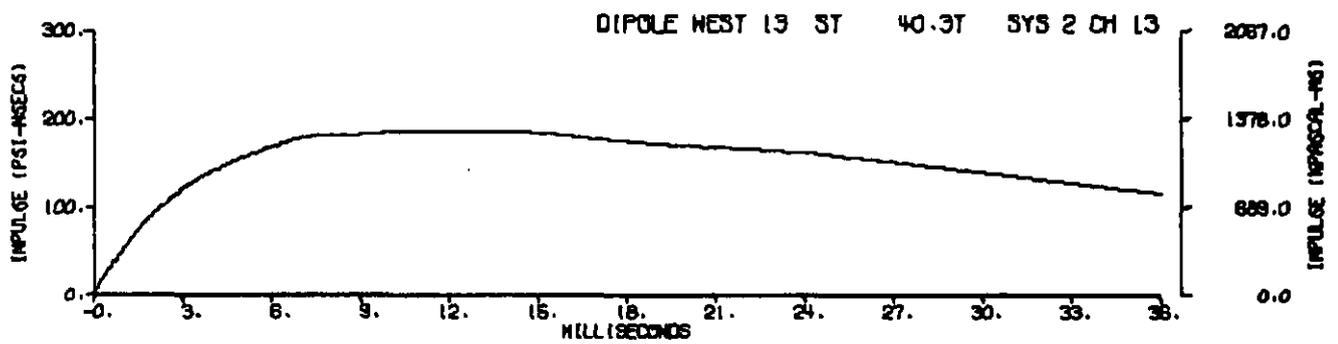
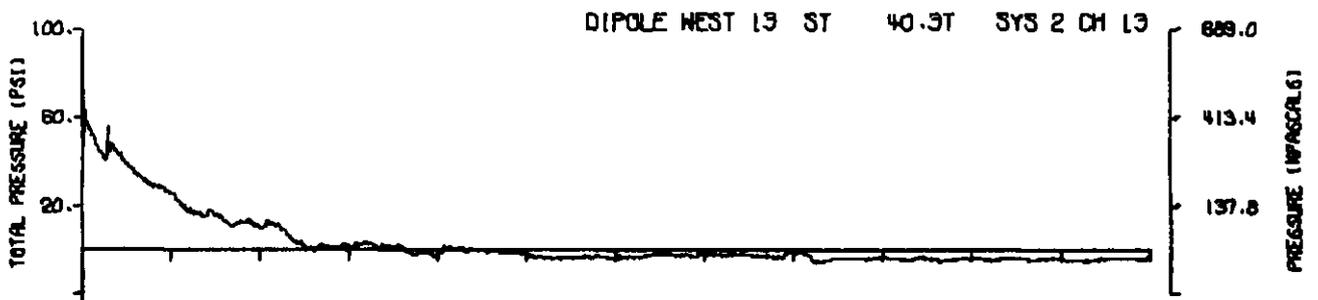
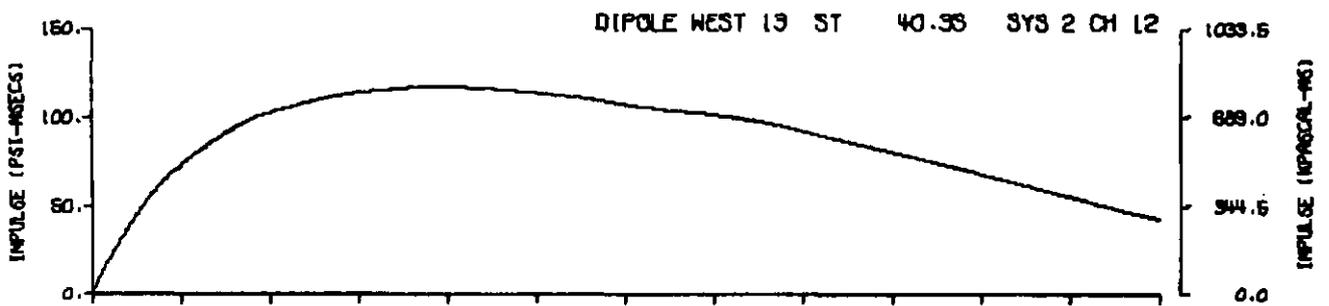
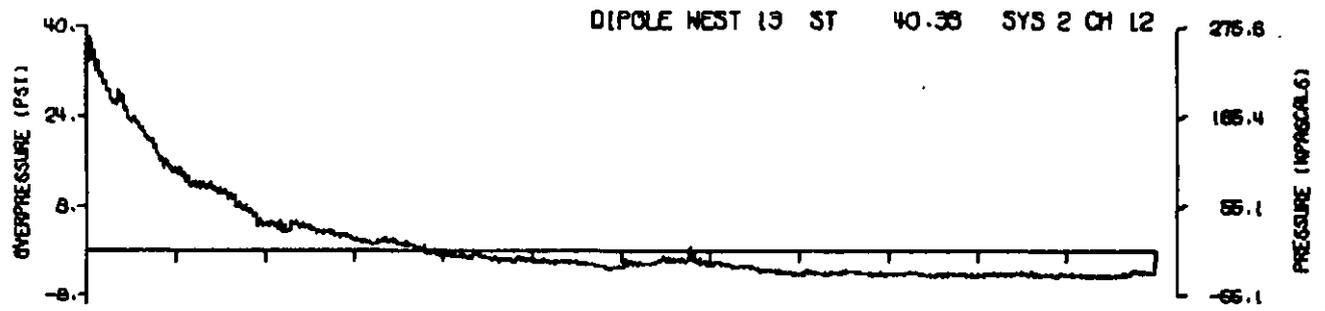
A13.18



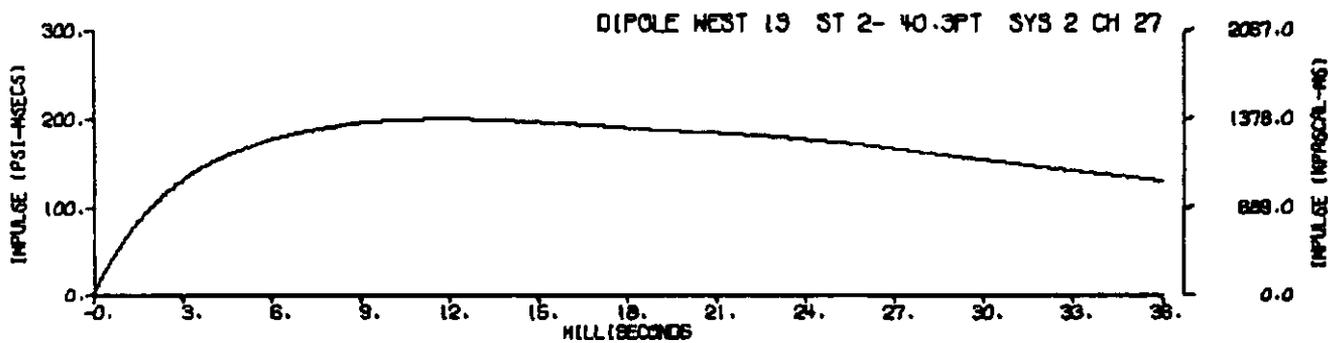
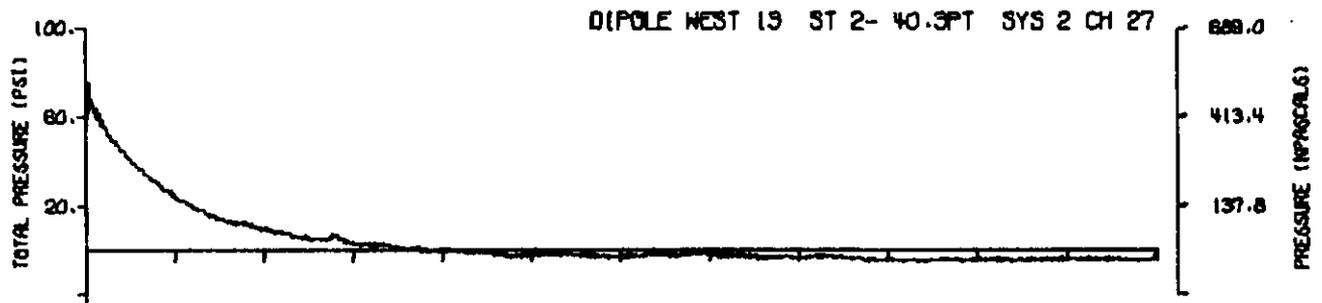
A13.19



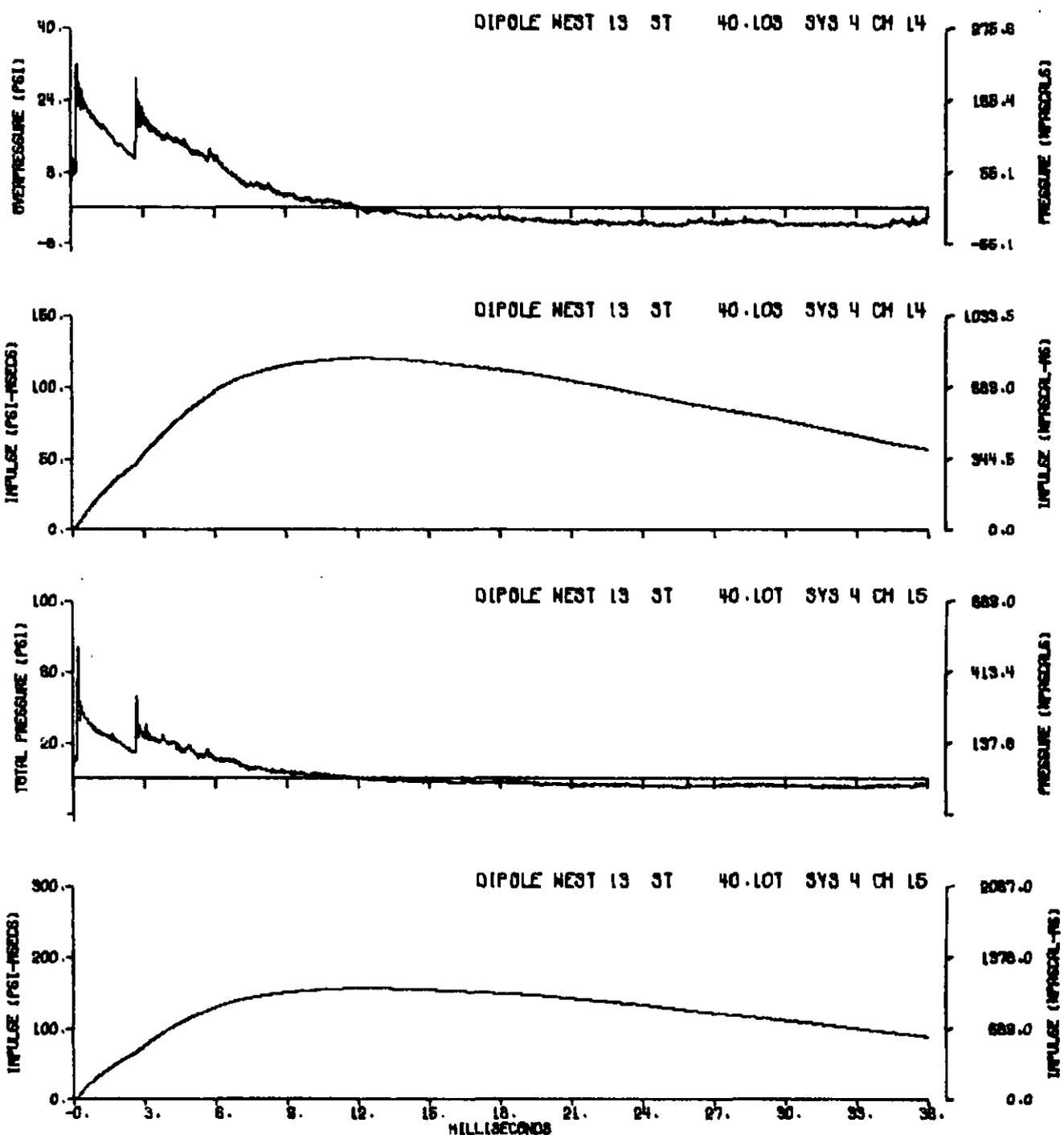
A13.20



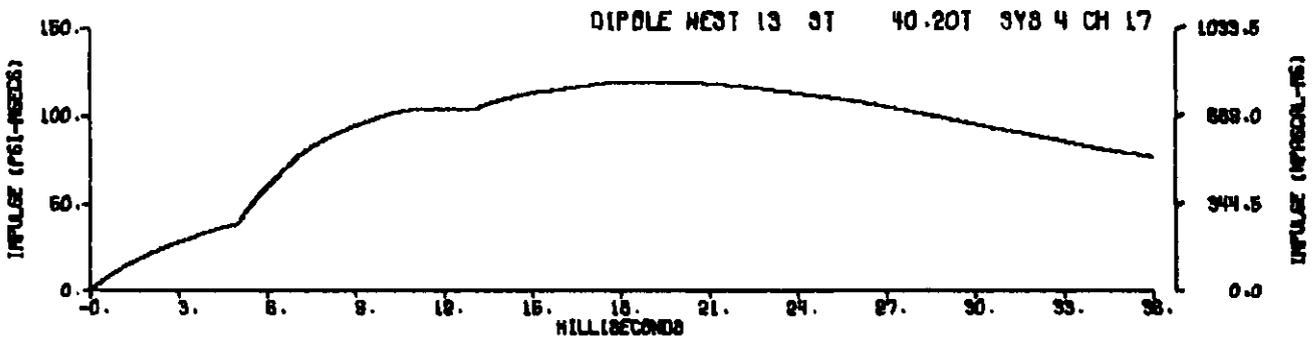
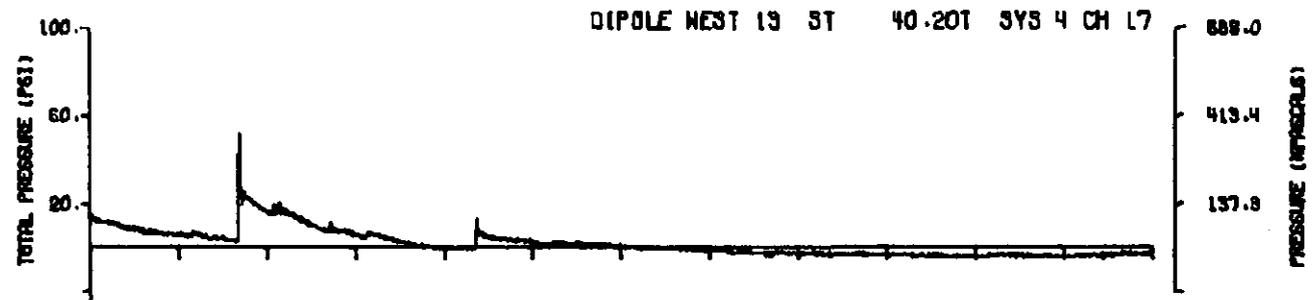
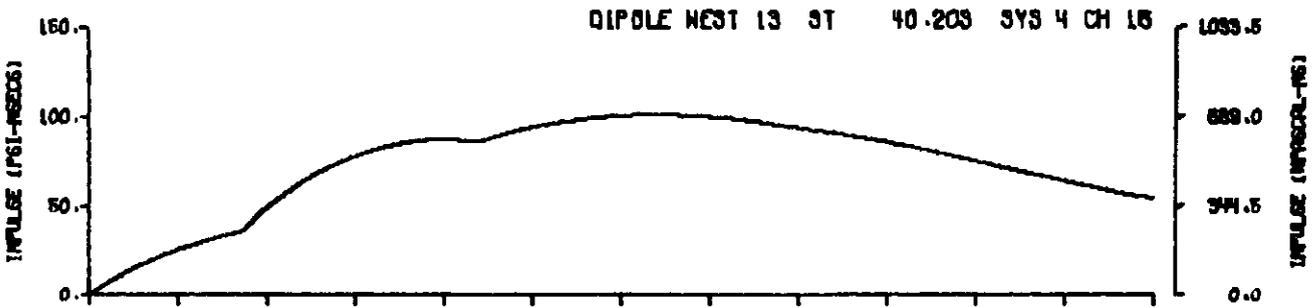
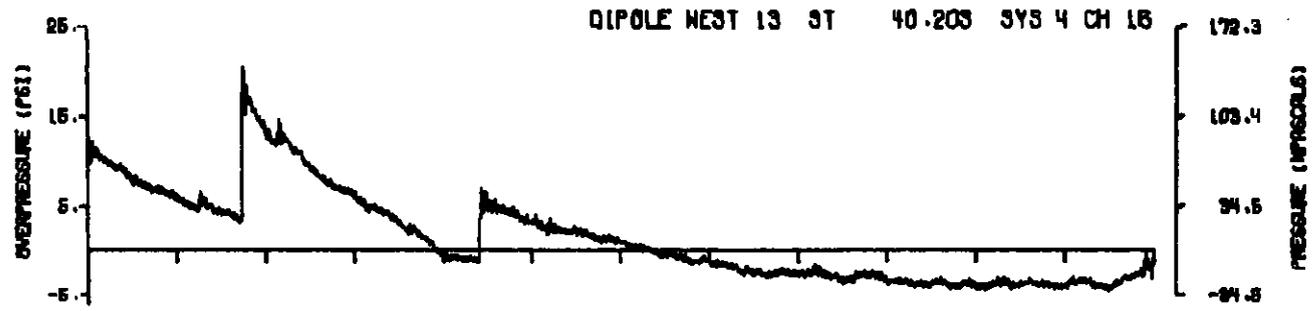
A13.21



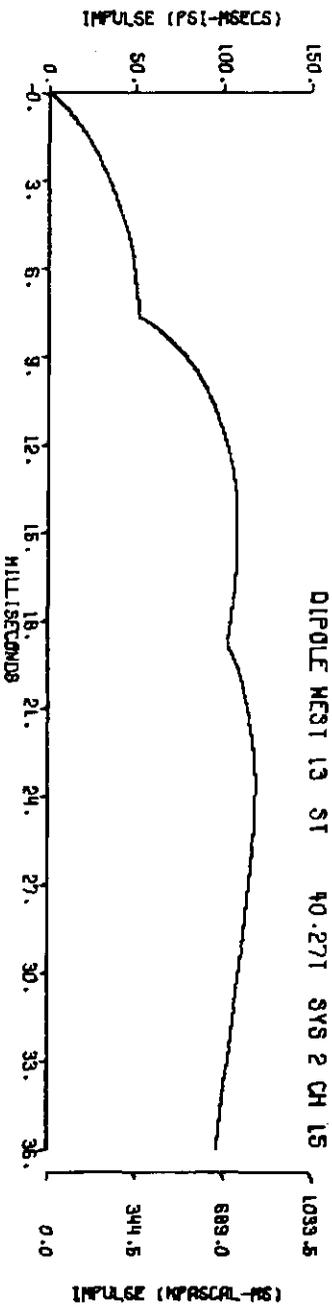
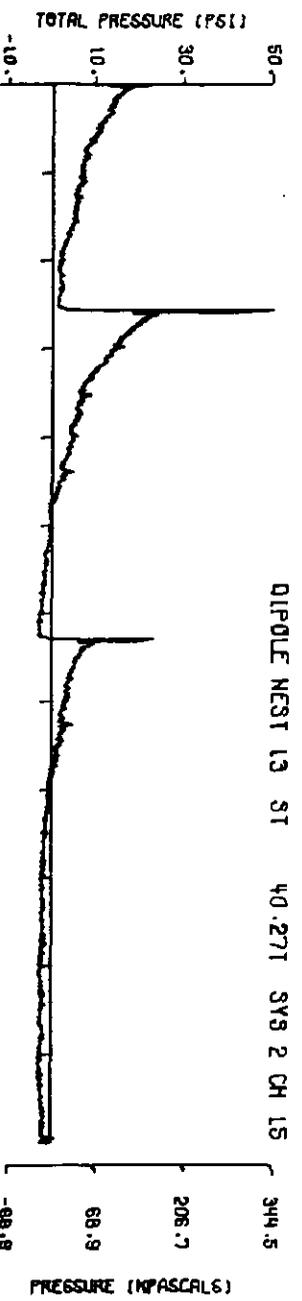
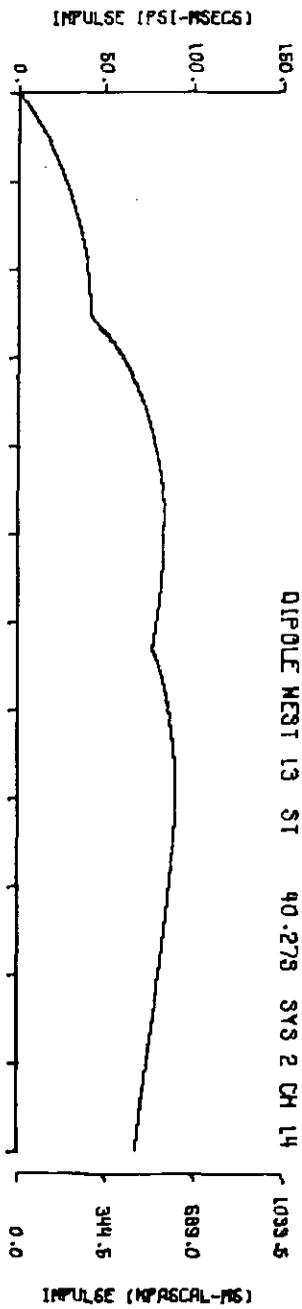
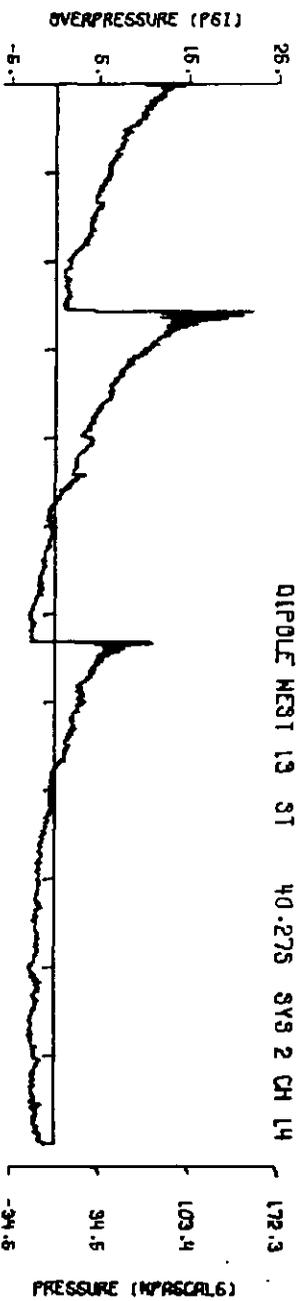
A13.22



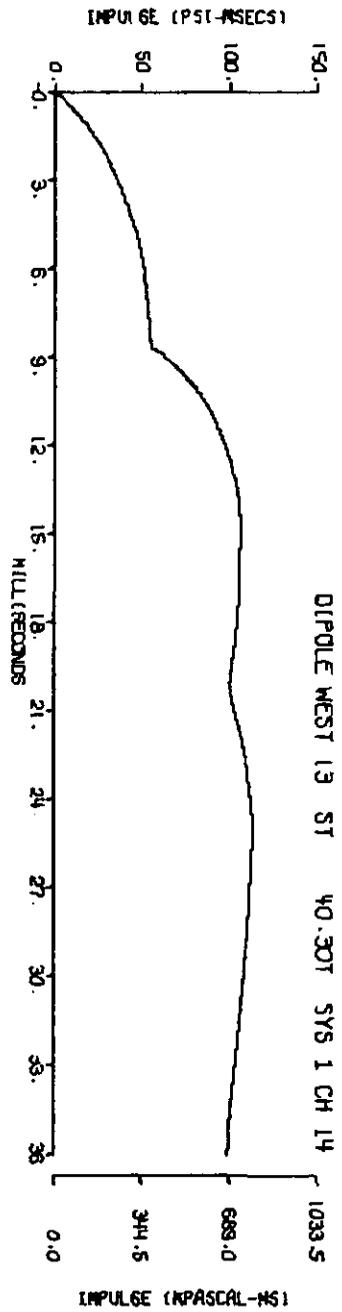
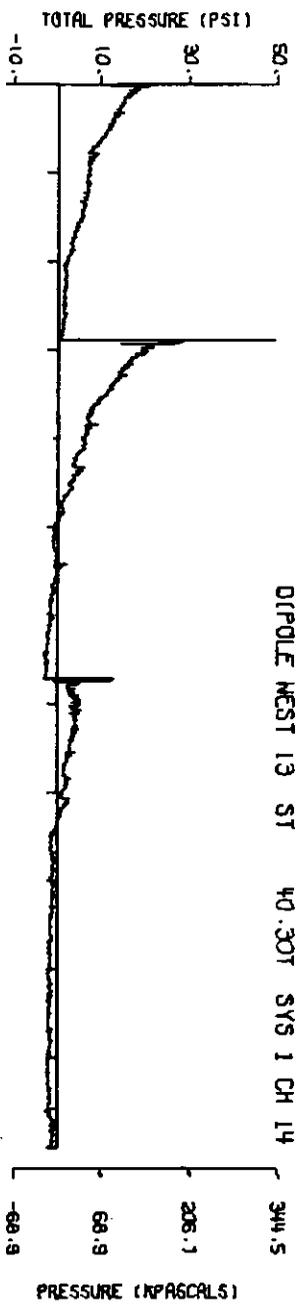
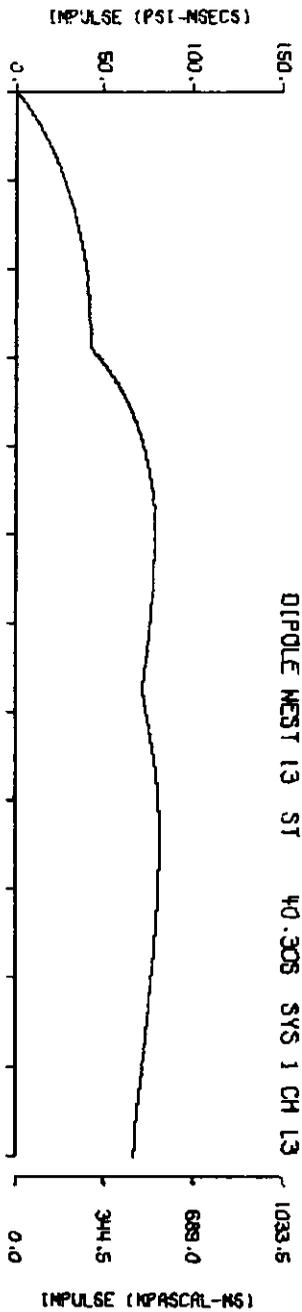
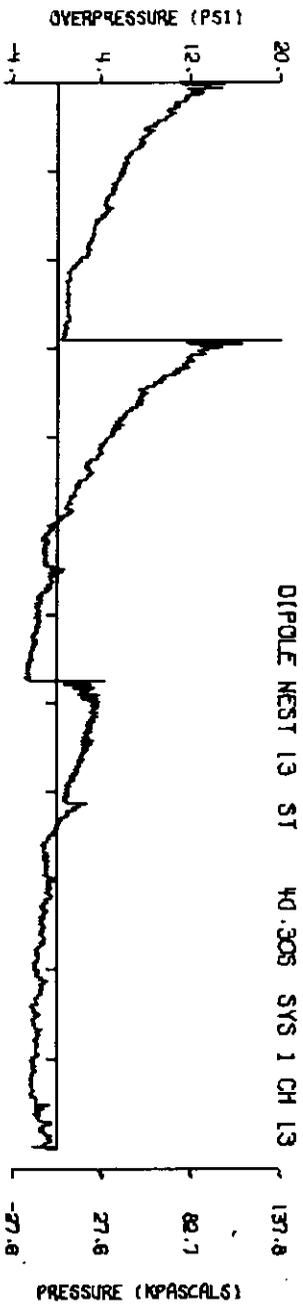
A13.23



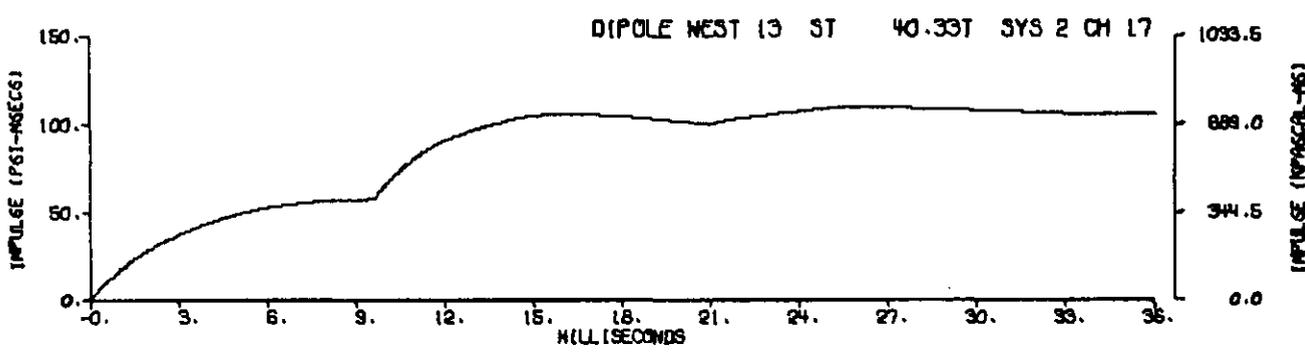
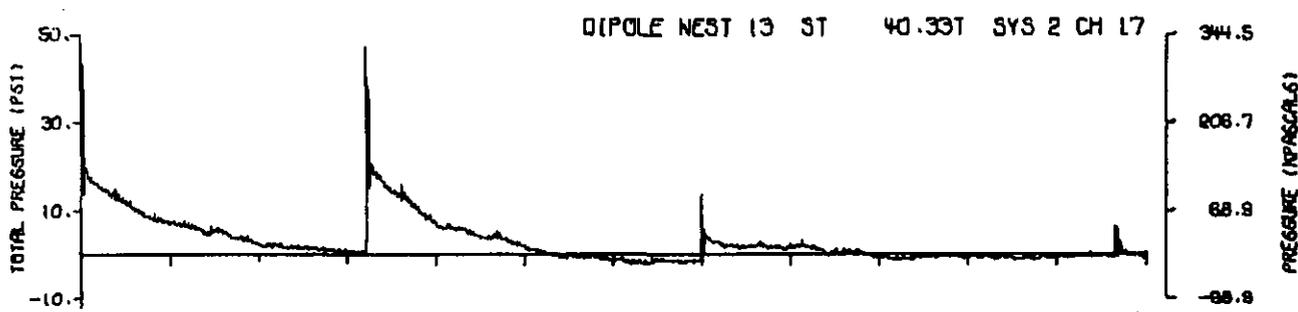
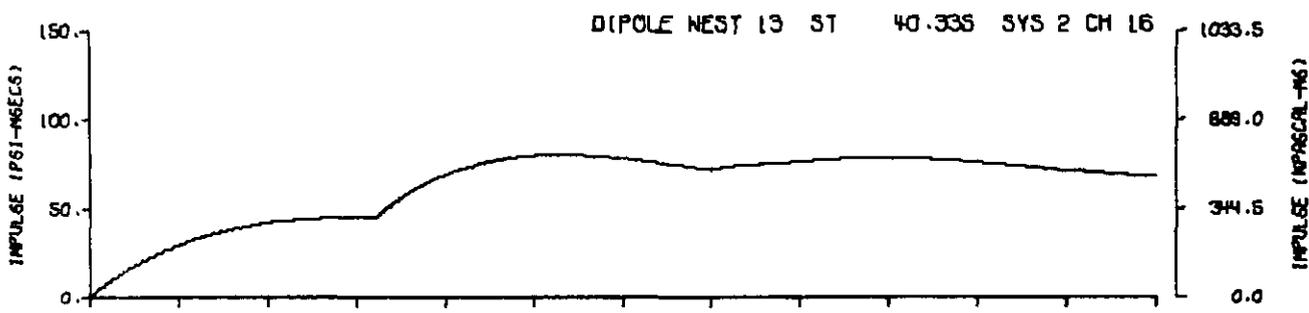
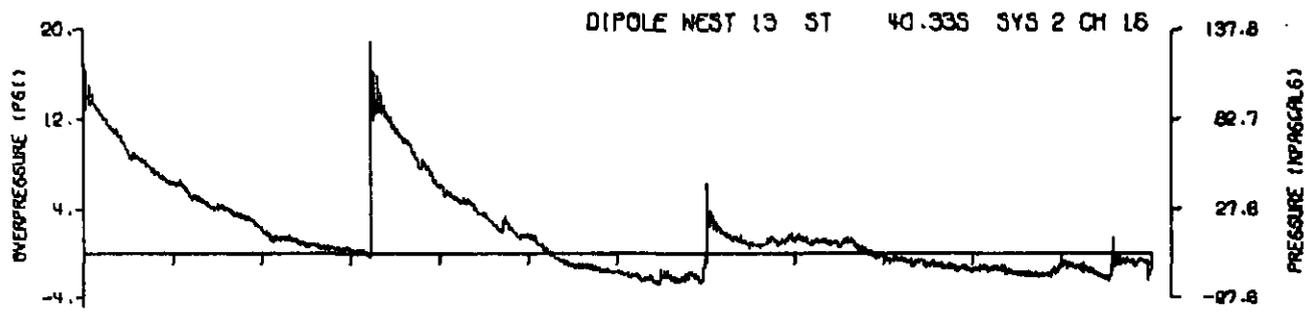
A13.24



A13.25

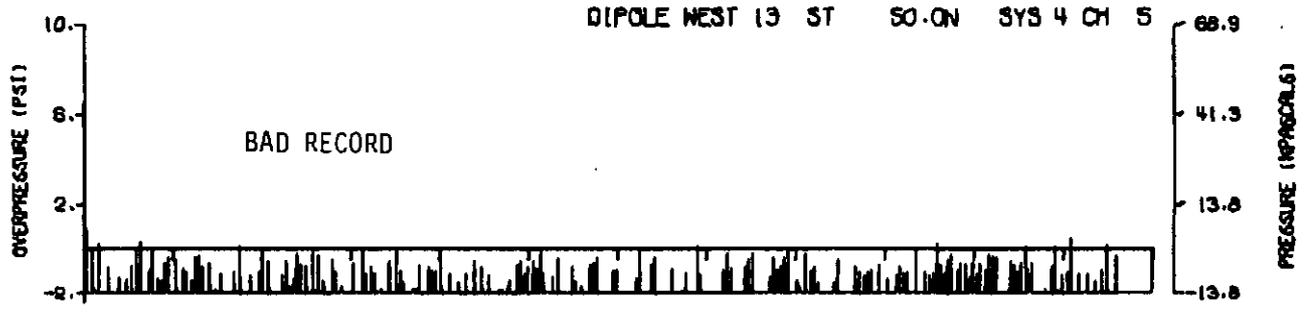


A13.26
226

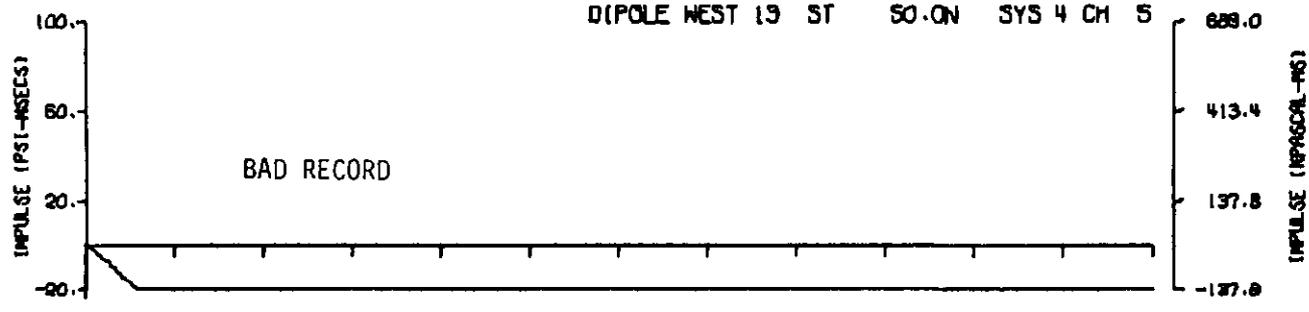


A13.27

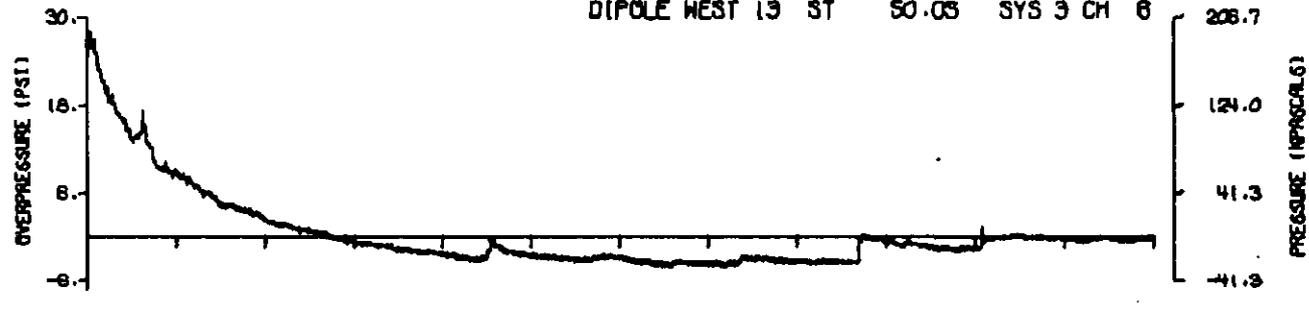
DIPOLE WEST 13 ST 50.0N SYS 4 CH 5



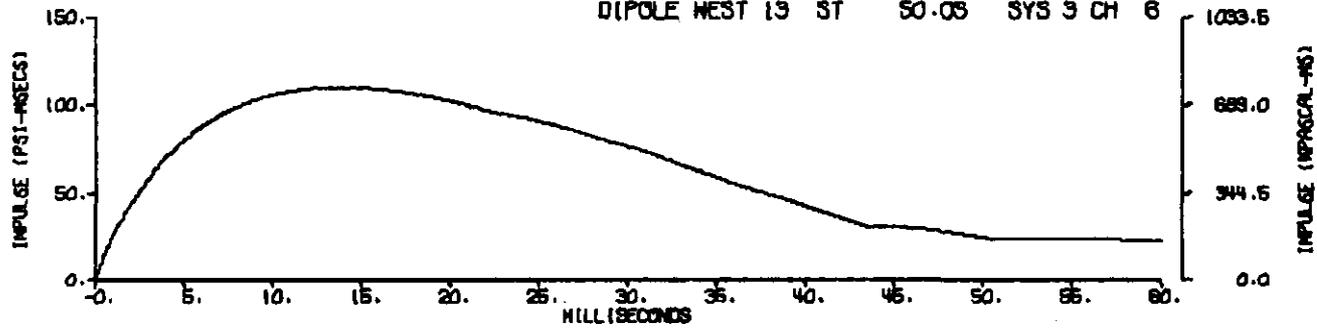
DIPOLE WEST 13 ST 50.0N SYS 4 CH 5

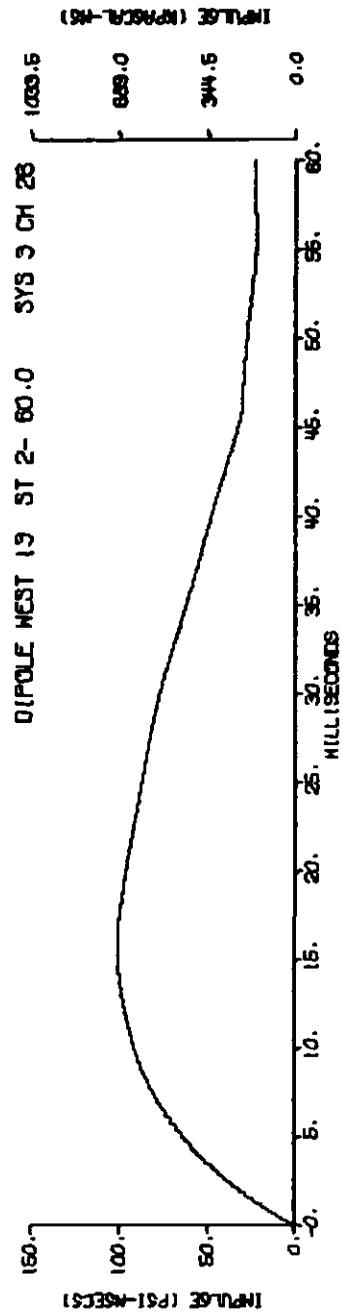
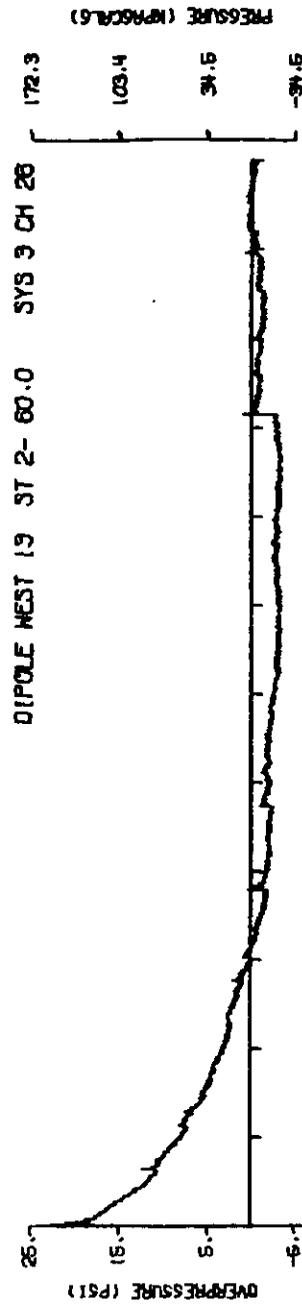
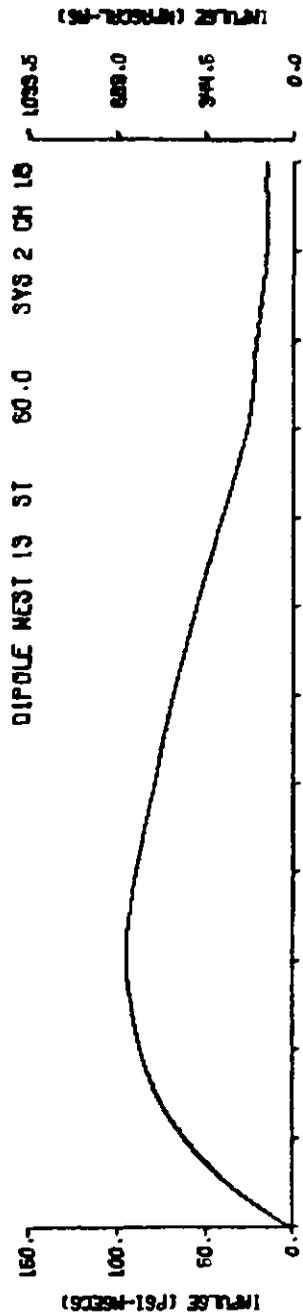
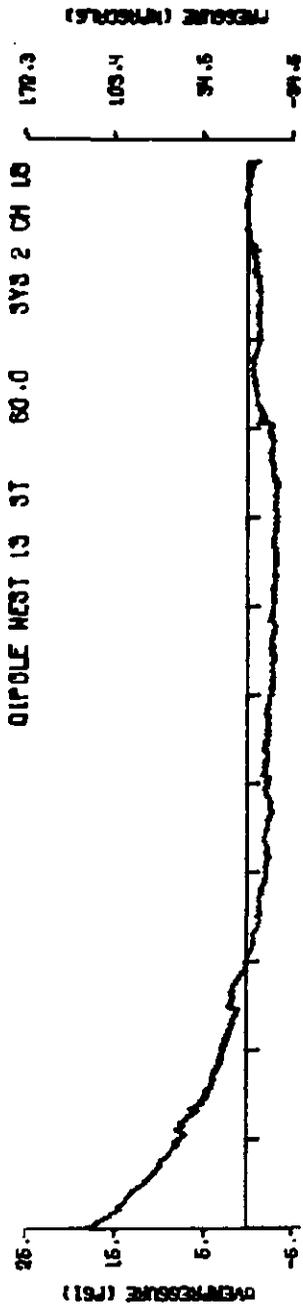


DIPOLE WEST 13 ST 50.0S SYS 3 CH 6

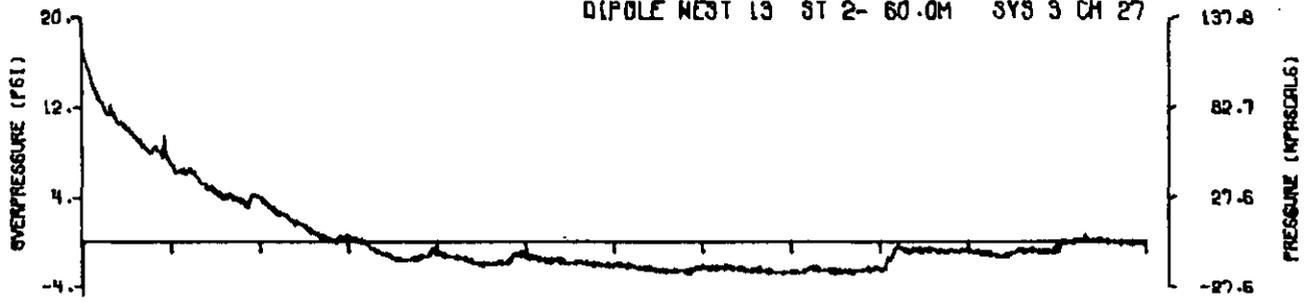


DIPOLE WEST 13 ST 50.0S SYS 3 CH 6

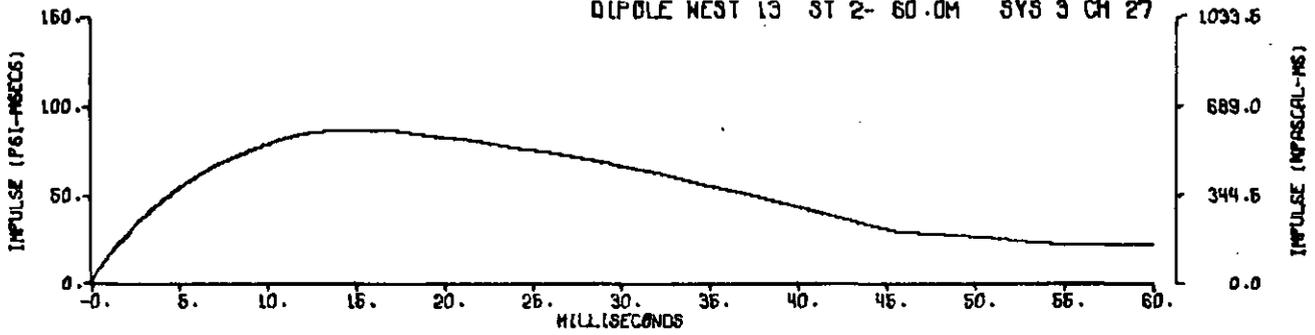


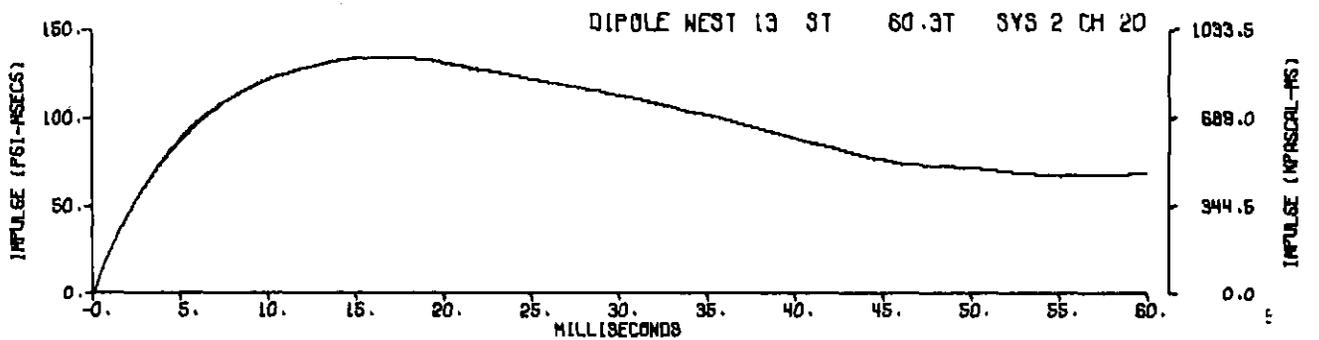
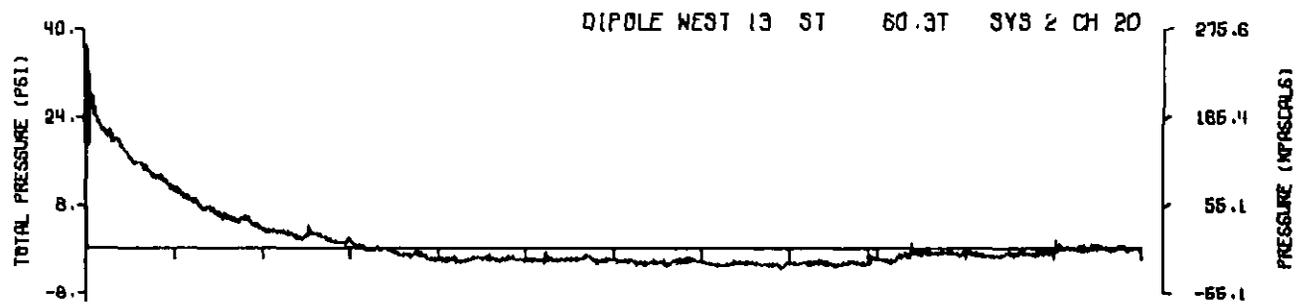
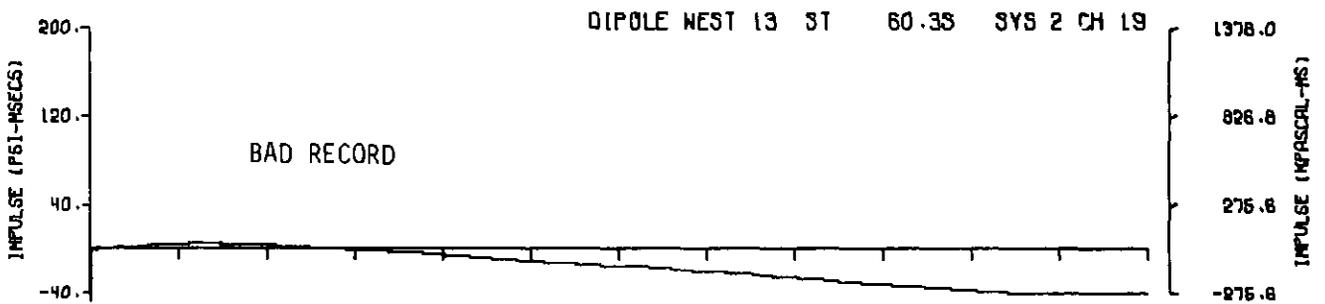
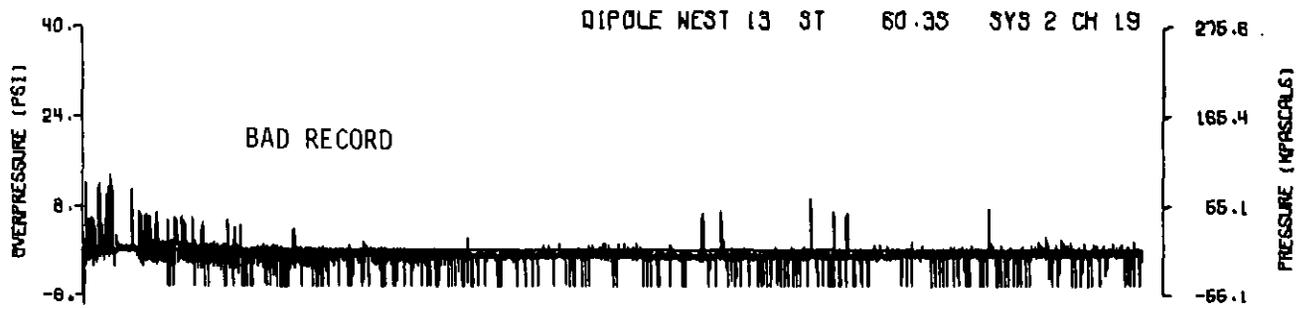


DIPOLE NEST 13 ST 2- 60.0M SYS 3 CH 27



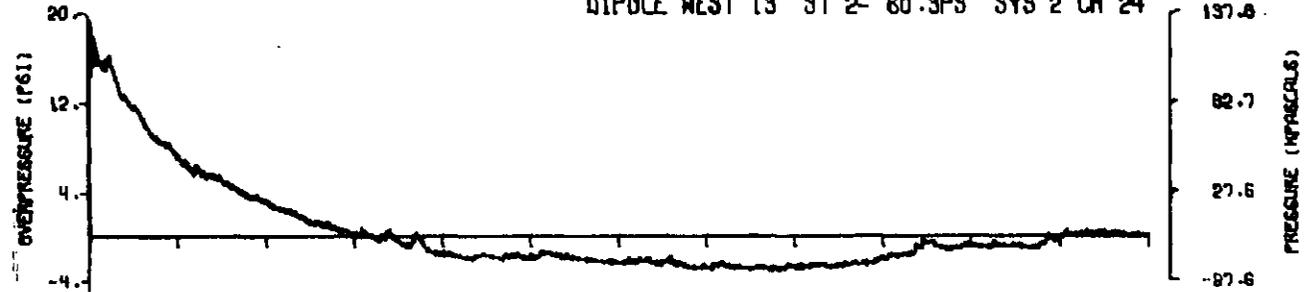
DIPOLE NEST 13 ST 2- 60.0M SYS 3 CH 27



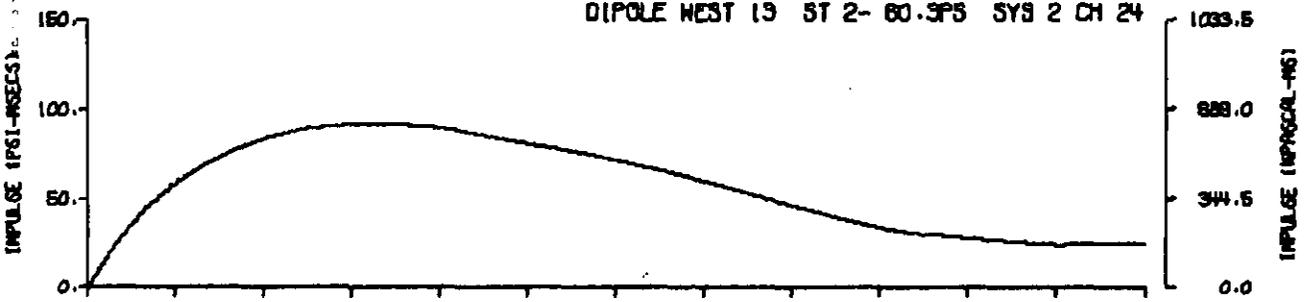


A13.31

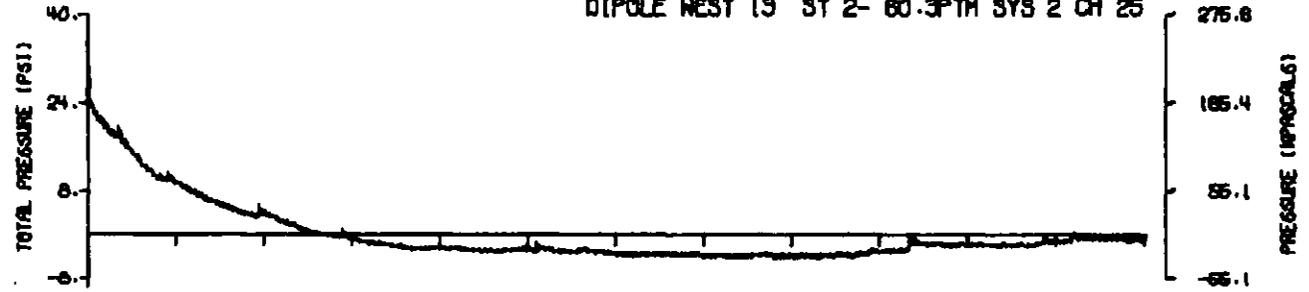
DIPOLE WEST 13 ST 2- 60.3PS SYS 2 CH 24



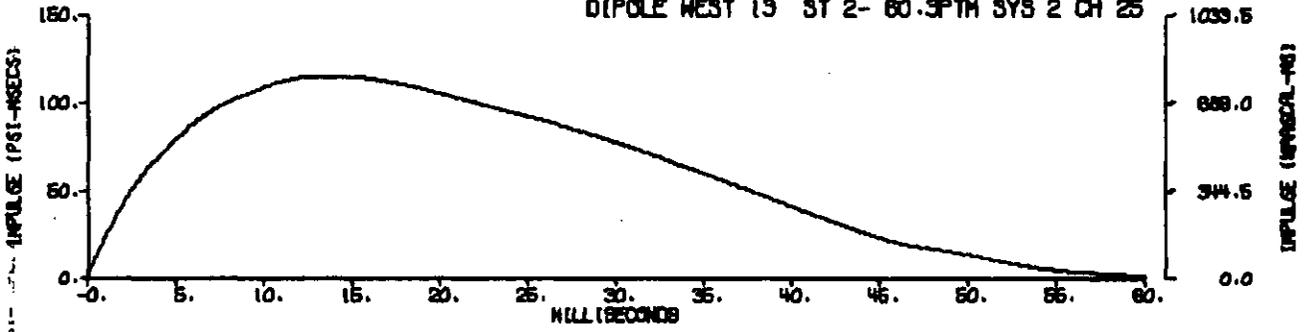
DIPOLE WEST 13 ST 2- 60.3PS SYS 2 CH 24

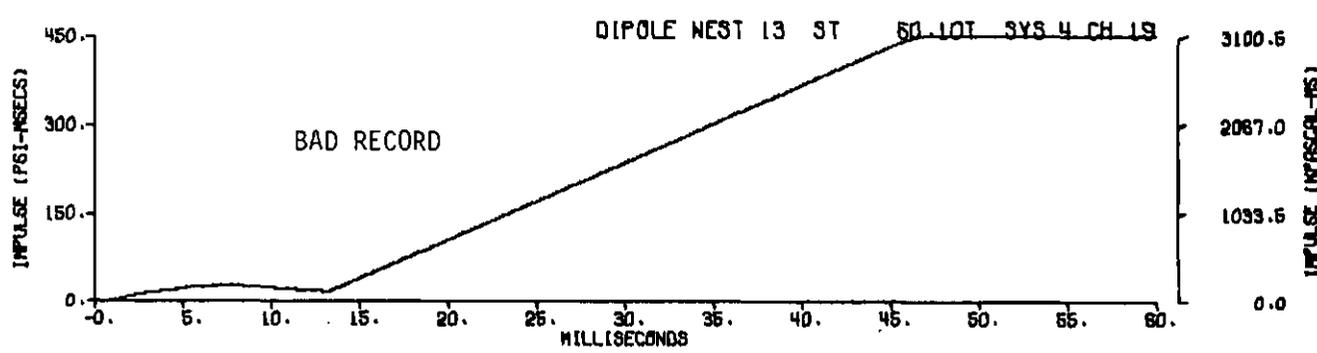
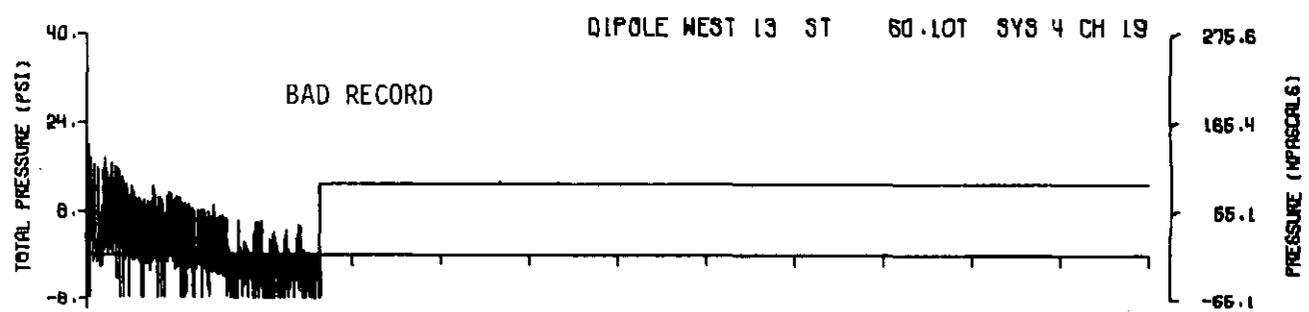
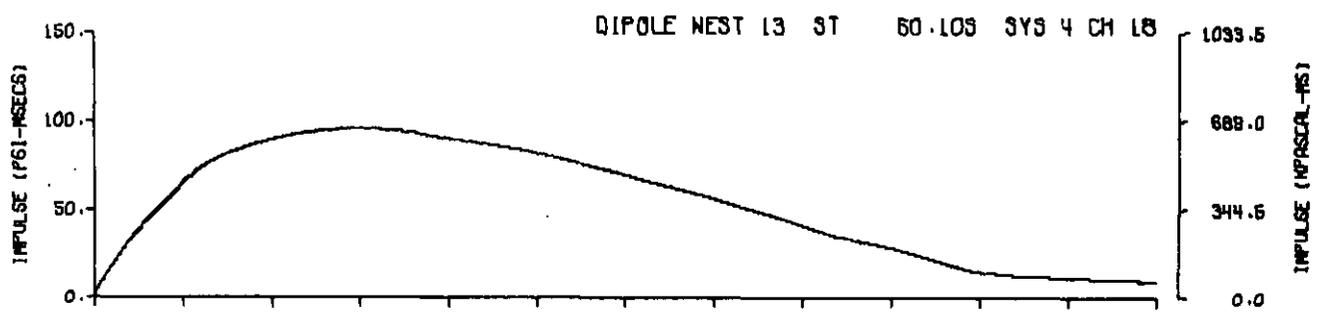
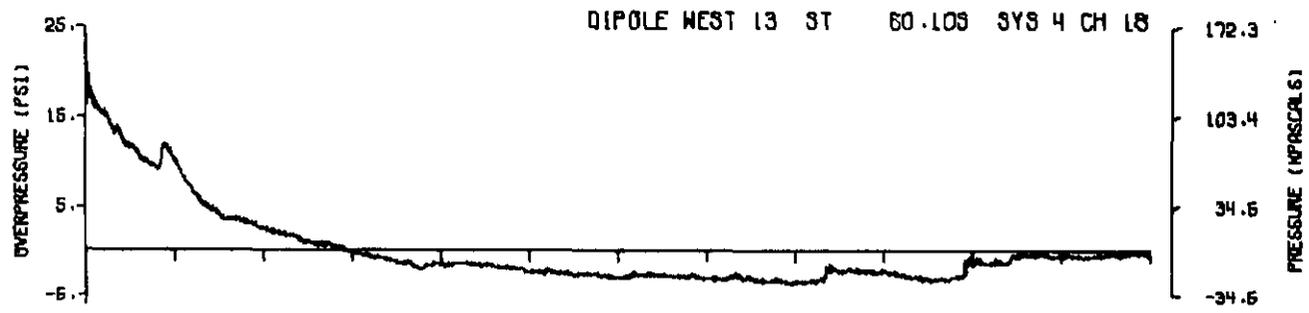


DIPOLE WEST 13 ST 2- 60.3PTH SYS 2 CH 25

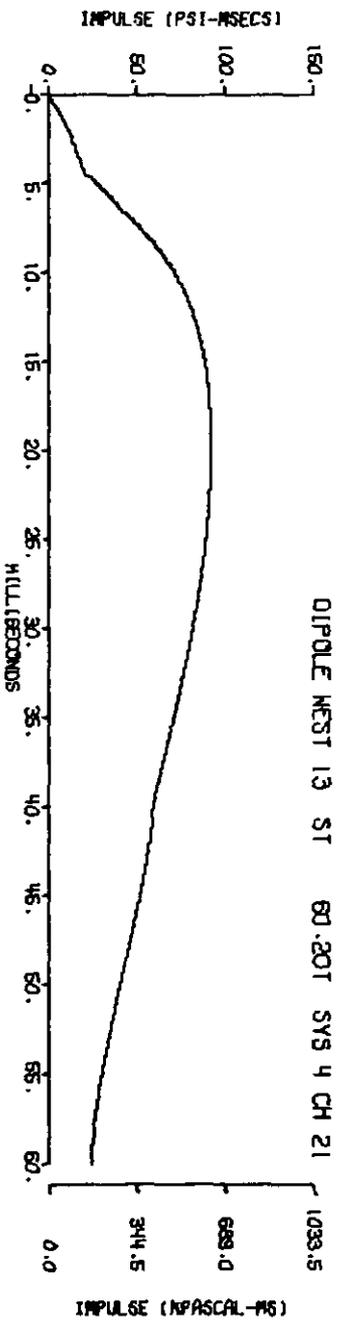
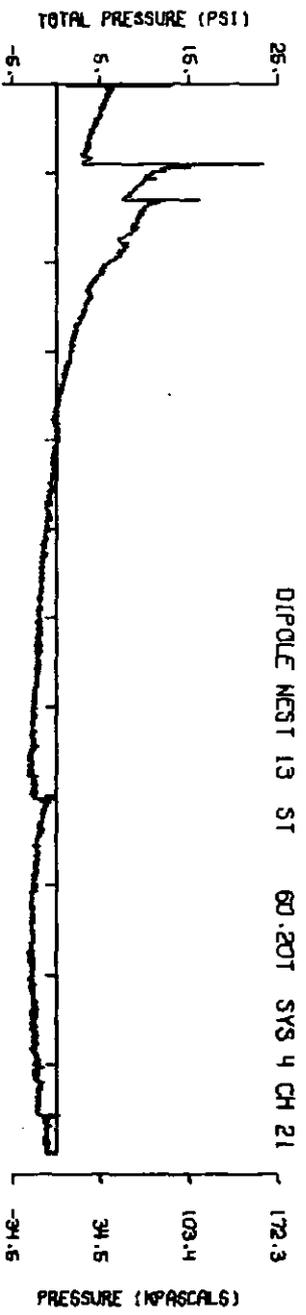
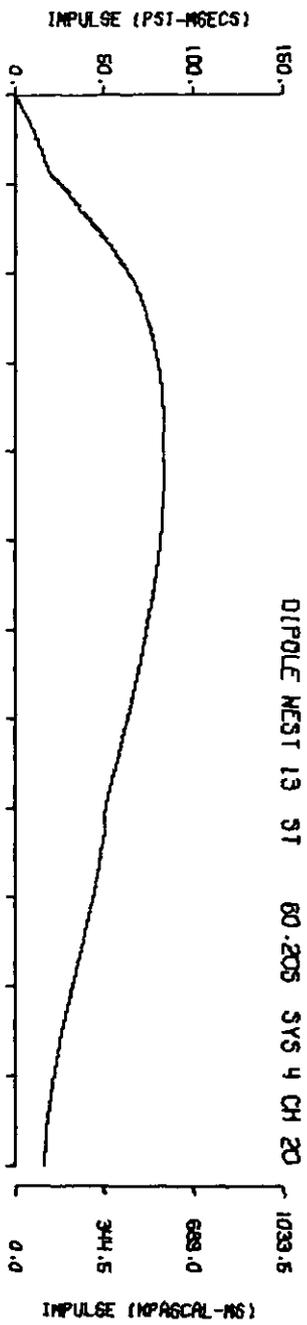
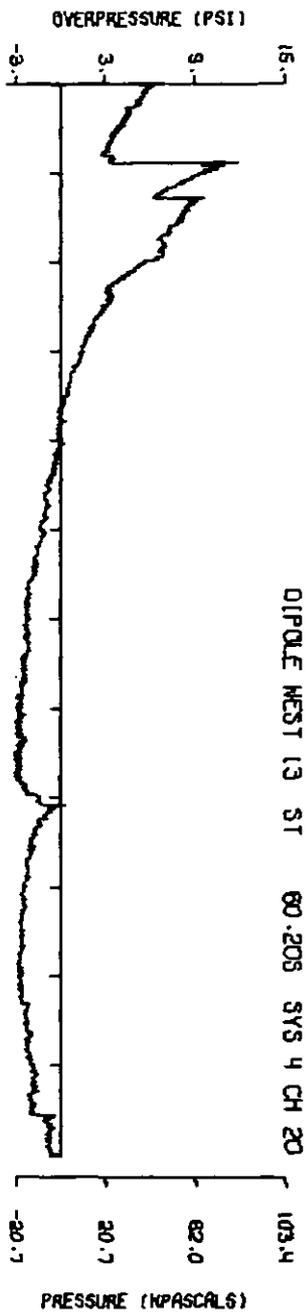


DIPOLE WEST 13 ST 2- 60.3PTH SYS 2 CH 25

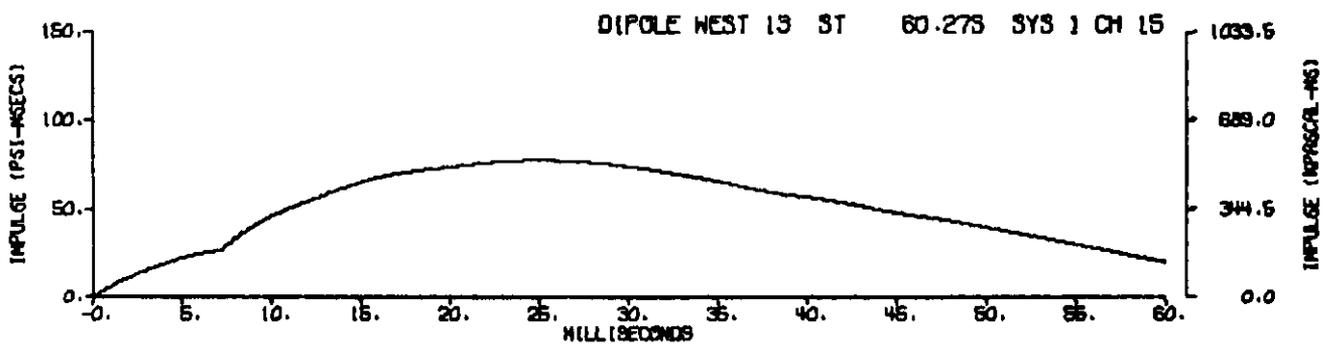
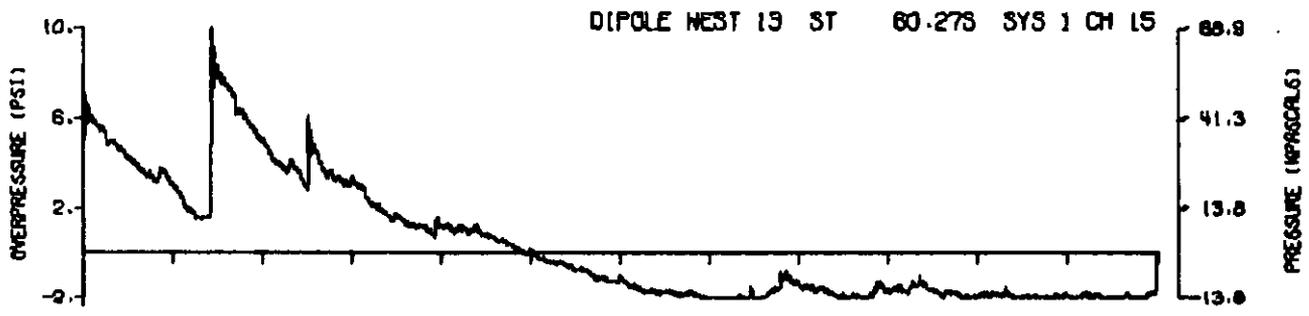




A13.33

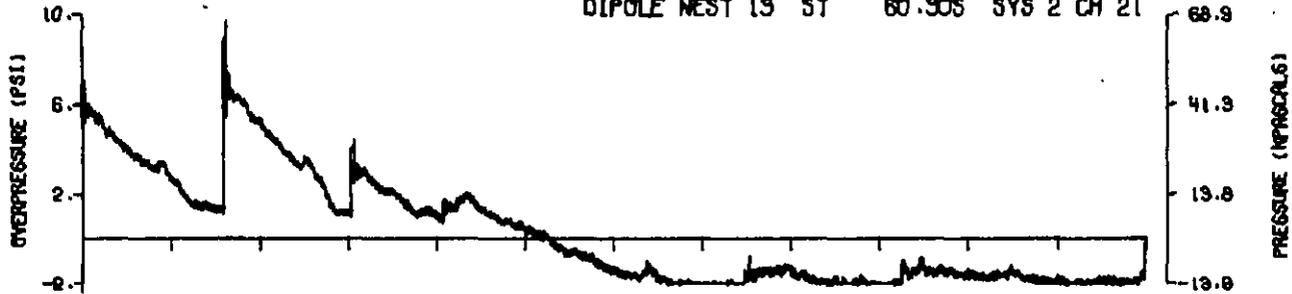


A13.34

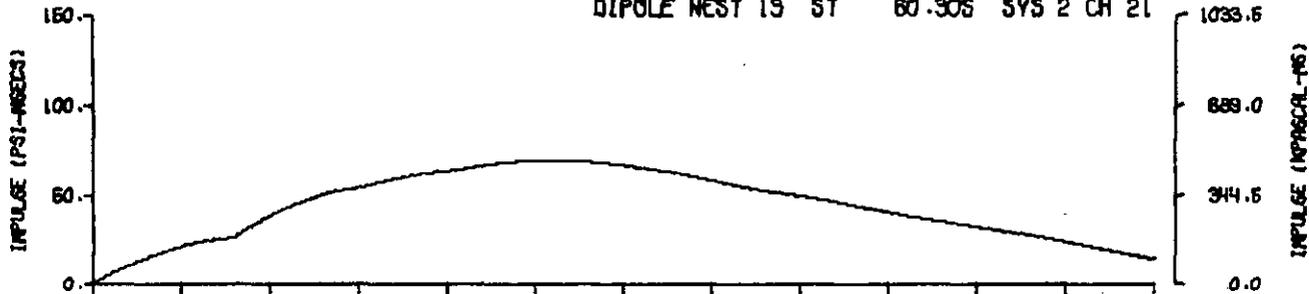


A13.35

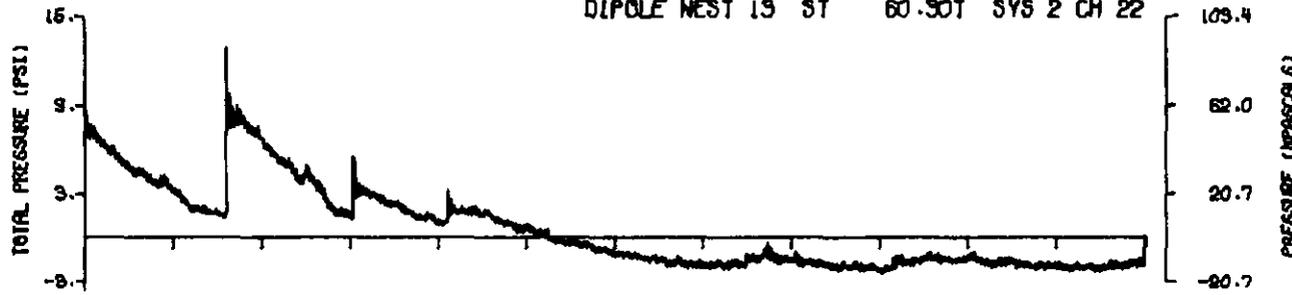
DIPOLE NEST 19 ST 60.305 SYS 2 CH 21



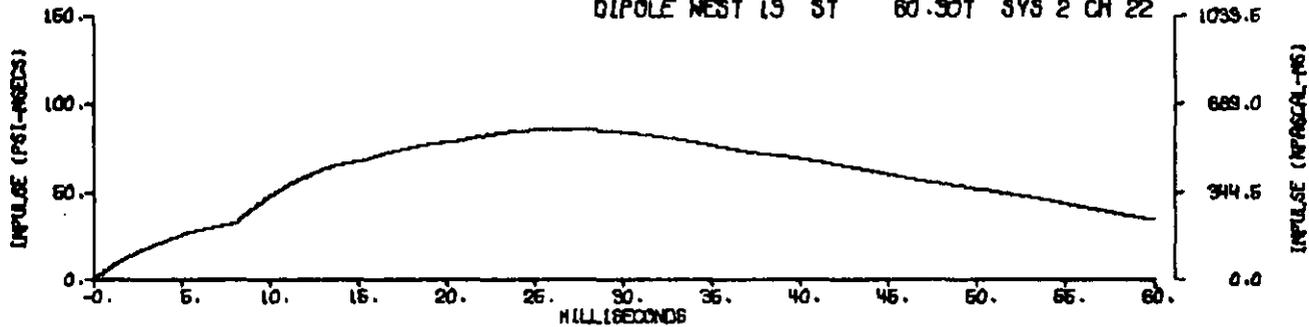
DIPOLE NEST 19 ST 60.305 SYS 2 CH 21



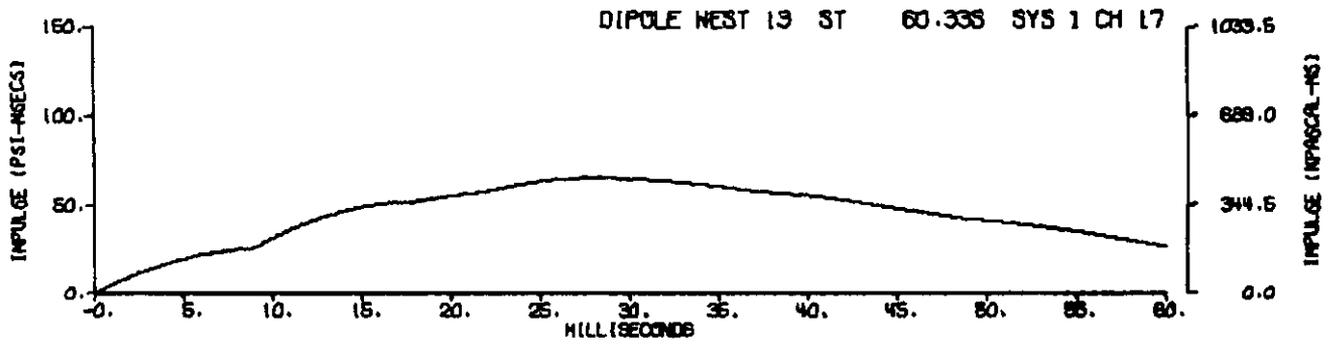
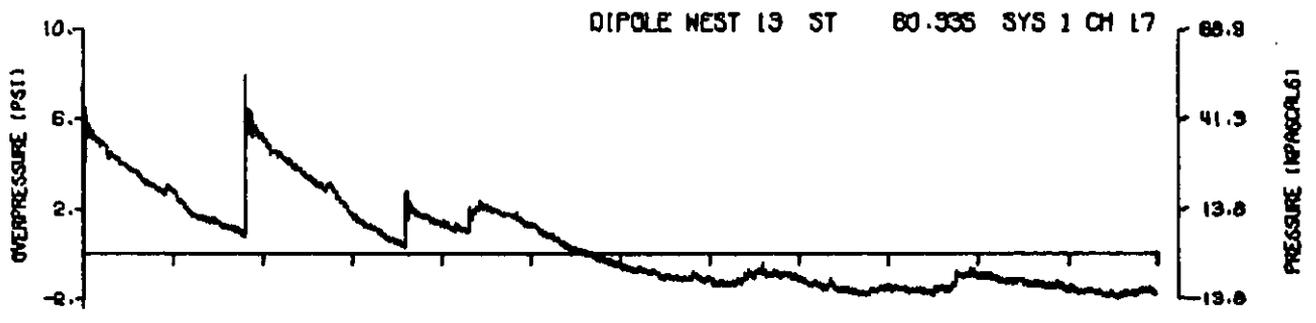
DIPOLE NEST 19 ST 60.307 SYS 2 CH 22



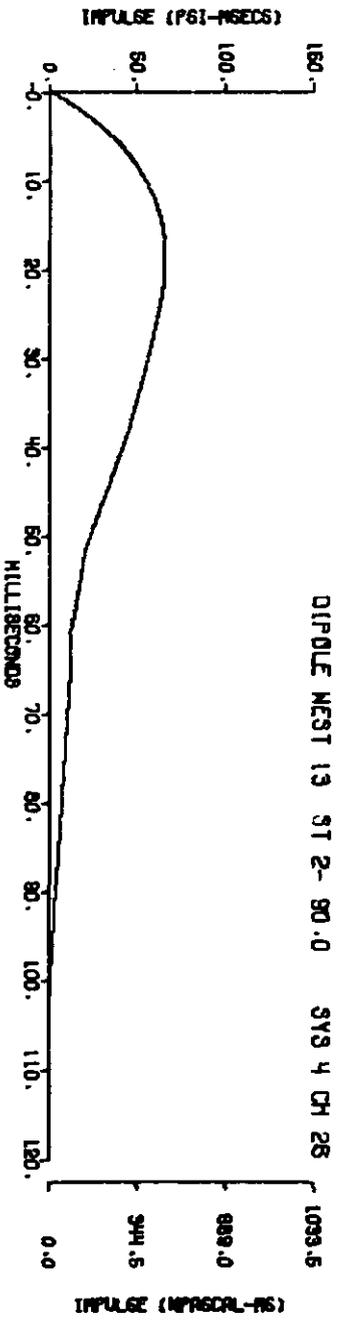
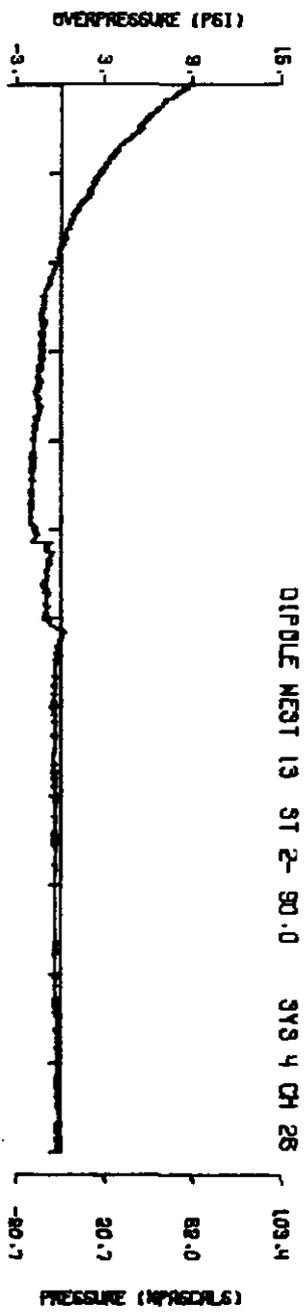
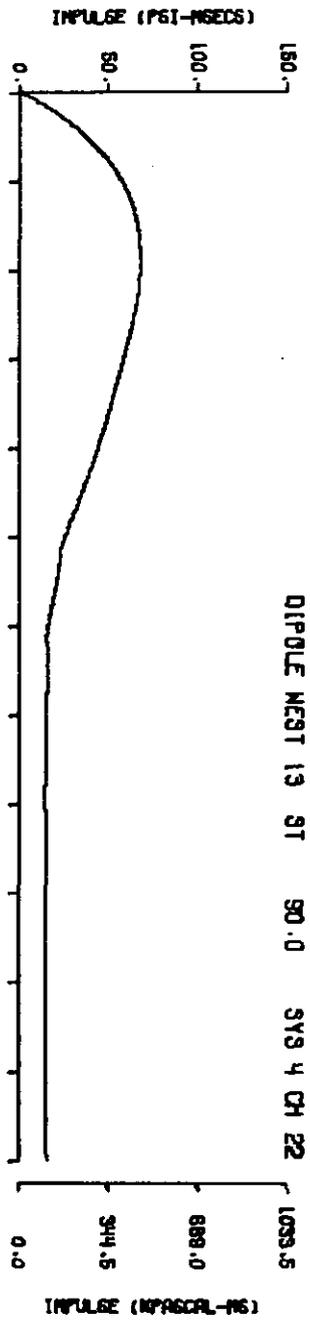
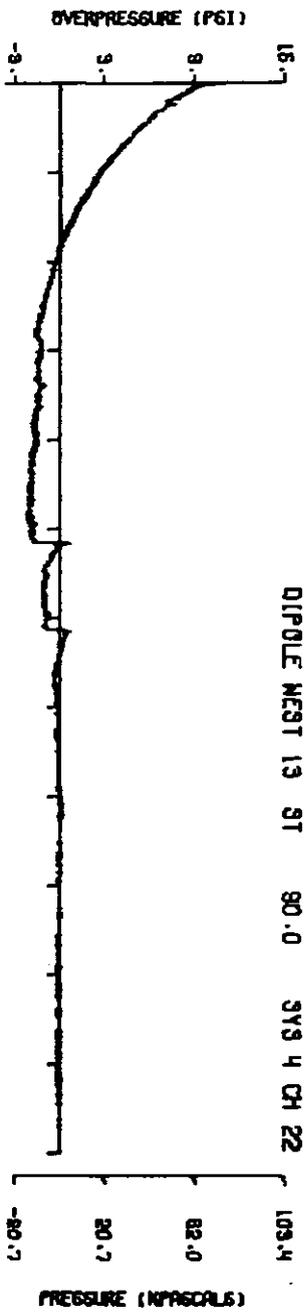
DIPOLE NEST 19 ST 60.307 SYS 2 CH 22



A13.36

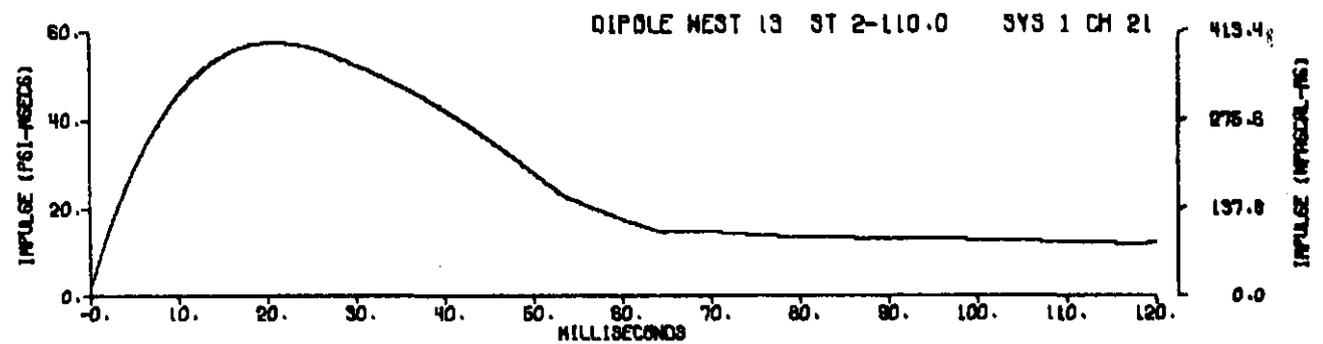
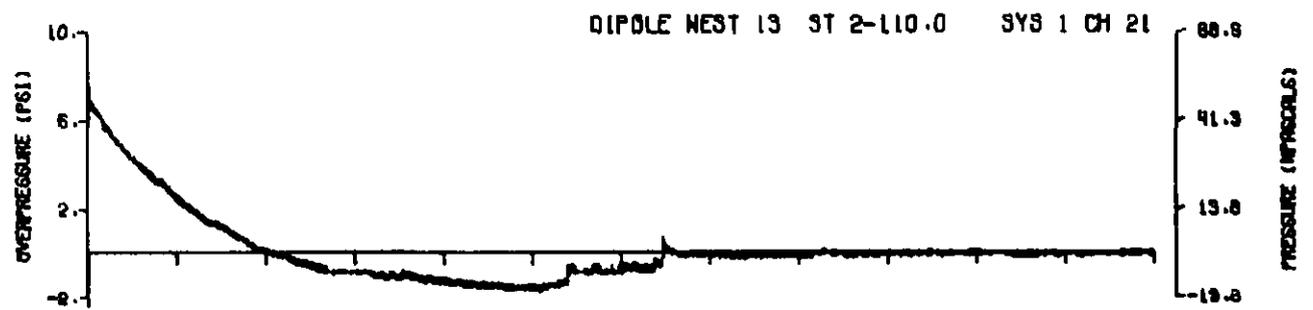
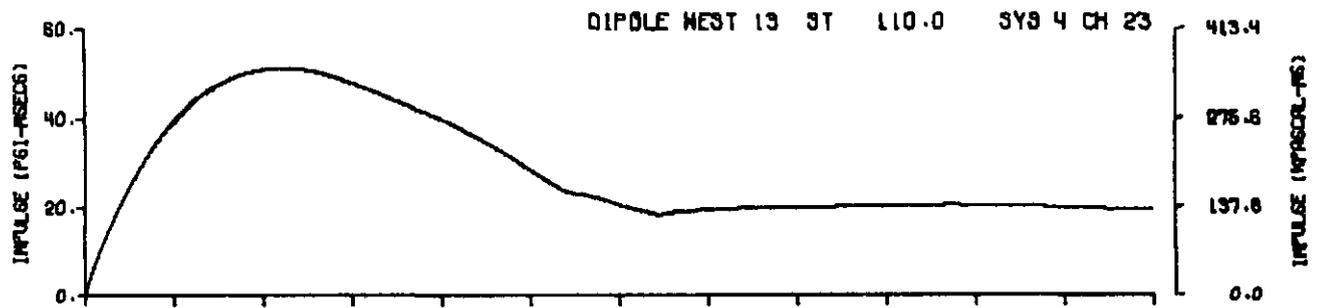
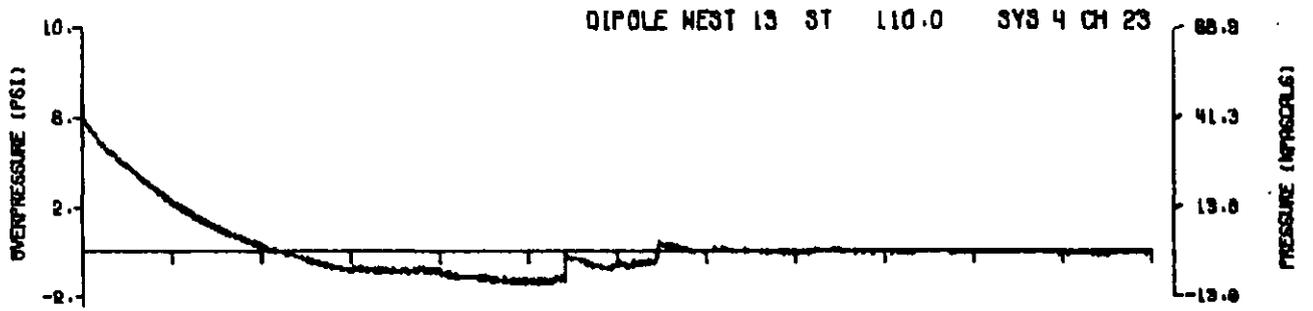


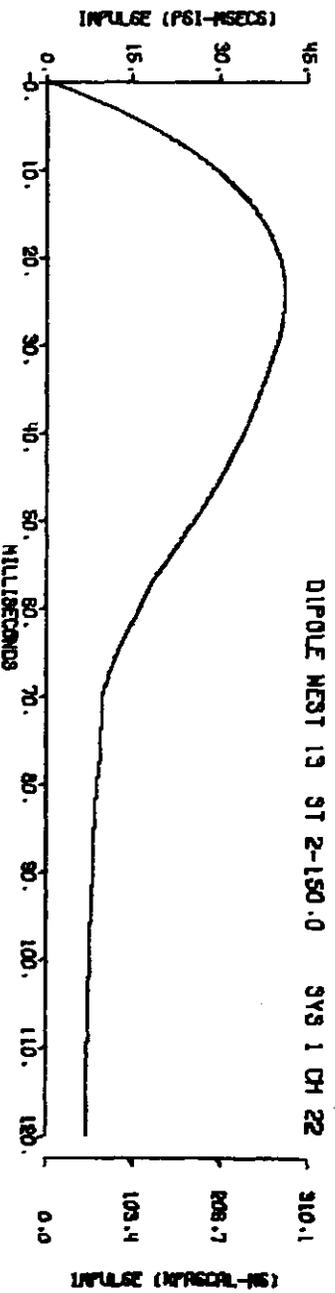
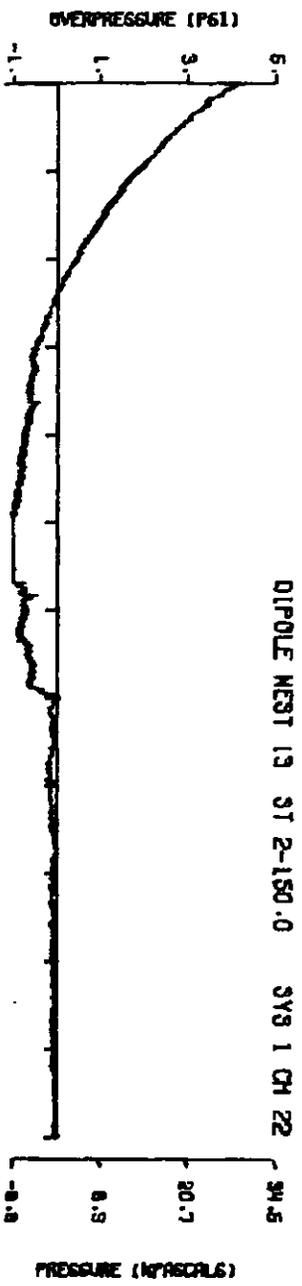
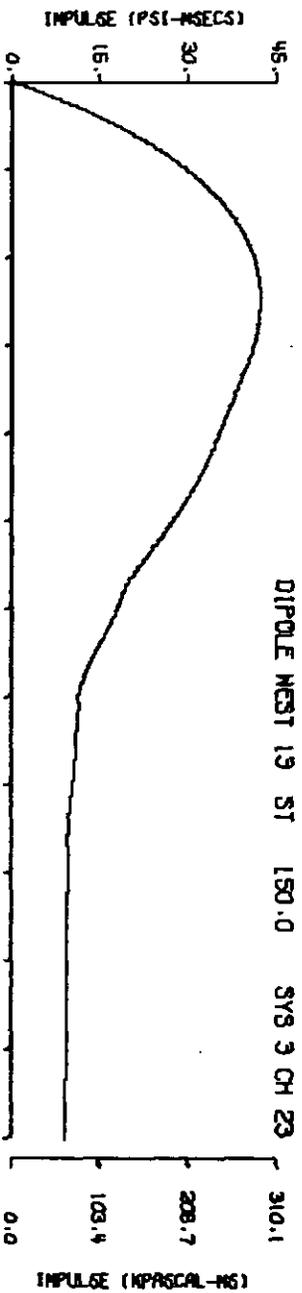
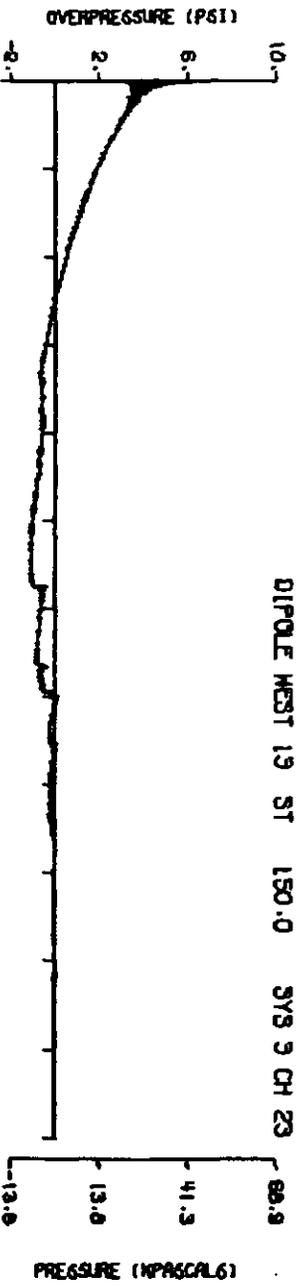
A13.37



A13.38

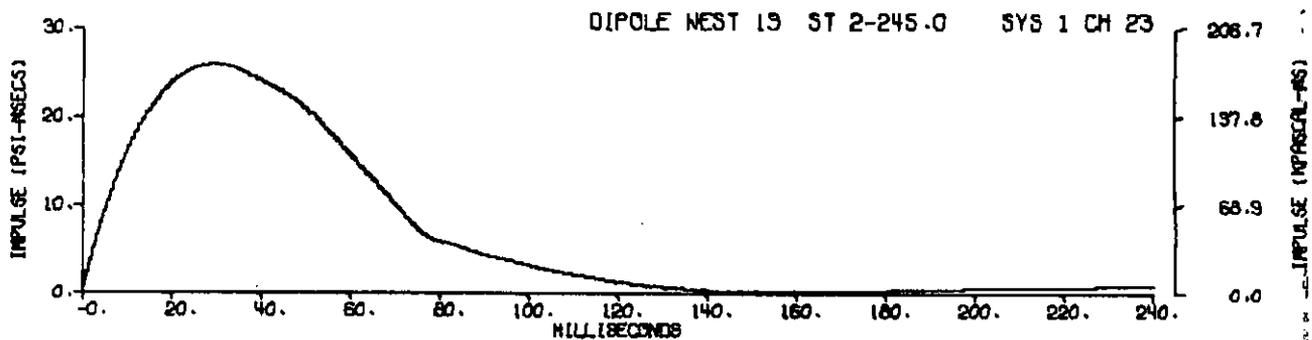
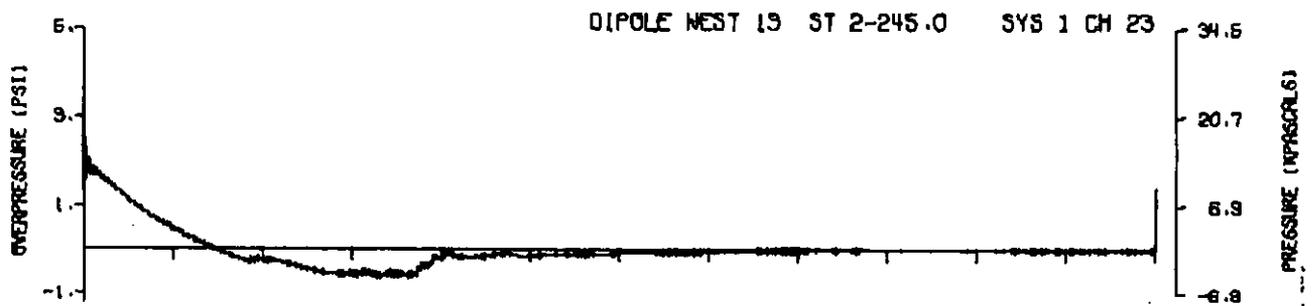
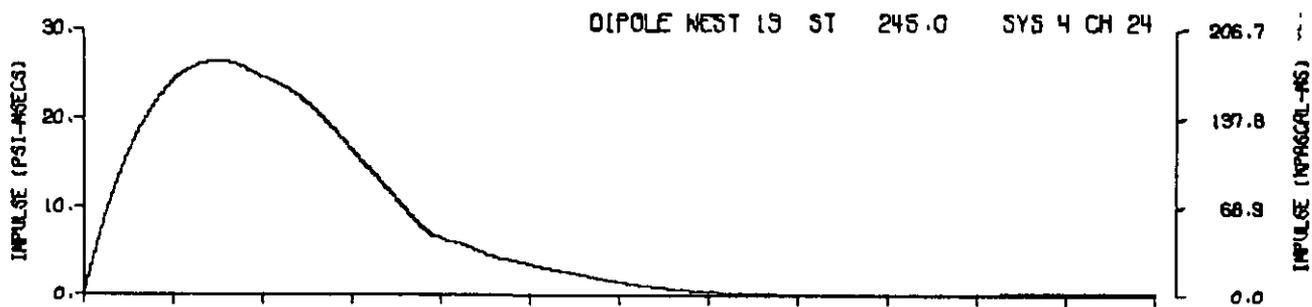
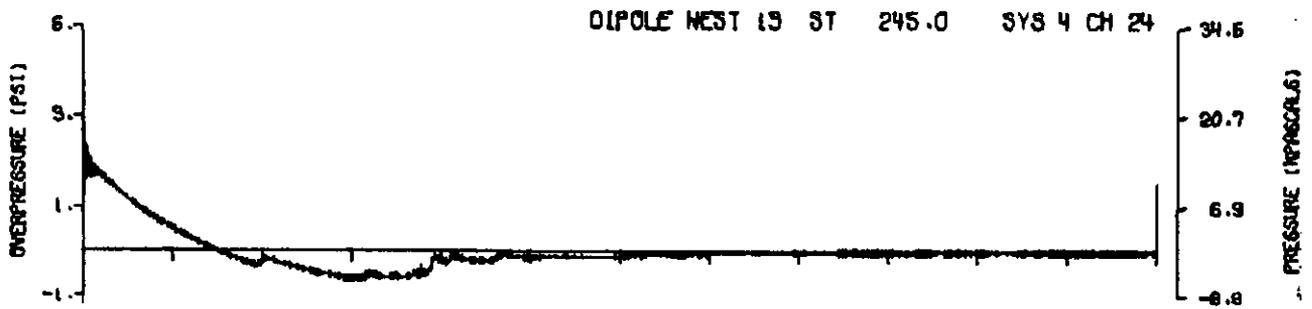
238



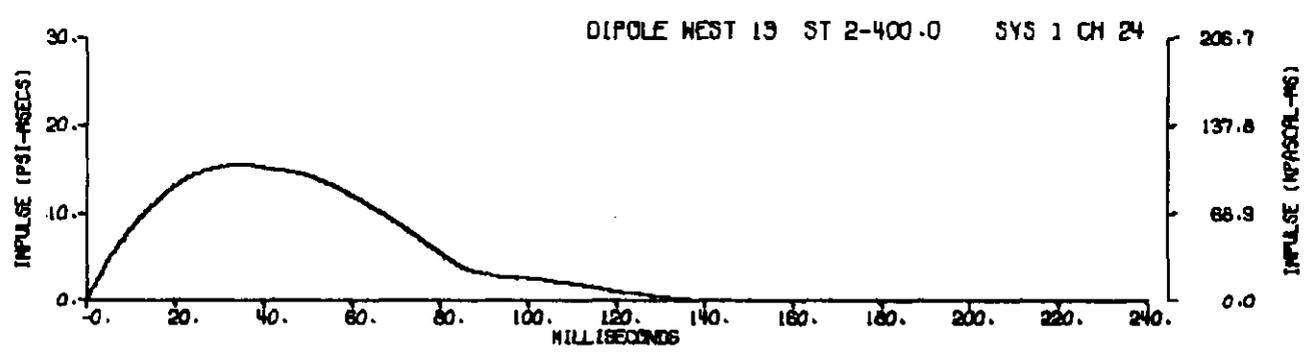
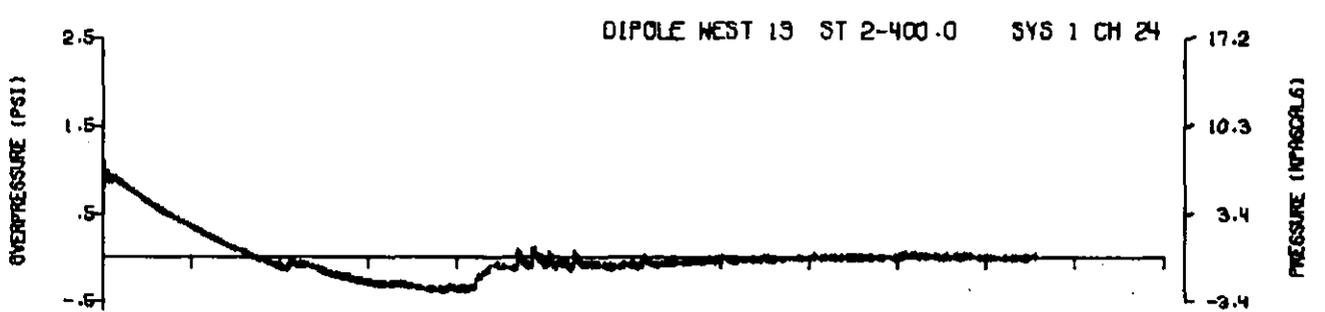
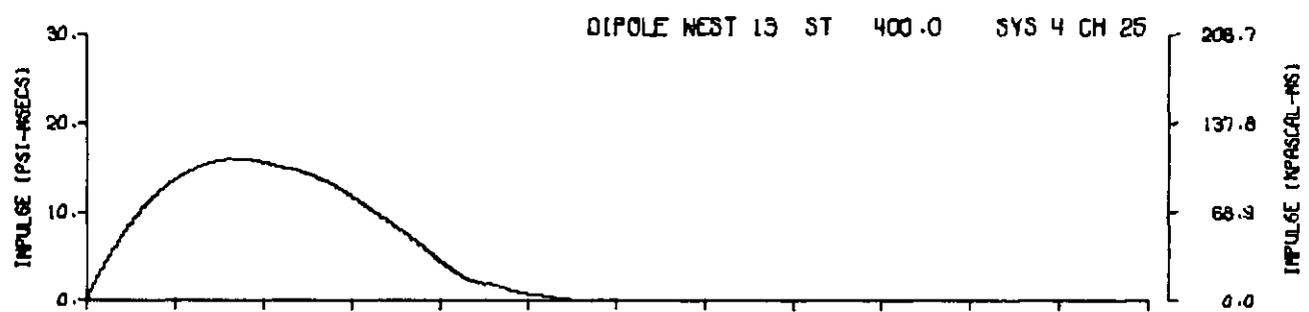
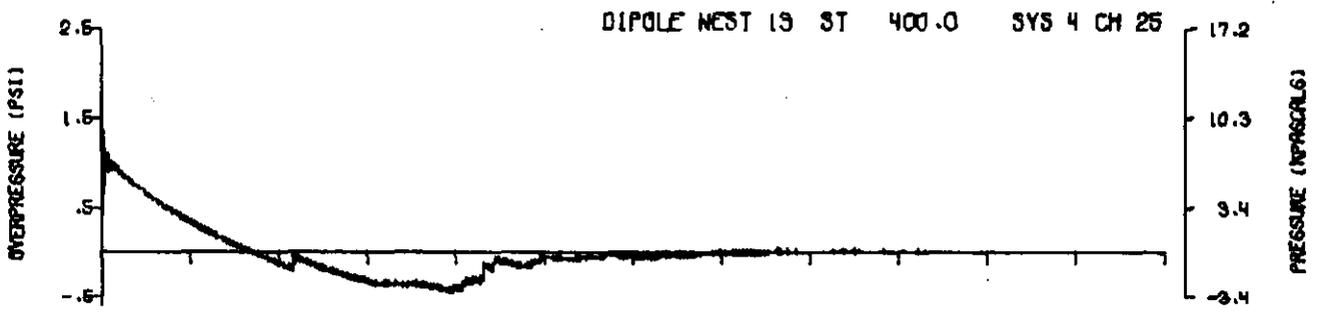


A13.40

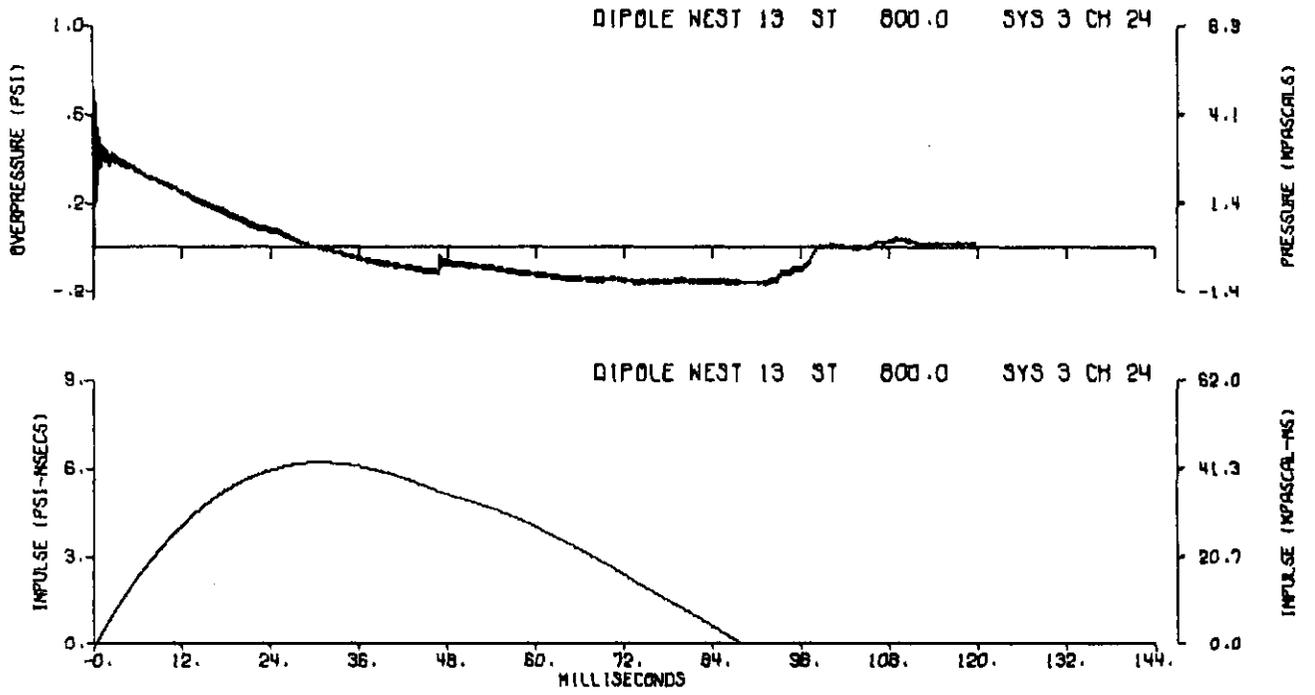
240



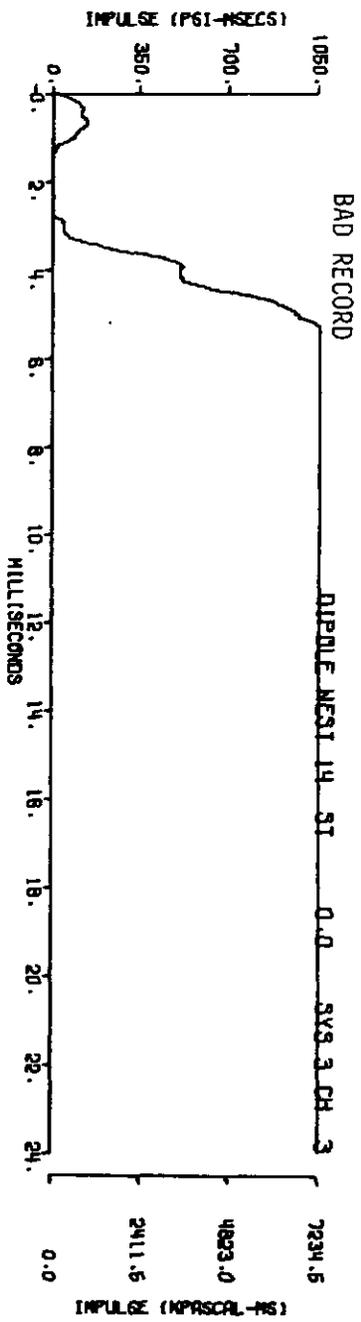
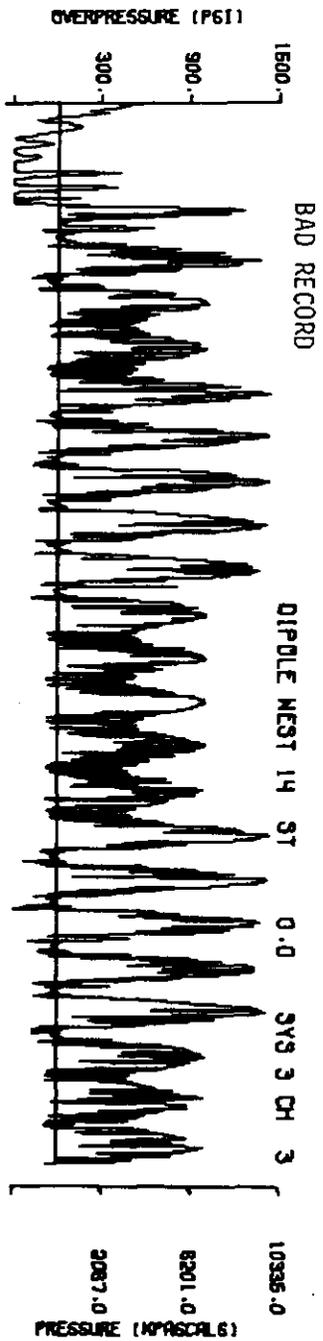
A13.41



A13.42

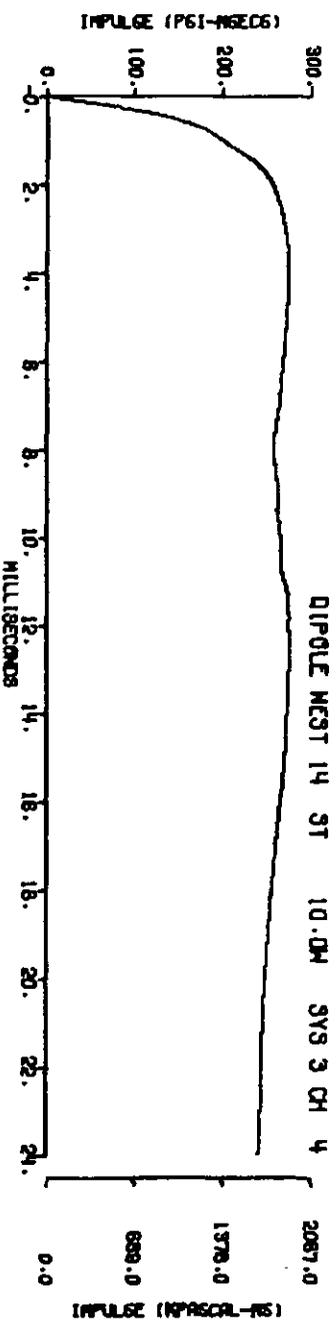
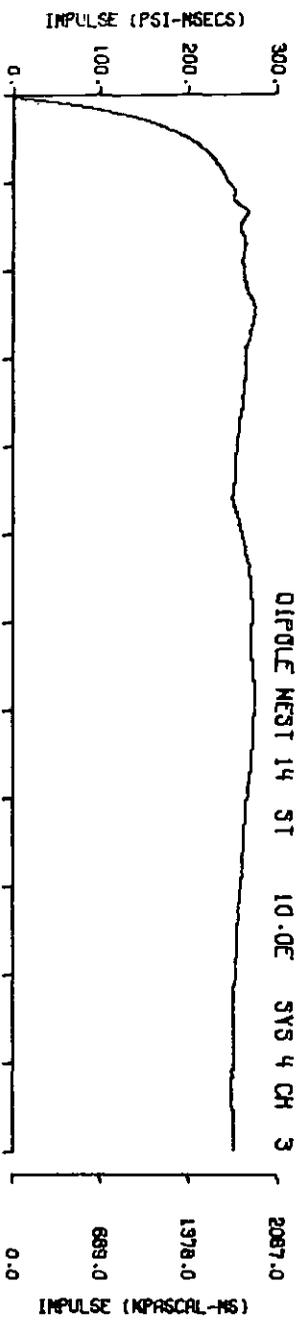
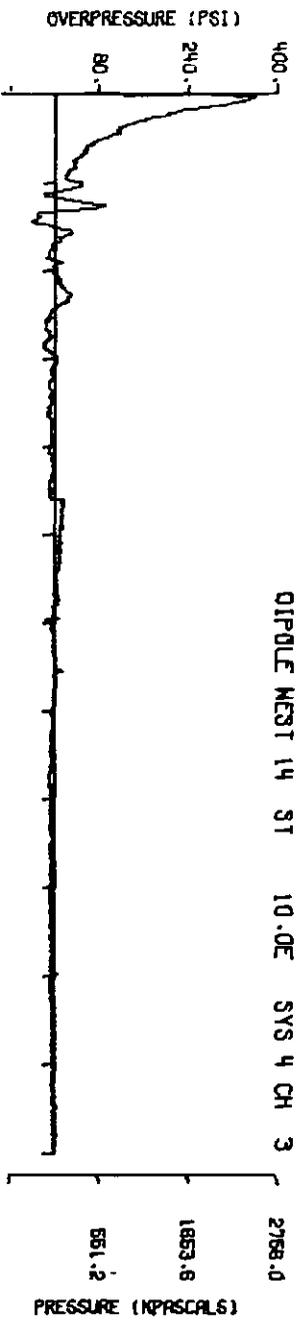


A13.43

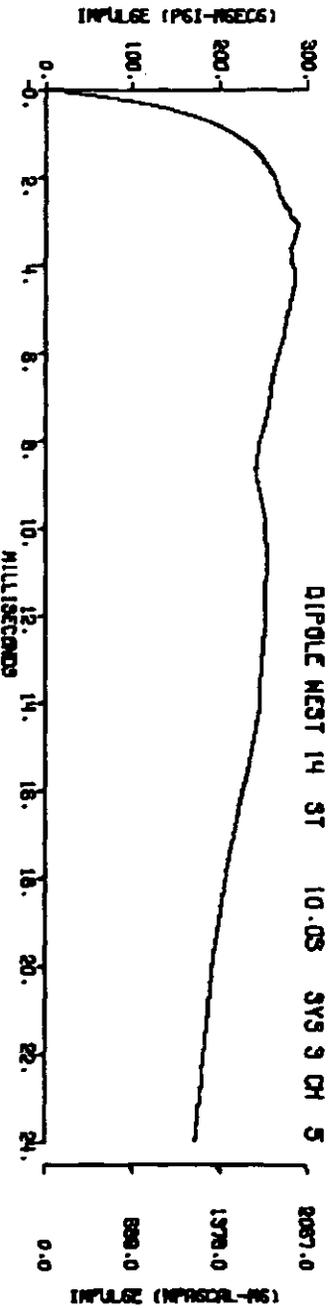
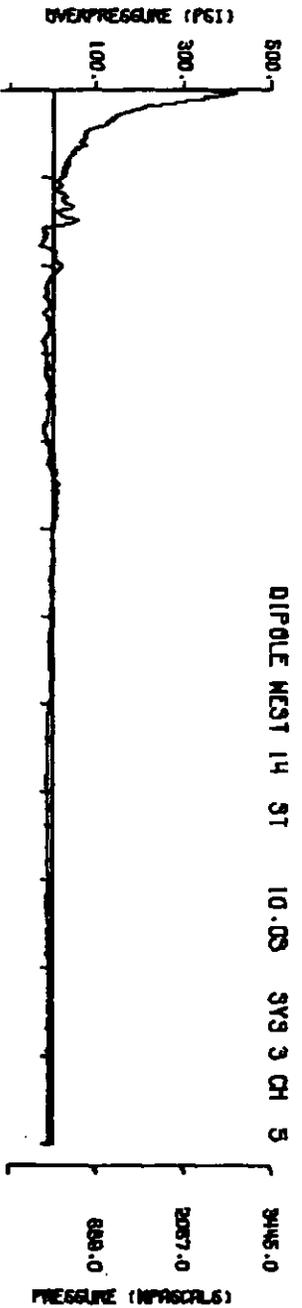
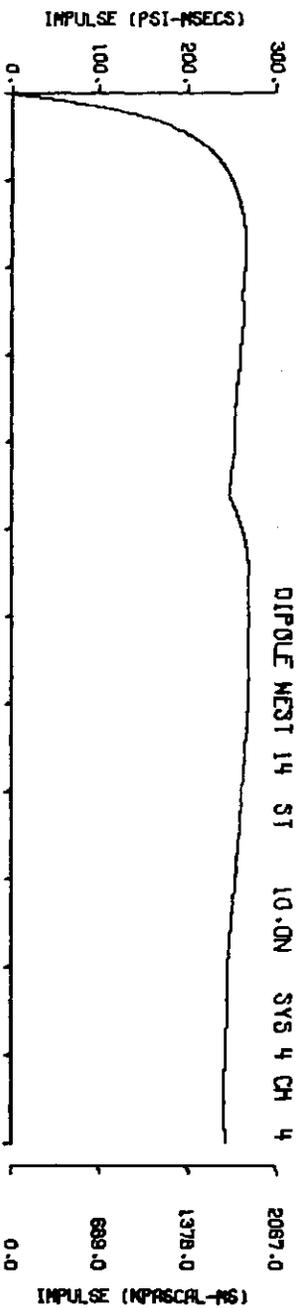
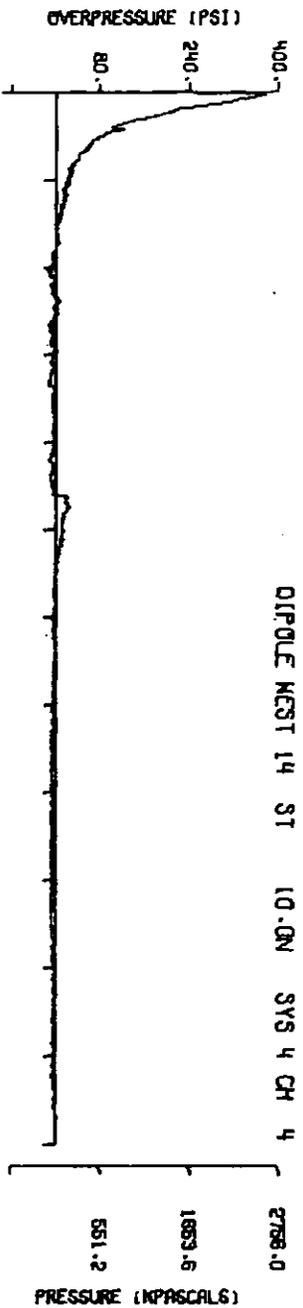


A14.1

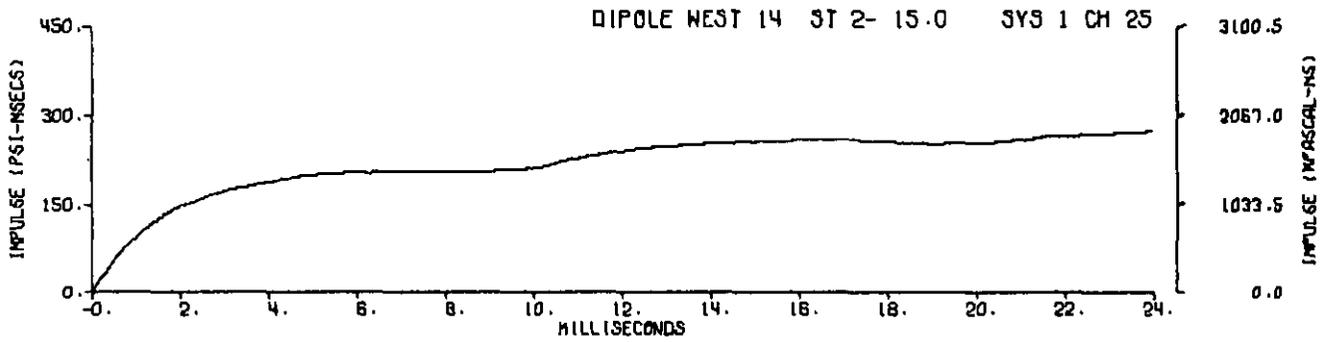
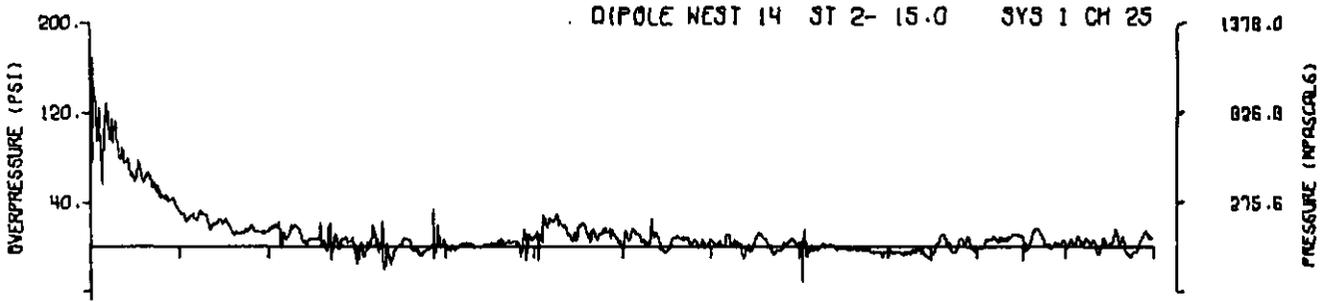
244



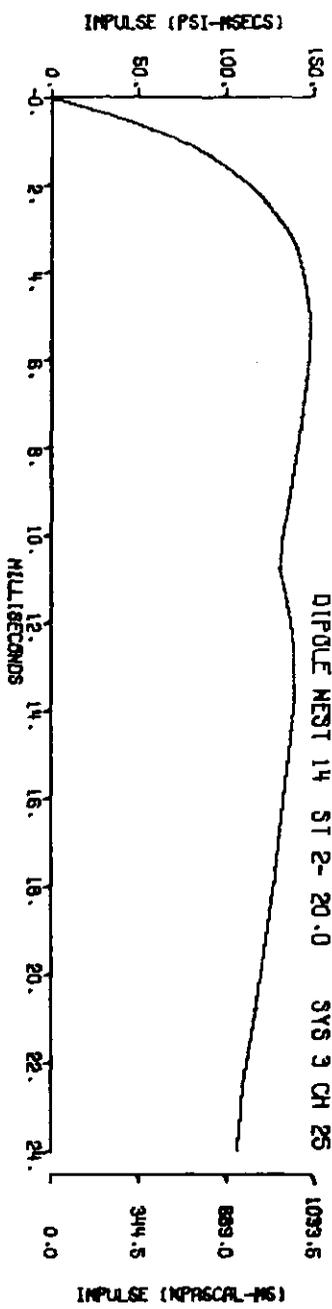
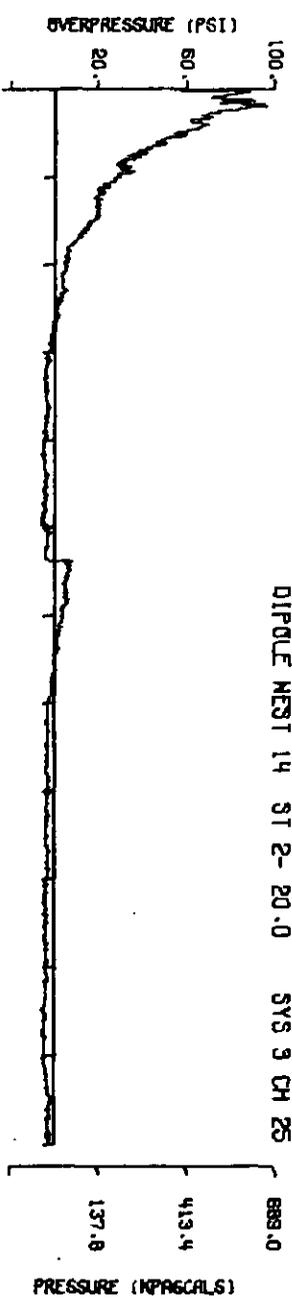
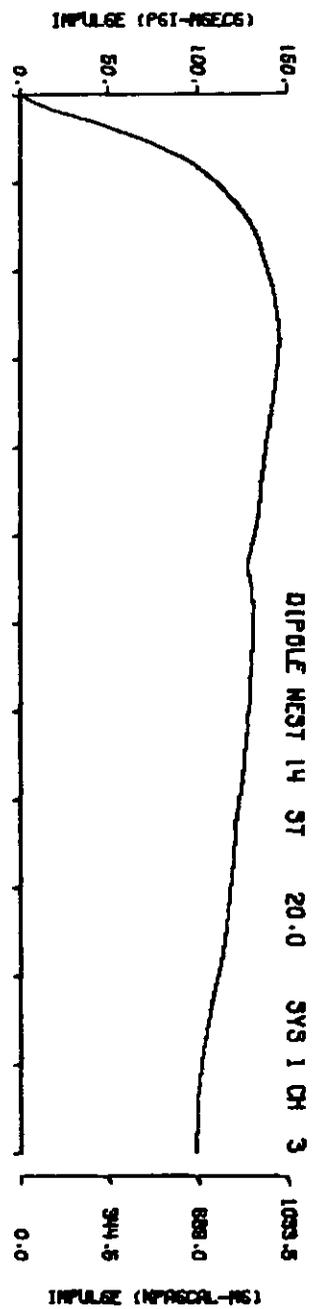
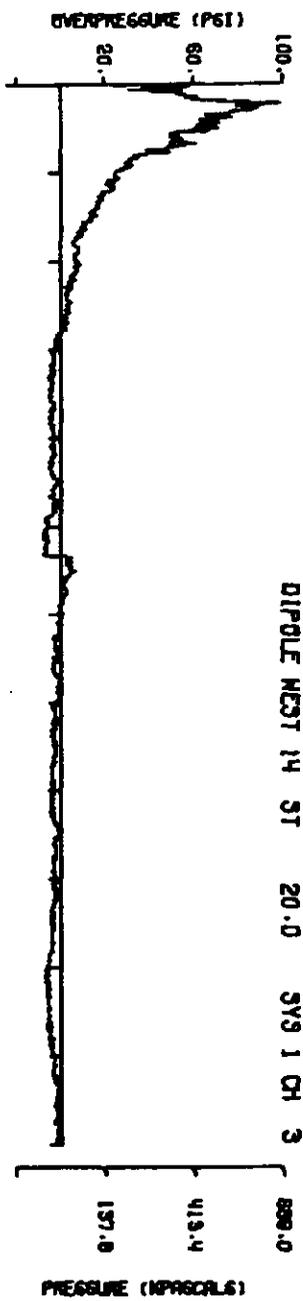
A14.2
245



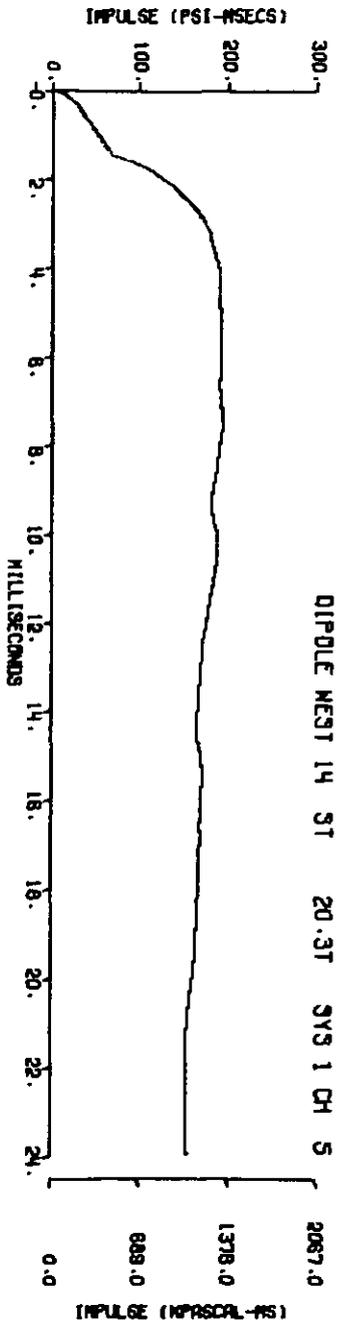
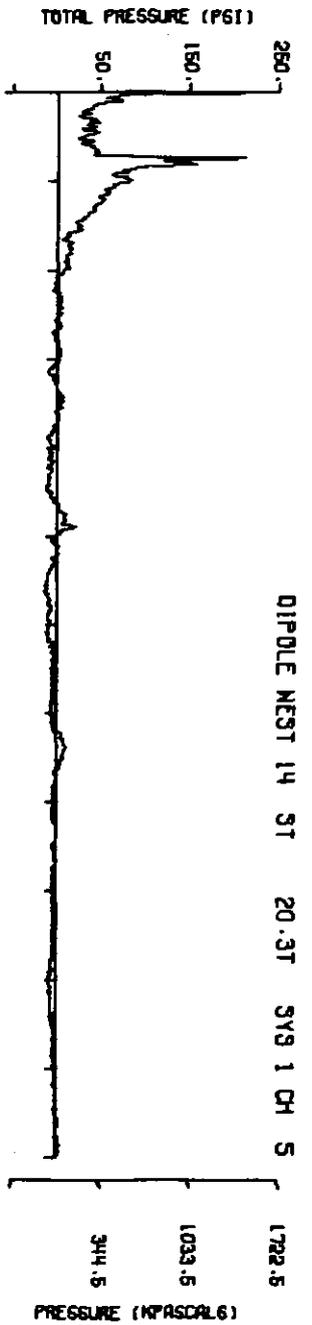
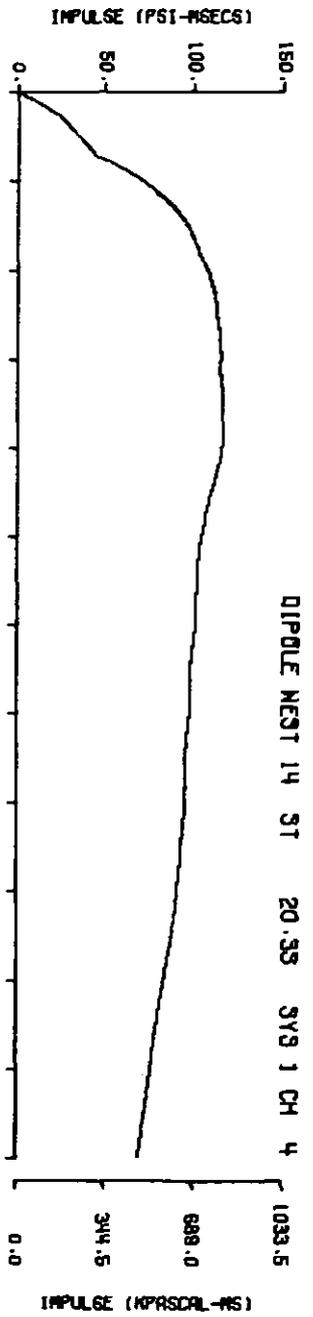
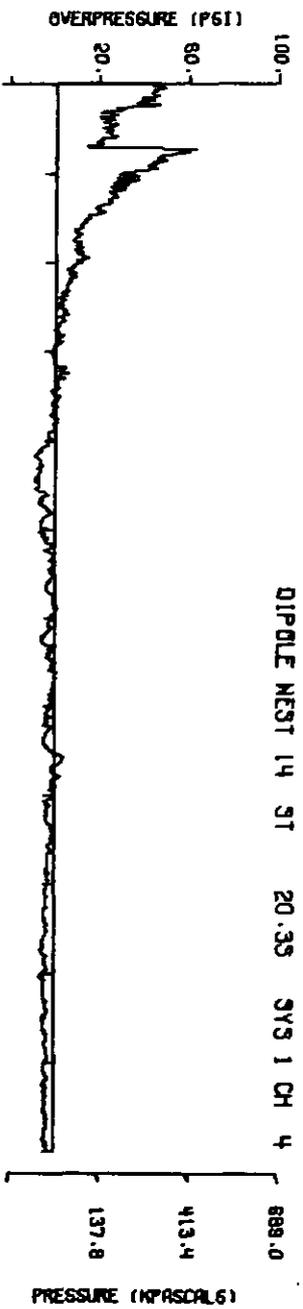
A14.3
246



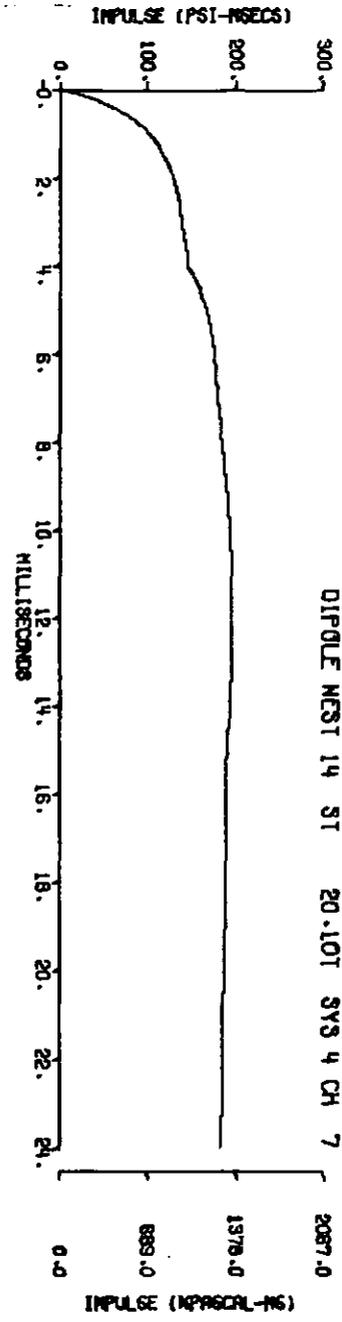
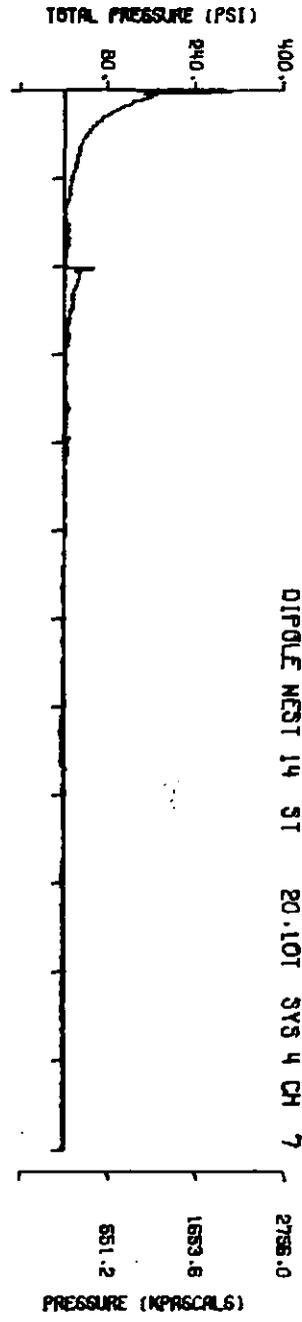
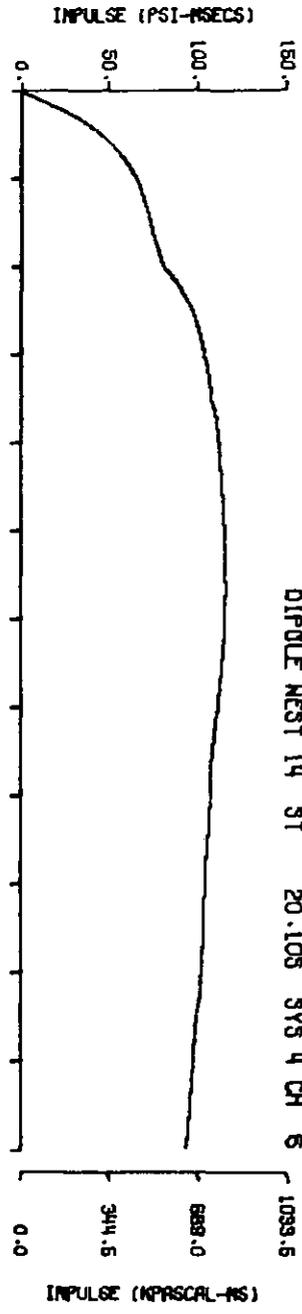
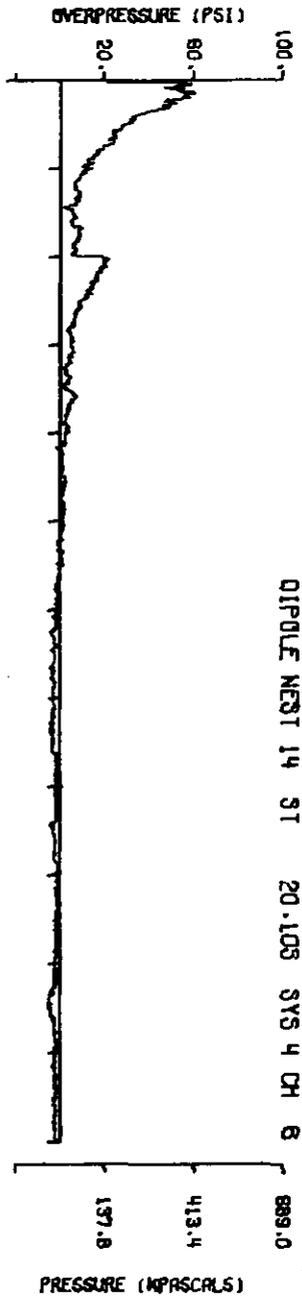
A14.4



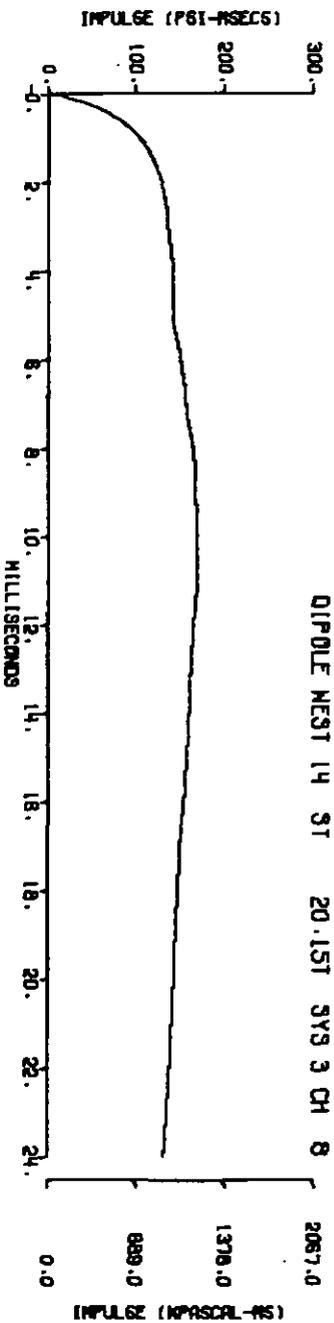
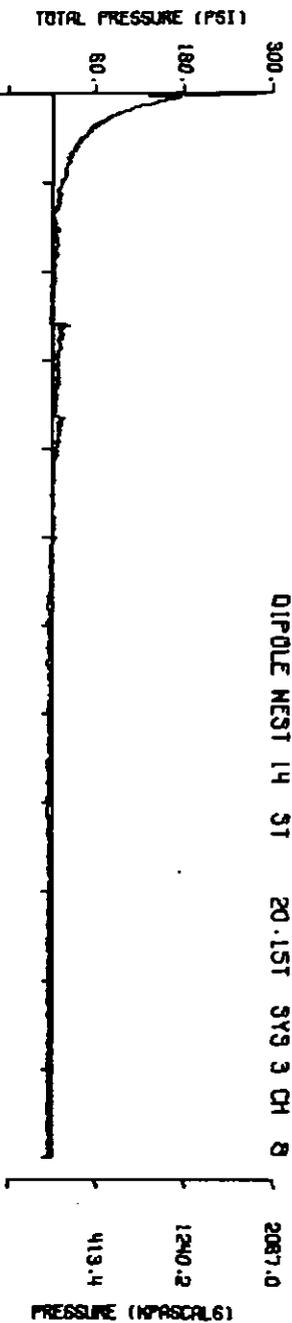
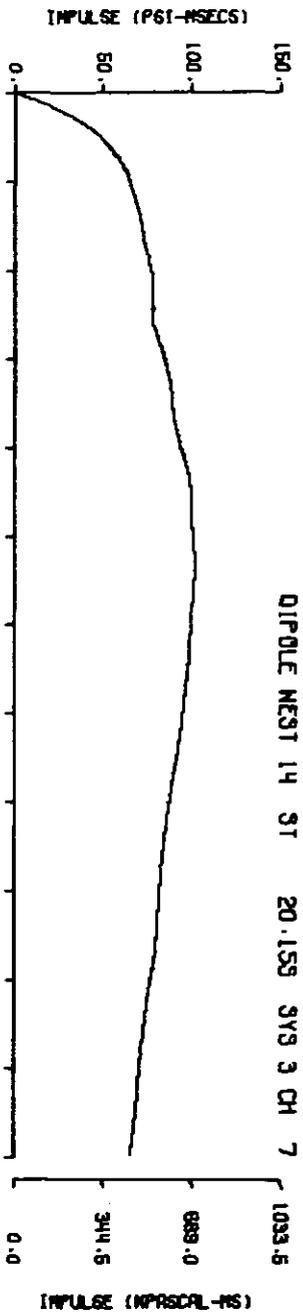
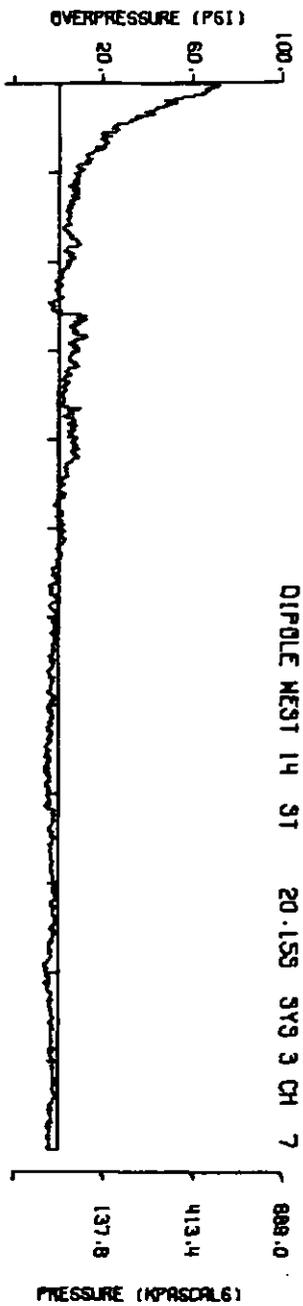
A14.5
248



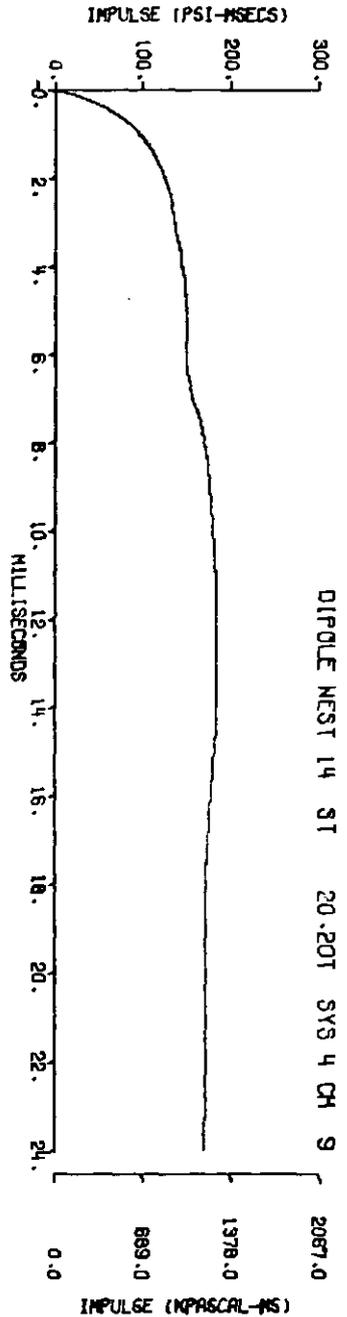
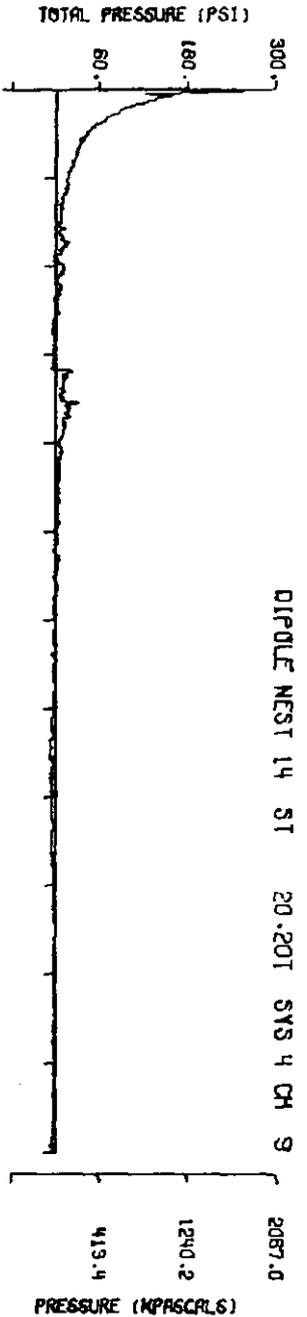
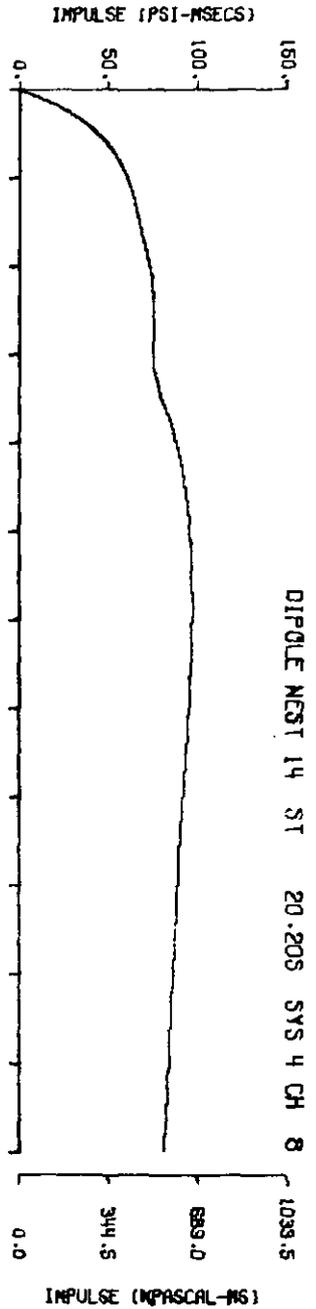
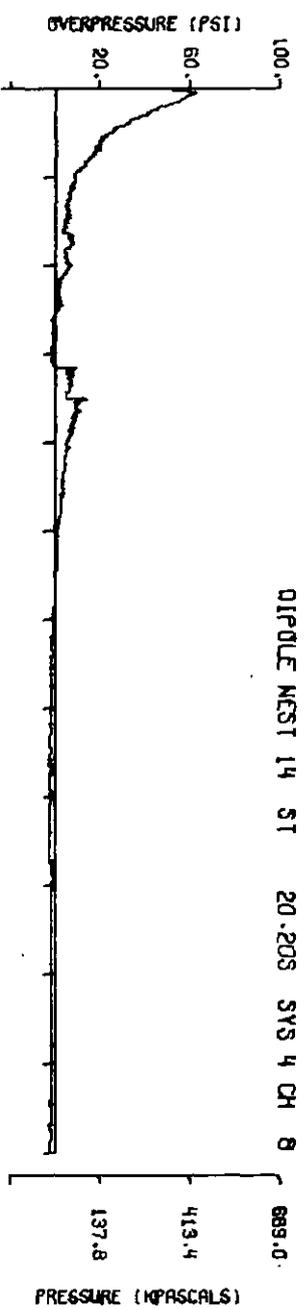
A14.6
249



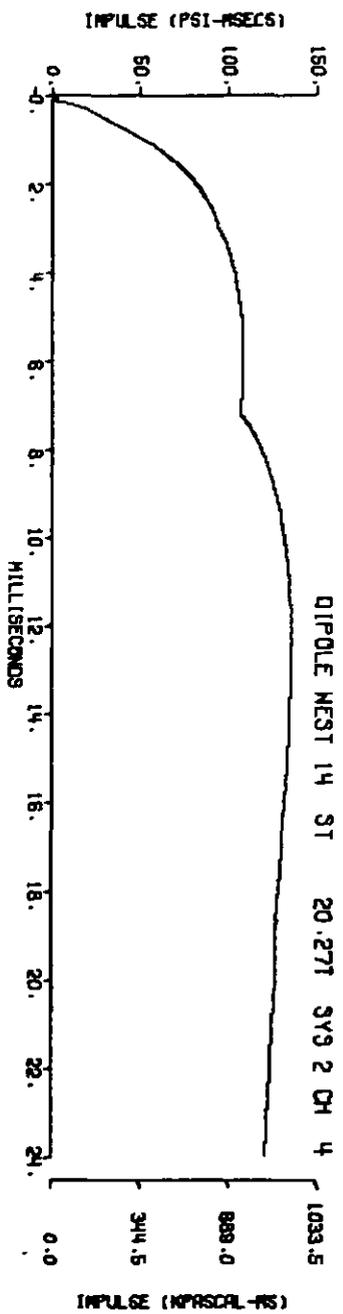
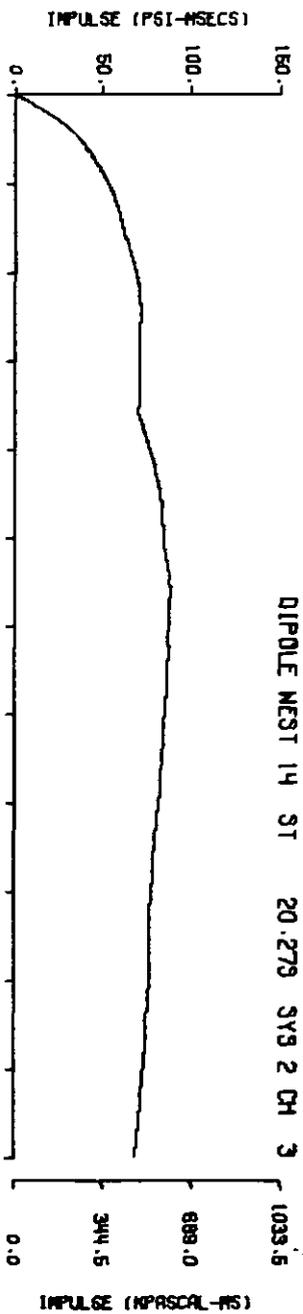
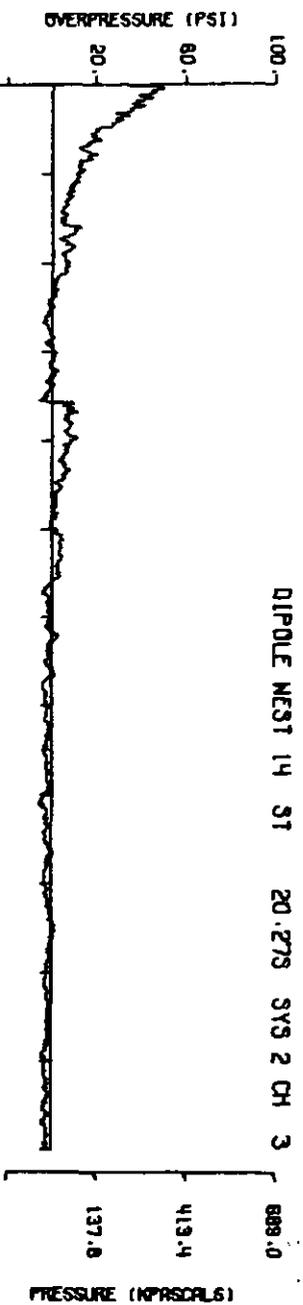
A14.7
250



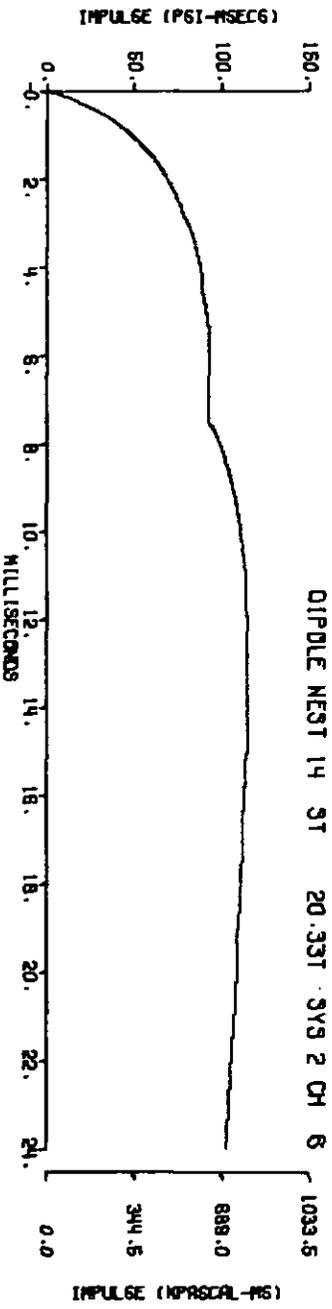
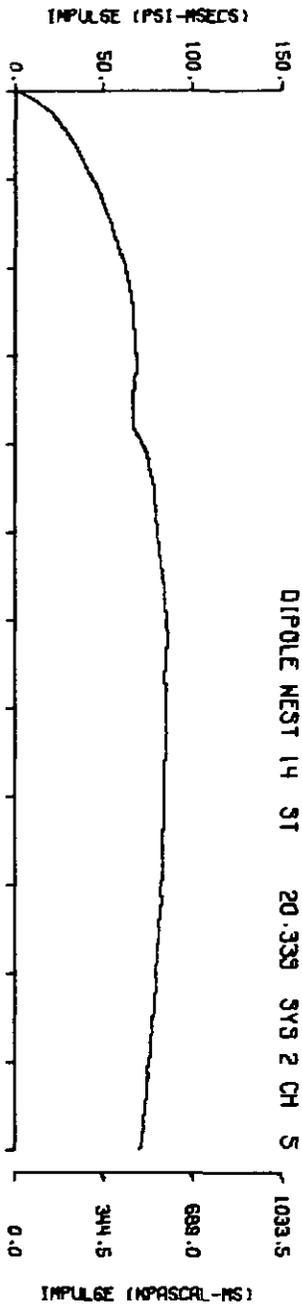
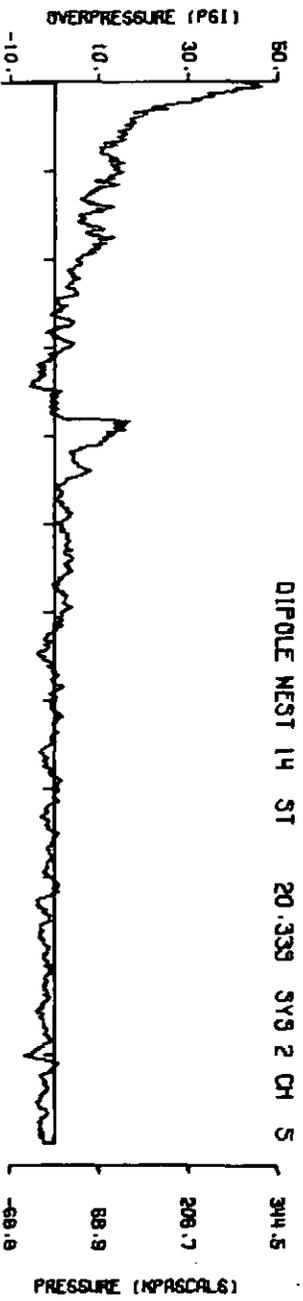
A14.8
251



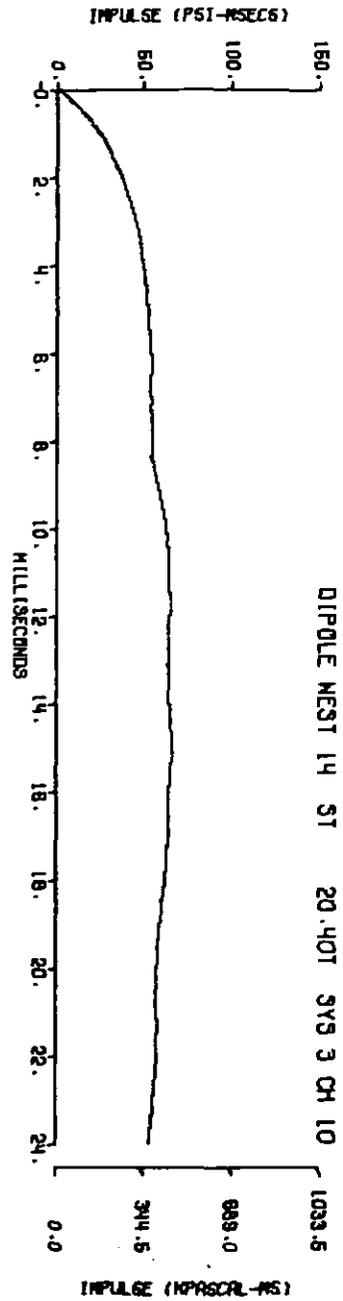
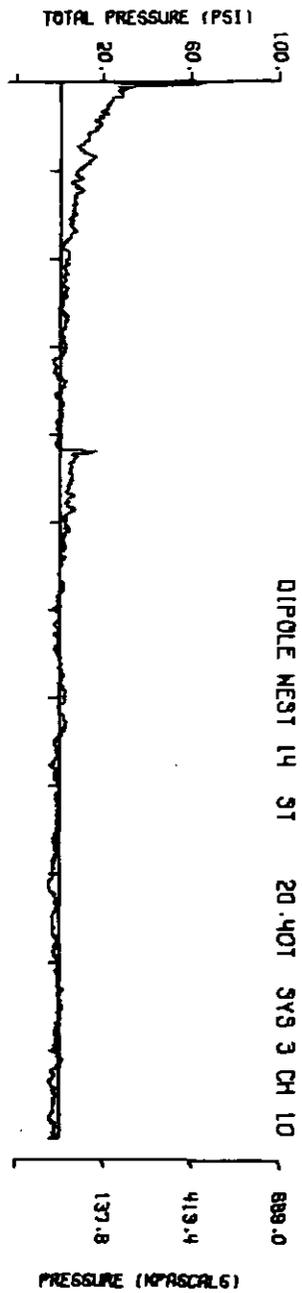
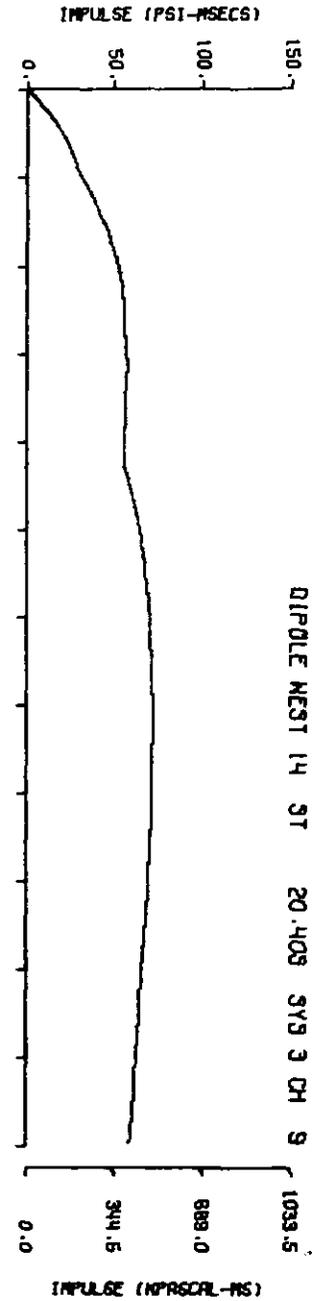
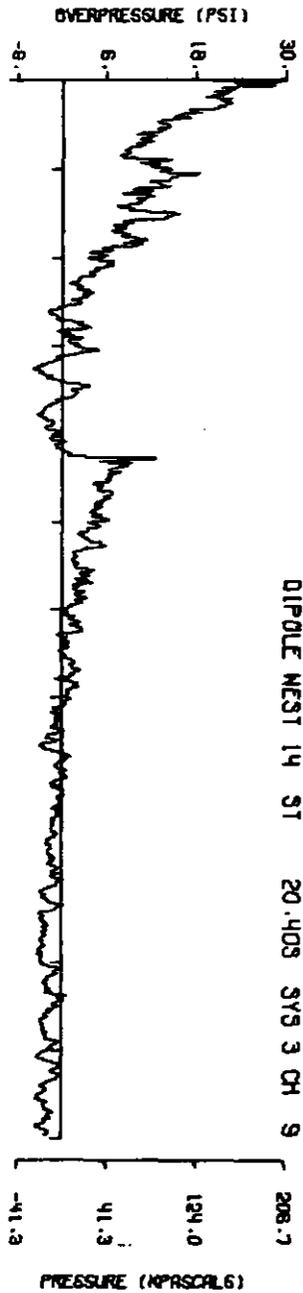
A14.9
252



A14.10

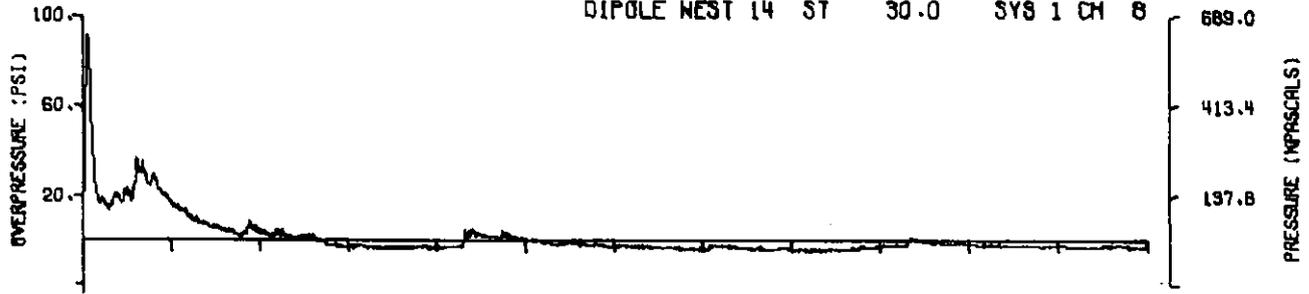


A14.11

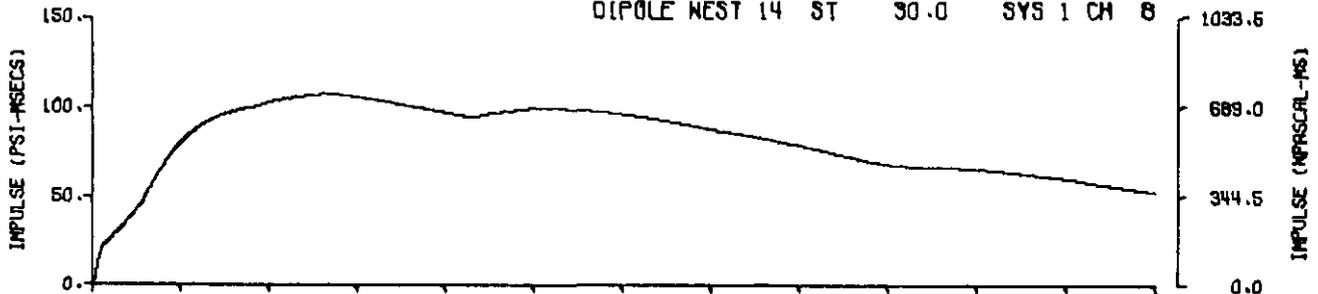


A14.12

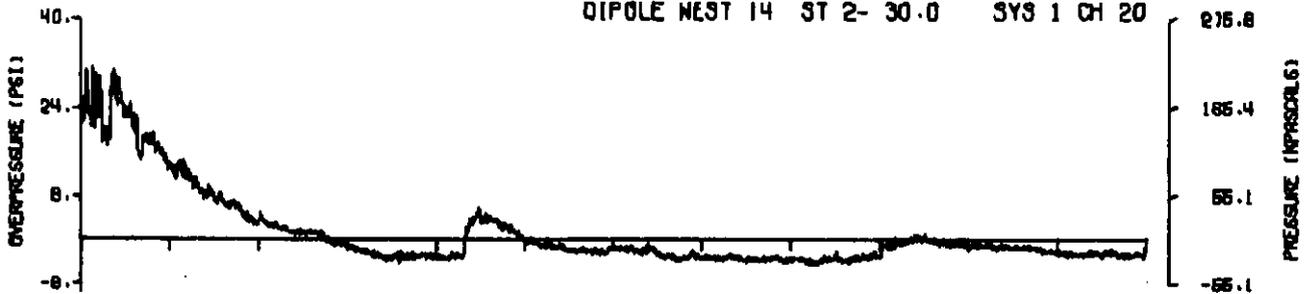
DIPOLE NEST 14 ST 30.0 SYS 1 CH 8



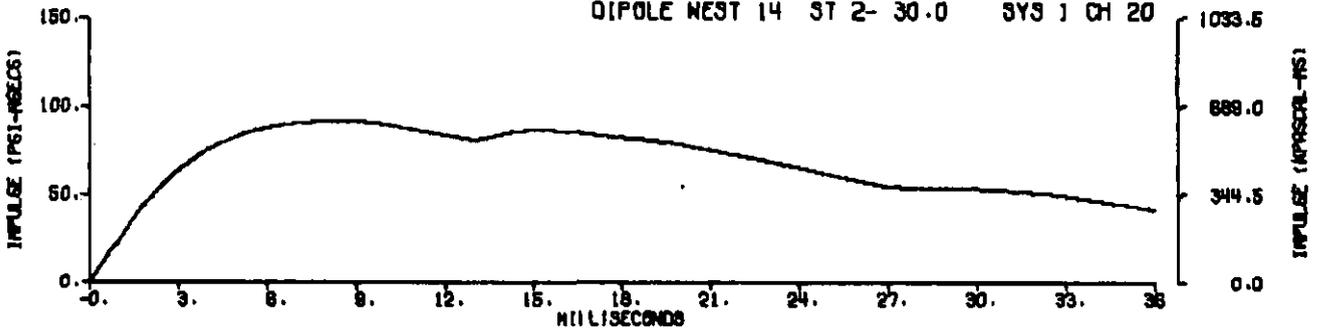
DIPOLE NEST 14 ST 30.0 SYS 1 CH 8



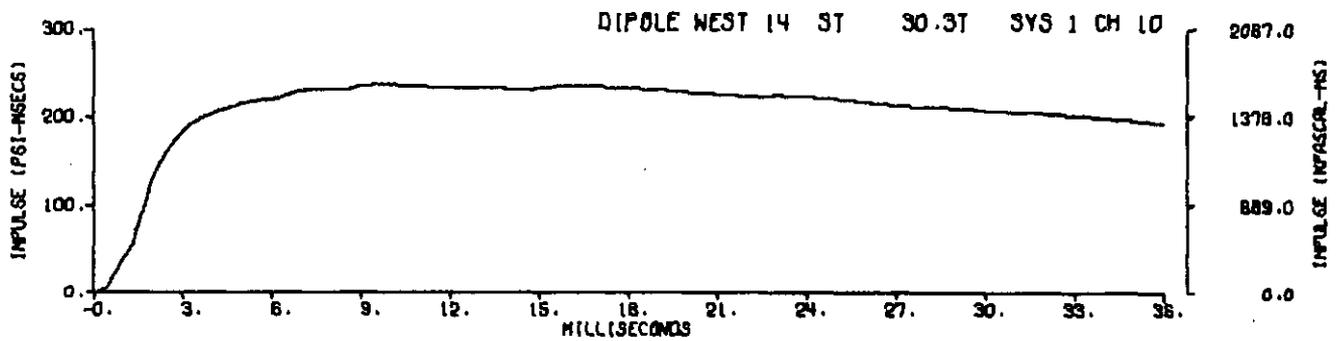
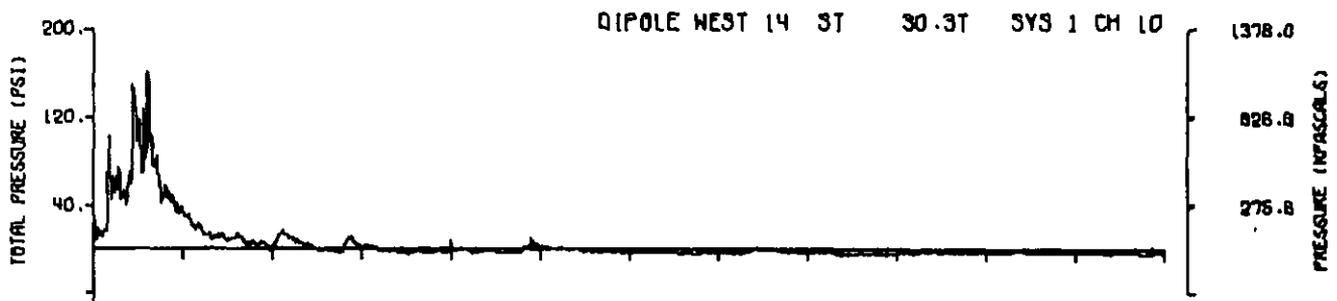
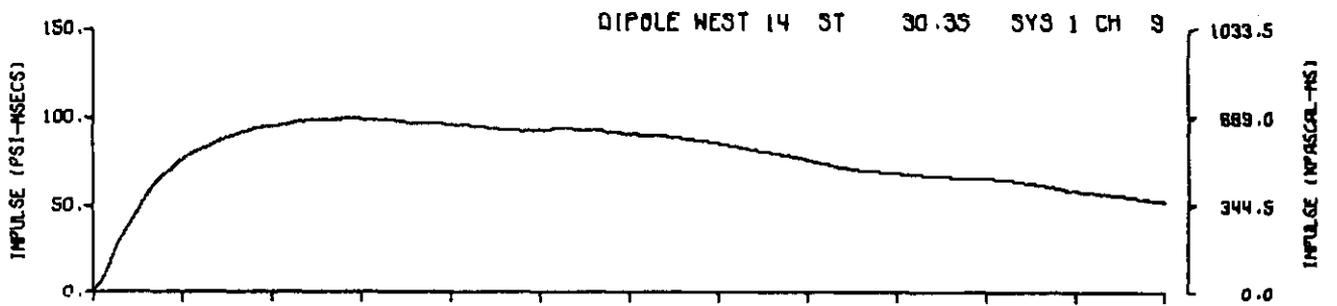
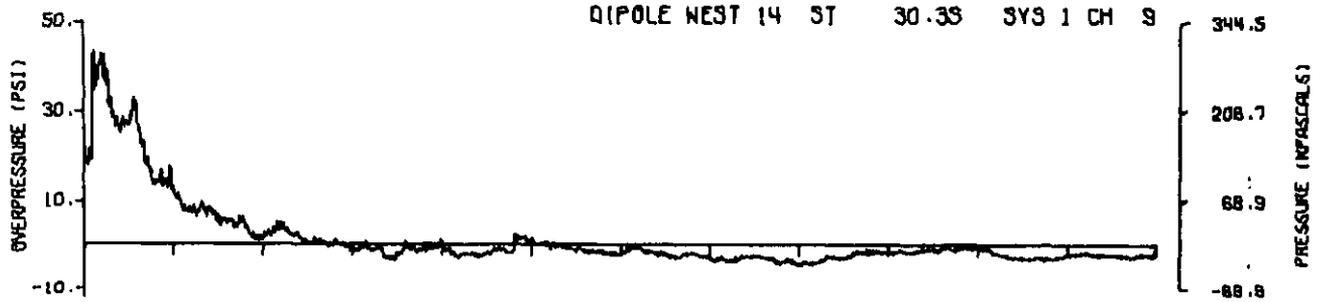
DIPOLE NEST 14 ST 2- 30.0 SYS 1 CH 20



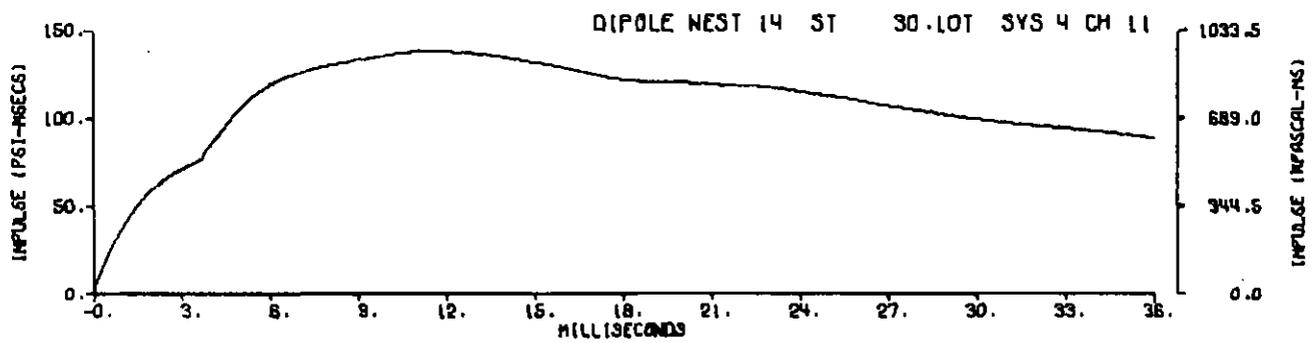
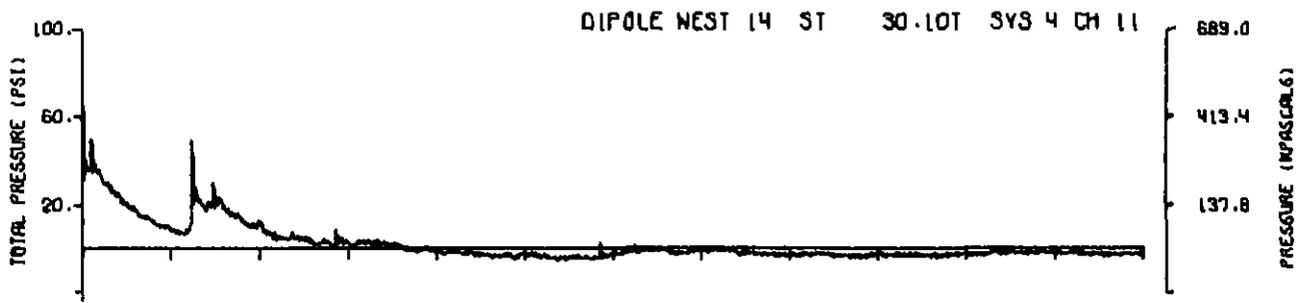
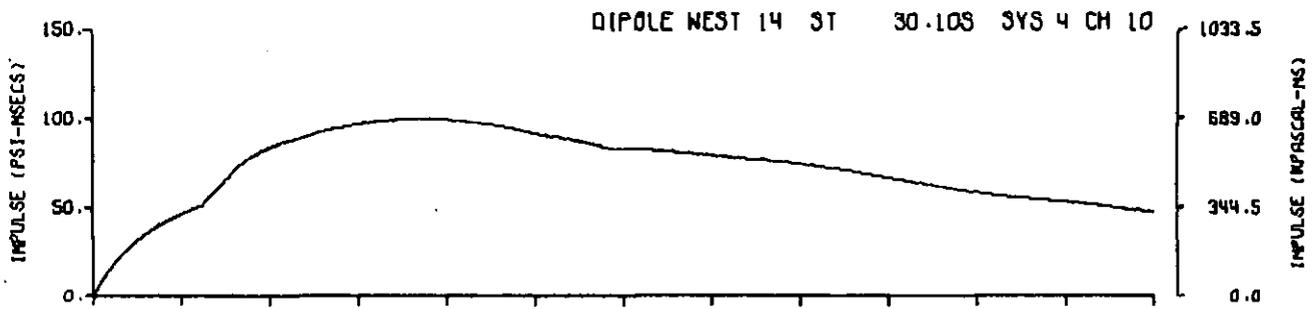
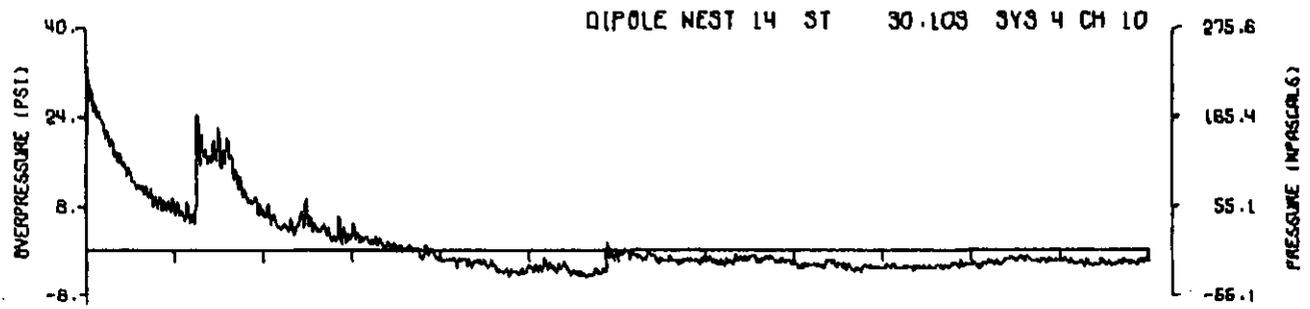
DIPOLE NEST 14 ST 2- 30.0 SYS 1 CH 20



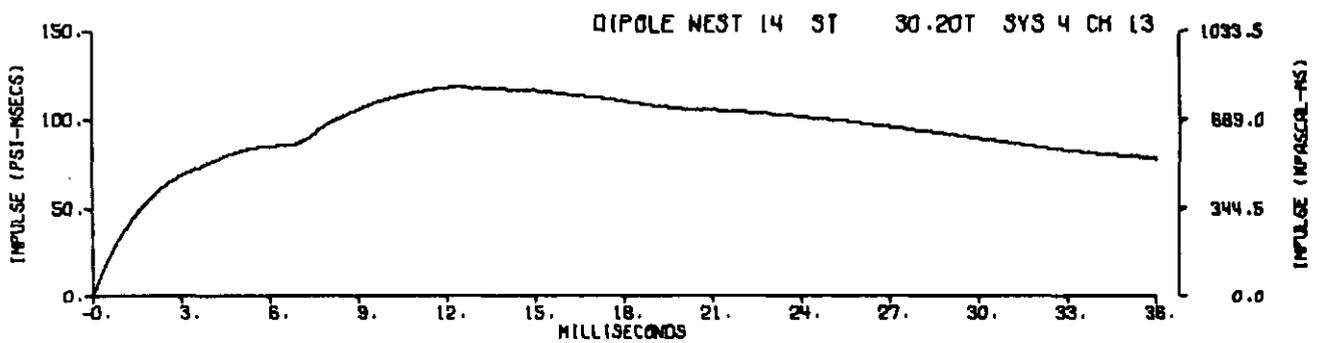
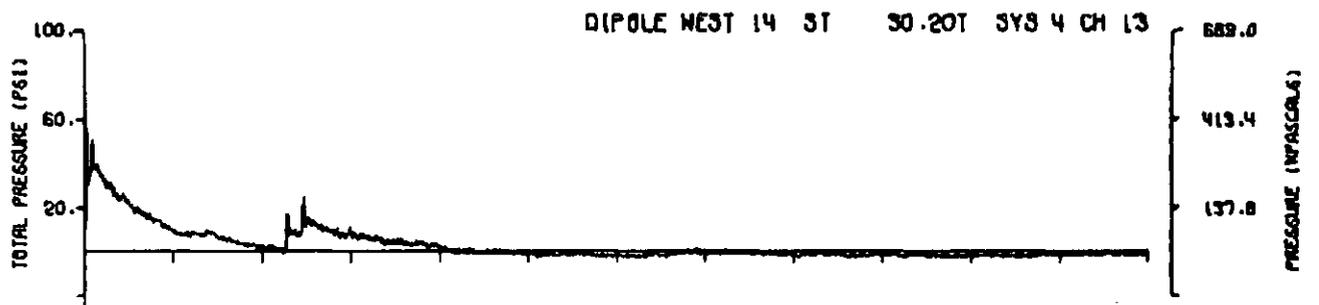
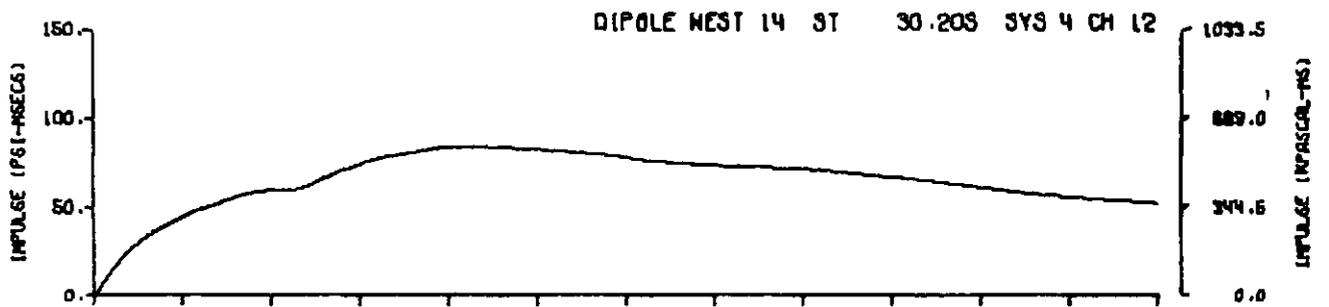
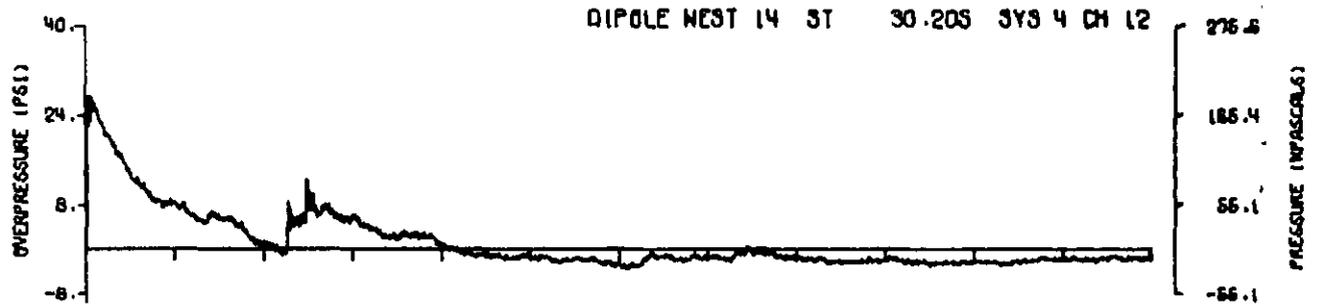
A14.13



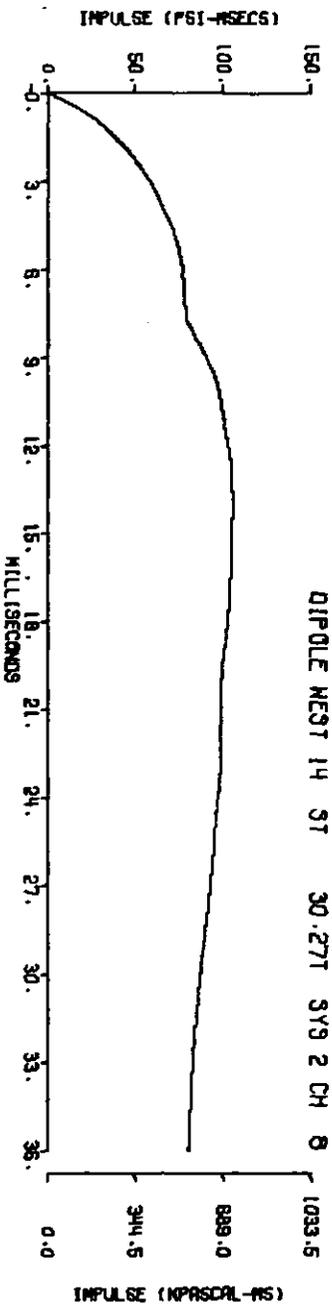
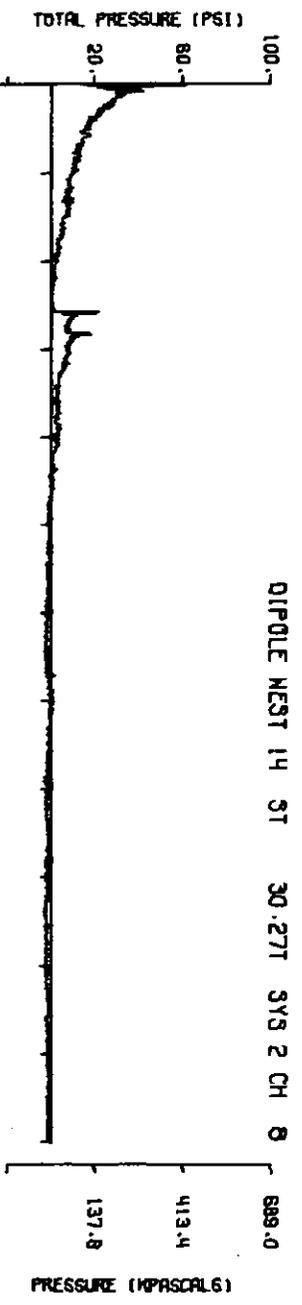
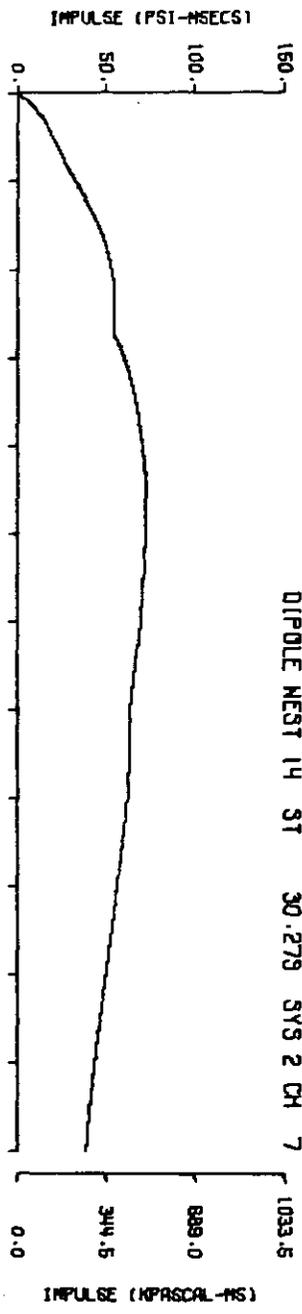
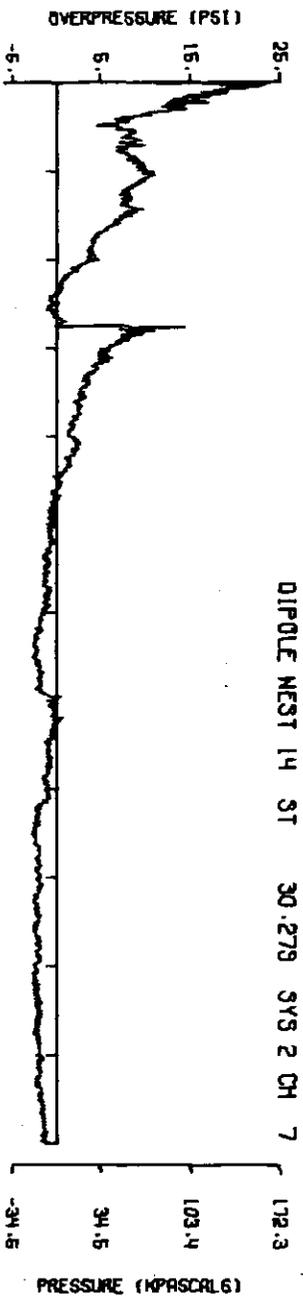
A14.14



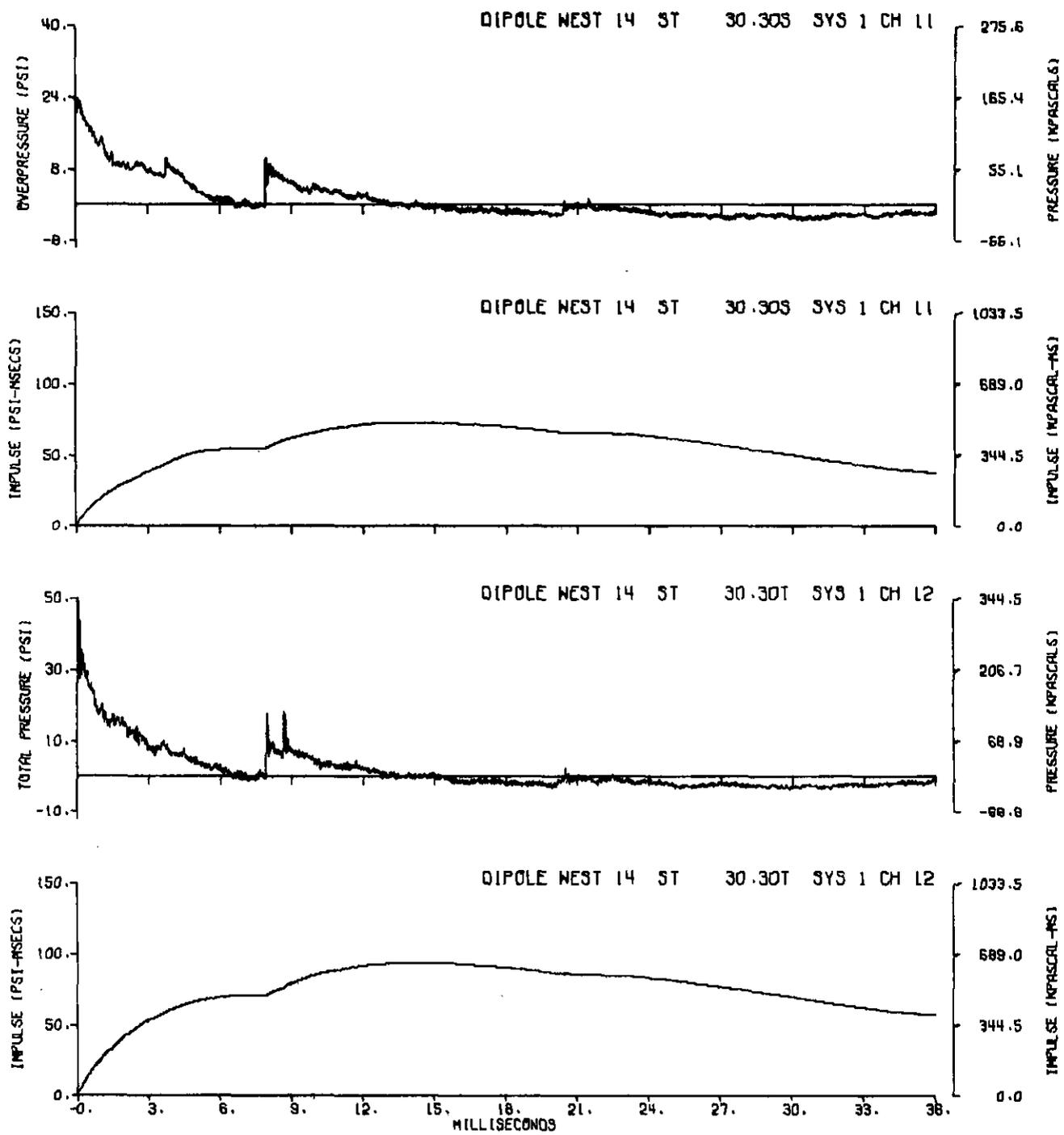
A14.15



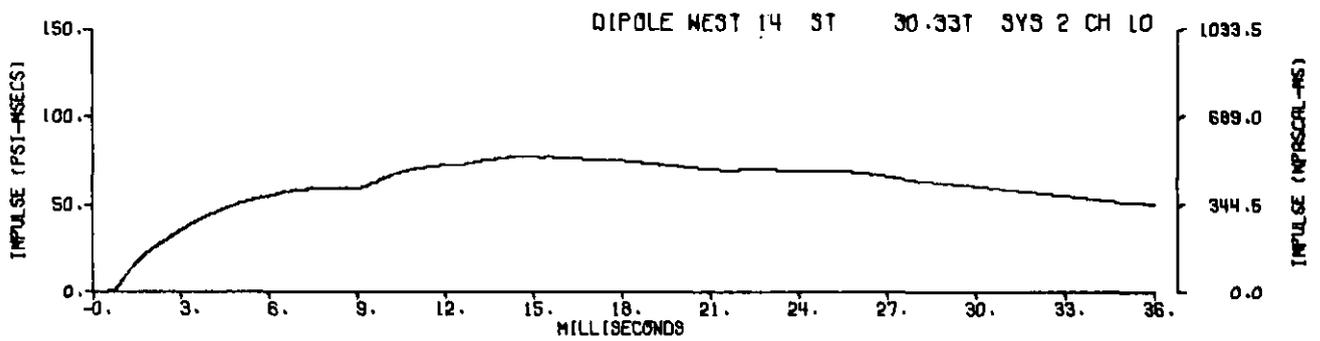
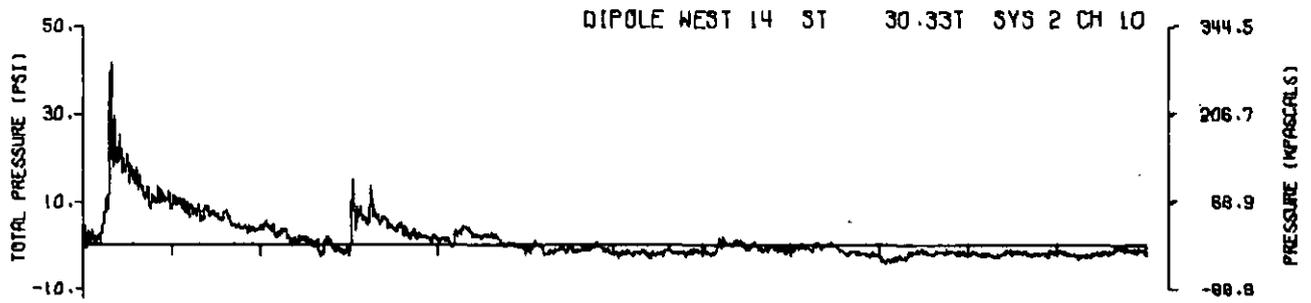
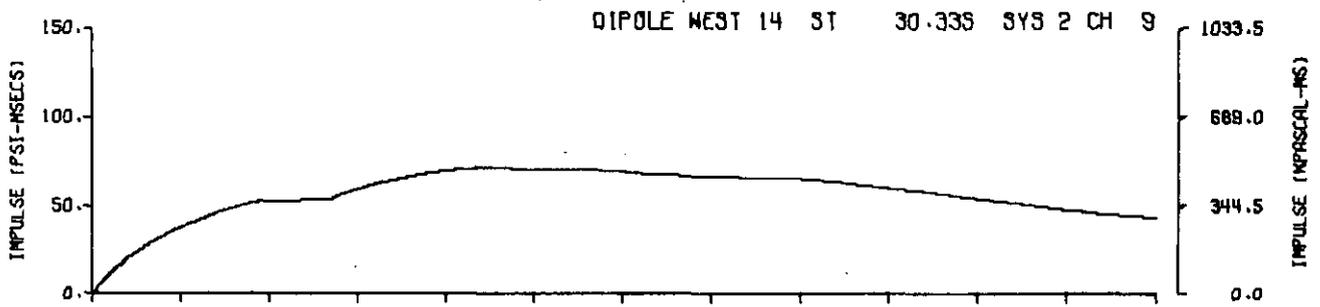
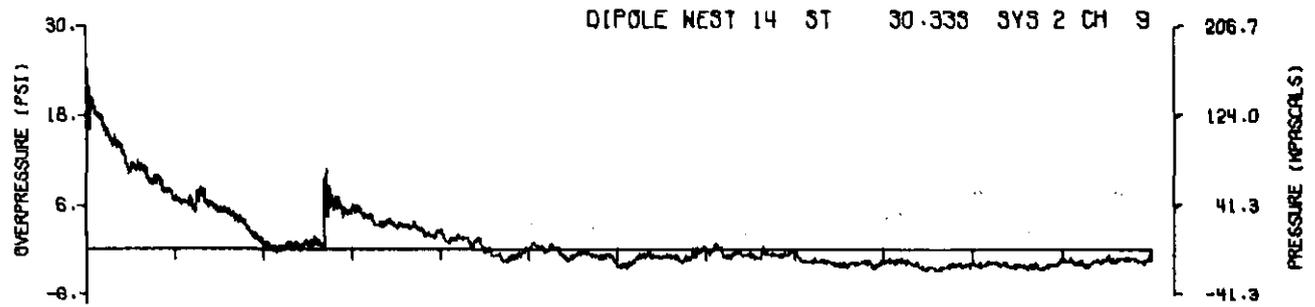
A14.16



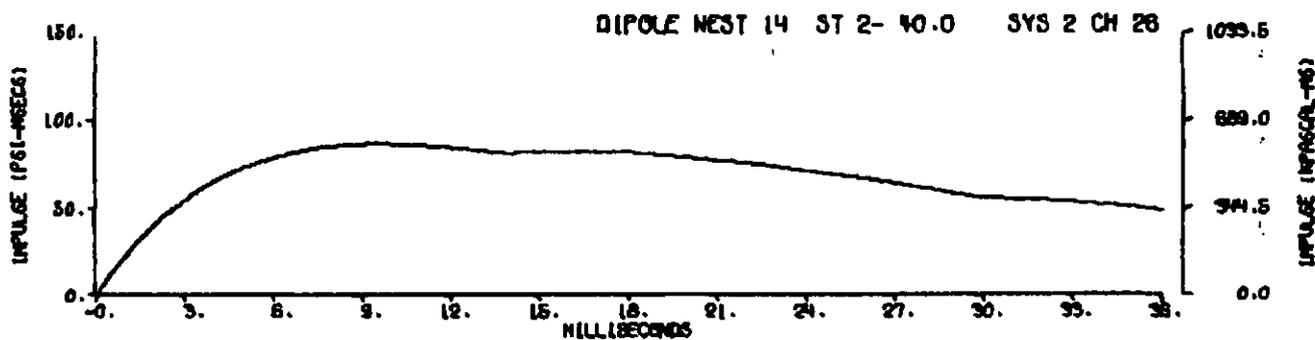
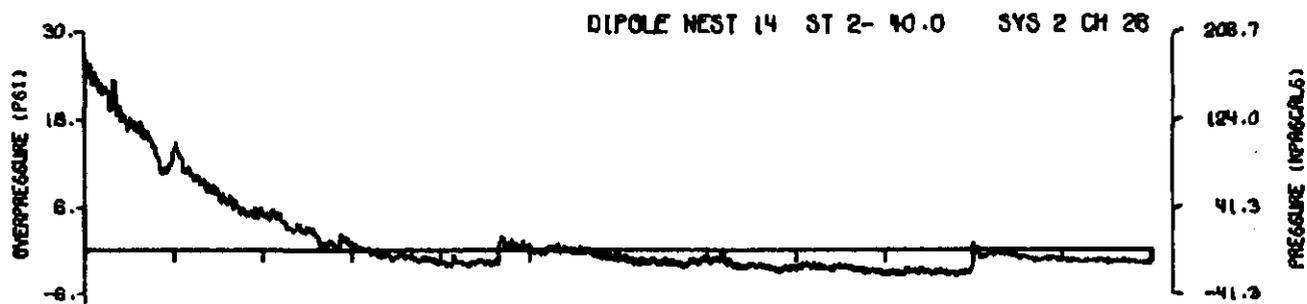
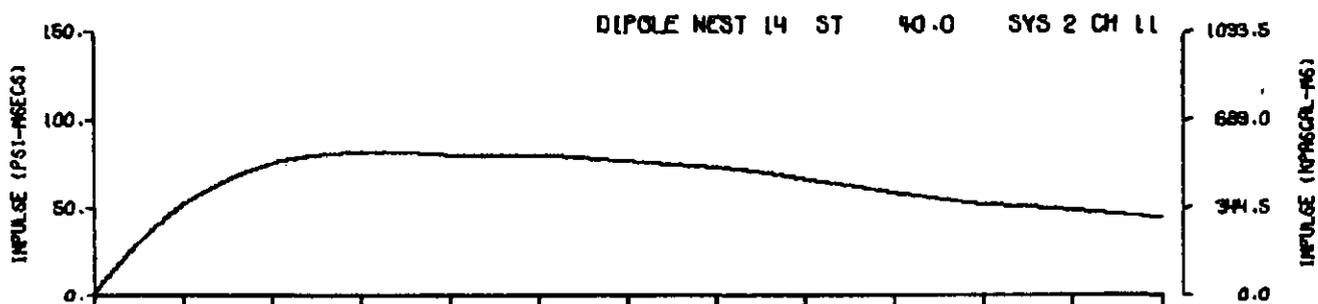
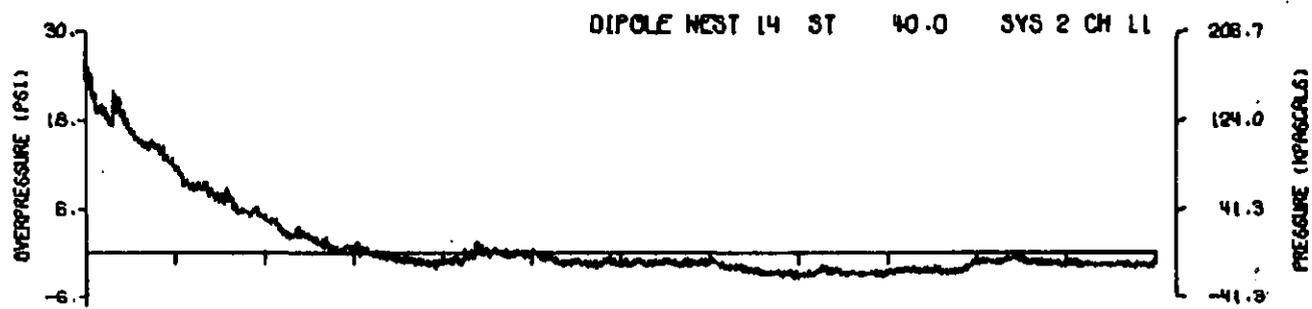
A14.17



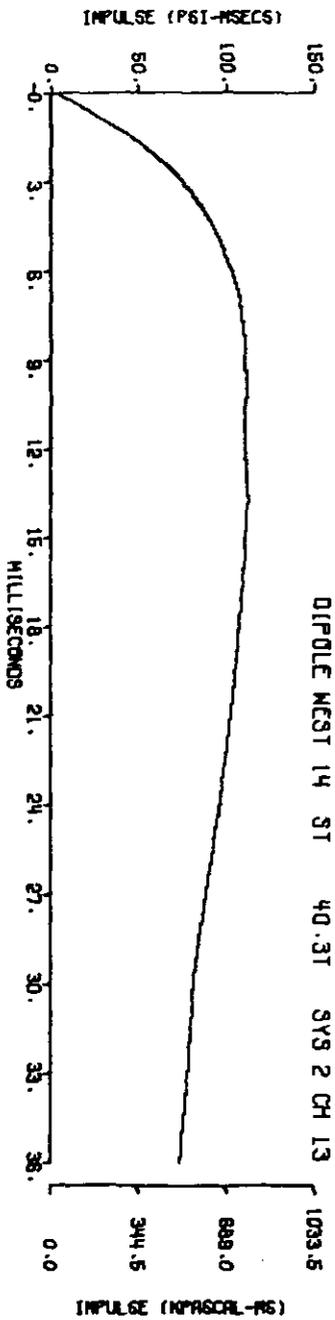
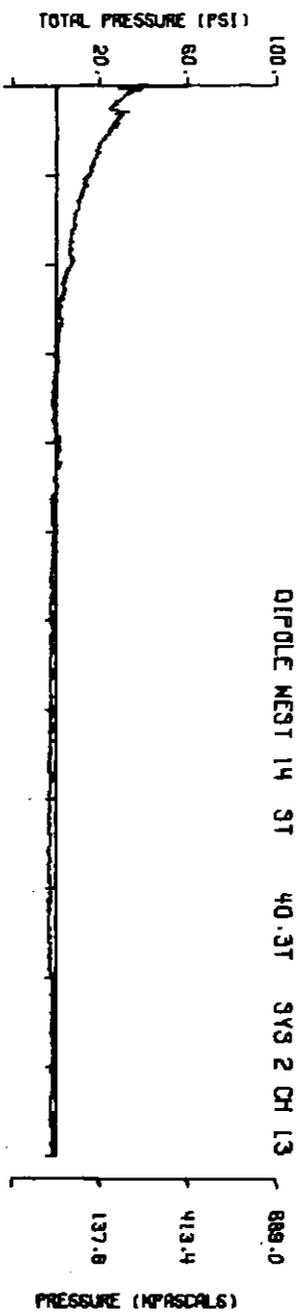
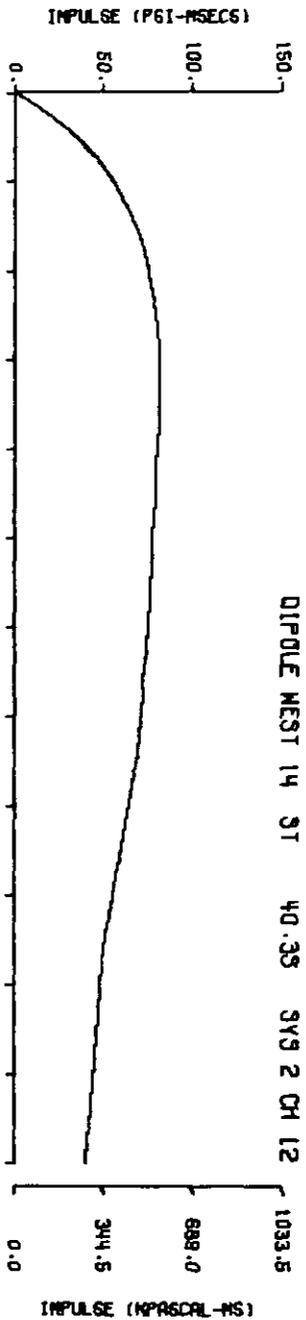
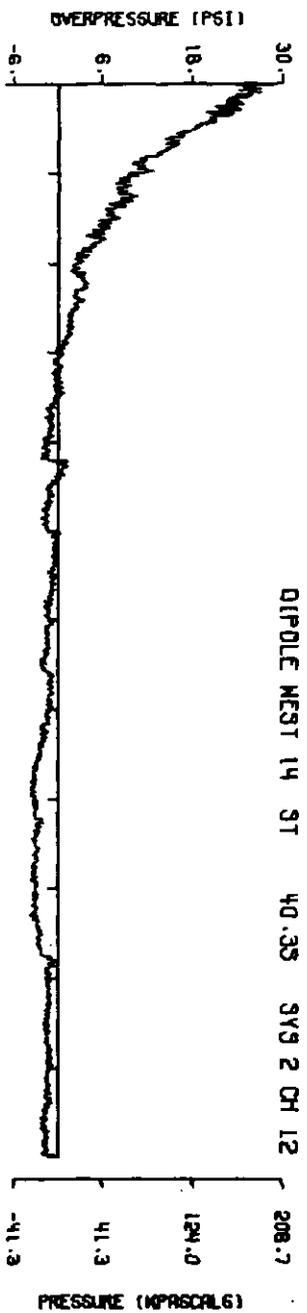
A14.18



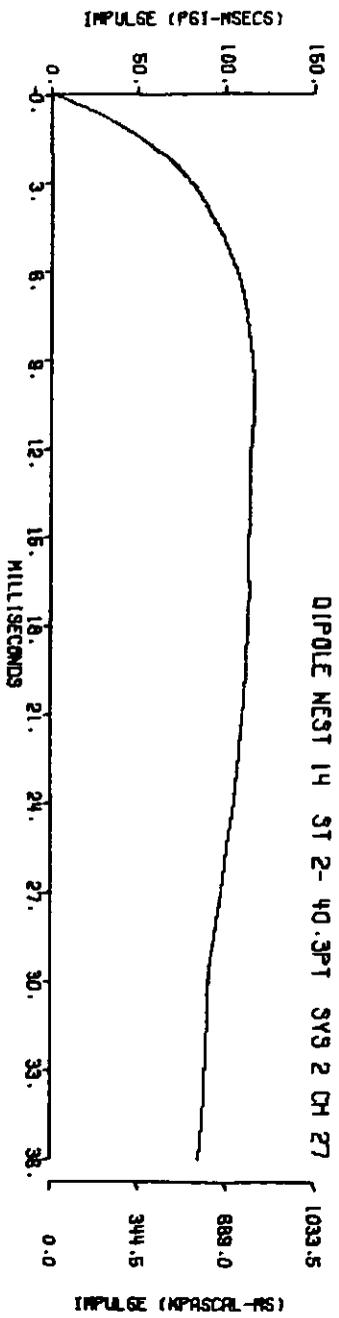
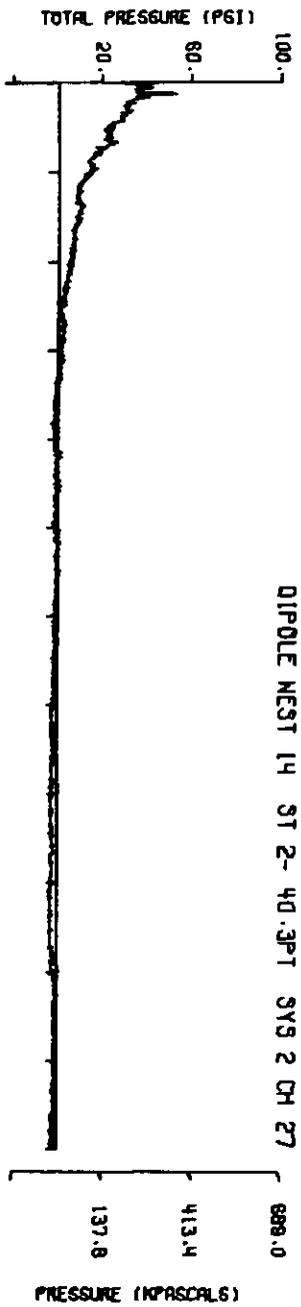
A14.19



A14.20

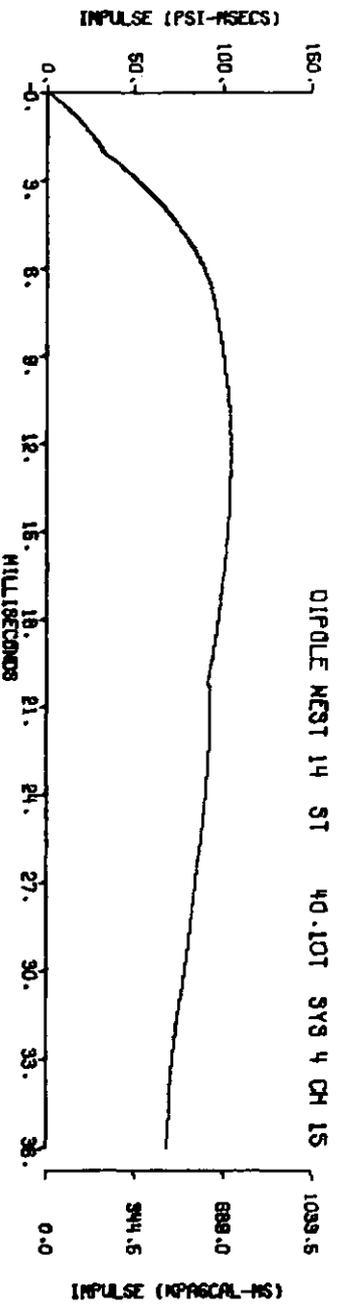
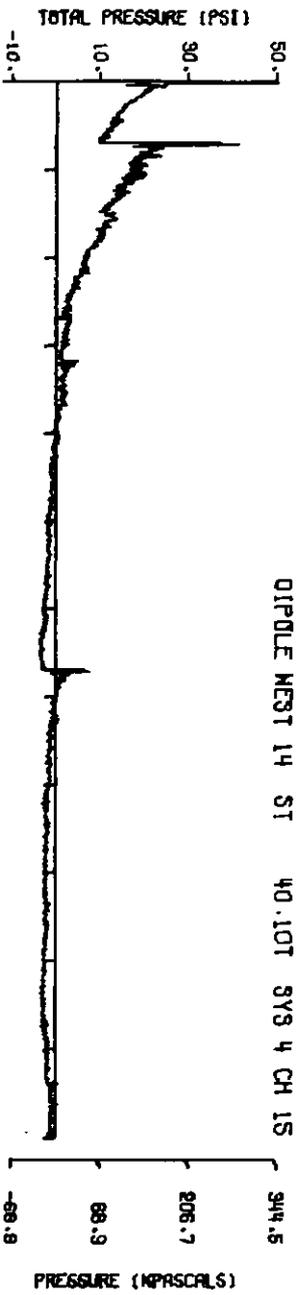
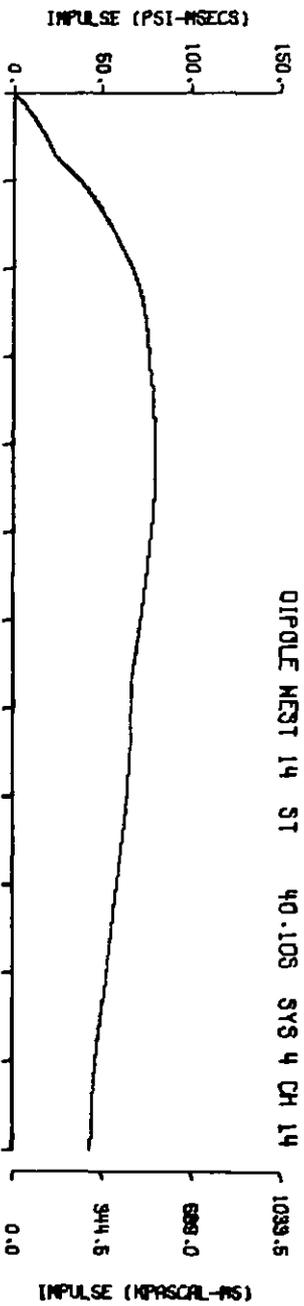
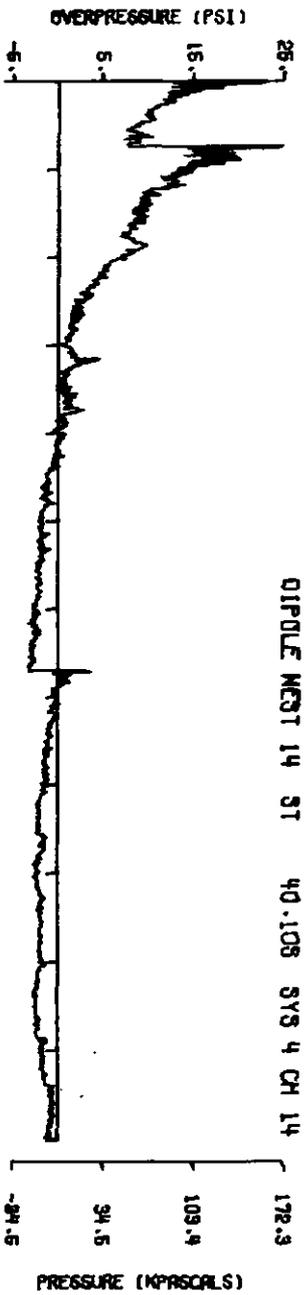


A14.21
264

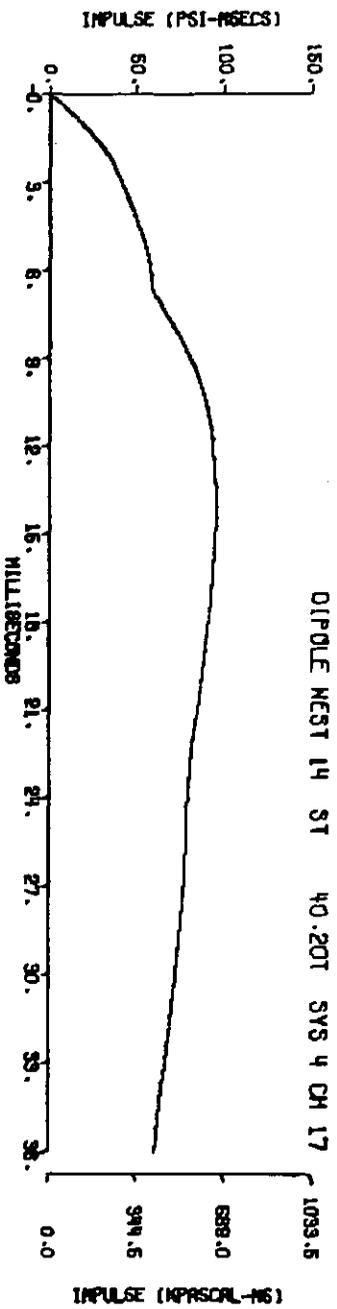
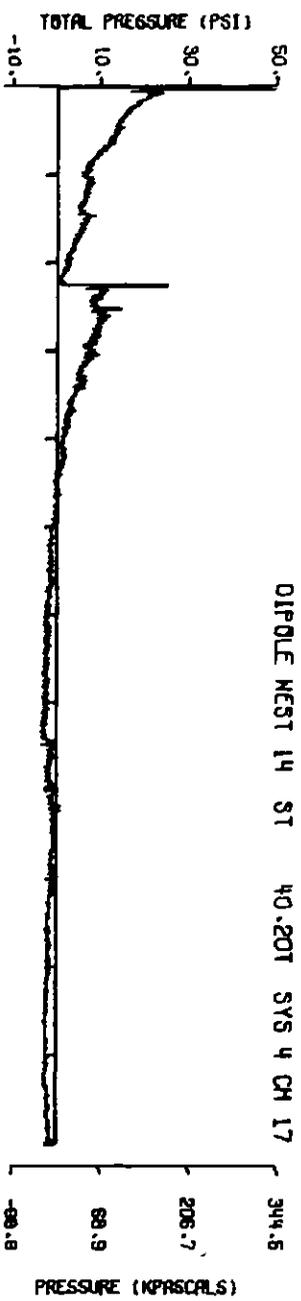
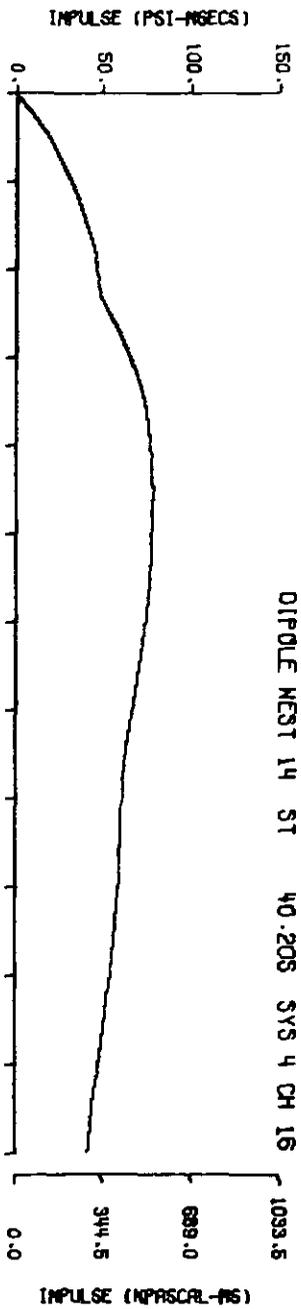
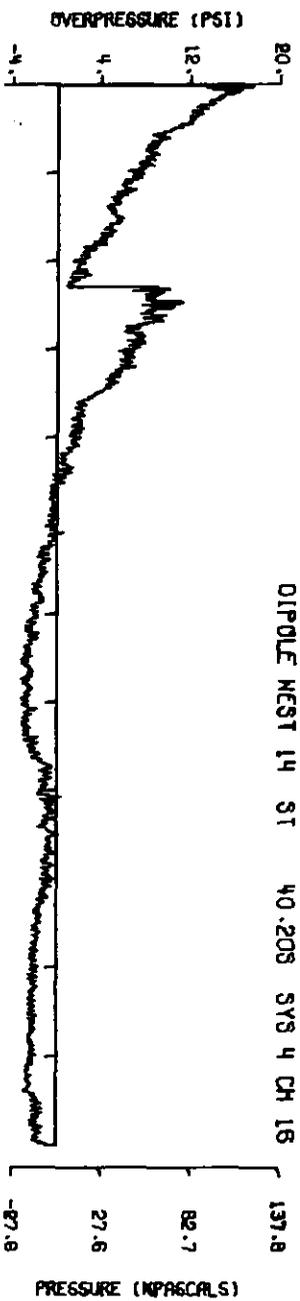


A14.22

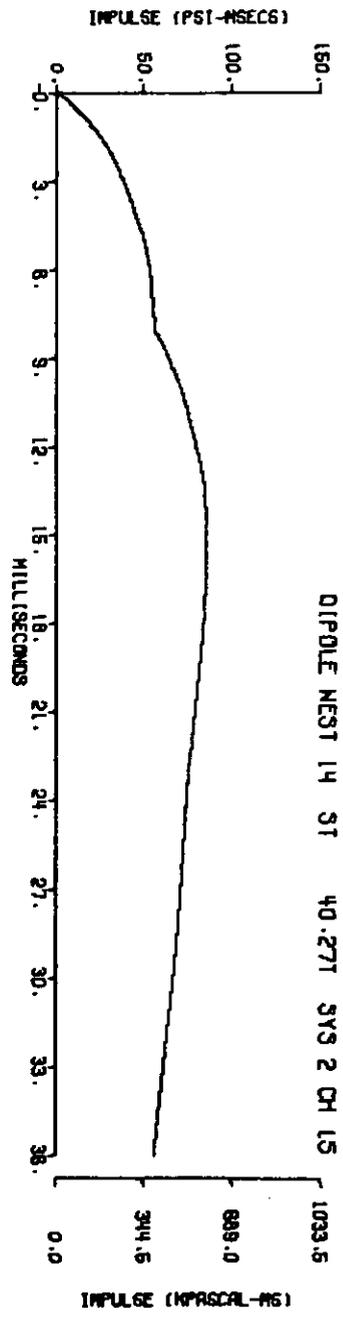
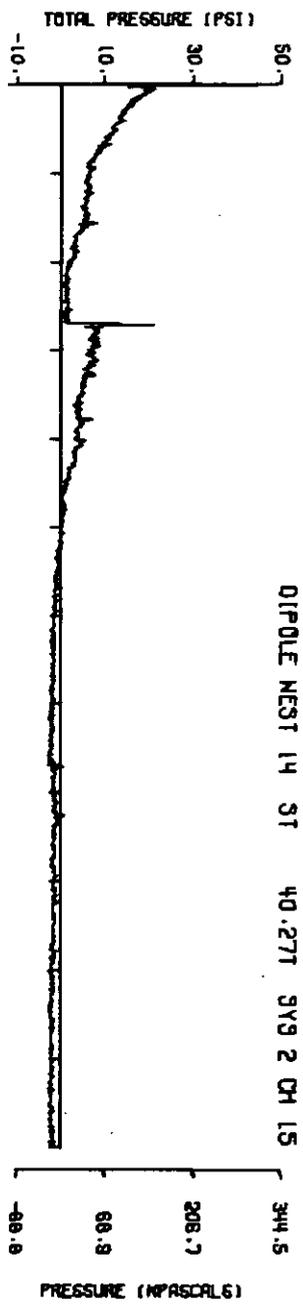
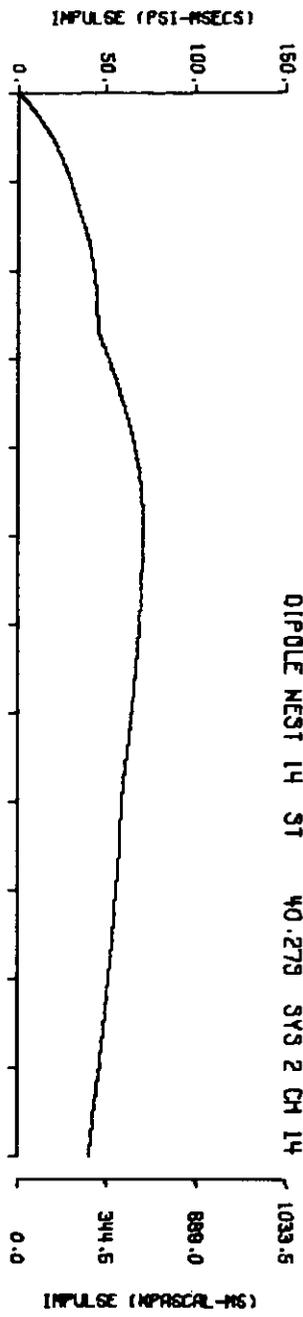
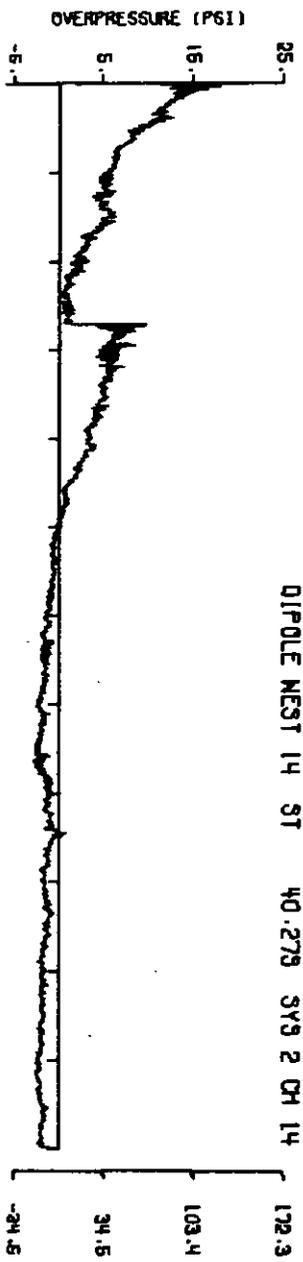
265



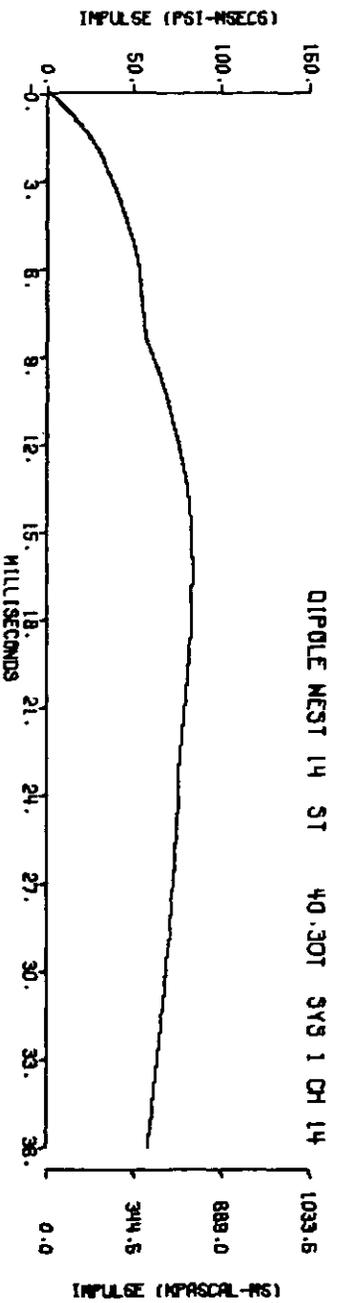
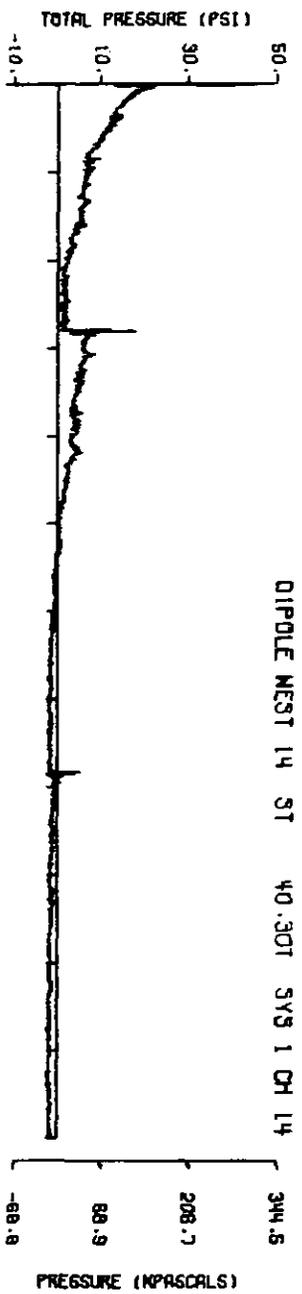
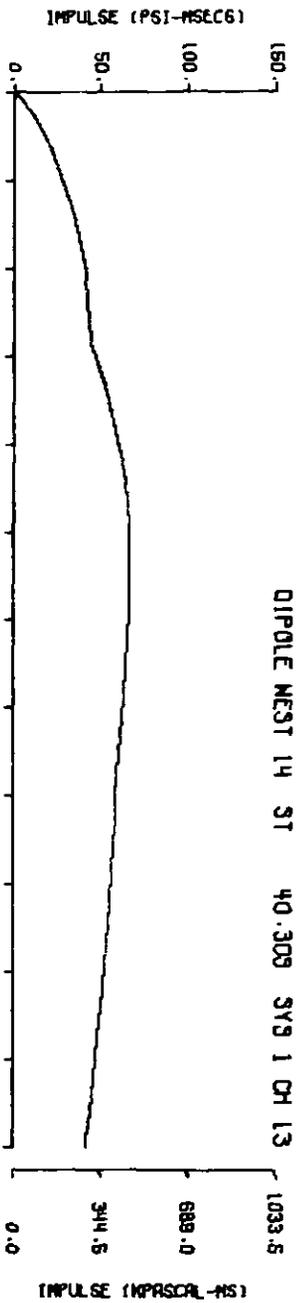
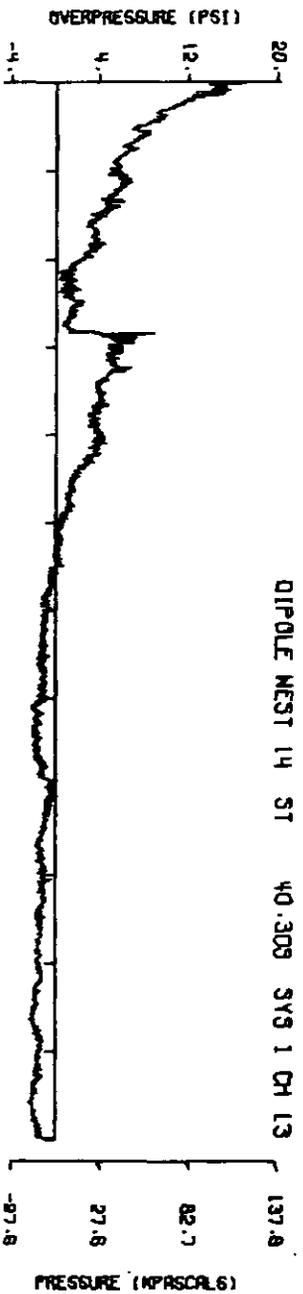
A14.23



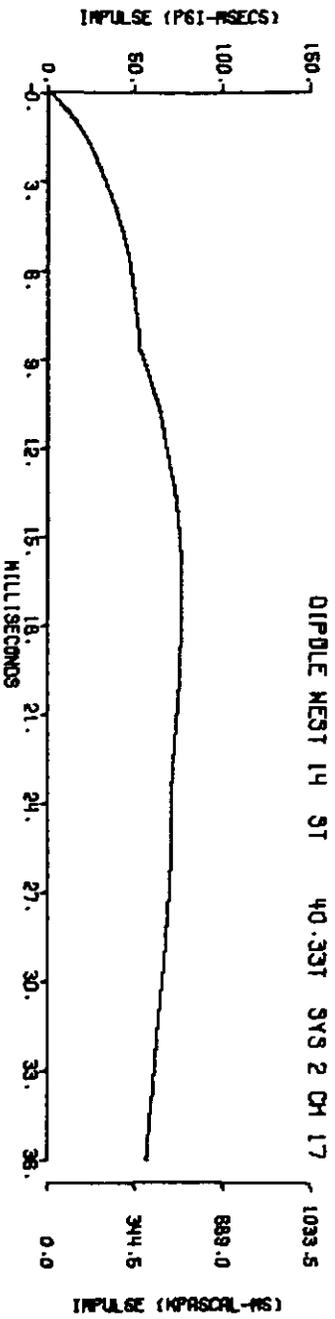
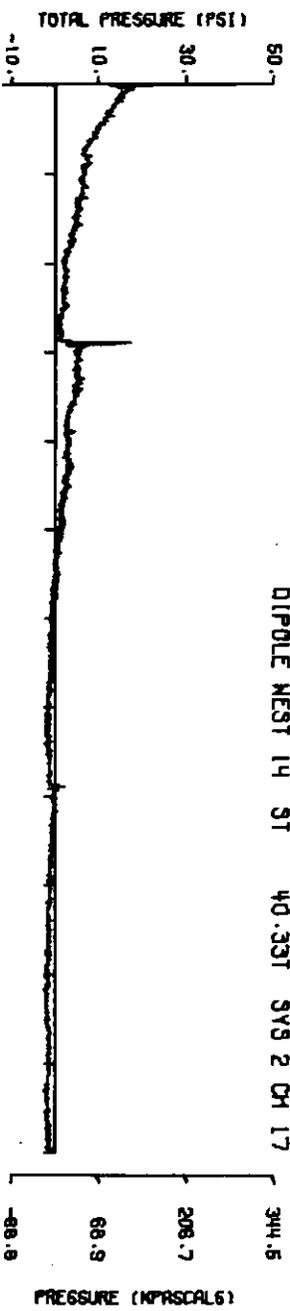
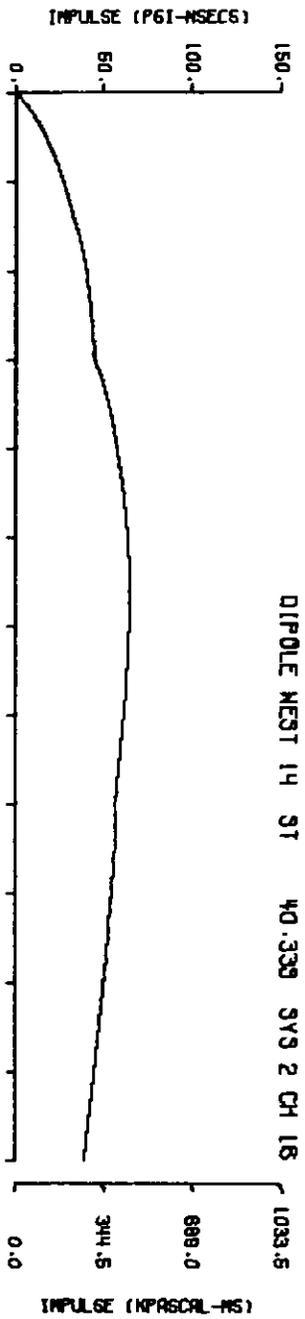
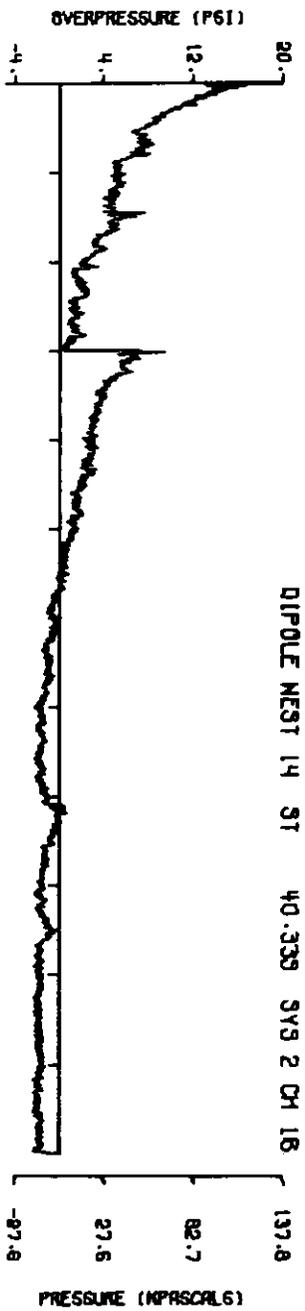
A14.24
267



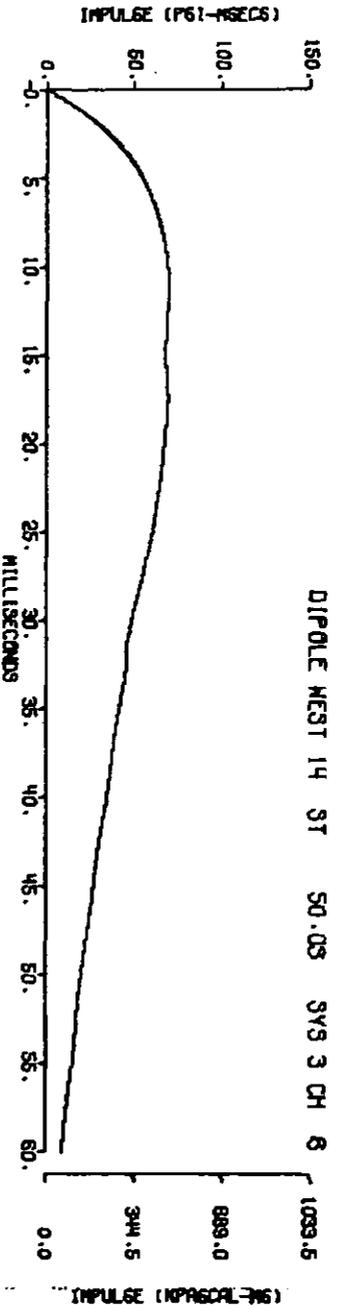
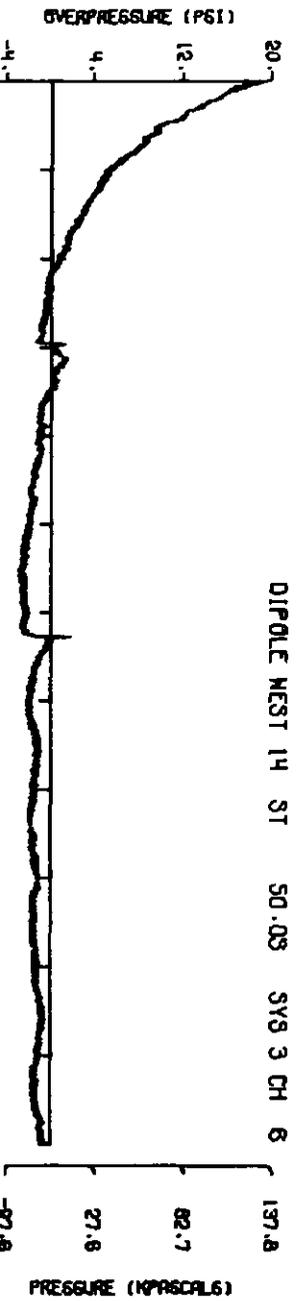
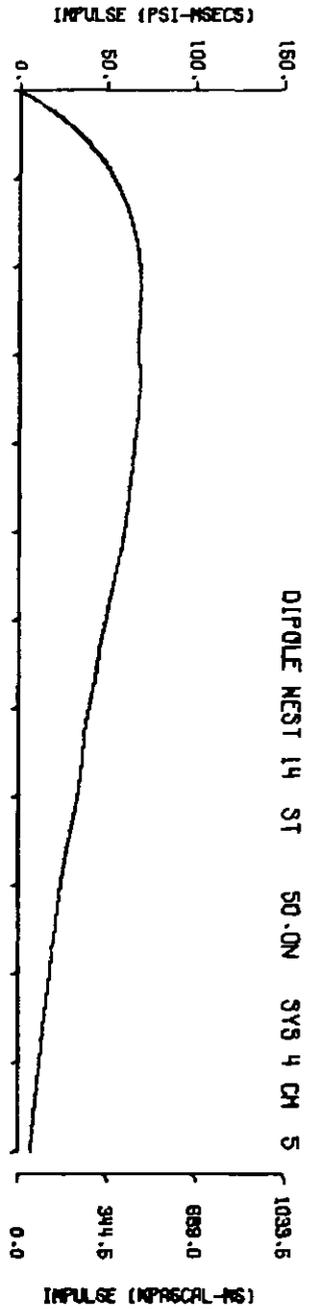
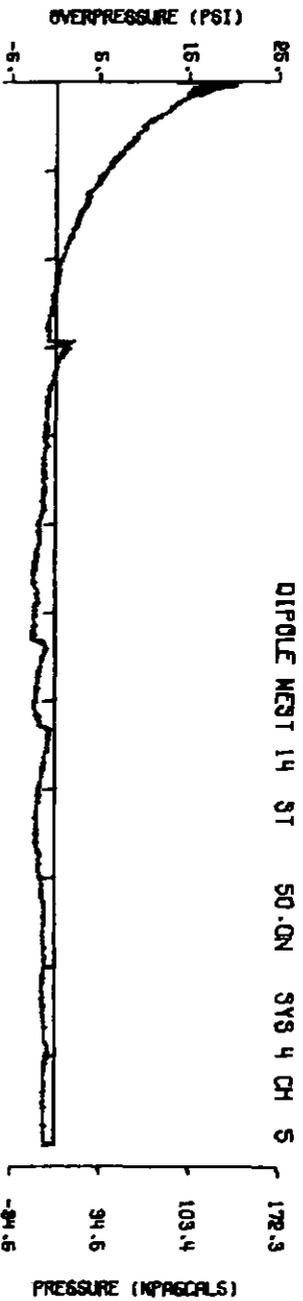
A14.25
268



A14.26
269



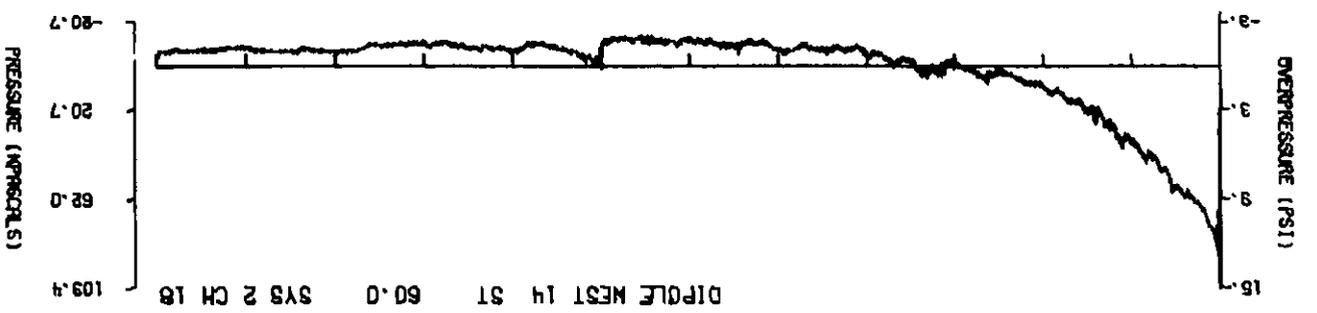
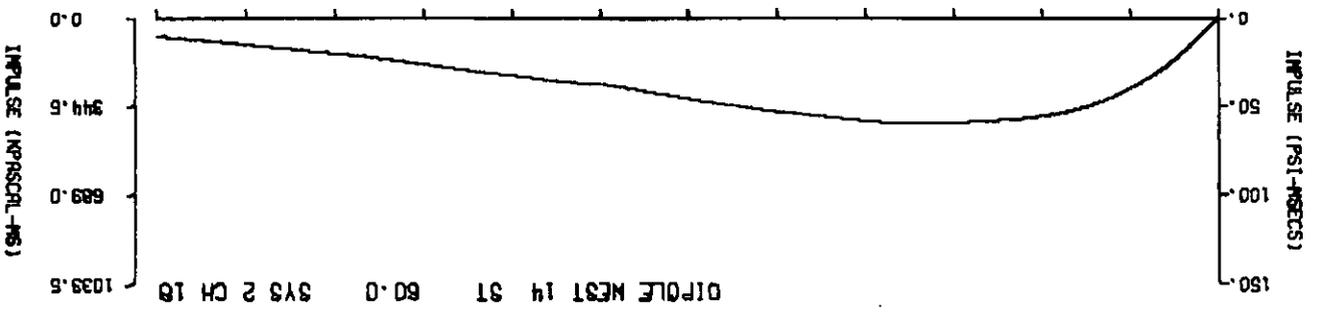
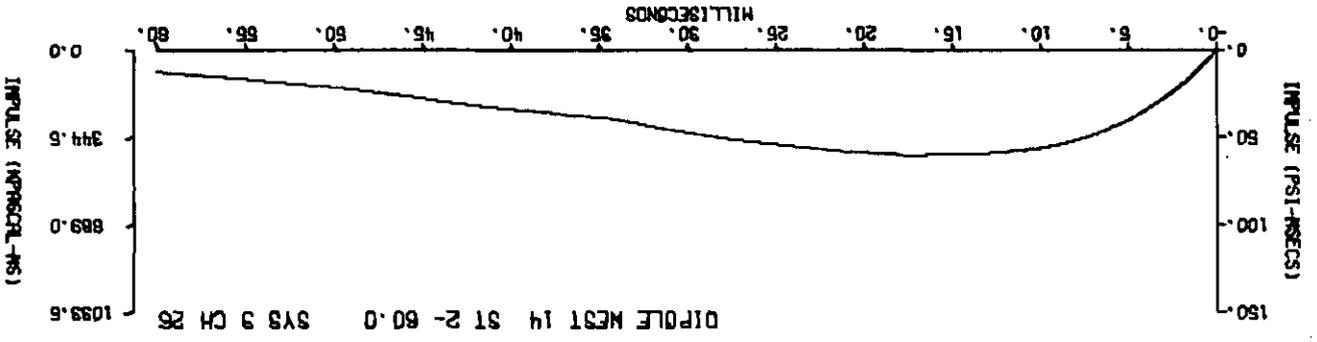
A14.27

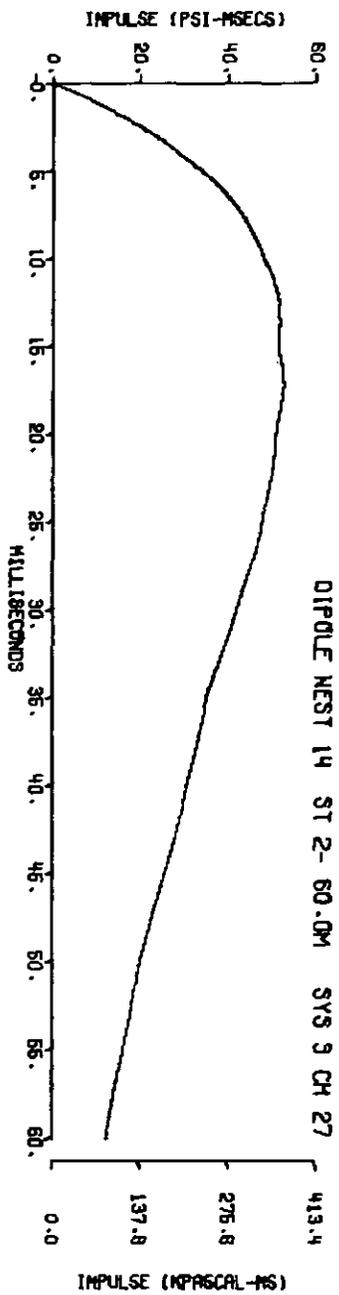
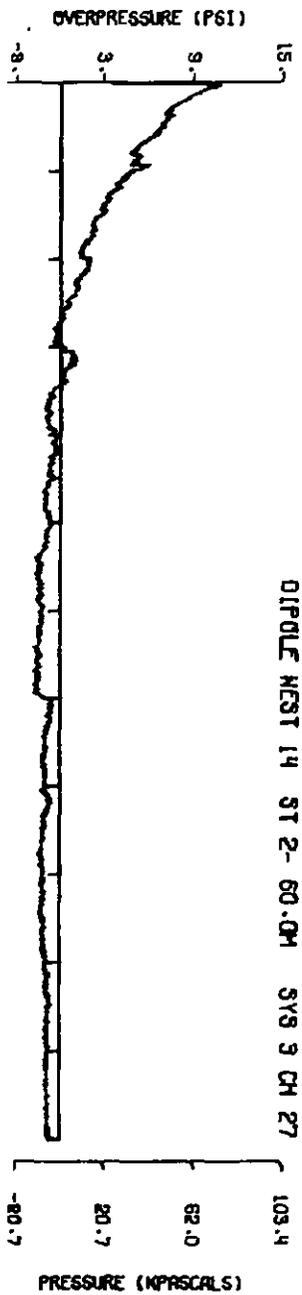


A14.28
271

272

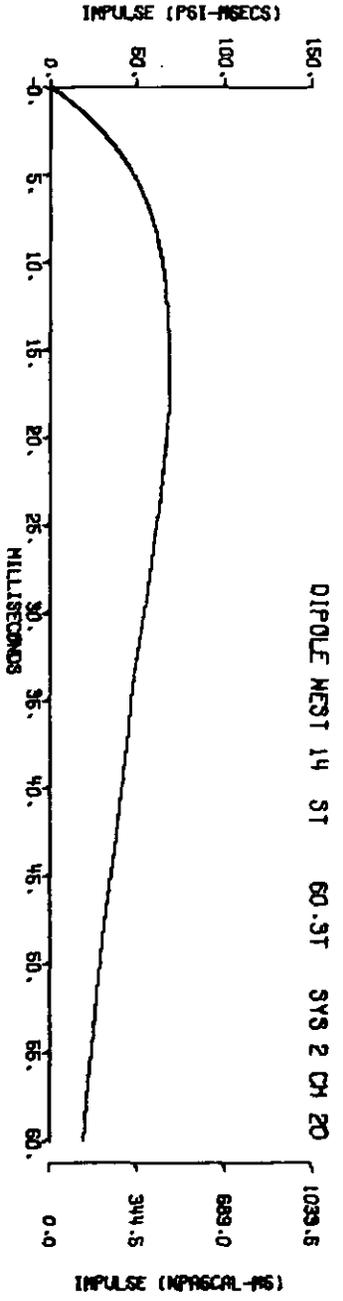
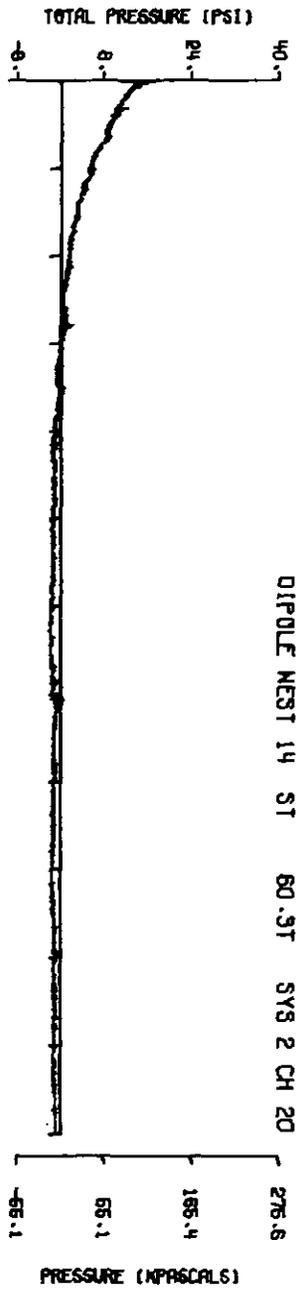
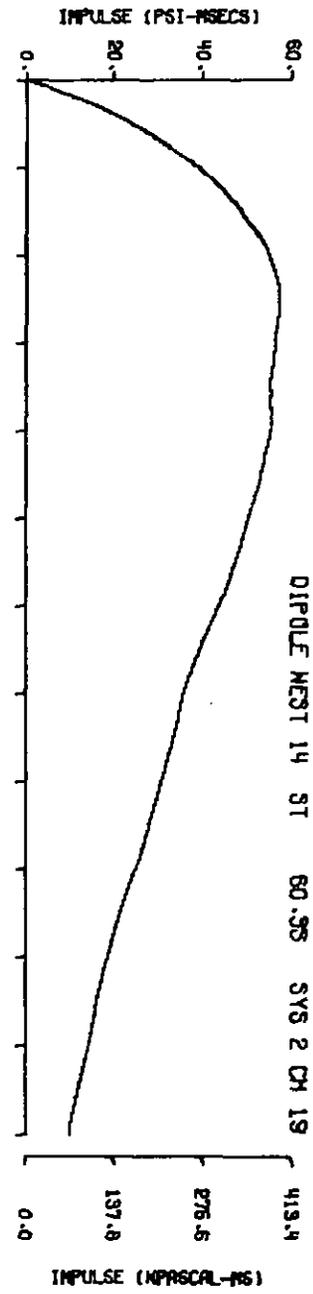
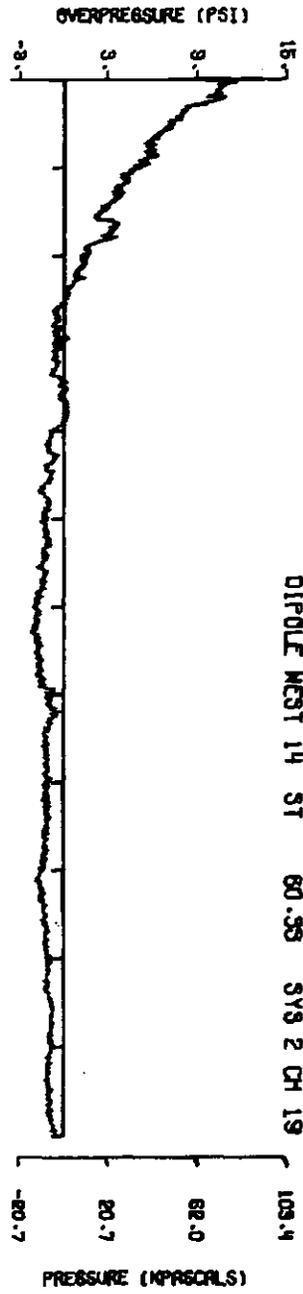
A14.29





A14.30

273



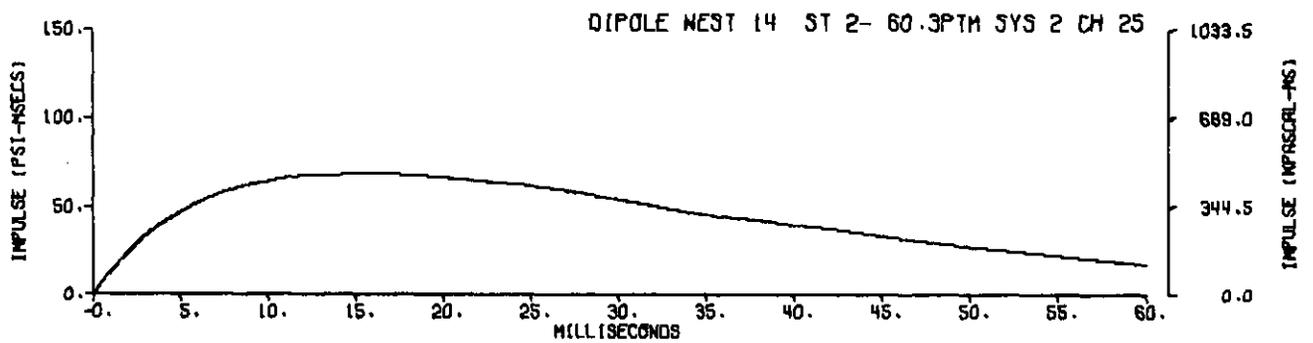
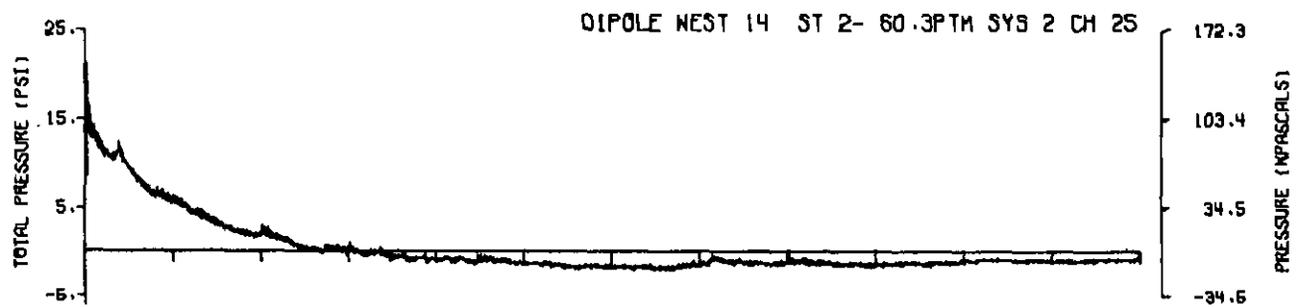
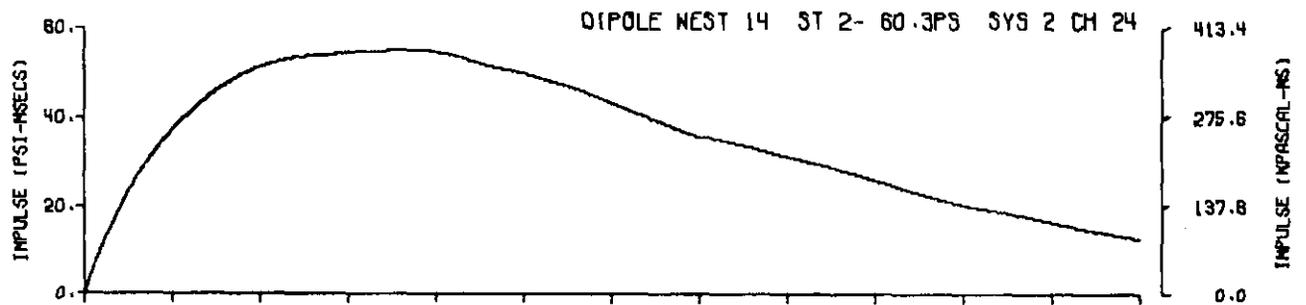
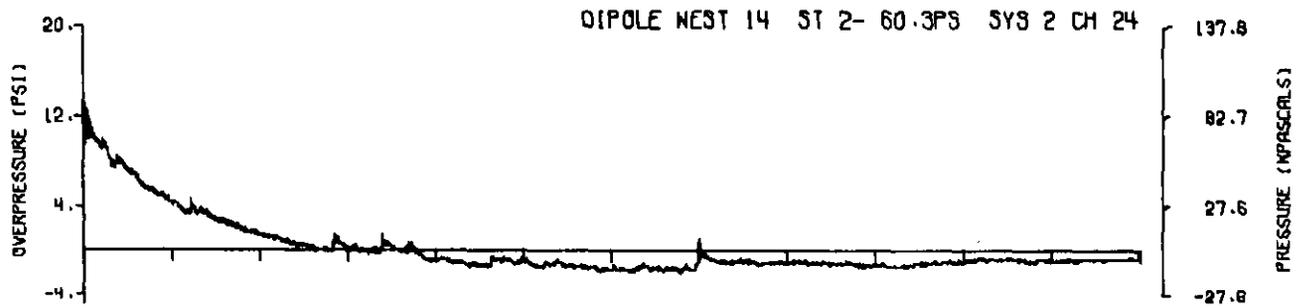
274
A14.31
MILLISECONDS

IMPULSE (MPASCAL-MS)

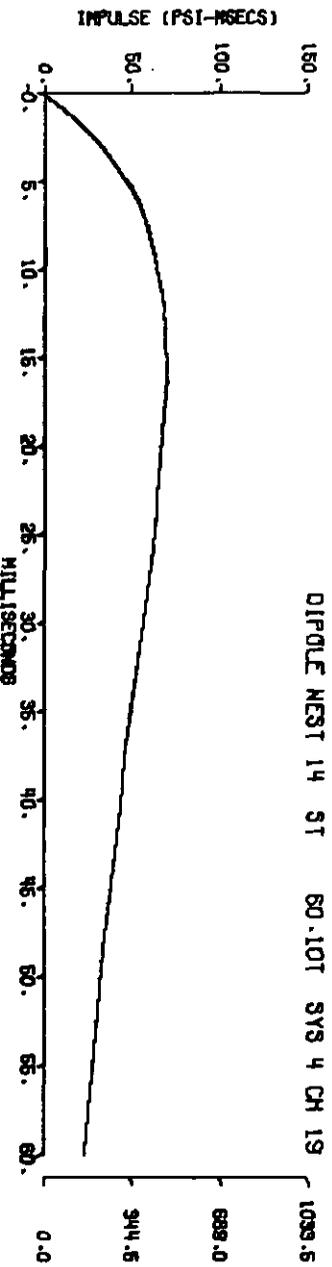
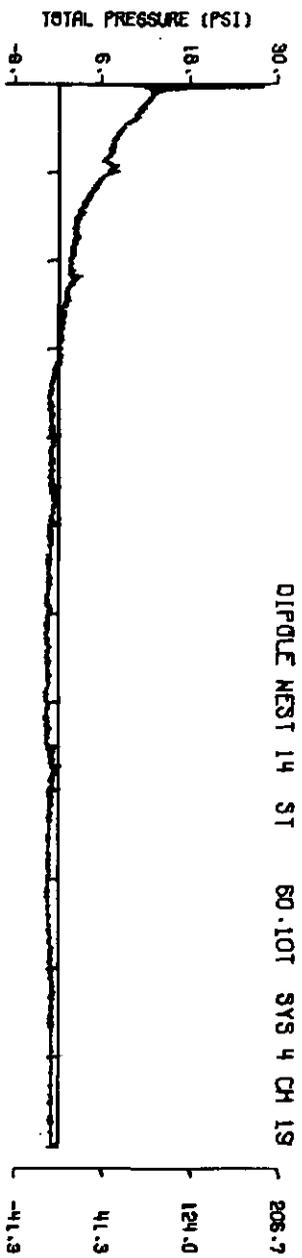
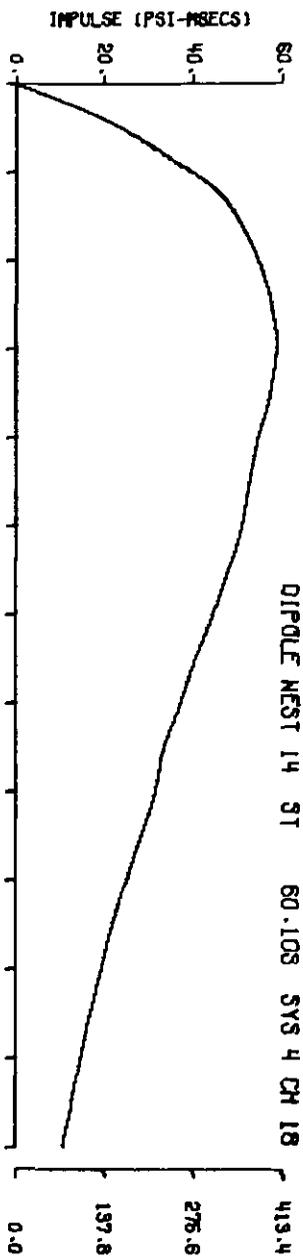
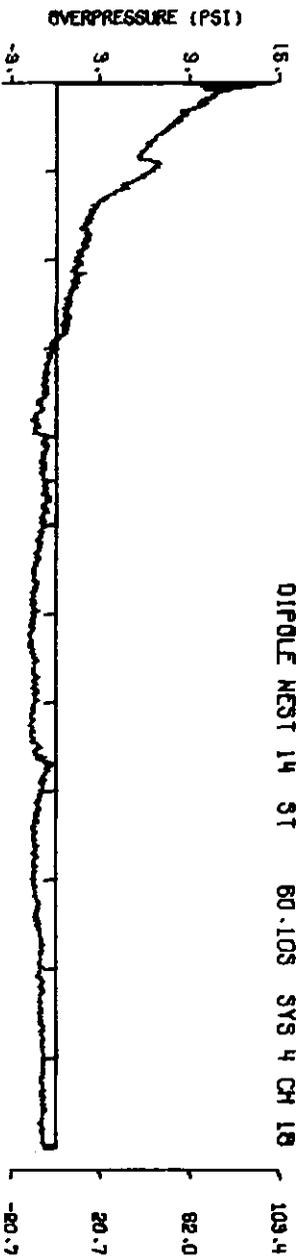
PRESSURE (MPASCALS)

IMPULSE (MPASCAL-MS)

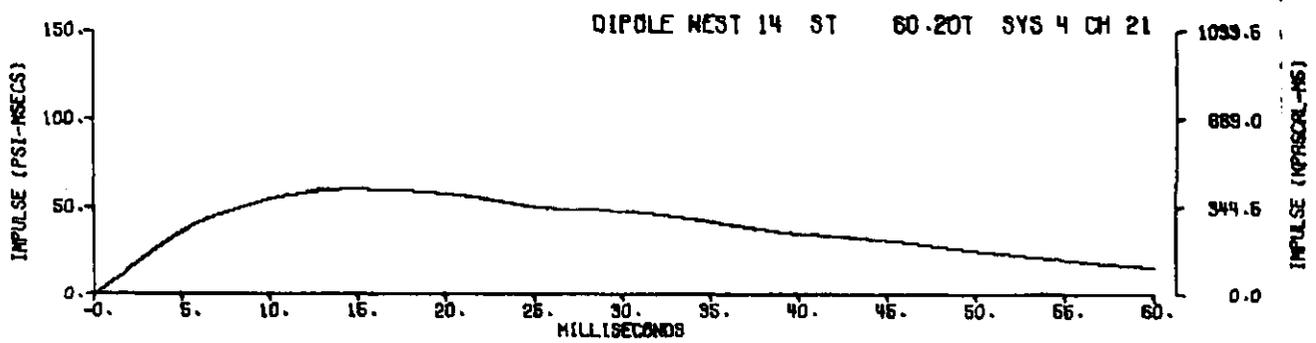
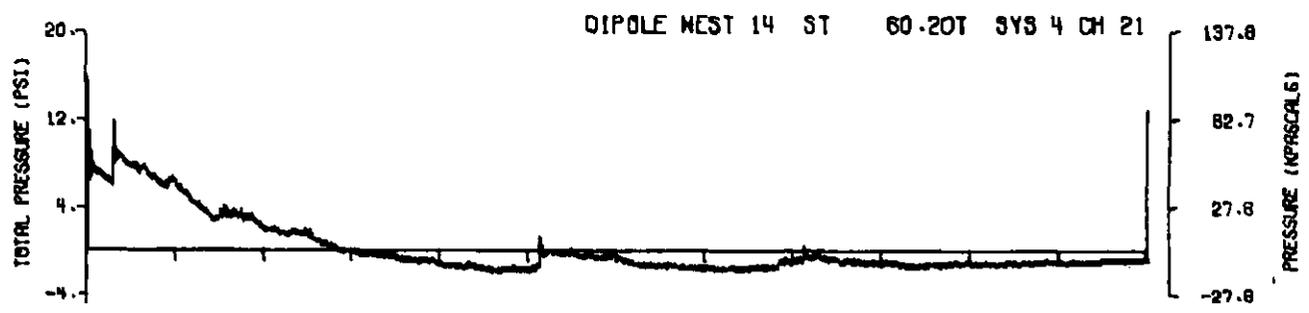
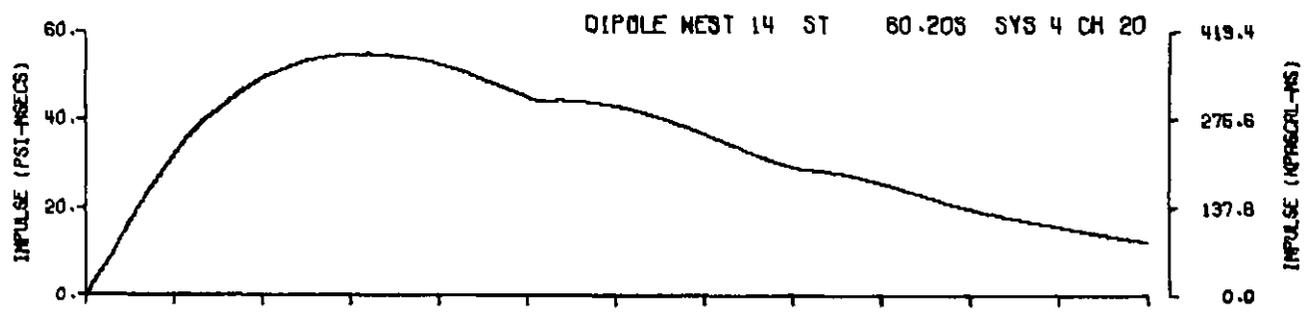
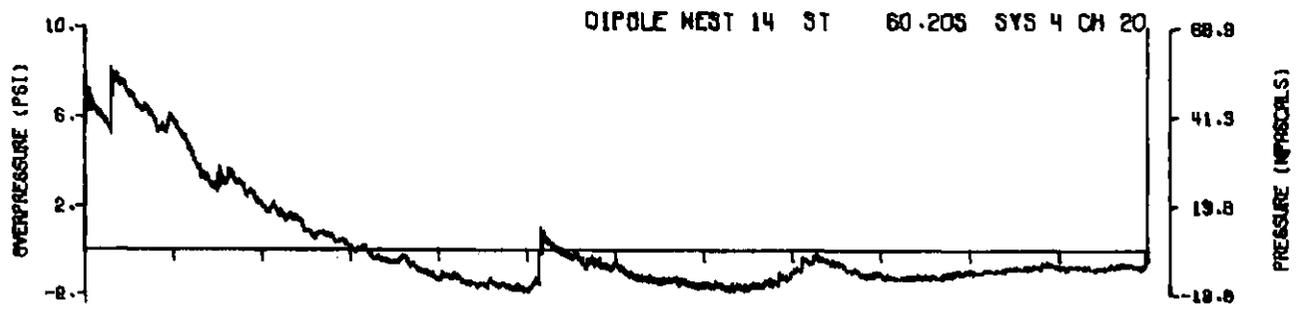
PRESSURE (MPASCALS)



A14.32

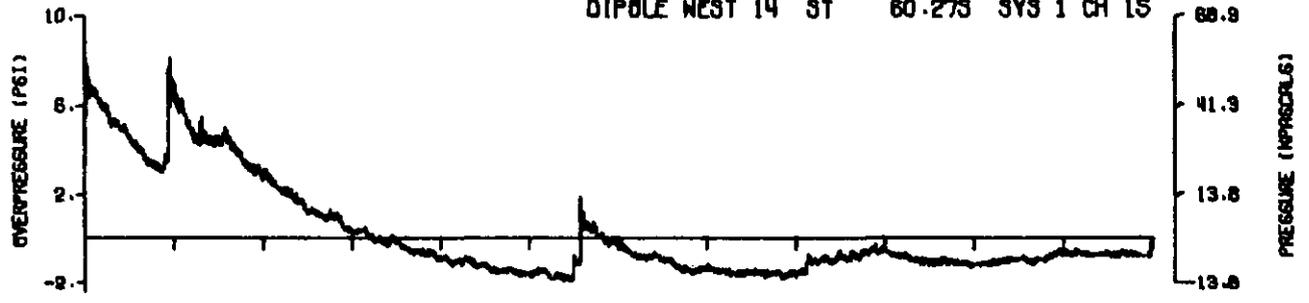


A14.33

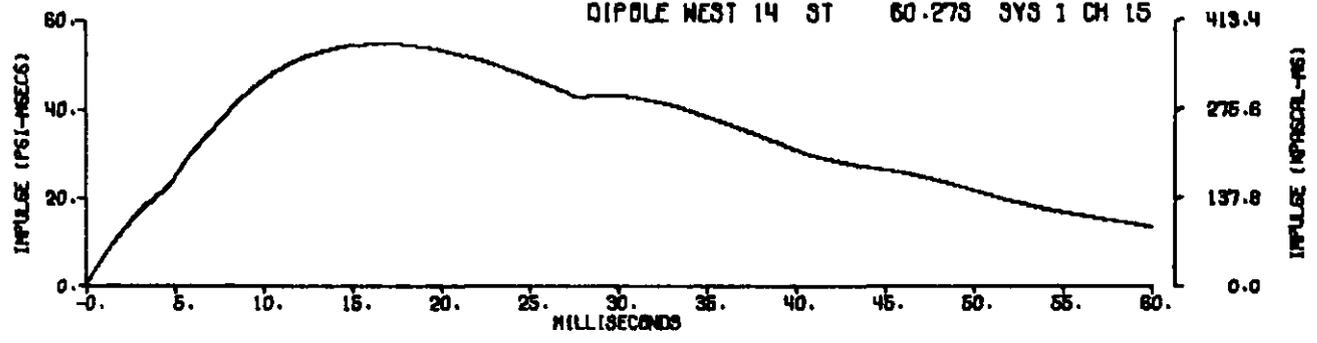


A14.34

DIPOLE WEST 14 ST 60.273 SYS 1 CH 15

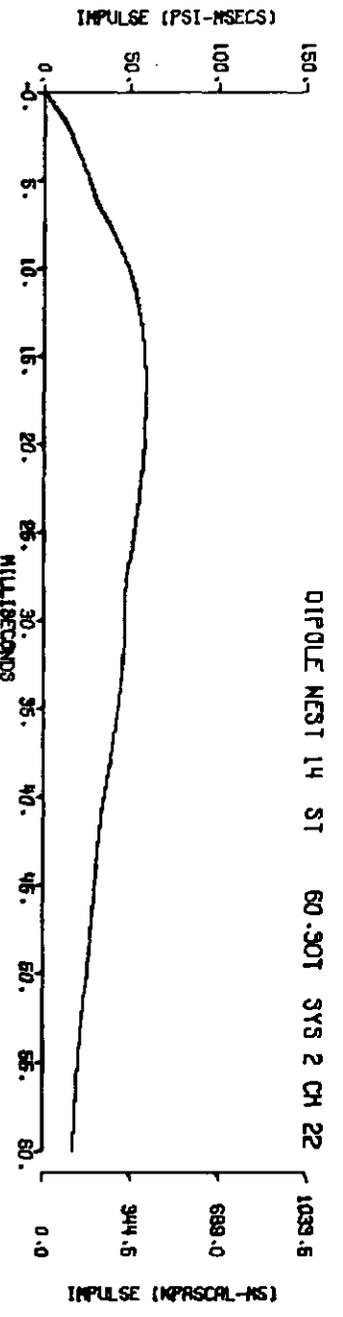
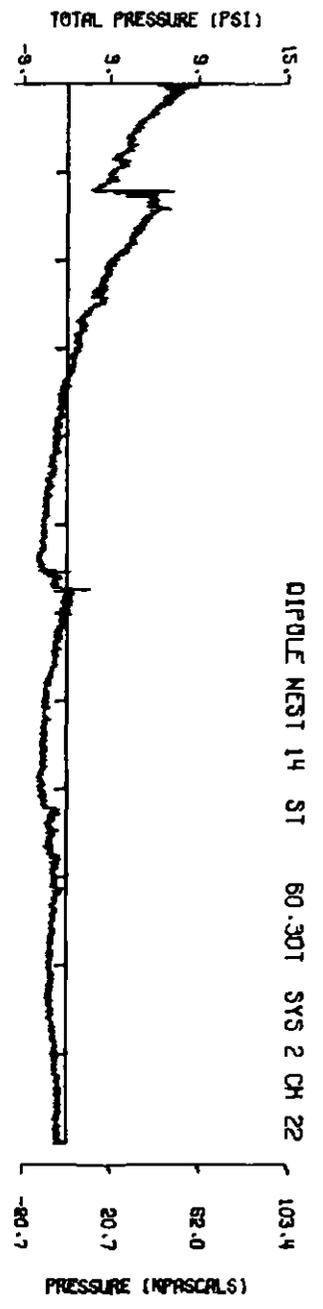
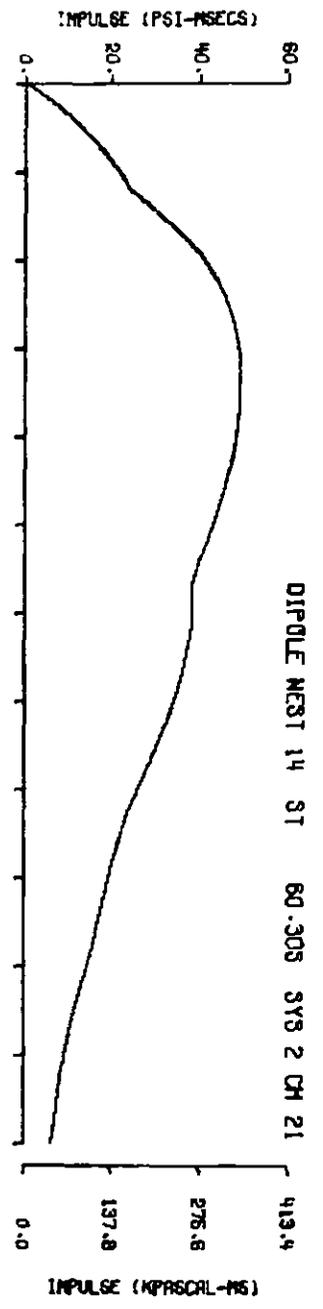
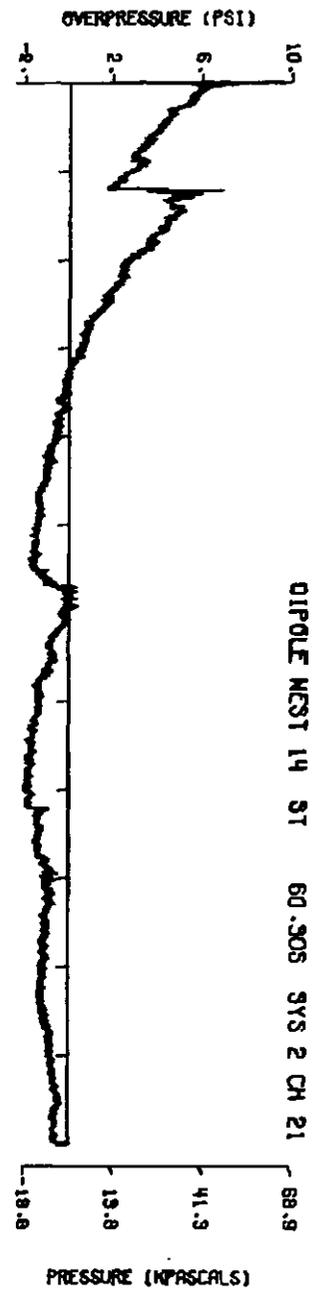


DIPOLE WEST 14 ST 60.273 SYS 1 CH 15

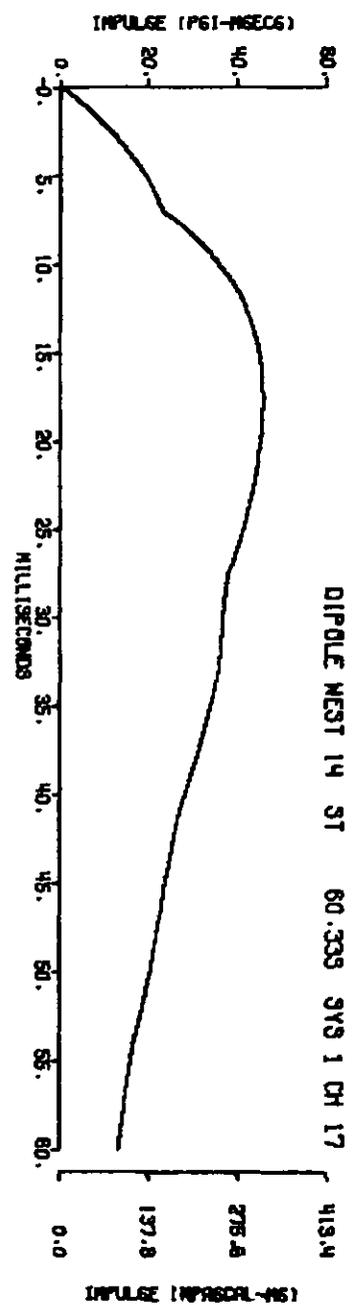
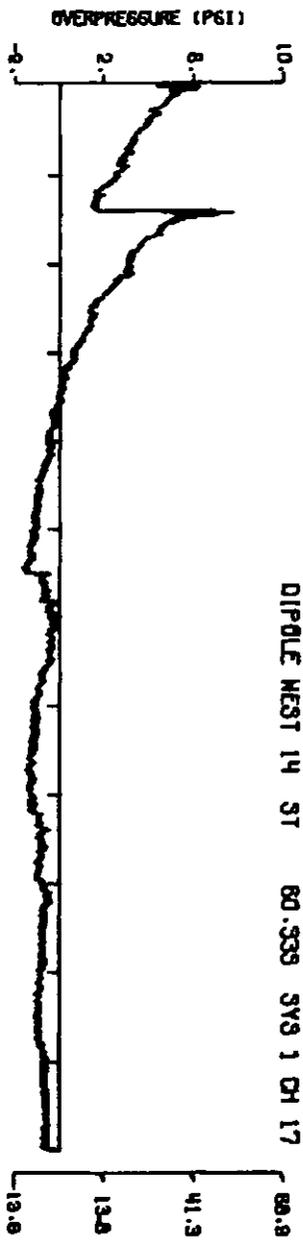


A14.35

278

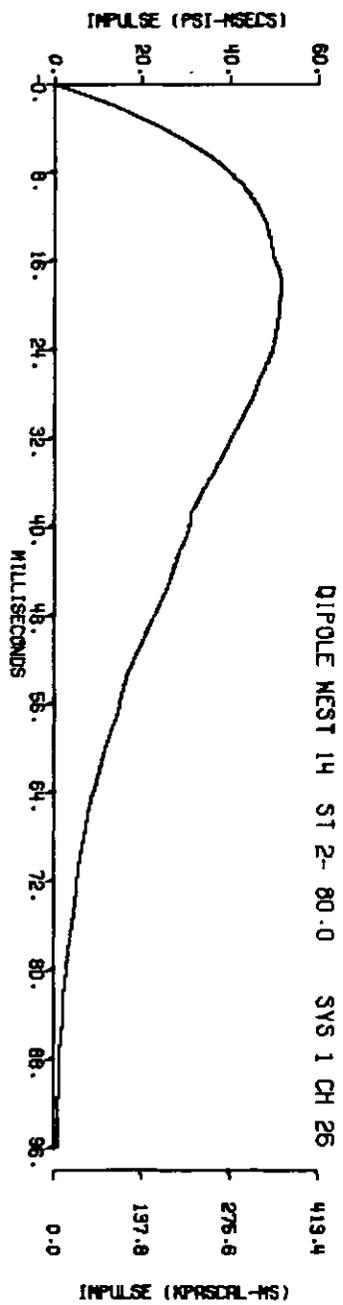
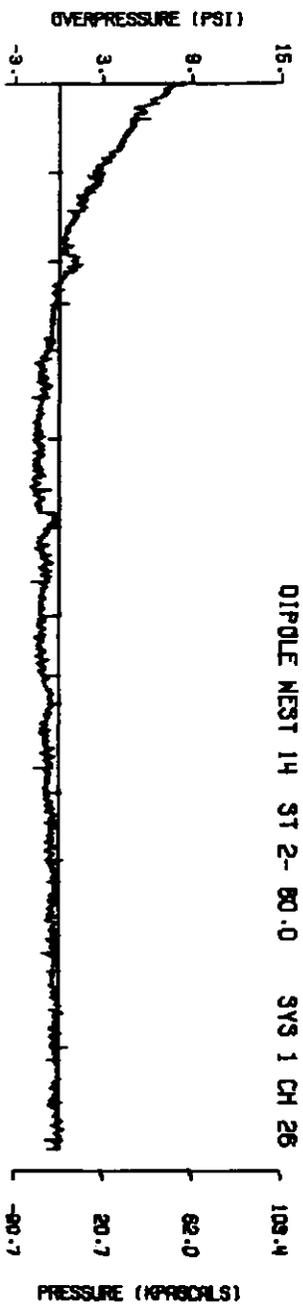


A14.36



A14.37

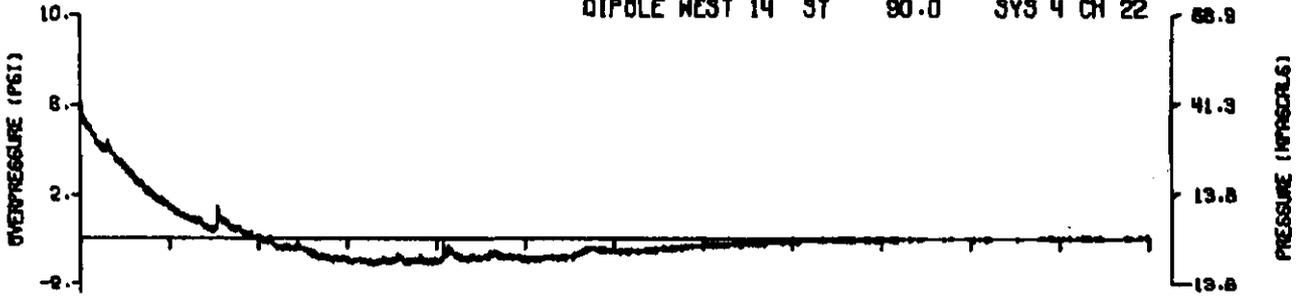
280



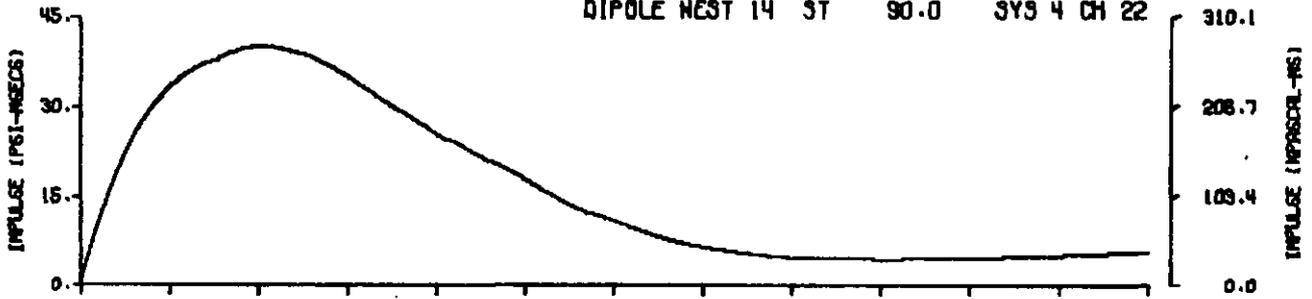
A14.38

281

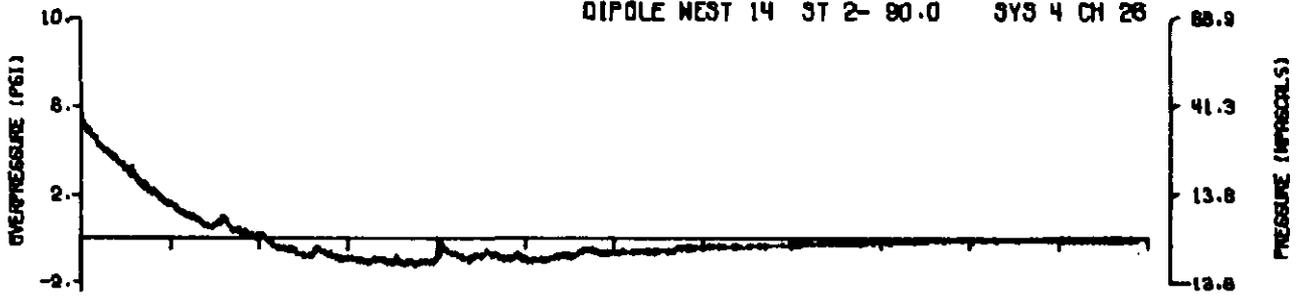
DIPOLE WEST 14 ST 90.0 SYS 4 CH 22



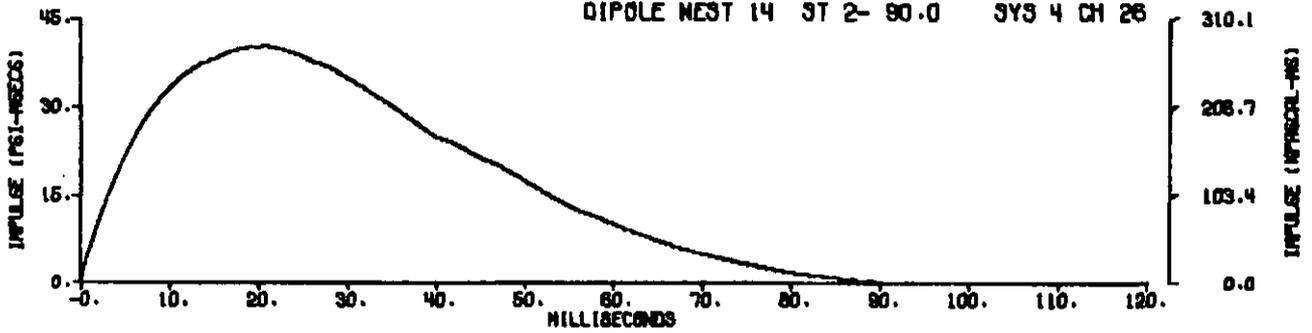
DIPOLE WEST 14 ST 90.0 SYS 4 CH 22



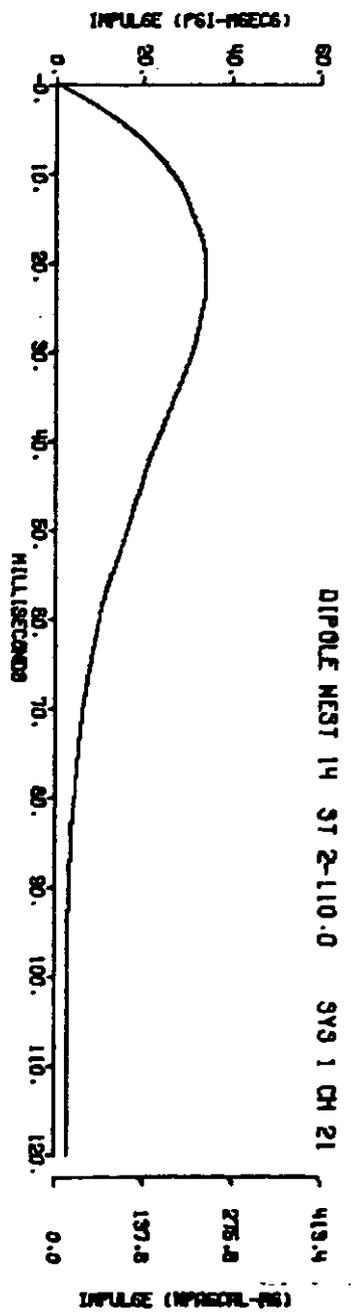
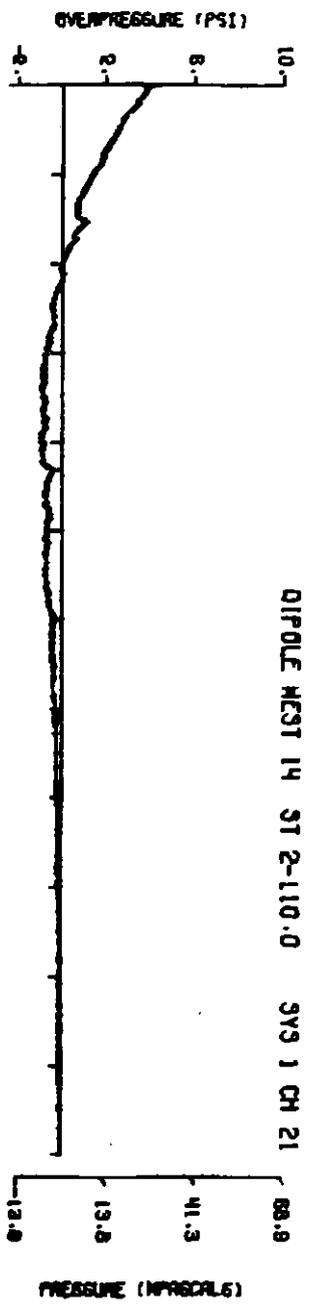
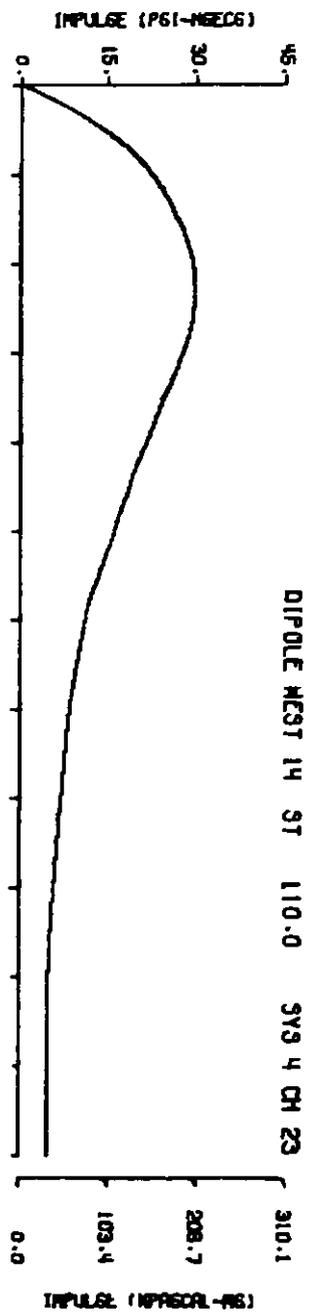
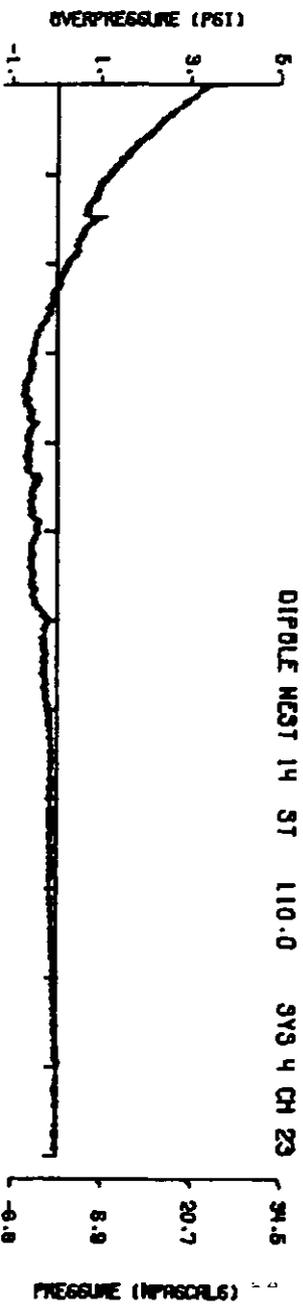
DIPOLE WEST 14 ST 2- 90.0 SYS 4 CH 26



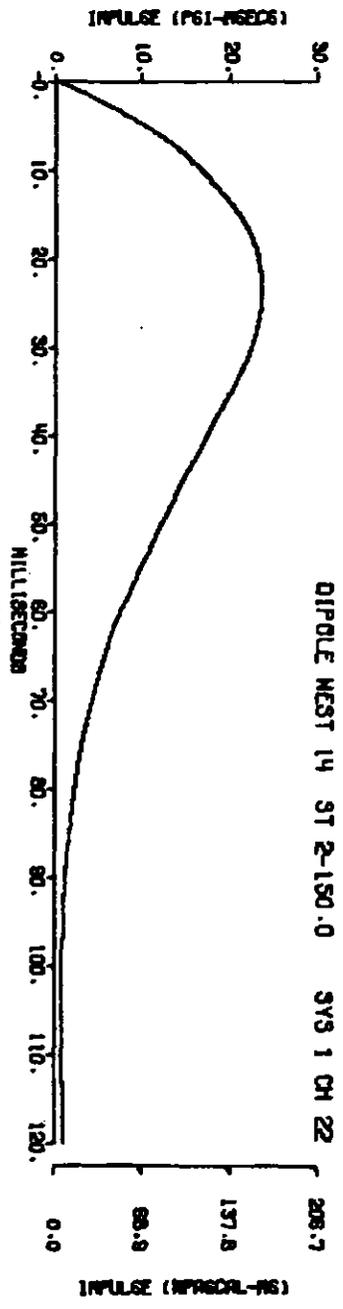
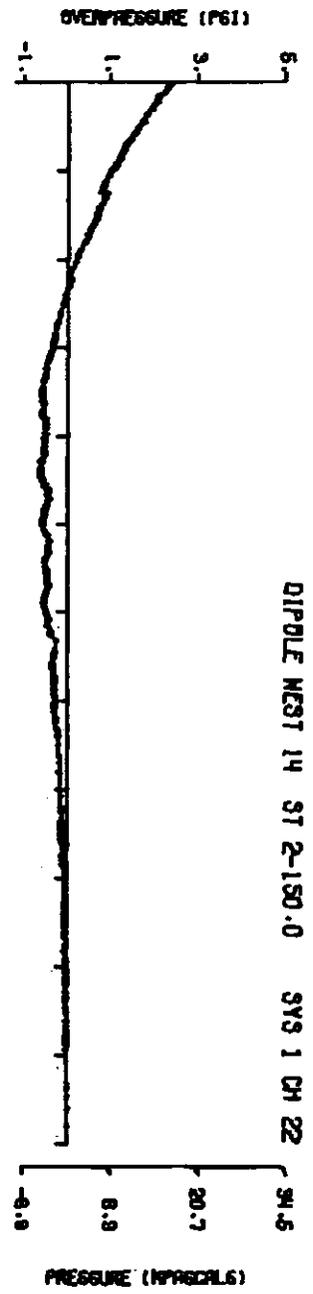
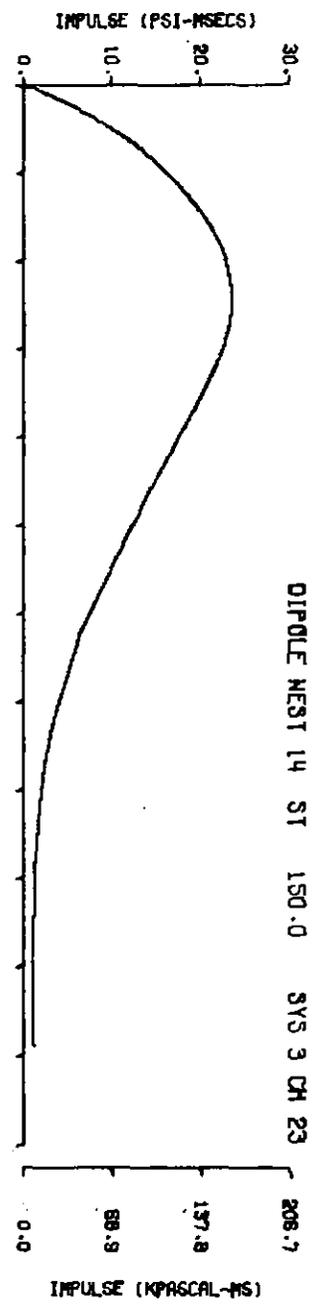
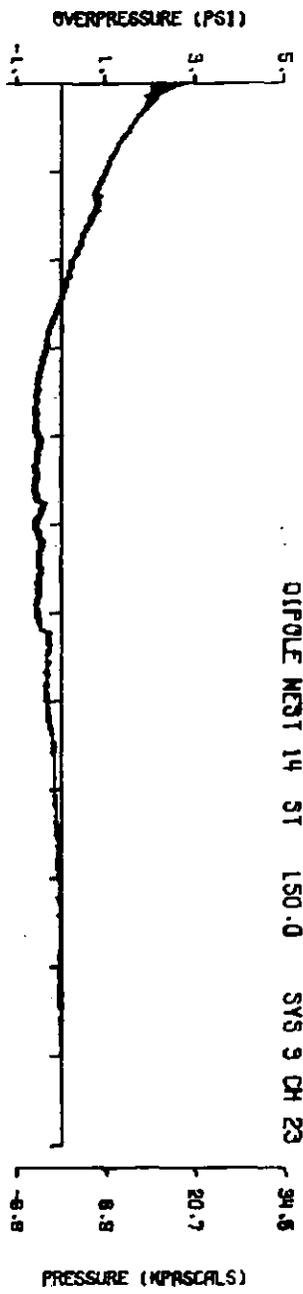
DIPOLE WEST 14 ST 2- 90.0 SYS 4 CH 26



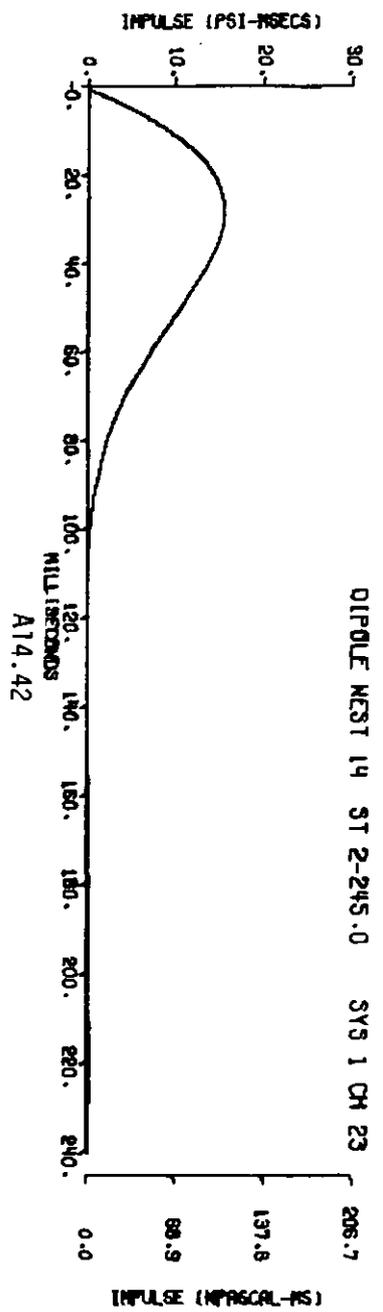
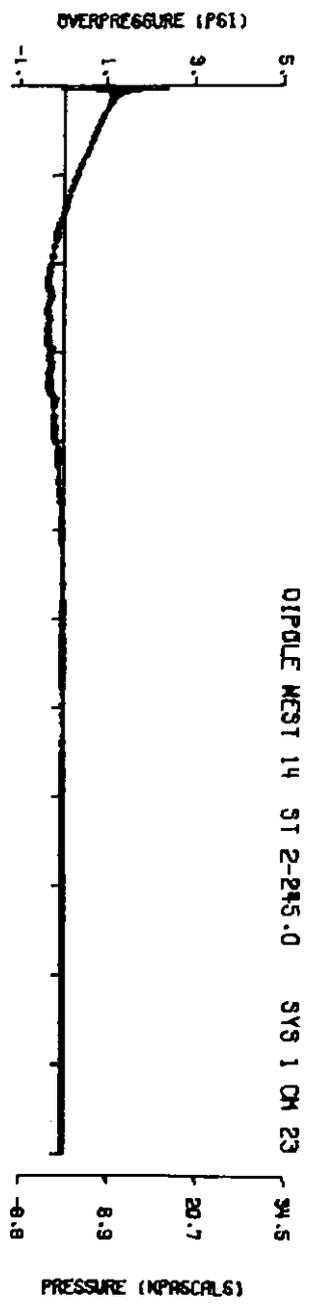
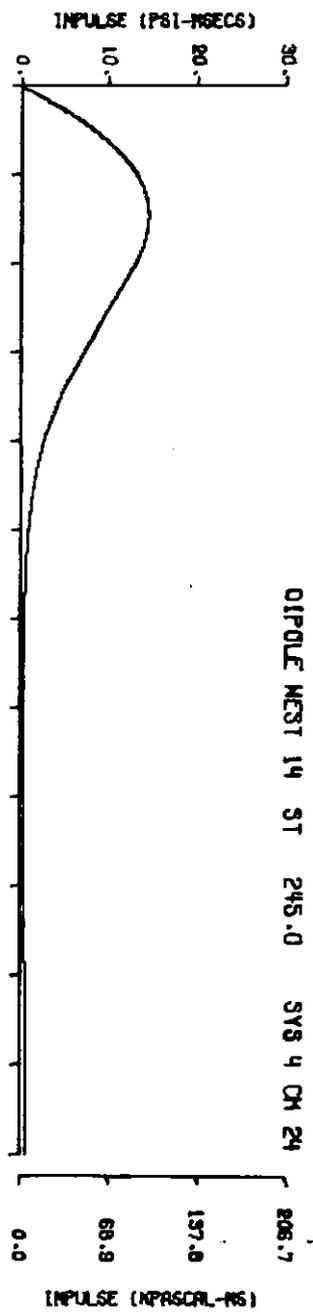
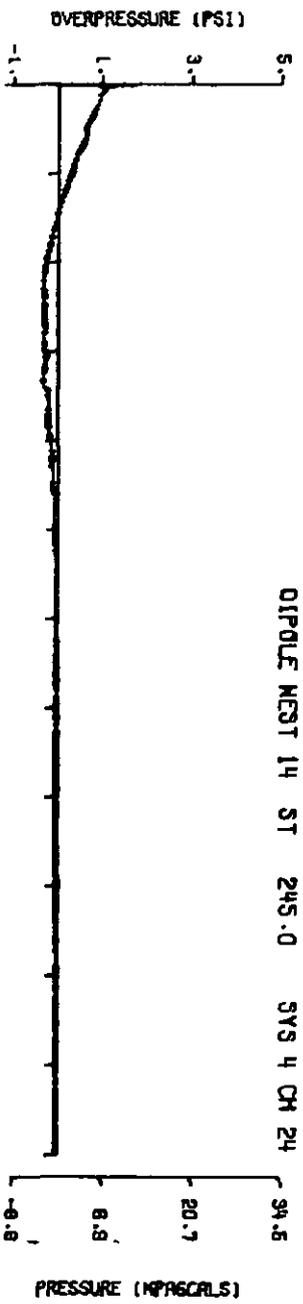
A14.39

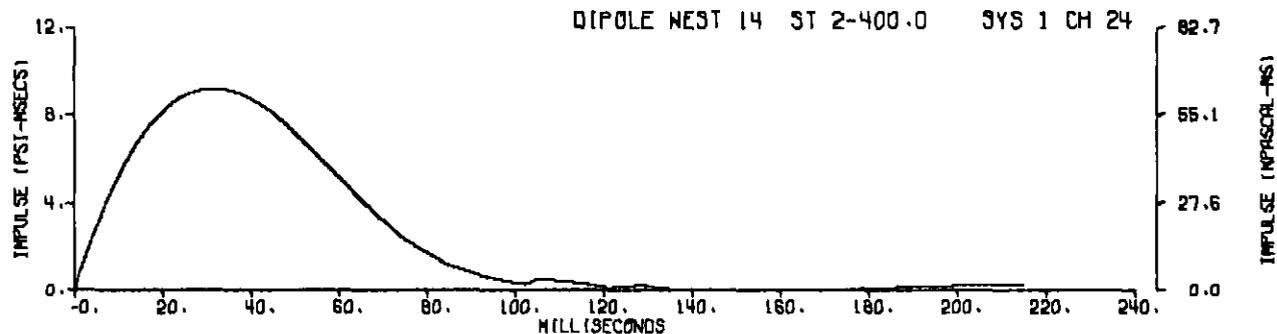
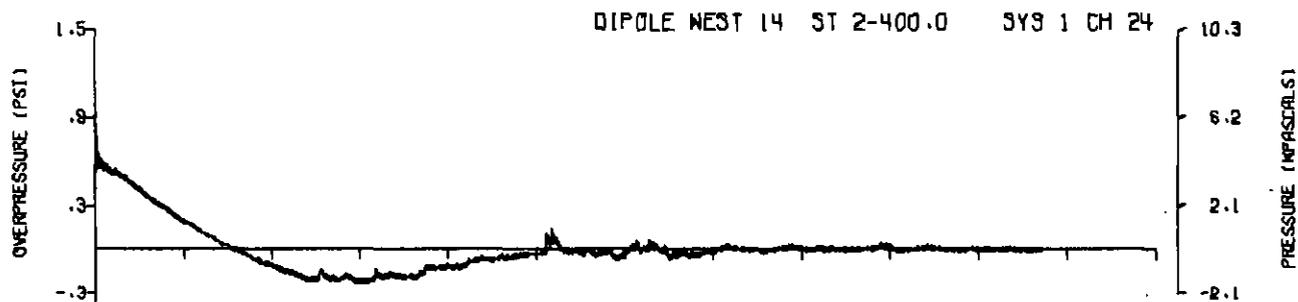
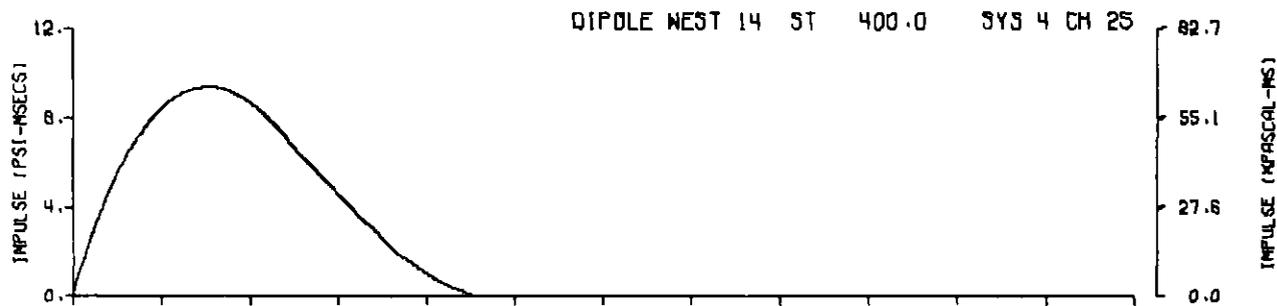
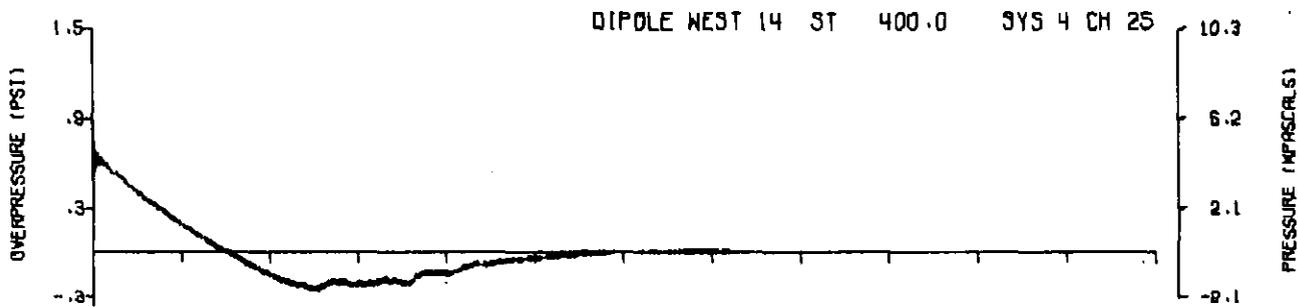


AT14.40

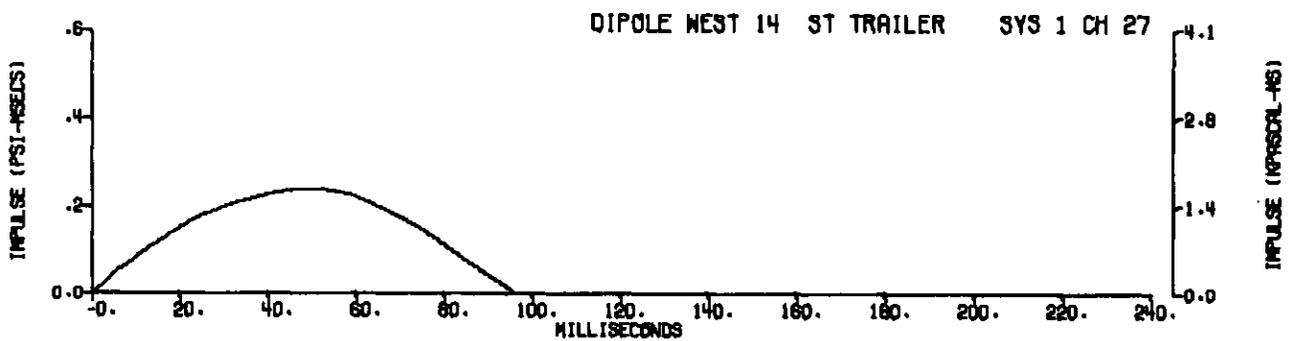
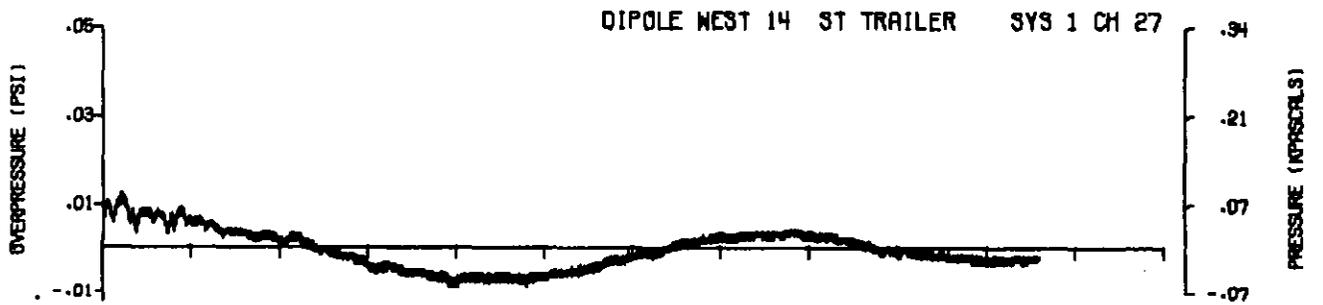
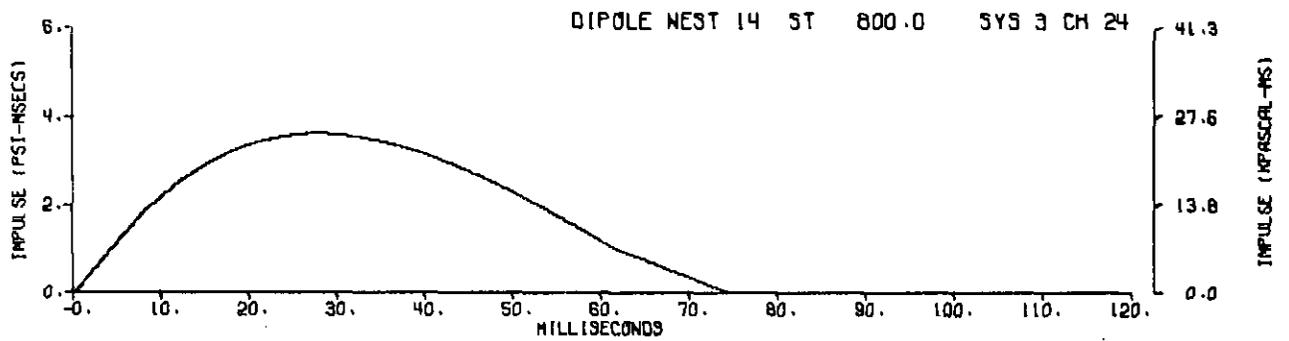
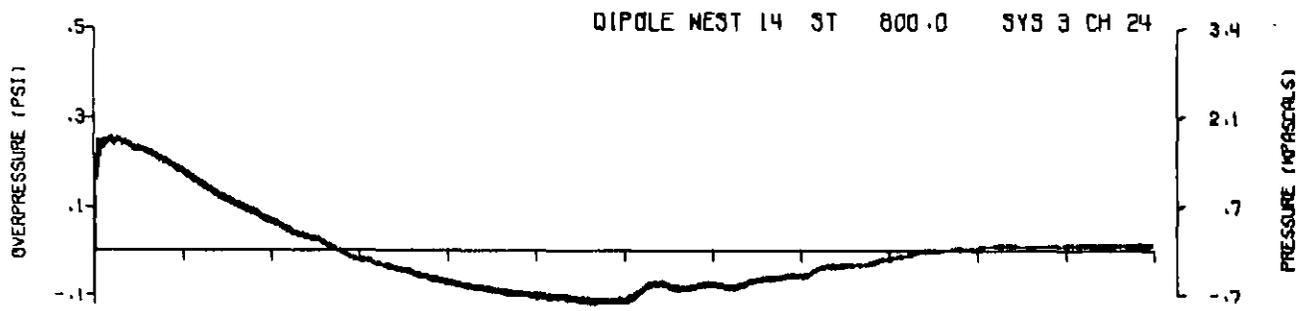


A14.47



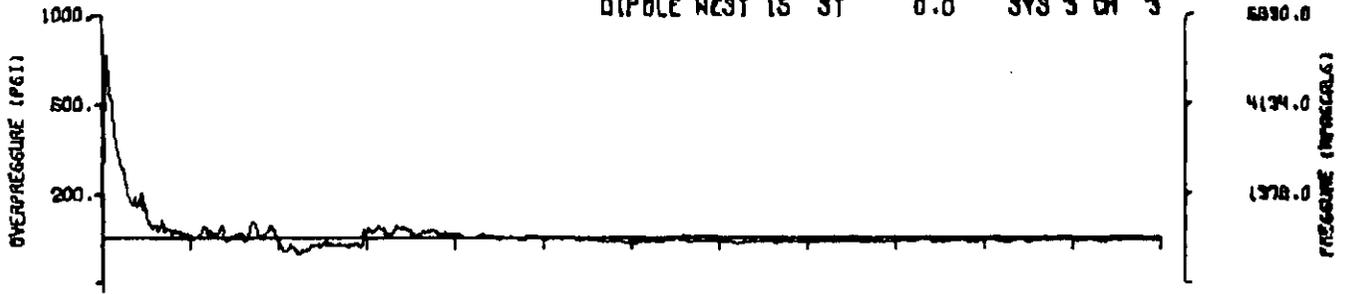


A14.43

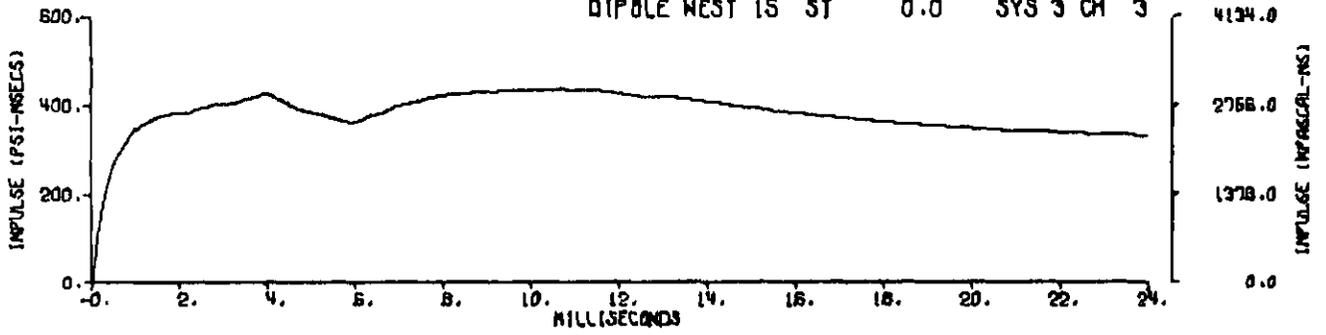


A14.44

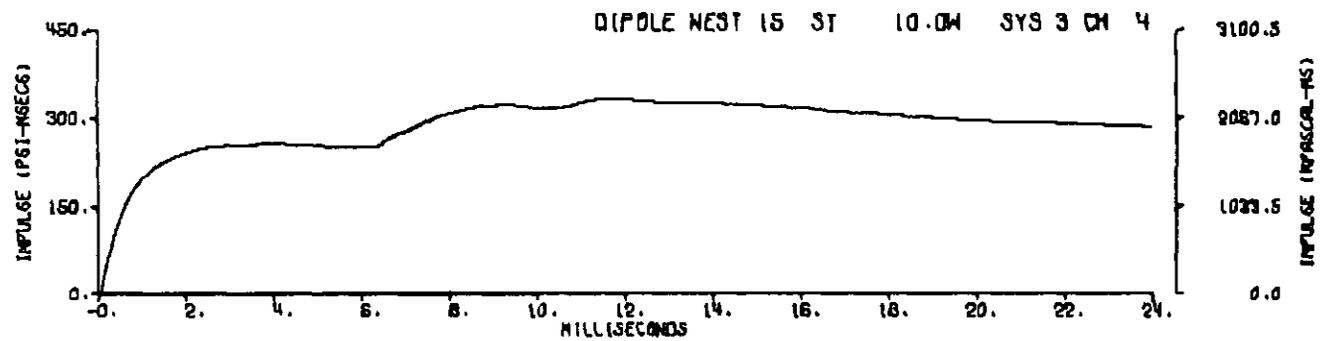
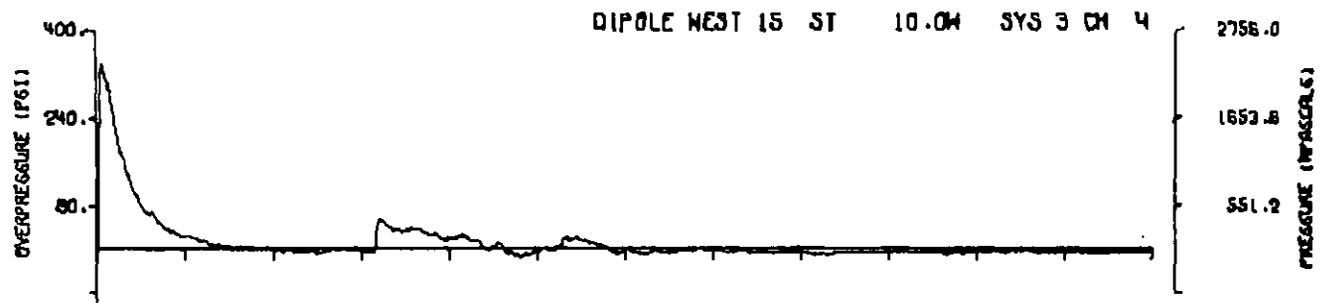
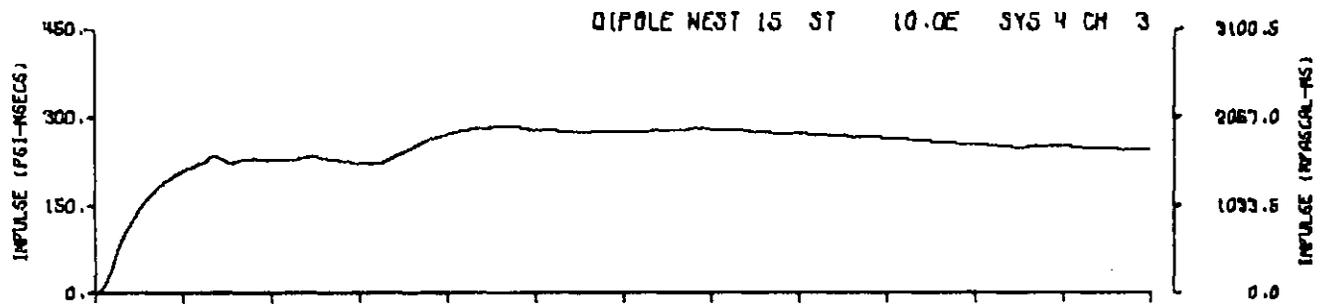
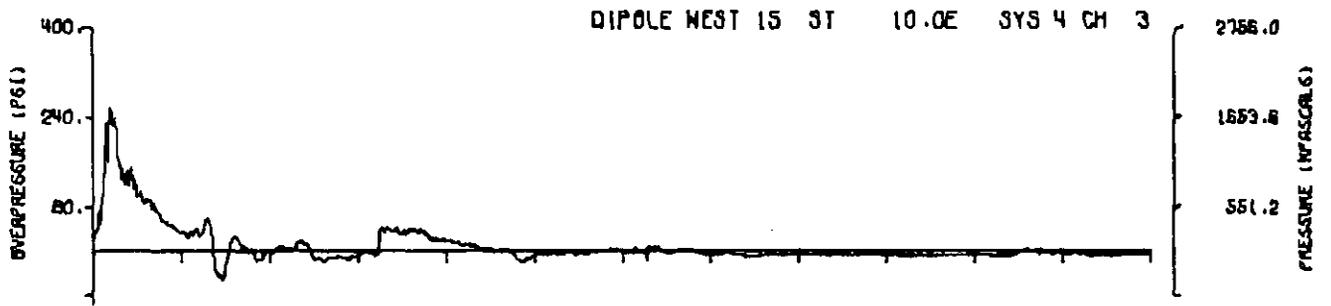
DIPOLE WEST 15 ST 0.0 SYS 3 CH 3



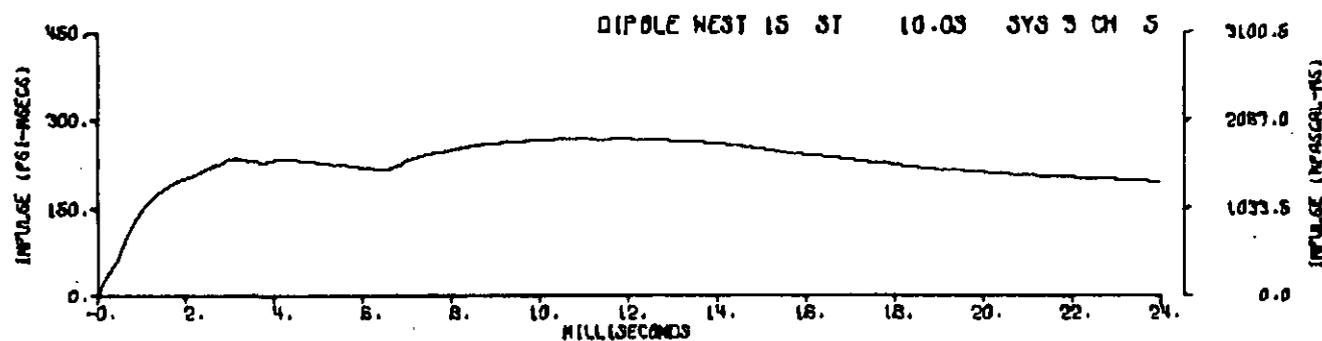
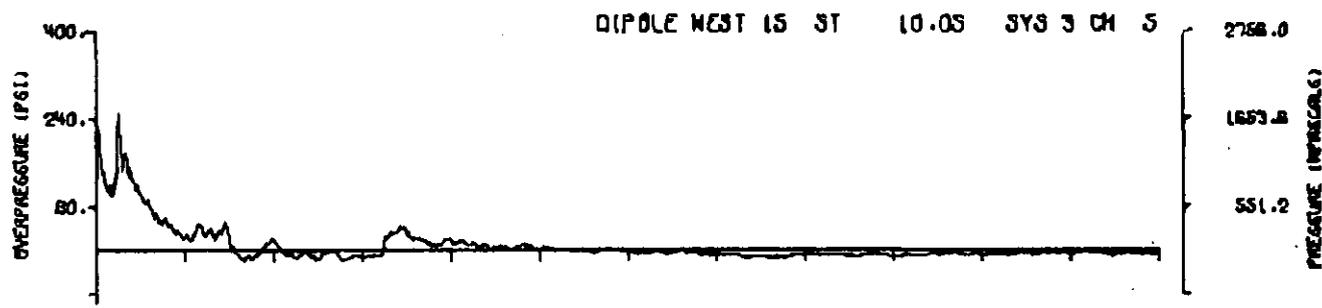
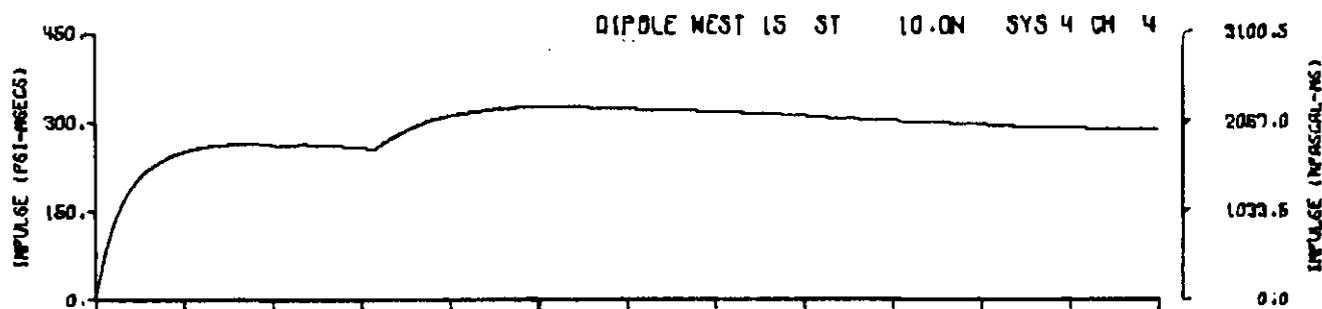
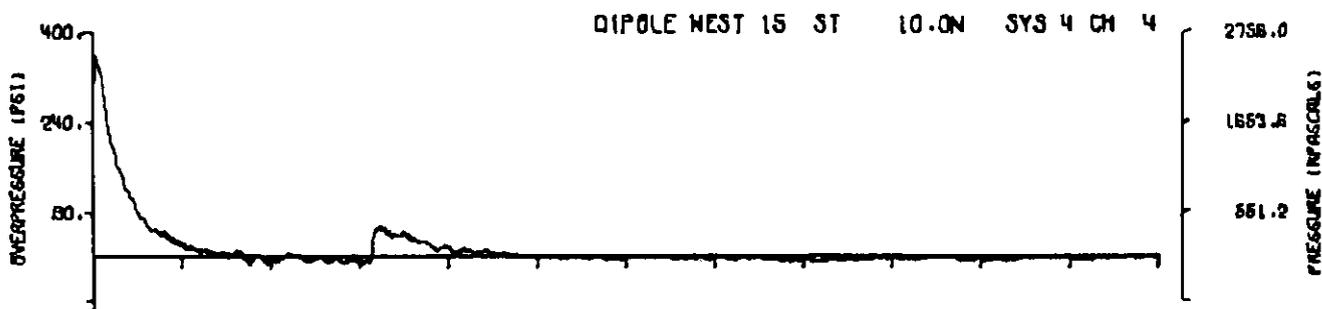
DIPOLE WEST 15 ST 0.0 SYS 3 CH 3



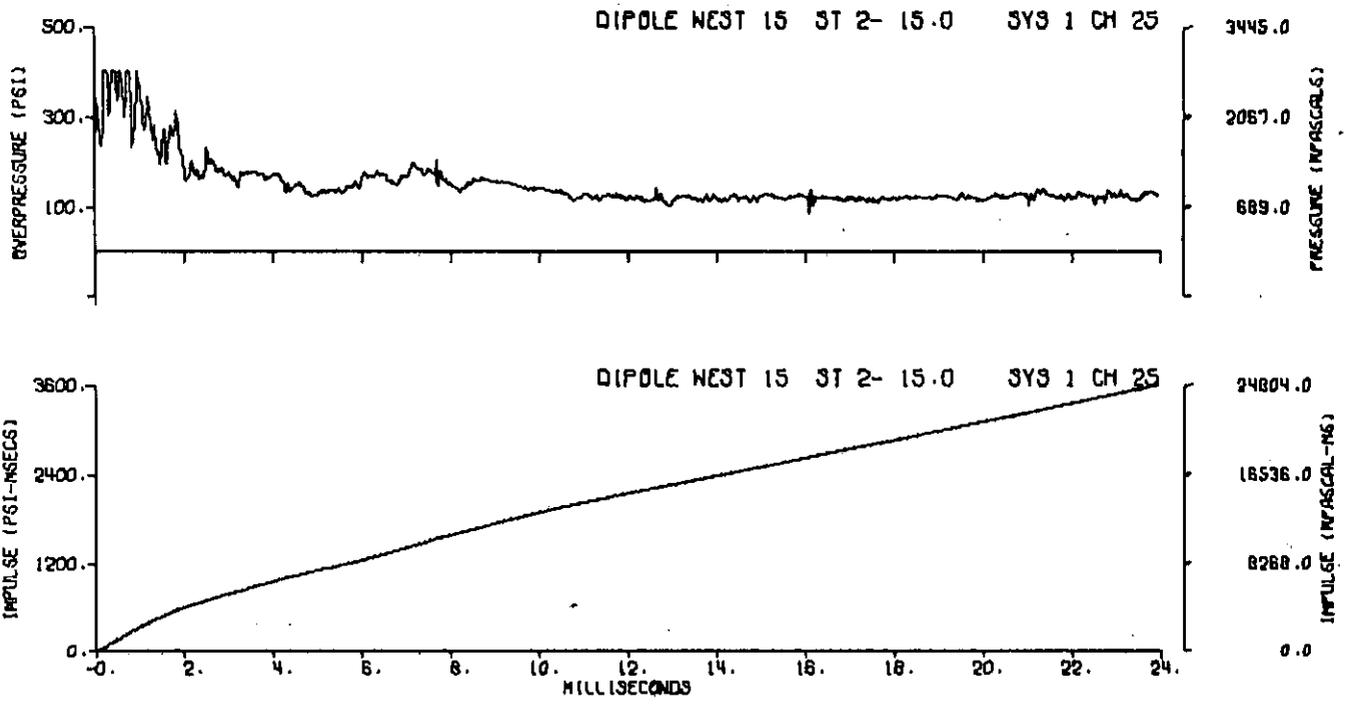
A15.1



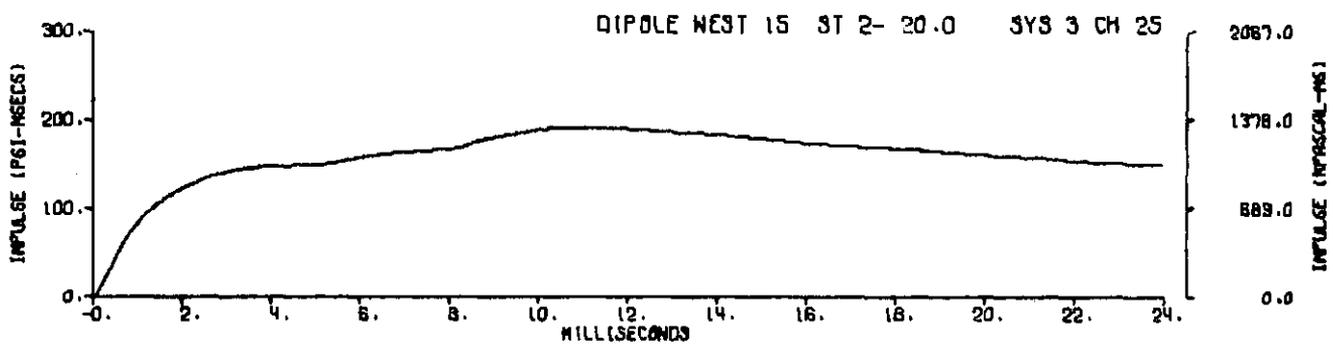
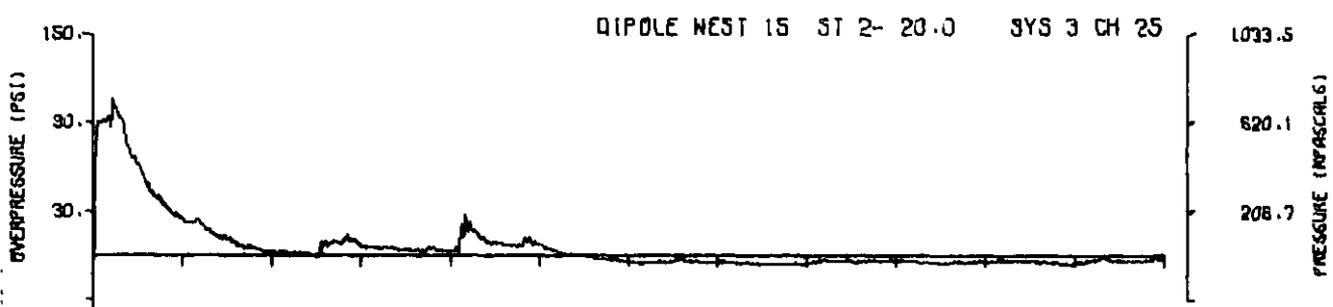
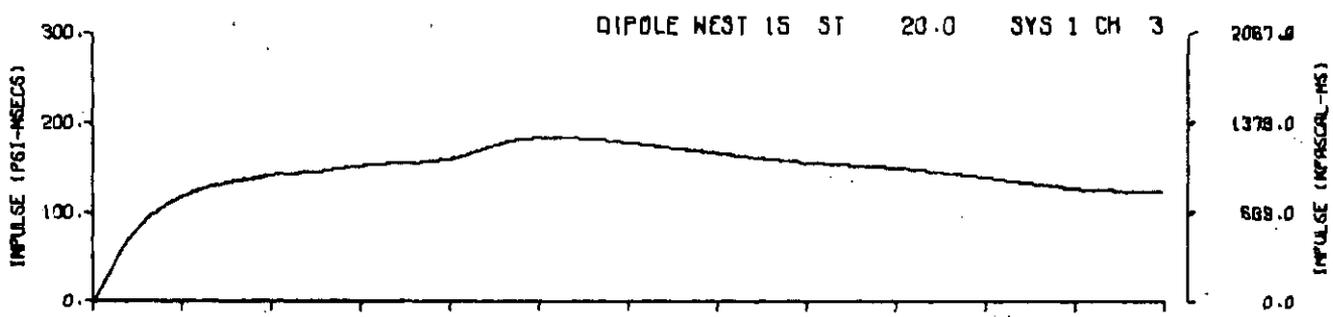
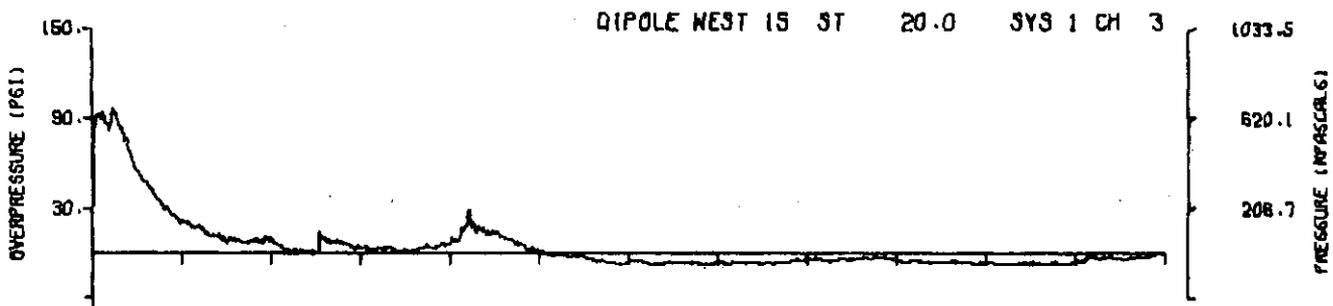
A15.2

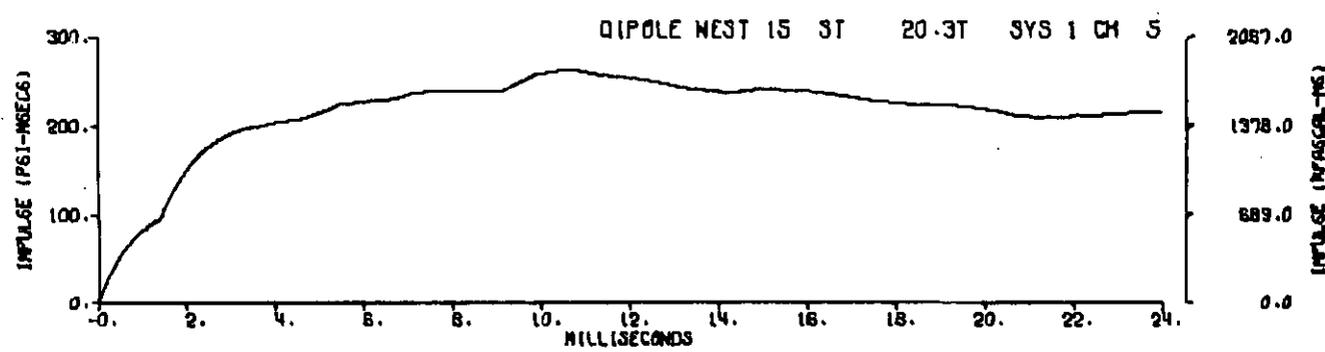
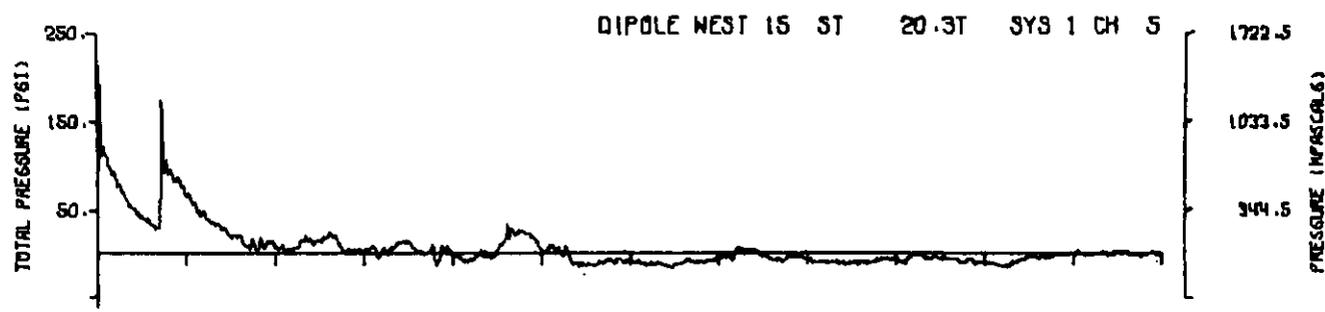
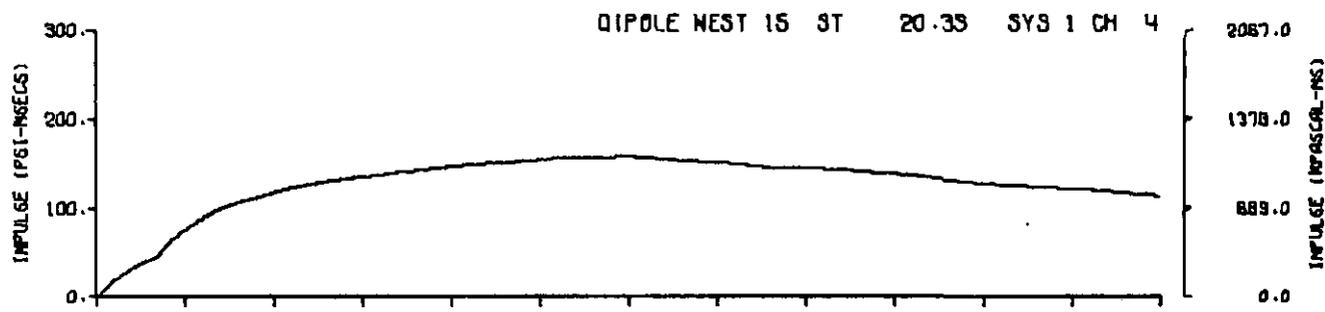
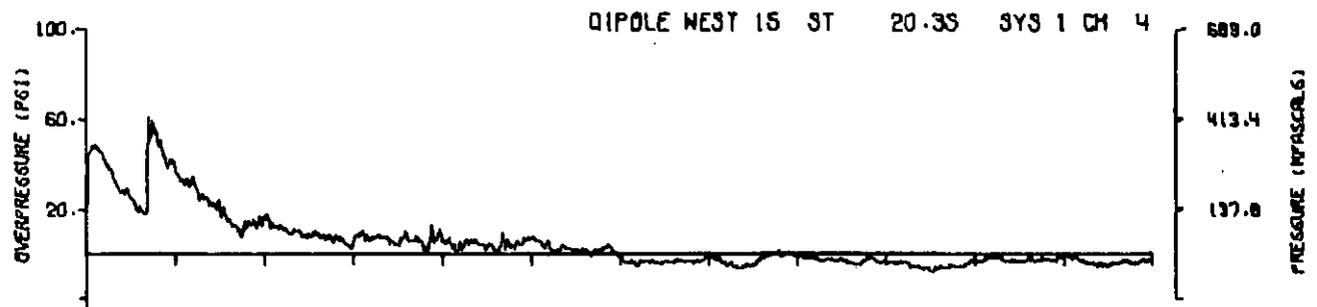


A15.3

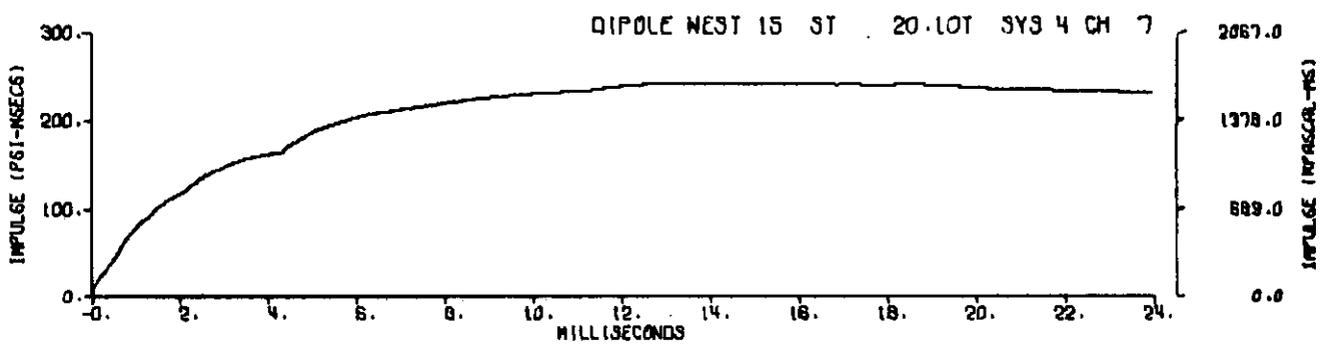
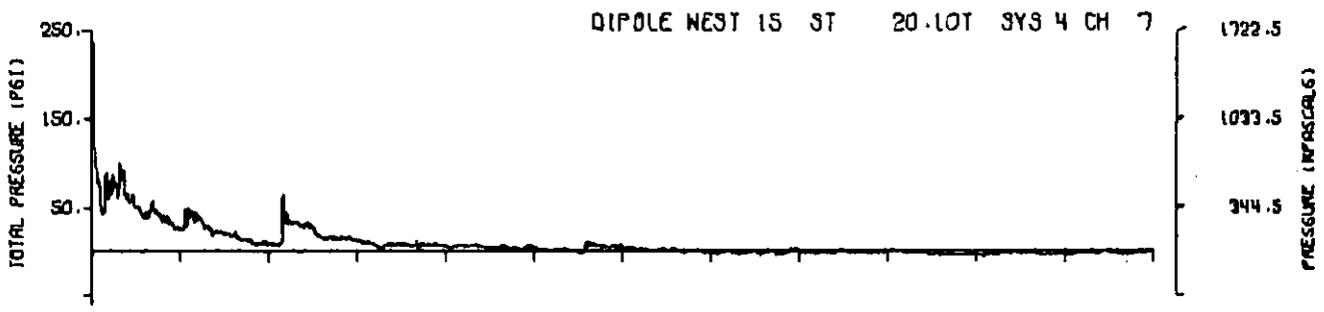
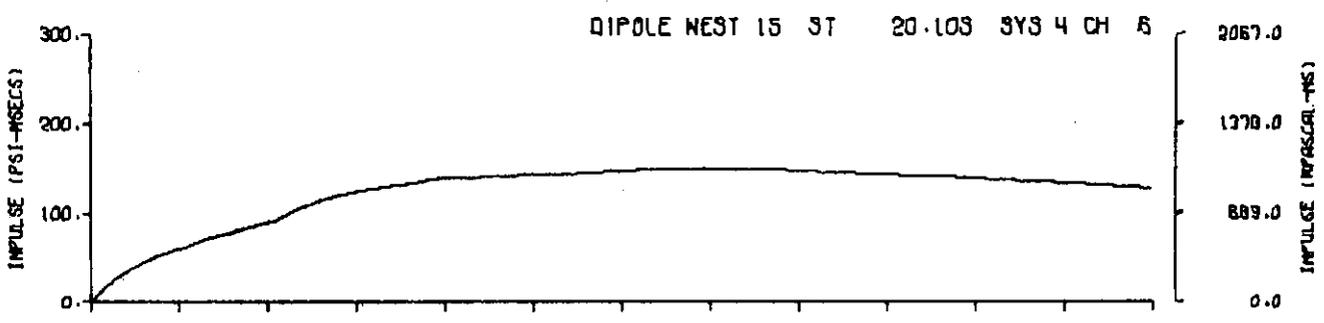
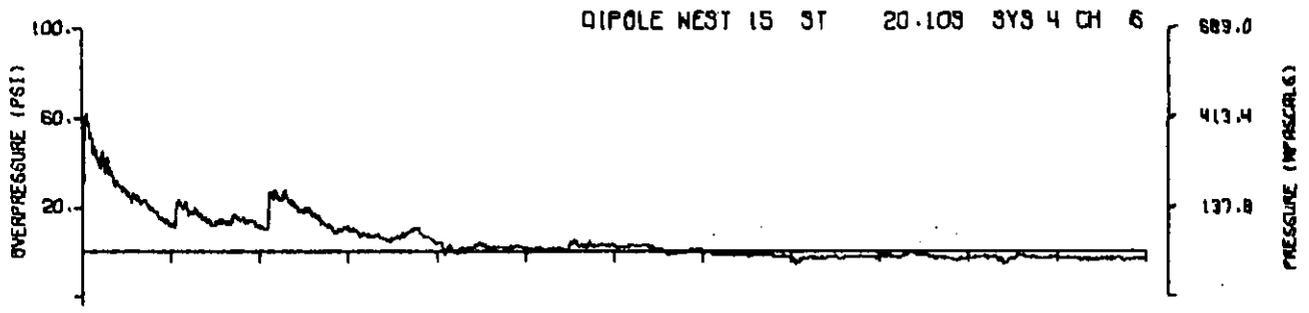


A15.4

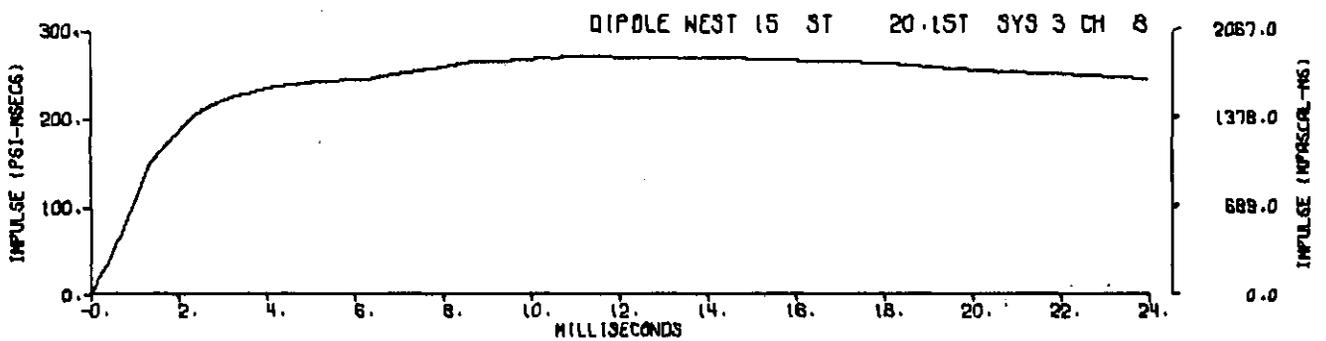
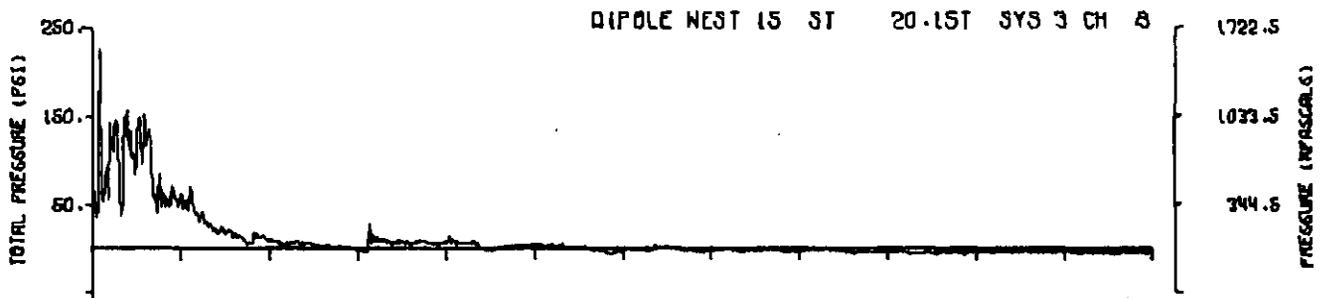
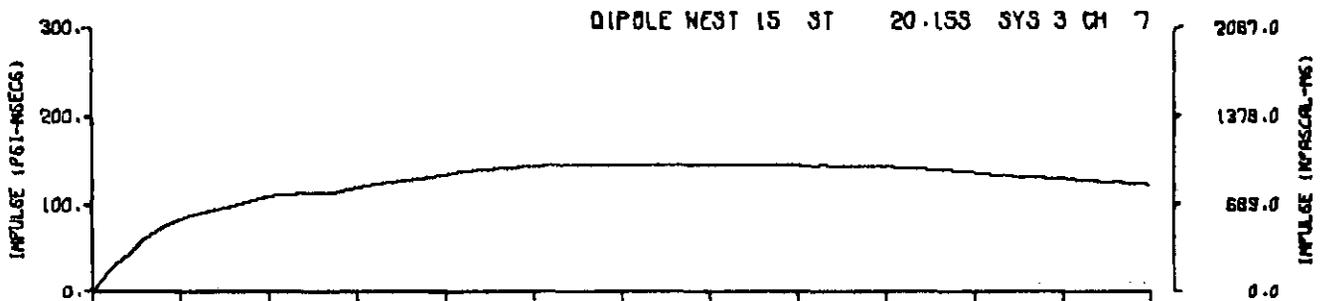
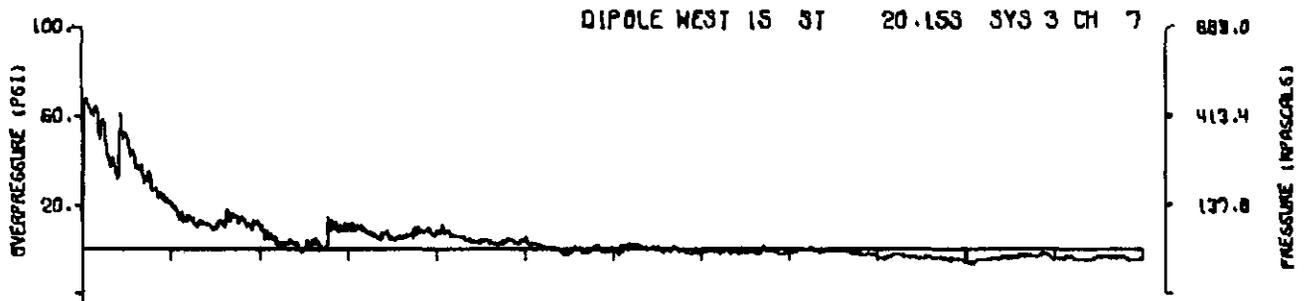




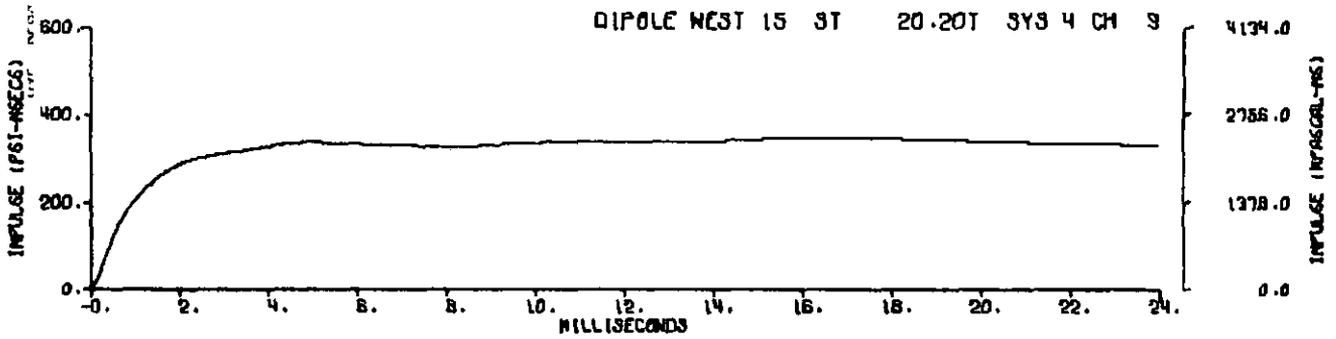
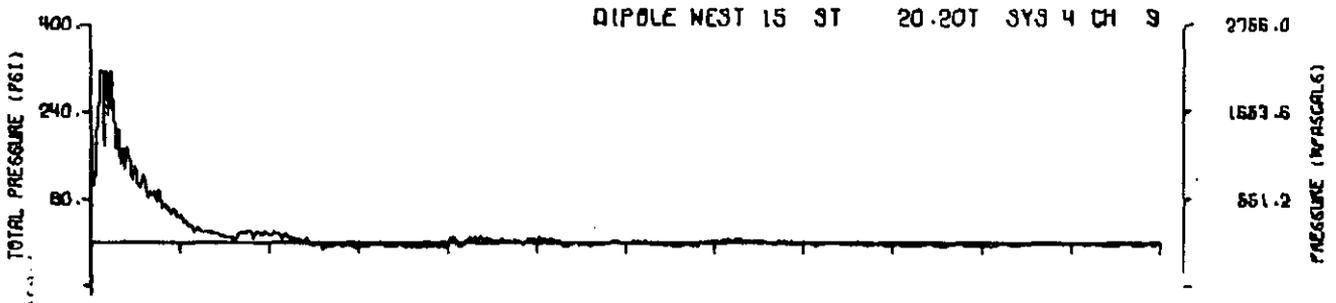
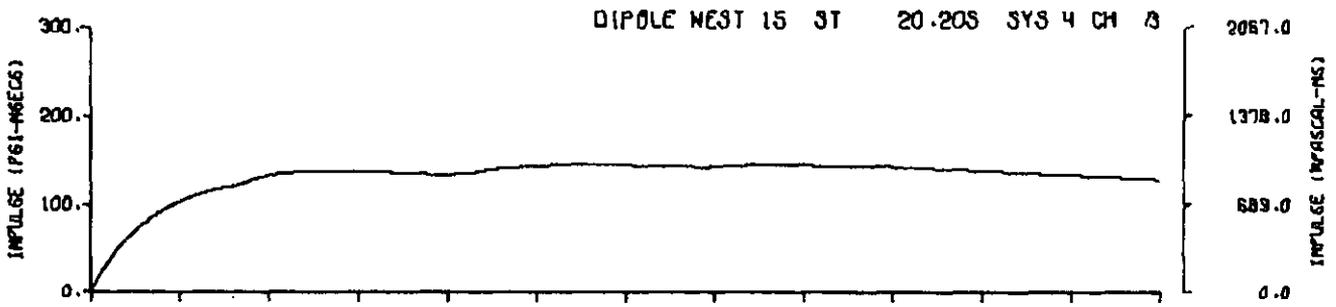
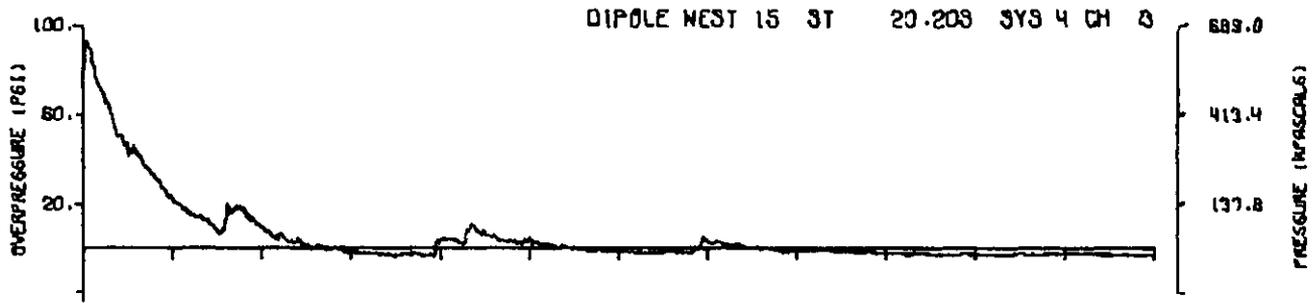
A15.6



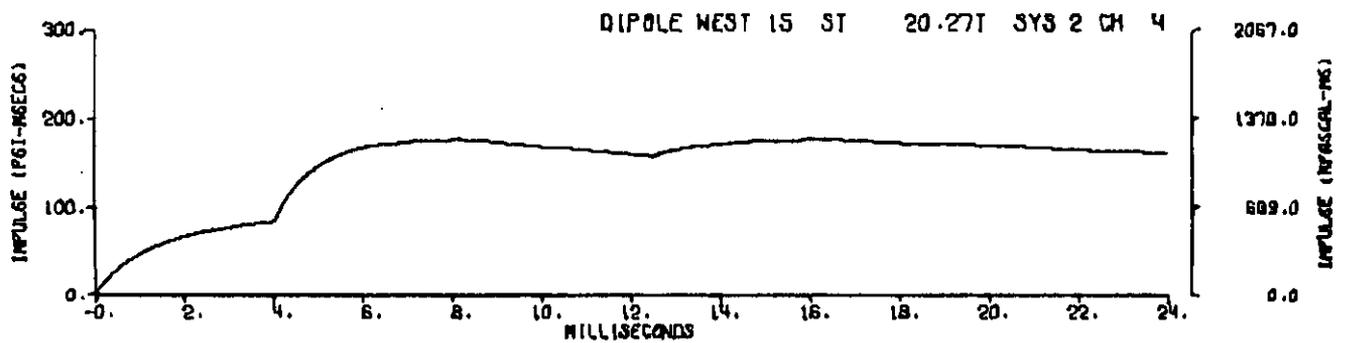
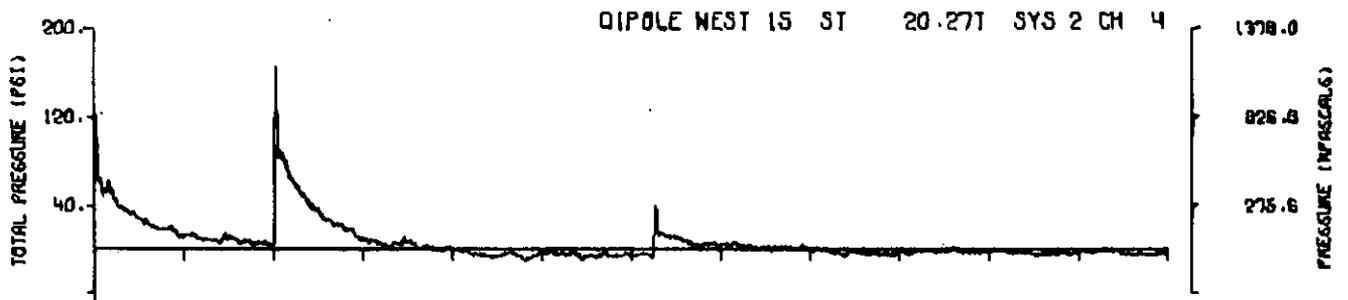
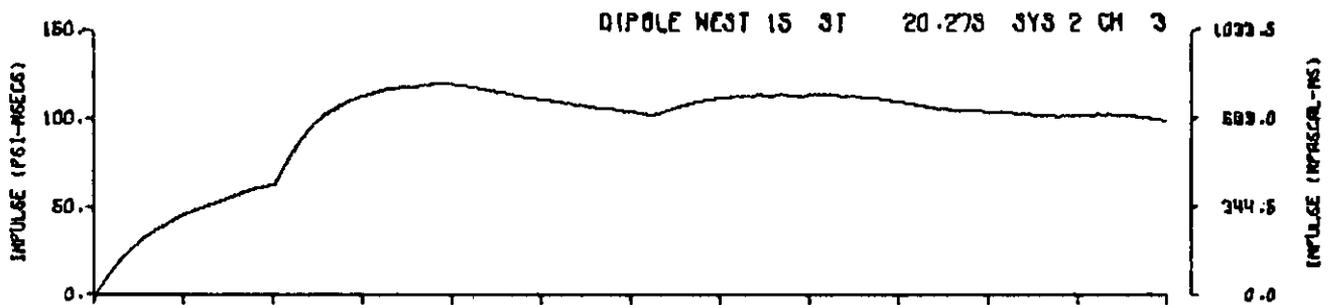
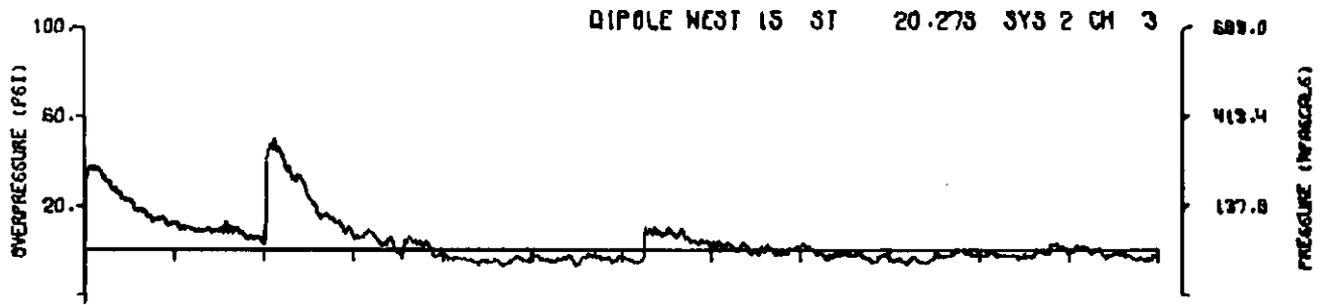
A15.7



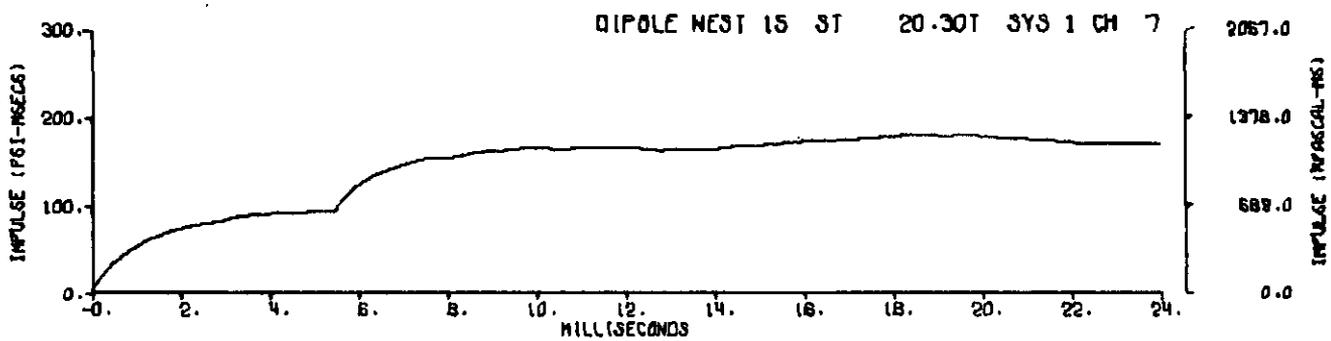
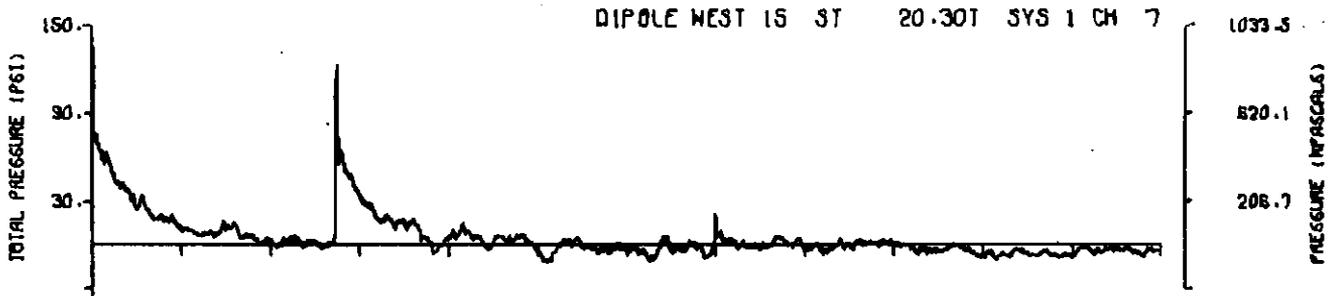
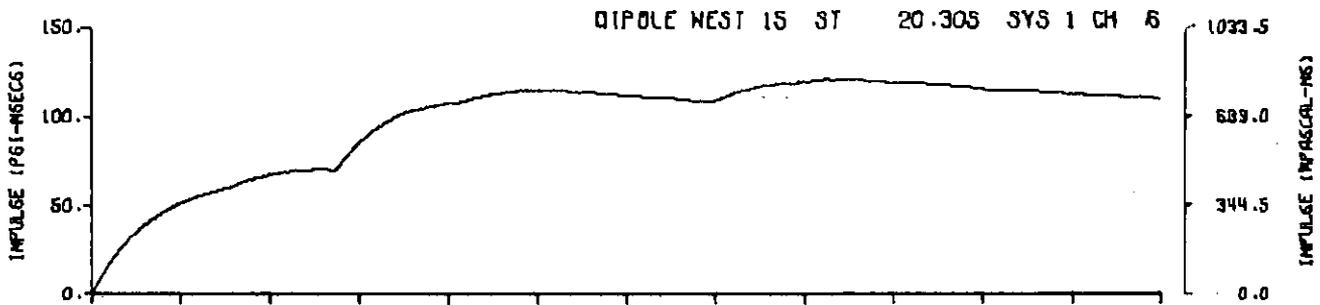
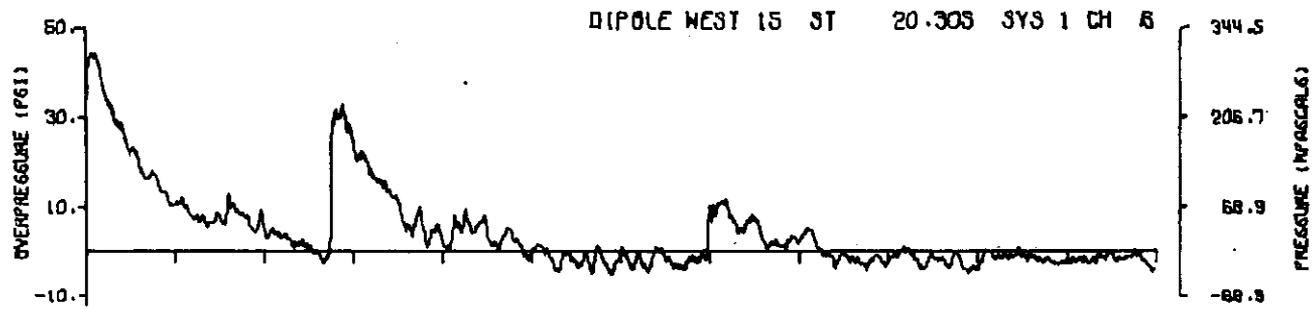
A15.8



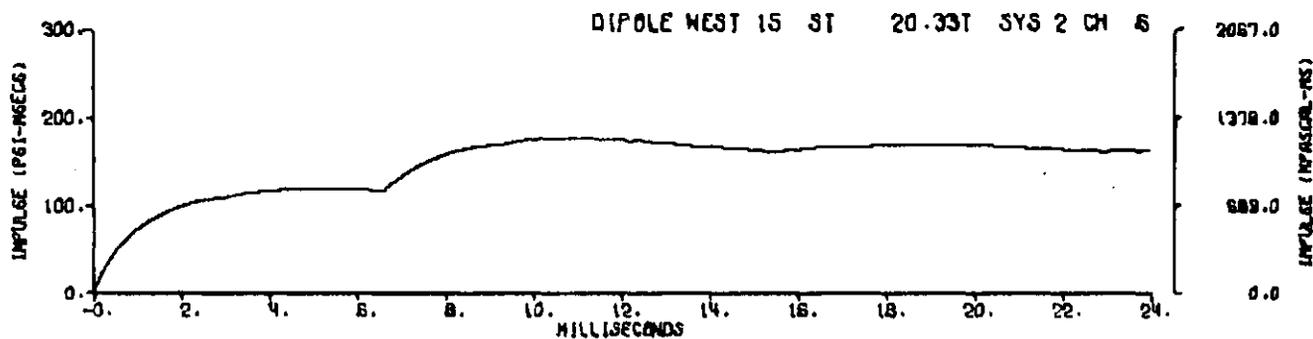
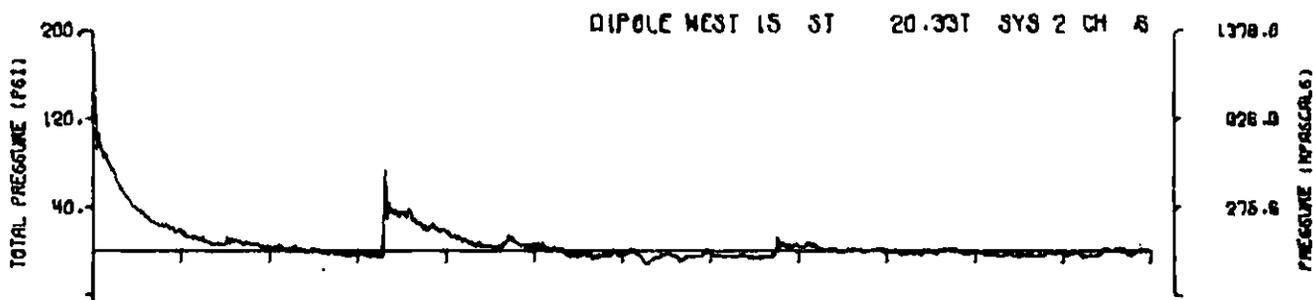
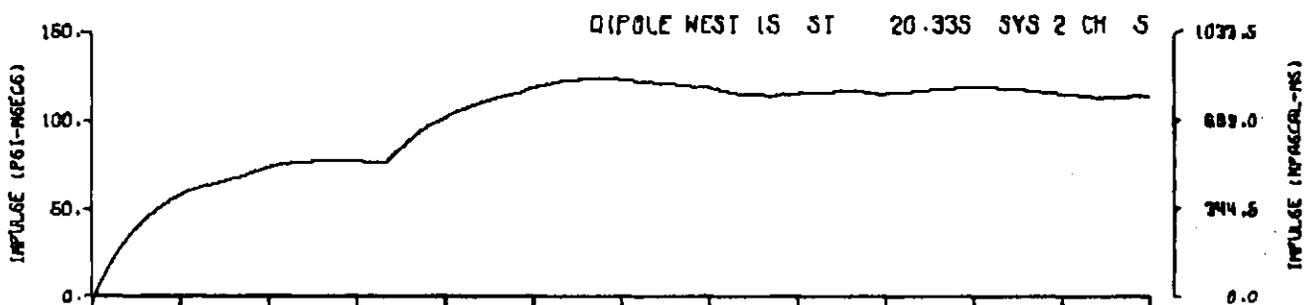
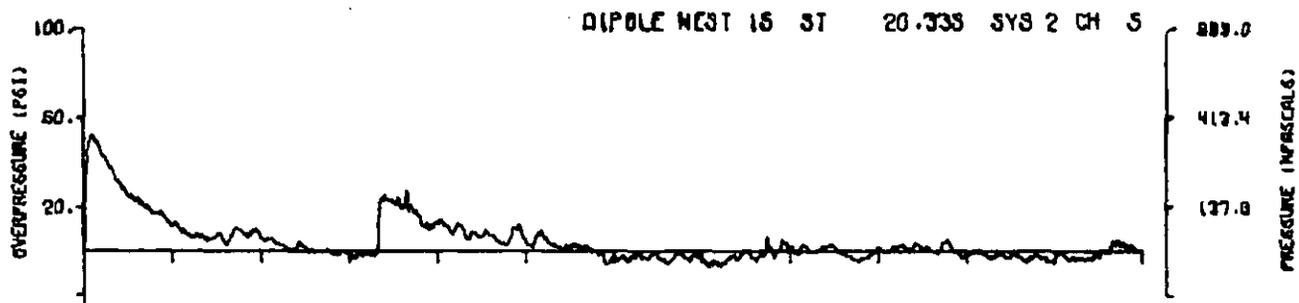
A15.9



A15.10

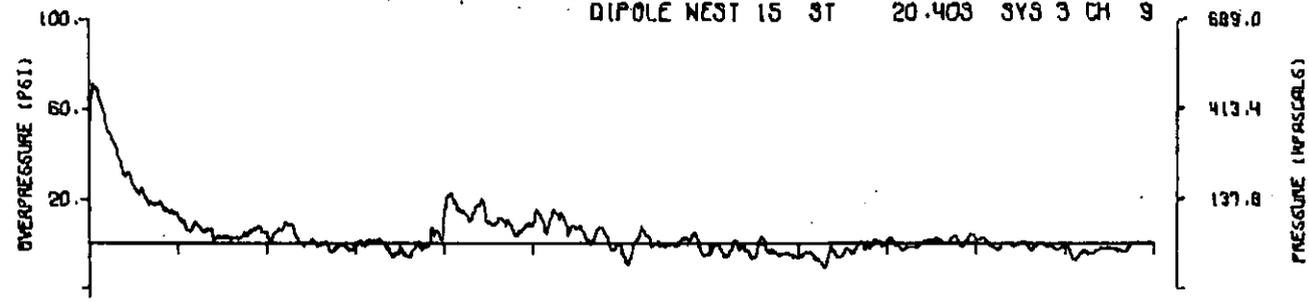


A15.11

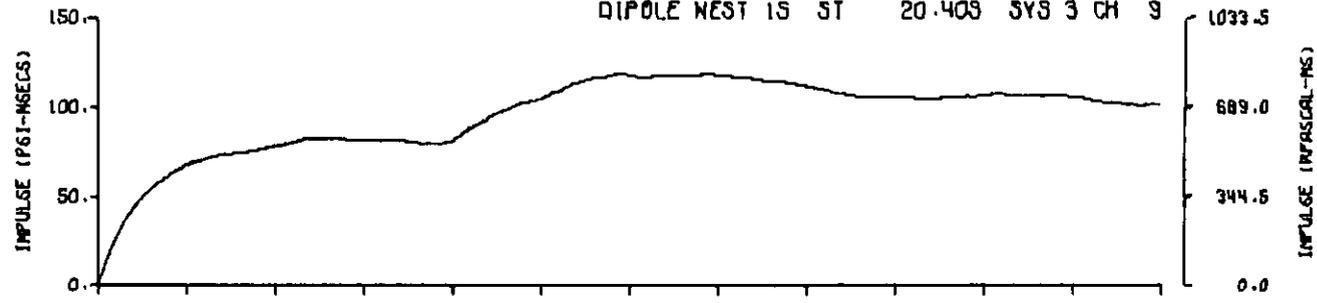


A15.12

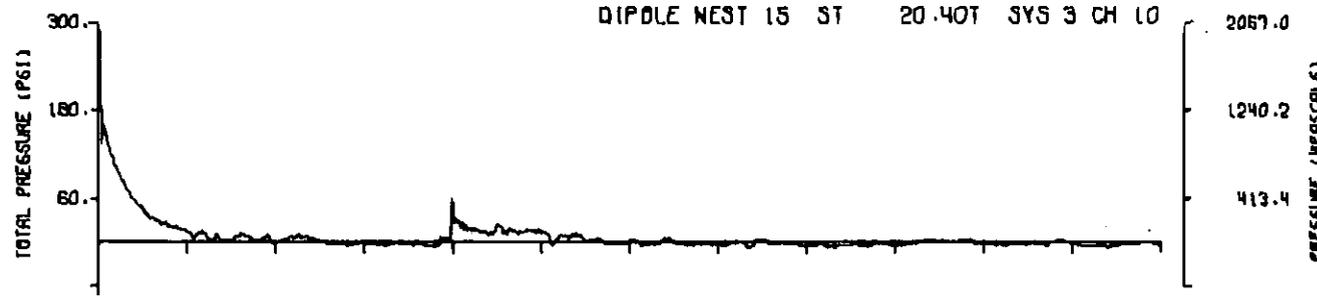
DIPOLE NEST 15 ST 20.403 SYS 3 CH 9



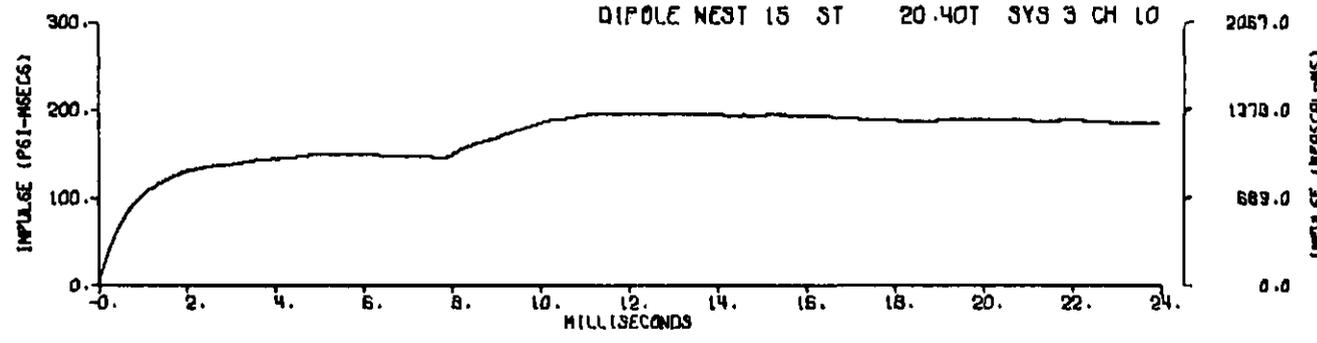
DIPOLE NEST 15 ST 20.403 SYS 3 CH 9



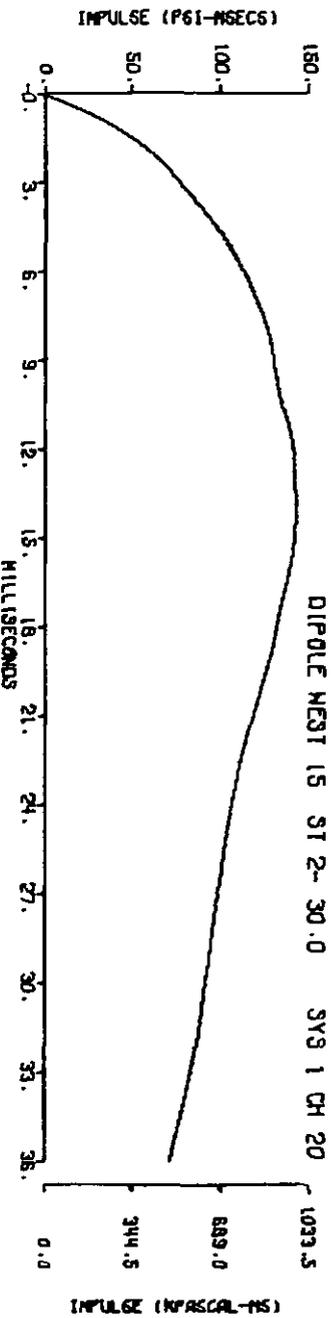
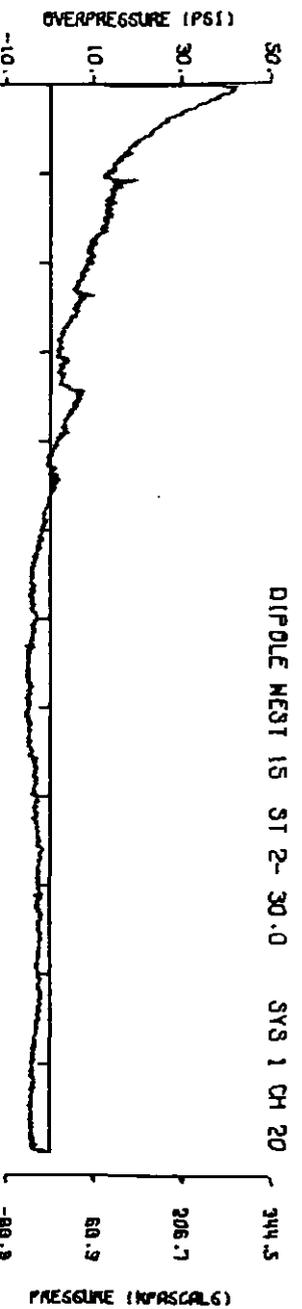
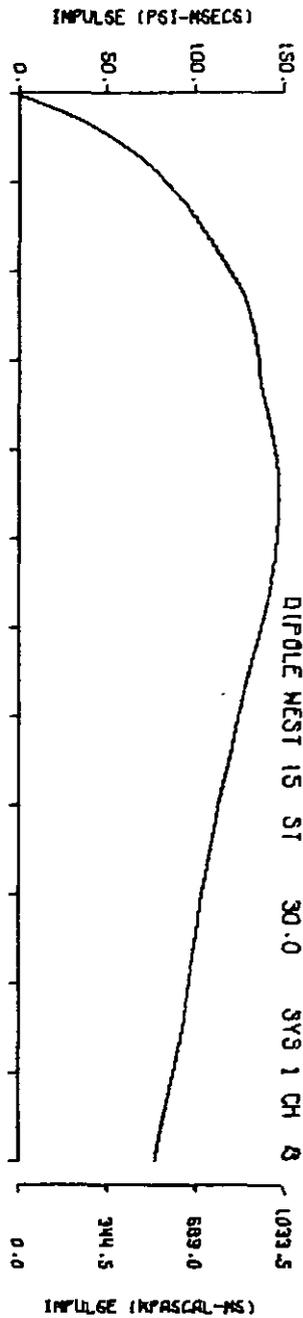
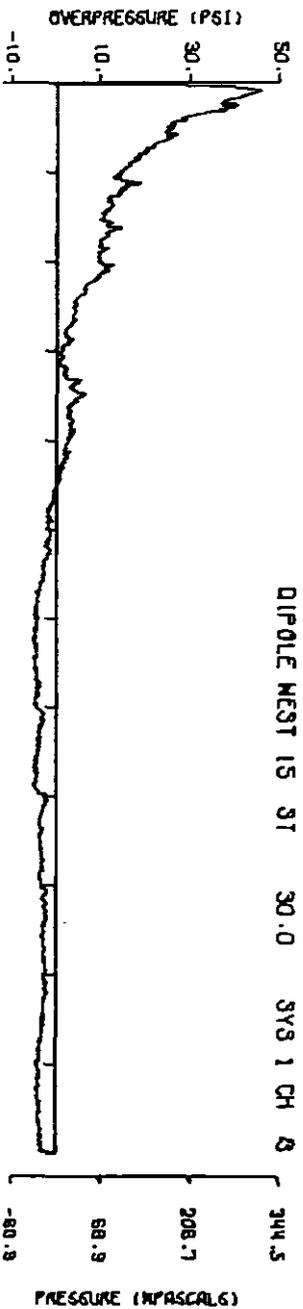
DIPOLE NEST 15 ST 20.407 SYS 3 CH 10



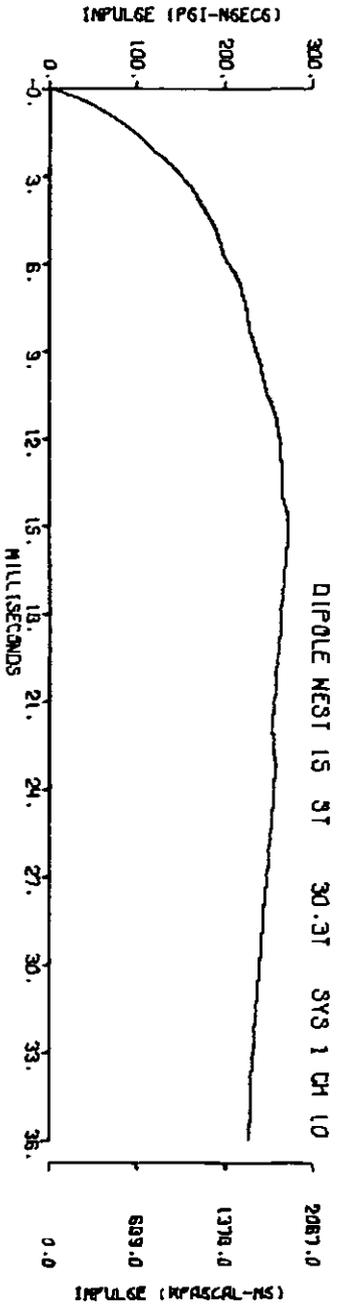
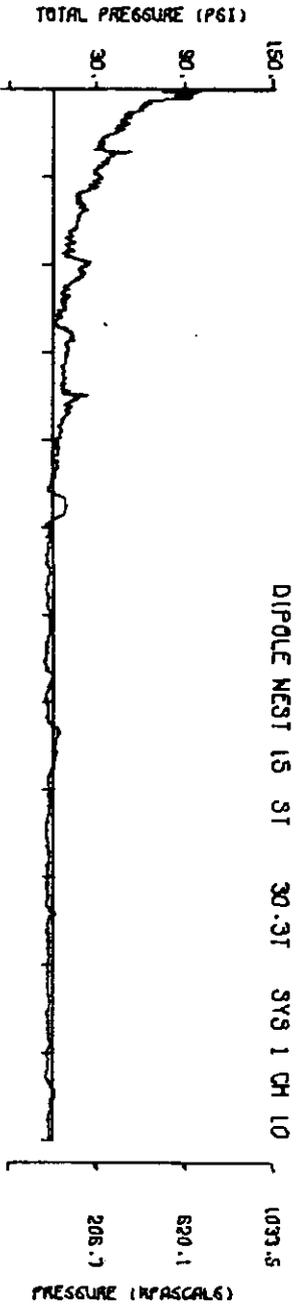
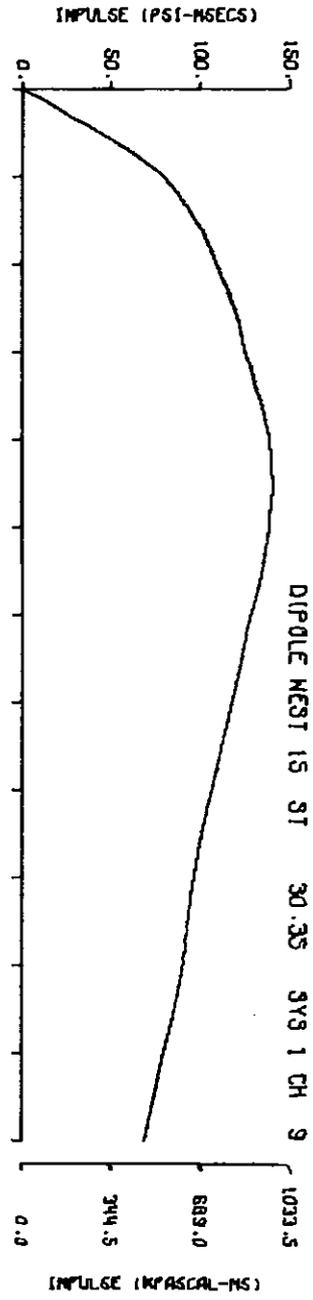
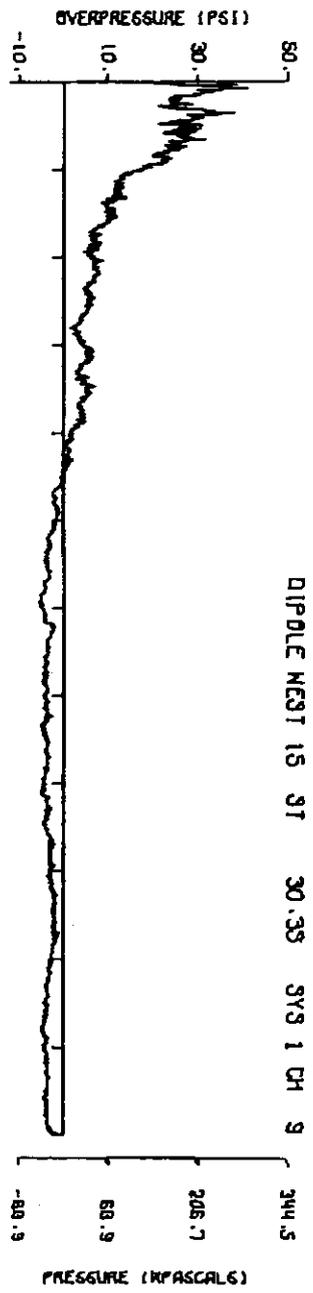
DIPOLE NEST 15 ST 20.407 SYS 3 CH 10



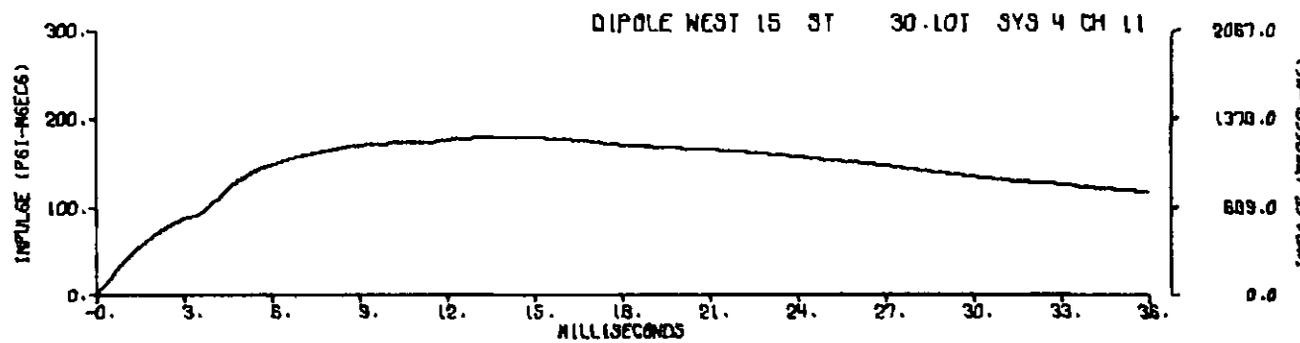
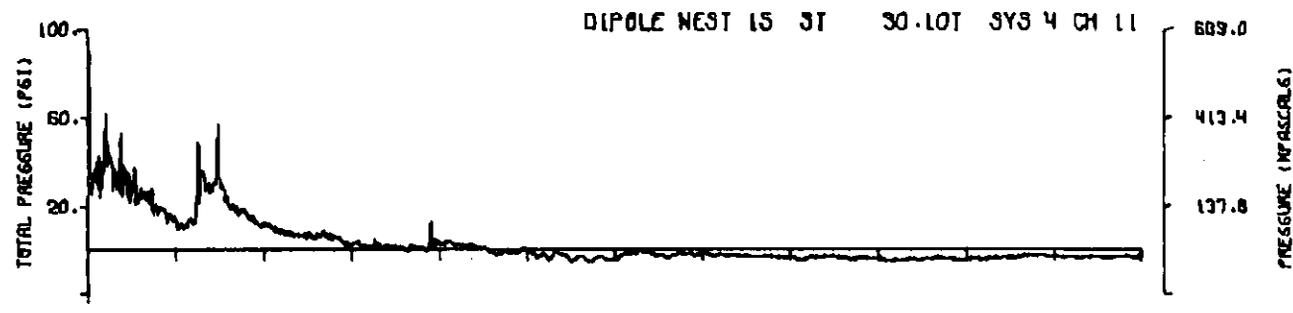
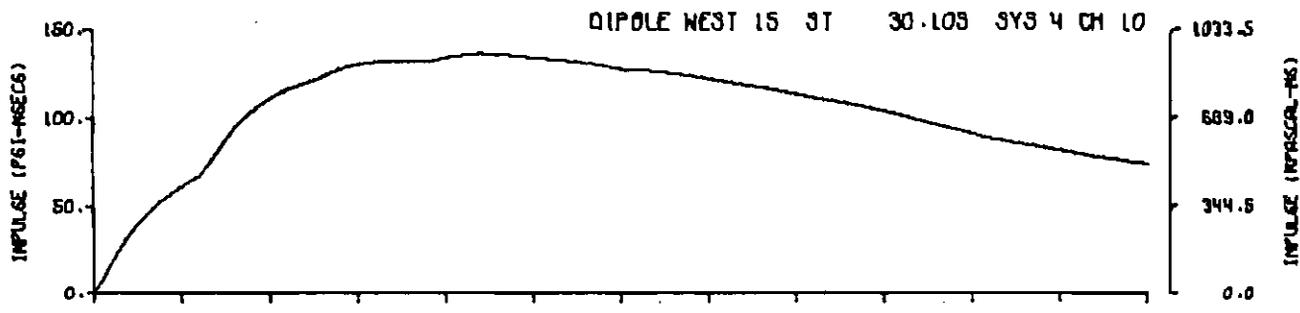
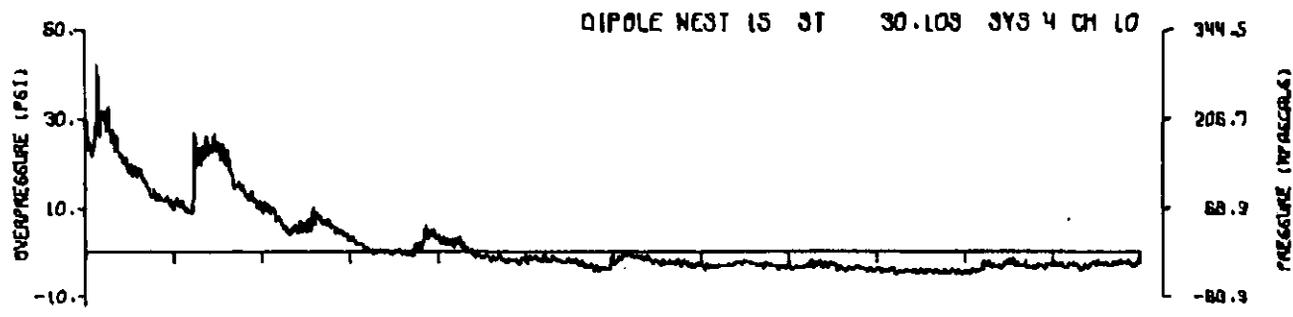
A15.13



A15.14
301

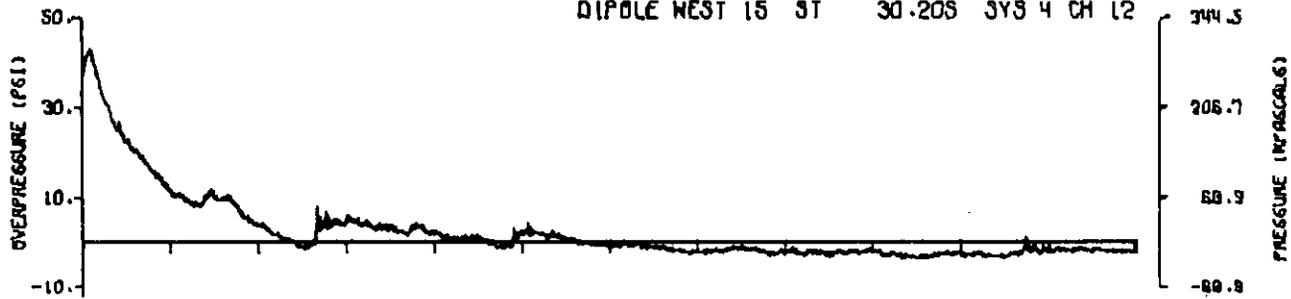


A15.15

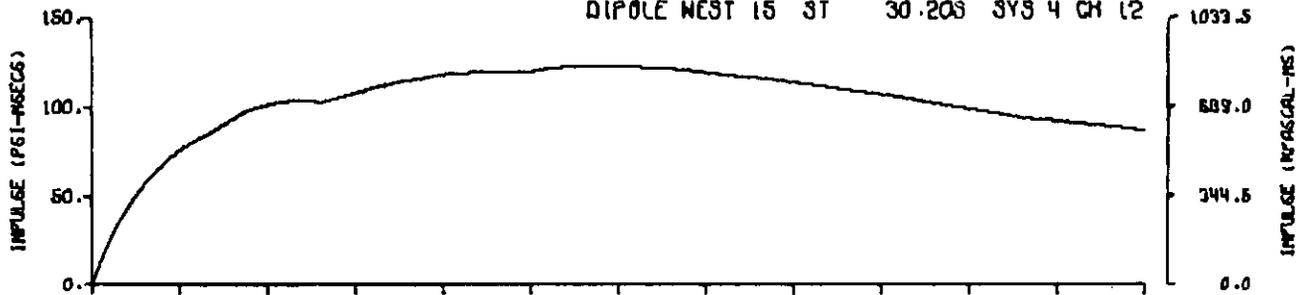


A15.16

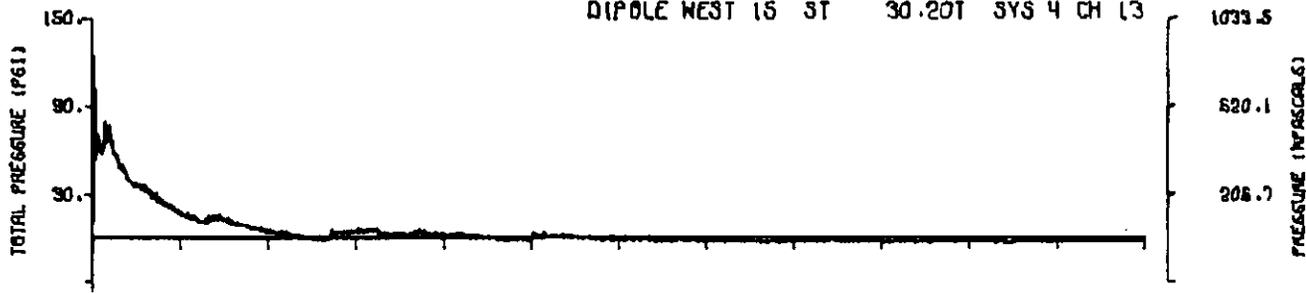
DIPOLE WEST 15 ST 30.20S SYS 4 CH 12



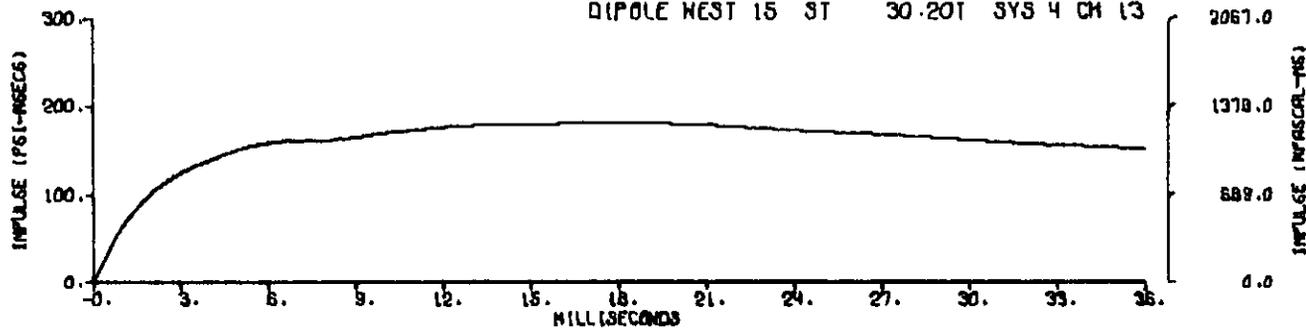
DIPOLE WEST 15 ST 30.20S SYS 4 CH 12



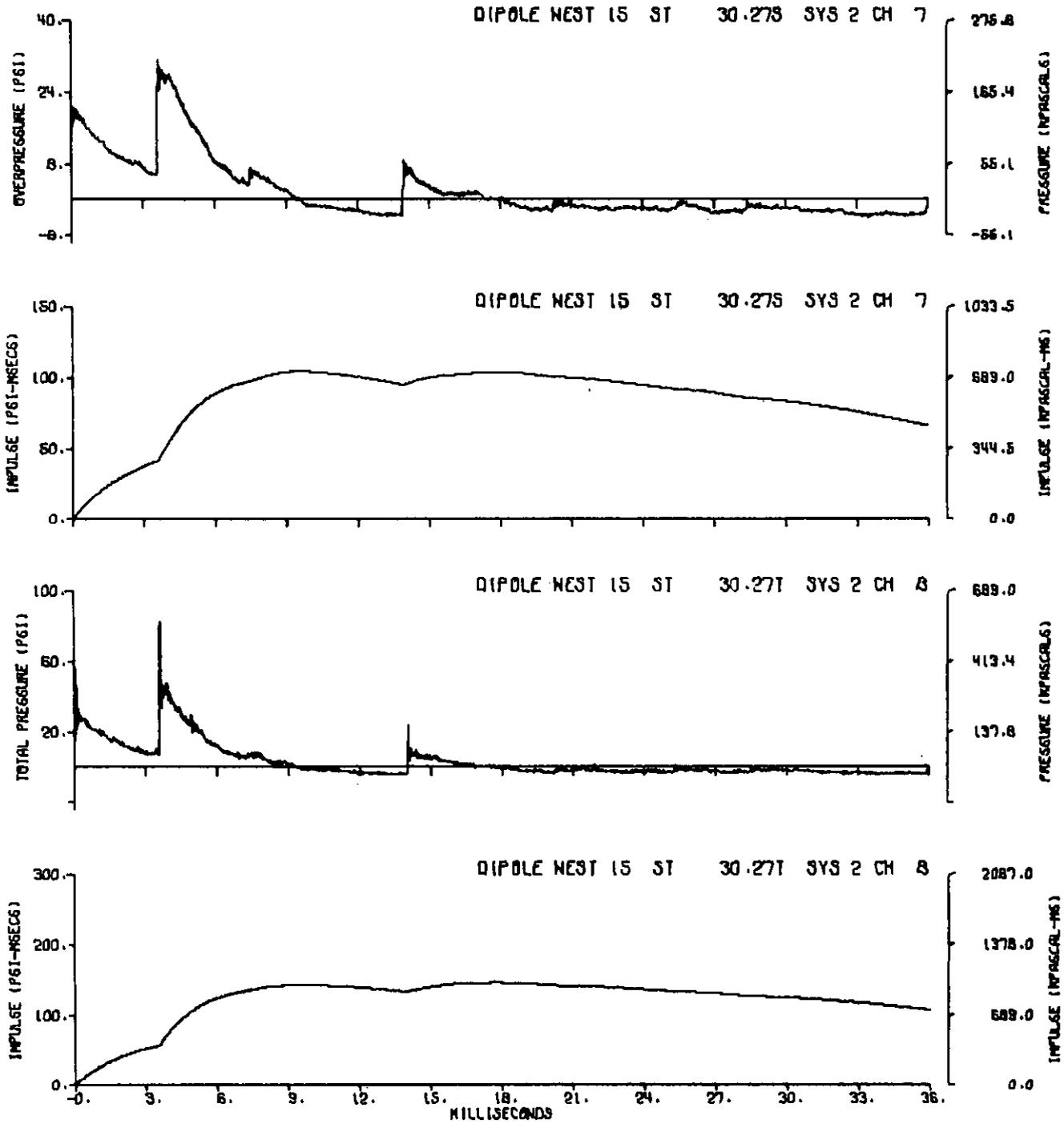
DIPOLE WEST 15 ST 30.20T SYS 4 CH 13



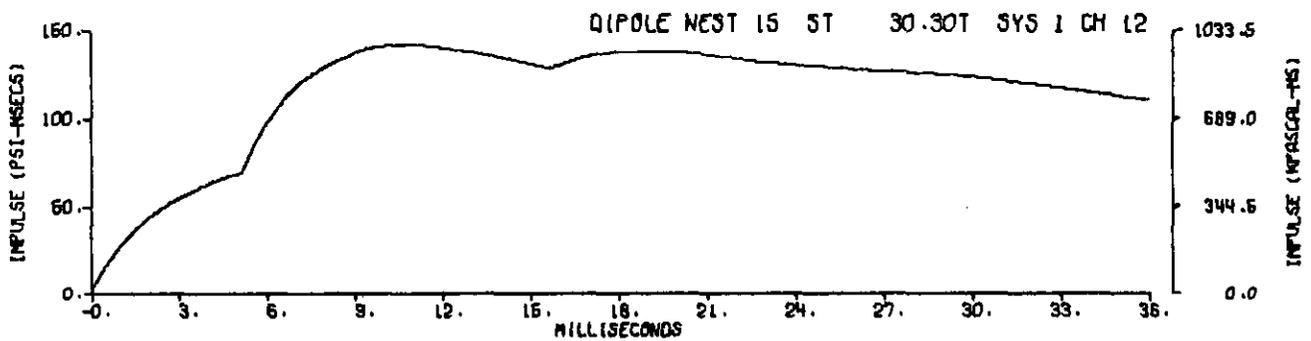
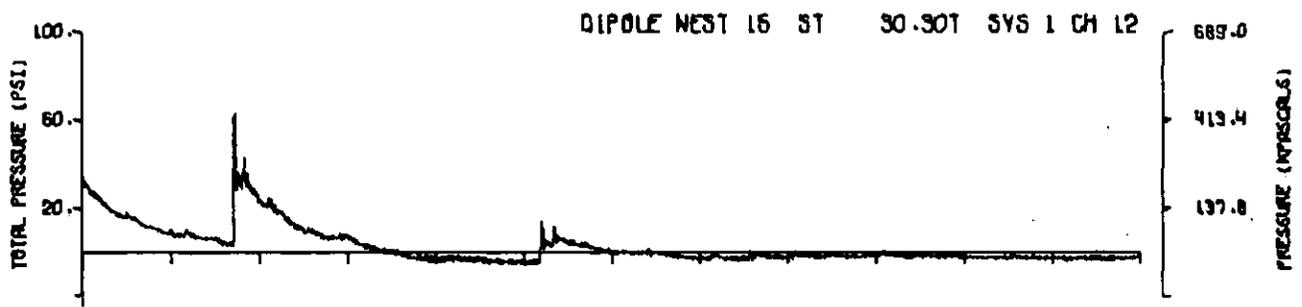
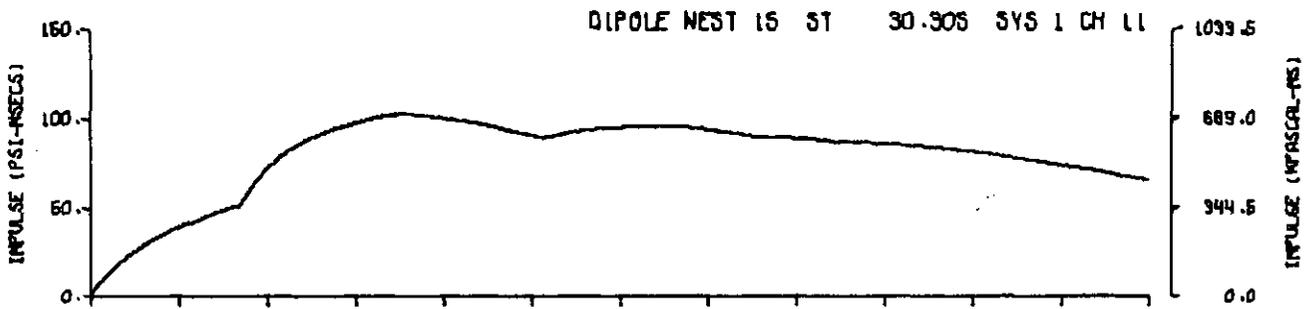
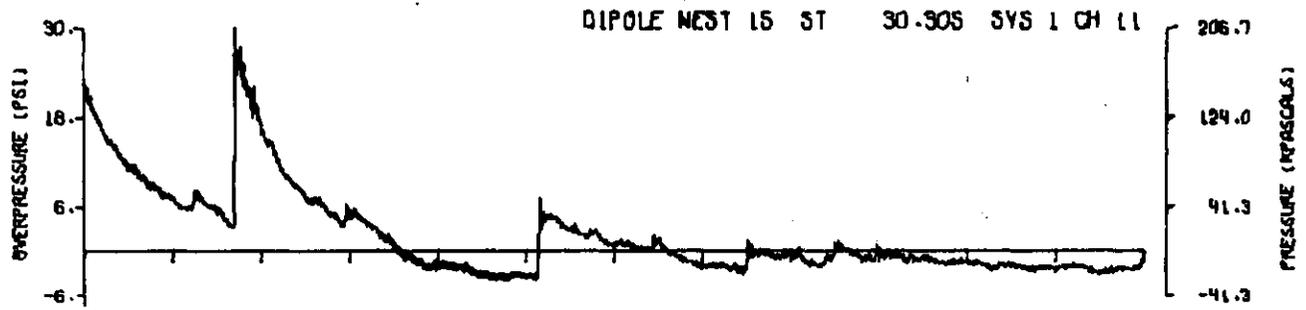
DIPOLE WEST 15 ST 30.20T SYS 4 CH 13



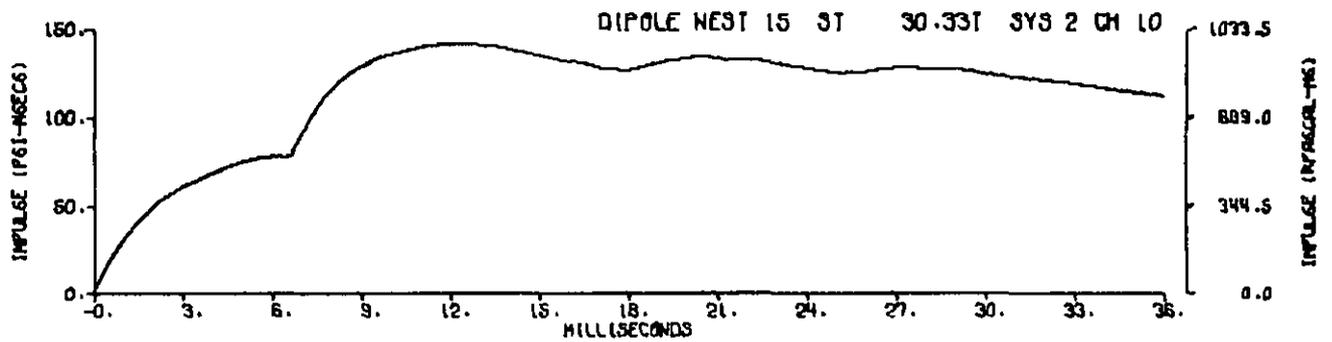
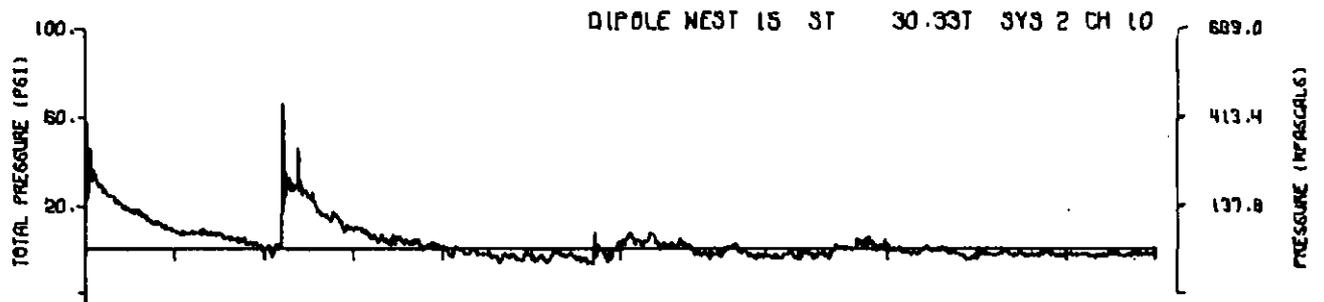
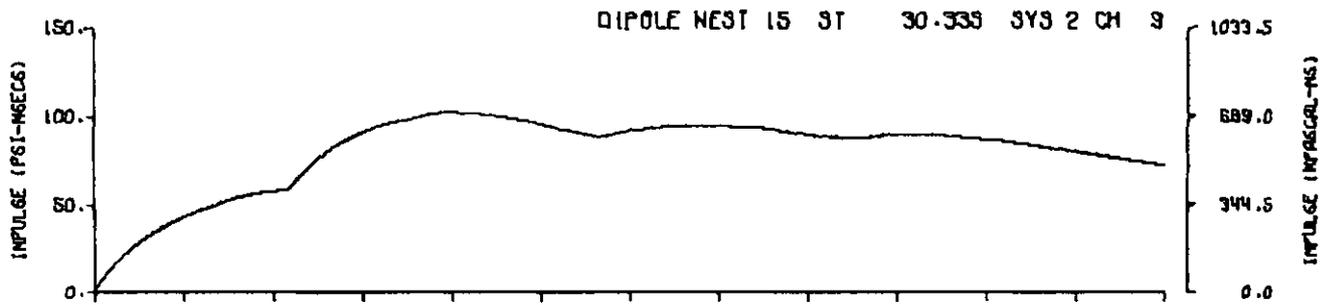
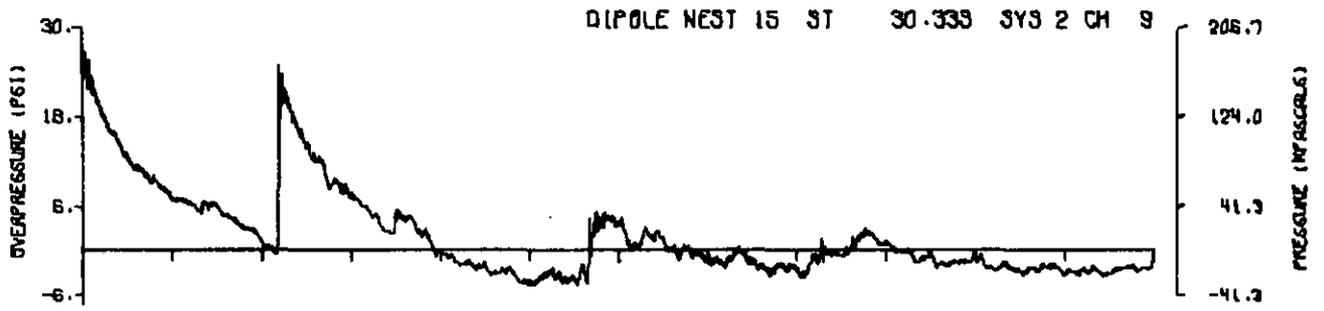
A15.17



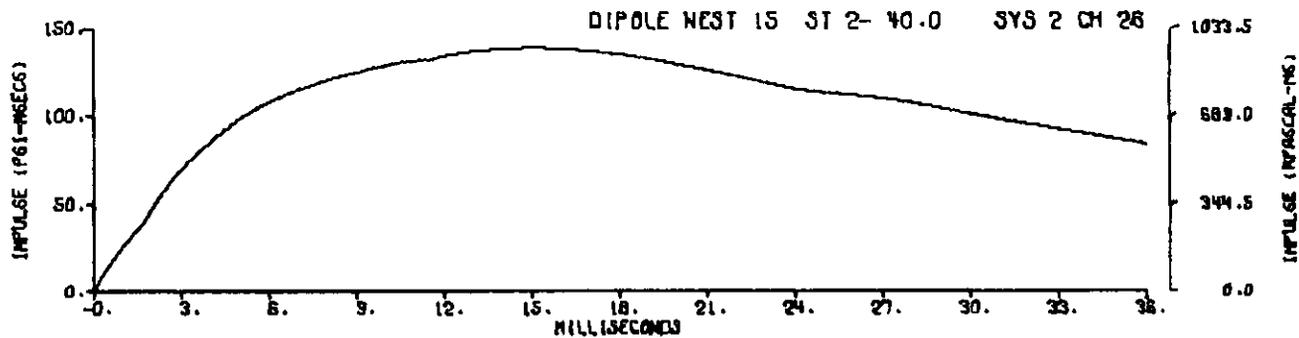
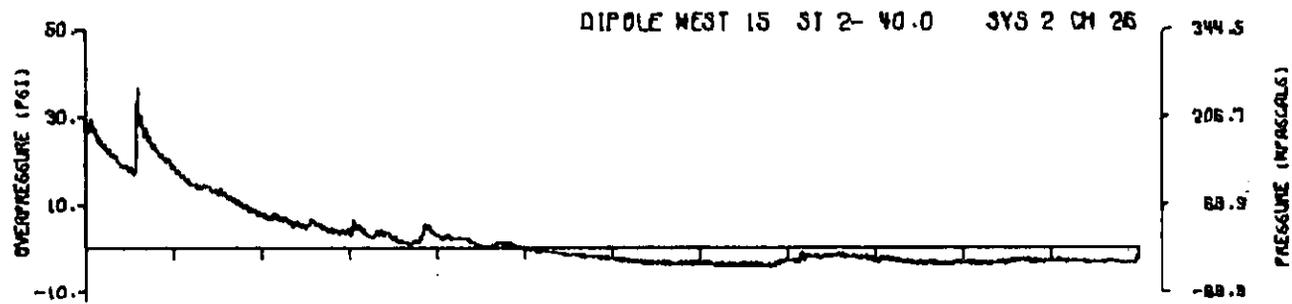
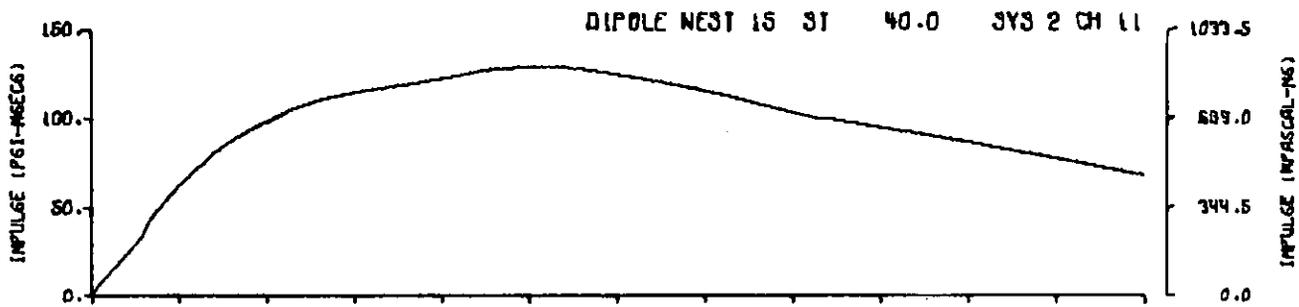
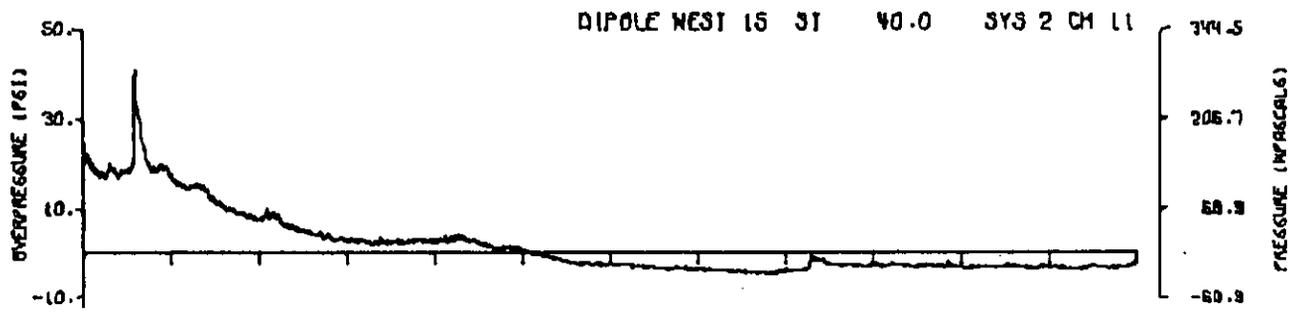
A15.18



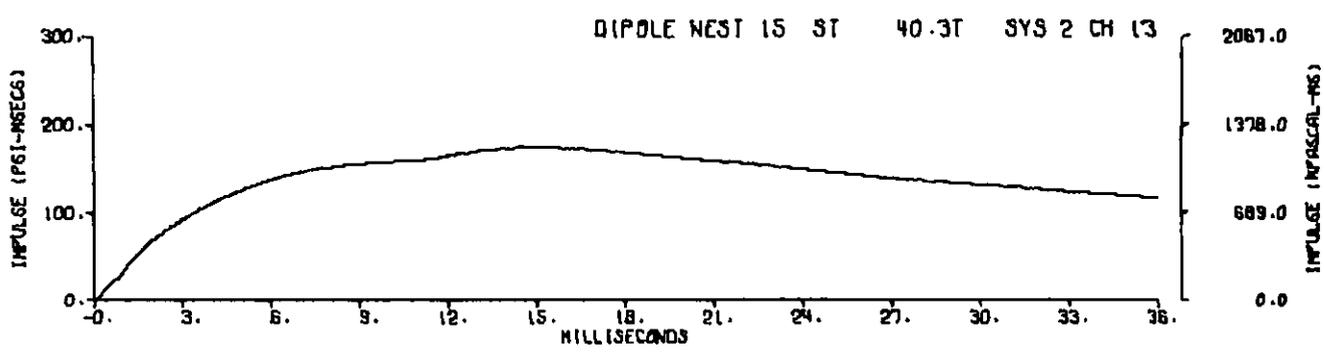
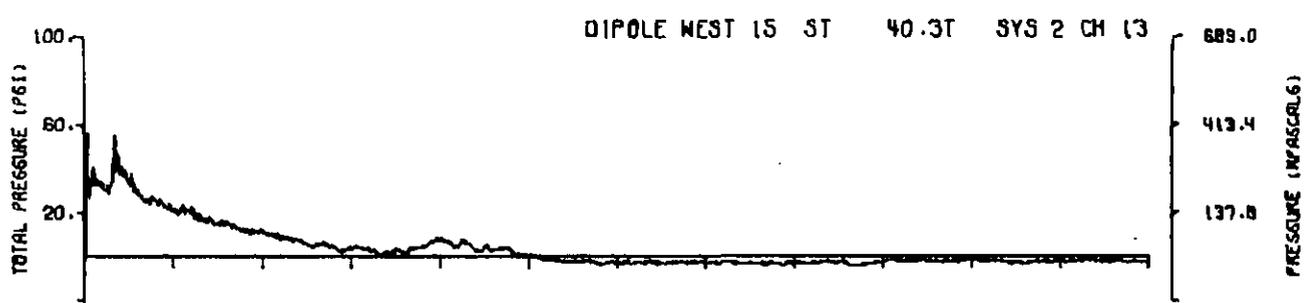
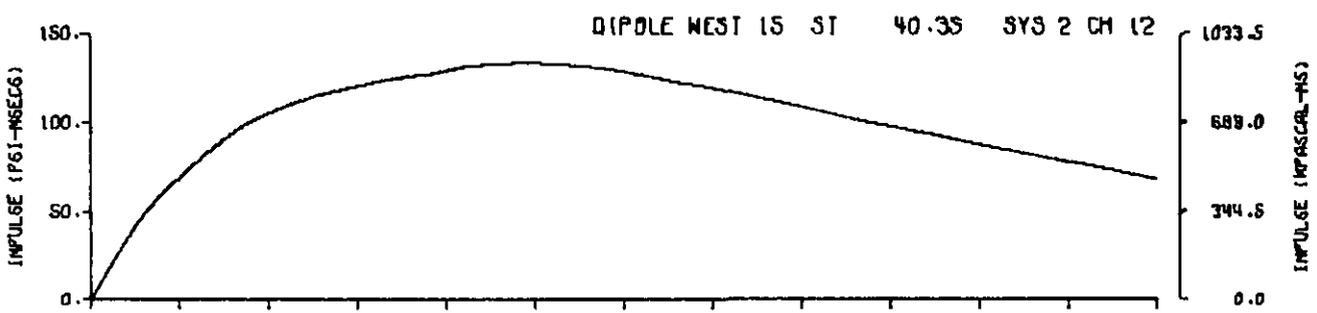
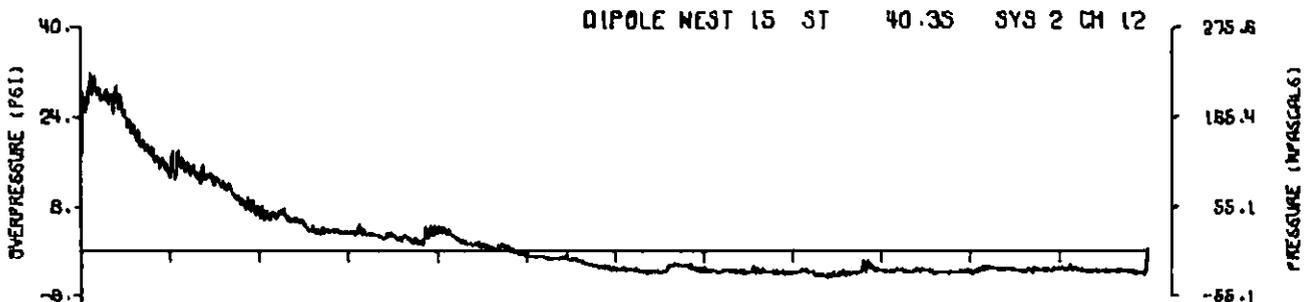
A15.19



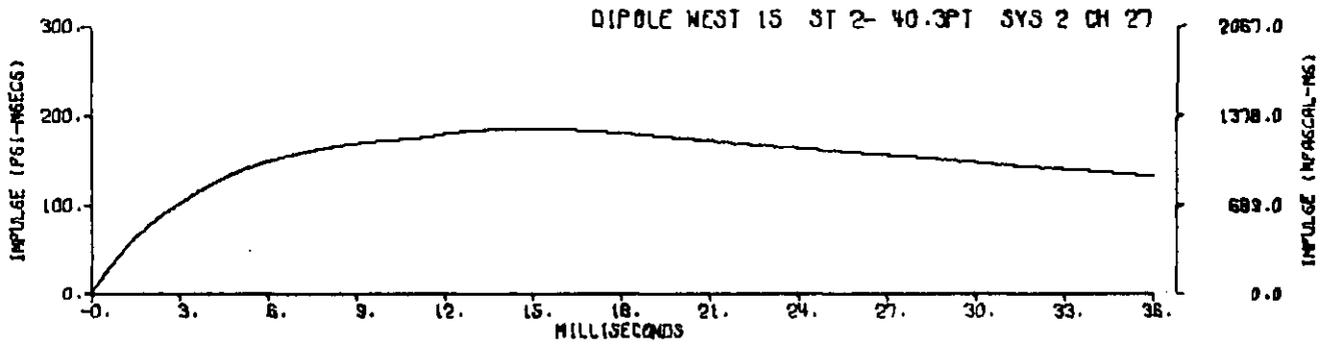
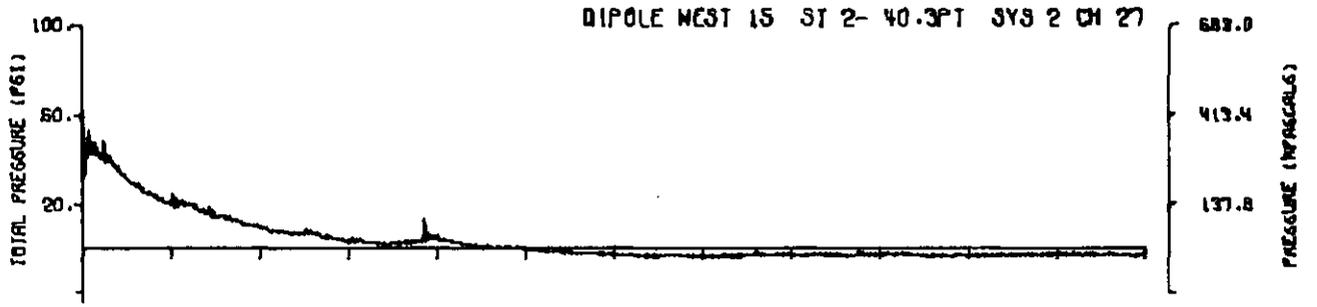
A15.20



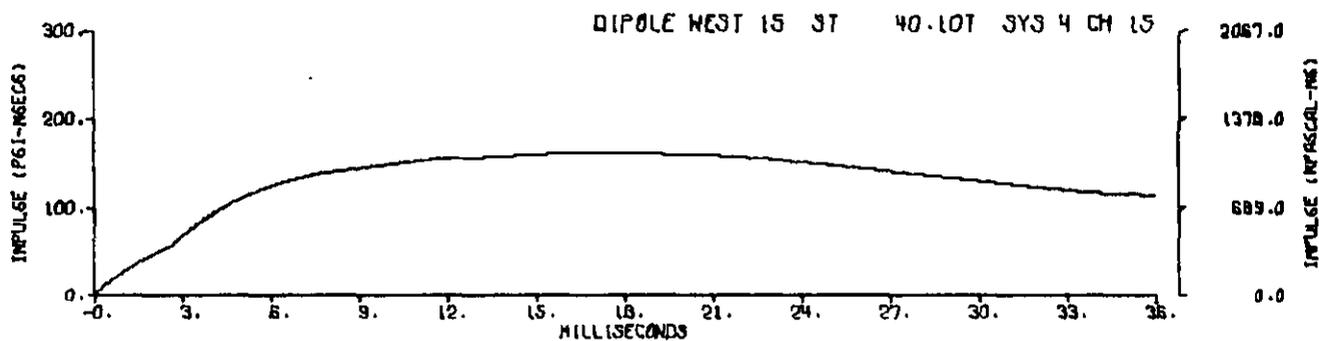
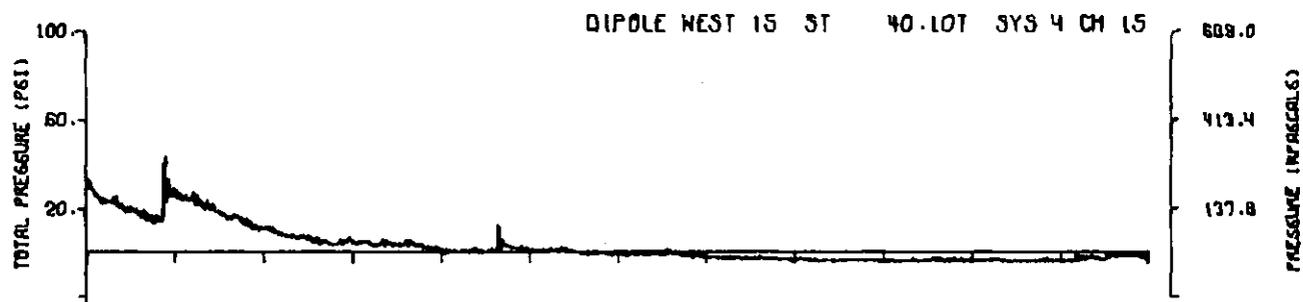
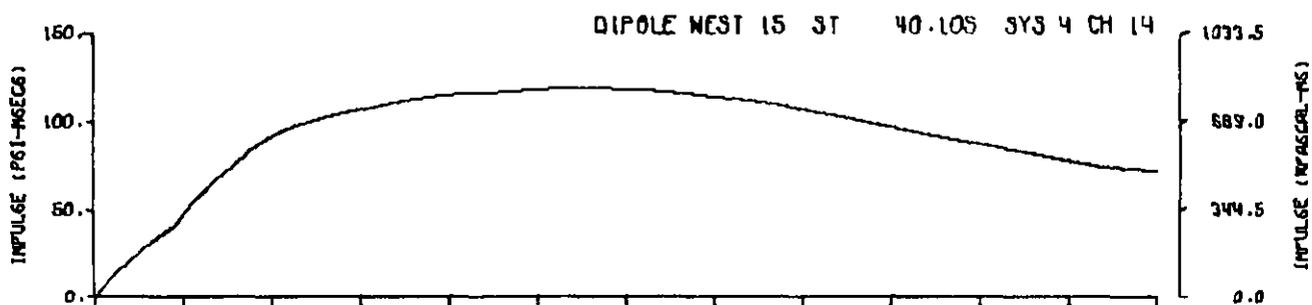
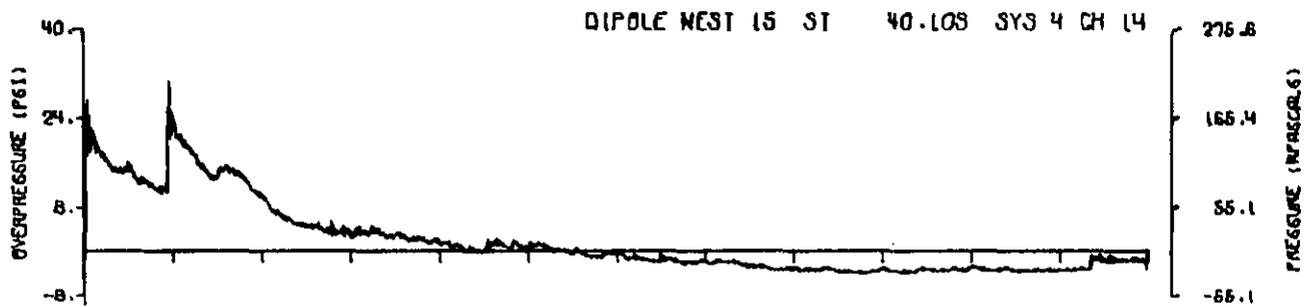
A15.21



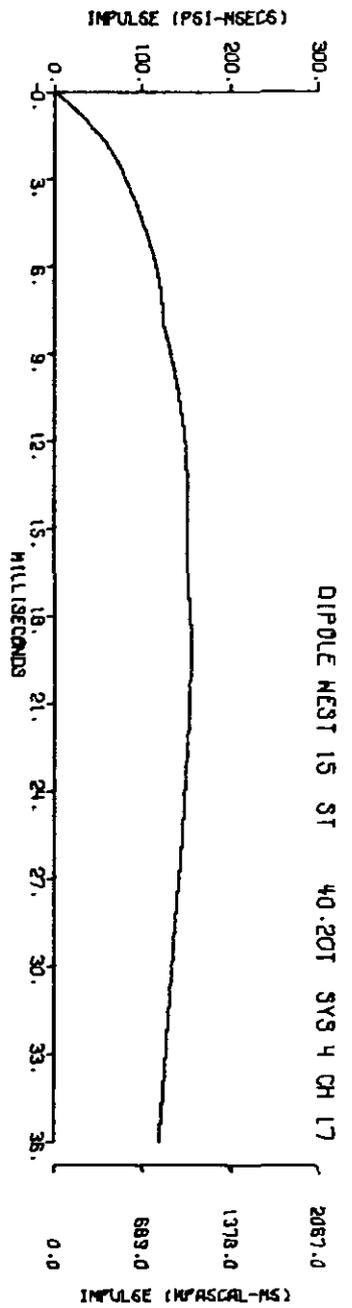
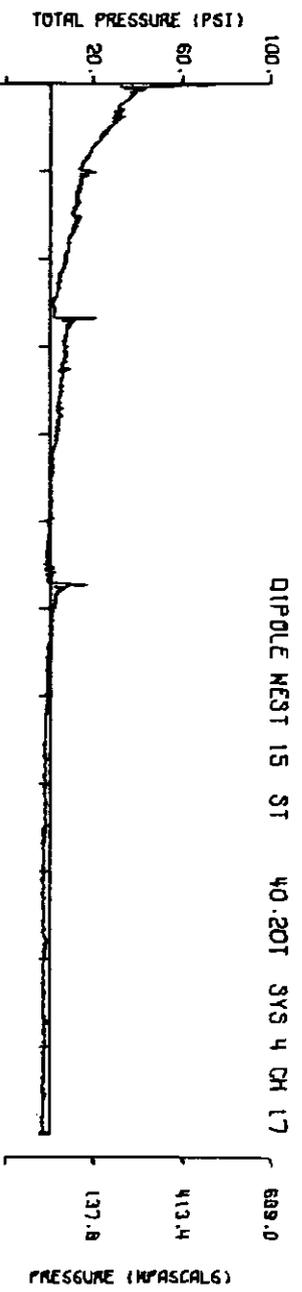
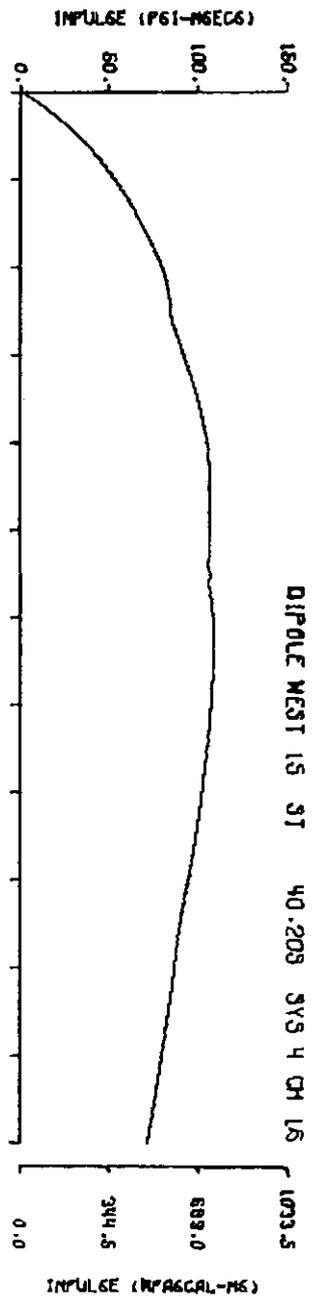
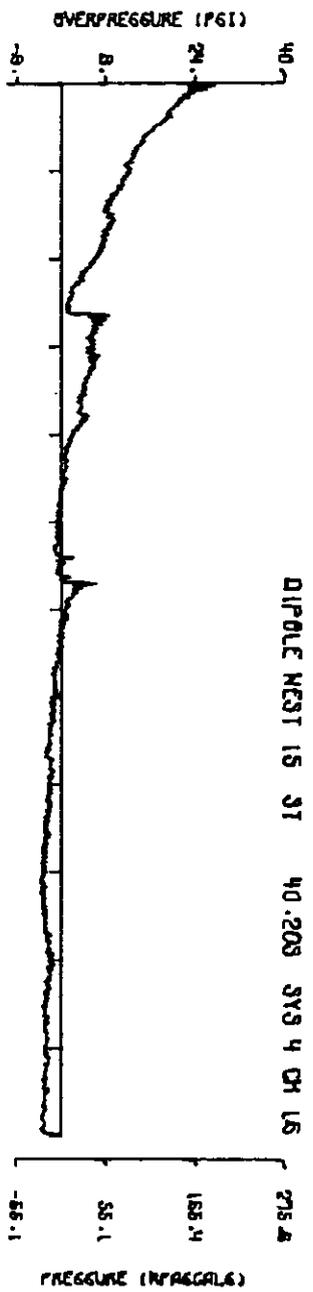
A15.22



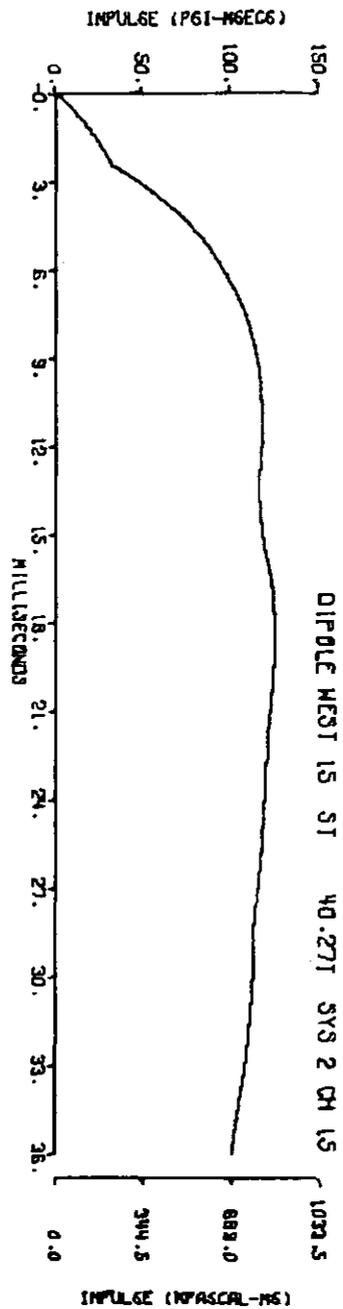
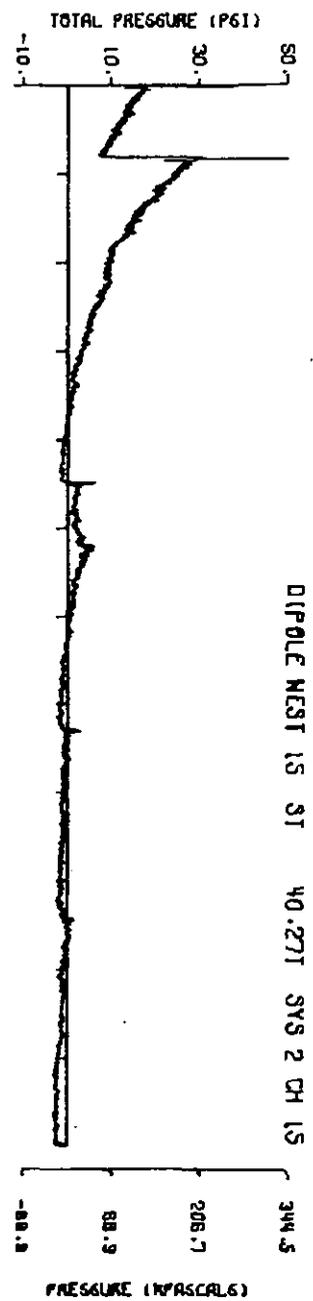
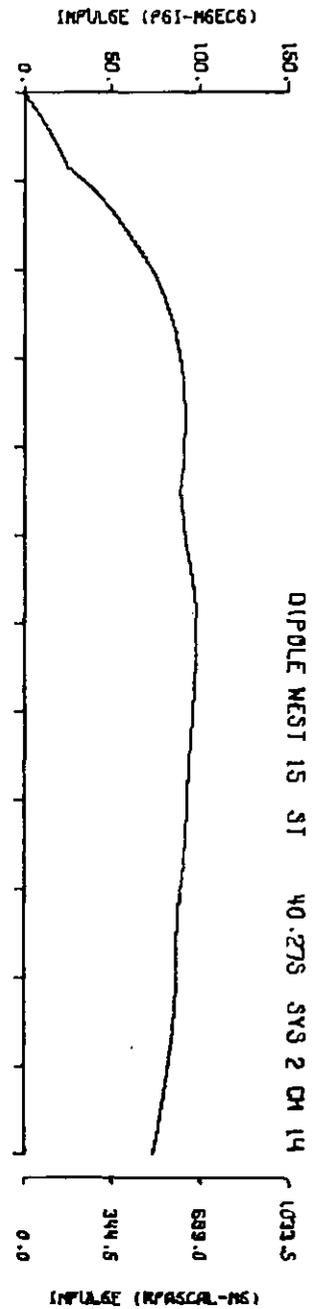
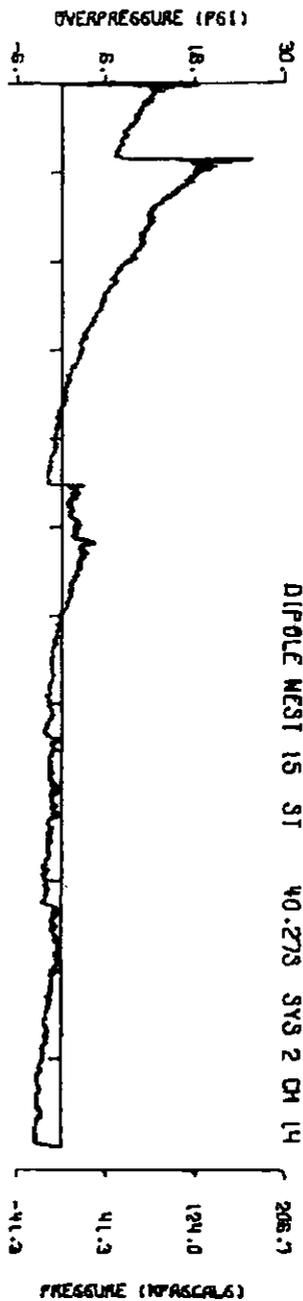
A15.23



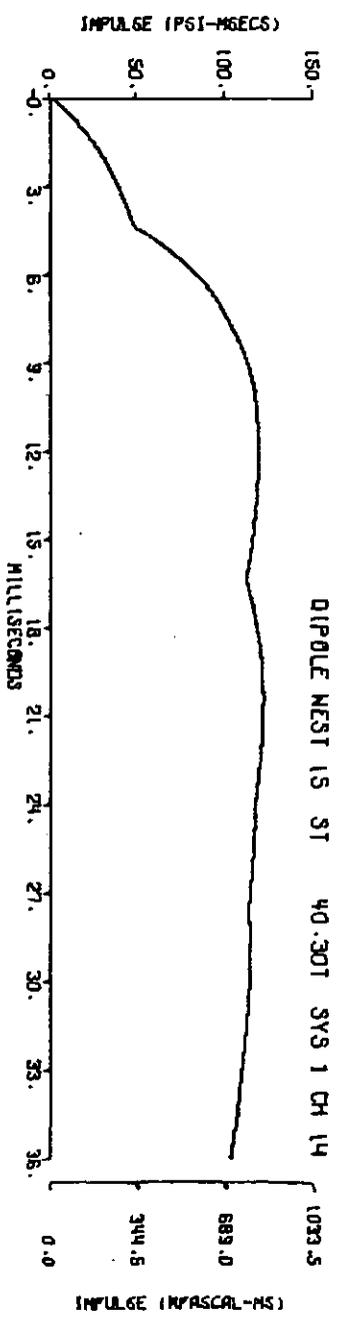
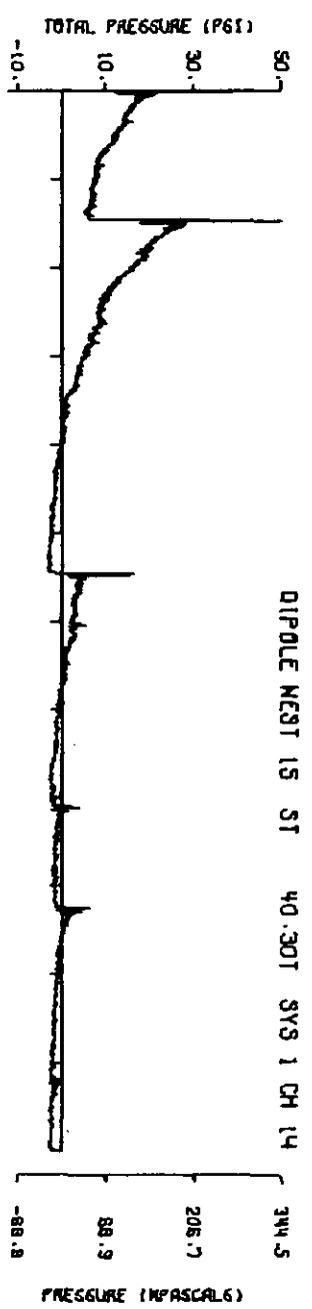
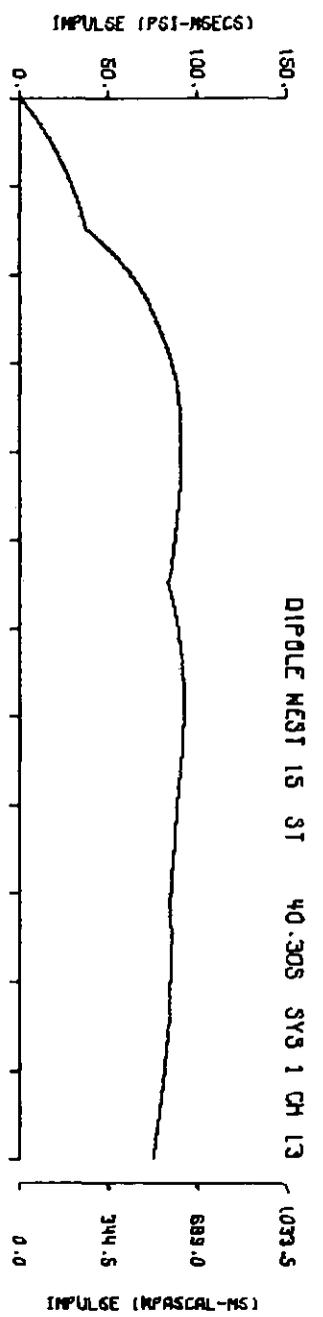
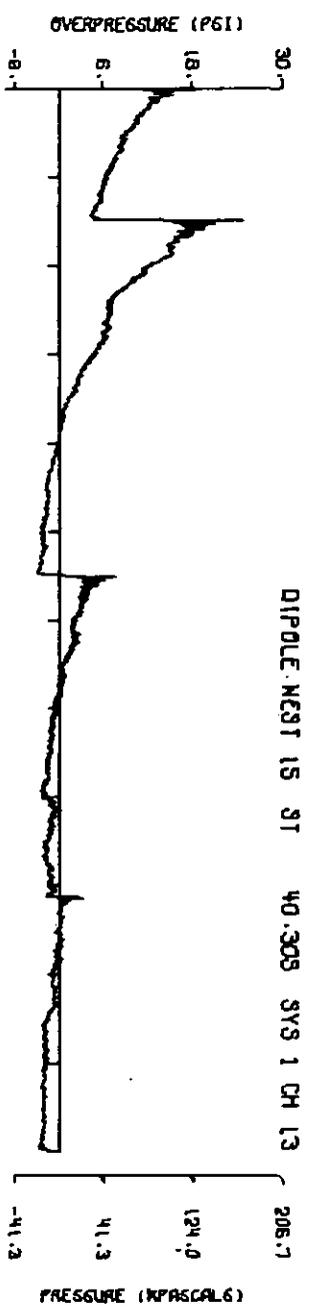
A15.24



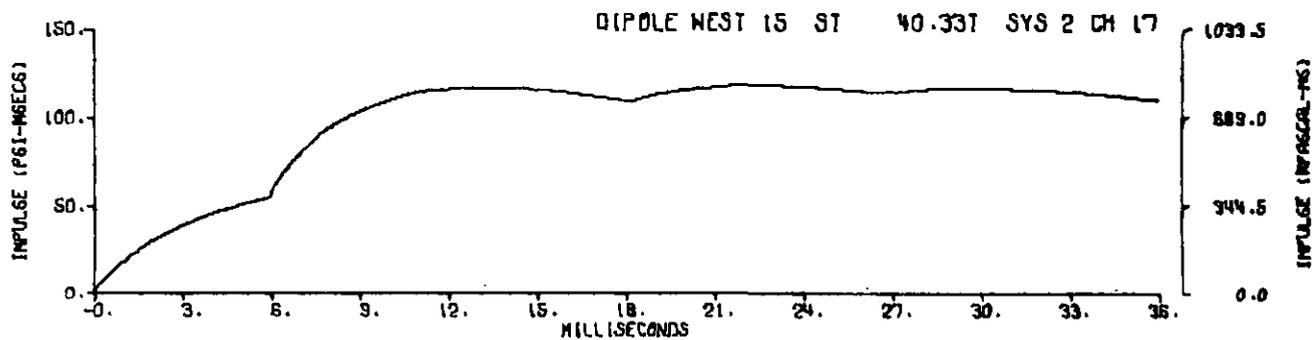
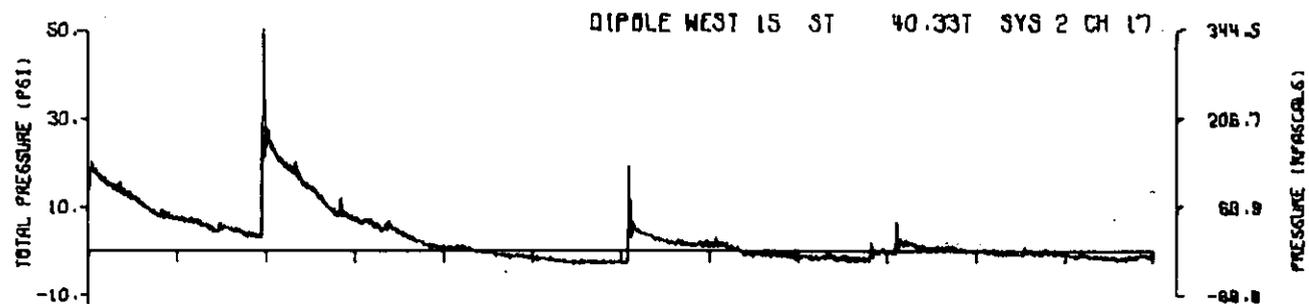
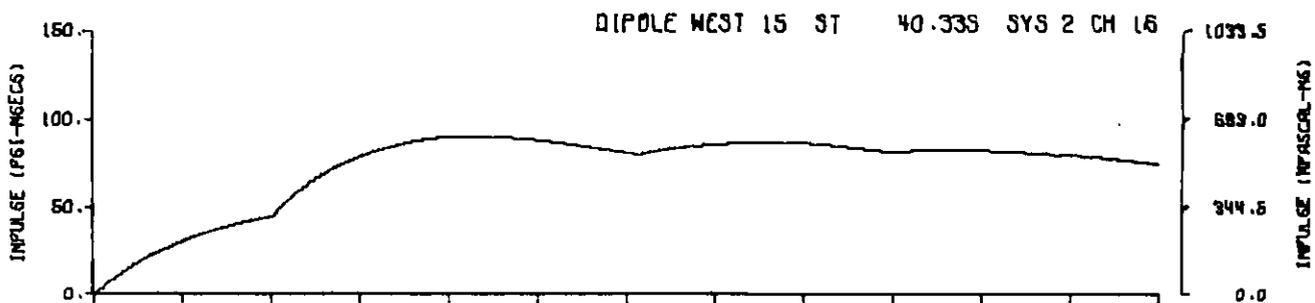
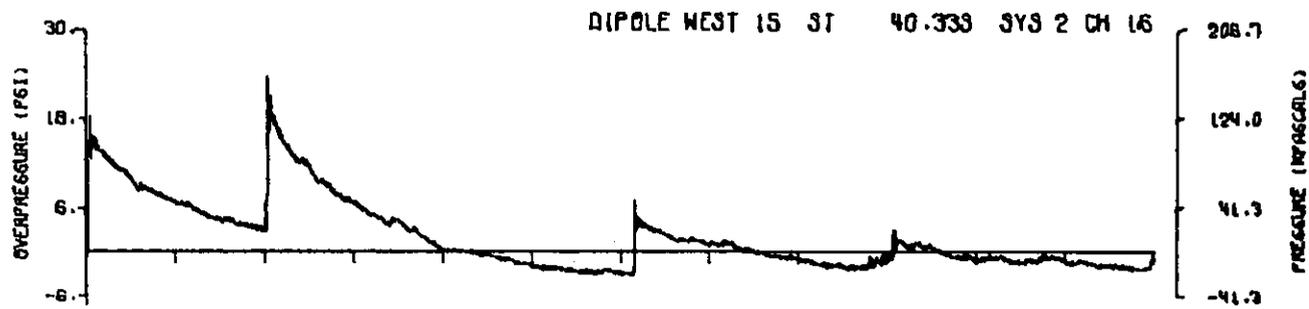
A15.25
312



A15.26

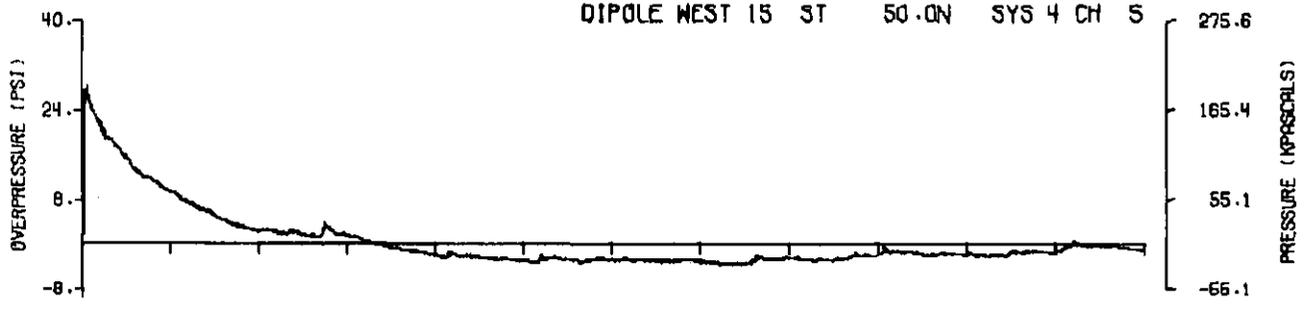


A15.27
314

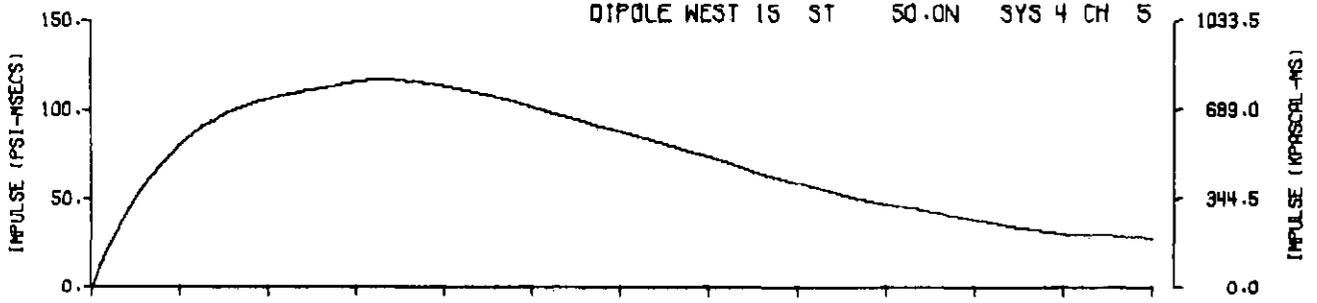


A15.28

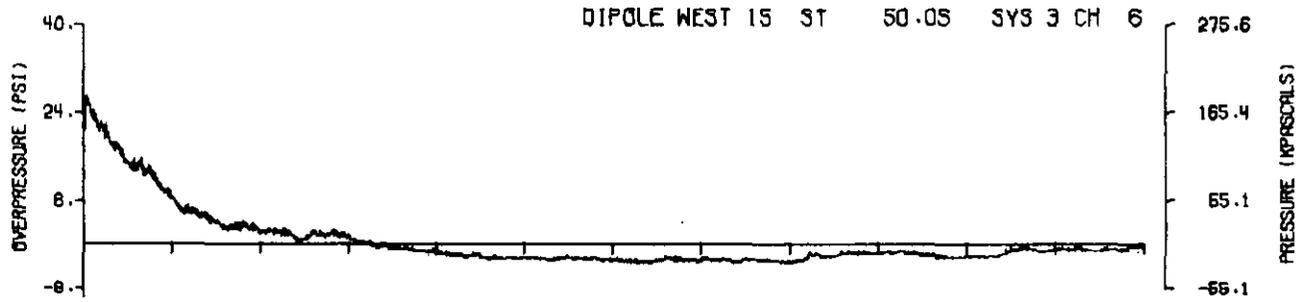
DIPOLE WEST 15 ST 50.0N SYS 4 CH 5



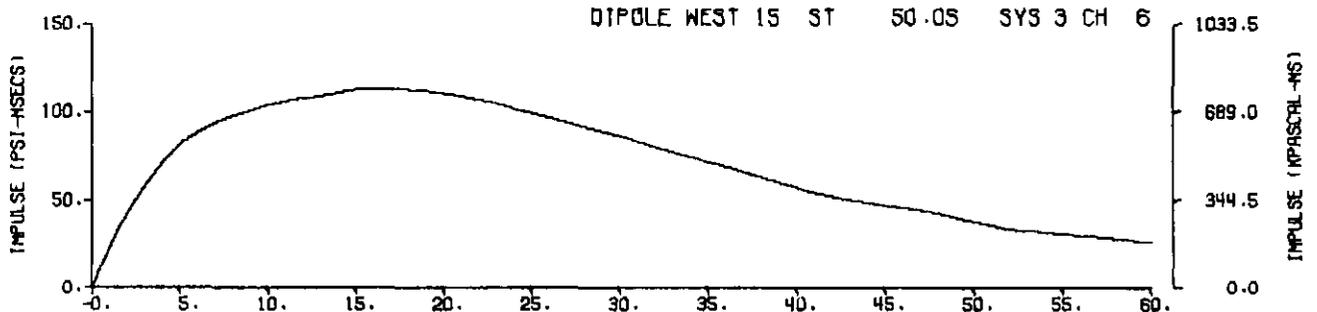
DIPOLE WEST 15 ST 50.0N SYS 4 CH 5



DIPOLE WEST 15 ST 50.0S SYS 3 CH 6



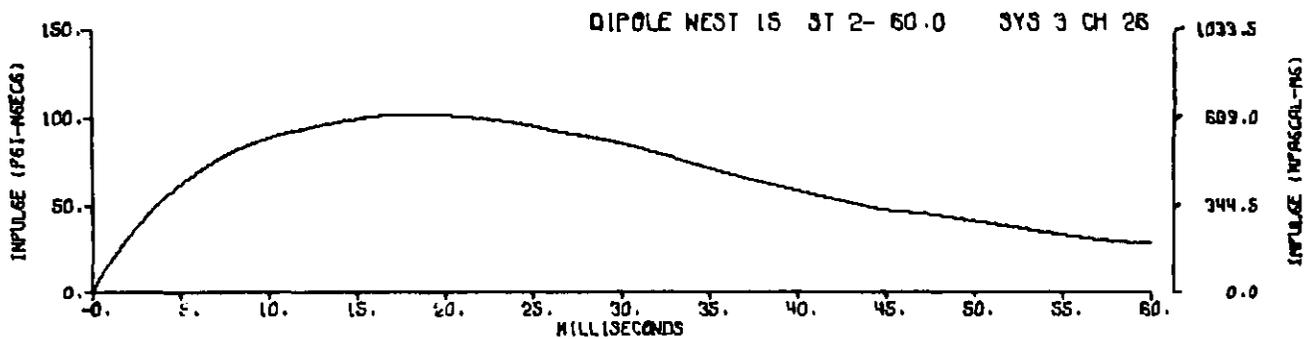
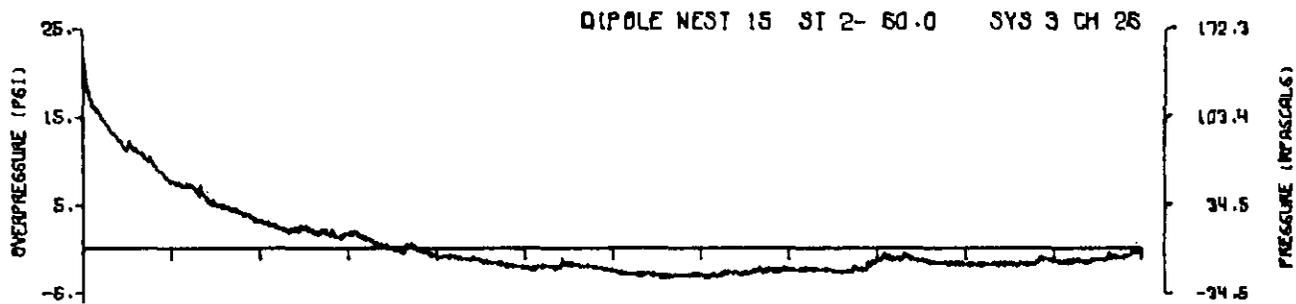
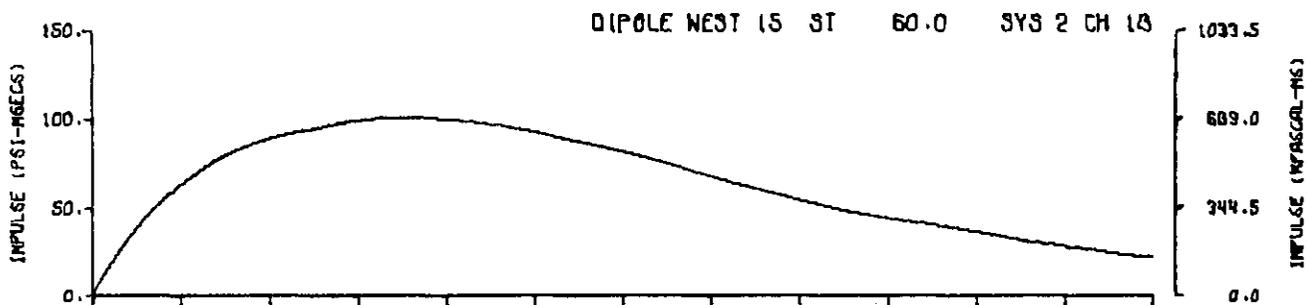
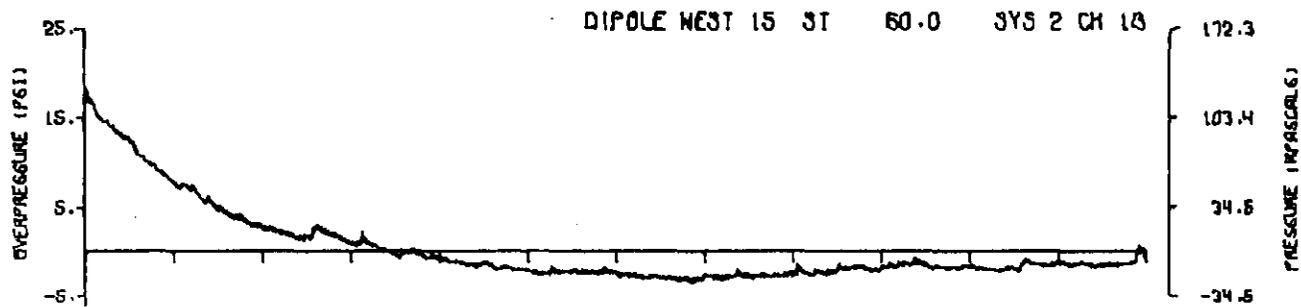
DIPOLE WEST 15 ST 50.0S SYS 3 CH 6



MILLISECONDS

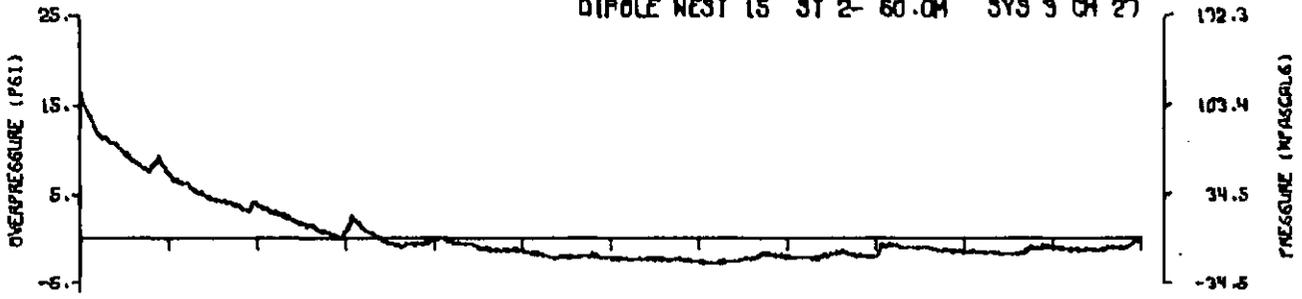
A15.29

316

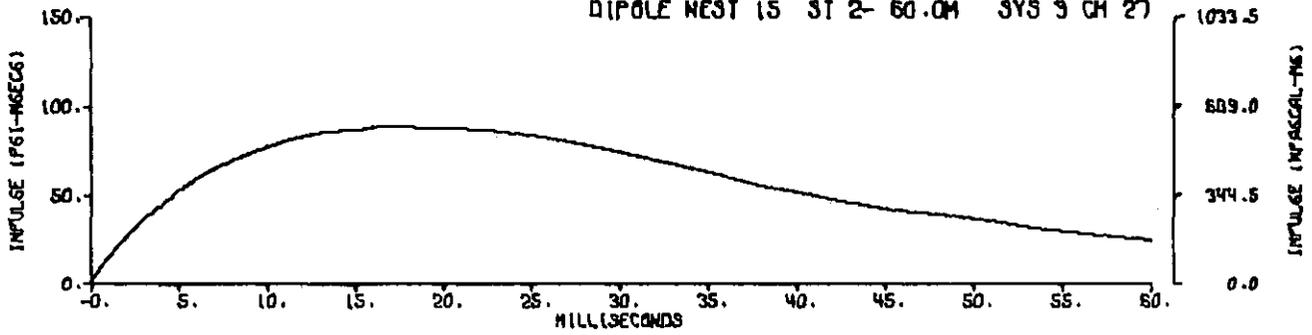


A15.30

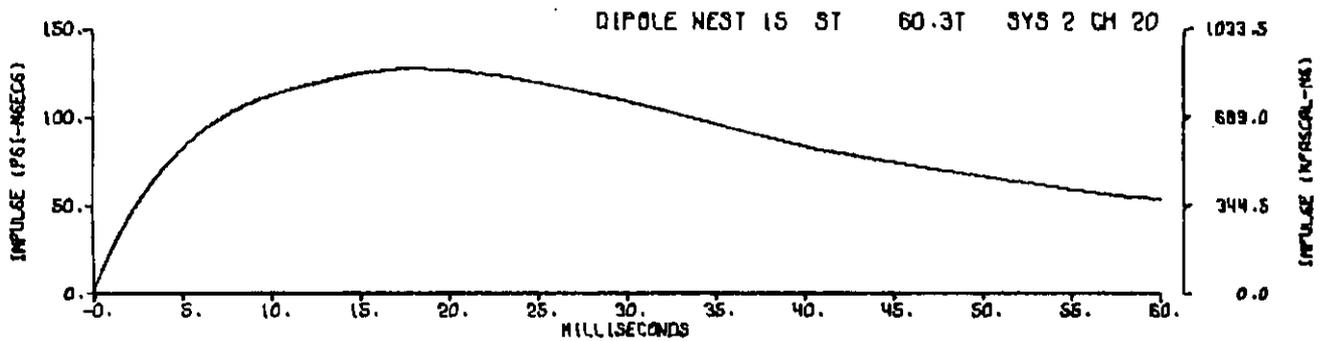
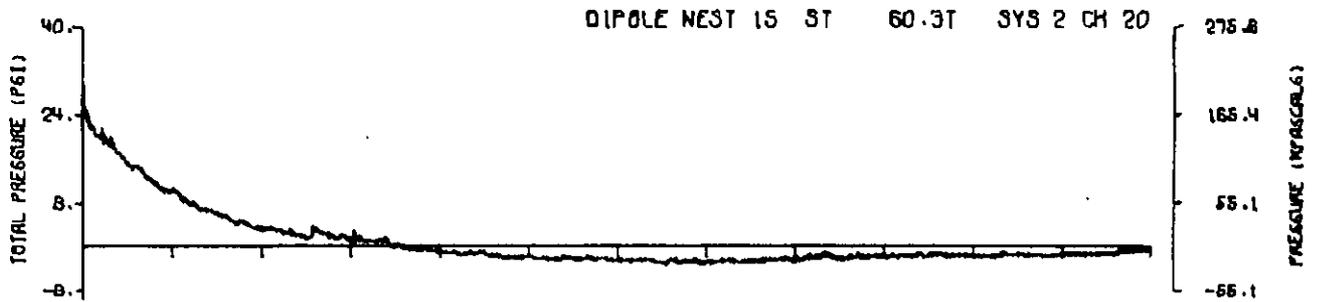
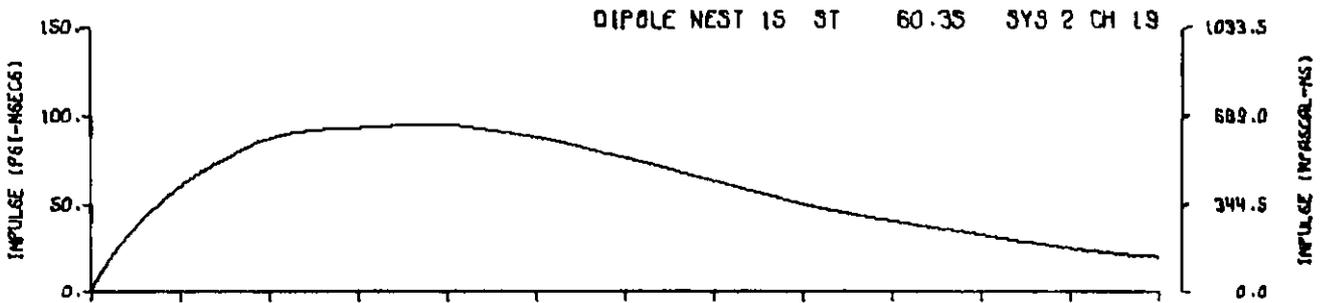
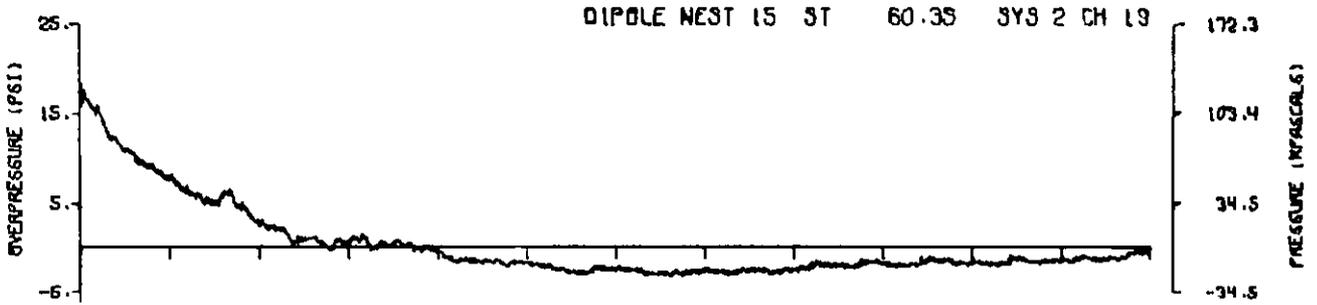
DIPOLE WEST 15 ST 2- 60.0M SYS 9 CH 27



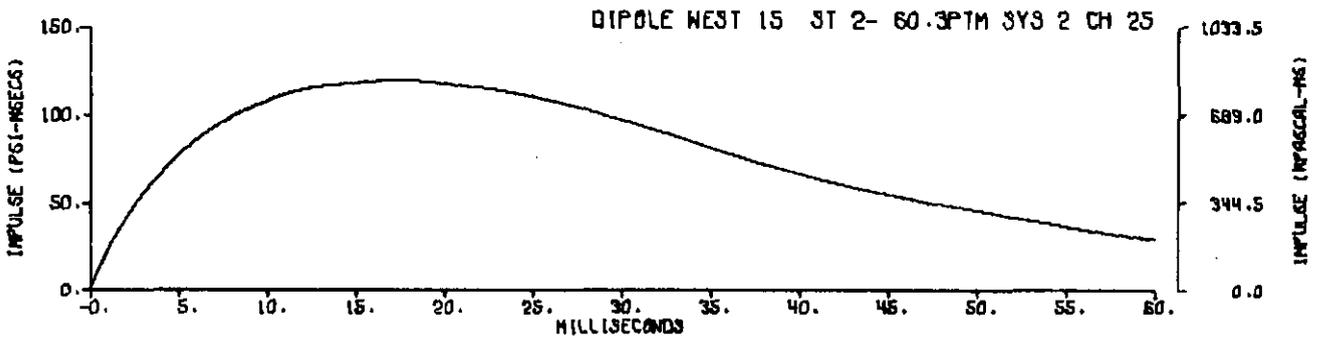
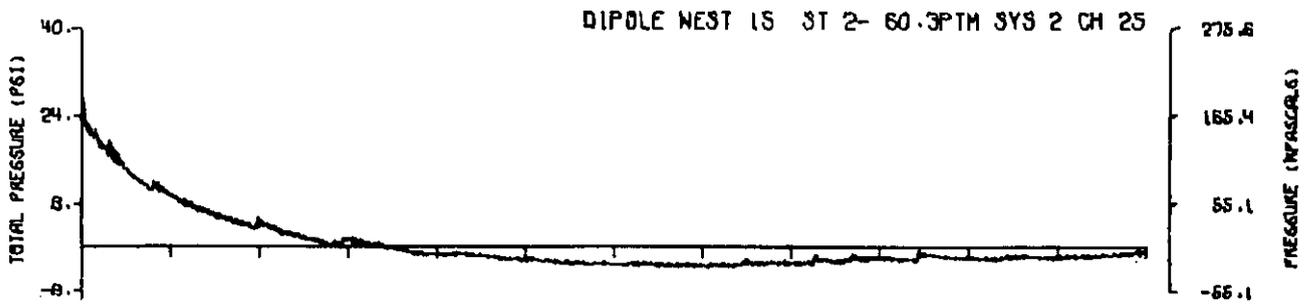
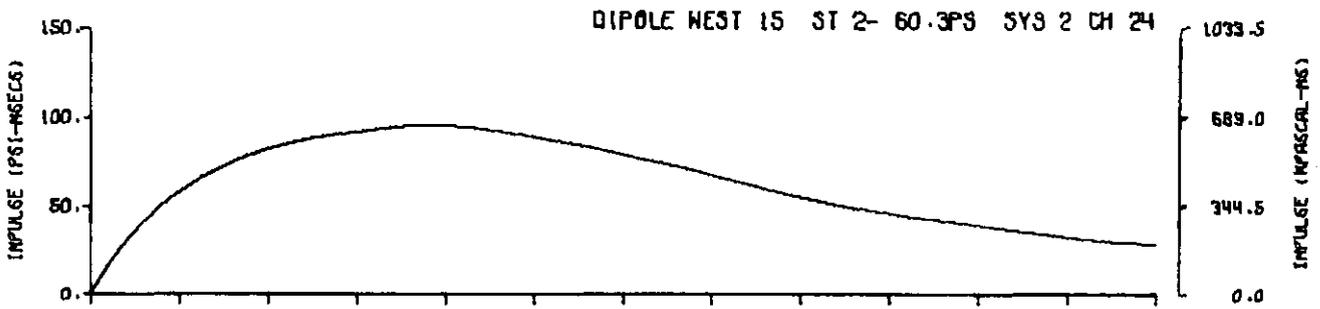
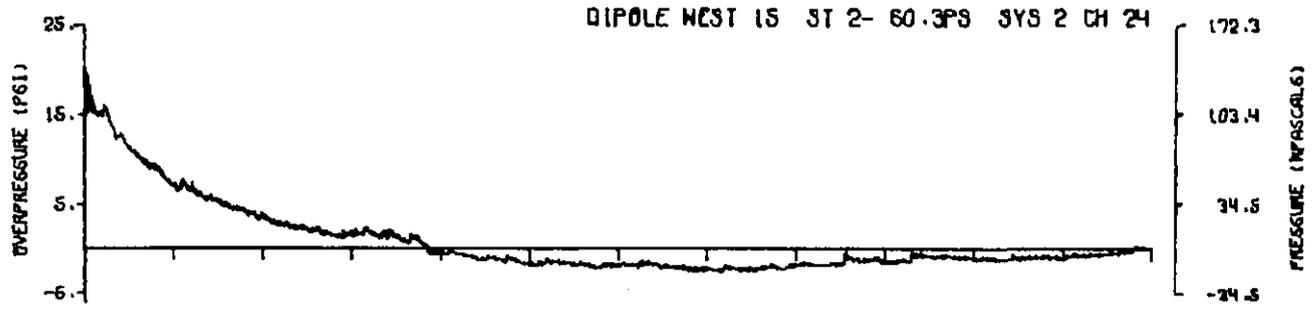
DIPOLE WEST 15 ST 2- 60.0M SYS 9 CH 27



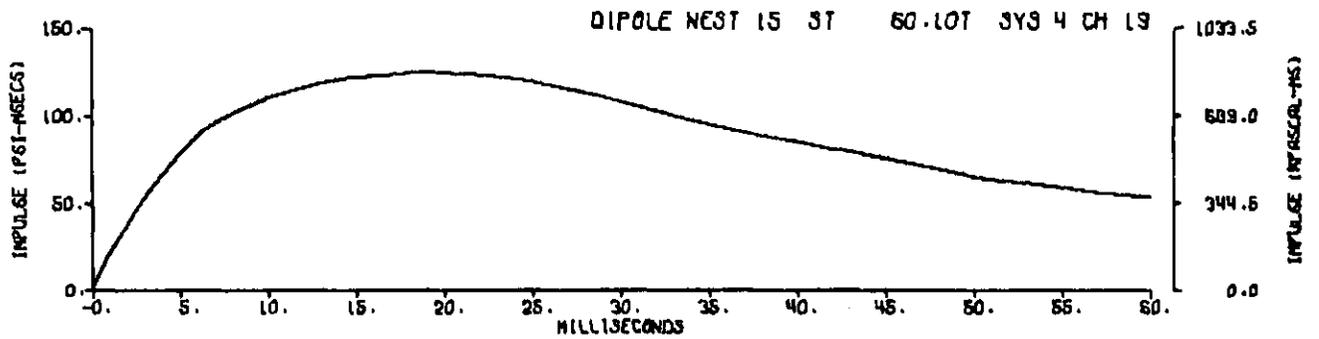
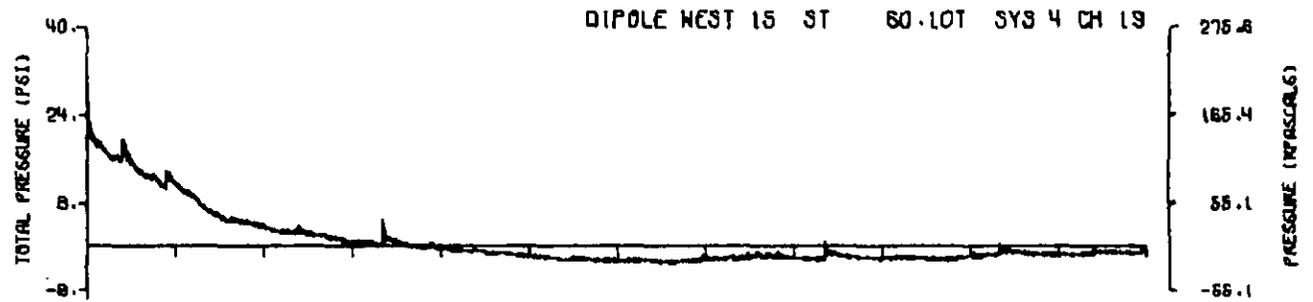
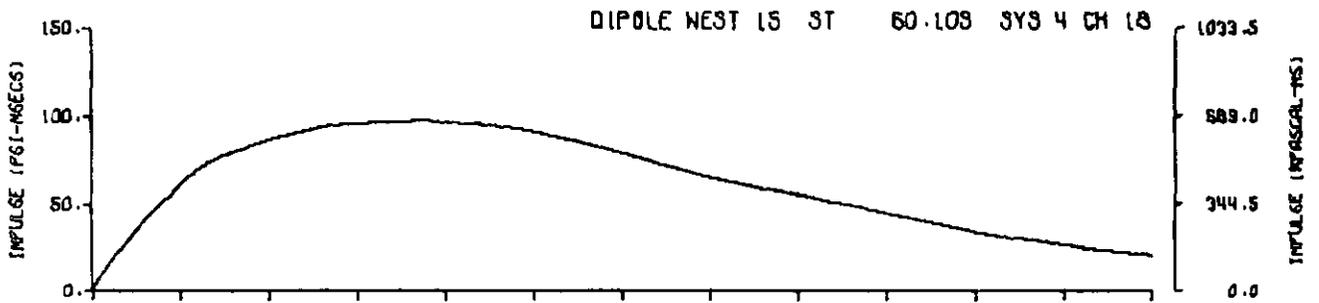
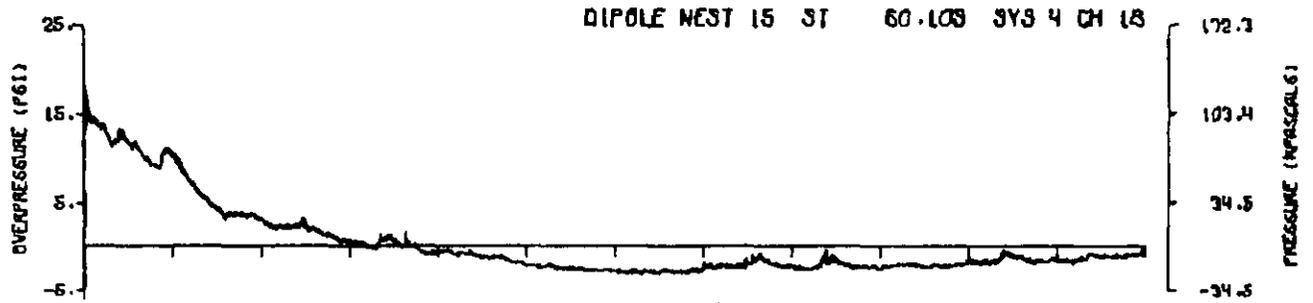
A15.31



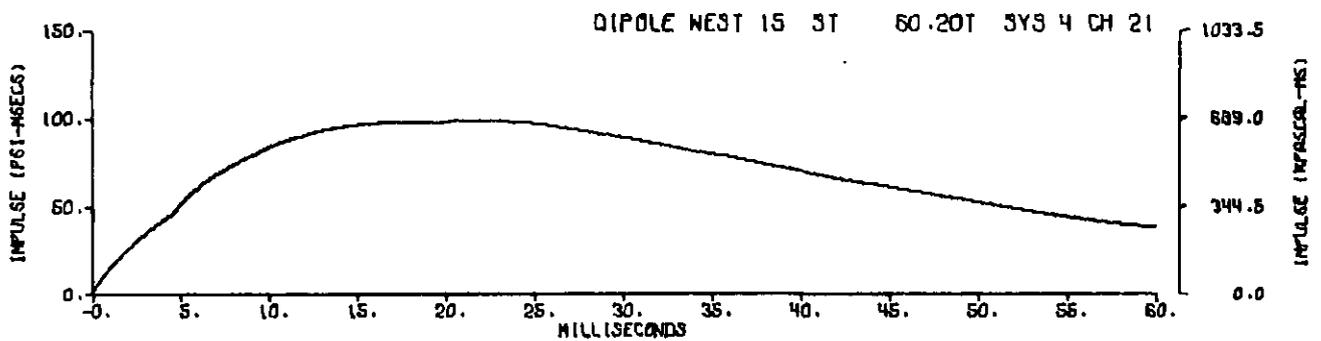
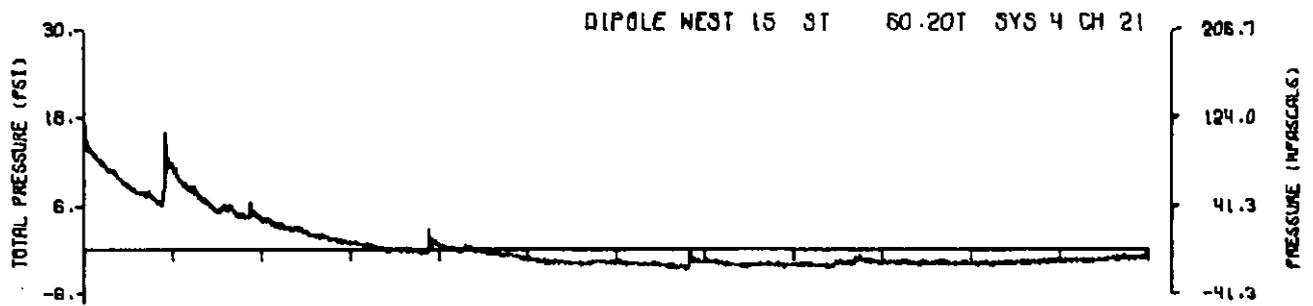
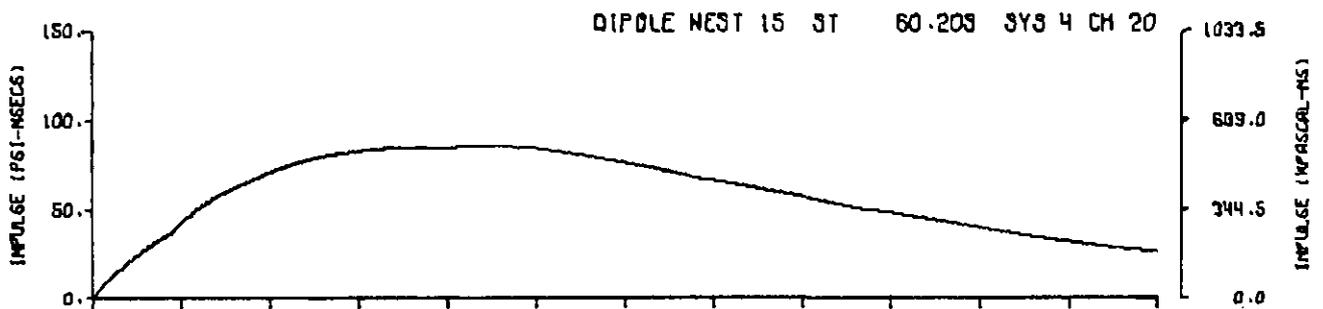
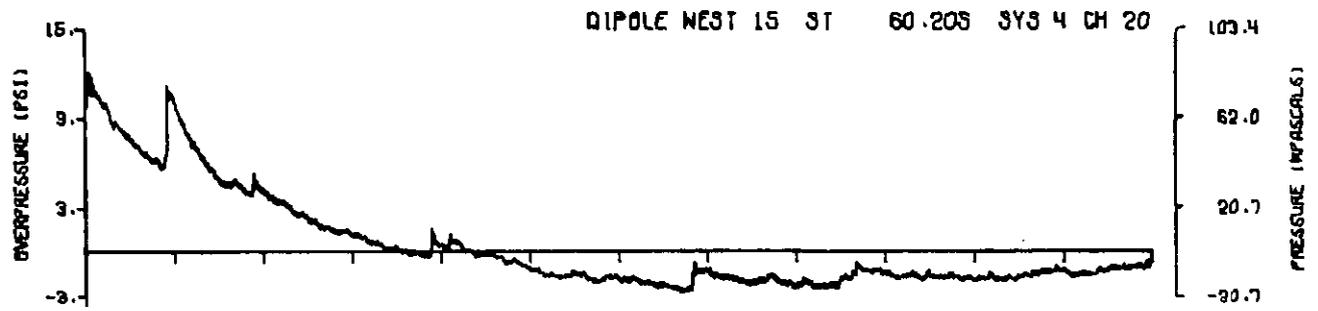
A15.32



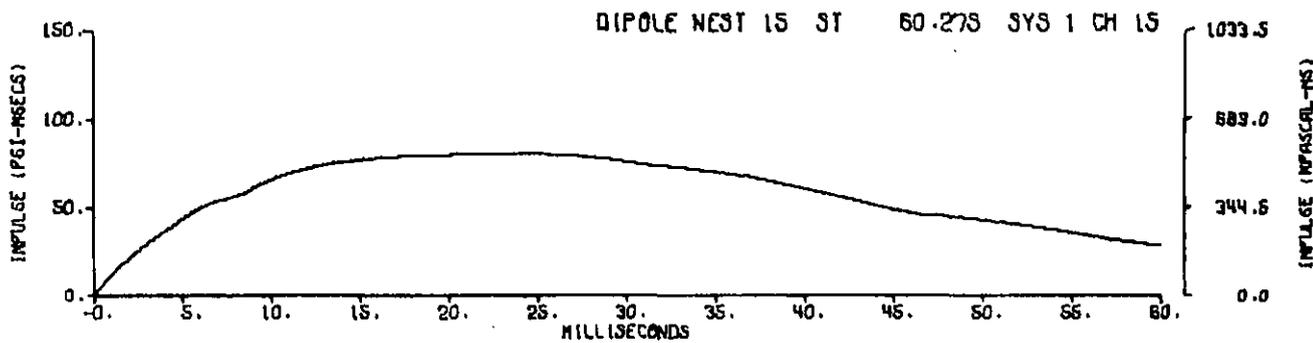
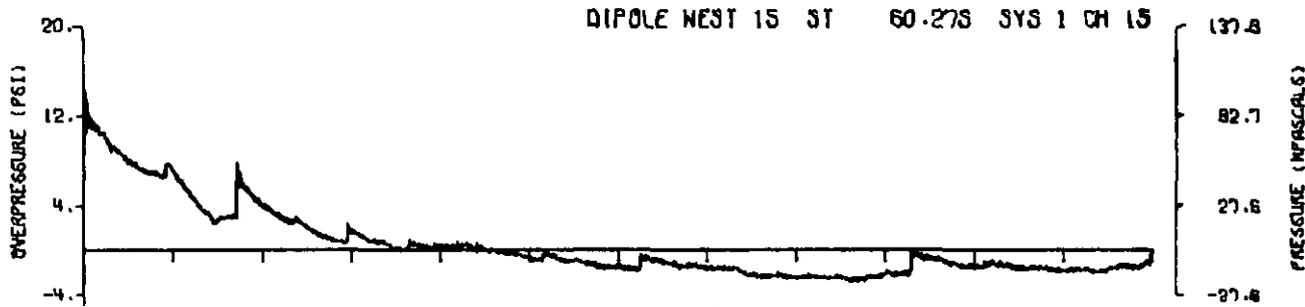
A15.33



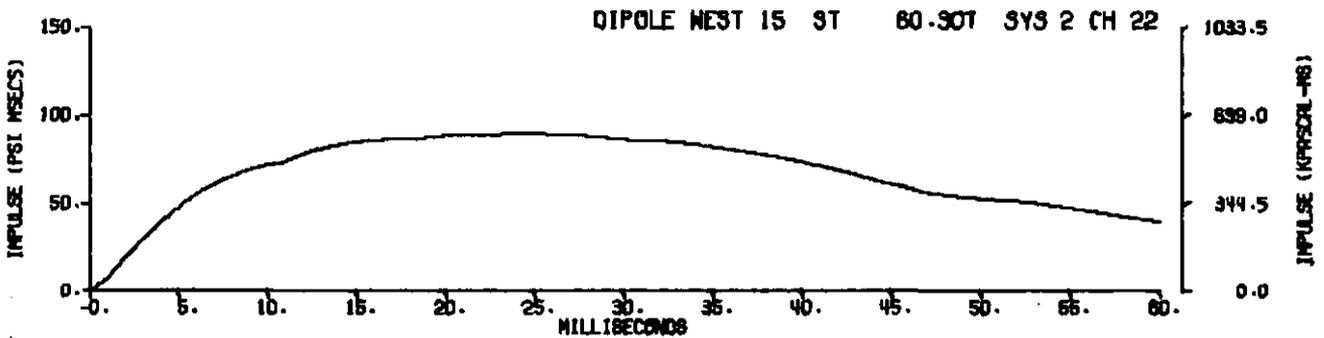
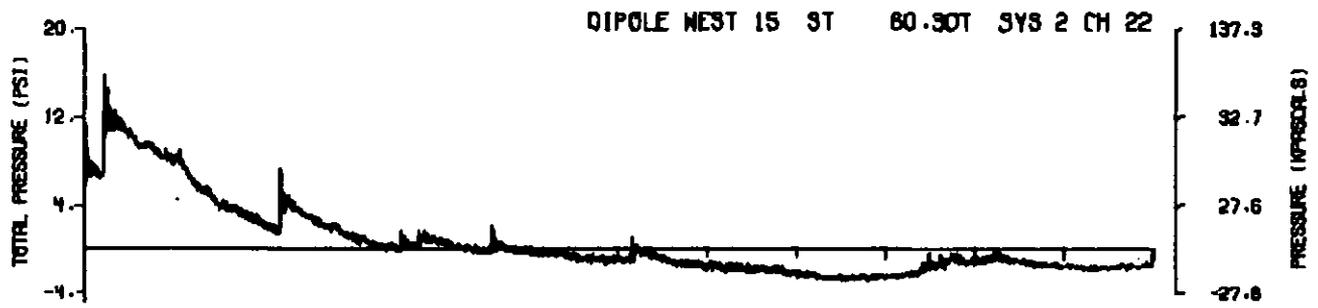
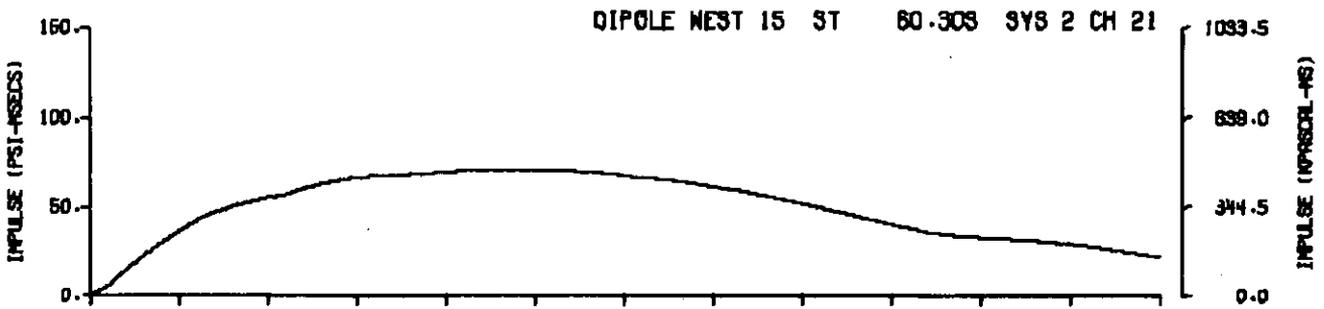
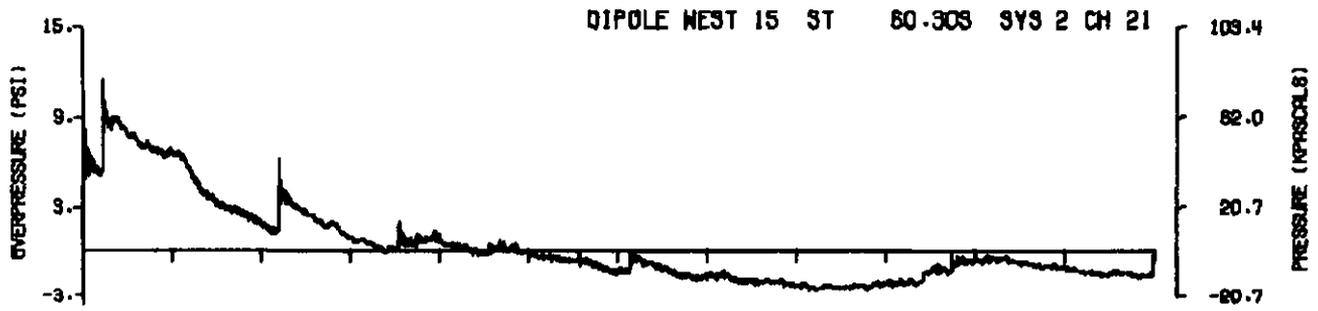
A15.34



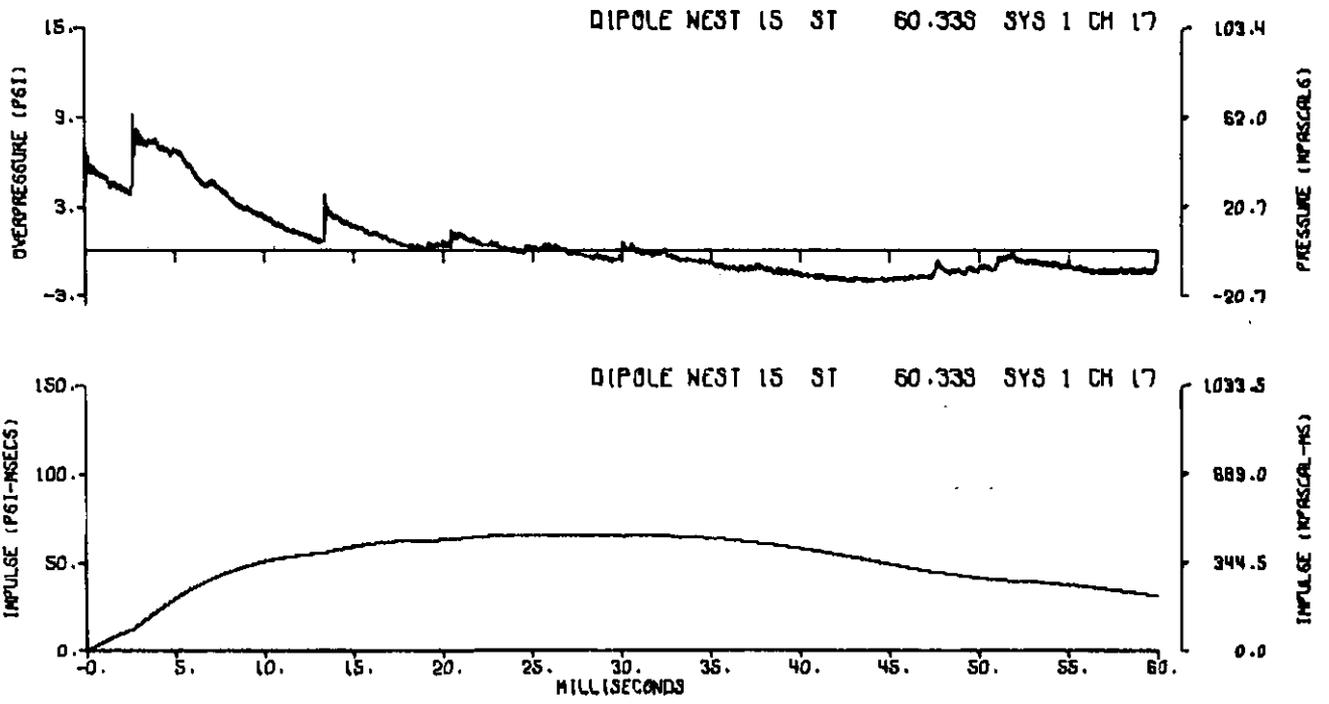
A15.35



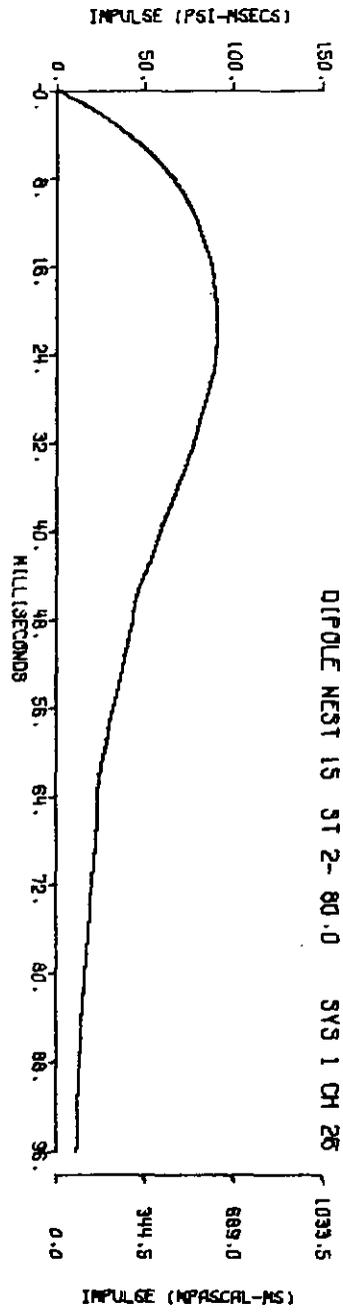
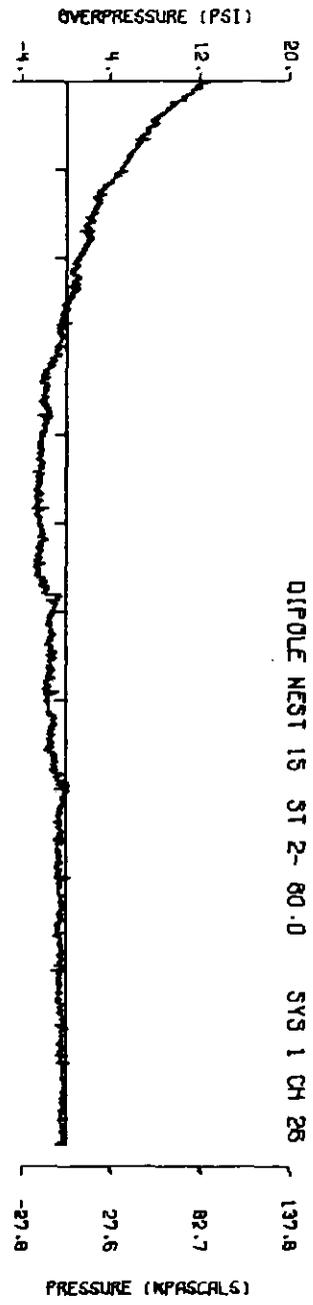
A15.36



A15.37

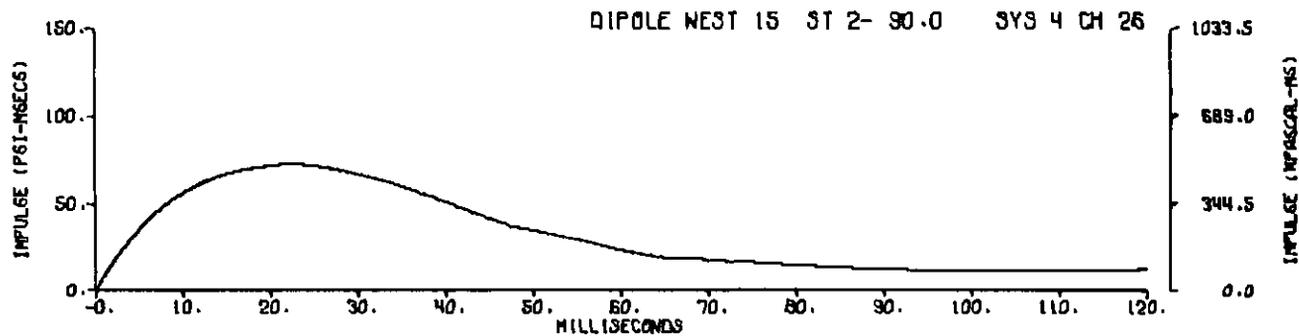
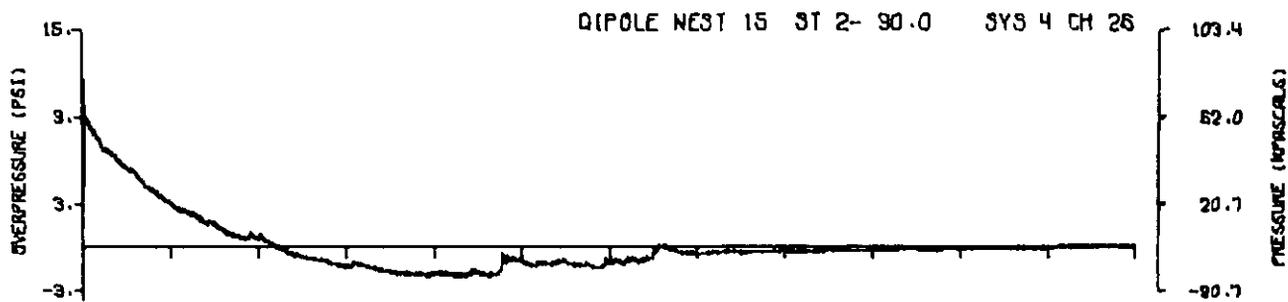
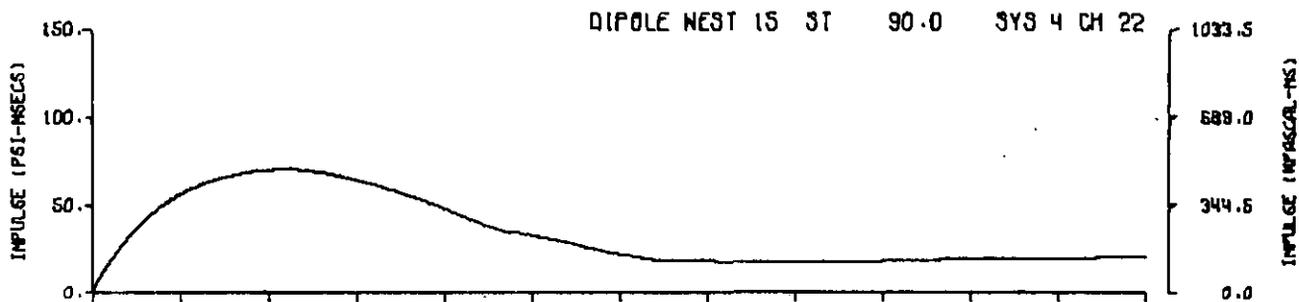
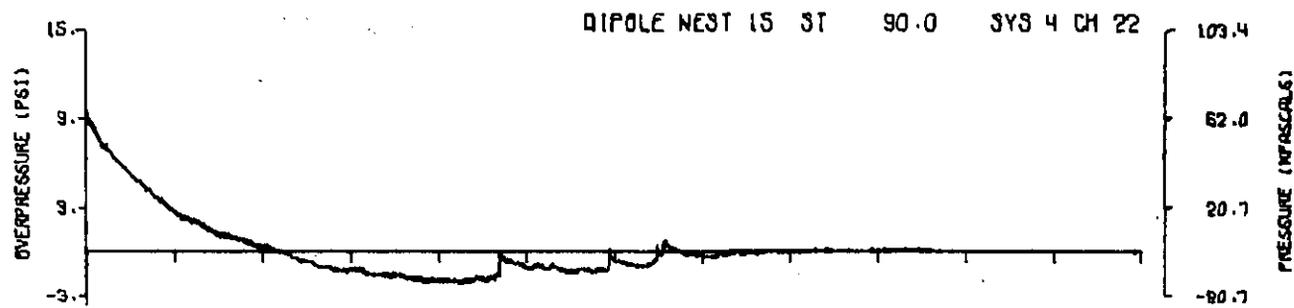


A15.38

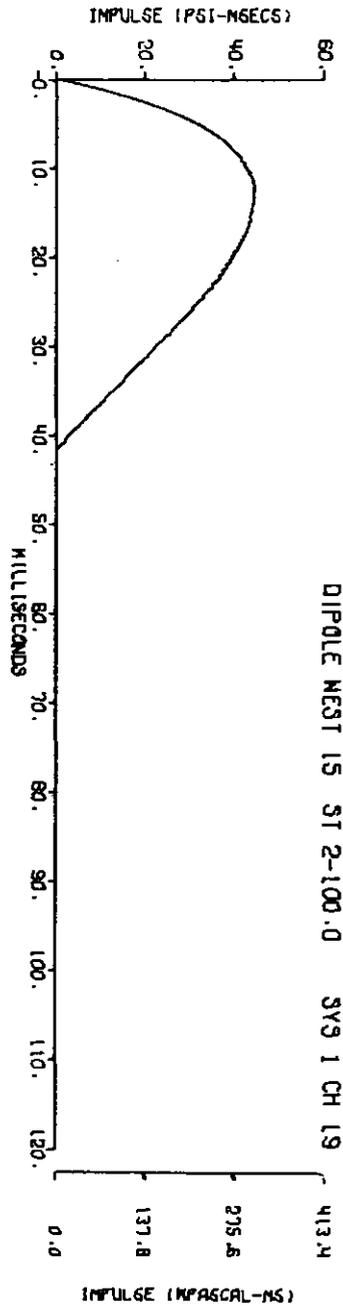
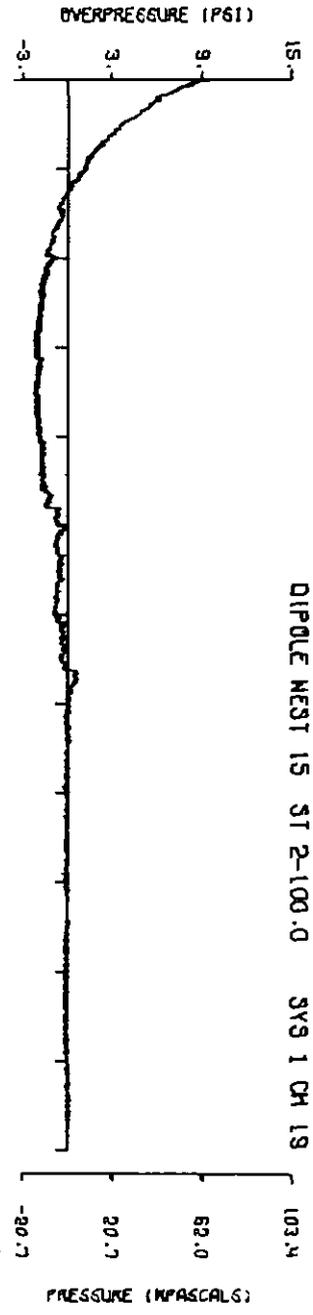


A15.39

326

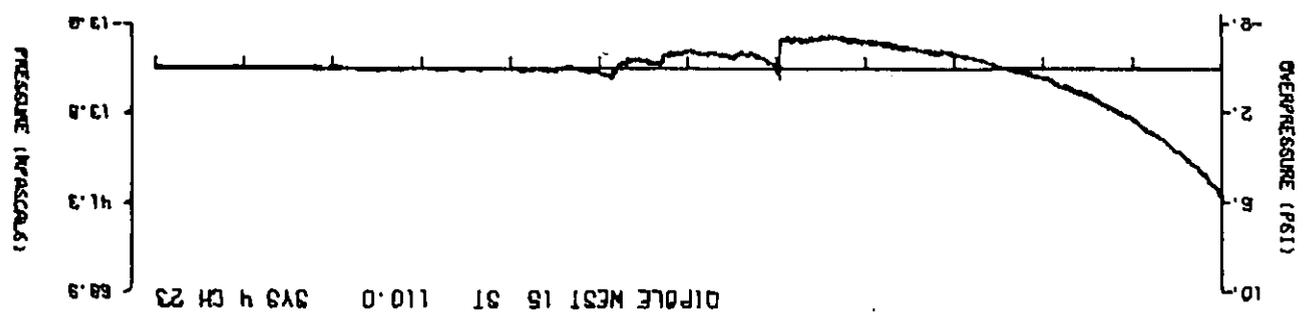
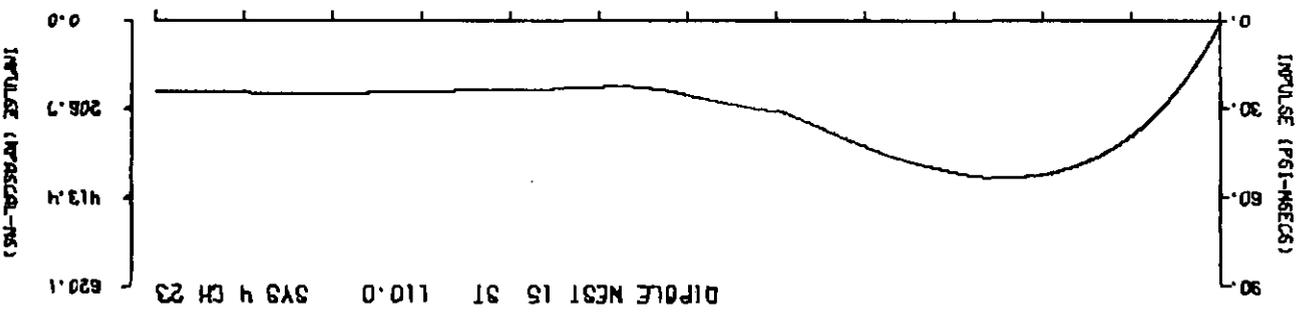
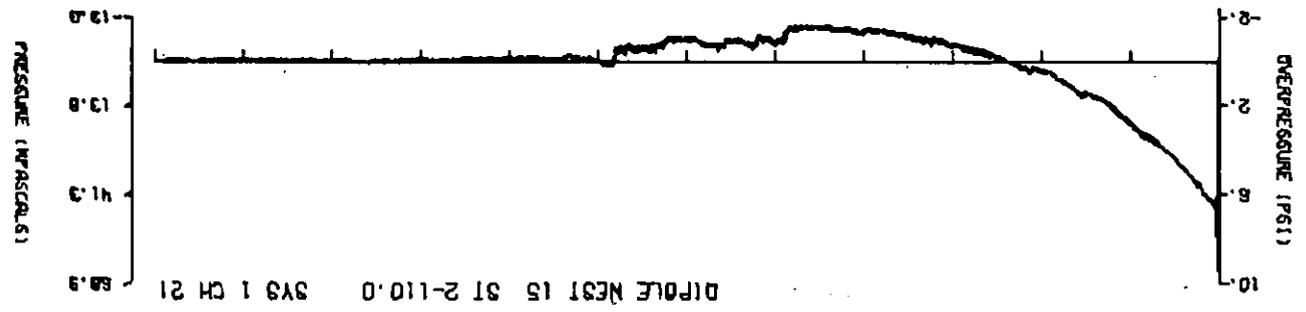
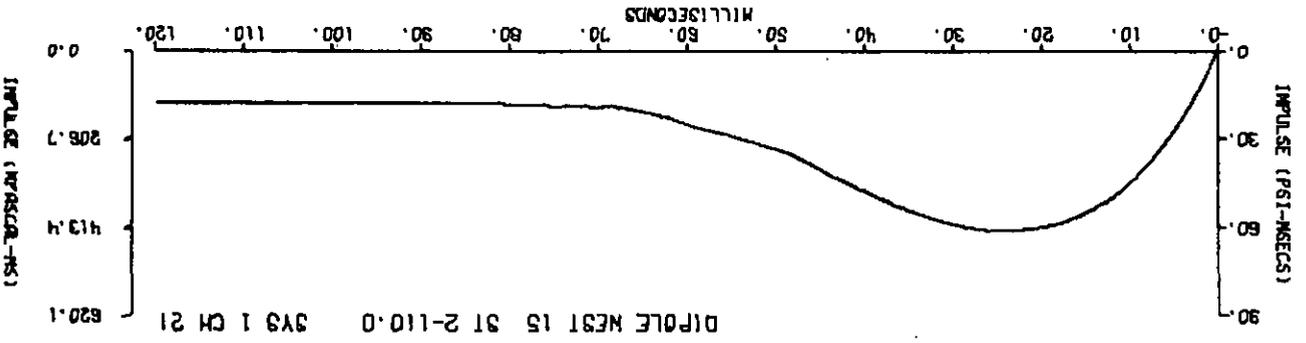


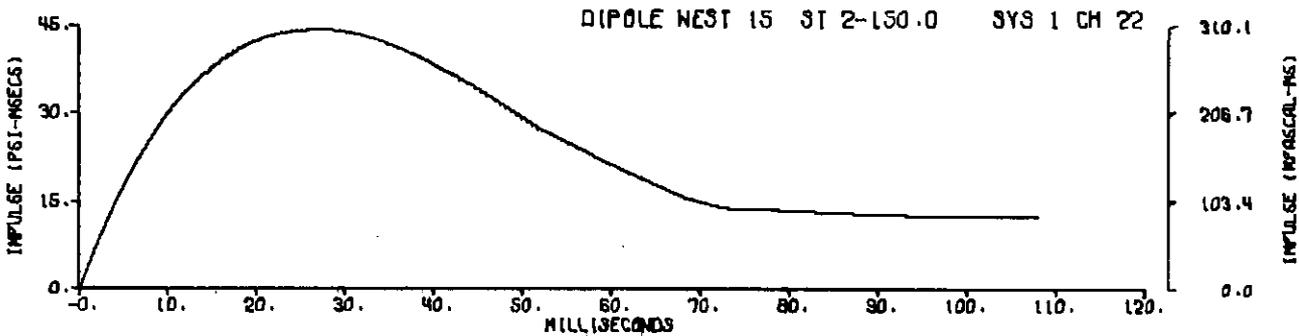
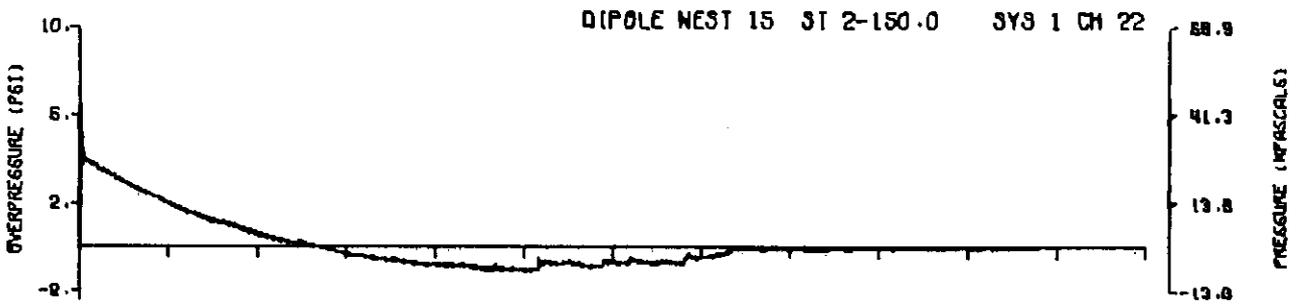
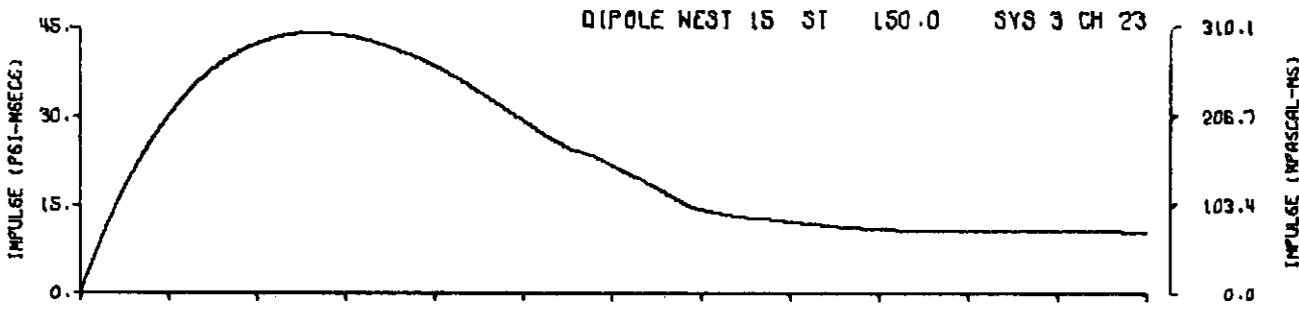
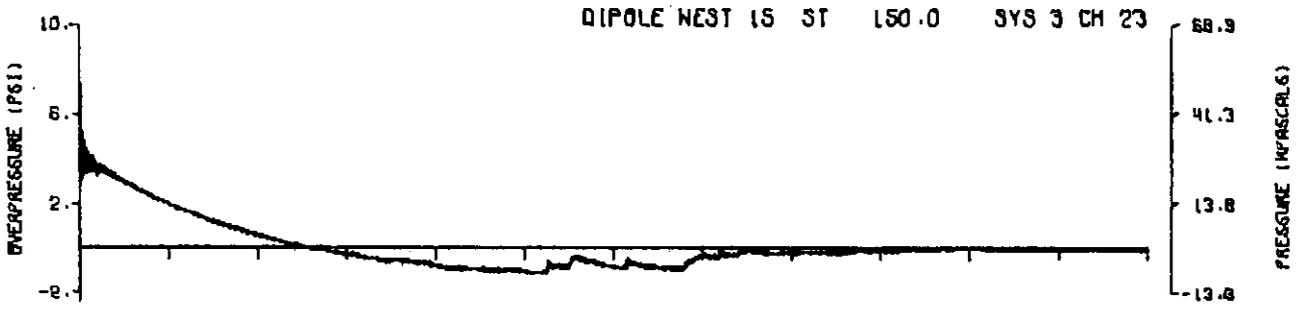
A15.40



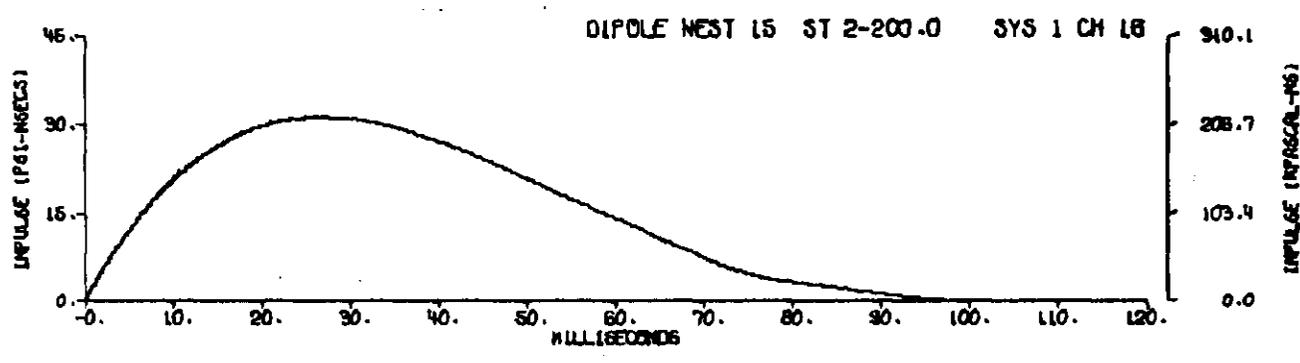
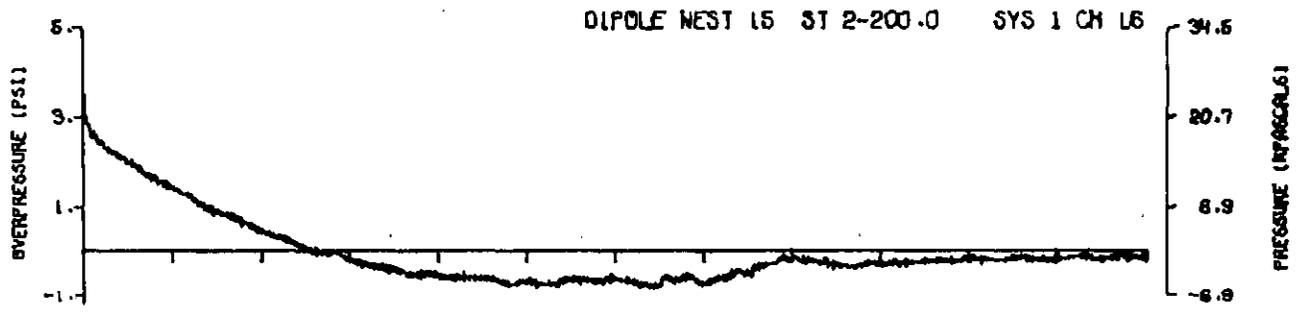
A15.41

328

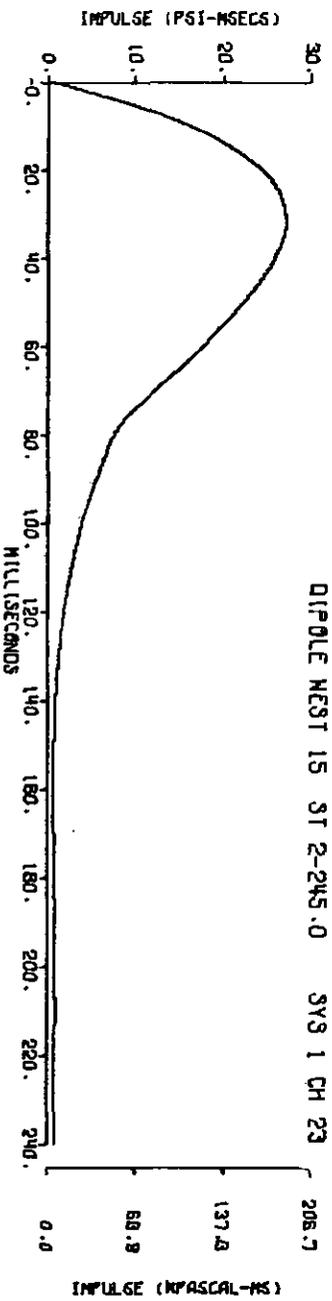
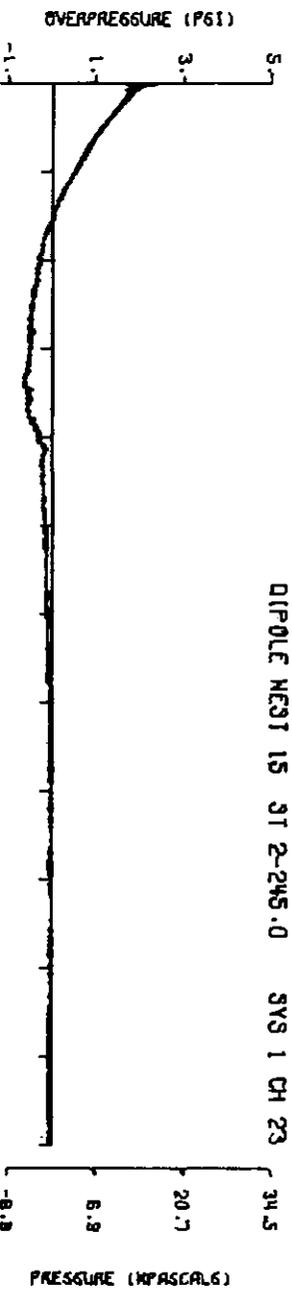
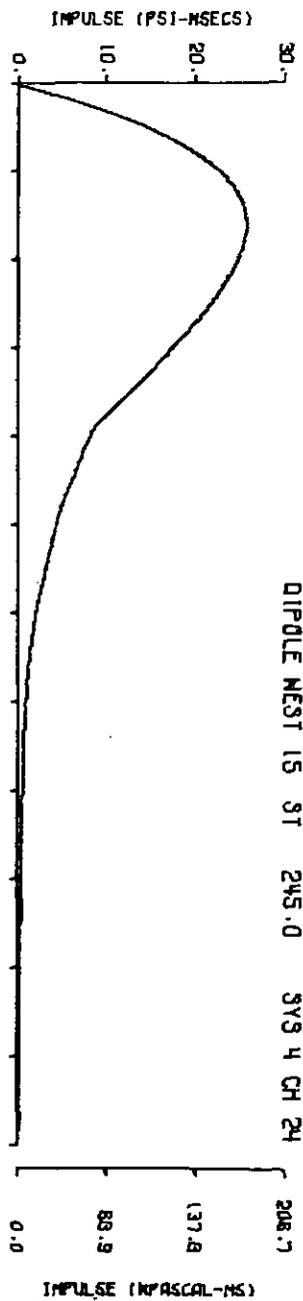
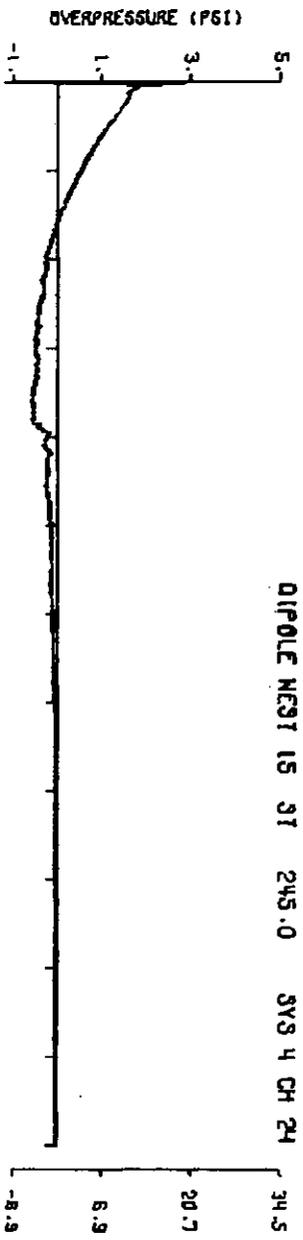




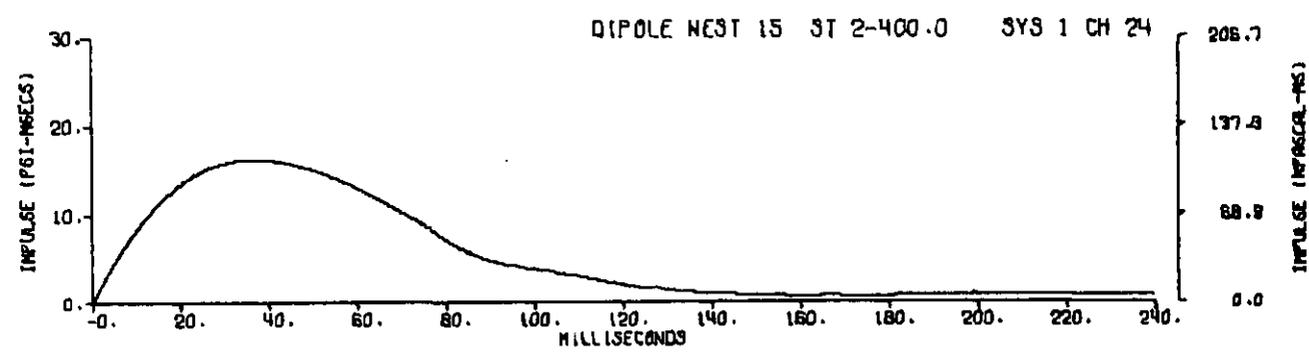
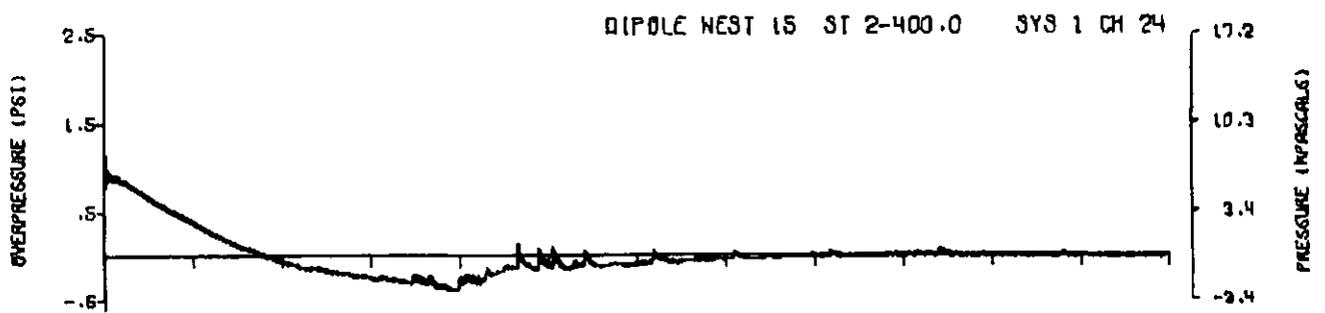
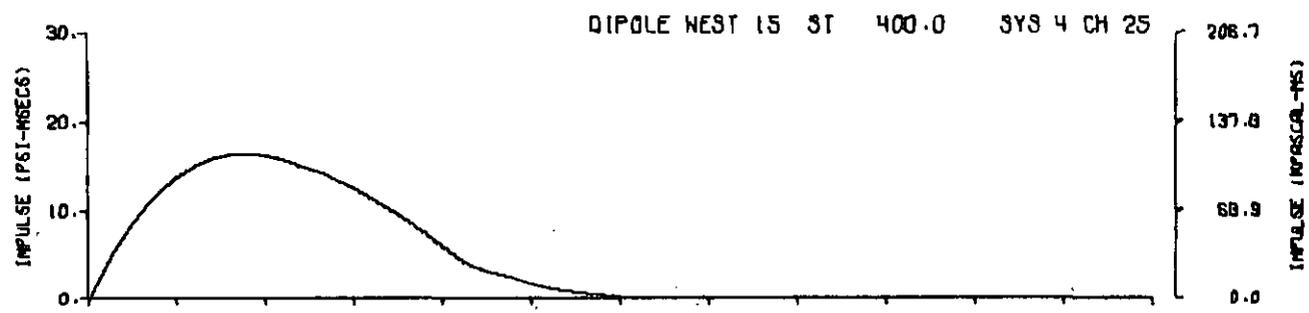
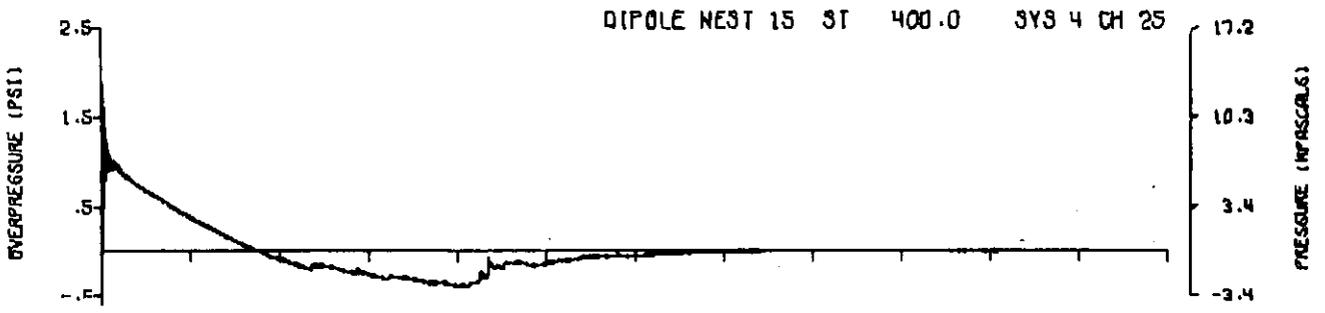
A15.43



A15.44

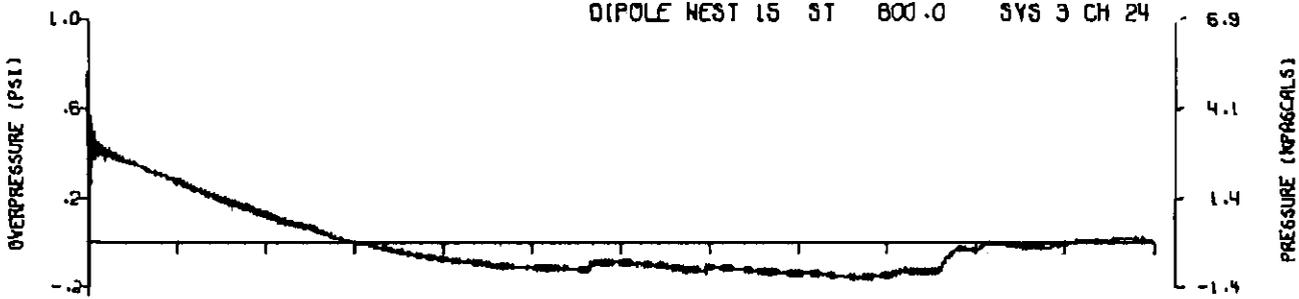


A15.45

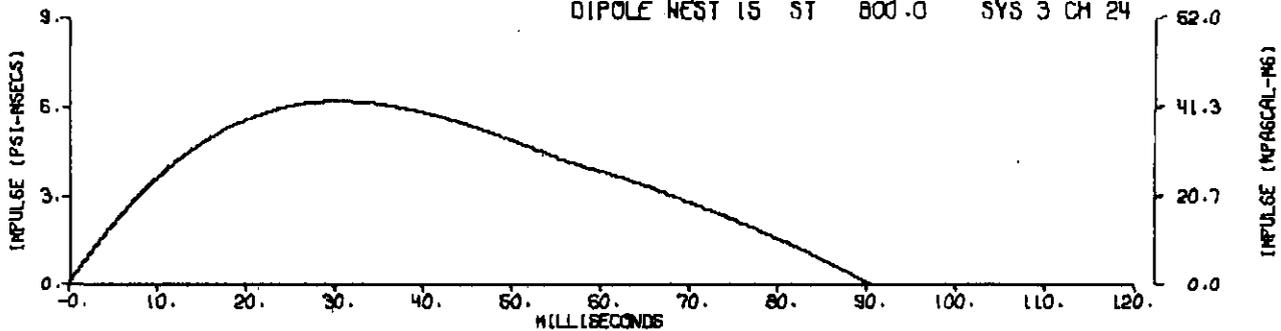


A15.46

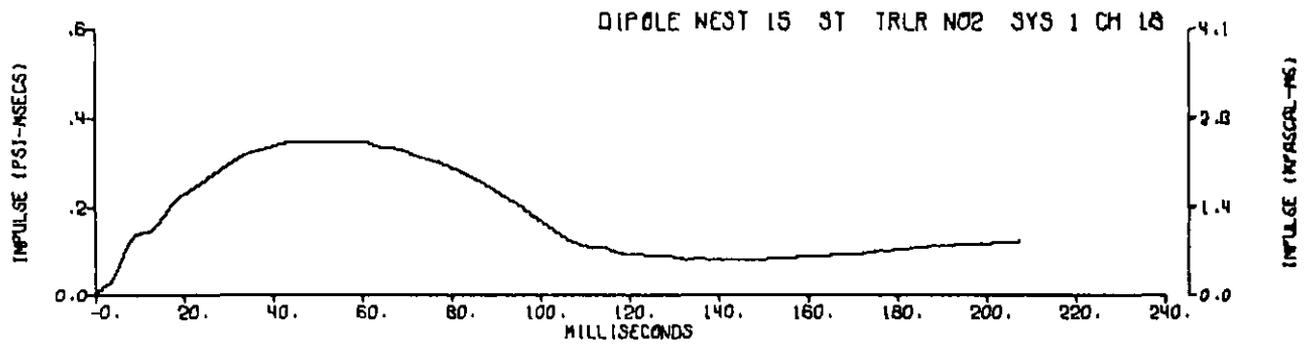
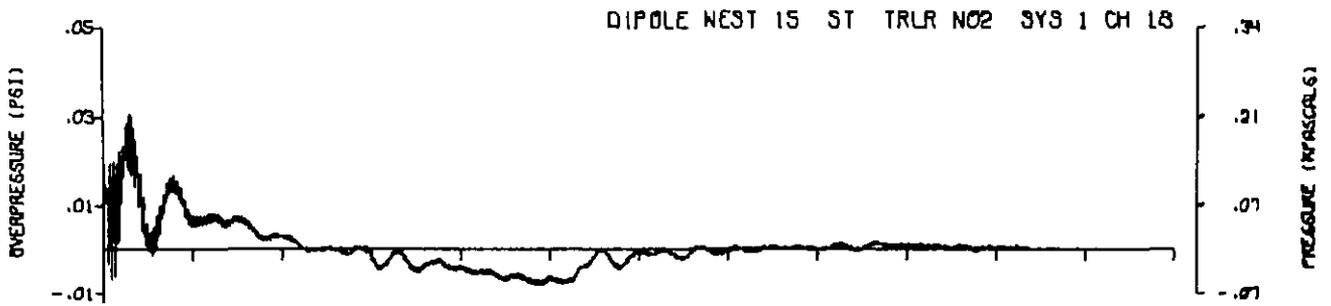
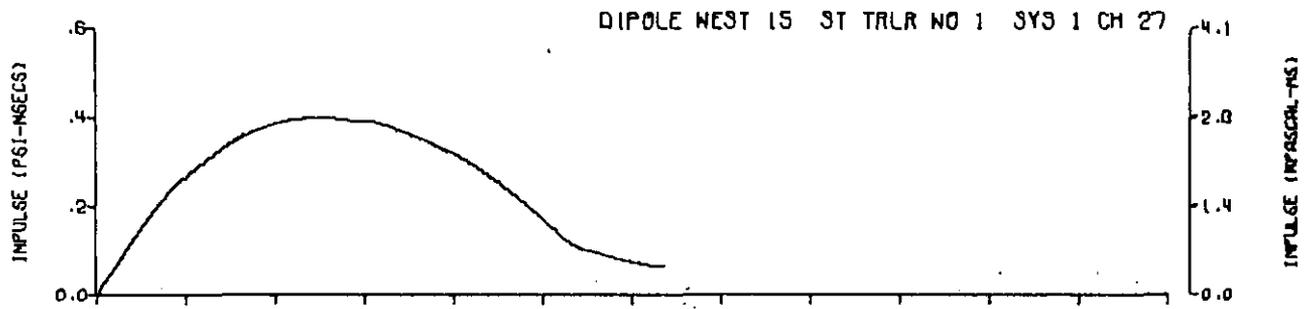
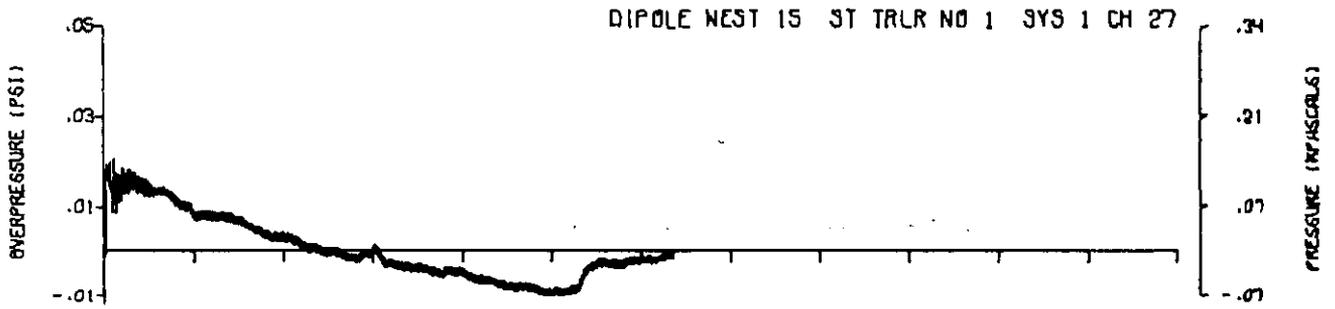
DIPOLE NEST 15 ST 800.0 SYS 3 CH 24



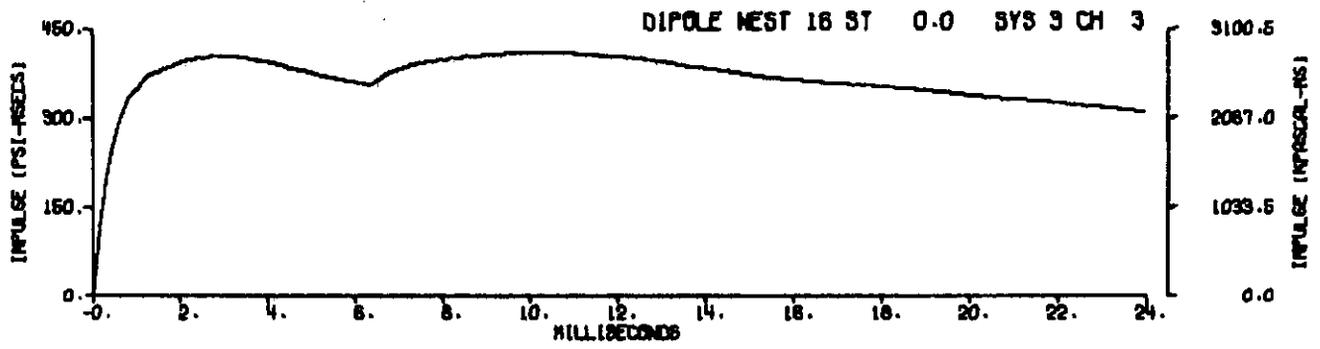
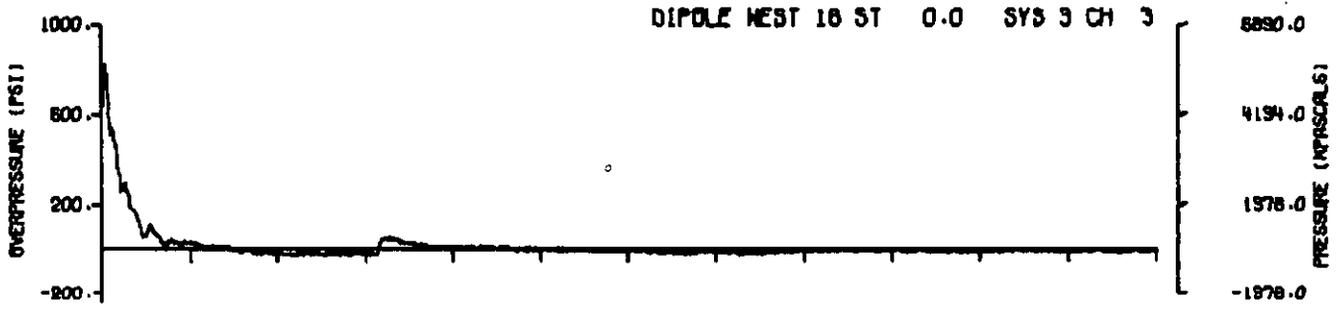
DIPOLE NEST 15 ST 800.0 SYS 3 CH 24



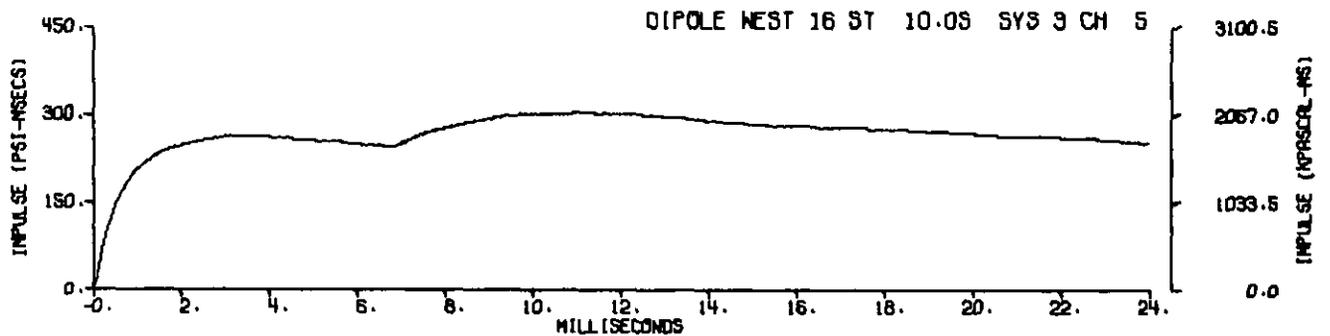
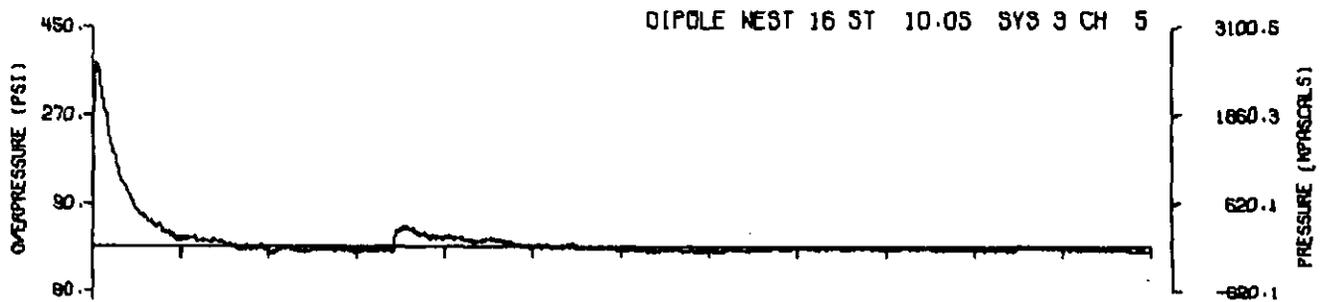
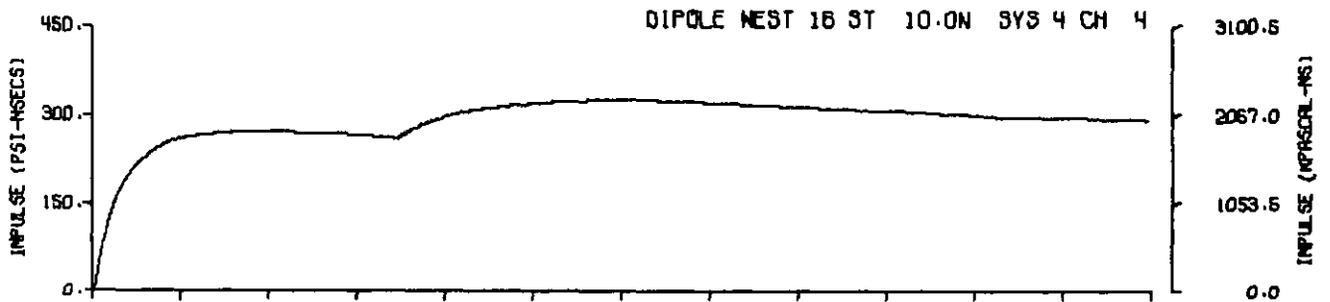
A15.47



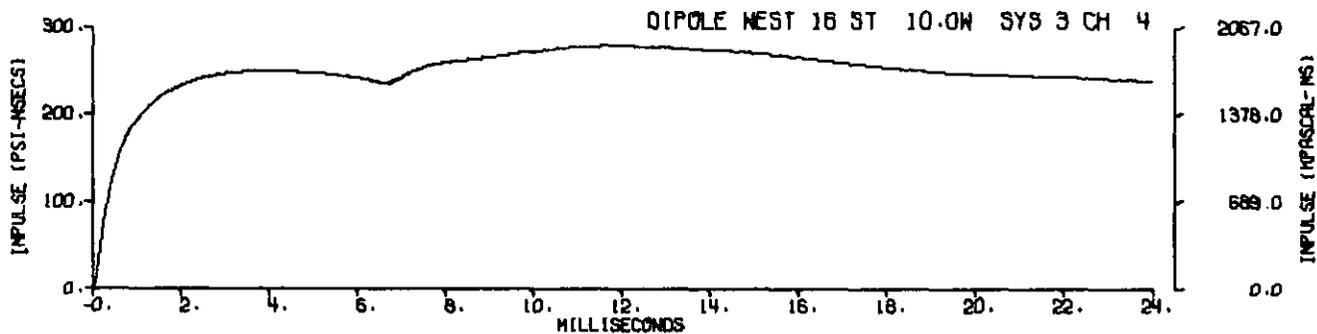
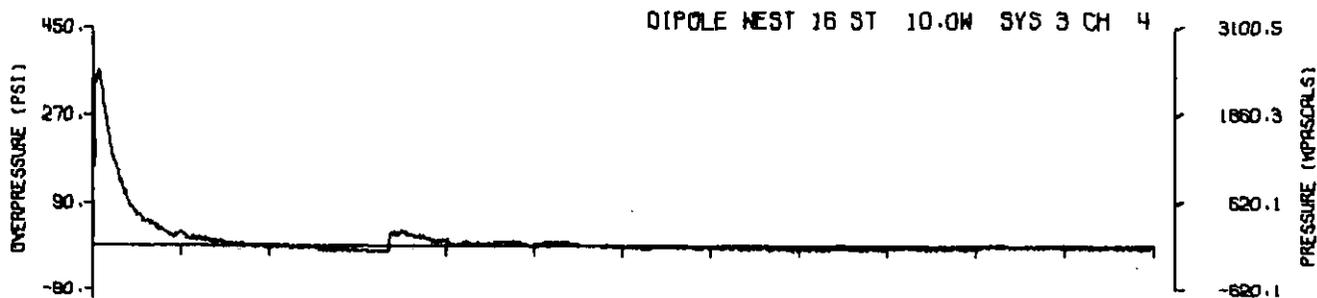
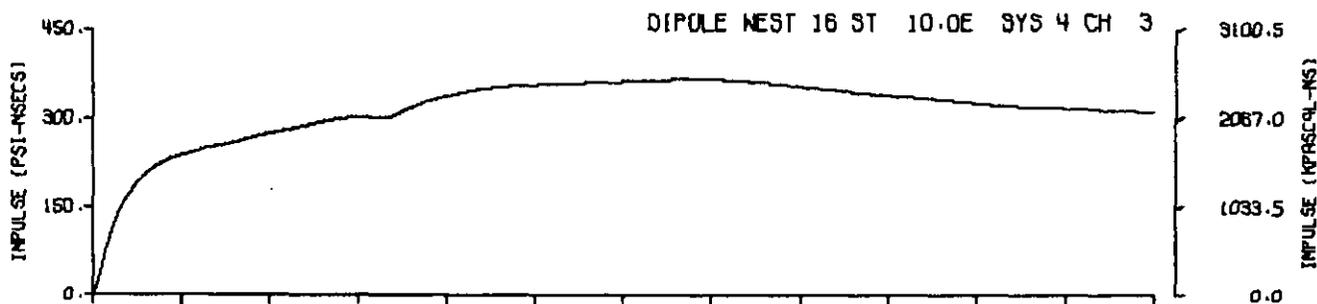
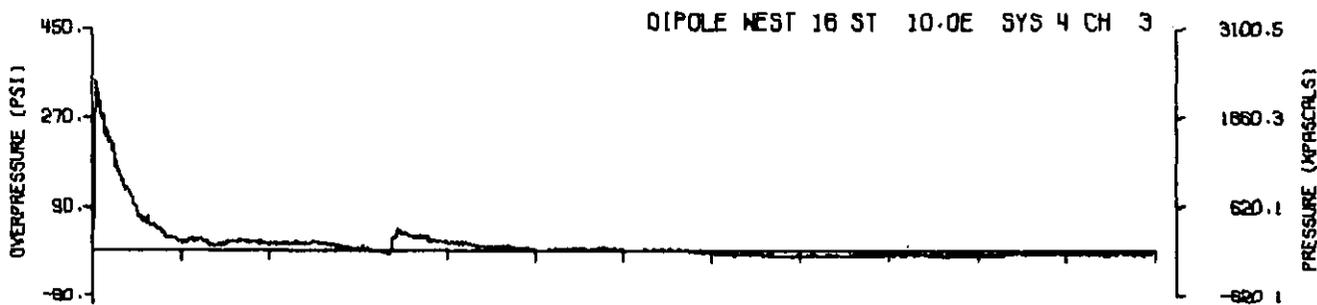
A15.48



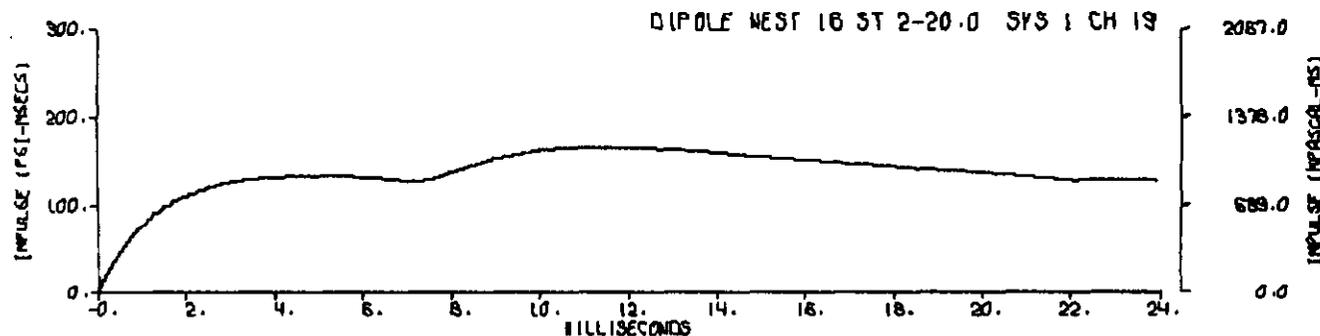
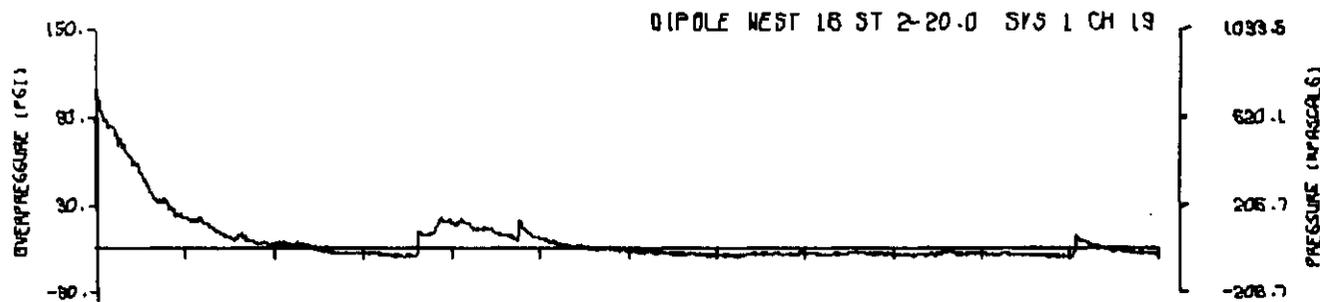
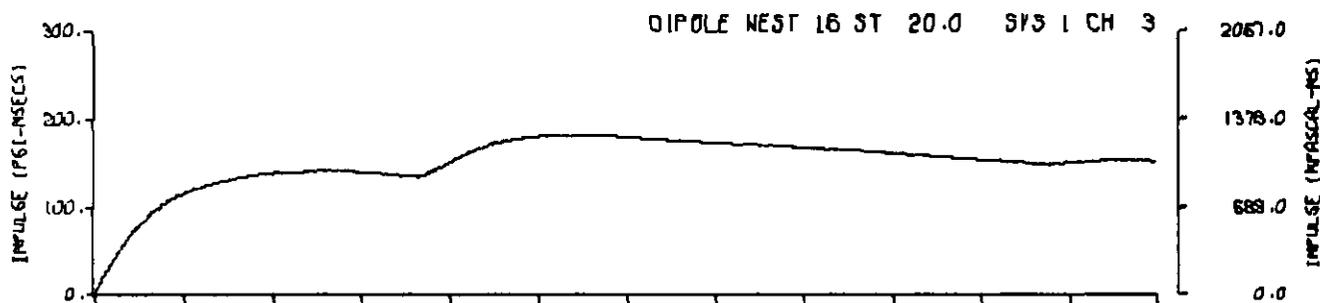
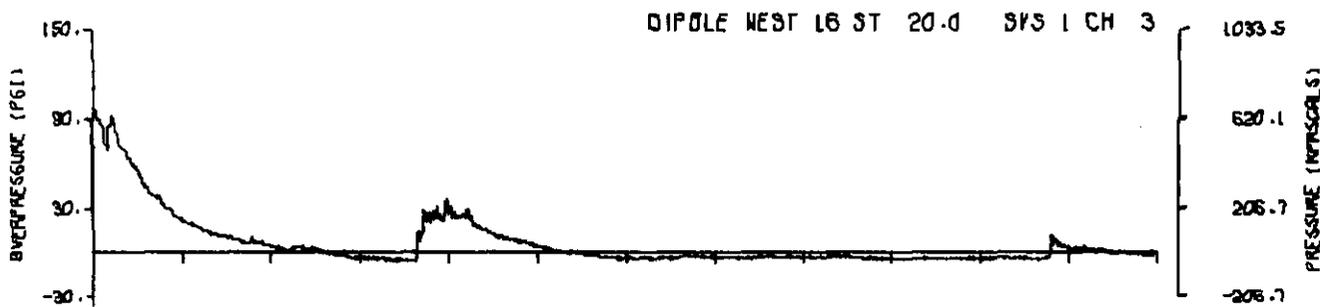
A16.1



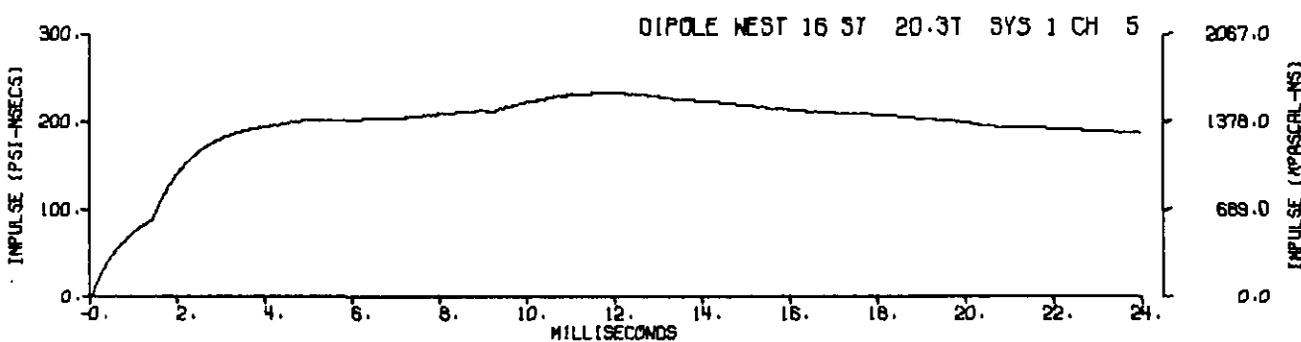
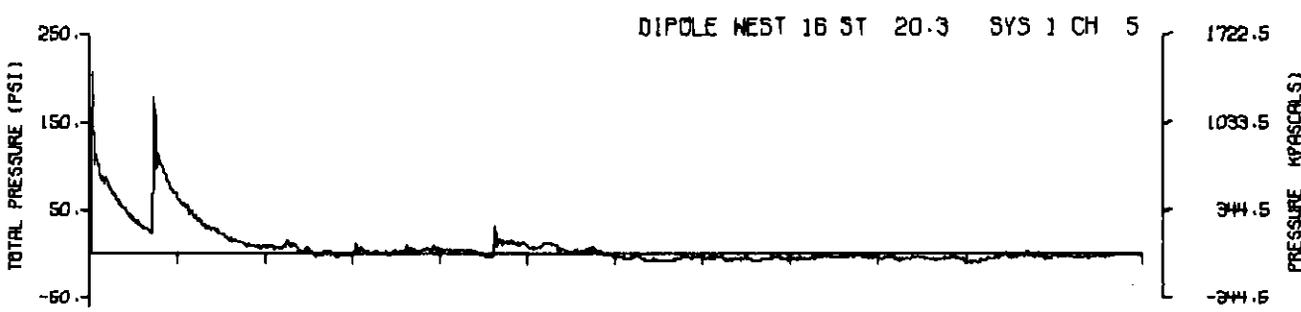
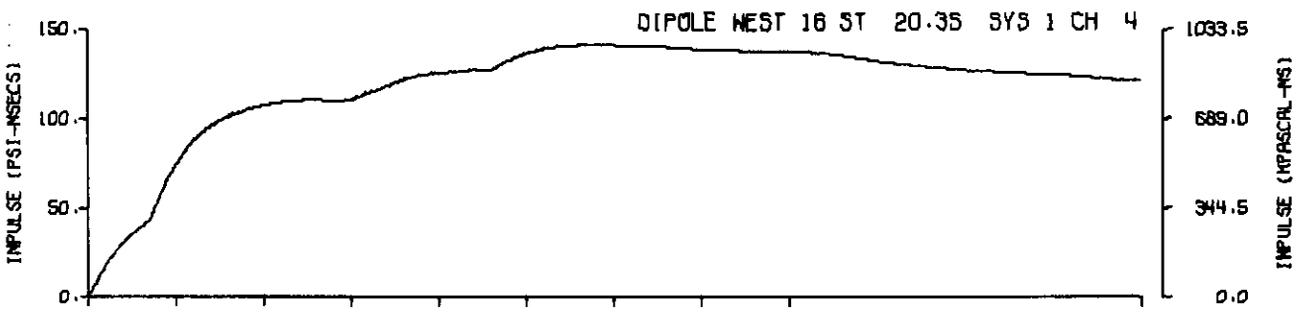
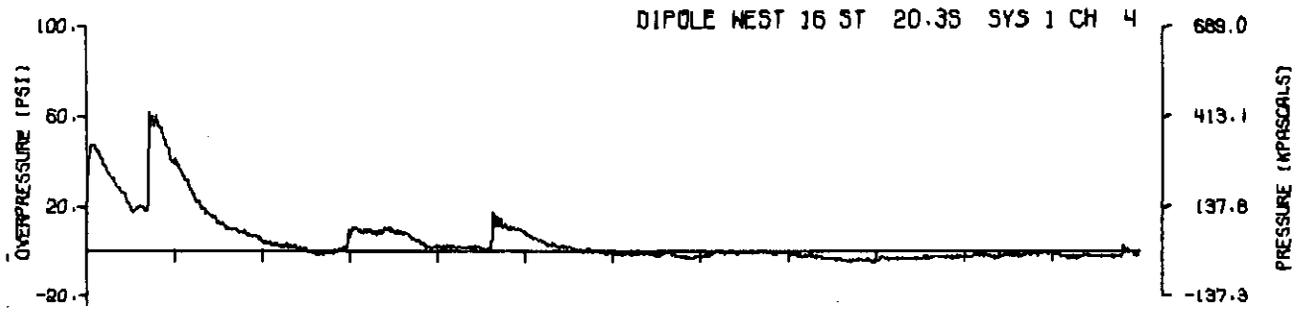
A16.2



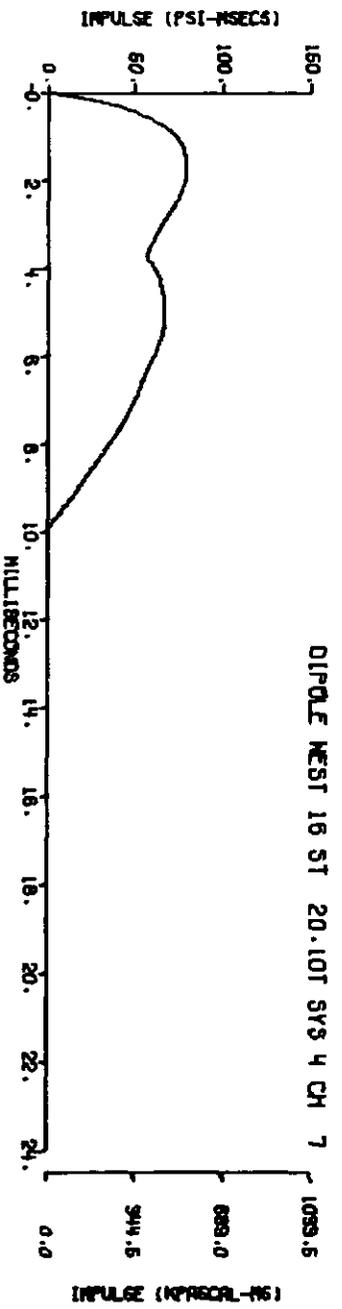
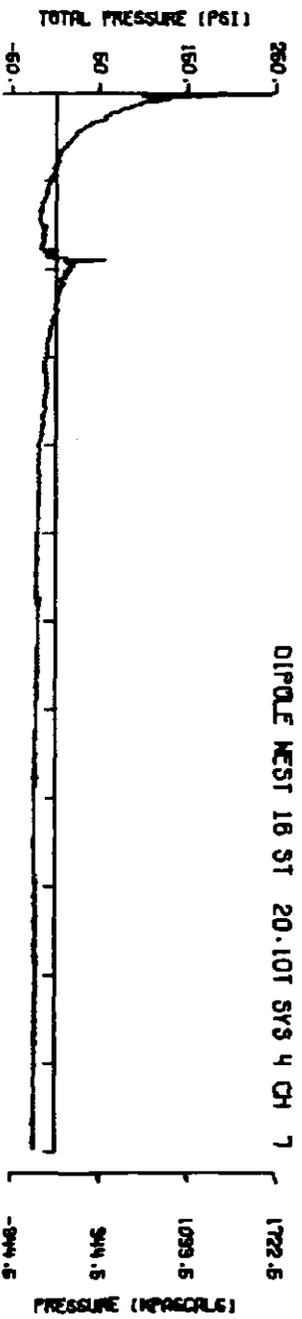
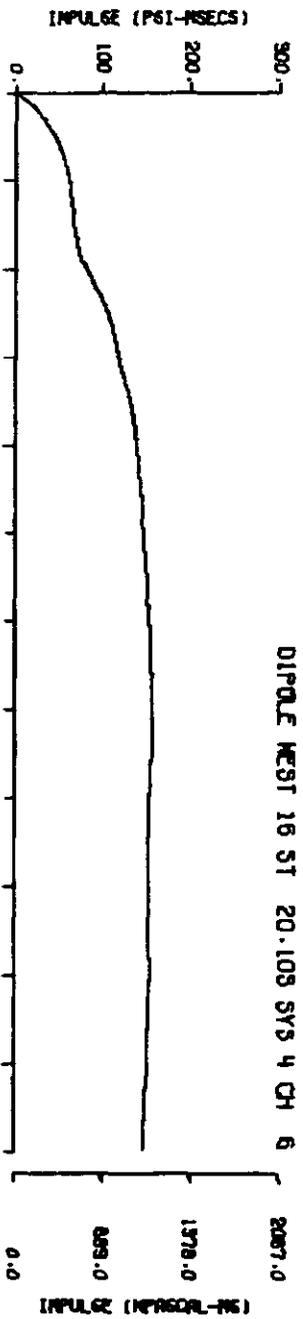
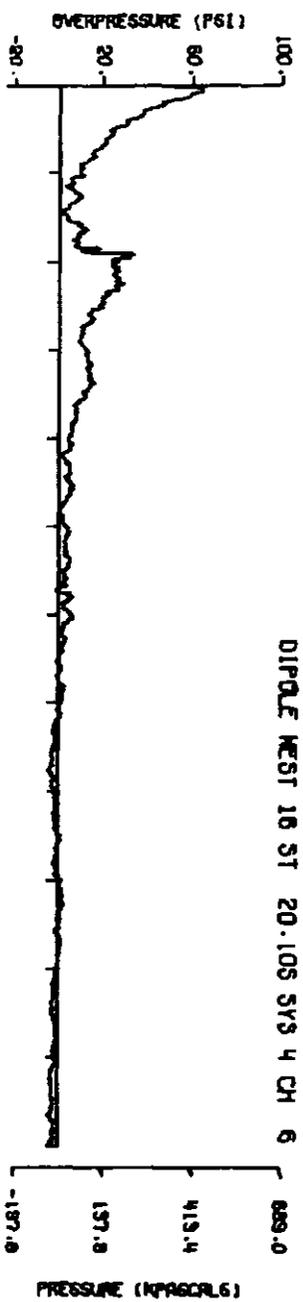
A16.3



A16.4

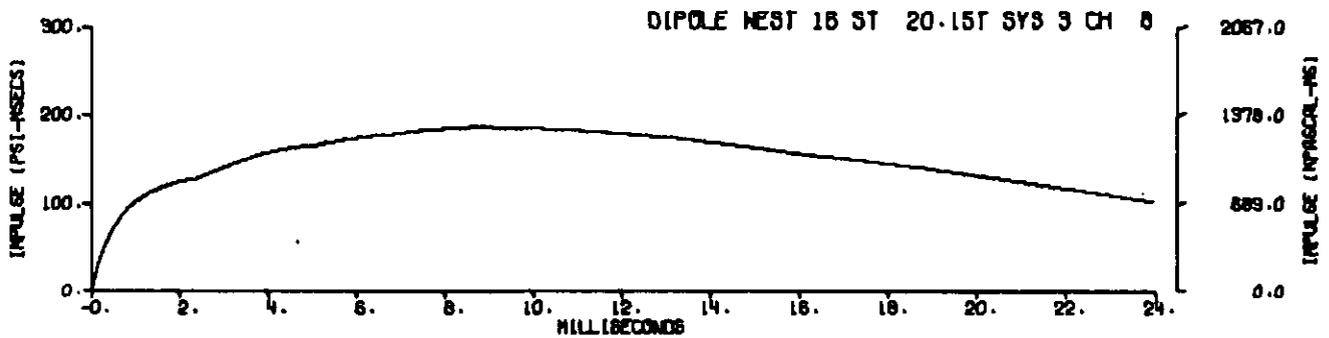
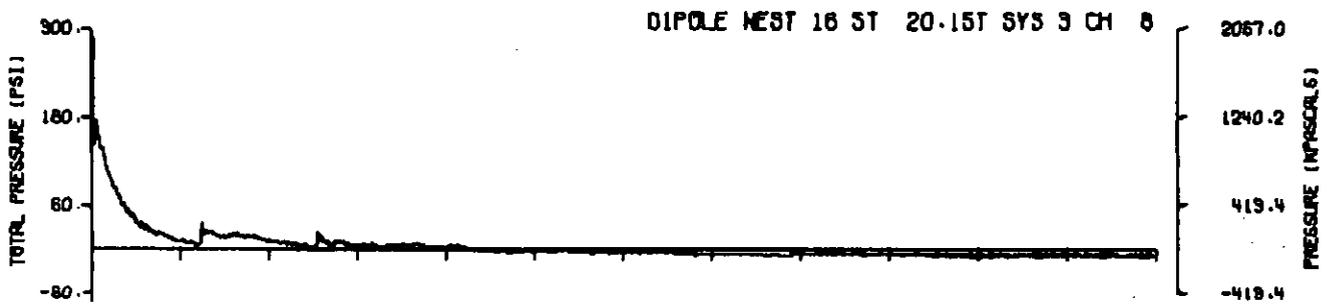
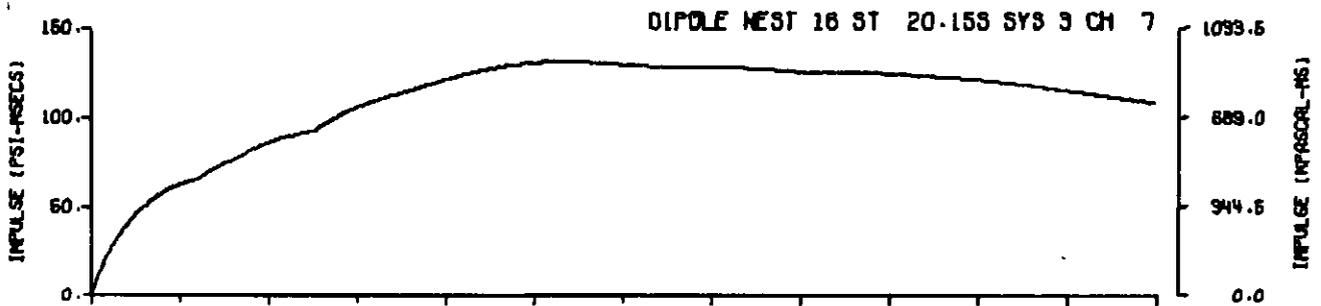
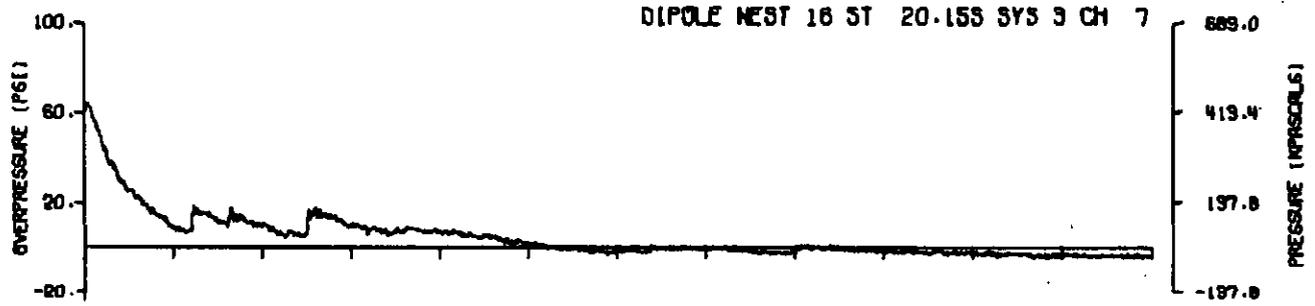


A16.5
340

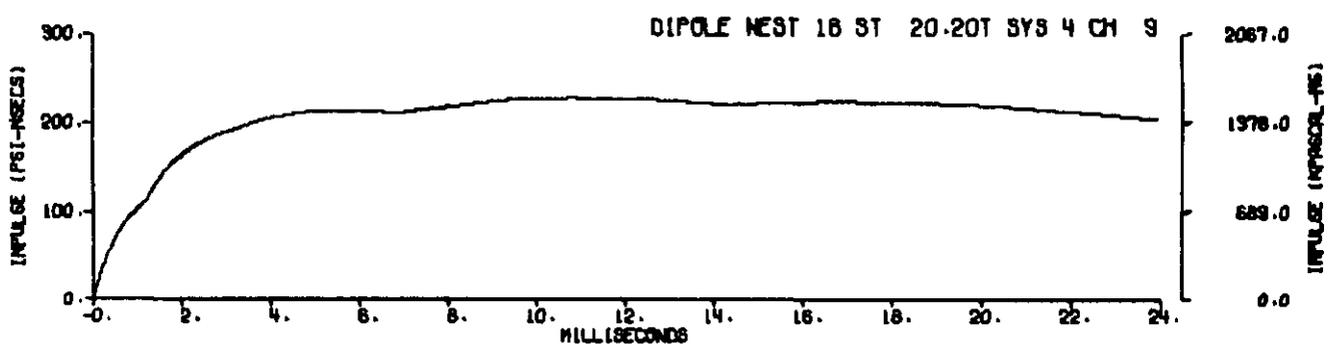
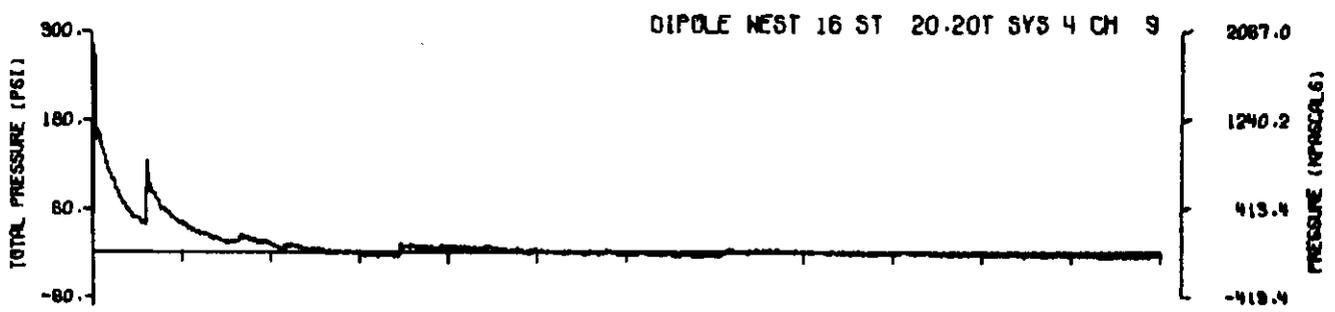
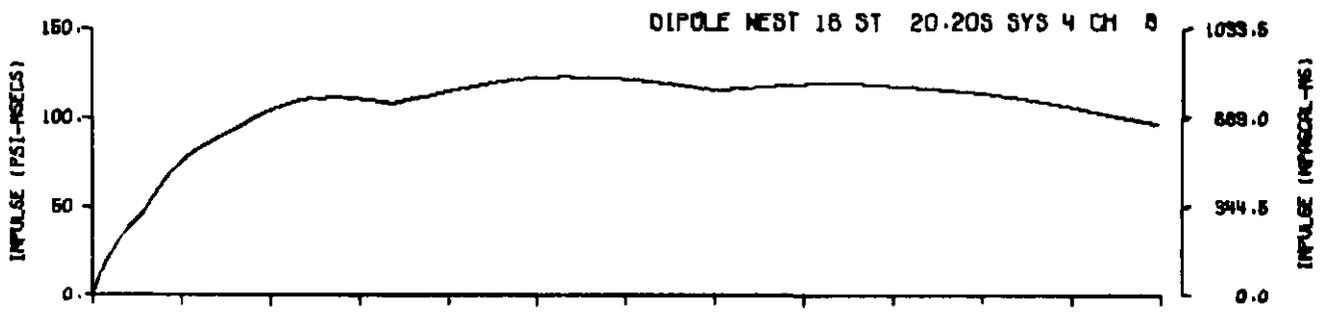
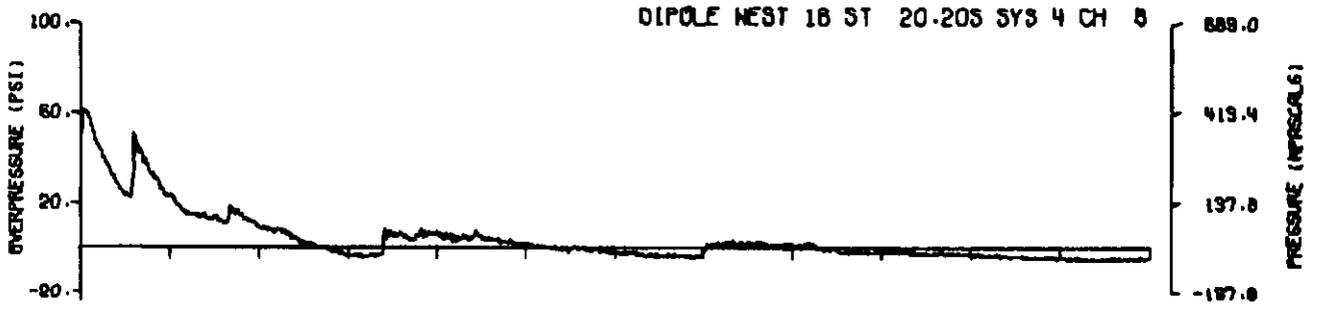


A16.6

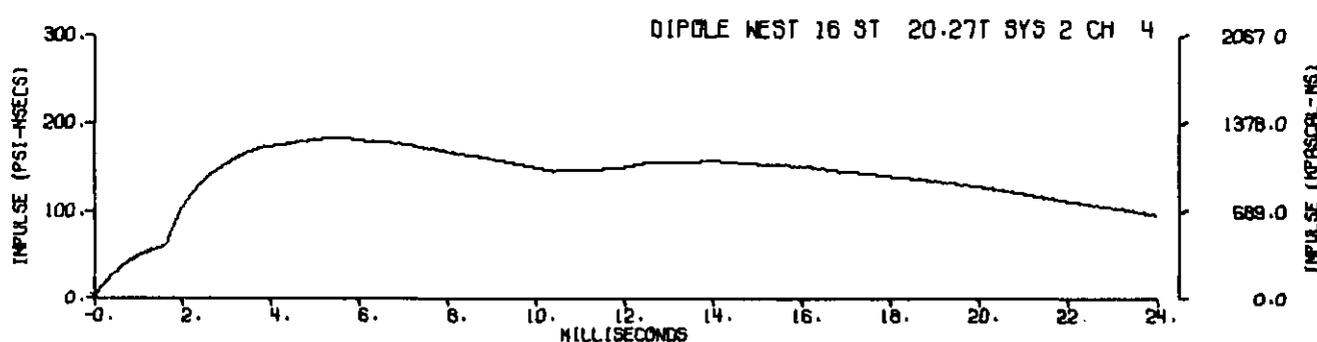
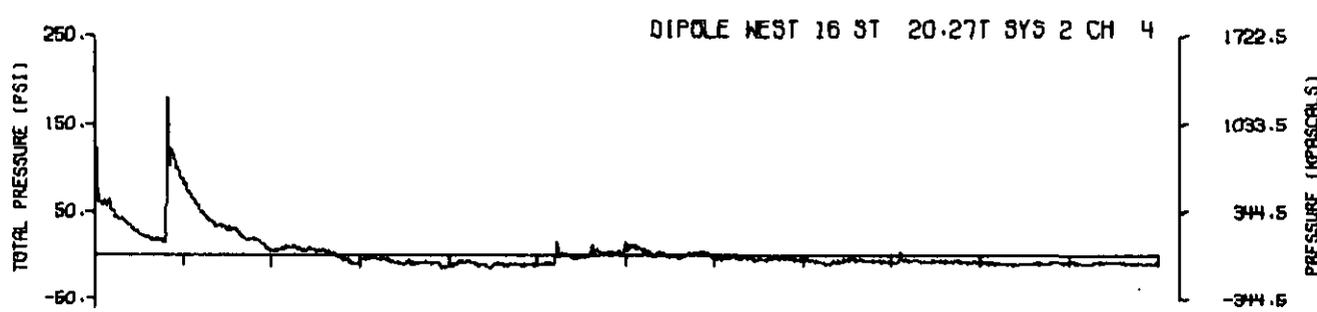
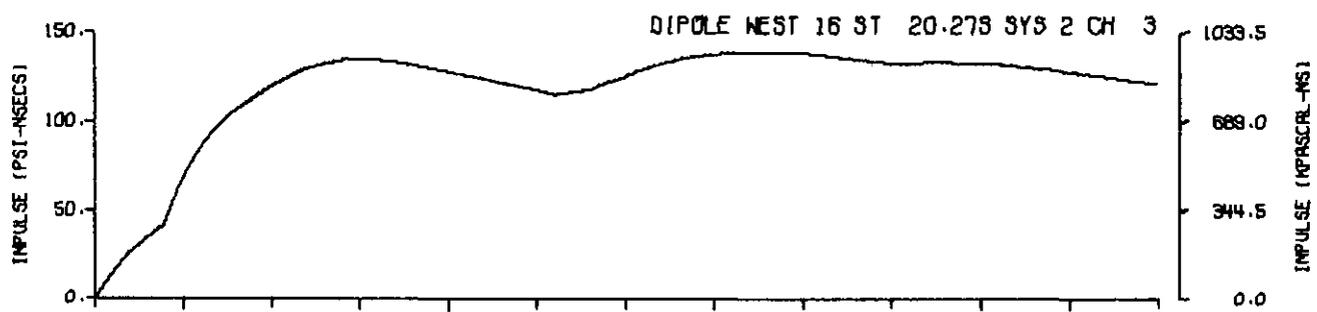
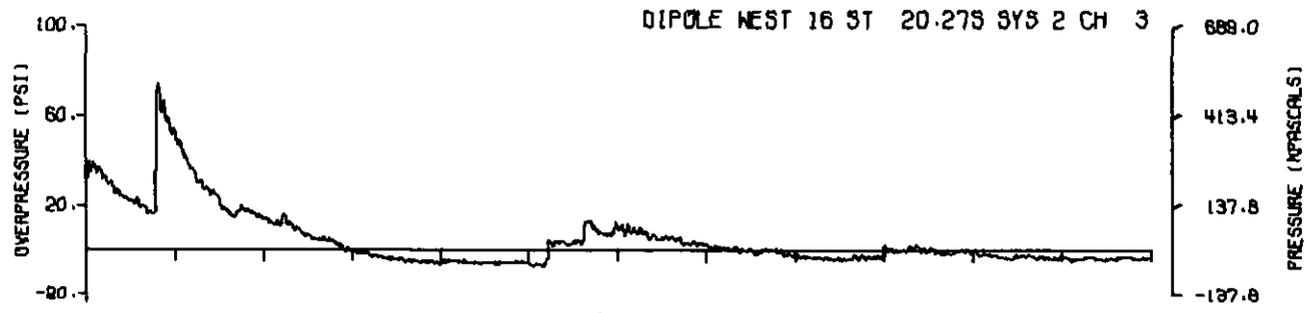
341



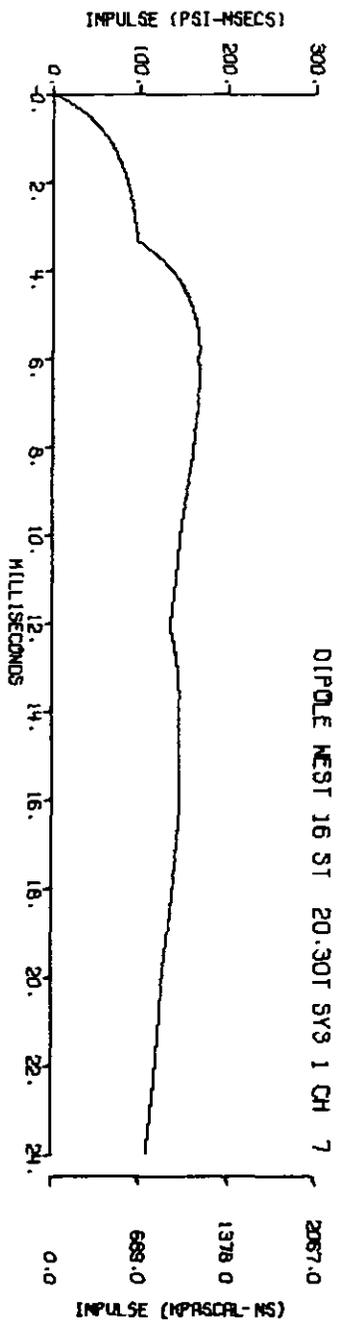
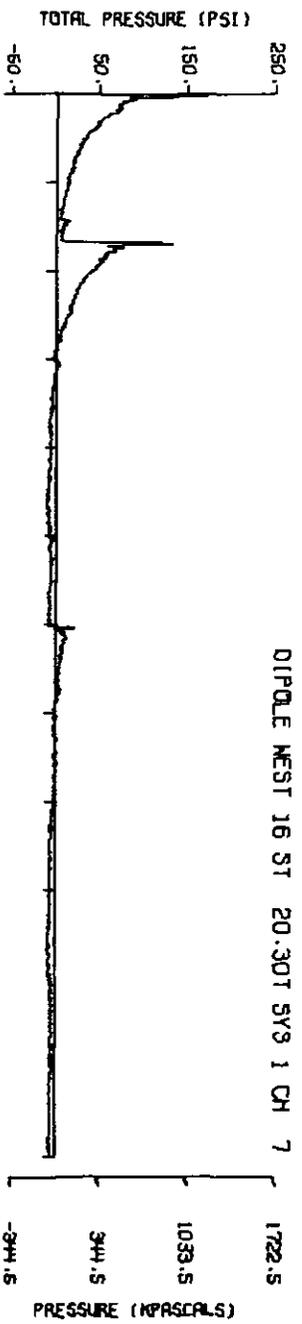
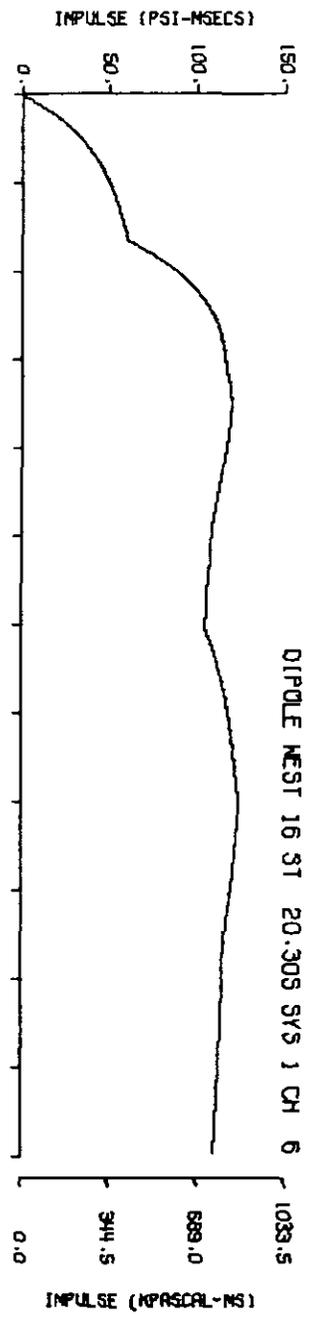
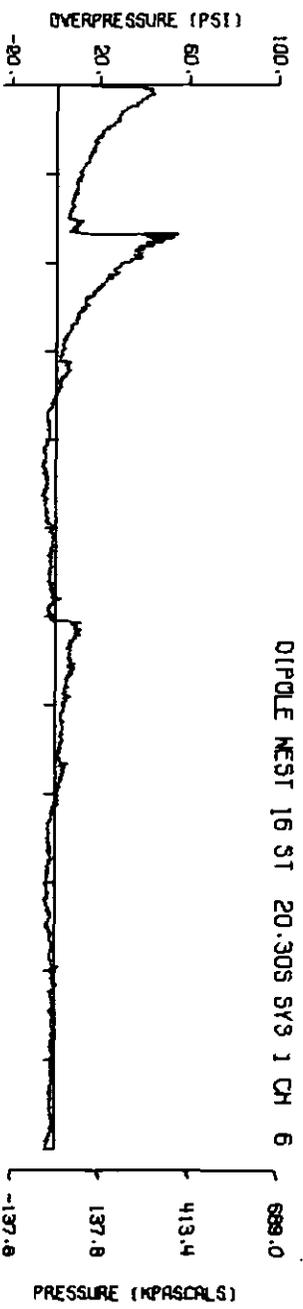
A16.7



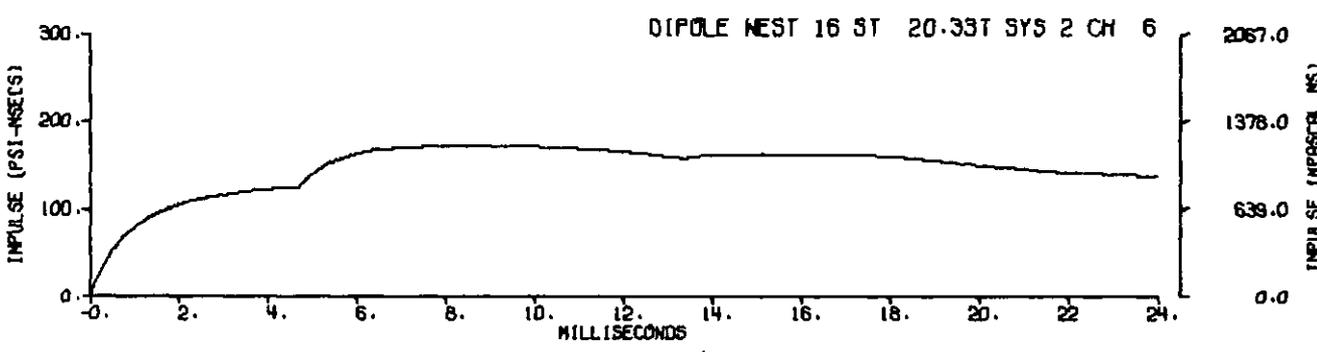
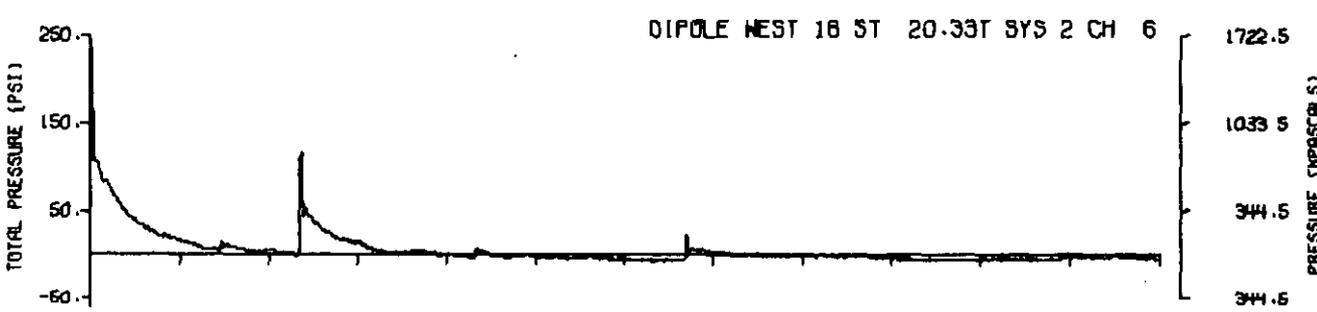
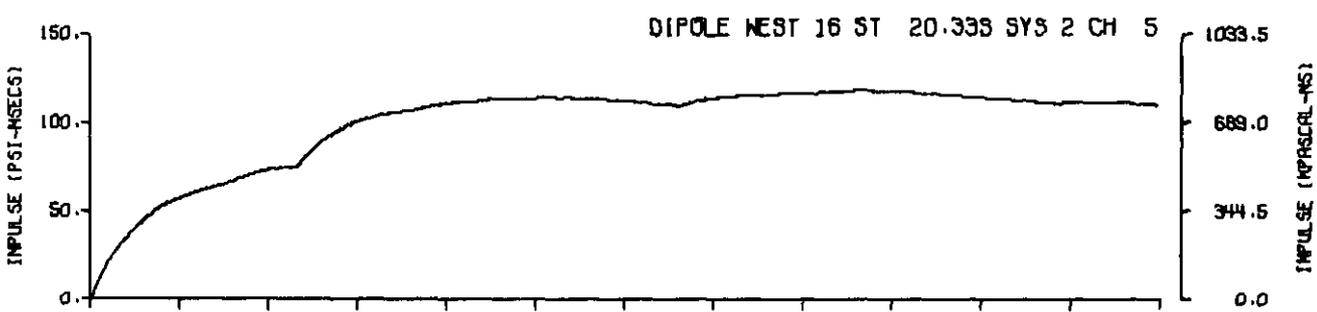
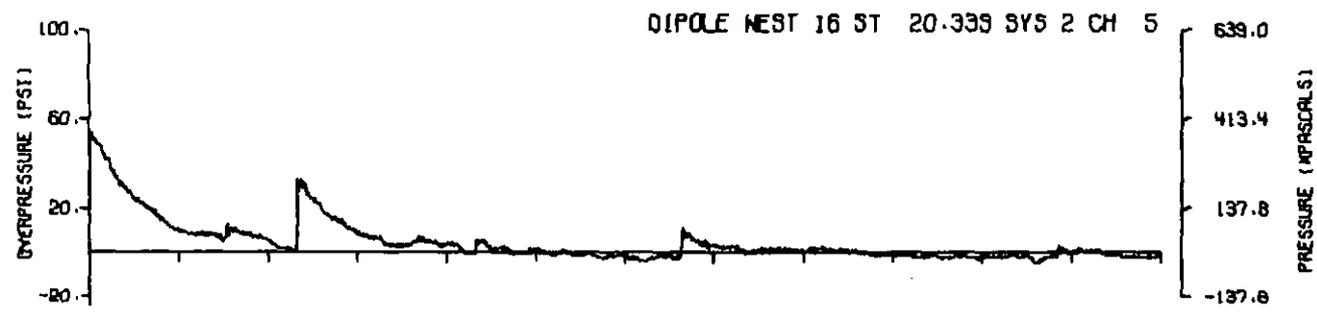
A16.8



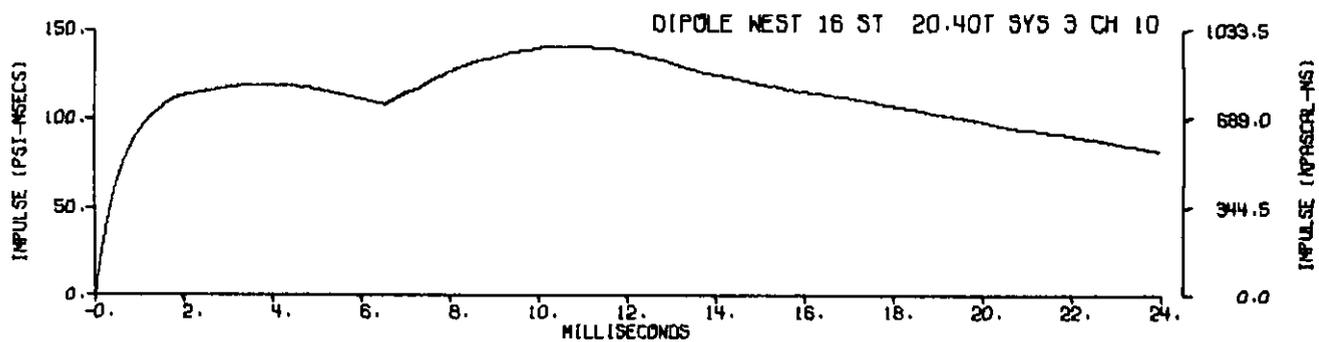
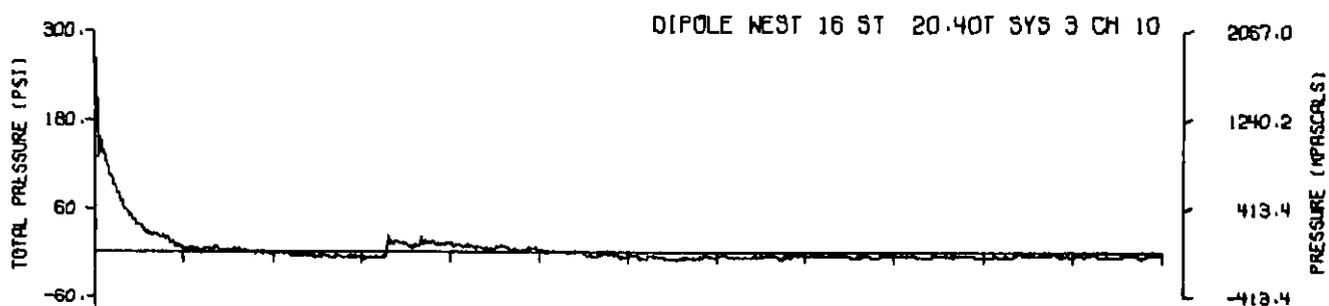
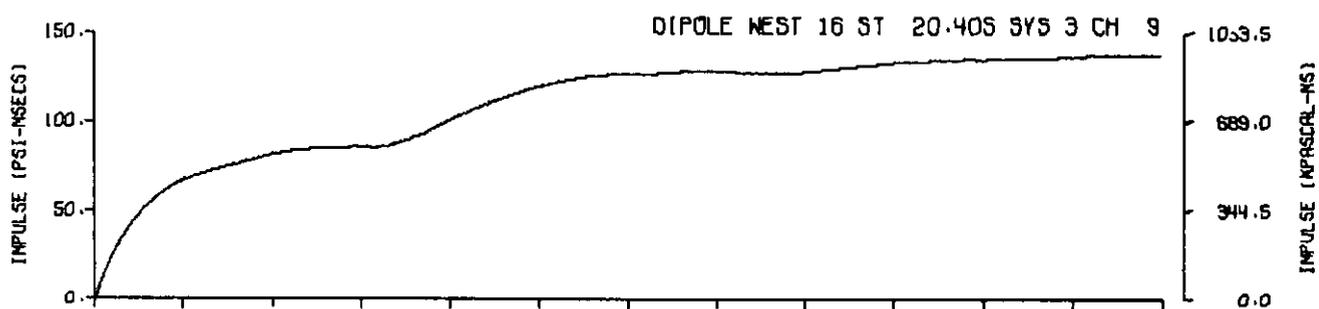
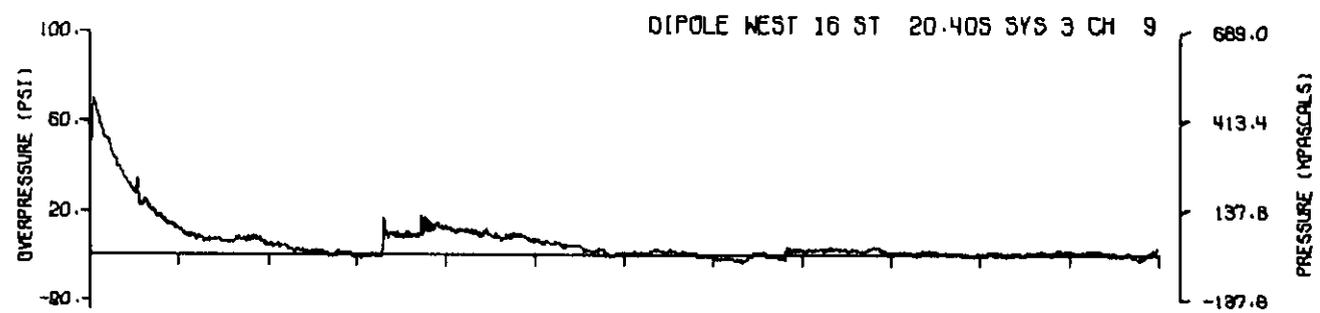
A16.9



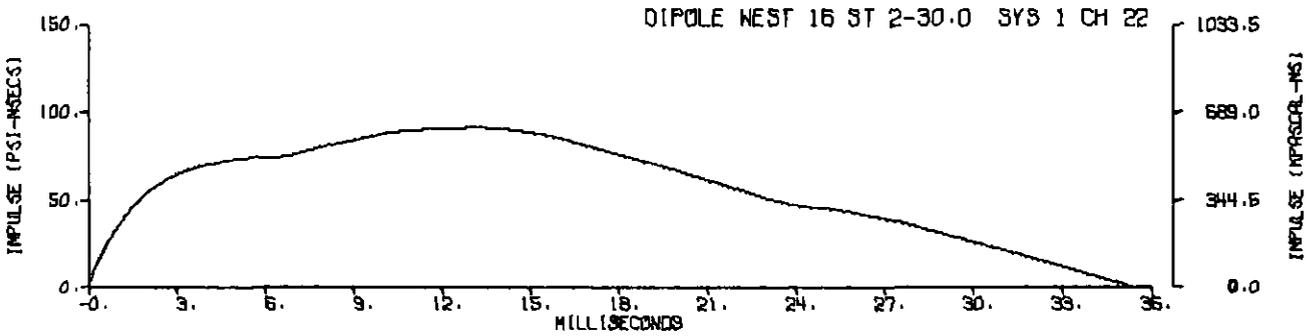
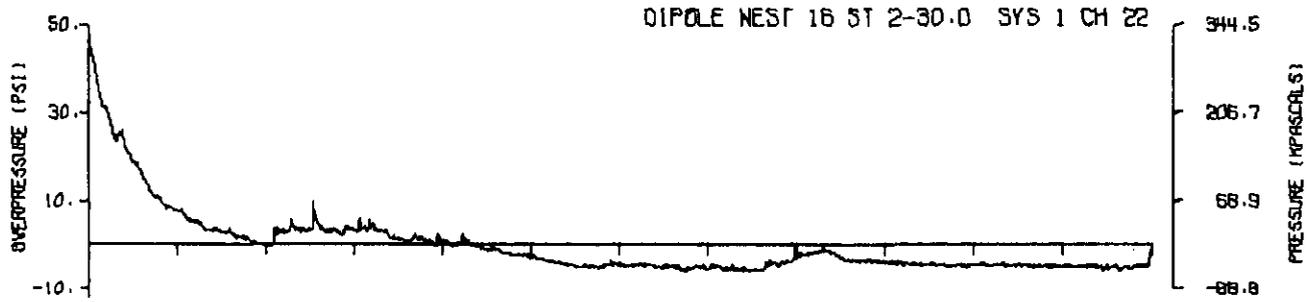
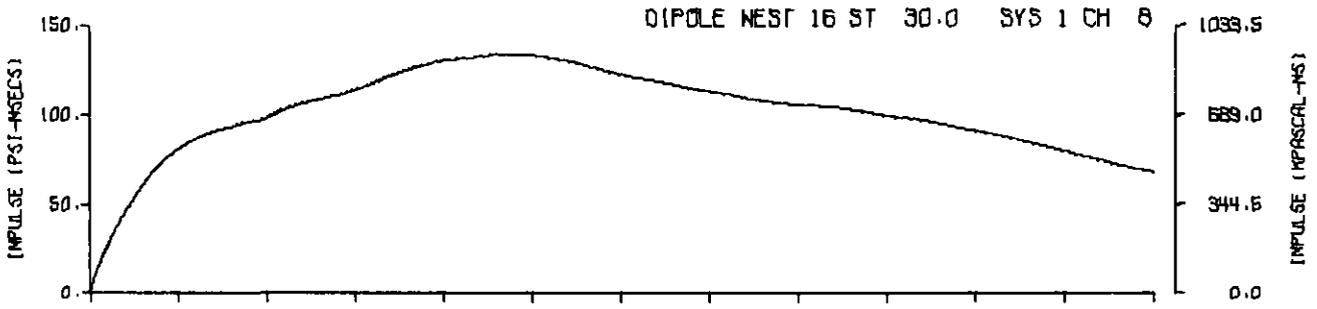
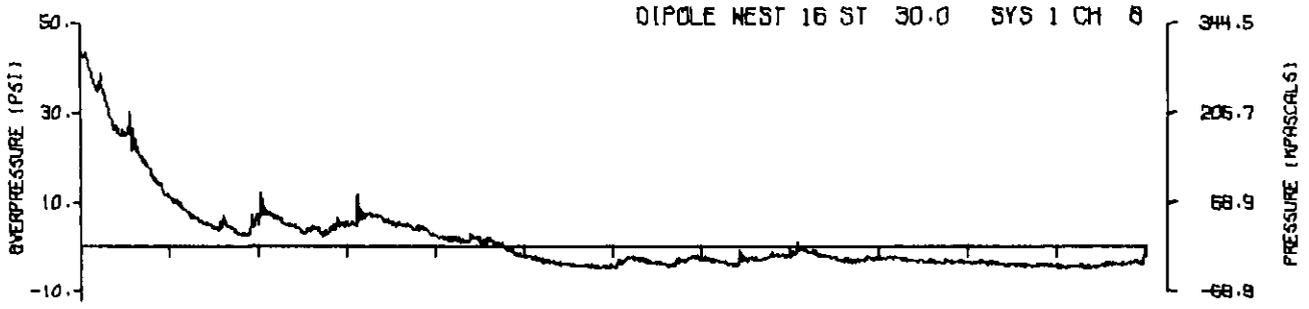
A16.10
345



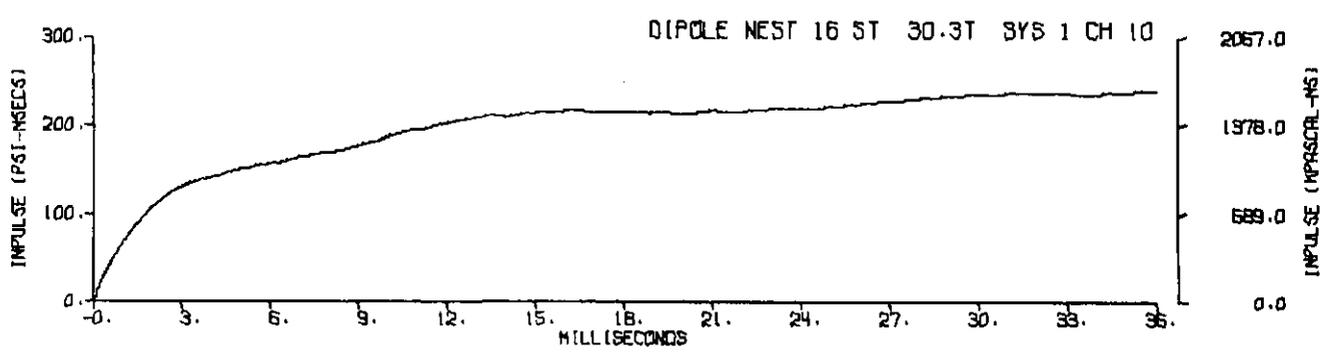
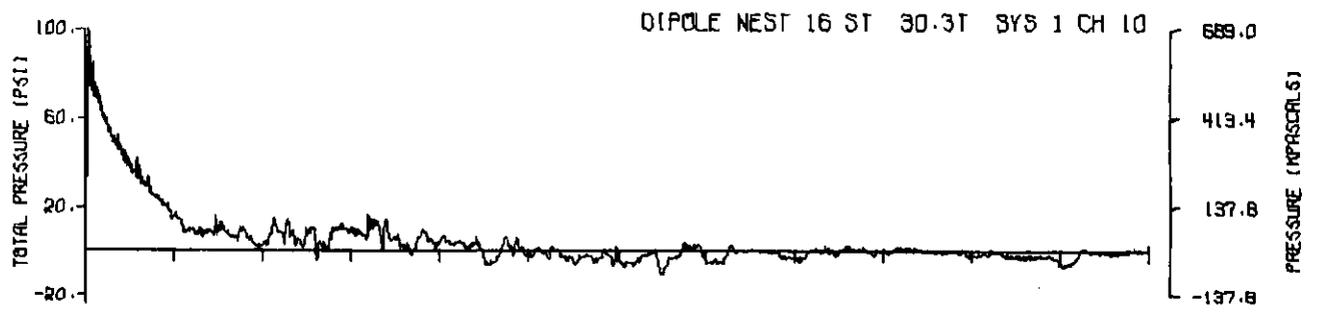
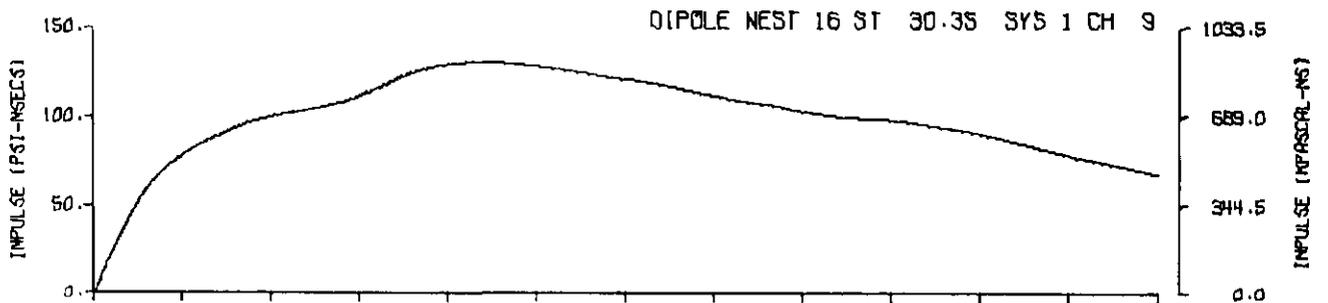
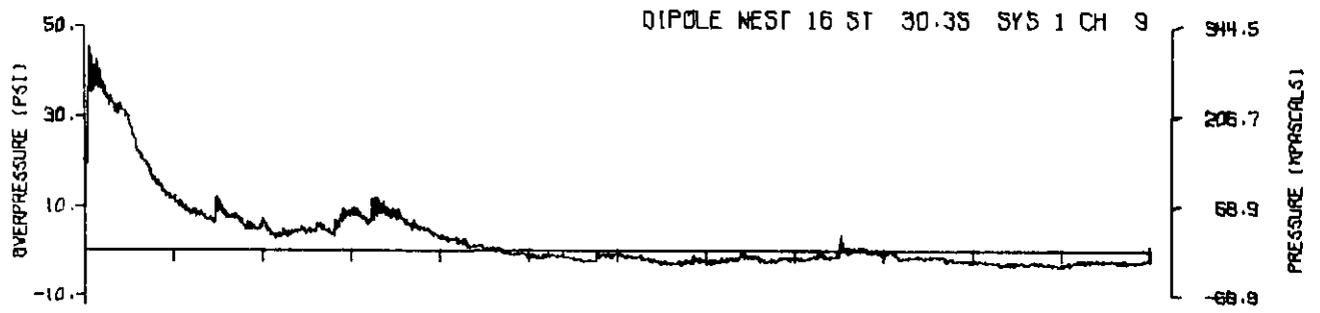
A16.11



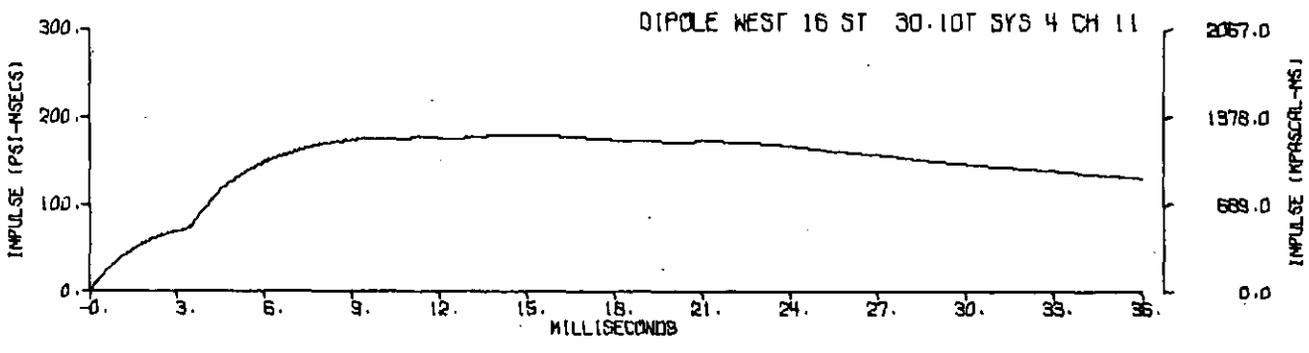
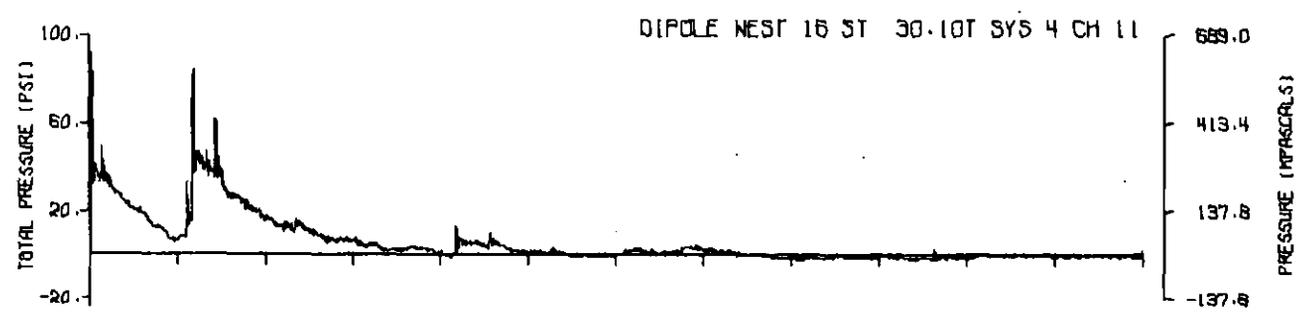
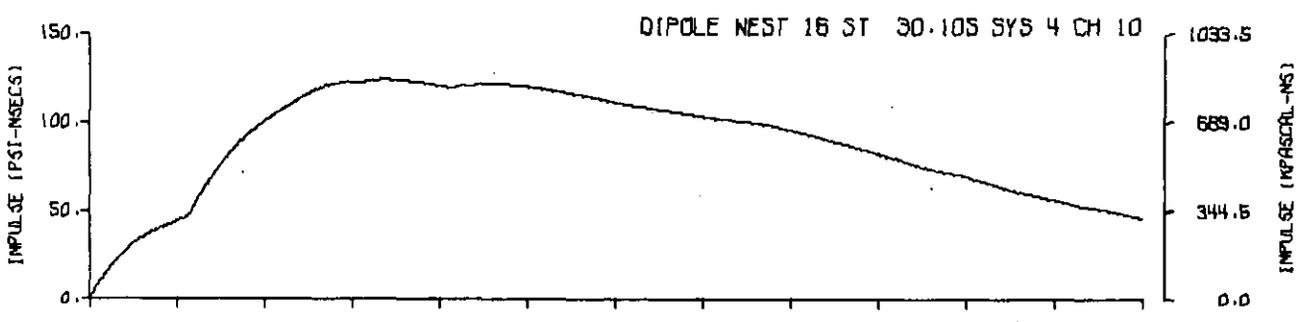
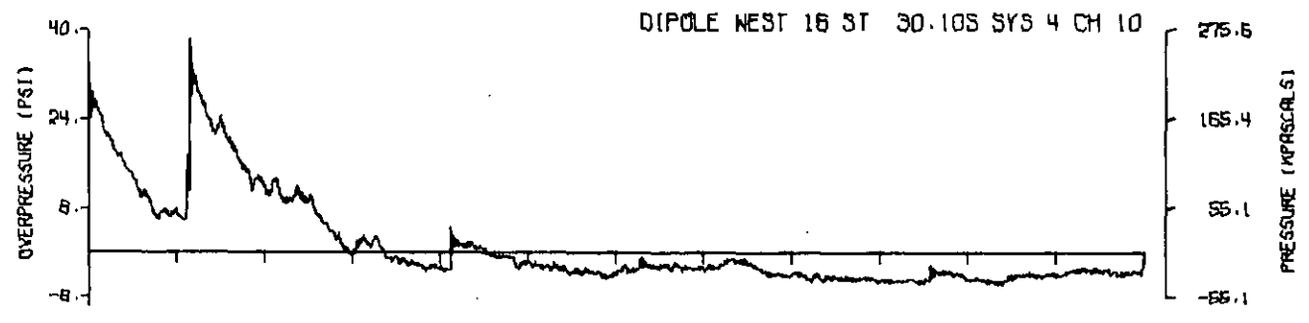
A16.12



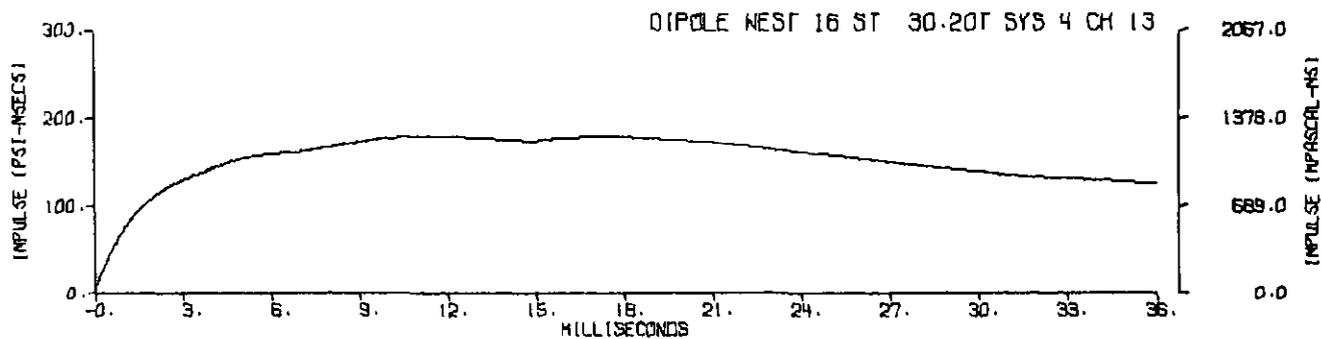
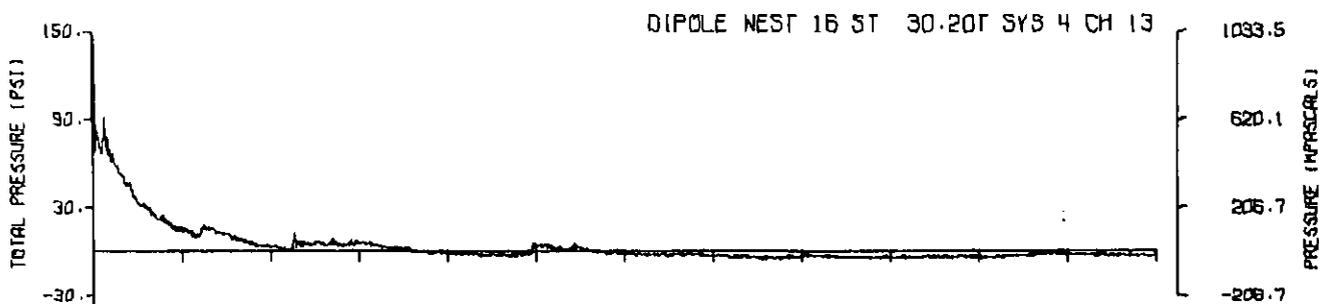
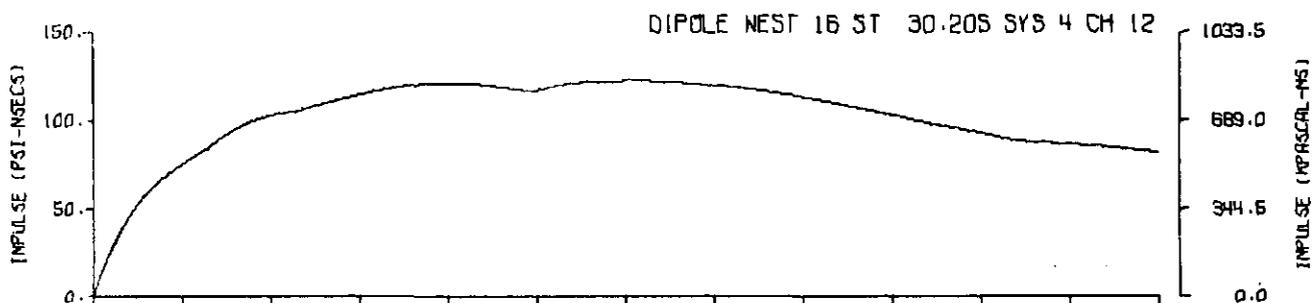
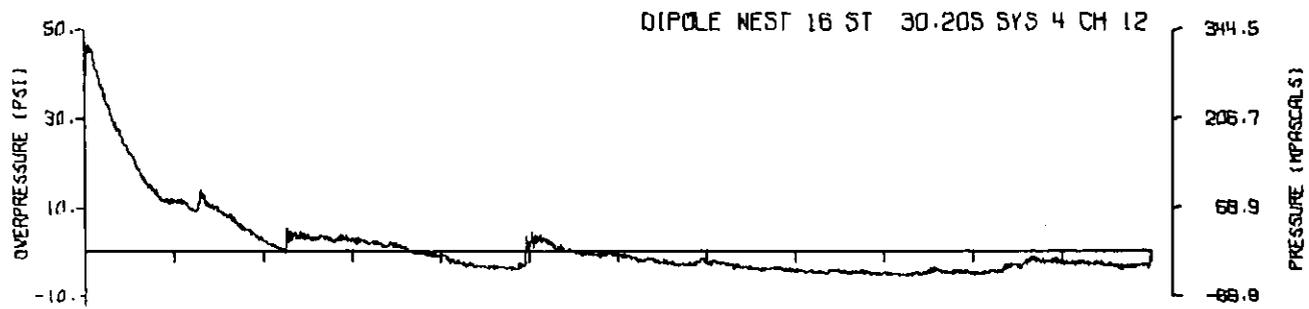
A16.13



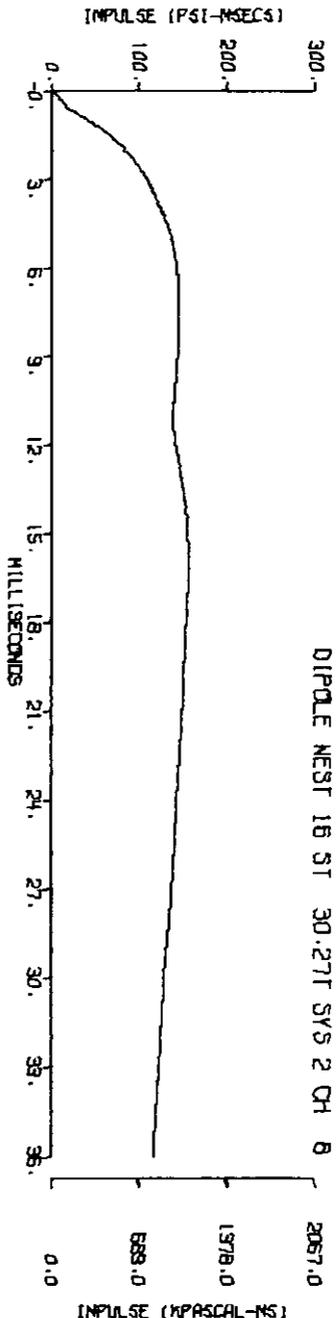
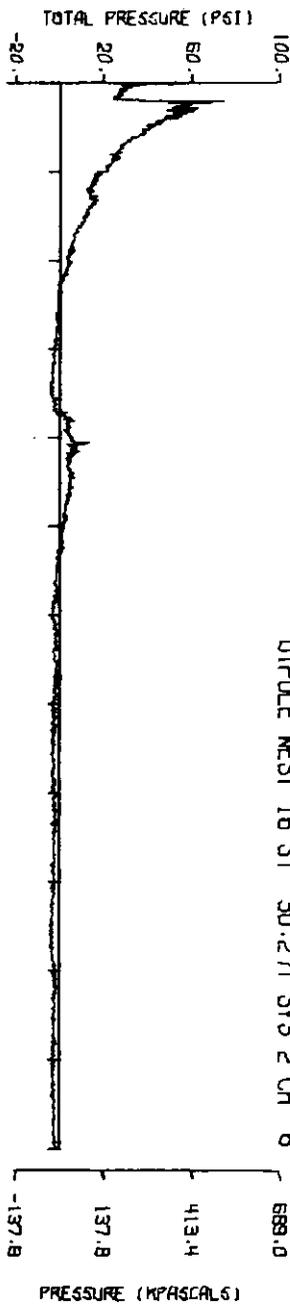
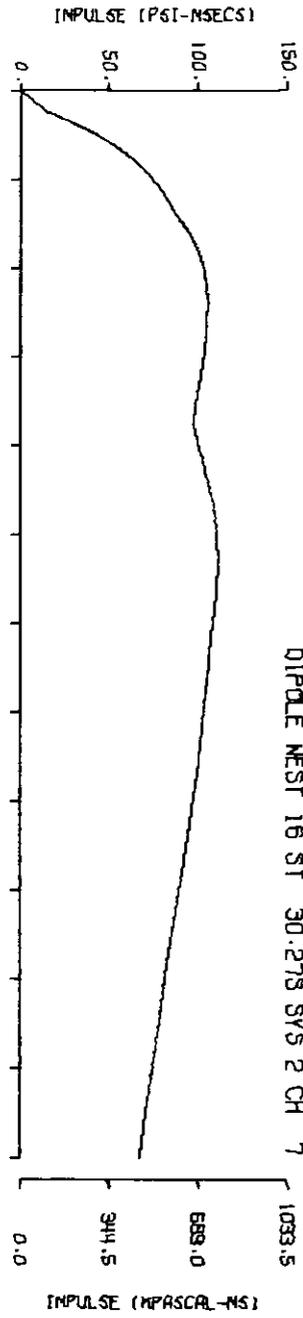
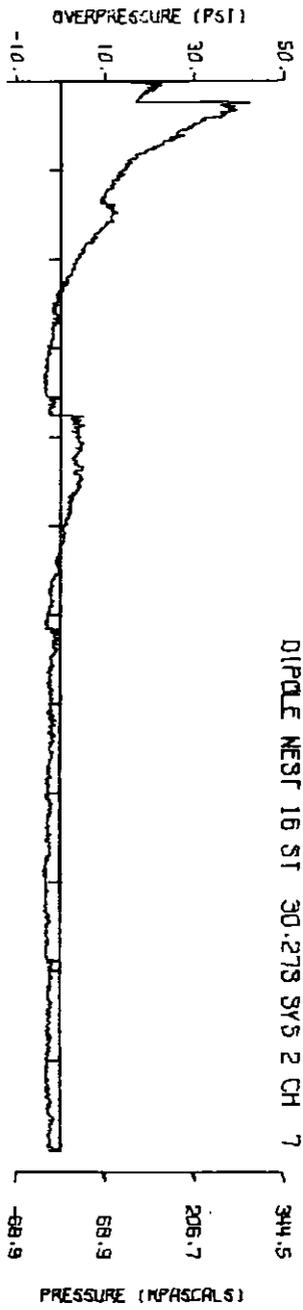
A16.14



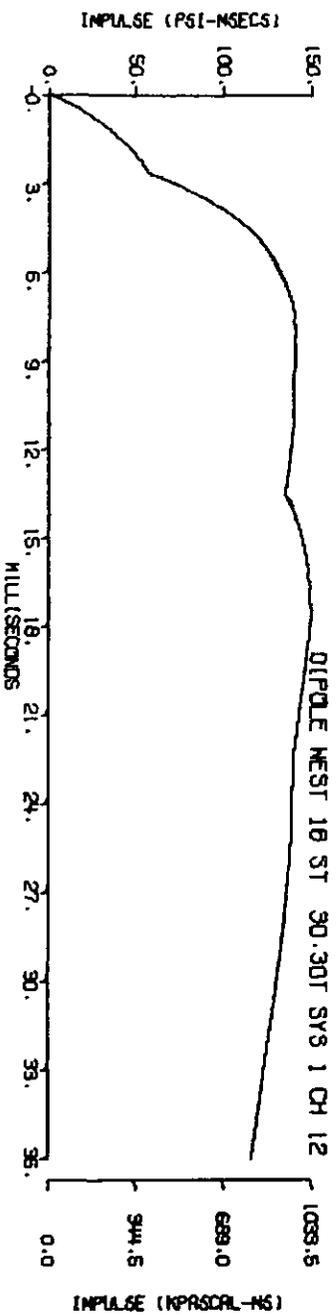
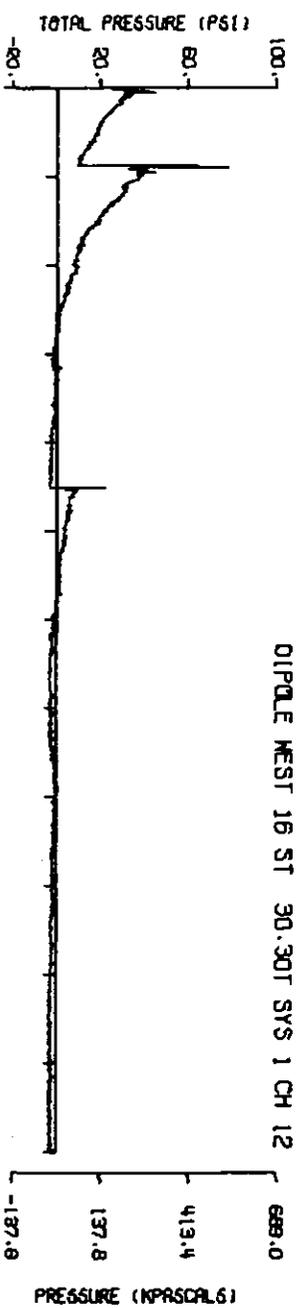
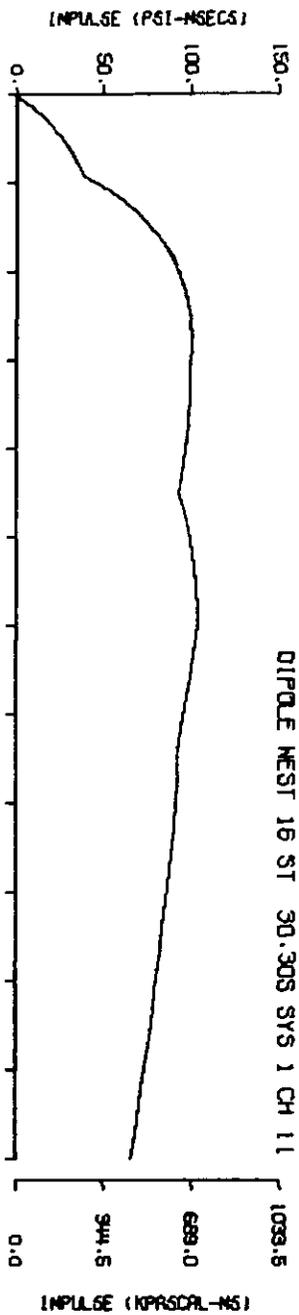
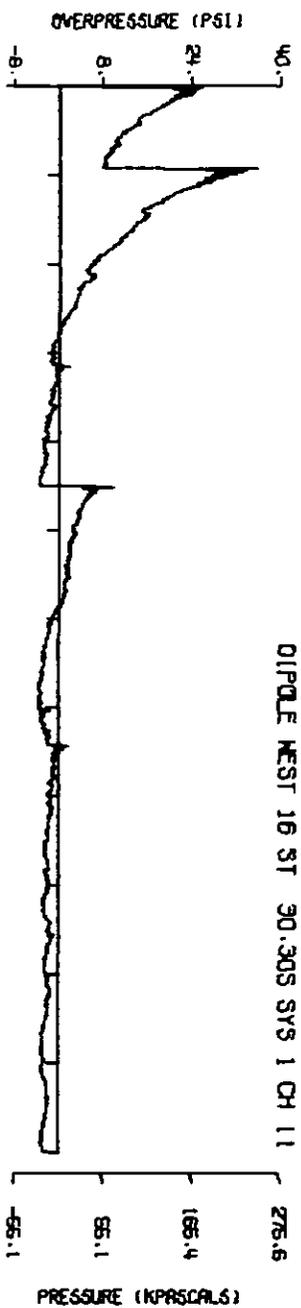
A16.15



A16.16

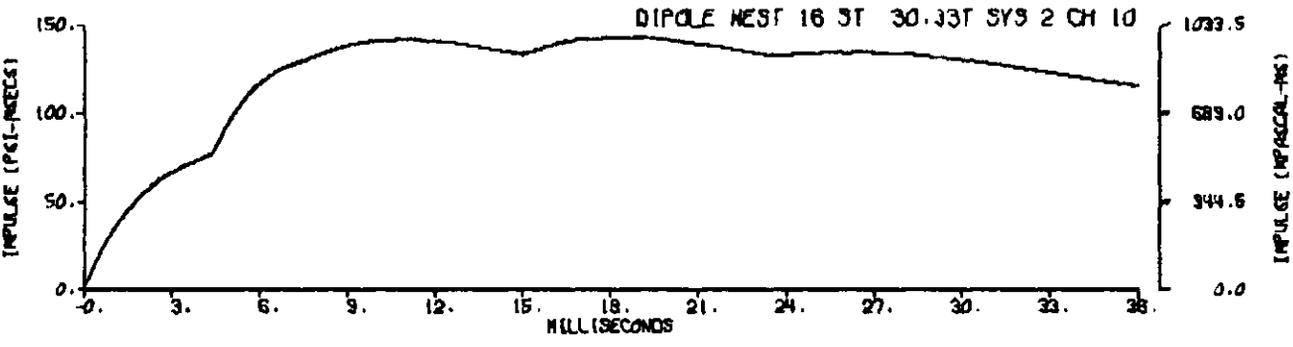
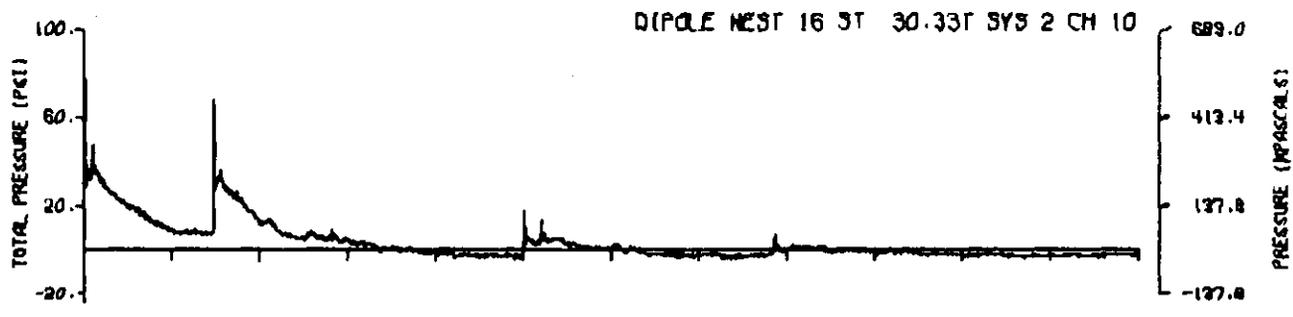
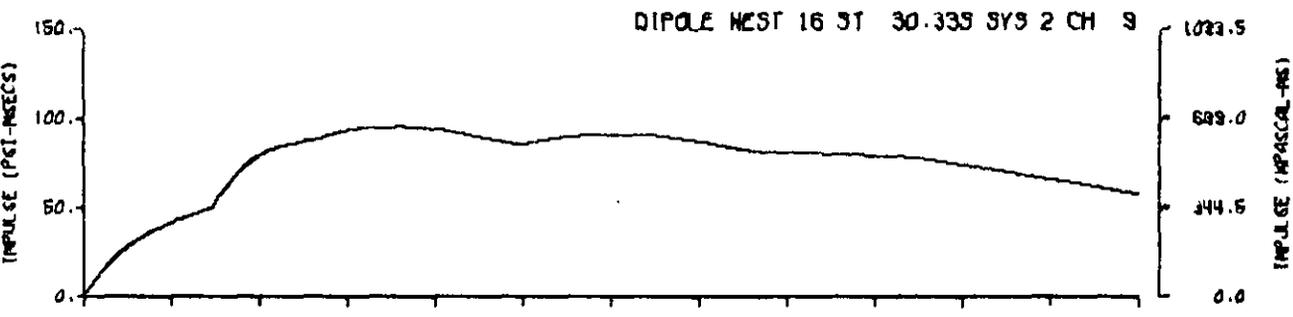
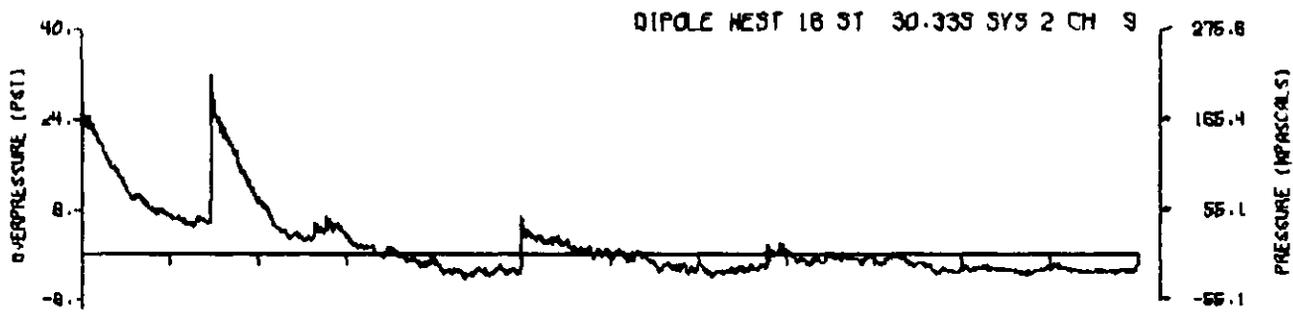


A16.17
352

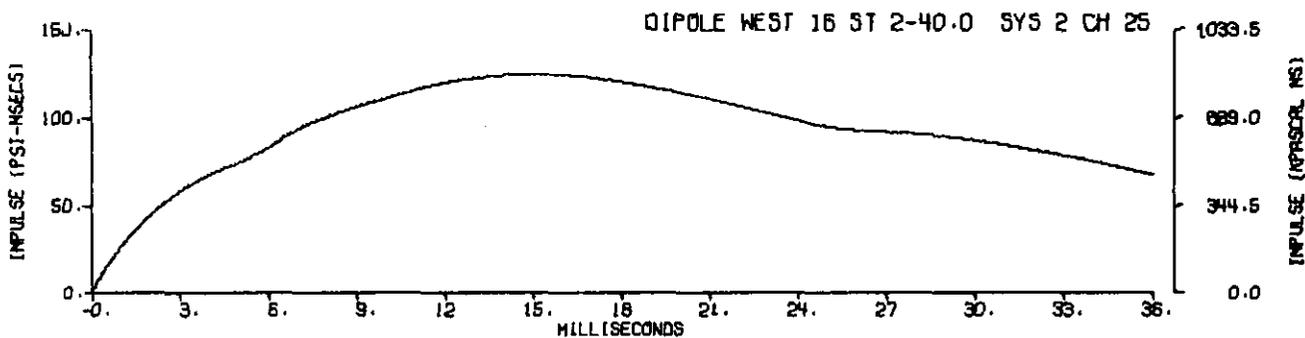
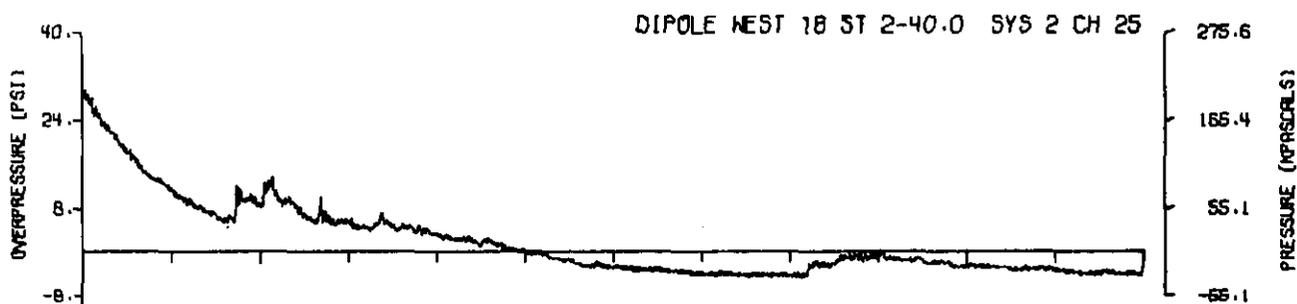
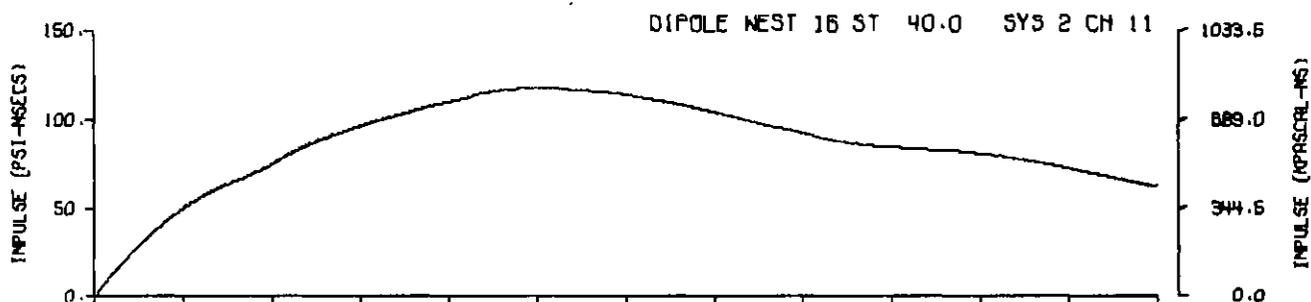
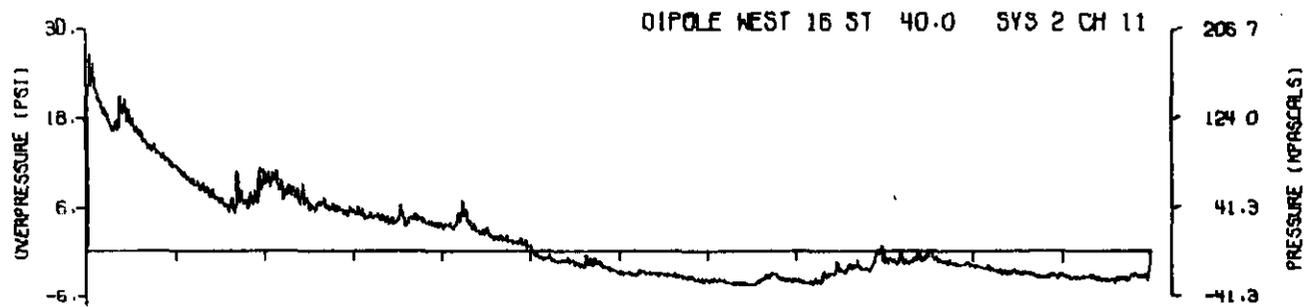


A16.18

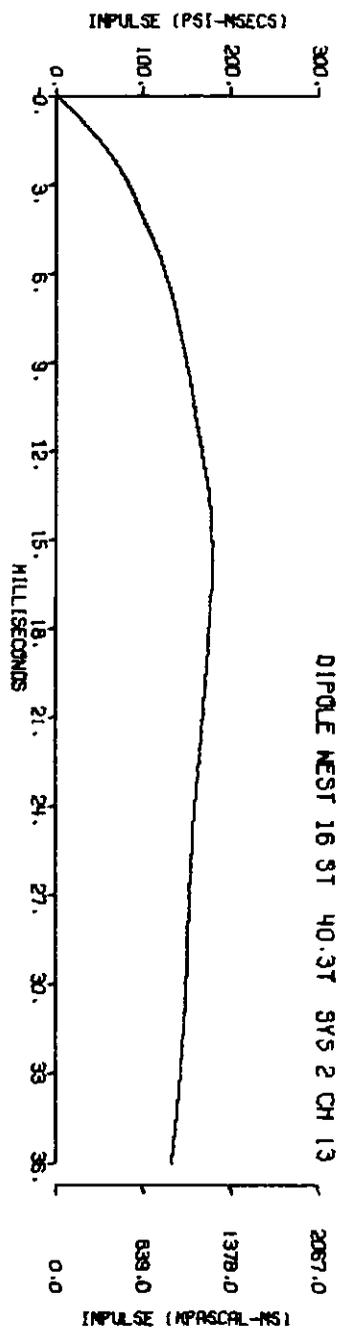
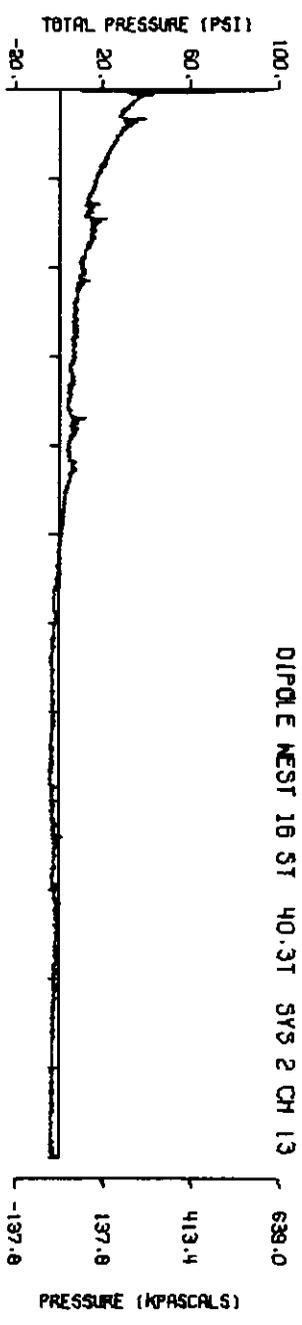
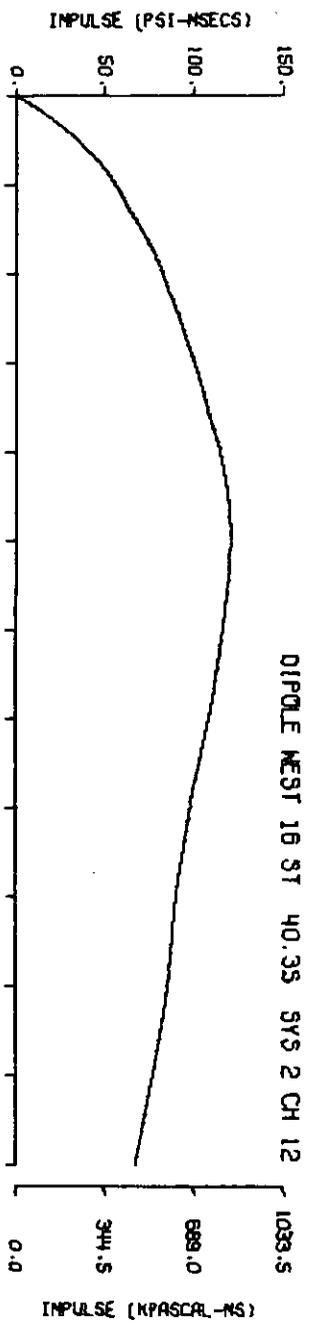
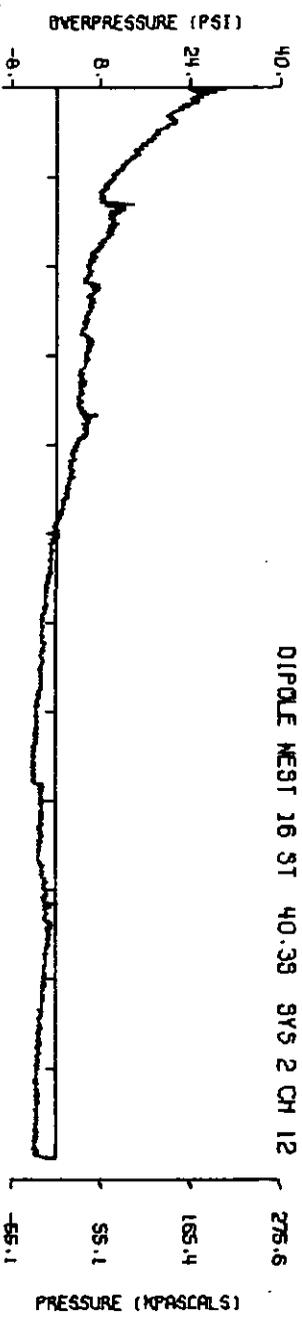
553



A16.19

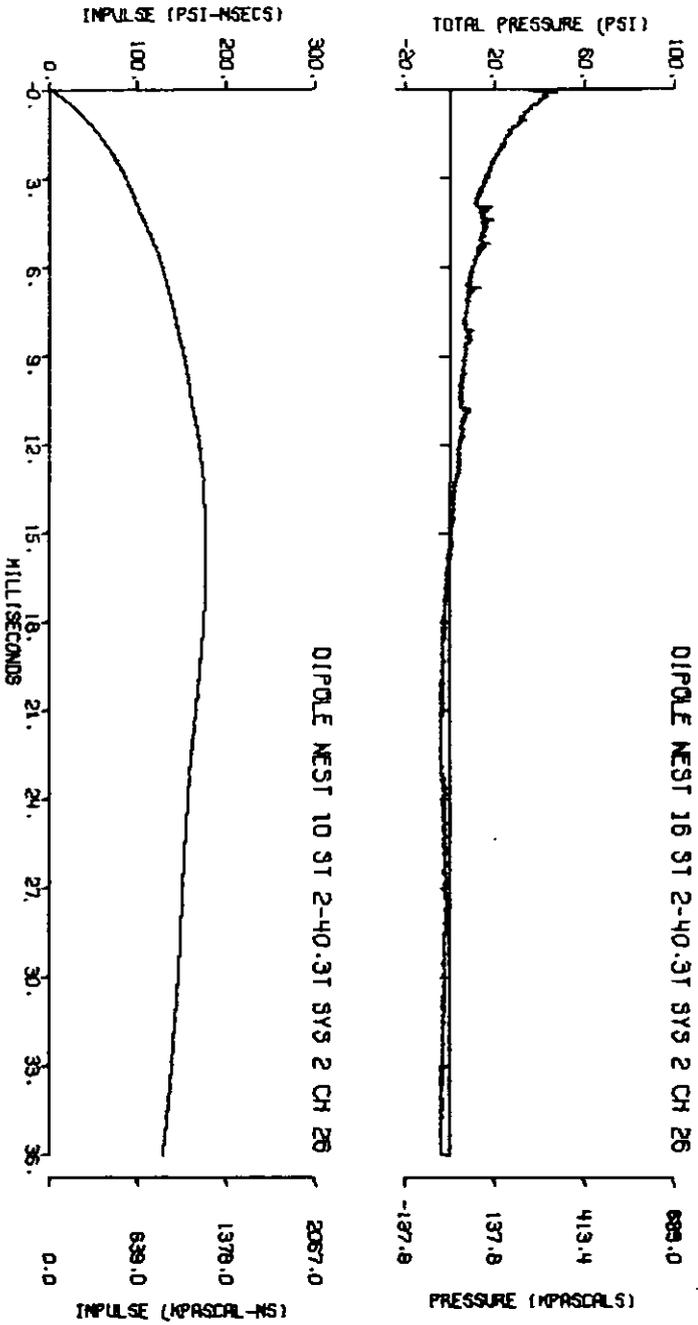


A16.20



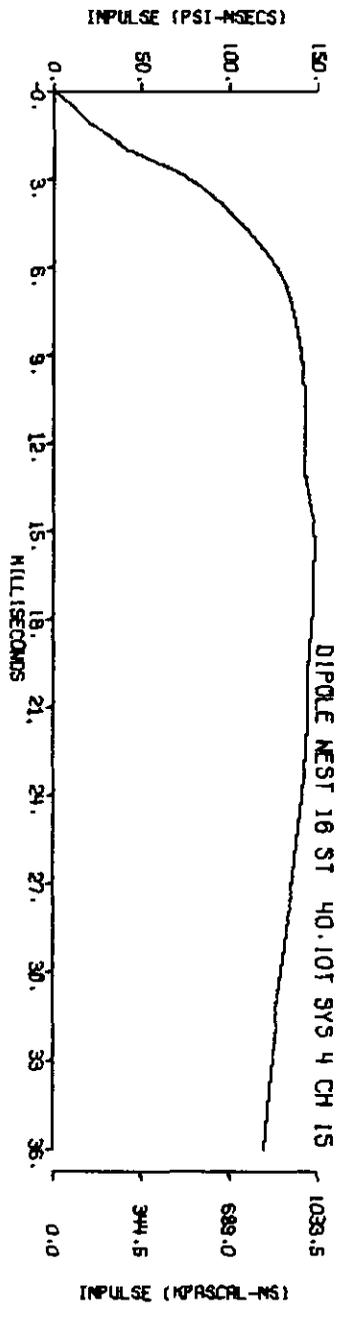
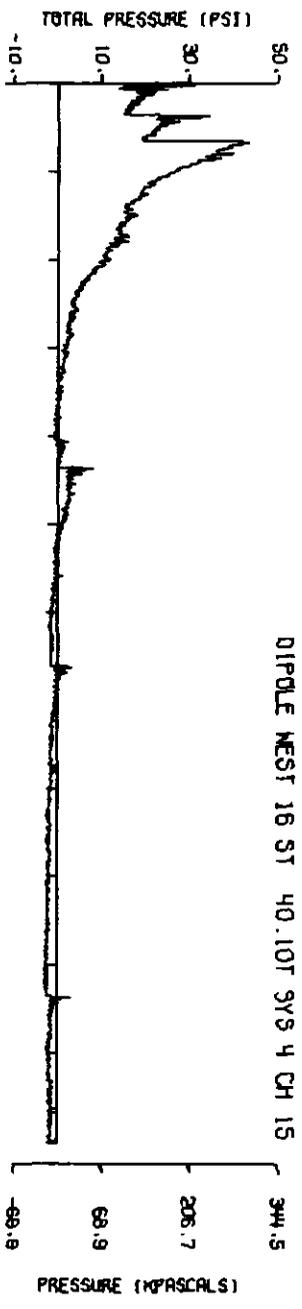
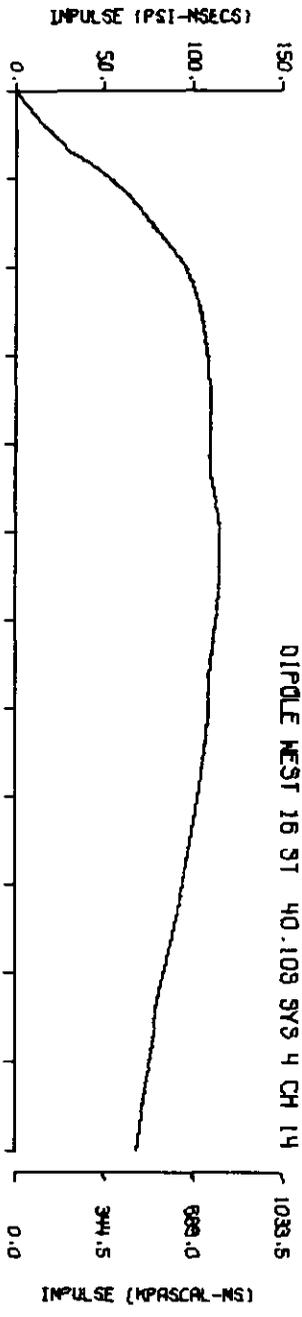
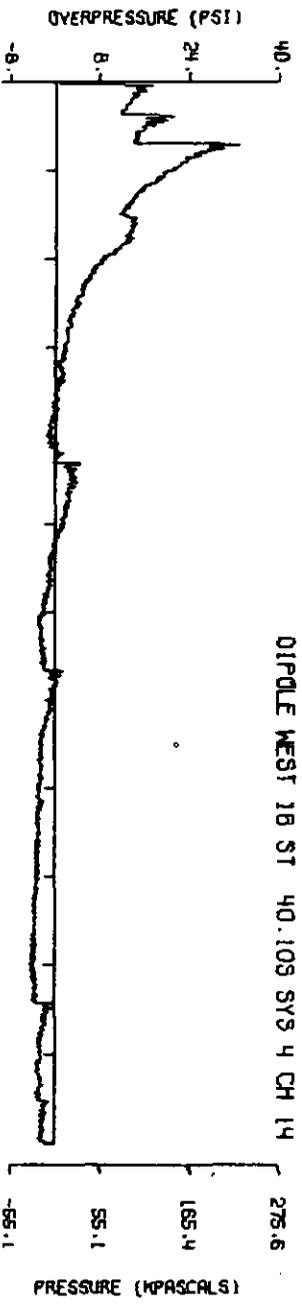
A16.21

356



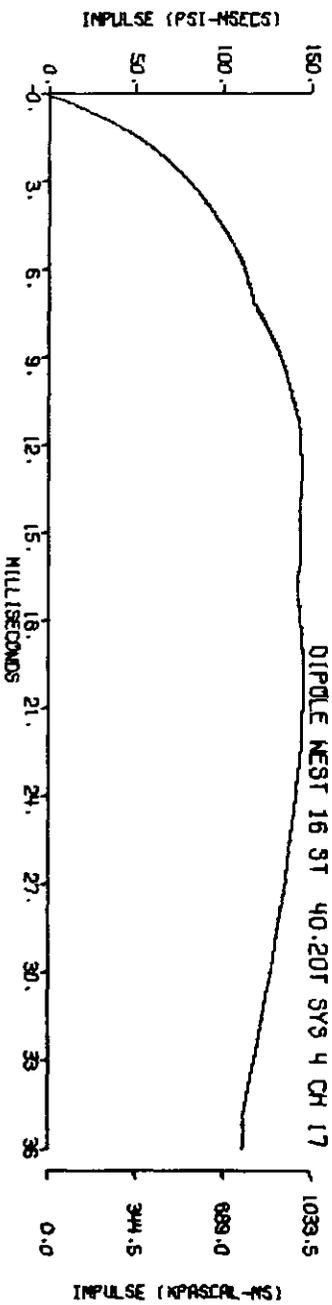
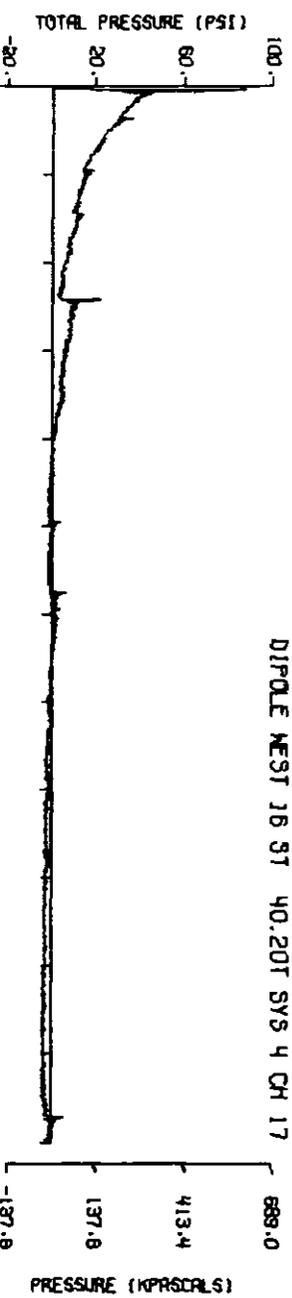
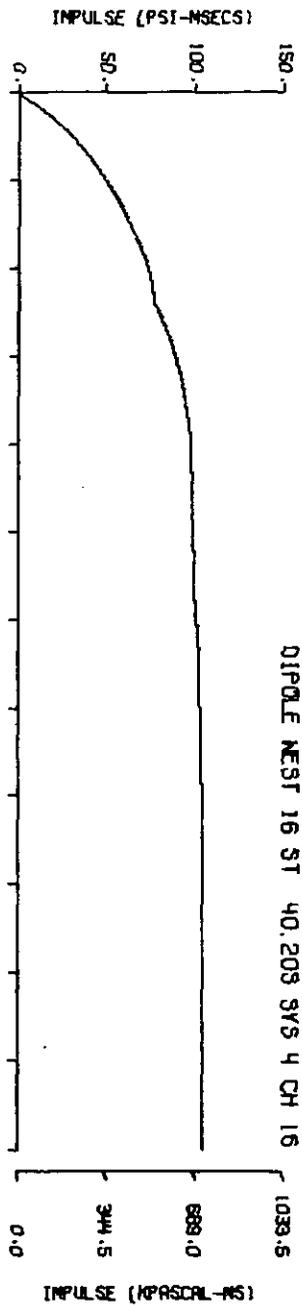
A16.22

357



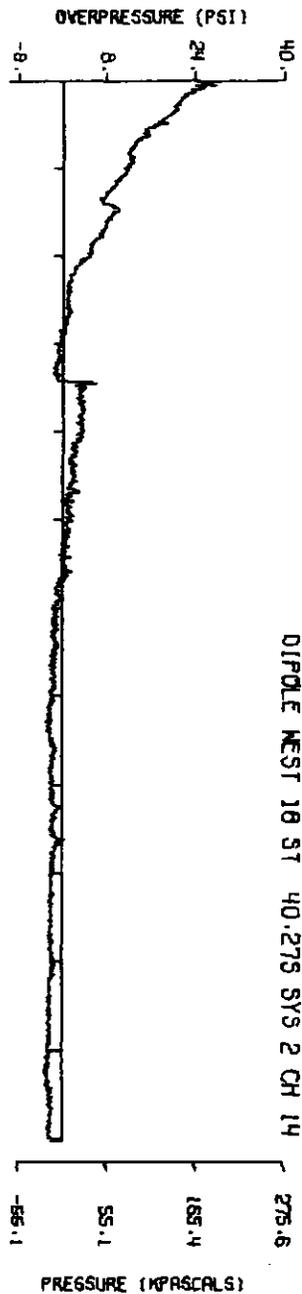
A16.23

358



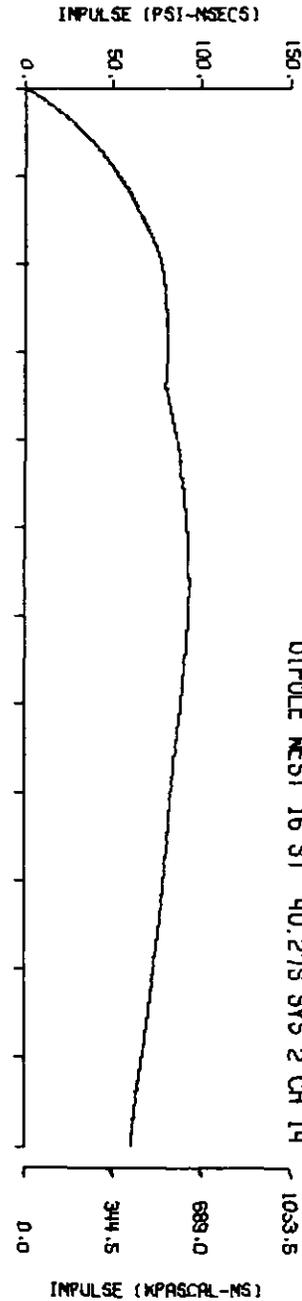
A16.24

359



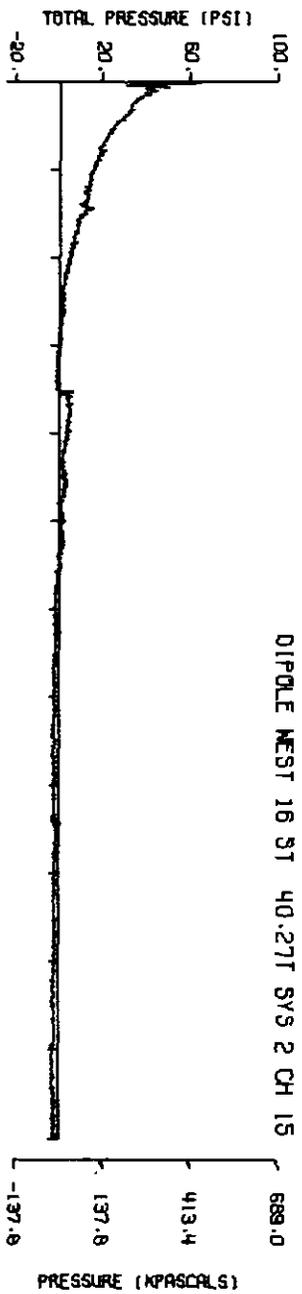
275.6
165.4
55.1
-55.1

PRESSURE (MPASCALS)



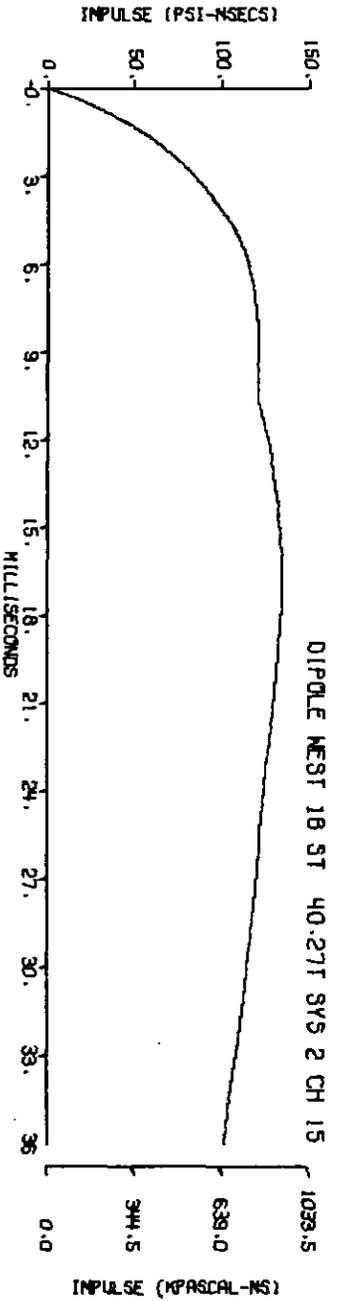
1053.5
689.0
344.5
0.0

IMPULSE (MPASCAL-NS)



689.0
413.4
137.8
-137.8

PRESSURE (MPASCALS)

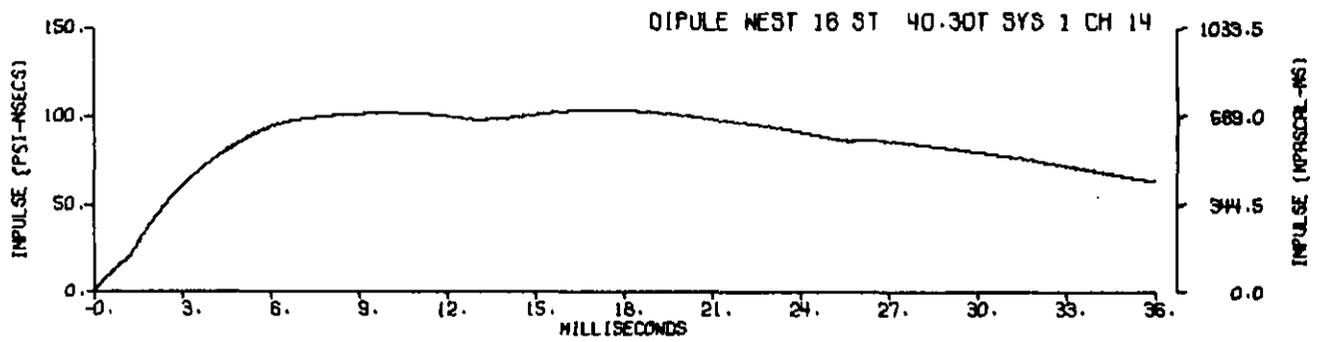
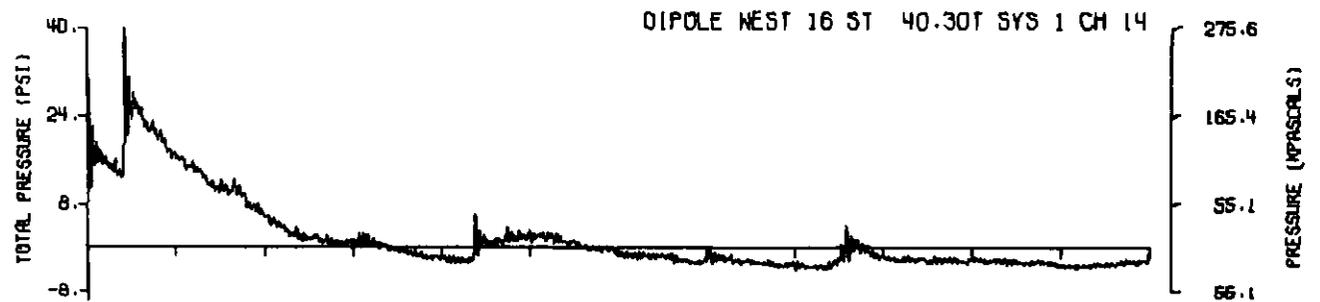
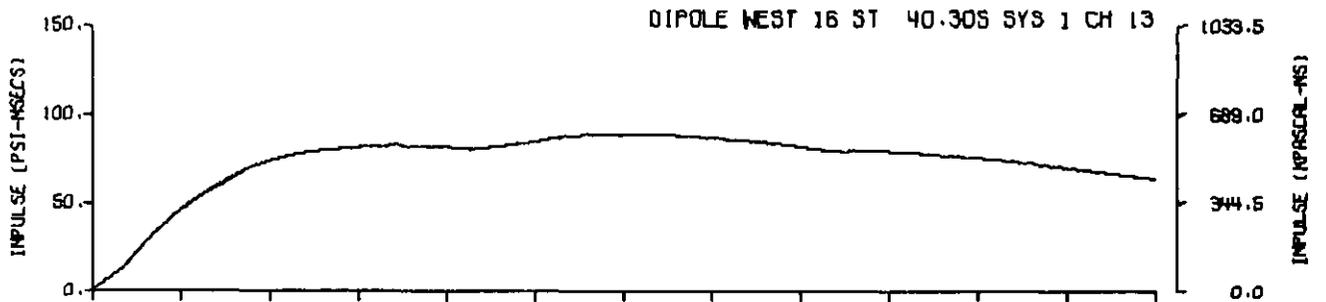
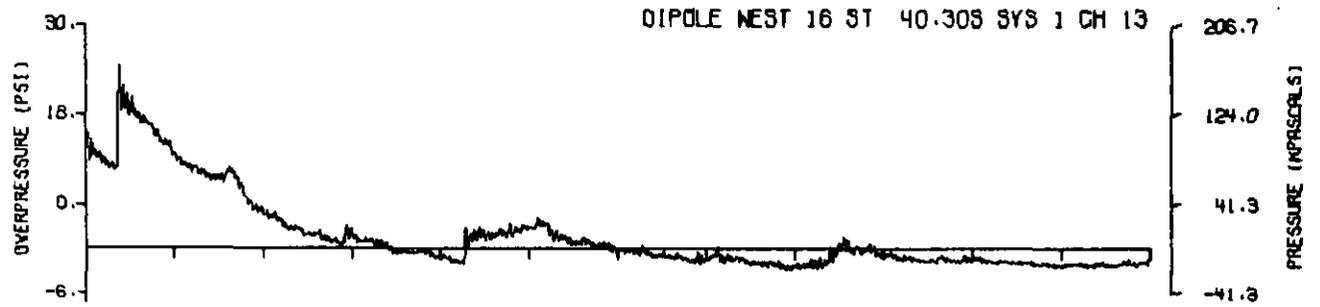


1039.5
639.0
344.5
0.0

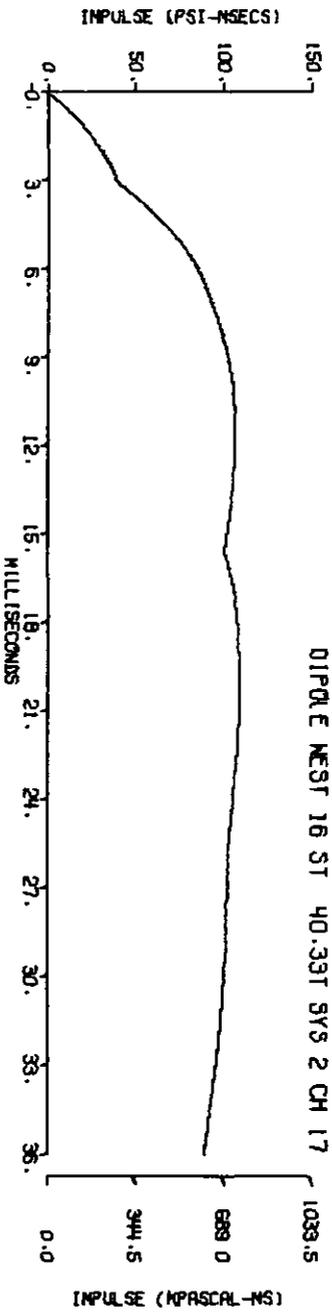
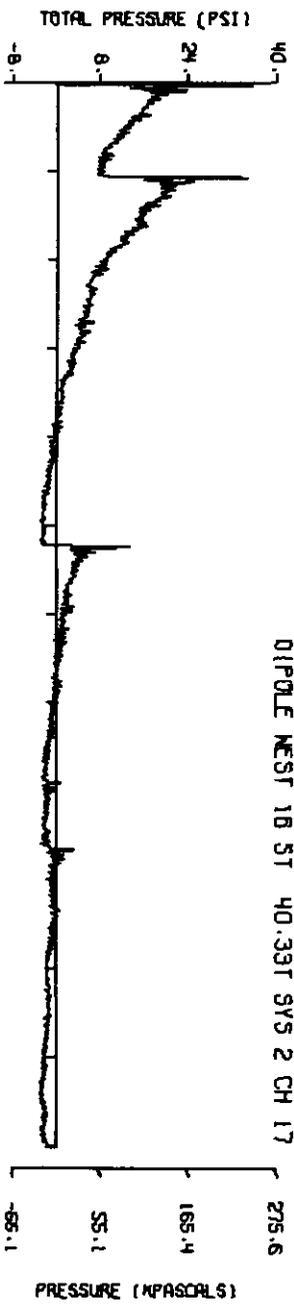
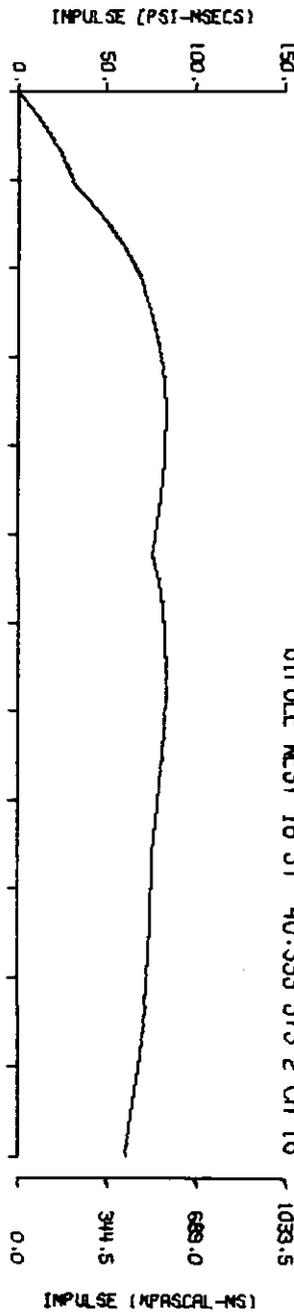
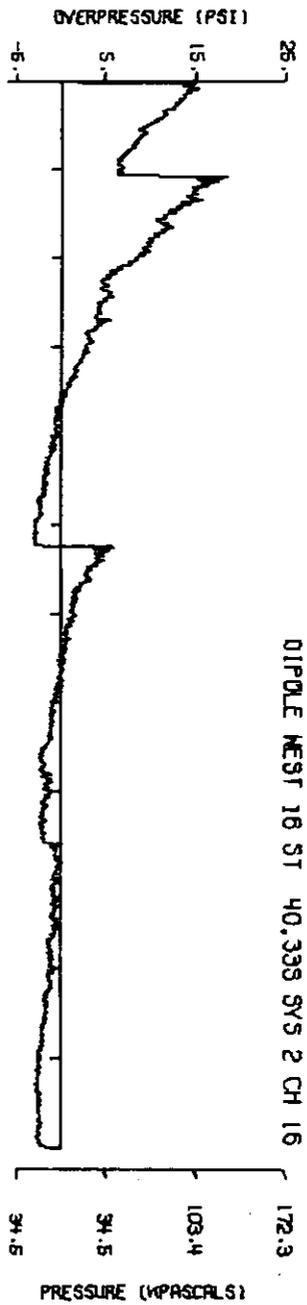
IMPULSE (MPASCAL-NS)

A16.25

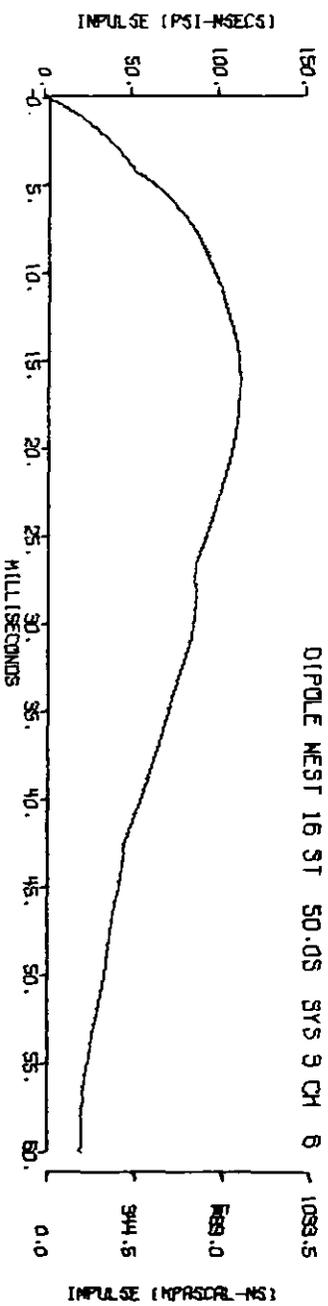
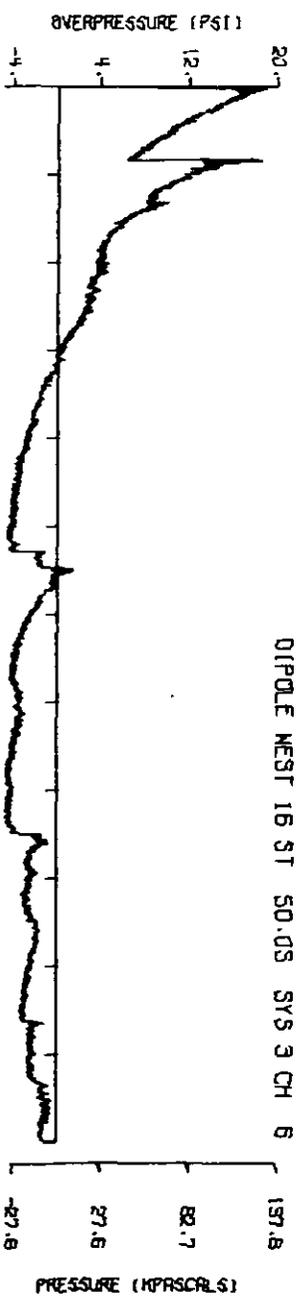
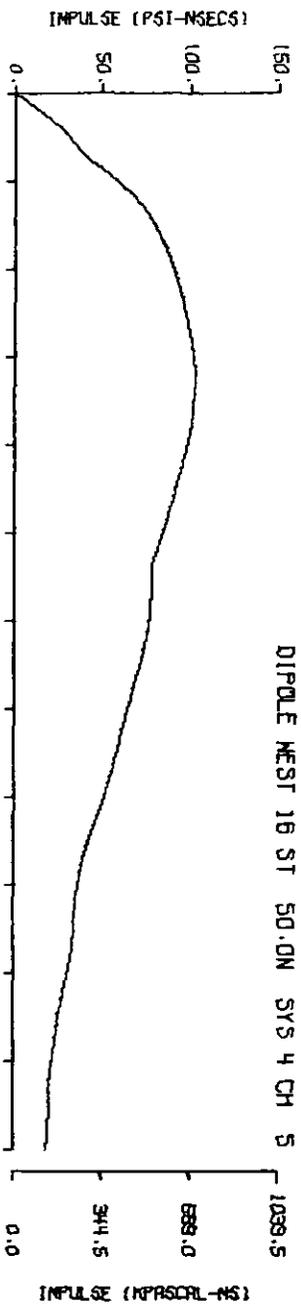
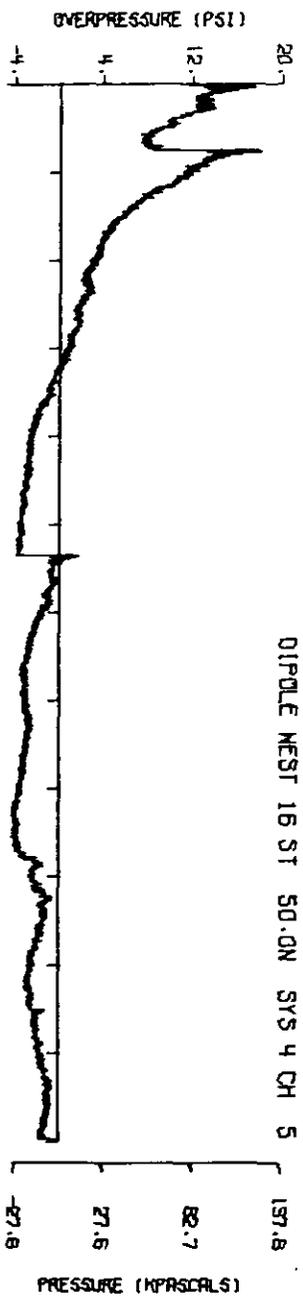
360



A16.26

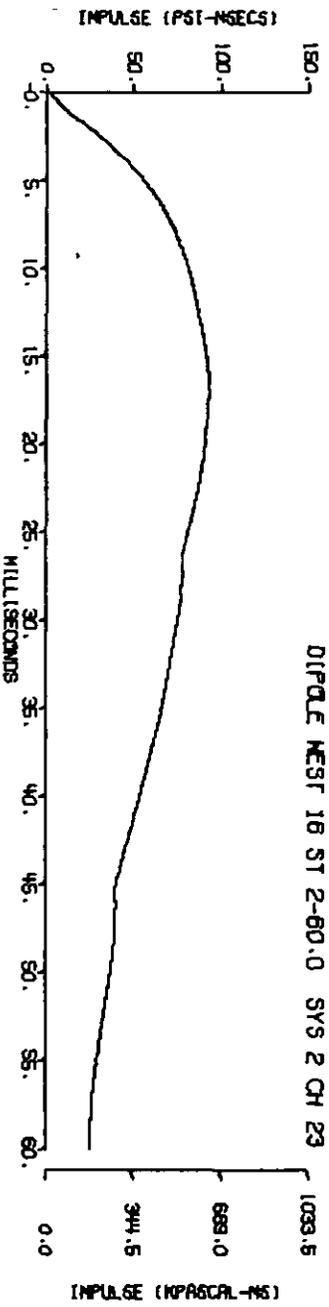
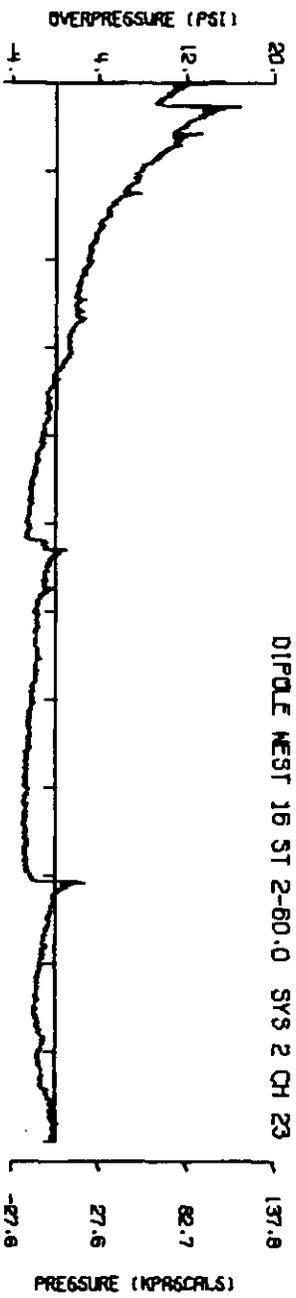
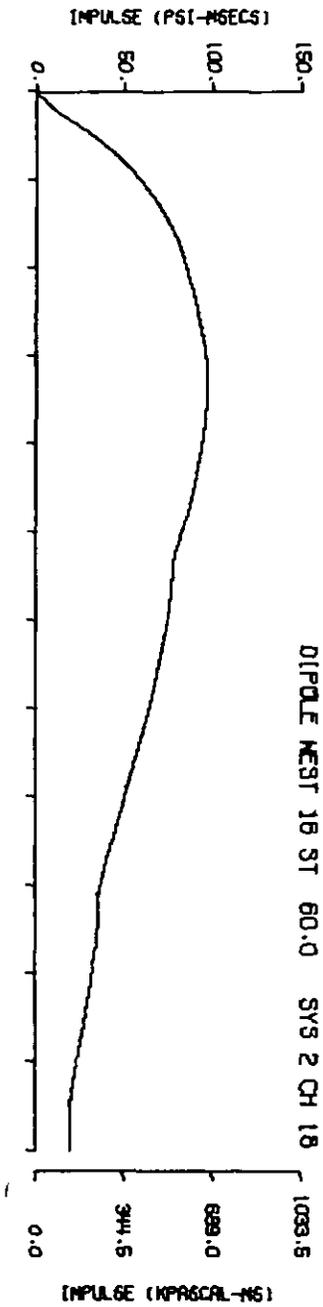
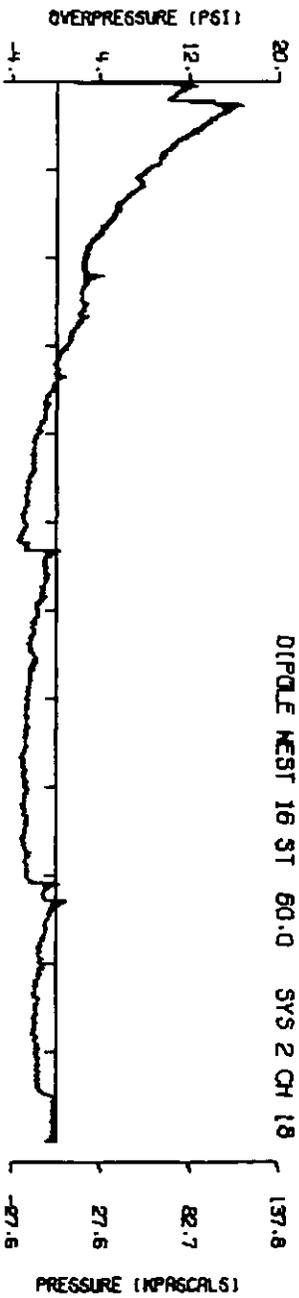


A16.27

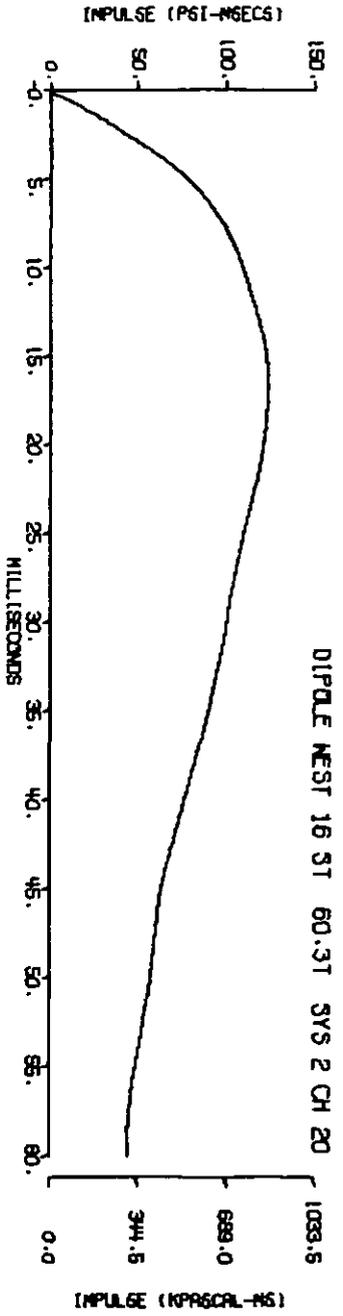
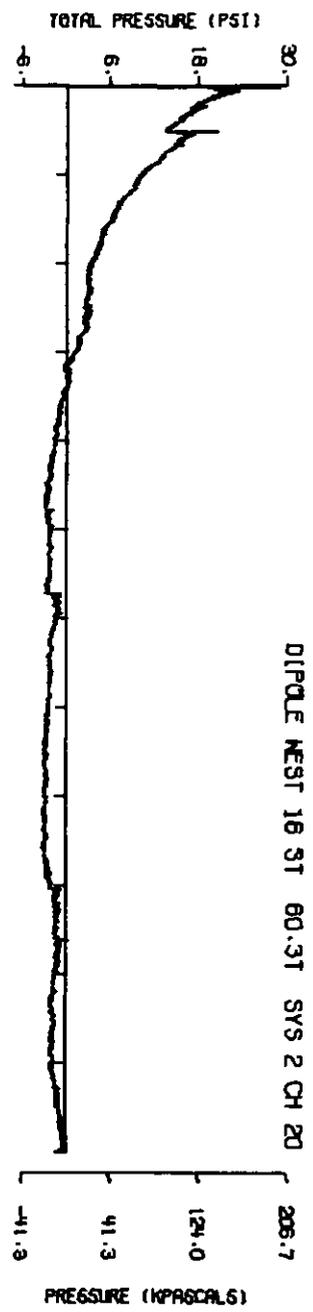
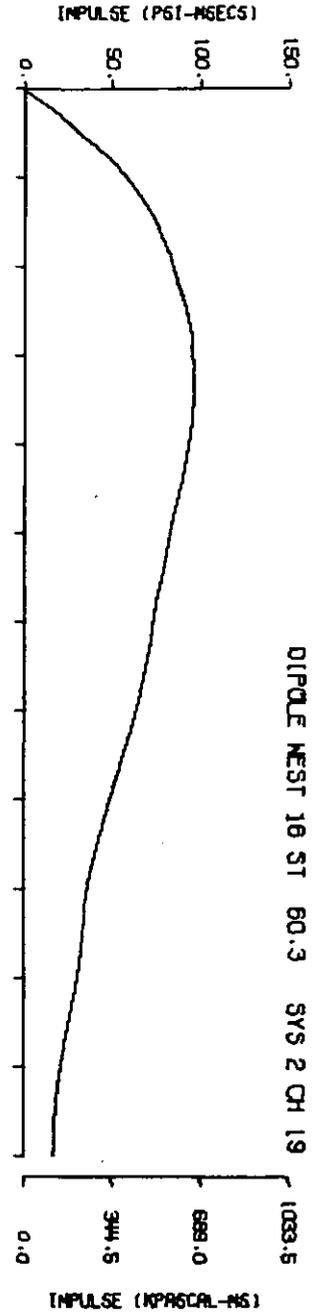
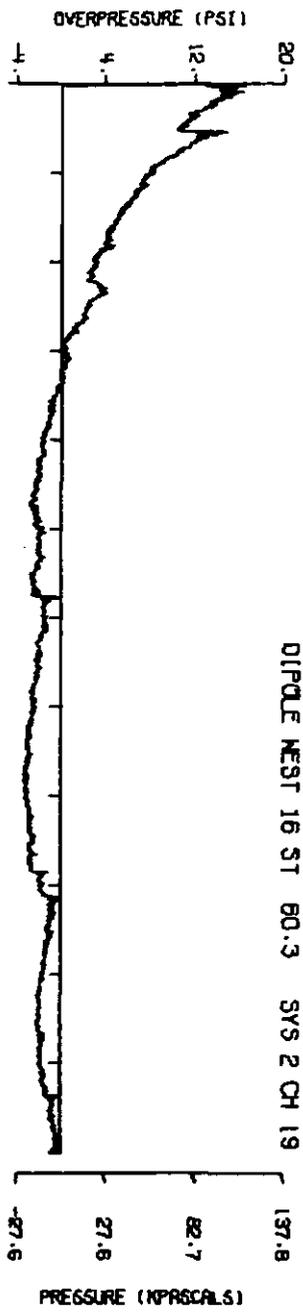


A16.28

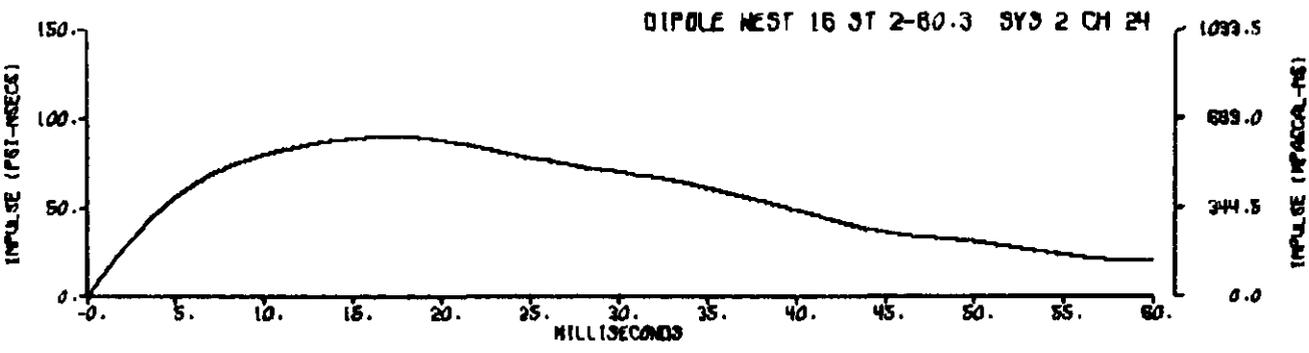
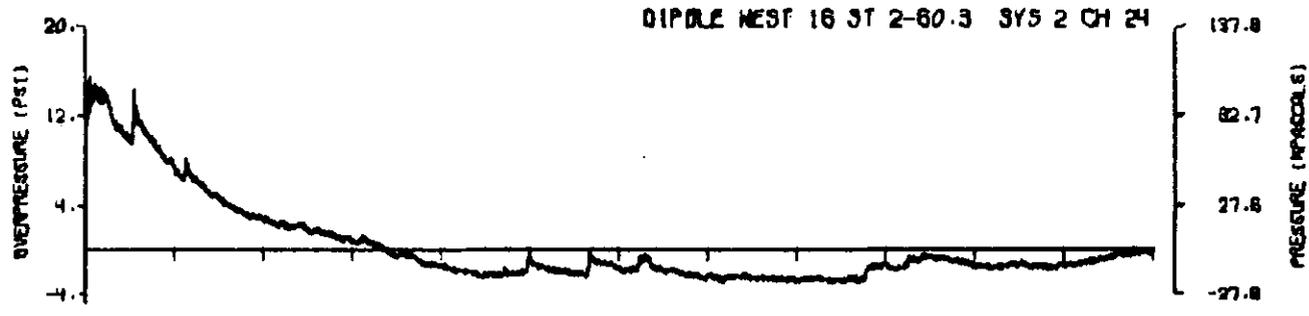
363



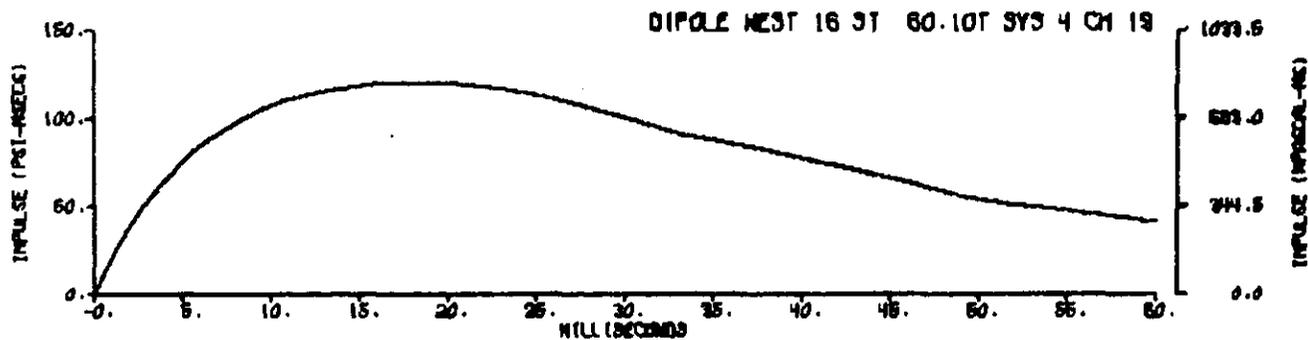
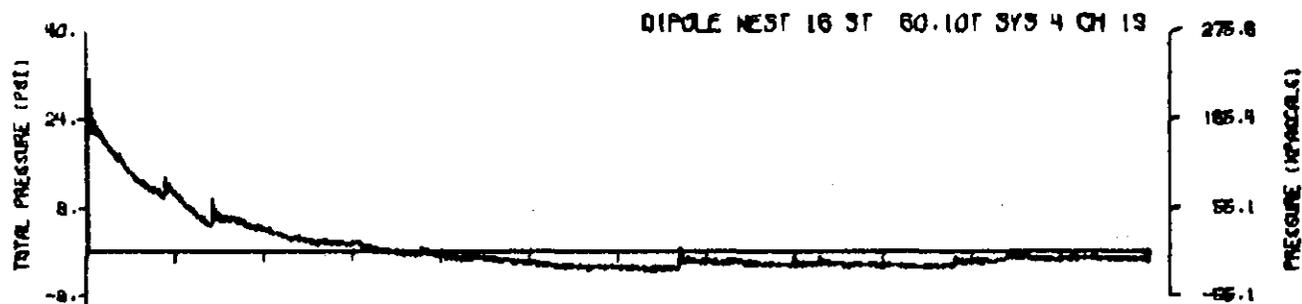
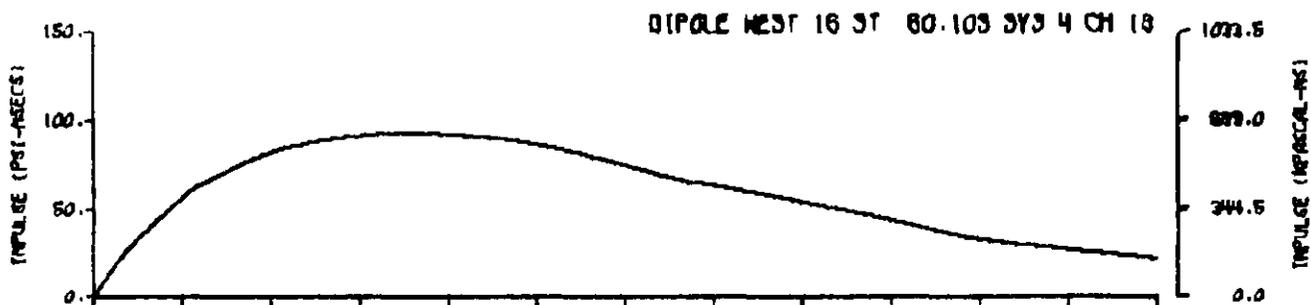
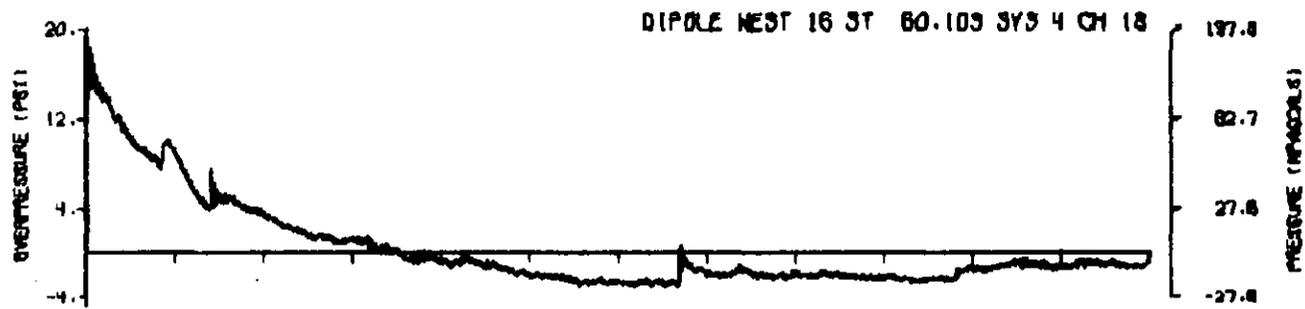
A16.29



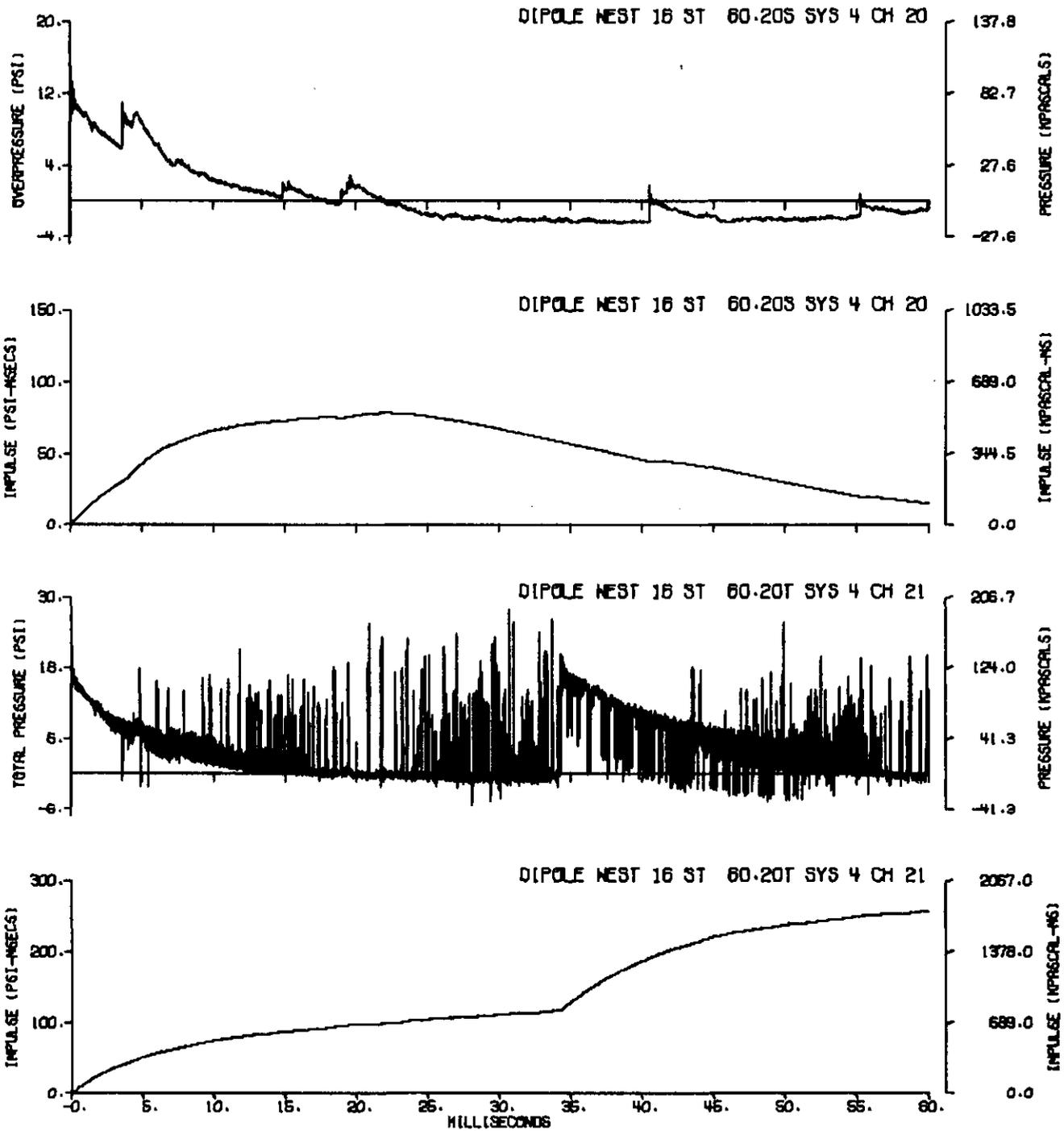
A16.30



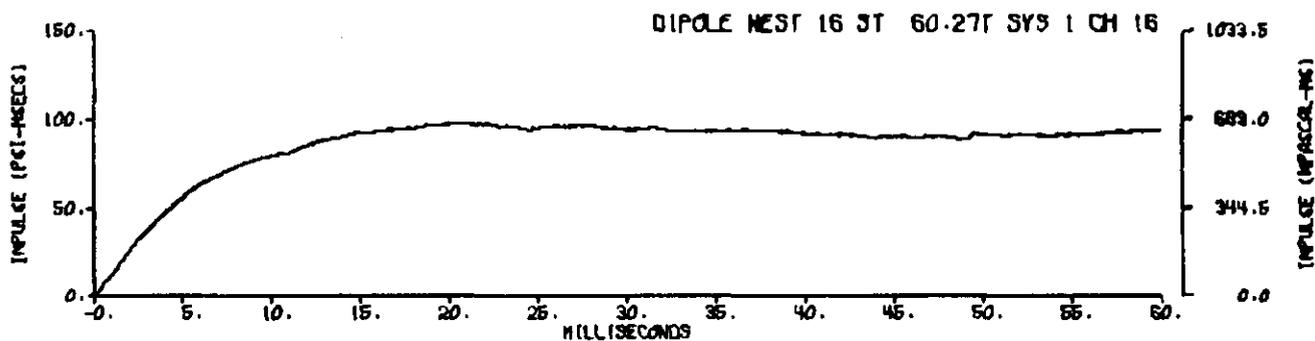
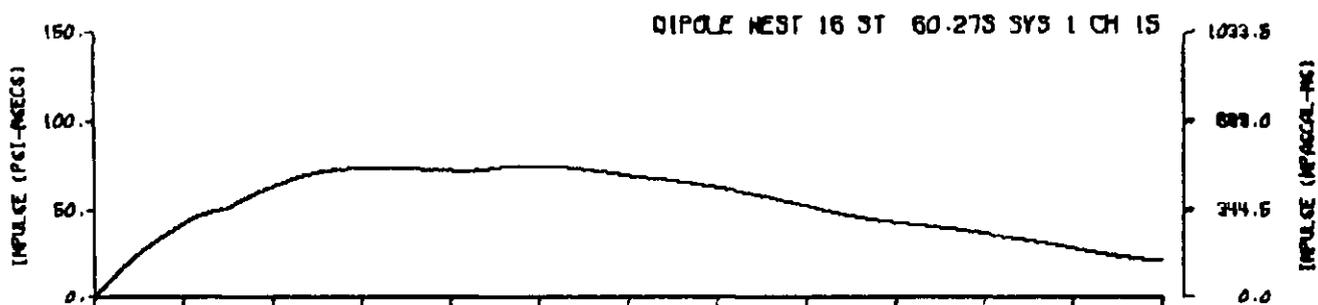
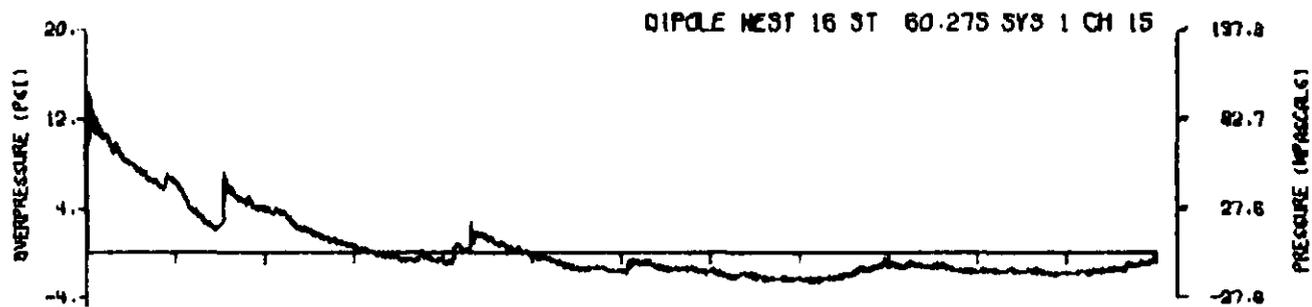
A16.31



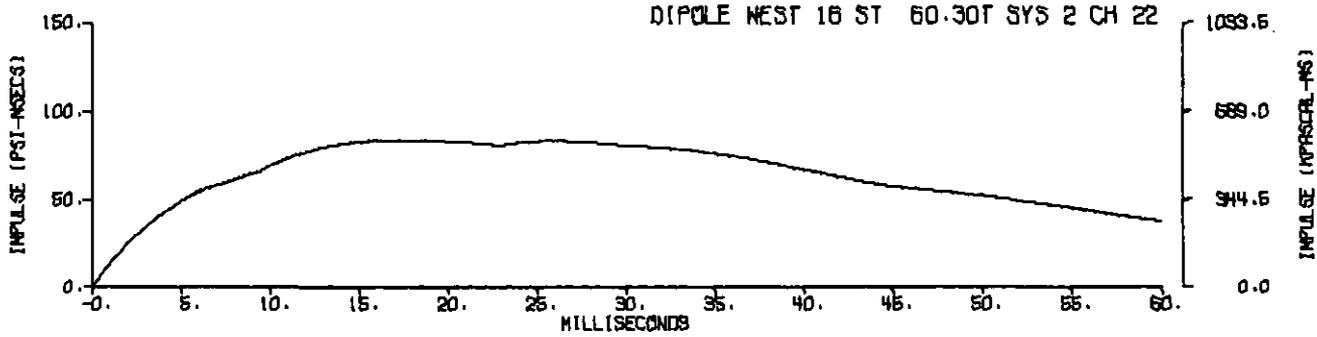
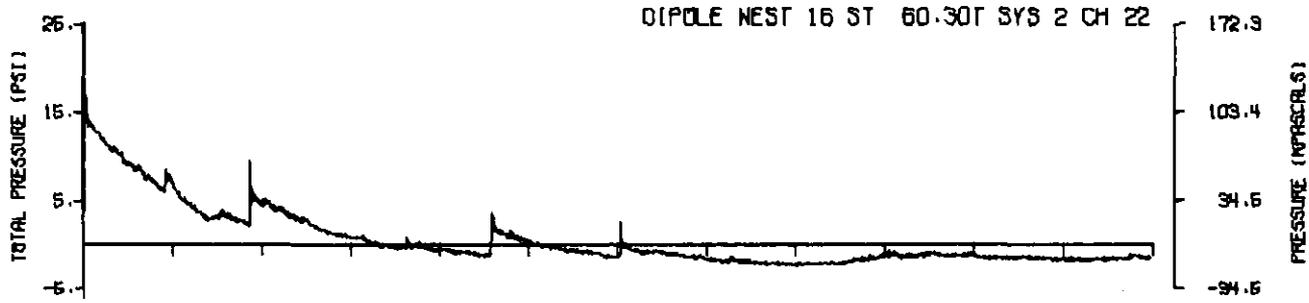
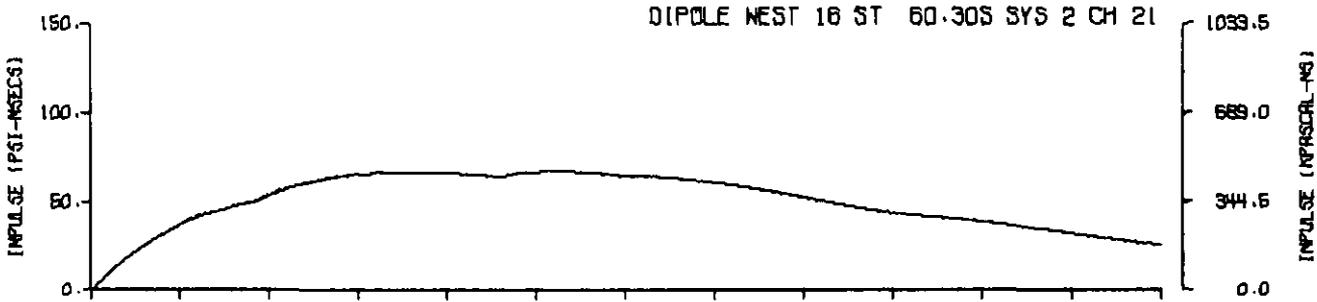
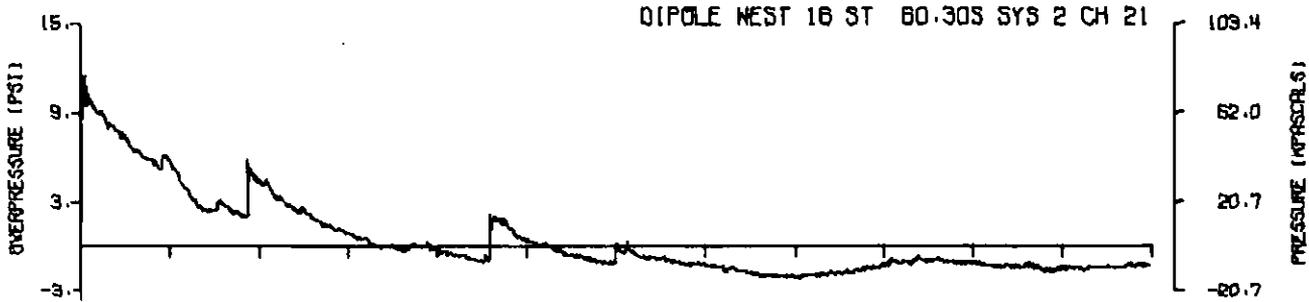
A16.32



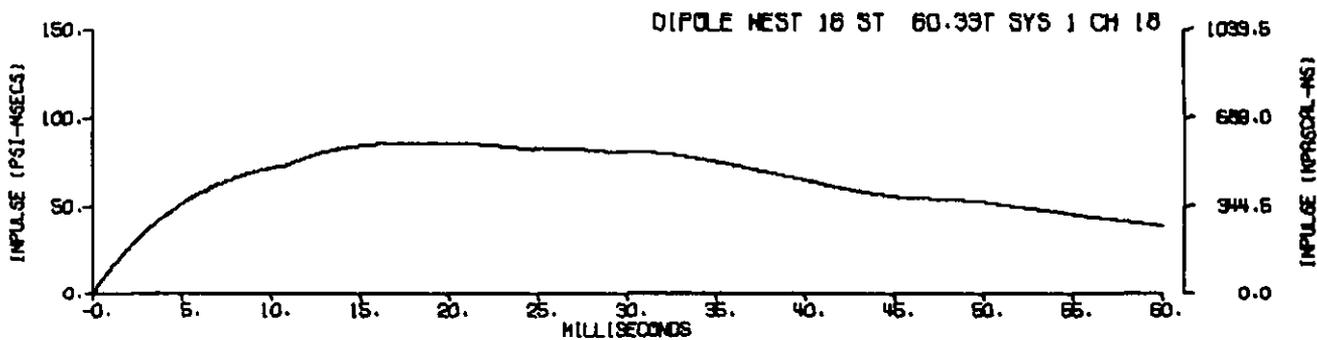
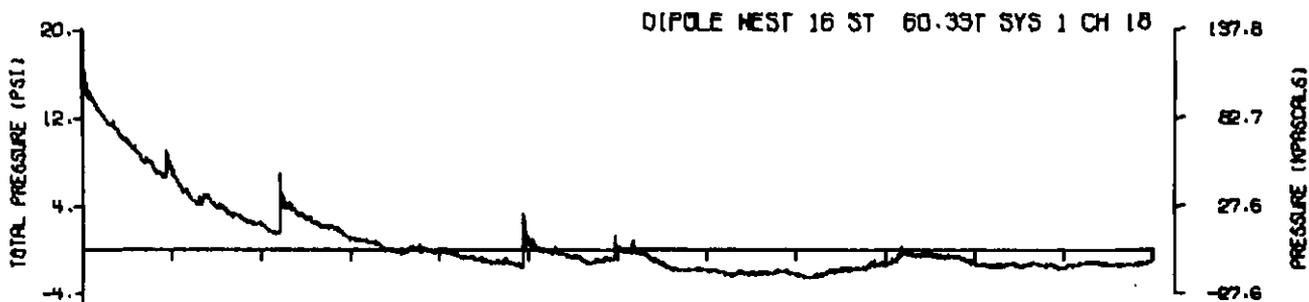
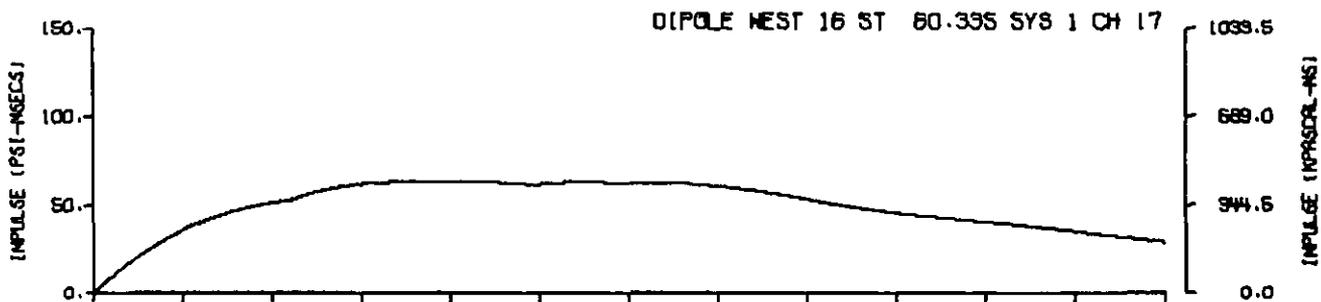
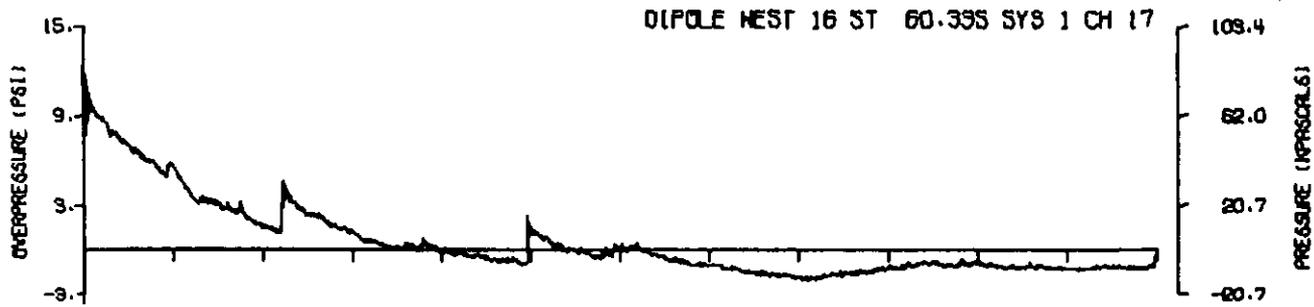
A16.33



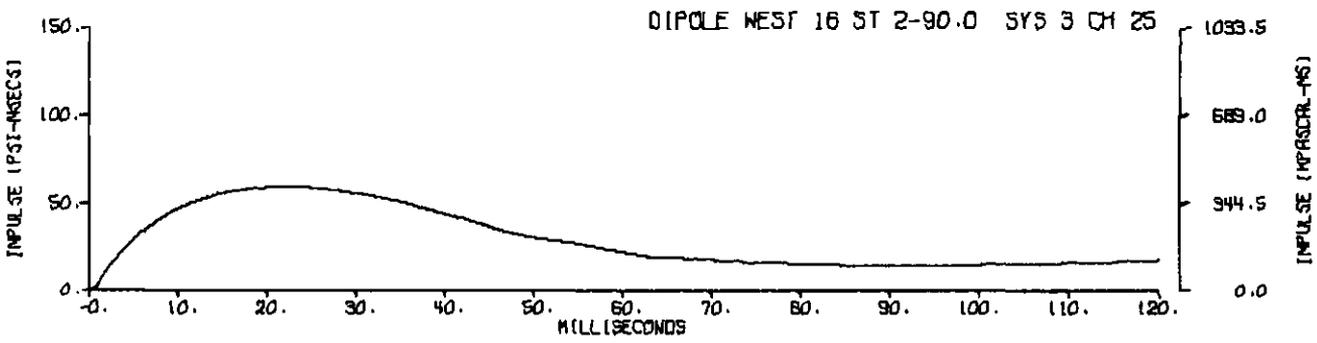
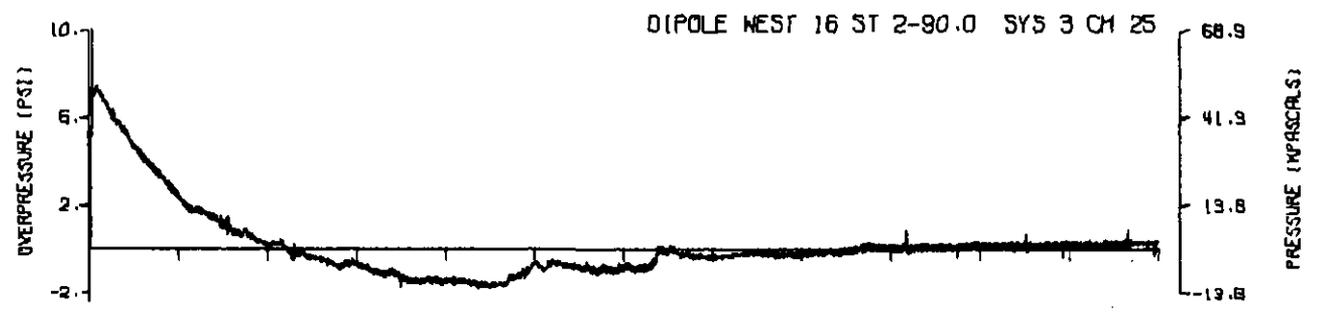
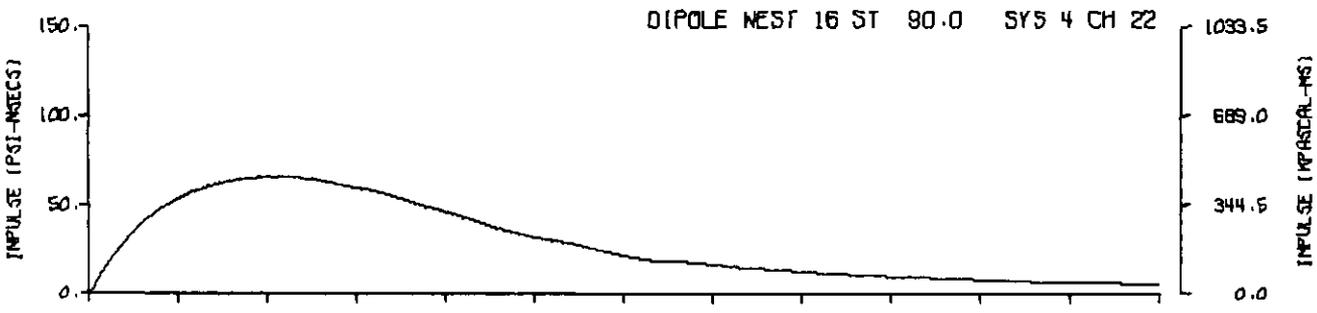
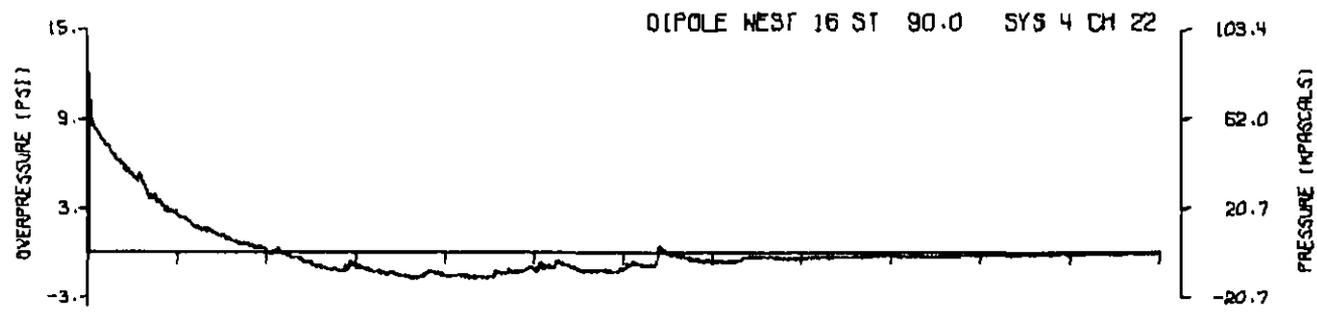
A16.34



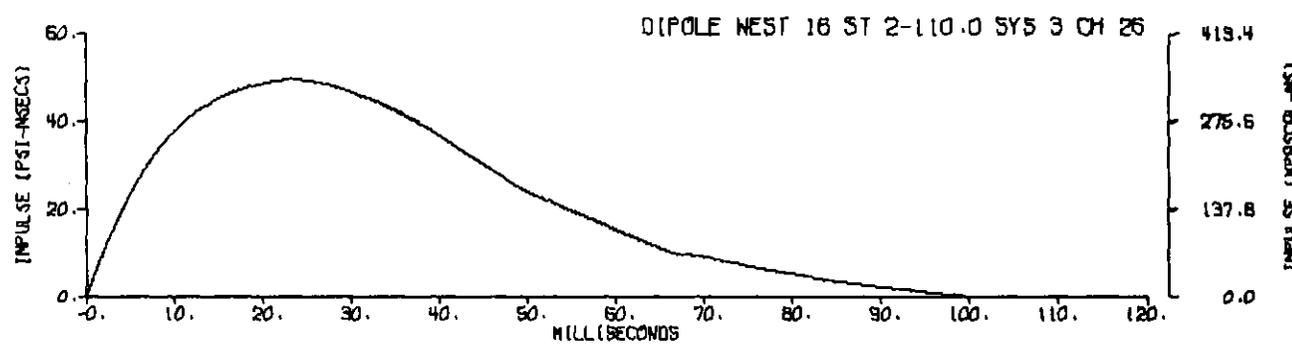
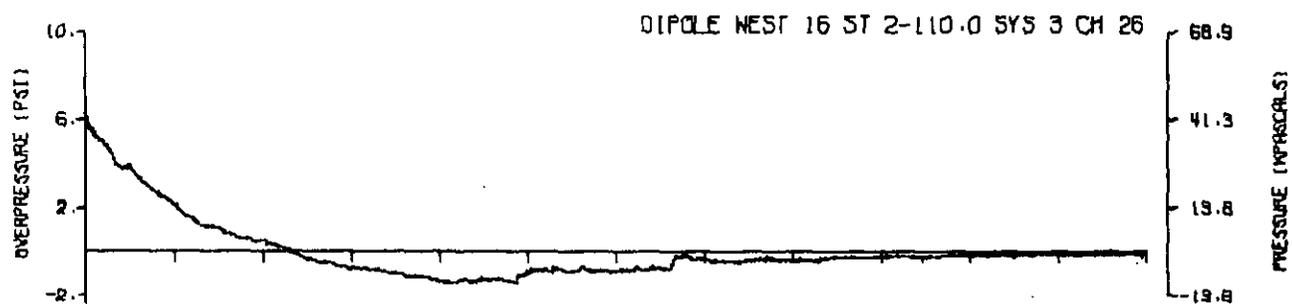
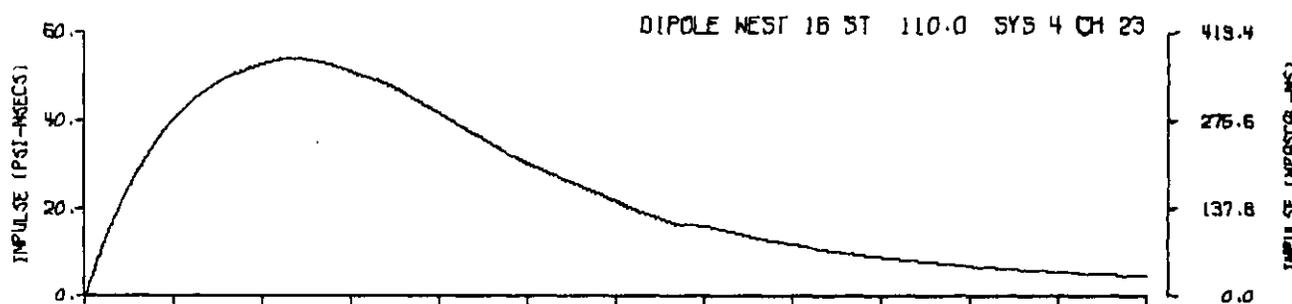
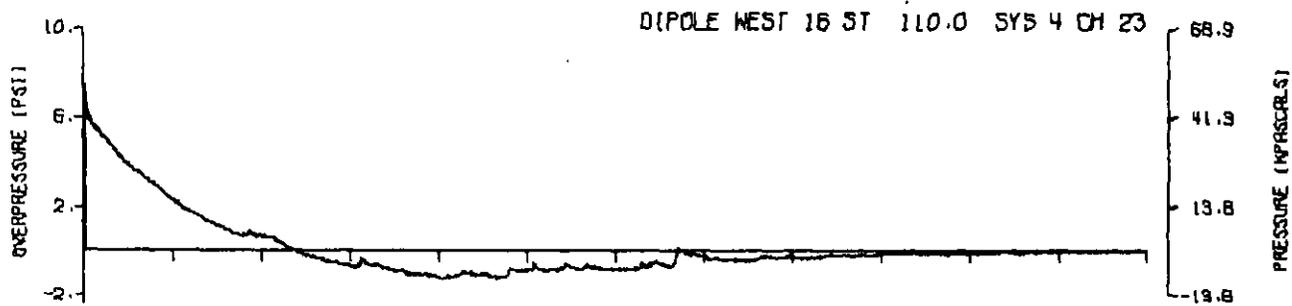
A16.35



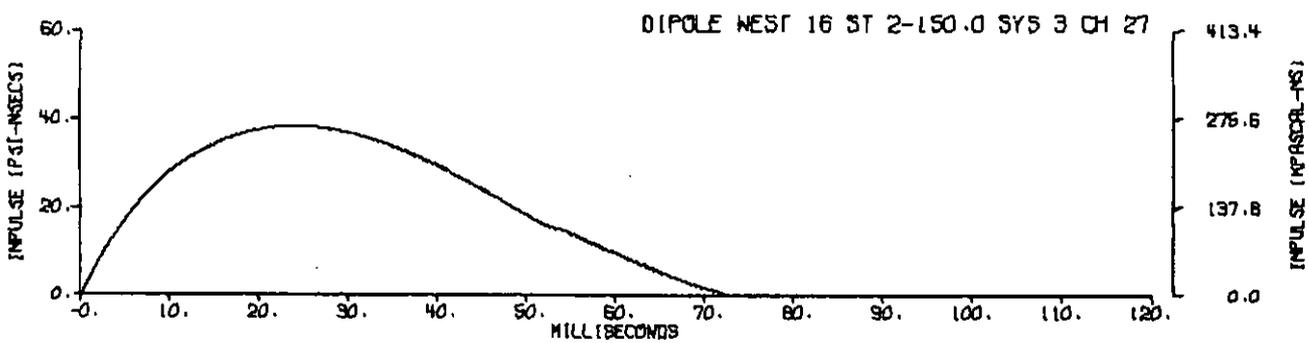
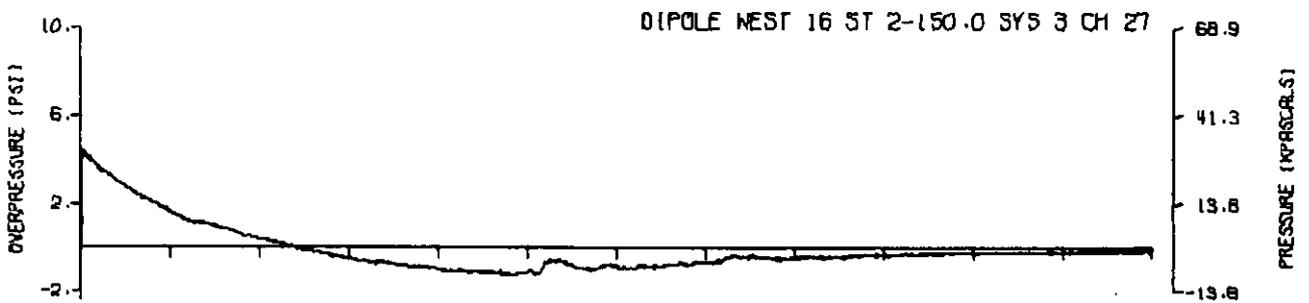
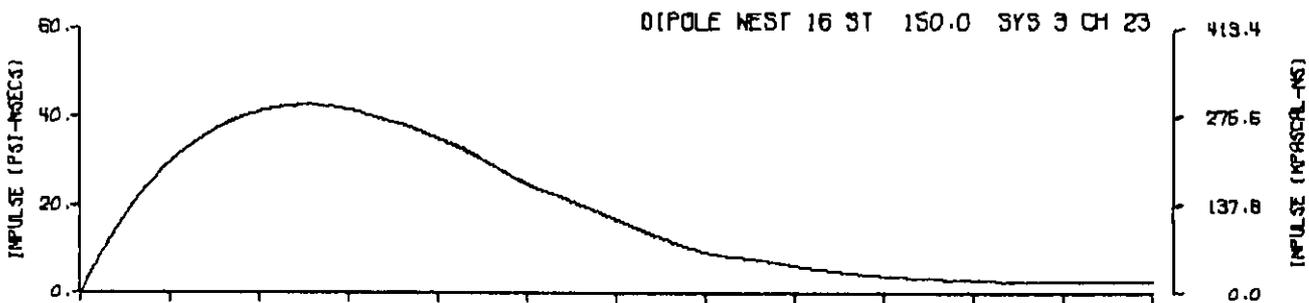
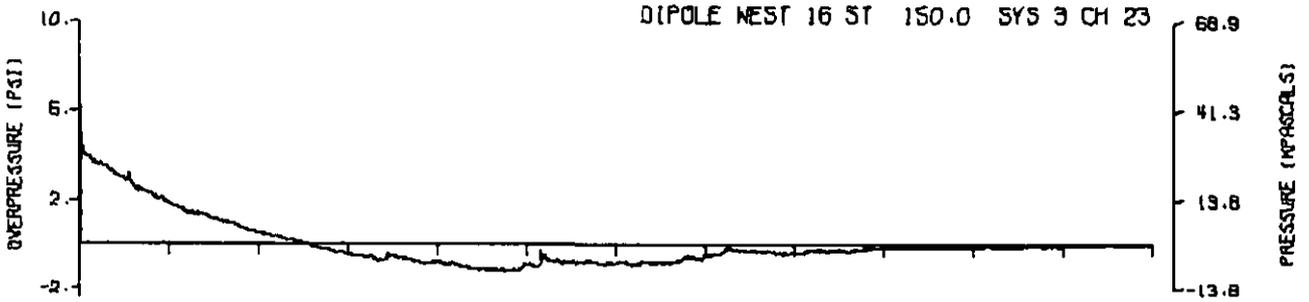
A16.36



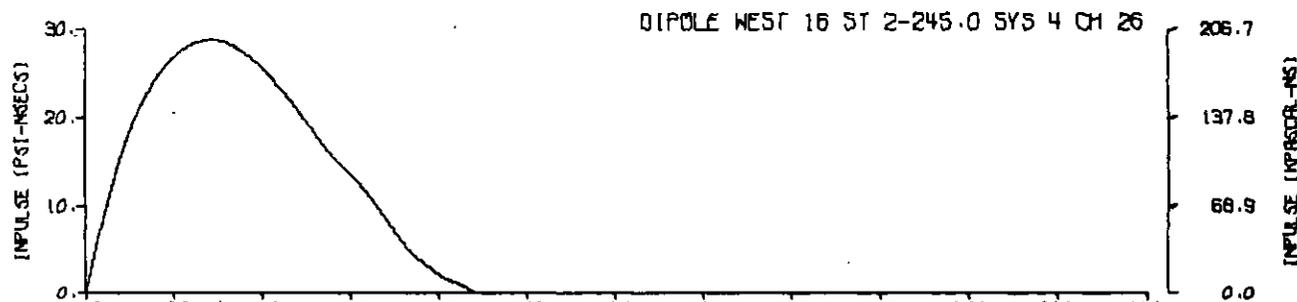
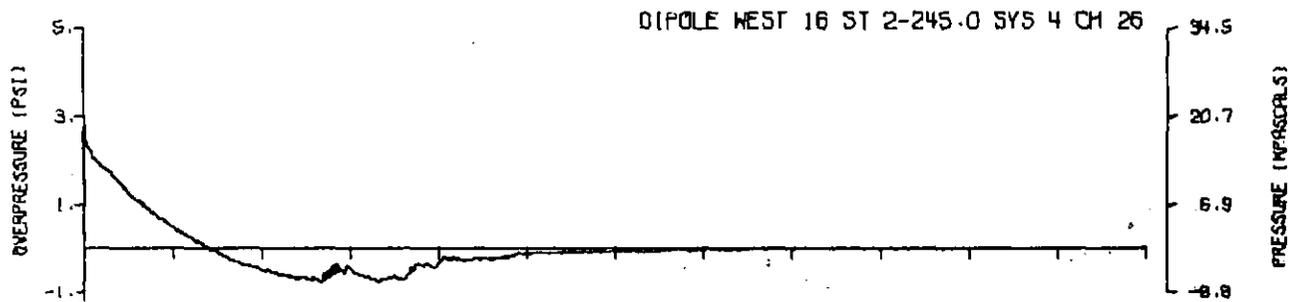
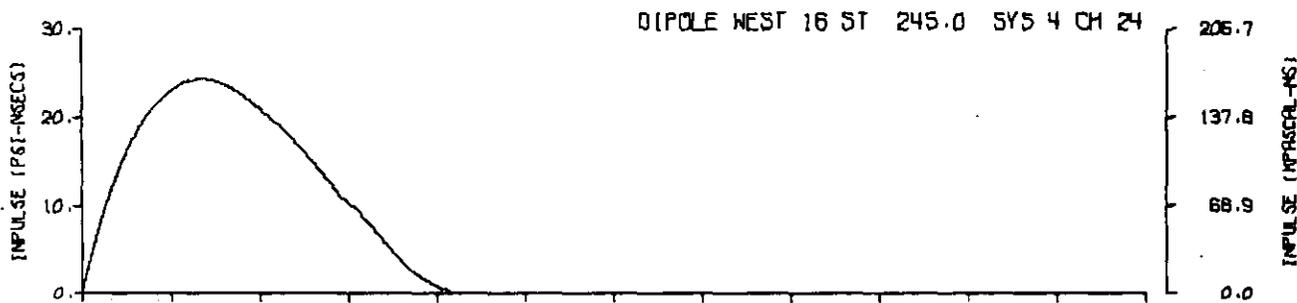
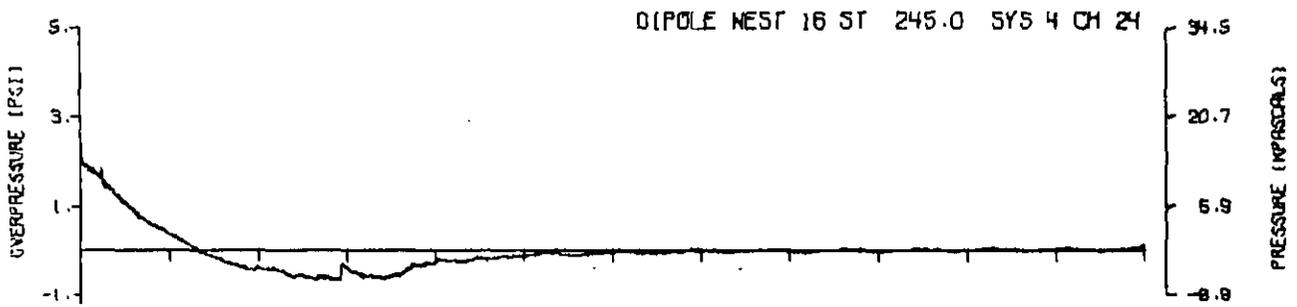
A16.37



A16.38



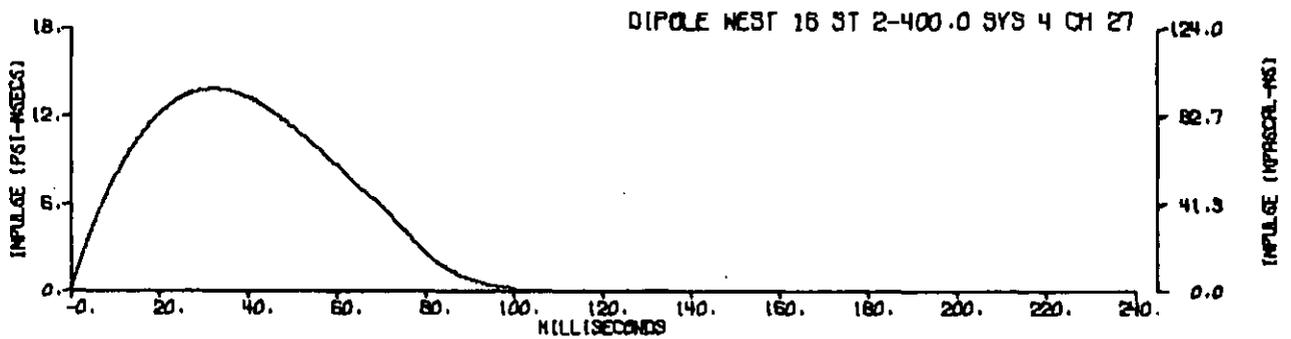
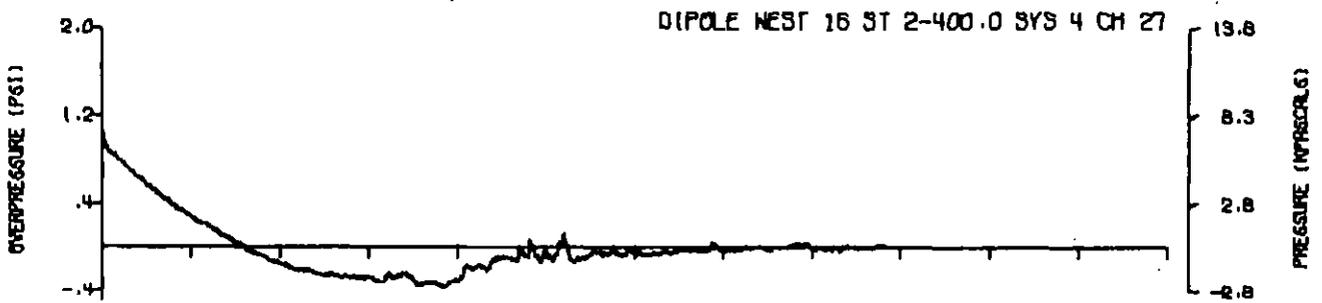
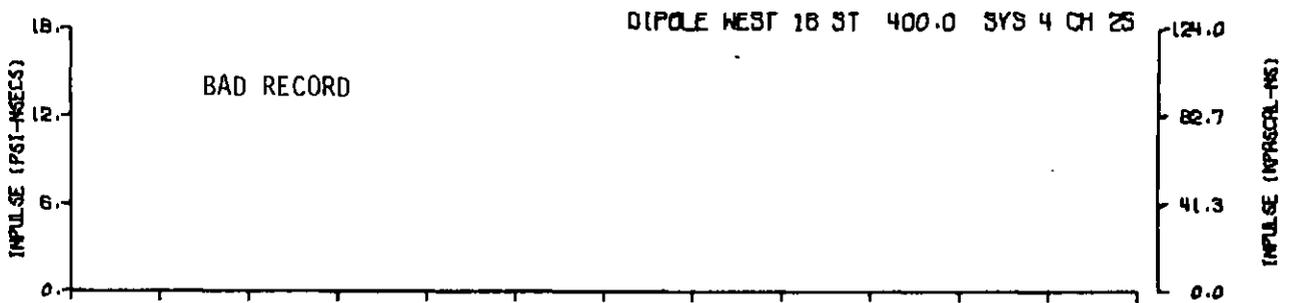
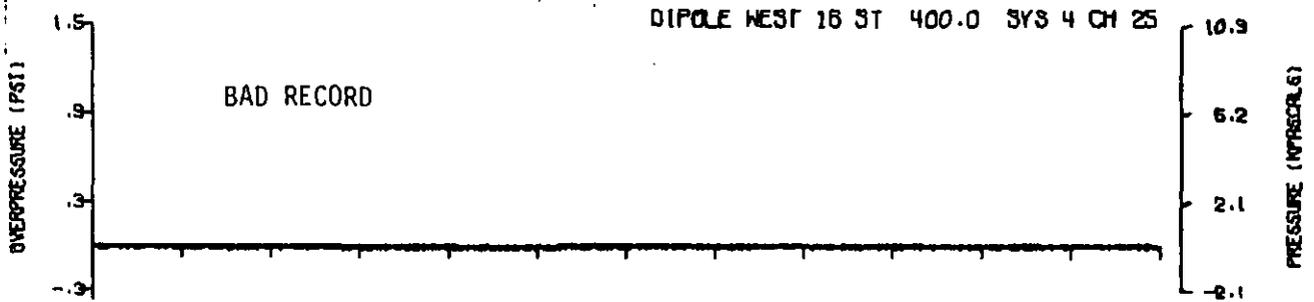
A16.39



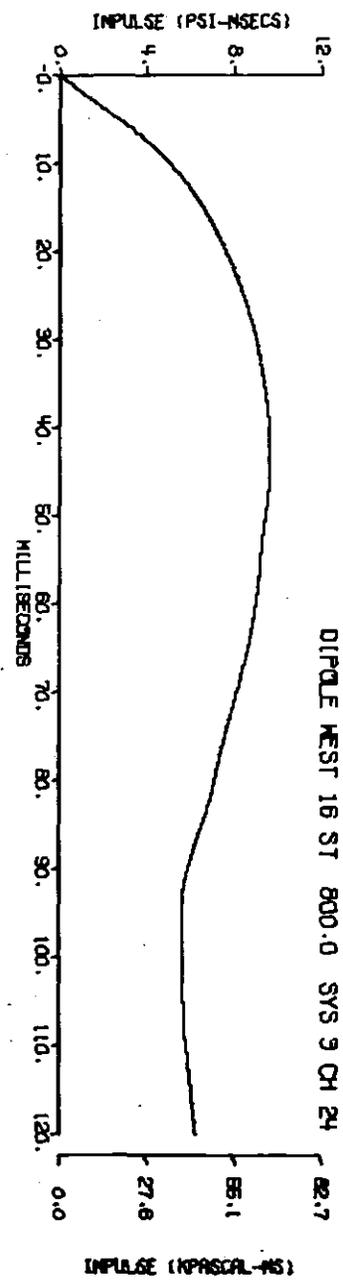
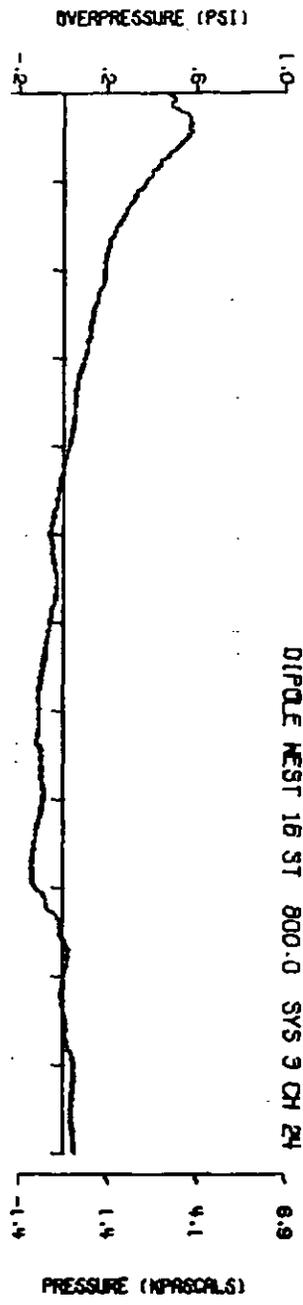
MILLISECONDS

A16.40

375

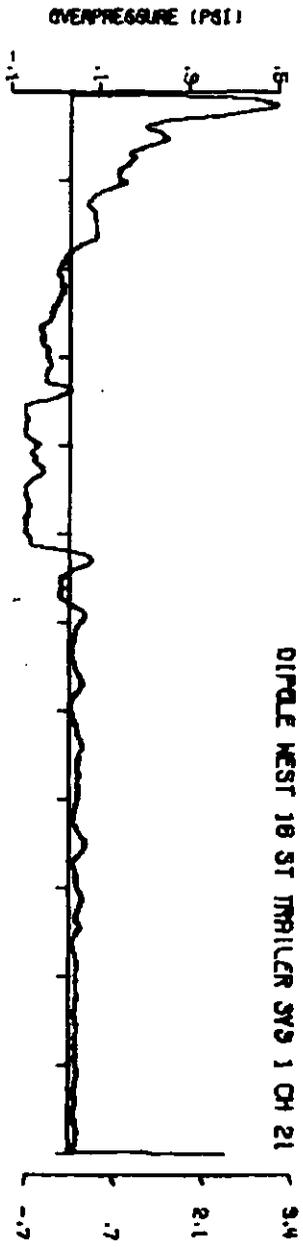


A16.41

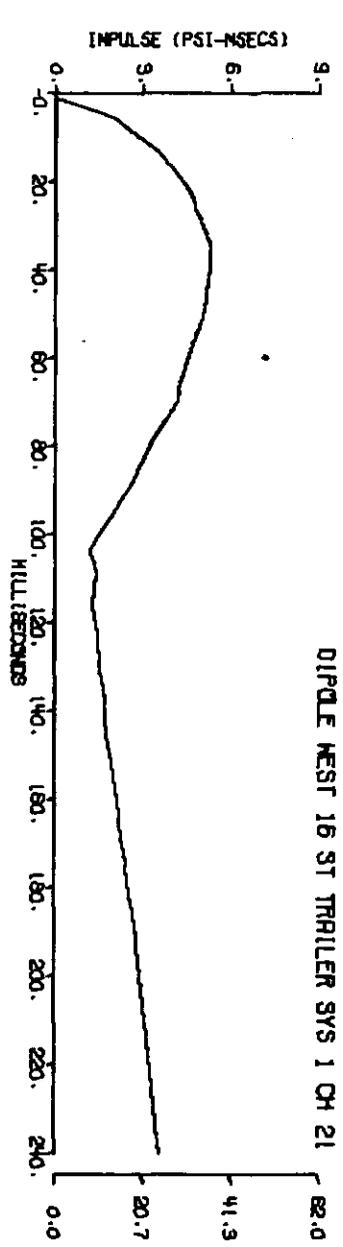


A16.42

377



PRESSURE (MPASCALS)



IMPULSE (MPASCAL-MS)

A16.43

378

DISTRIBUTION LIST

<u>No. of Copies</u>	<u>Organization</u>	<u>No. of Copies</u>	<u>Organization</u>
12	Commander Defense Documentation Center ATTN: DDC-TCA Cameron Station Alexandria, VA 22314	1	Commander US Army Materiel Development and Readiness Command ATTN: DRCDMA-ST 5001 Eisenhower Avenue Alexandria, VA 22333
4	Director of Defense Research and Engineering ATTN: DD/TWP DD/S&SS DD/T&SS AD/SW Washington, DC 20301	1	Commander US Army Aviation Systems Command ATTN: DRSAV-E 12th and Spruce Streets St. Louis, MO 63166
6	Director Defense Nuclear Agency ATTN: STTL (Tech Lib, 2 cys) SPAS, Mr. J. Moulton Mr. D. Kohler DDST, Mr. P. H. Haas SPTD, Mr. J. Kelso Washington, DC 20305	1	Director US Army Air Mobility Research and Development Laboratory Ames Research Center Moffett Field, CA 94035
3	Director Defense Advanced Research Projects Agency ATTN: Tech Library NMRO PMO 1400 Wilson Boulevard Arlington, VA 22209	4	Commander US Army Electronics Command ATTN: DRSEL-RD DRSEL-IR, J. Roma DRSEL-TL, S. Kronenberg R. Freiberg Fort Monmouth, NJ 07703
2	Commander Field Command, DNA ATTN: FCTA-C (Lib) Mr. Noel Ganick Kirtland AFB, NM 87115	4	Commander US Army Missile Command ATTN: DRSMI-S, Ch Scientist DRSMI-R DRSMI-RR, L. Lively DRSMI-RKP, W. Thomas Redstone Arsenal, AL 35809
2	Department of Defense Explosives Safety Board ATTN: R. Perkins Dr. Tom Zaker Room GB-270, Forrestal Building Washington, DC 20314	2	Commander US Army Tank Automotive Development Command ATTN: DRDTA-RHT, LT P. Hasek DRDTA-RWL Warren, MI 48090

DISTRIBUTION LIST

<u>No. of Copies</u>	<u>Organization</u>	<u>No. of Copies</u>	<u>Organization</u>
2	Commander US Army Mobility Equipment Research & Development Center ATTN: Tech Docu Cen, Bldg 315 DRSME-RZT Fort Belvoir, VA 22060	1	Director US Army TRADOC Systems Analysis Activity ATTN: ATAA-SA White Sands Missile Range NM 88002
1	Commander US Army Armament Command ATTN: SARRI-LR/Mr. B. Morris Rock Island, IL 61202	3	Commander US Army Nuclear Agency ATTN: ATCN-W/CPT M. Bowling CDINS-E Technical Library Fort Bliss, TX 79916
2	Commander US Army Picatinny Arsenal ATTN: P. Angelotti SARPA - Mr. G. Demitrack Dover, NJ 07801	1	Director US Army Advanced BMD Technology Center ATTN: Technical Library Commonwealth Building 1320 Wilson Boulevard Arlington, VA 22209
5	Commander US Army Harry Diamond Labs ATTN: DRXDO-TI DRXDO-TI/012 DRXDO-NP, F. N. Wimenitz Jim Gaul J. H. Gwaltney 2800 Powder Mill Road Adelphi, MD 20783	3	Director US Army Advanced BMD Technology Center ATTN: Mr. B. E. Kelley Mr. M. Capps Mr. Marcus Whitfield P.O. Box 1500 Huntsville, AL 35807
1	Director US Army Materials and Mechanics Research Center ATTN: Technical Library Watertown, MA 02172	1	Commander US Army Ballistic Missile Defense Program Office ATTN: DACS-SAE-S, J. Shea Commonwealth Building 1300 Wilson Boulevard Arlington, VA 22209
1	Commander US Army Foreign Science and Technology Center ATTN: Research & Data Branch 220 - 7th Street, NE Charlottesville, VA 22901		

DISTRIBUTION LIST

<u>No. of Copies</u>	<u>Organization</u>	<u>No. of Copies</u>	<u>Organization</u>
3	Commander US Army Ballistic Missile Defense Systems Command ATTN: SSC-DRS, J. G. Buxbaum SSC-DH, H. L. Solomonson SSC-HS, H. Porter P.O. Box 1500 Huntsville, AL 35807	3	Commander US Naval Surface Weapons Center ATTN: Code 1224, Navy Nuclear Programs Office Code 241, J. Petes Code 730, Tech Lib Silver Spring, MD 20910
1	Commander US Army Ballistic Missile Defense Systems Evaluation Agency ATTN: Mr. R. E. Dekinder, Jr. White Sands Missile Range NM 88002	1	Commander Naval Weapons Evaluation Facility ATTN: Document Control Kirtland AFB, NM 87117
1	HQDA (DAMA-AR, NCB Div.) Washington, DC 20310	2	Commander Naval Civil Engineering Lab ATTN: Dr. W. A. Shaw, Code L31 R. Seabold Port Hueneme, CA 93041
2	Commander US Army Engineer Waterways Experiment Station ATTN: Library Mr. W. Flateau P.O. Box 631 Vicksburg, MS 39180	3	Director US Naval Research Laboratory ATTN: M. Persechino G. Cooperstein Tech Library/Code 2027 Washington, DC 20390
3	Chief of Naval Research Department of the Navy ATTN: T. Quinn, Code 464 Technical Library J. L. Warner, Code 464 Washington, DC 20360	1	Commander Charleston Navy Shipyard ATTN: H. Shuler Charleston, SC 29451
2	Commander Naval Ship Engineering Center ATTN: J. R. Sullivan, NSEC 6105-G Technical Library Hyattsville, MD 20782	1	HQ USAFSC (DLCAW, Tech Library) Andrews AFB Washington, DC 20331
		1	AFOSR (OAR) Bolling AFB, DC 20332
		1	RADC (Documents Library) FMTLD Griffiss AFB, NY 13440
		4	AFWL (WLRE, Dr. A. Guenther; DYT, Charles Needham; DYT, MAJ G. Ganong DYT, Burt Chambers Kirtland AFB, NM 87117

DISTRIBUTION LIST

<u>No. of Copies</u>	<u>Organization</u>	<u>No. of Copies</u>	<u>Organization</u>
1	AFGL (F. Doherty) Hanscom AFB, MA 01731	2	Los Alamos Scientific Laboratory ATTN: Dr. J. Taylor Technical Library P.O. Box 1663 Los Alamos, NM 87544
1	SAMSO (RSSE, MAJ R. Rene) P.O. Box 92960 Los Angeles, CA 90009	1	National Academy of Sciences ATTN: Dr. Donald Groves 2101 Constitution Avenue, NW Washington, DC 20418
3	AFTAC (K. Rosenlof, R. McBryde, G. Leies) Patrick AFB, FL 32925	1	Aerojet-General Corporation ATTN: Dr. G. Woffinden 11711 South Woodruff Avenue Downey, CA 92041
2	AFML (G. Schmitt, MAS; D. Schmidt) Wright-Patterson AFB, OH 45433	1	Aerospace Corporation ATTN: Dr. Michael Kausch Bldg 105, Rm 2220 P.O. Box 92957 Los Angeles, CA 90009
1	Department of the Interior US Geological Survey ATTN: Dr. D. Roddy 601 East Cedar Avenue Flagstaff, AZ 86001	1	Agbabian Associates ATTN: Dr. J. Malthan 250 N. Nash Street El Segundo, CA 90245
2	Energy Research and Development Administration Dept of Military Applications ATTN: R&D Branch Library Branch, G-043 Washington, DC 20545	1	AVCO Government Projects Group ATTN: Dr. W. Bade 201 Lowell Street Wilmington, MA 01887
1	Director National Aeronautics and Space Administration ATTN: Code 04.000 Langley Research Center Langley Station Hampton, VA 23365	1	AVCO-Everett Research Laboratory ATTN: Technical Library 2385 Revere Beach Parkway Everett, MA 02149
1	Director NASA Scientific and Technical Information Facility ATTN: SAK/DL P.O. Box 8757 Baltimore/Washington International Airport, MD 21240	1	Battelle Memorial Institute ATTN: Technical Library 505 King Avenue Columbus, OH 43201

DISTRIBUTION LIST

<u>No. of Copies</u>	<u>Organization</u>	<u>No. of Copies</u>	<u>Organization</u>
1	Bell Telephone Laboratories ATTN: Mr. E. Witt Whippany Road Whippany, NJ 07981	1	Hughes Aircraft Company Systems Development Laboratory ATTN: Dr. A. Puckett Centinela and Teale Streets Culver City, CA 90232
1	John A. Blume and Associates ATTN: Dr. John A. Blume Sheraton - Palace Hotel 100 Jessie Street San Francisco, CA 94105	1	Ion Physics Corporation ATTN: Technical Library South Bedford Street Burlington, MA 01803
1	Calspan Corporation ATTN: Library P.O. Box 235 Buffalo, NY 14221	3	Kaman Sciences Corporation ATTN: Dr. D. Williams Dr. F. Shelton Dr. D. Sachs 1500 Garden of the Gods Road Colorado Springs, CO 80907
1	Effects Technology, Inc. ATTN: E. Anderson 5383 Holister Avenue Santa Barbara, CA 93105	2	Kaman Avidyne, Division of Kaman Sciences ATTN: Dr. Normal Hobbs Dr. J. Ray Ruetenik 83 Second Avenue, NW Industrial Park Burlington, MA 01803
1	Fairchild Hiller, Republic Aviation Division ATTN: Engr Library Farmingdale, NY 11735	1	KTECH Corporation ATTN: Dr. Donald V. Keller 911 Pennsylvania, NE Albuquerque, NM 87110
1	General Electric Co., TEMPO ATTN: DASIAC 816 State Street, Drawer QQ Santa Barbara, CA 93102	2	Lockheed Missiles and Space Company, Inc. Division of Lockheed Aircraft Corporation ATTN: J. Nickell L. Hearne P.O. Box 504 Sunnyvale, CA 94088
3	General Electric Co., TEMPO ATTN: Dr. Craig Hudson Dr. Lynn Kennedy Mr. Gerald L. E. Perry 7800 Marble Avenue, NW, Suite 5 Albuquerque, NM 87110	2	Lovelace Foundation ATTN: Dr. D. Richmond Dr. R. Fletcher 4800 Gibson Boulevard, SE Albuquerque, NM 87108
1	H. J. Wiggins Company ATTN: Dr. J. H. Wiggins, Jr. 2516 Via Tejon Palos Verdes Estates CA 92074		

DISTRIBUTION LIST

<u>No. of Copies</u>	<u>Organization</u>	<u>No. of Copies</u>	<u>Organization</u>
3	Martin Marietta Aerospace Orlando Division ATTN: A. Ossin H. Sugiuchi C. Washburn P.O. Box 5837 Orlando, FL 32805	1	Science Applications, Inc. ATTN: Dr. T. Stefansky 1261 Birchwood Drive Sunnyvale, CA 94086
1	Maxwell Laboratories, Inc. ATTN: A. Kolb 9244 Balboa Avenue San Diego, CA 92123	1	Shock Hydrodynamics, Inc. ATTN: L. Zernow 4710-16 Vineland Avenue North Hollywood, CA 91602
1	McDonnell Douglas Astronautics Corporation ATTN: Technical Library 5301 Bolsa Avenue Huntington Beach, CA 92647	1	Systems, Science & Software, Inc. ATTN: H. E. Read P.O. Box 1620 La Jolla, CA 92037
1	Philco-Ford Corporation Aeronutronic Division ATTN: L. K. Goodwin Newport Beach, CA 92663	2	Teledyne-Brown Engineering ATTN: Dr. M. Batel Dr. R. Patrick Research Park Huntsville, AL 35807
2	Physics International Company ATTN: Document Control F. Sauer 2700 Merced Street San Leandro, CA 94577	1	Union Carbide Corporation Oak Ridge National Laboratory ATTN: J. Auxier P.O. Box X Oak Ridge, TN 37830
1	R&D Associates ATTN: Technical Library P.O. Box 3580 Marina del Rey, CA 90403	1	URS Research Company ATTN: Technical Library 155 Bovet Road San Mateo, CA 94002
4	Sandia Laboratories ATTN: Dr. C. Broyles Dr. D. McCloskey Mr. Jack W. Reed Dr. J. Kennedy P.O. Box 5800 Albuquerque, NM 87115	1	Denver Research Institute University of Denver ATTN: Mr. John Wisotski P.O. Box 10127 Denver, CO 80210
		2	IIT Research Institute ATTN: Dr. Robert Denne Technical Library 10 West 35th Street Chicago, IL 60616

DISTRIBUTION LIST

<u>No. of Copies</u>	<u>Organization</u>	<u>No. of Copies</u>	<u>Organization</u>
1	The John Hopkins University Dept of Mechanics and Material Sciences ATTN: Dr. F. D. Bennett 34th and Charles Streets Baltimore, MD 21218	1	Temple University Department of Physics ATTN: Prof T. Korneff Philadelphia, PA 19122
1	Applied Physics Laboratory The Johns Hopkins University Johns Hopkins Road Laurel, MD 20810	1	Research Institute of Temple University ATTN: Technical Library Philadelphia, PA 19144
1	Louisiana State University ATTN: Dr. O. Nance P.O. Box 16006 Baton Rouge, LA 70803	1	Texas Technical University Depart of Civil Engineering ATTN: Mr. Joseph E. Minor Lubbock, TX 79409
1	Massachusetts Institute of Technology Aerophysics Laboratory Cambridge, MA 02139	1	University of Arkansas Department of Physics ATTN: Prof O. Zinke Fayetteville, AR 72701
1	Northwestern Michigan College ATTN: Prof D. C. Kennard, Jr. Traverse City, MI 49684	2	University of California Lawrence Livermore Laboratory Technical Information Division ATTN: Technical Library Dr. Donald N. Montan P.O. Box 808 Livermore, CA 94550
1	Southwest Research Institute ATTN: Dr. W. Baker 8500 Culebra Road San Antonio, TX 78206	1	University of Maryland Department of Physics ATTN: Dr. E. Oktay College Park, MD 20742
1	Stevens Institute of Technology Department of Elect Engrg ATTN: Prof R. Geldmacher Castle Point Station Hoboken, NJ 07039	1	University of Oklahoma Department of Physics ATTN: Prof R. Fowler Norman, OH 73069
1	Syracuse University Department of Physics ATTN: Prof C. Bachman Syracuse, NY 13201		<u>Aberdeen Proving Ground</u> Marine Corps Ln Ofc Dir, USAMSAA ATTN: Dr. J. Sperrazza Mr. R. Norman, WSD